



HAL
open science

Identification of new levers to fight muscle atrophy: benefit of the hibernating brown bear model.

Laura Cussonneau

► **To cite this version:**

Laura Cussonneau. Identification of new levers to fight muscle atrophy: benefit of the hibernating brown bear model.. Tissues and Organs [q-bio.TO]. 2022. hal-04129120

HAL Id: hal-04129120

<https://hal.inrae.fr/hal-04129120v1>

Submitted on 15 Jun 2023

HAL is a multi-disciplinary open access archive for the deposit and dissemination of scientific research documents, whether they are published or not. The documents may come from teaching and research institutions in France or abroad, or from public or private research centers.

L'archive ouverte pluridisciplinaire **HAL**, est destinée au dépôt et à la diffusion de documents scientifiques de niveau recherche, publiés ou non, émanant des établissements d'enseignement et de recherche français ou étrangers, des laboratoires publics ou privés.

ECOLE DOCTORALE DES SCIENCES DE LA VIE, SANTE
AGRONOMIE, ENVIRONNEMENT

Thèse

Présentée à l'Université Clermont Auvergne

Pour l'obtention du grade de

DOCTEUR D'UNIVERSITE

Spécialité : Biologie cellulaire et Physiologie

Présentée et soutenue publiquement par

Laura CUSSONNEAU

Le 15 décembre 2022

Identification of new levers to fight muscle atrophy: benefit
of the hibernating brown bear model.

Rapporteurs : **Pr. Jean-Paul THISSEN**, Clinique Saint-Luc / Université catholique de Louvain (Belgique)
Dr. Audrey BERGOUIGNAN, IPHC / CNRS U7178 / Université de Strasbourg (France)

Examineurs : **Dr. Jennifer RIEUSSET**, CarMeN / Inserm U1060 / Université Lyon 1 (France)
Dr. Cédric CHAVEROUX, CRCL / Inserm U1052 CNRS 5286 / Université Lyon 1 (France)

Directeurs de thèse : **Dr. Lydie COMBARET**, UNH / INRAE U1019 / Université Clermont Auvergne (France)
Dr. Etienne LEFAI, UNH / INRAE U1019 / Université Clermont Auvergne (France)

[...]

*Sans la curiosité de l'esprit, que serions-nous ?
Telle est bien la beauté et la noblesse de la
science: désir sans fin de repousser les
frontières du savoir, de traquer les secrets de
la matière et de la vie sans idée préconçue des
conséquences éventuelles.*

Marie Skłodowska-Curie, 1938

1. Acknowledgements

Aux membres du jury, le Pr Jean-Paul Thissen, la Dr Audrey Bergouignan, la Dr Jennifer Rieusset et le Dr Cédric Chaveroux

Je suis très honorée de vous compter parmi les membres de mon jury. Un immense merci pour votre temps que je sais très précieux. Un grand merci également pour votre expertise apportée sur mon travail qui, je l'espère, vous apportera satisfaction.

A ma directrice et directeur de thèse, la Dr Lydie Combaret et le Dr Etienne Lefai

Lydie, Etienne, je vous remercie de l'immense confiance que vous m'avez accordée pendant ces trois ans de thèse. J'ai beaucoup appris à vos côtés et vous m'avez permis de vivre des expériences de vie inoubliables. Il est difficile de retracer en seulement quelques lignes trois ans de partage, d'échange et d'écoute dont vous avez fait preuve. Merci pour vos grandes qualités humaines qui ont fait de cette thèse un moment de ma vie que je n'oublierai jamais.

A l'équipe Protéostasis

Merci à tous les membres de l'équipe Protéostasis, on ne peut pas espérer un meilleur cadre de travail, joie et bonne humeur sont les maîtres mots de cette équipe. Je vous souhaite à tous le meilleur dans vos vies professionnelles et personnelles. J'aimerais remercier tout particulièrement certaines personnes. Merci à Pierre le chef d'équipe, alias Pr Dumbledore, pour tes conseils scientifiques toujours très avisés, et pour tes histoires de vie toujours très passionnantes. Merci à Christiane, pour ton aide technique, mais surtout pour ta générosité et ta gentillesse, j'ai beaucoup appris à tes côtés et je te souhaite la plus formidable des retraites. Merci à Cécile, ma partenaire de pilate et de stretching, pour ton aide en histologie mais aussi pour nos franches rigolades et confessions. Et merci à Lolo, pour ta bonne humeur et ton écoute, tu m'auras tellement fait rire, tu as été mon soleil du labo.

Aux animaliers de l'INRAE de Theix

Merci à toute l'équipe de l'animalerie de Theix qui fournit un travail formidable. Un merci tout spécial à Mehdi et Yoann, vous m'avez bien fait rire pendant ces trois ans, et également bien aidé avec mes souris suspendues, ce fût un réel plaisir de travailler avec vous. Vous me croyez maintenant, je n'étais pas une stagiaire !

A l'équipe du Brown Bear Project

Merci à toute l'équipe du BBP, sans qui ce projet de thèse n'aurait jamais existé. Cette équipe de vétérinaires, de rangers et de scientifiques expérimentés permet à ce consortium de vivre et de faire naître de beaux projets scientifiques.

A Fabrice Bertile et Damien Freyssenet

Merci à Fabrice Bertile et Damien Freyssenet pour les échanges scientifiques de qualité que l'on a pu avoir lors de mes comités scientifiques de thèse. Merci à toi Fabrice également pour ton implication dans le BBP, et l'inoubliable expérience que tu m'as offerte avec Etienne lors de notre voyage en Suède.

A l'IUT Génie Biologique de Clermont-Ferrand

Merci à l'IUT Génie Biologique de Clermont-Ferrand, et spécialement à Mathilde Bonnet et Jérémy Denizot pour leur confiance en m'accordant un poste de vacataire pendant deux ans, ce fût une belle expérience qui a confirmé mon souhait de devenir enseignante chercheuse.

Aux étudiant.es de l'équipe de passage ou de plus longue durée

Merci aux doctorants qui ont partagé pendant trois ans cette incroyable expérience. Merci à Christian, même si tu râles beaucoup tu es très attachant, il faudrait te créer si tu n'existais pas. Merci à Aurore pour ta bienveillance et surtout tes conseils de maman chat quand je le suis devenue également. Merci à Ghita, pour ta présence et ton écoute. On aura partagé de jolis moments, je regrette déjà ta tajine somptueuse, tes appels avec ton franco-arabe qui me faisaient tant rigoler, tu vas beaucoup me manquer. Merci à Guillaume, mon petit frère ours, pour ces moments de franche rigolade au labo et en dehors, j'espère que tu t'occuperas bien de papa ours en mon absence. Merci à Maelle, ça a été un plaisir de travailler avec toi pendant quelques mois, et de partager de jolis moments de vie ensemble dans notre immeuble. Et merci à Maxime, alias Ludovic, Pierre, Enguerrand Raucroy, merci pour tous ces moments de rire, d'avoir relu mon manuscrit, de m'avoir consolée quand je doutais, et merci de m'avoir donné un peu plus confiance en moi.

A Dulce

Il était nécessaire de faire un paragraphe à part pour toi ma Dutz. Merci d'avoir été la première personne que j'ai rencontré dans cette ville, tu as transformé mon expérience Clermontoise et mon expérience de thèse comme je ne l'aurais jamais imaginé. Merci d'avoir partagé ces rires, ces doutes, ces questionnements et ces confessions pendant trois ans dans notre bureau, dans nos appartements ou pendant notre traversée de la Corse à pied. Je suis extrêmement chanceuse d'avoir croisé ton chemin. Te quiero mucho como la trucha y el trucho.

A mon fils

A mon petit chat Bibi, auvergnat d'origine, qui me rappellera à vie ce souvenir indélébile de l'Auvergne. Merci pour tous ces câlins réconfortants et ta présence de tout instant.

Aux KAPAK

Ces trois ans n'auraient pas été les mêmes si je n'avais pas pu m'évader dans ma passion de toujours, la danse. Alors un immense merci à Yohann Sebileau, le meilleur professeur de danse contemporaine de la Terre, je pleure déjà la fin de tes cours, tu m'auras tellement fait progresser, merci pour tes chorées et ton engagement, merci pour ces moments sur scène gravés à tout jamais. Et merci à mes copines Tia et Claire pour ces jolis moments de danse partagés en cours, sur scène et en dehors.

A mes ami.es clermontois.es

Merci à Alexis, mon compère de soirées et de confidences, tes petits plats vont terriblement me manquer mais pas plus que toi. Merci à ma copine Melu, pour ton soutien, ton amitié, ces soirées à refaire le monde et à rêver ensemble. Et merci au groupe des Théseux pour la bonne humeur et les galères de thèse partagées ensemble.

A mes ami.es de longue date

A Chachou, Dédoule et Cass, mes meilleures amies depuis tant d'années maintenant, votre amour et soutien sont sans faille, vous êtes mes piliers de vie, merci pour tout. Merci à Ele, ma précieuse amie, pour nos week-ends évasion et dégustation de vin. Merci à ma Caice pour ta joie de vivre et tes mots réconfortants. Merci à mes copains de master Juju, Roro, Fabi, Val et Mauricette pour nos week-ends découverte de la France et votre présence depuis Lyon. Et merci à mes copains bourguignons, à nos soirées au Galopin ou à la cocoloc, ces moments de franche rigolade m'ont permis de tenir le choc pendant trois ans.

A ma famille

Merci à ma famille, pour votre soutien et amour inconditionnel depuis 26 ans. A mon papa et ma maman, qui ont toujours les mots qu'il faut pour apaiser mes angoisses et doutes. A mes deux petites sœurs Marine et Ema, qui me comblent de bonheur. A ma tata Séverine, mon tonton Pascal et à ma mamie MC pour votre présence et votre amour, et à mon papi parti pendant ma thèse qui je sais aurait été très fier de moi.

2. Contents

2.1 Table of contents

1. ACKNOWLEDGEMENTS	3
2. CONTENTS	6
2.1 TABLE OF CONTENTS	6
2.2 PUBLICATIONS	8
2.2.1 Publications directly associated with the thesis work.....	8
2.2.2 Other publication	8
2.3 ORAL COMMUNICATIONS	9
2.3.1 National and International congresses	9
2.3.2 Invited conferences.....	9
2.3.3 Communication towards the general public.....	10
2.3.4 Congress organisation	10
2.4 LIST OF FIGURES	11
2.5 LIST OF ABBREVIATIONS	13
3. PREFACE	15
4. STATE OF THE ART	16
4.1 SKELETAL MUSCLE: THE HOLY GRAIL FOR WHOLE-BODY HOMEOSTASIS	16
4.1.1 Introduction	16
4.1.2 Muscle protein turnover	20
4.1.3 Muscle atrophy	26
4.2 A PIVOTAL ROLE FOR THE TGF-β SUPERFAMILY IN SKELETAL MUSCLE HOMEOSTASIS	31
4.2.1 Overview	31
4.2.2 TGF- β signalling: The master regulator of skeletal muscle atrophy.....	33
4.2.3 BMP signalling: The silver bullet for muscle atrophy ?	37
4.2.4 A finely tuned balance between TGF- β and BMP signalling.....	40
4.3 THE INTEGRATED STRESS RESPONSE SIGNALLING: BENEFICIAL OR HARMFUL FOR SKELETAL MUSCLE?	43
4.3.1 Overview	43
4.3.2 The ISR pathway involvement in autophagy and mitochondrial homeostasis	47
4.3.3 The ISR pathway implication in muscle atrophy	48
4.4 A NATURAL MODEL OF MUSCLE ATROPHY RESISTANCE: THE HIBERNATING BROWN BEAR	53
4.4.1 Getting inspired by the oldest research laboratory: Nature	53
4.4.2 Hibernation: a bioinspired approach for human challenges	53
4.4.3 Hibernation in bears.....	54
4.4.4 Skeletal muscle features in hibernating bears	58
4.4.5 Circulating antiproteolytic compounds in hibernating bear serum	63
4.4.6 The ISR and TGF- β superfamily signalling regulation in hibernating mammal muscles.....	64
5. OBJECTIVES AND STRATEGIES	66
6. STUDY 1: CONCURRENT BMP SIGNALING MAINTENANCE AND TGF-β SIGNALING INHIBITION IS A HALLMARK OF NATURAL RESISTANCE TO MUSCLE ATROPHY IN THE HIBERNATING BEAR	68
6.1 OBJECTIVE AND STRATEGY	68
6.2 EXPERIMENTAL PROTOCOL	68

6.3	PAPER	71
6.4	DISCUSSION AND PERSPECTIVES	97
6.4.1	Hibernation induces a transcriptomic reprogramming in genes related to protein synthesis and RNA metabolism in bear muscles	97
6.4.2	Hibernation induces a transcriptomic reprogramming in TGF- β superfamily-related genes in bear muscles	99
7.	STUDY 2: INDUCTION OF ATF4 ATROGENES IS UNCOUPLED FROM DISUSE-INDUCED MUSCLE ATROPHY IN HALOFUGINONE-TREATED MICE AND IN HIBERNATING BROWN BEAR	110
7.1	OBJECTIVE AND STRATEGY	110
7.2	PAPER	111
7.3	DISCUSSION AND PERSPECTIVES	141
7.3.1	Halofuginone mechanism of action in skeletal muscle	141
7.3.2	Biological effects of halofuginone on skeletal muscle	144
7.3.3	The dual role of ATF4 signalling in skeletal muscle	146
7.3.4	Halofuginone-like compound enriched in bear food	149
8.	STUDY 3: WINTER BEAR SERUM INDUCES SIMILAR CHARACTERISTICS IN HUMAN MUSCLE CELLS AS THOSE FOUND NATURALLY IN HIBERNATING BEAR MUSCLE	151
8.1	OBJECTIVE AND STRATEGY	151
8.2	RESULTS, DISCUSSION AND PERSPECTIVES	151
8.2.1	Analysis of microarrays in human muscle cells cultivated with WBS.....	151
8.2.2	Optimisation of tools for the screening active compounds in WBS.....	152
8.2.3	Perspective on identifying the circulating active compound in WBS.....	154
9.	GENERAL CONCLUSION	156
10.	APPENDIX	157
10.1	MATERIALS AND METHODS DISCUSSION 1	157
10.1.1	Identification of BMP target genes in skeletal muscle.....	157
10.1.2	Is SMAD4 recruited more by TGF- β or BMP signalling: Co-immunoprecipitation	158
10.1.3	Is GDF5 synthesised and released by adipose tissue: GDF5 ELISA.....	159
10.2	MATERIALS AND METHODS DISCUSSION 2	159
10.2.1	Complementary RT-qPCR and Western blots of study 2	159
10.2.2	ATF4 signalling in hibernating bear muscles	160
10.3	MATERIALS AND METHODS DISCUSSION 3	160
10.3.1	Optimisation of tools for screening active compounds in WBS.....	160
10.4	REVIEW	163
10.5	PAPER	201
10.6	RESUME DE LA THESE EN FRANÇAIS	216
10.6.1	Introduction bibliographique.....	216
10.6.2	Objectifs et stratégies	232
10.6.3	Résultats	235
10.6.4	Conclusion générale.....	240
11.	REFERENCES	241

2.2 Publications

2.2.1 Publications directly associated with the thesis work

Cussonneau, L.; Coudy-Gandilhon, C.; Deval, C.; Chaouki, G.; Djelloul-Mazouz, M.; Delorme, Y.; Hermet, J.; Gauquelin-Koch, G.; Polge, C.; Taillandier, D.; et al. *Induction of ATF4-Regulated Atrogenes Is Uncoupled from Muscle Atrophy during Disuse in Halofuginone-Treated Mice and in Hibernating Brown Bears*. IJMS 2022, 24, 621, doi:10.3390/ijms24010621.

Cussonneau, L.; Boyer, C.; Brun, C.; Deval, C.; Loizon, E.; Meugnier, E.; Gueret, E.; Dubois, E.; Taillandier, D.; Polge, C.; et al. *Concurrent BMP Signaling Maintenance and TGF- β Signaling Inhibition Is a Hallmark of Natural Resistance to Muscle Atrophy in the Hibernating Bear*. Cells 2021, 10, 1873, doi:10.3390/cells10081873.

Peris-Moreno, D.; **Cussonneau, L.;** Combaret, L.; Polge, C.; Taillandier, D. *Ubiquitin Ligases at the Heart of Skeletal Muscle Atrophy Control*. Molecules 2021, 26, 407, doi:10.3390/molecules26020407.

Boyer, C.; **Cussonneau, L.;** Brun, C.; Deval, C.; Pais de Barros, J.-P.; Chanon, S.; Bernoud-Hubac, N.; Daira, P.; Evans, A.L.; Arnemo, J.M.; et al. *Specific Shifts in the Endocannabinoid System in Hibernating Brown Bears*. Front Zool 2020, 17, 35, doi:10.1186/s12983-020-00380-y.

2.2.2 Other publication

Piecyk, M.; Triki, M.; Laval, P.-A.; Dragic, H.; **Cussonneau, L.;** Fauvre, J.; Duret, C.; Aznar, N.; Renno, T.; Manié, S.N.; et al. *Pemetrexed Hinders Translation Inhibition upon Low Glucose in Non-Small Cell Lung Cancer Cells*. Metabolites 2021, 11, 198, doi:10.3390/metabo11040198.

2.3 Oral communications

2.3.1 National and International congresses

2.3.1.1 Orals

Cussonneau, L. ; Boyer, B. ; Meugnier, E. ; Gauquelin-Koch, G. ; Arnemo, J. ; Lefai, E. ; Bertile, F. ; Combaret, L.; *Concurrent BMP signaling maintenance and TGF- β signaling inhibition is a hallmark of natural resistance to muscle atrophy*, Congrès des Jeunes Chercheurs en Auvergne-Rhône-Alpes, on-line (France), June 2021, oral.

Cussonneau, L. ; Dubois, E. ; Arnemo, J. ; Bertile, F. ; Lefai, E. ; Combaret, L.; *Concurrent BMP maintenance and TGF- β inhibition is a hallmark of bear resistance to muscle atrophy*, 16th International Hibernation Symposium, Groningen (Netherlands), August 2021, oral plenary session.

Cussonneau, L. ; Dubois, E. ; Arnemo, J. ; Bertile, F. ; Lefai, E. ; Combaret, L.; *Concurrent BMP maintenance and TGF- β inhibition is a hallmark of bear resistance to muscle atrophy*, 18^{ème} Journées de la Société Française de Myologie, Saint-Etienne (France), November 2021, oral plenary session.

2.3.1.2 Posters

Cussonneau, L. ; Boyer, B. ; Deval, C. ; Meugnier, E. ; Gueret, E. ; Dubois, E. ; Béchet, D. ; Polge, C. ; Taillandier, D. ; Arnemo, J. ; Bertile, F. ; Lefai, E. ; Combaret, L.; *Genetic reprogramming involving a shift from TGF- β to BMP signaling for muscle mass maintenance in hibernating brown bear*, 23rd Day of the Doctoral School SVSAE, Clermont-Ferrand (France), October 2020, poster session and speed poster, best poster prize.

Cussonneau, L. ; Dubois, E. ; Arnemo, J. ; Boyer, B. ; Deval, C. ; Taillandier, D. ; Polge, C. ; Béchet, D. ; Bertile, F. ; Lefai, E. ; Combaret, L.; *Concurrent BMP Signaling Maintenance and TGF- β Signaling Inhibition Is a Hallmark of Natural Resistance to Muscle Atrophy in the Hibernating Bear*, 9th International Congress Proteasome and Autophagy, Clermont-Ferrand (France), October 2021, poster session and speed poster.

2.3.2 Invited conferences

Scientific seminar, *Get inspired by living: BMP/TGF- β balance for muscle atrophy resistance in hibernating bear muscle* , I-SITE CAP 20-25, Clermont-Ferrand (France), June 2022, oral.

Scientific seminar, *BMP maintenance and TGF- β inhibition in the hibernating bear: a key to muscle atrophy resistance*, for the Institute of Arctic Biology, University of Alaska Fairbanks, on-line (Fairbanks, Alaska), October 2022, oral.

2.3.3 Communication towards the general public

Science Festival, *Studying animals to go to Mars: a story with rockets, men and bears*, audience of middle and high school students, Clermont-Ferrand (France), October 2019.

Participation at the international competition "My Thesis in 180s", Internet Users Prize and 2nd Jury Prize at Clermont-Ferrand final, Clermont-Ferrand (France), March 2021 (<https://www.youtube.com/watch?v=2ssYh-TnhEM&t=1s>).

"Partenaire scientifique pour la classe" program with *Maison pour la Science en Auvergne*, scientific interventions in kindergarten classes, Saint-Saturnin (France), January-March 2021.

2.3.4 Congress organisation

Organising committee for the 9th International Congress Proteasome and Autophagy, Clermont-Ferrand (France), October 2021.

2.4 List of figures

State of the art

Figure 1. Skeletal muscle organisation and contractile apparatus structure* ¹	17
Figure 2. Myokinome overview of muscle-organ crosstalk*	19
Figure 3. Myokinome overview of muscle autocrine/paracrine crosstalk*	20
Figure 4. Muscle protein balance in physiological conditions*	21
Figure 5. mTORC1 and mTORC2 intracellular organisation and their biological effects*	22
Figure 6. Autophagy-lysosomal system*	24
Figure 7. Ubiquitin-proteasomal system*	25
Figure 8. Muscle protein imbalance in pathophysiological conditions leading to muscle atrophy*	27
Figure 9. Histopathological characteristics of healthy muscle (A) versus atrophied muscle (B) with a decrease of myofiber cross sectional area (CSA)*	28
Figure 10. Overview of anabolic and catabolic signalling pathways involved in muscle protein homeostasis.....	30
Figure 11. TGF- β superfamily organisation and signal transduction*	32
Figure 12. TGF- β superfamily regulation by E3-ubiquitin ligase and deubiquitinase enzymes*	33
Figure 13. TGF- β signalling involvement in muscle atrophy*	35
Figure 14. BMP signalling involvement in muscle hypertrophy*	39
Figure 15. SMAD4 recruitment in muscle in basal (A) or muscle wasting (B) conditions*	40
Figure 16. Non-SMAD TGF- β /BMP signalling and its dual involvement in muscle homeostasis*	42
Figure 17. The Integrated Stress Response pathway organisation and signal transduction*	44
Figure 18. ATF4 mRNA sequence and its translation upon (A) basal condition or (B) stress condition.*	45
Figure 19. The Integrated Stress Response involvement in muscle homeostasis*	50
Figure 20. Pictures of hibernating brown bear dens in North Sweden.	55
Figure 21. Main physiological characteristics of hibernating bears.....	57
Figure 22. Overview of the spectacular characteristics of bears resistance to physiological damage during hibernation*	58
Figure 23. Protein content in bear muscles in summer, early denning and late denning.	59
Figure 24. Protein turnover in bear muscles in summer, early denning and late denning.	61
Figure 25. A complex and non-exhaustive overview of the mechanisms identified in bears to save muscle protein content during hibernation*	62
Figure 26. Winter bear serum promotes hypertrophy in human muscle cells.....	64

Study 1

Figure 27. Schema of the experimental strategy of study 1*	68
Figure 28. Hindlimb suspension model in laboratory mice.	69
Figure 29. Pictures from the collection of free-ranging bears samples in the forest of Northern Sweden as part of the Brown Bear Research Project.	70
Figure 30. Graphical abstract of the study 1*	97
Figure 31. Detailed enriched terms from the biological processes “Protein metabolism” and “RNA metabolism” from the differentially expressed genes in Cussonneau et al., 2021.	99
Figure 32. Western blots of total and phosphorylated SMAD1/5, and SMAD4 in CCL136 human muscle cells expressing an inactive BMP receptor.....	101

¹ * schemas created with BioRender.com

Figure 33. Co-immunoprecipitation of SMAD4 with SMAD1/5 or SMAD2/3 in bear muscles.	102
Figure 34. SMAD4 linker protein sequences in different species.	103
Figure 35. SMAD4 degradation involving MAPK, GSK3 and β -TrCP proteins*.	104
Figure 36. Hypothetical schema to explain the denervation-induced muscle atrophy resistance in the hibernating brown bears muscles*.	107
Figure 37. Hypothetical schema of the origin of muscle transcriptomic changes of TGF- β superfamily*.	108

[Study 2](#)

Figure 38. Schema of the experimental strategy of study 2*	110
Figure 39. Graphical abstract of the study 2*	141
Figure 40. Chemical structures of febrifugine and halofuginone.	142
Figure 41. Effect of halofuginone treatment prior to hindlimb suspension on extracellular matrix components expression in gastrocnemius muscle in mice.	143
Figure 42. Halofuginone treatment for 2 weeks prior to hindlimb suspension mitigates atrophy in gastrocnemius muscle in mice.	144
Figure 43. Effect of halofuginone treatment prior to hindlimb suspension in soleus muscle.	145
Figure 44. Effect of halofuginone treatment prior to hindlimb suspension on autophagy-lysosomal system in gastrocnemius muscle.	147
Figure 45. ATF4 signalling regulation in atrophy-resistant muscle of the hibernating bear.	148
Figure 46. Worldwide geographic repartition of (A) <i>Hydrangea macrophylla</i> and (B) brown bear living area (<i>Ursus arctos</i>).	150
Figure 47. Hypothetical halofuginone and halofuginone-like molecular mechanisms in skeletal muscle*.	150

[Study 3](#)

Figure 48. Schema of the experimental strategy of study 3*	151
Figure 49. Human myotubes cultivated with winter bear serum induces similar transcriptional changes than those occurring in hibernating bears muscles.	152
Figure 50. Winter bear serum mimics in human muscle cells what occurs naturally in the muscles of hibernating bears.	153

2.5 List of abbreviations

4E-BP1: 4E-binding protein 1	ER stress: endoplasmic reticulum stress
AA: amino acid	FBS: fetal bovine serum
ACVR1B: activin receptor type-1B	FBXO30/32: F-Box Protein 30/32
ActR-2A/B: activin receptor type-2A/B	FC: fold change
ACVR2A/B: activin A receptor type 2A/B	FFA: free fatty acid
AKT: protein kinase B	FGF-2/21: fibroblast growth factor-2/21
ALS: autophagy-lysosomal system	FOXO1/3: forkhead Box-O 1/3
AMH: anti-müllerian hormone	FST: follistatin
AMPK: AMP(5'-adenosine monophosphate)-activated protein kinase	FSTL-1: follistatin-related protein 1
ATF4: activating transcription factor 4	GADD34: growth arrest and DNA damage-inducible 34
ATG: autophagy related genes	GADD45A: growth arrest and DNA damage inducible alpha
ATP: adenosine triphosphate	GCN2: general control nonderepressible 2
BAIBA: beta-aminoisobutyric acid	GDF1/5/7/10/11: growth differentiation factor 1/5/7/10/11
BCL2: B-cell lymphoma-2	GDP: guanosine diphosphate
BDNF: brain-derived neurotrophic factor	GFP: green fluorescent protein
BMP: bone morphogenetic protein	GSK3: glycogen synthase kinase-3
BMPR1A/B: bone morphogenetic protein receptor type 1A/B	GSH/GSSG: glutathione/oxidized glutathione ratio
BNIP3: BCL2 Interacting Protein 3	GTP: guanosine-5'-triphosphate
BRE: BMP response element	HDAC4: histone deacetylase 4
BSA: bovine serum albumin	HF: halofuginone
bZIP: basic leucine zipper	HM: human myotube
C/EBPβ: CCAAT enhancer binding protein β	HRI: heme-regulated inhibitor
CARE: C/EBP-ATF response elements	HS: hindlimb suspension
CCN2/4: cellular communication network factor 2/4	I-SMAD: inhibitory SMAD
CDKN1A: cyclin-dependent kinase inhibitor 1	IB: immunoblotting
CDS: coding sequence	IBA: interbout arousal
ChIP: chromatin immunoprecipitation	ID1-4: DNA-binding protein inhibitor 1-4
CLOCK: clock circadian regulator	IGF-1: insulin growth factor-1
COL1A1: collagen type 1 alpha 1 chain	IL-4/6/7/10/15/1ra: interleukin 4/6/7/10/15/1ra
CREB: cyclic AMP response element binding	INHBA/B: inhibin subunit beta A/B
CSA: cross sectional area	IP: immunoprecipitation
CTGF: connective tissue growth factor	ISR: integrated stress response
DEG: differentially expressed gene	JAK: janus kinase
DHA: docosahexaenoic acid	KD: kinase dead
DMEM: dulbecco's modified eagle medium	KO: knockout
DUB: deubiquitinase or deubiquitinating enzyme	LIF: leukemia inhibitory factor
ECM: extracellular matrix	Luc: luciferase
eIF2α: eukaryotic translation initiation factor 2 alpha	MAP1LC3A: microtubule associated protein 1 light chain 3 alpha
eIF4E: eukaryotic translation initiation factor 4E	MAPK: mitogen-activated protein kinase
EIF4EBP1: eukaryotic translation initiation factor 4E binding protein 1	MEF2: myogenic enhancer factor 2
ELISA: enzyme linked immunosorbent assays	MEKK4: mitogen-activated protein kinase kinase kinase 4

MPB: muscle protein breakdown
MPS: muscle protein synthesis
MR: metabolic rate
mRNA: messenger ribonucleic acid
MSTN: myostatin
mTOR: mechanistic target of rapamycin
mTORC 1/2: mechanistic target of rapamycin complex 1/2
MuRF1: muscle ring finger-1
MUSA1: muscle ubiquitin ligase of SCF complex in atrophy-1
MuSK: muscle-specific kinase
MYH: myosin heavy chain
MyoD: myoblast determination protein
NF- κ B: nuclear factor-kappa B
NMJ: neuromuscular junction
NOG: noggin
NRF2: NFE2 (nuclear factor erythroid 2)-related factor 2
NUPR1: nuclear protein 1 transcriptional Regulator
OXPHOS: oxidative phosphorylation
PAX3: paired box 3
PBS: phosphate buffered saline
pcDNA: plasmid cloning desoxyribonucleic acid
PDK4: pyruvate dehydrogenase kinase isoenzyme 4
PERK: PKR-like ER kinase
PGC-1 α : peroxisome proliferator-activated receptor-gamma coactivator 1
PI3K: phosphoinositide 3-kinase
PINK1: PTEN (phosphatase and TENsin homolog) induced kinase 1
PKR: double-stranded RNA-dependent protein kinase
PPAR- α : peroxisome proliferator-activator receptor
PPP1R15A: protein phosphatase 1 regulatory subunit 15A
ProRS: prolyl-tRNA synthetase
PVDF: polyvinylidene difluoride
R-SMAD: receptor-regulated SMAD
RBM3: RNA binding motif protein 3
ROS: reactive species oxygen

RPS6: ribosomal protein S6
RPS2/4X/5/7/A: ribosomal protein of the small subunit 2/4X/5/7/A
RT-qPCR: reverse transcription and quantitative polymerase chain reaction
S: summer
S6K1: ribosomal protein S6 kinase 1
SARA: SMAD anchor for receptor activation
SBE: SMAD binding element
SBS: summer bear serum
SDS-PAGE: sodium dodecyl sulfate-polyacrylamide gel electrophoresis
SMAD: SMAD family member
SMOX: spermine oxidase
STAT: signal transducers and activators of transcription
sWAT: subcutaneous white adipose tissue
TAK1: TGF- β -activated kinase 1
Tb: body temperature
TBS-T: tris-buffered saline tween-20
TCA: tricarboxylic acid cycle
TFE3: transcription factor binding to IGHM enhancer 3
TFEB: transcription factor EB
TG: triglyceride
TGF- β : transforming growth factor- β
TGFBR1: transforming growth factor beta receptor 1
TGX: tris-glycine eXtended
TNF- α : tumor necrosis factor- α
TRAF6: TNF Receptor Associated Factor 6
TRIB3: tribbles pseudokinase 3
TRIM63: tripartite motif containing 63
Ub: ubiquitin
UCP3: uncoupling protein 3
ULK1: unc-51 like autophagy activating kinase
uORF: upstream open reading frame
UPR: unfolded protein response
UPS: ubiquitin-proteasomal system
W: winter
WAT: white adipose tissue
WBS: winter bear serum
WNT/FZD: wingless/int1-frizzled

3. Preface

Muscle wasting results from a wide range of pathophysiological conditions such as cancer and renal failure, but also microgravity, bed rest or inactivity. Muscle wasting is associated with adverse health effects such as a decline in independence and an increased morbidity and mortality. With increasing physical inactivity and improved life expectancy, muscle wasting is a major public health problem. Muscle atrophy results from an imbalance between protein synthesis and degradation, and a variety of intracellular players are involved in this dysregulation, including the TGF- β superfamily and the ATF4 pathway. Their biological roles in muscle physiology are mainly described in humans or laboratory rodents. Despite the wealth of knowledge on this subject, an approved and readily available therapeutic or preventive treatment is still lacking. Hibernating brown bears are fascinating mammals because they naturally resist muscle atrophy although they remain completely inactive and starved for 5-7 months during the hibernation period. The main objective of this thesis was to find new underlying mechanisms that could become therapeutic targets to combat muscle atrophy in humans. To achieve this goal, we (1) used a comparative physiology approach in hibernating bears naturally resistant to atrophy, (2) investigated the role of the interaction between the ATF4 and the TGF- β /BMP pathways in unloaded mice susceptible to atrophy, and finally (3) initiated experiments in human muscle cells to validate hypotheses arising from the first two studies.

This manuscript is therefore a compilation of all the work carried out during my 3-year thesis on the regulation of the TGF- β superfamily and ATF4 signalling pathways in the skeletal muscle of the hibernating brown bear and the unloaded mouse. It will be divided into 3 distinct parts. First, a state-of-the-art of (1) skeletal muscle physiology and muscle atrophy, (2) TGF- β superfamily and ATF4 signalling pathways, and their pivotal roles in muscle homeostasis, as well as (3) bear hibernation and the first clues to explain its resistance to muscle atrophy. In the second part, two studies will be presented. The first one is a published article on the transcriptomic analysis of muscles of brown bears during hibernation and of mice during unloading. The second study is a paper currently under review on the effect of ATF4 induction on skeletal muscle in both healthy and unloaded mice, and also in hibernating brown bears. A discussion of perspectives and questions arising from the data follows both studies. Finally, the last part consists of the presentation and discussion of the preliminary results of the effect of bear serum on human muscle cells. This thesis is written in english, and therefore a substantial abstract in french requested by the doctoral school is included in the Appendix, together with 2 articles of which I am co-author: one is an original article related to tissue adaptations (muscle, adipose tissue and serum) in the hibernating brown bear and the other is a review on ubiquitin ligases and their role in muscle atrophy.

4. State of the art

4.1 Skeletal muscle: The Holy Grail for whole-body homeostasis

4.1.1 Introduction

4.1.1.1 Skeletal muscle physiology

The word “muscle” was first used by Middle French speakers in the 14th century, from the existing Latin words *mus* meaning “mouse” and *musculus* which translates to both “little mouse” and “muscle.” Ancient Romans thought that some muscles, especially the biceps, looked like little mice running under a person’s skin. Our organism contains about 600 “little mice” accounting for approximately 40% of our total body weight, making skeletal muscle the most abundant tissue in the human body.

Generalities. Two types of muscles coexist: (1) the so-called smooth muscles located in walls of hollow organs (e.g intestine, stomach) under involuntary control, and (2) the striated muscles divided into two types, the cardiac muscles which also contract spontaneously, and the skeletal muscles which cover our skeleton and allow movements under voluntary control. Skeletal muscle is a very dynamic and plastic tissue. It is essential for movement, gesture and posture for functional autonomy. It also acts as the main tissue for energy metabolism, with heat production and absorption, use and storage of energy substrates (i.e. glucose, lipids and amino acids). Skeletal muscle is composed of water (75%), proteins (20%) and other constituents such as carbohydrates, lipids and minerals. It accounts for approximately 50-75% of body proteins and 30-50% of whole-body protein turnover [1,2].

Organisation. Skeletal muscle is a highly organised tissue containing several bundles of myofibers with each layer successively surrounded by the extracellular matrix (Figure 1). Myofibers are multinucleated and post-mitotic cells and contain adult stem cells called satellite cells that contribute to muscle growth and repair. Each myofiber contains thousands of myofibrils which are composed of the basic cellular unit of muscle, the sarcomere. The sarcomere itself is composed of billions of myofilaments, both thick (myosin) and thin (actin), which are essential for muscle contraction requiring high ATP consumption (Figure 1). Myofilaments represent the main protein content of muscle (i.e. 70-80% of the total protein content of a single fibre) [1,2]. The size of the muscle is primarily determined by the number and the size (i.e. cross-sectional area, CSA) of each myofiber, although fat and extracellular matrix infiltration can also influence its size [1,2].

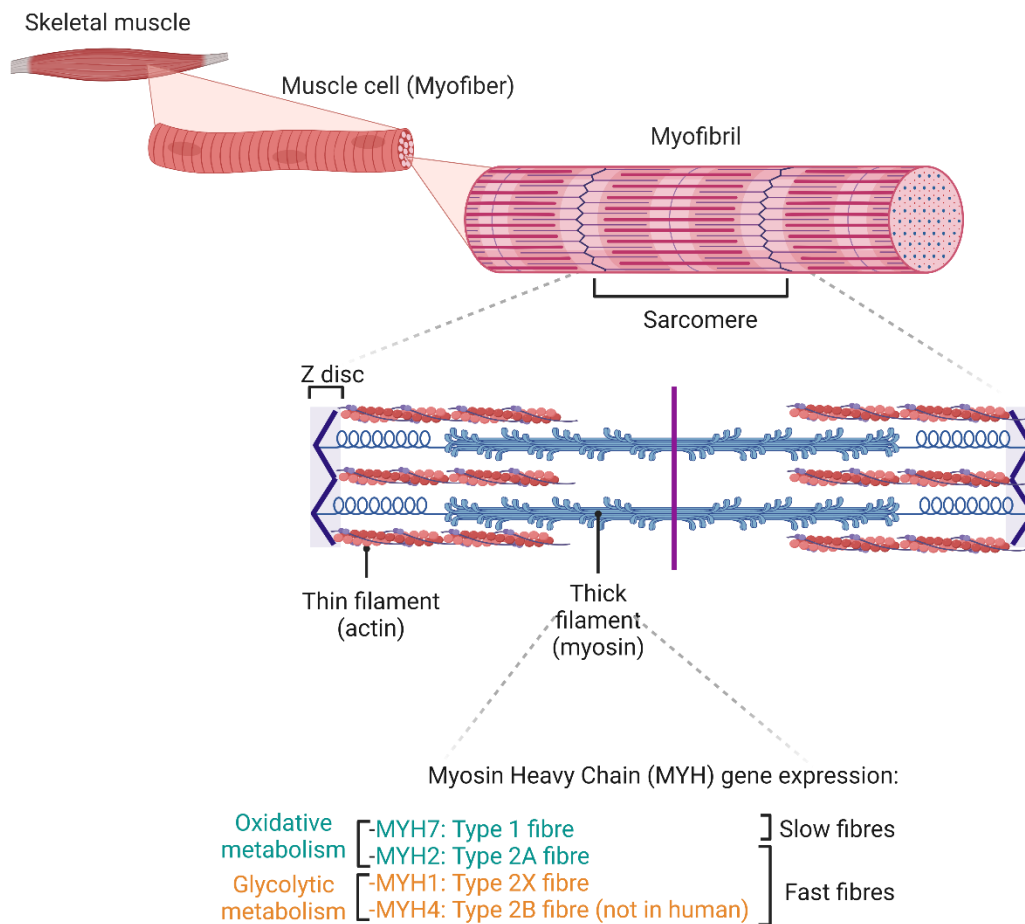


Figure 1. Skeletal muscle organisation and contractile apparatus structure.

Typology. Myofibers are classified into different types, with different characteristics such as the sarcomeric myosin heavy chain (MYH) gene expression, strength-velocity, response to neural inputs, or metabolic properties [3] (Figure 1). Since the first half of the 19th century, scientists have distinguished skeletal muscles based on their colours and contractile properties: (1) red muscles composed of slow-twitch fibres (i.e. type 1) rich in mitochondria with oxidative metabolism and (2) white muscles composed of fast-twitch fibres (i.e. type 2) poor in mitochondria with glycolytic metabolism [4]. Over the past 40 years, this oversimplified schema has evolved with the notion of diversity of muscle fibre types, and four major fibre types have been identified in adult mammalian skeletal muscle (i.e. types 1, 2A, 2X, and 2B) (Figure 1). Humans, however, lack type 2B fibres, and the proportion of MYH within the same muscle may differ between mammals [3,5]. Skeletal muscle fibre type and mitochondrial function are sometimes uncoupled, for example for fast type 2A fibres with abundant mitochondrial content [2,3,6] (Figure 1). Based on differential MYH expression, a muscle may also consist of hybrid fibres (i.e., 1/2A, 2A/2X, 2X/2B), which allow muscles to utilise ATP in a nearly continuous gradient and thus be endowed with a fast type 2B to slow type 1 muscle contraction rate [2,3]. The heterogeneity of muscle fibres is the basis for the flexibility to use the same muscle for a

variety of tasks, from fast and intense contraction (e.g. jumping) to slow and low-intensity activity (e.g. posture).

Mitochondria. Skeletal muscles are highly vascularised and innervated, and contain components of the metabolic machinery (e.g. mitochondria, sarcoplasmic reticulum), allowing efficient energy production. The precise coordination of activity between each of these components is essential to maintain muscle homeostasis and associated motor activity. The energy requirement during an intense contraction increases the normal ATP consumption in skeletal muscle by 100-fold [7]. To support this high energy demand, skeletal muscle relies in part on mitochondrial oxidative phosphorylation (OXPHOS) for ATP production. Adult myofibers exhibit specific subcellular localisation of distinct populations of mitochondria, namely subsarcolemmal (i.e. just below the plasma membrane) and intermyofibrillar. These two distinct populations of mitochondria are functionally highly interconnected but have a specific shape and exhibit differences in their biochemical and functional properties [8–11]. The morphology, arrangement, and connectivity of the mitochondrial network are adapted to the specific functional needs of each fibre type. For example, oxidative fibres have a grid-like organisation with elongated mitochondria oriented both parallel and perpendicular to the muscle contraction axis, in contrast to the mitochondrial network of glycolytic fibres, which is fragmented and oriented perpendicular to the muscle contraction axis [12]. Maintaining a functional mitochondrial network in skeletal muscle is fundamental to fulfilling the metabolic demands imposed by contraction, thereby regulating fuel utilisation, energy expenditure, and overall metabolism. Mitochondrial integrity and function are highly regulated by quality control systems (e.g., mitochondrial biogenesis, dynamics, and degradation) to maintain homeostasis [2,13]. Moreover, mitochondrial dysfunction has been linked to several human muscle diseases called mitochondrial myopathies [14–19].

4.1.1.2 Muscle-organ crosstalk

Myokine. Over the past decades, skeletal muscle has been extensively studied for its role as an endocrine organ, producing and secreting hundreds of cytokines and other peptides, i.e. myokines, with autocrine, paracrine, or endocrine effects [20–23] (Figure 2). The first myokine described was myostatin [24] followed by interleukin-6 (IL-6). The latter is increased 100-fold in the bloodstream during exercise and shows multiple metabolic effects at the whole the body level [25,26]. Given the broad physiological and metabolic effects of physical activity throughout the body, it was clear that there was more than one myokine [27,28]. The biological name myokine provided a new concept for understanding how muscles communicate with the rest of the body, and more than 650 myokines have been identified [20–23] (Figure 2). Myokines (e.g. myostatin, IL-6, cathepsin B, irisin, IL-15) are

synthesised and released from myofibers during muscle contraction and provide communication between skeletal muscles and other organs, including the brain, adipose tissue, bone, liver, intestine, pancreas, endothelial cells, and skin, as well as communication within the muscle itself [20–22] (Figure 2, Figure 3). The biological roles of myokines include widespread body functions such as cognition, lipid and glucose metabolism, white fat browning, bone formation, endothelial cell function, hypertrophy, and skin structure (Figure 2, Figure 3). For muscle itself, myokines play a role in mitochondrial biogenesis, fat oxidation and glucose metabolism, and act as signals for muscle hypertrophy or atrophy [20,21,29] (Figure 3). It should be noted that most of the myokines are not yet sufficiently well characterised with respect to their biological functions [20–23]. Establishing proper crosstalk between body organs and muscles is essential for whole-body homeostasis [20–23].

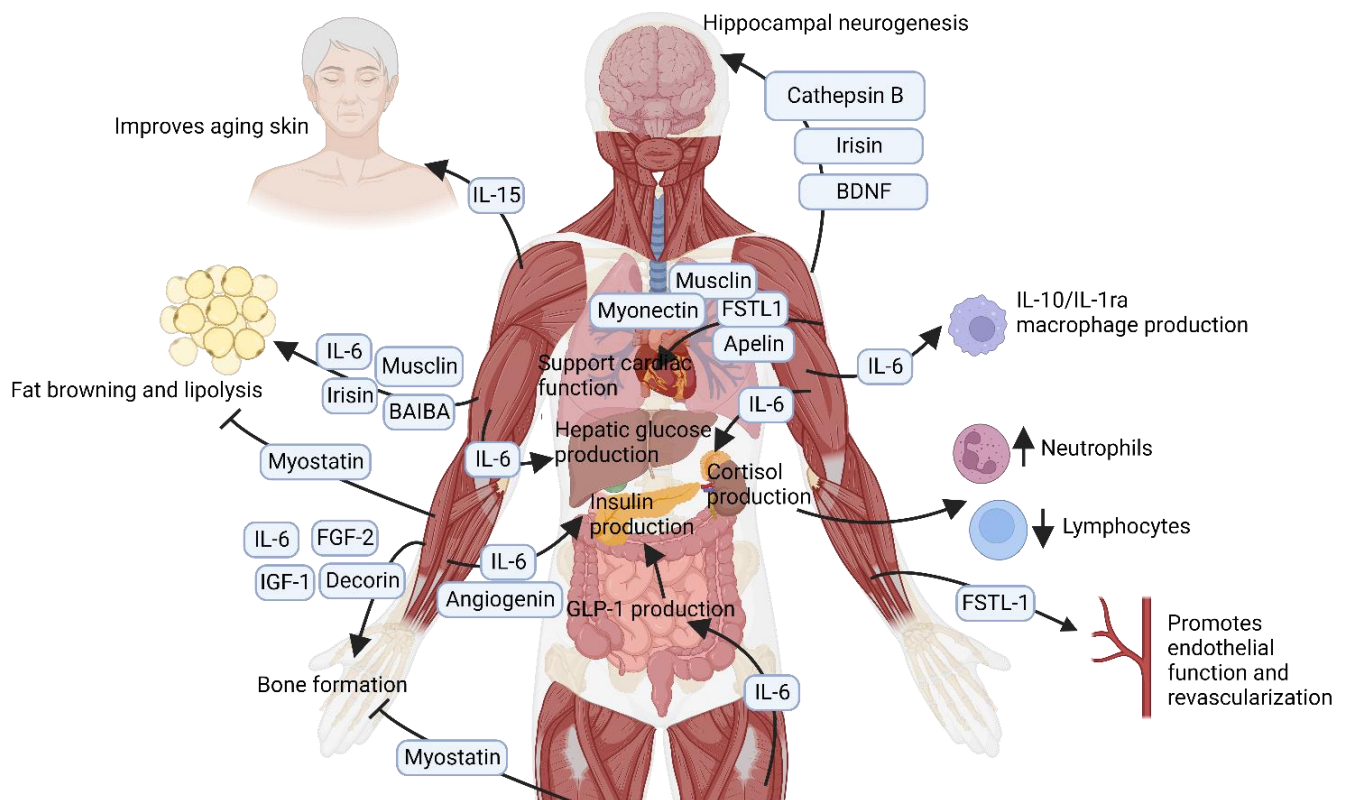


Figure 2. Myokinome overview of muscle-organ crosstalk.

Amino acid reservoir. Another major role of skeletal muscle is to be a reservoir of amino acids. Muscle amino acids can be mobilised in the absence of an adequate nutrient supply or in situations of increased need in other tissues to maintain their protein mass [30–32]. For example, obese individuals maintain normal plasma amino acid concentrations even after 60 days of total fasting [33]. Studies conducted by Jewish physicians in concentration camps during World War 2 suggested that death by starvation (i.e. uncomplicated by severe disease) occurred when amino acids mobilised from muscle proteins became insufficient to maintain the precursors necessary for gluconeogenesis. Indeed, amino

acids released from muscles serve as precursors for the maintenance of blood glucose levels through hepatic gluconeogenesis during starvation [34]. In the context of disease prevention and health maintenance, reduced muscle mass compromises the body's ability to respond to stress and chronic disease due to inappropriate crosstalk between muscles and organs. Therefore, loss of muscle mass is incompatible with life, and maintenance of muscle protein content through appropriate turnover is vital to maintain whole body homeostasis (see section 4.1.3).

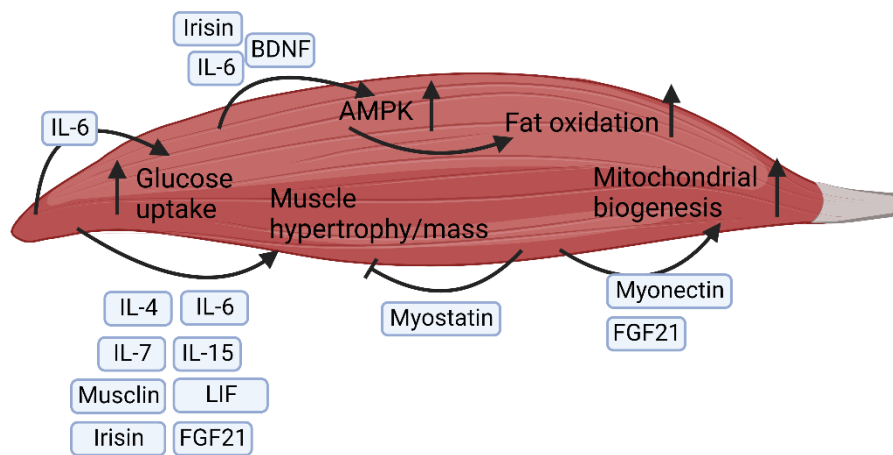


Figure 3. Myokine overview of muscle autocrine/paracrine crosstalk.

4.1.2 Muscle protein turnover

During embryonic and early postnatal development, muscle growth occurs primarily through myogenesis and fusion of satellite cells [35,36]. In adult organisms, regulation of muscle mass results from growth within existing myofibers primarily via cellular pathways that control protein turnover [37,38] (see Appendix 10.4). Muscle proteins are constantly renewed, i.e. synthesised and degraded (Figure 4). The balance between the rates of muscle protein synthesis (MPS) and muscle protein breakdown (MPB), i.e. the net muscle protein balance, determines muscle protein content and homeostasis (Figure 4). MPS and MPB are sensitive to many factors, including nutritional status, hormonal balance, physical activity, injury or diseases. A decrease in muscle size in fully mature organisms, i.e. muscle atrophy (see section 4.1.3), results from a negative protein balance, whereas an increase in muscle size, i.e. hypertrophy, results from a positive protein balance. Muscle hypertrophy,

in response to physical activity or a high-protein diet, is an interesting field of investigation that is of clinical interest in the search for treatments to limit or prevent muscle wasting.

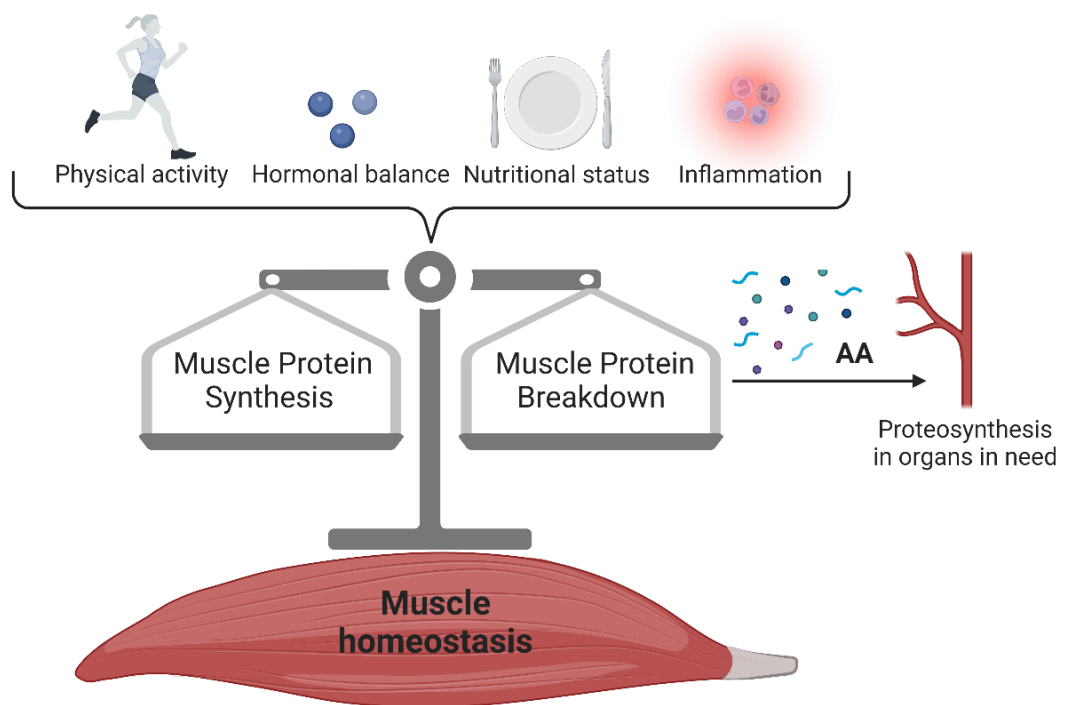


Figure 4. Muscle protein balance in physiological conditions.

AA: amino acid

4.1.2.1 Muscle protein synthesis

External stimuli. Amino acids (AA) provided by an appropriate diet act as extra- and intra-cellular anabolic molecules and are essential for inducing MPS [39,40] (Figure 4). High-protein diets do not enhance MPS as long as energy and protein requirements are met in the muscles and other organs. Amino acids bioavailability is strongly influenced by protein source, digestibility, and protein intake pattern, and is important for optimising MPS [40,41]. Mechanical cues are also considered anabolic stimuli, based on two basic lines of evidence: (1) muscles atrophy when mechanical load is reduced (e.g. bed rest) [42] and (2) muscle overload is sufficient for skeletal muscle hypertrophy [43,44]. Life on Earth has evolved in a 9.8m/s^2 environment that loads organisms. Therefore, cells have evolved with a plethora of sensors that detect mechanical stimuli. These mechanosensors help cells to adapt not only directly to the force produced by the contraction of a muscle fibre but also to more indirect mechanical signals, such as the stiffness of the extracellular matrix (ECM) that surrounds each cell [44,45]. However, these mechanical signals remain incompletely characterised. The increase in MPS after food intake is a systemic transient phenomenon, whereas physical activity stimulates a long-term

local adaptive response. Furthermore, adequate nutrition after physical activity can take advantage of anabolic pathways initiated by physical activity [41,46,47].

mTOR. One of the most recognized players in MPS is the mechanistic target of rapamycin (mTOR), which controls anabolic and catabolic signalling in skeletal muscle, resulting in the modulation of muscle hypertrophy and wasting [48,49] (Figure 5). mTOR inhibition by rapamycin or genetic invalidation respectively reduces the increase in MPS and/or muscle size after exercise in humans [50], or results in severe myopathy leading to premature death in mice [51]. mTOR is a serine/threonine kinase that (1) senses a variety of environmental and intracellular changes, including nutrient availability, energy status and mechanical stimulation, and (2) coordinates a variety of cellular processes, including cell growth and survival, differentiation and autophagy [48,49,52]. There are two biochemically and functionally distinct mTOR complexes, namely mTORC1 and mTORC2 [48,52] (Figure 5). Both complexes share the mTOR catalytic subunit and are distinguished by their accessory proteins, and their unique substrates and functions [48,52] (Figure 5).

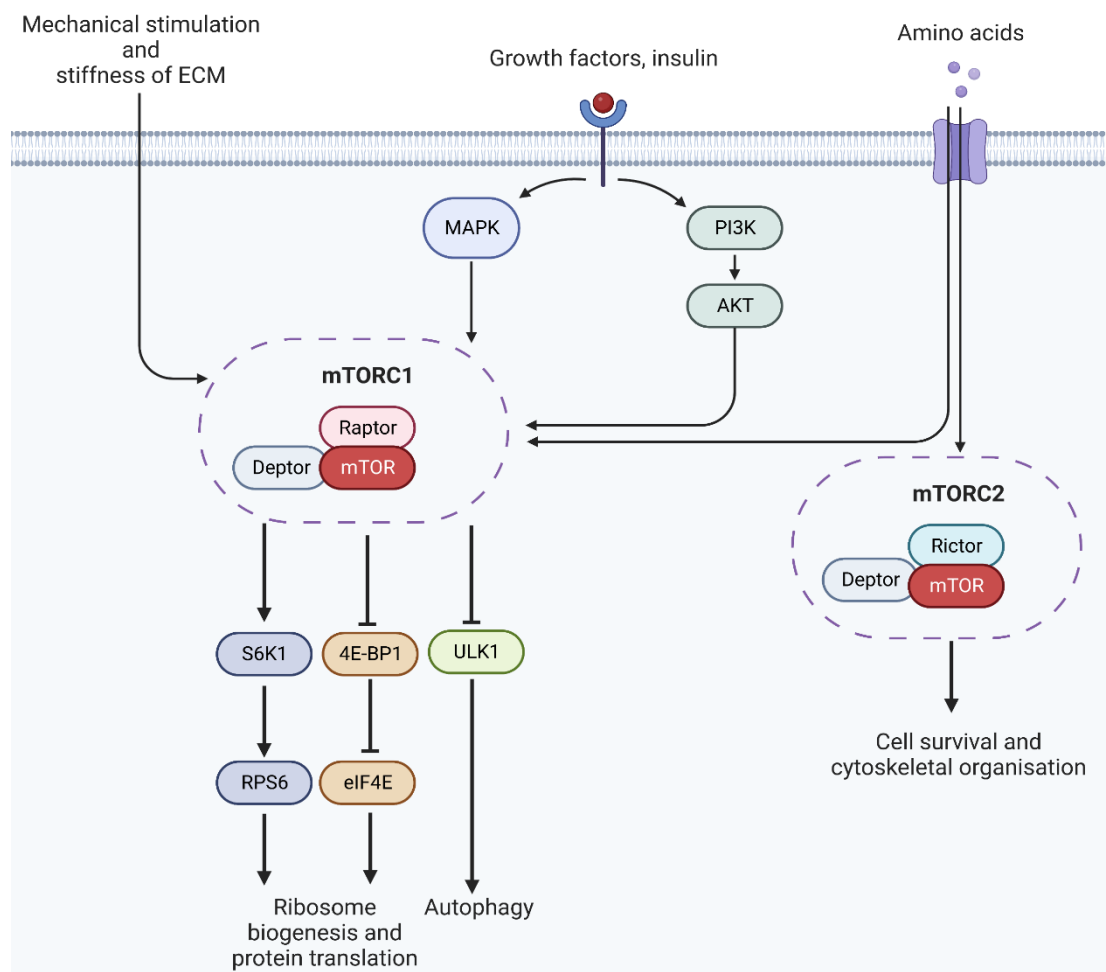


Figure 5. mTORC1 and mTORC2 intracellular organisation and their biological effects.

On one hand, mTORC2 regulates cell survival and cytoskeleton organisation [48,52]. On the other hand, mTORC1 controls protein synthesis by activating S6K1², which promotes ribosome biogenesis, and by inhibiting 4E-BP1³ leading to protein translation (Figure 5). mTORC1 also promotes muscle hypertrophy by phosphorylating and suppressing ULK1⁴ activity resulting in the inhibition of autophagy, one of the major protein degradation processes in muscle [48,52] (Figure 5).

4.1.2.2 Muscle protein breakdown

Physical activity, nutritional interventions, hormonal balance or inflammation also influence muscle protein breakdown (MPB) (Figure 4). The mechanisms are much less understood than for MPS, mainly because MPB measurement is technically more challenging than for MPS [53,54]. The main systems that contribute to MPB in skeletal muscle are the autophagy-lysosomal system (ALS) and the ubiquitin-proteasomal system (UPS).

Autophagy-lysosomal system. The word autophagy is derived from two Greek words *auto* meaning “self”, and *phagy* meaning “eating”. Three different systems of autophagy have been described in mammals: macroautophagy, chaperone-mediated autophagy, and microautophagy. In this manuscript, ALS will refer to macro-autophagy, the most explored system in MPB. ALS involves the formation of a nascent membrane structure, i.e. the phagophore, surrounding bulk intracellular components, such as organelles, damaged proteins, or other target proteins (e.g. transporters, ion channels, receptors) (Figure 6). The origin of the membrane, i.e. endosomal, trans-golgi, nuclear or *de novo* synthesis, is unclear. After maturation of the autophagosome, it fuses with lysosomes to generate an autolysosome (Figure 6). Finally, activation of lysosomal proteases, i.e. cathepsins, or other enzymes such as DNases or lipases, leads to the degradation of the autolysosome content and recycling of AAs [55] (Figure 6). It should be noted that ALS cannot degrade proteins in intact myofibrils; therefore, additional catabolic pathways are required [56,57]. Under normal conditions, ALS primarily prevents the accumulation of damaged organelles and misfolded proteins, but also degrades glycogen and lipid droplets, thus providing glucose, free fatty acids (FFAs), or AAs to the entire body to support basic cellular metabolism. In response to different stresses, such as starvation, ALS acts as a pro-survival mechanism in skeletal muscle, providing metabolic substrates [55]. Skeletal muscle is one of the organs with the highest rate of autophagy flux when nutrients are lacking [58]. In particular, basal autophagic flux is higher in glycolytic fibres than in oxidative fibres [59]. This is particularly important

² ribosomal protein S6 kinase 1

³ eukaryotic translation initiation factor 4E binding protein 1

⁴ unc-51-like autophagy activating kinase

because muscles may regulate ALS differently during specific stresses depending on their fibre type composition. Additionally, because muscle cells are highly sensitive to insulin [60], known to inhibit ALS [61], the autophagy flux fluctuates according to the food intake throughout the day and the level of physical activity [62,63]. While too much autophagy flux contributes to muscle wasting (see section 4.1.3), inhibition of ALS also leads to muscle atrophy [64]. In addition, inhibition of ALS leads to the accumulation of abnormal mitochondria, oxidative stress and protein aggregates, causing degeneration, weakness and premature death of myofibers [62–65]. Therefore, proper autophagic flux is required to maintain healthy muscle cells [62,63].

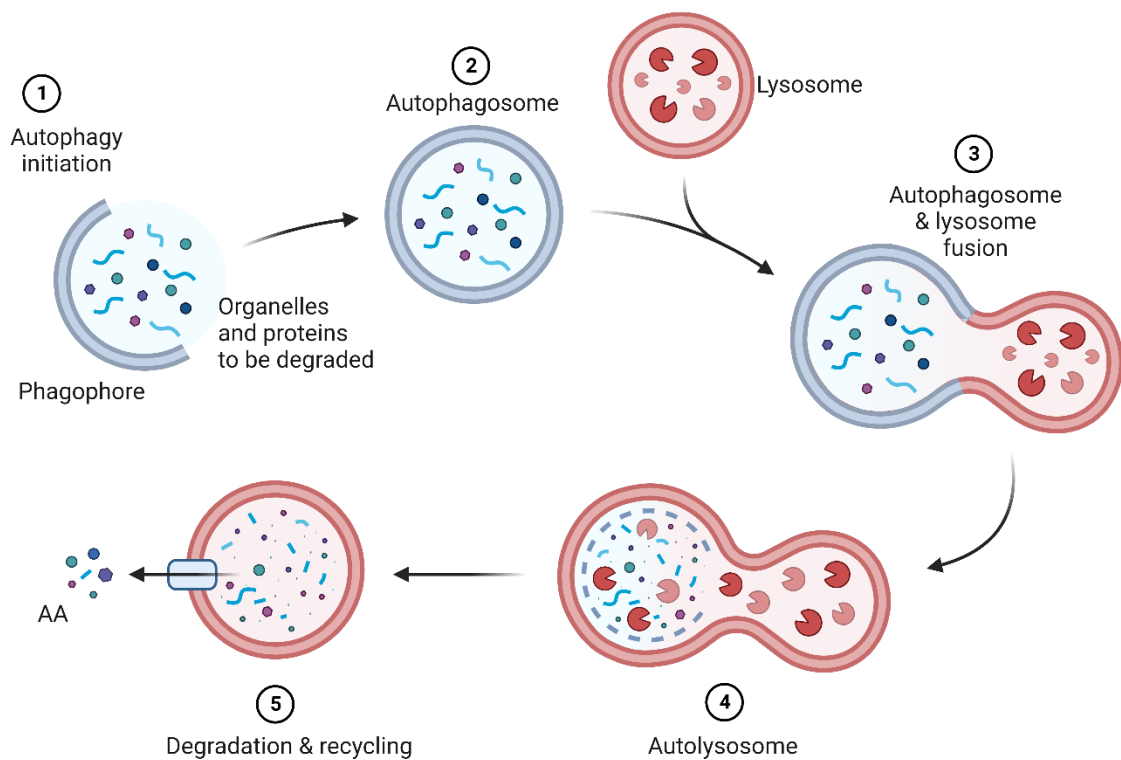


Figure 6. Autophagy-lysosomal system.

AA: amino acids

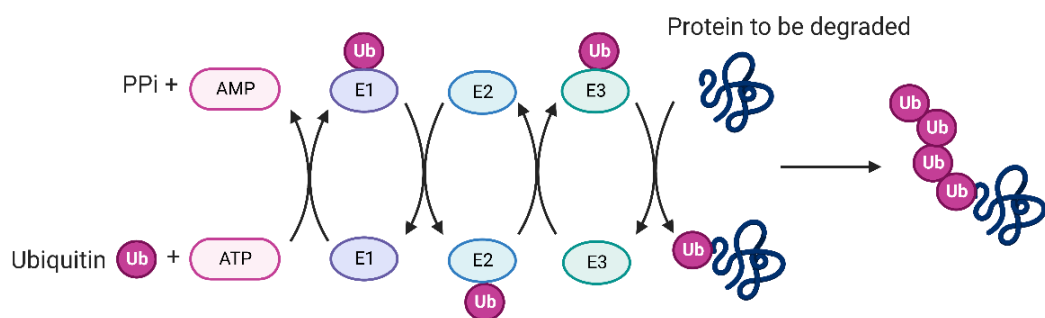
Mitophagy. In healthy skeletal muscles, damaged and depolarized mitochondria are selectively removed by the mitophagy process, which is a selective form of autophagy. The most studied mitophagy involves the ubiquitin-protein ligase Parkin and the mitochondrial kinase PINK1⁵ [13,19,66]. Studies have demonstrated that mitochondrial dynamics and mitophagy are essential for skeletal muscle homeostasis [13,19,66]. There is a growing body of evidence that alterations in mitophagy or mitochondrial distribution and dynamics are present in muscles during wasting conditions (e.g. ageing,

⁵ PTEN induced kinase 1

disuse or cancer cachexia) [66–68]. Importantly, enhancing mitophagy through genetic or nutritional approaches improves skeletal muscle function in aged rodents [13,19,66]. Thus, improving mitophagy in skeletal muscle appears to be a promising therapeutic target to prevent or even treat skeletal muscle dysfunction.

Ubiquitin-proteasomal system. The UPS is perhaps the best-known cellular proteolytic system and is responsible for degrading the majority of misfolded or defective proteins in all cell types. The UPS plays a fundamental role in normal muscle physiology, including degrading myofibrillar proteins [69,70]. Most proteins undergo degradation by being targeted to the 26S proteasome through the covalent attachment of a multi-ubiquitin chain (Figure 7). Protein ubiquitination involves the action of 3 enzymes: ubiquitin-activating enzymes E1, ubiquitin-conjugating enzyme E2, and ubiquitin-ligase E3 (Figure 7). The ubiquitin-tagged proteins are then recognized by the 26S proteasome, which initiates the ATP-dependent degradation process within the catalytic core (Figure 7). Through this mechanism, the UPS performs substrate-specific proteolysis [71]. Protein ubiquitination is both dynamic and reversible. Deubiquitinase or deubiquitinating enzymes (DUB) catalyze the removal of ubiquitin from target proteins and are also involved in ubiquitin maturation, recycling and editing. Several reports have demonstrated a relationship between UPS and lifespan, with proteasome activity decreasing with age in skeletal muscle, causing dysfunction [72]. Moreover, inhibition of proteasome activity in skeletal muscle is associated with a defect in muscle growth and shortened lifespan in rodent models [70,73].

1 Ubiquitination



2 Protein degradation

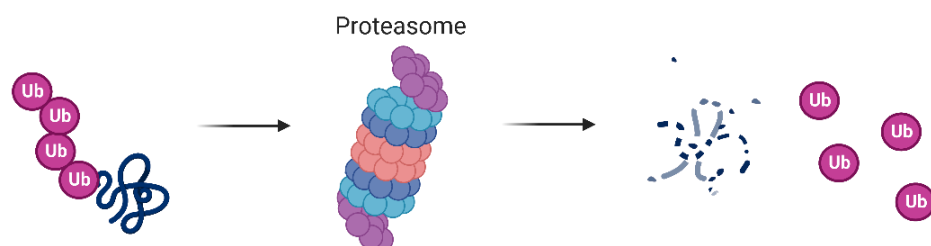


Figure 7. Ubiquitin-proteasomal system.

UPS and ALS crosstalk. UPS and ALS have long been considered independent. However, emerging evidence suggests that there is a crosstalk between both pathways in skeletal muscle. Although ALS had been thought to be a non-specific degradation system, it has also been reported to degrade ubiquitinated proteins [74]. Studies also suggest that ALS and UPS are complementary because proteasome-deficient mice exhibit increased autophagic flux [70,73]. Therefore, the UPS and ALS are compensatory mechanisms, both essentials to sustain muscle homeostasis and integrity. However, since they are important for the health of skeletal muscle, dysfunctions in both systems lead to muscle pathological conditions.

4.1.3 Muscle atrophy

4.1.3.1 Causes and consequences

Causes. The loss of muscle mass and strength in the adult body is referred to as muscle atrophy. Muscle loss arises from inherited (congenital or genetic) or acquired conditions (pathological or physiological conditions) [75] (Figure 8). In addition, older adults exhibit age-induced muscle atrophy, primarily due to anabolic resistance, which may predispose this population to more pronounced muscle loss when exposed to periods of reduced physical activity [76]. Pathological conditions that cause muscle atrophy include cancer cachexia [77], chronic obstructive pulmonary disorders [78], diabetes and obesity [79], chronic kidney diseases [80], heart failure [81], sepsis [82], burns [83], and conditions associated with anorexia or malnutrition [84]. Physical inactivity also leads to muscle wasting, especially following leg fractures, immobilisation and bed rest [85–90] and even in those with sedentary lifestyles, as observed during COVID-19 home confinement [91]. It should be noted that 60-85% of people worldwide lead a sedentary lifestyle (World Health Organisation). Muscle atrophy results from an imbalance between MPS and MPB, with a negative balance in favour of protein breakdown [75] (Figure 8). Data suggest that both (1) decreased MPS and (2) increased MPB contribute to muscle loss and that the relative contribution of each process to muscle loss depends on the pathophysiological condition [92–94]. During this thesis, we were primarily interested in disuse-induced muscle atrophy.

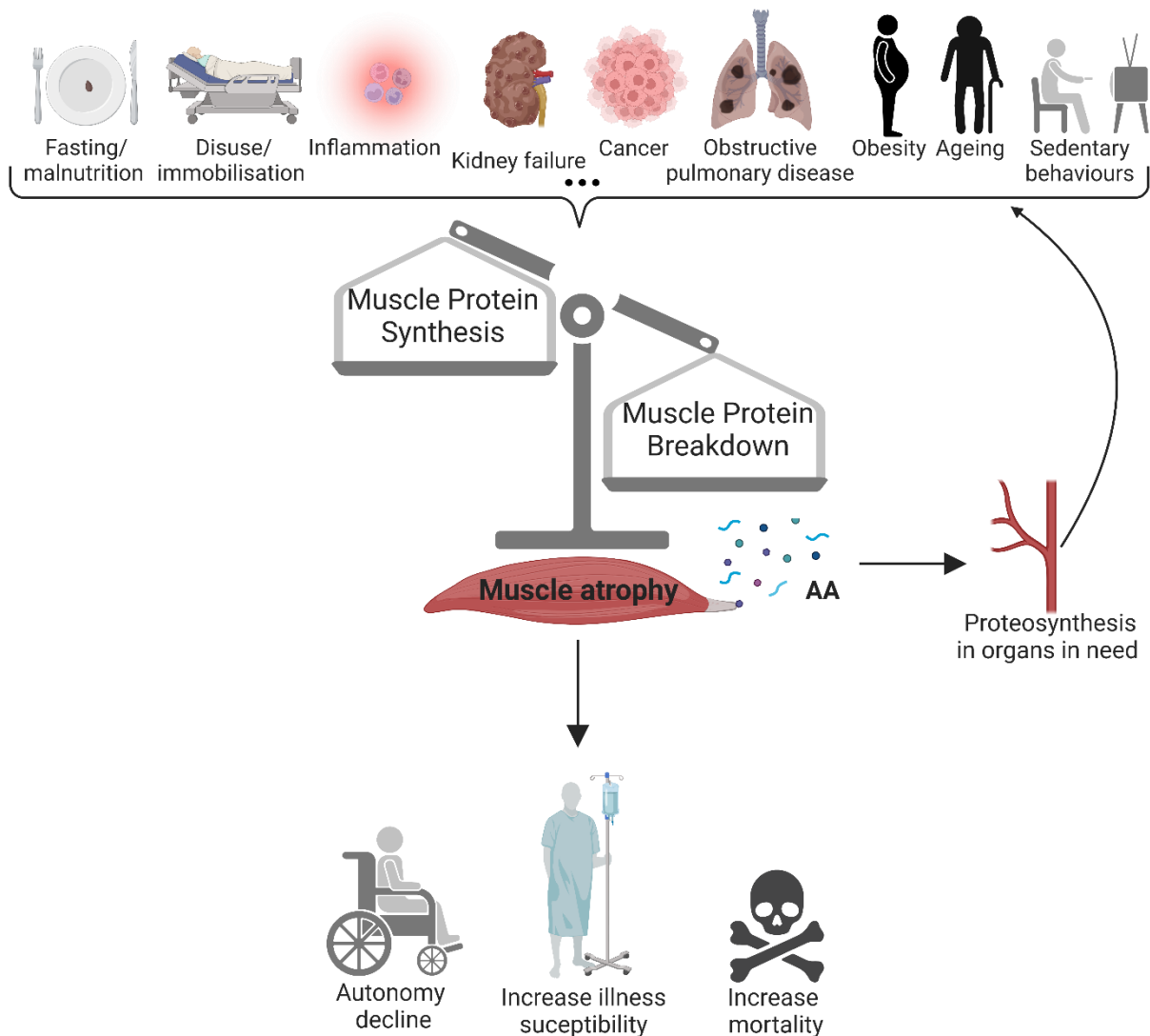
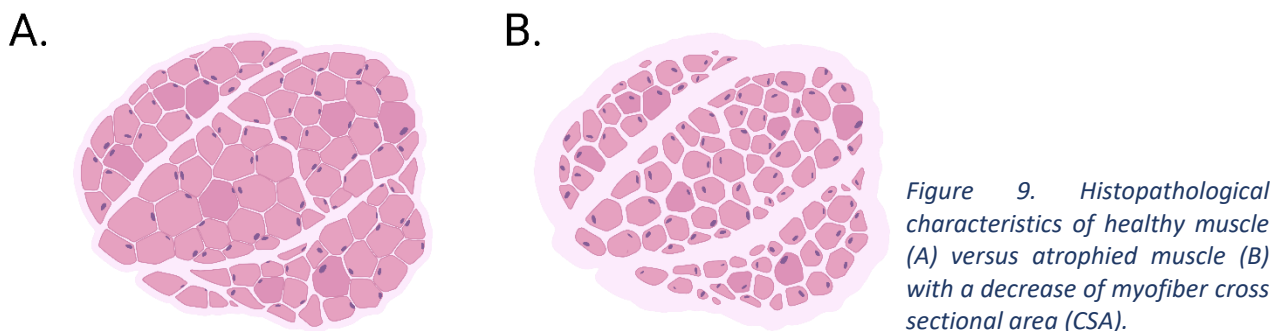


Figure 8. Muscle protein imbalance in pathophysiological conditions leading to muscle atrophy.

AA: amino acid

Consequences and treatments. The resulting muscle wasting is characterised by muscle alterations such as myofiber shrinkage, changes in fibre types or myosin isoforms, and net losses of cytoplasm, organelles, and total proteins. Loss of myofibers and/or a decrease in myofiber diameter are the most prominent histopathologic features of skeletal muscle atrophy (Figure 9). As mentioned above, skeletal muscle plays a central and major role in whole-body homeostasis. Lack of physical activity is associated with a wide network of diseases, including type 2 diabetes, cardiovascular diseases, cancer, dementia, and osteoporosis [22,95]. These adverse effects are likely, to some extent, mediated by a lack of release of myokines and/or resistance to their effects [20,23]. In addition, skeletal muscle is a major organ of insulin-induced glucose metabolism. Therefore, a loss of muscle mass is closely related to insulin resistance and metabolic syndrome [96]. Muscle atrophy limits daily activities, reduces quality

of life and lengthens recovery time after illness, while increasing morbidity and mortality (Figure 8). Given its adverse consequences, increasing sedentary lifestyle and life expectancy worldwide, muscle wasting affects millions of people and remains a major economic and social burden. Currently, strategies for treating skeletal muscle atrophy include physical exercise, nutritional interventions and some medications [75]. In addition, natural products have a wide range of effects on muscle function. However, their low bioavailability and low intestinal absorption limit their application [97]. To date, no drugs have been approved for clinical use, no effective remedies for muscle atrophy have been discovered, and exercise or nutritional interventions are strategies that are not suitable for all patients (e.g., immobilised or intensive care unit patients). Thus, although our understanding has improved considerably over the last two decades, mainly through the use of laboratory models inducing muscle atrophy, there is still a need to discover new targets and drugs to combat it.



4.1.3.2 An interconnected network of cellular actors

Signalling pathways. MPS and MPB are influenced by a wide range of external and internal molecular actors. External stimuli (1) include mechanical load, inflammatory factors such as cytokines (e.g. IL-6, TNF- α ⁶), endocrine factors such as growth factors (e.g. IGF-1⁷, insulin), catecholamines and angiotensin, and (2) activate various intracellular pathways (Figure 10). This interconnected network of intracellular actors contributes to the regulation of muscle protein balance by working in synergy or in antagonism to promote anabolism or catabolism [2,37,38,75] (see Appendix 10.4). In the context of muscle atrophy, dysregulation of one or more of these actors results in a blunting of anabolic signalling in favour of catabolism leading to either MPS inhibition, UPS and ALS overactivation, or both [2,37,38,75] (see Appendix 10.4) (Figure 10). In brief, anabolic pathways suppressed in many atrophy

⁶ tumor necrosis factor α

⁷ insulin growth factor-1

conditions include signalling from PI3K⁸-AKT⁹-mTORC1, β 2-adrenergic, WNT/FZD¹⁰, calcineurin, hippo and bone morphogenetic protein (BMP). In contrast, catabolic pathways overactivated in many cases of atrophy include signalling from transforming growth factor- β (TGF- β), AMPK¹¹, NF- κ B¹², glucocorticoid receptors, angiotensin, IL-6-JAK/STAT¹³, kinin, sphingolipids, notch or activating transcription factor 4-endoplasmic reticulum stress (ATF4 and ER stress) [2,37,38,75] (see Appendix 10.4) (Figure 10). The precise interconnection and biological actions of these actors still need to be fully elucidated. A detailed description of their regulation is beyond the scope of this manuscript. Nevertheless, a review of which I am a co-author is appended for more details (see Appendix 10.4).

Atrogenes. Atrogenes (i.e. atrophy-related genes) are referred to as a set of genes whose expression changes in different catabolic situations associated with muscle wasting. Regulation at the protein level is sometimes more complex to elucidate [98,99]. The atrogenes belong to different cellular pathways, mainly the UPS and ALS proteolytic systems, and include the E3-ubiquitin ligases containing tripartite motif 63 (TRIM63)/muscle ring finger-1(MuRF1) and F-Box protein 32 (FBXO32)/Atrogin-1, as well as some autophagy players such as cathepsin L and BCL2-interacting protein 3 (BNIP3) [99]. For example, TRIM63/MuRF1 targets myofibrillar proteins (i.e. thin and thick filaments), as well as sarcomere structural components such as telethonin, for UPS-dependent degradation [100]. FBXO32/Atrogin-1 is involved in the degradation of ribosomal proteins and translation initiation factors, as well as several other proteins such as myoblast determination protein (MyoD), desmin, and vimentin (i.e. the intermediate filament in muscle). Thus, overexpression of FBXO32/Atrogin-1 in the context of muscle atrophy may reduce MPS and regeneration and thus leads to muscle wasting [101]. Atrogenes are markers of atrophy, but their involvement as active inducers of atrophy remains an open question. Furthermore, whether rodent atrogenes are shared with humans remains to be established for most of them.

Drugs targeting. Several actors in this interconnected network have been proven effective when targeted to limit or counteract skeletal muscle atrophy in rodent models. For instance, targeting myostatin ligand or its activin receptor type 2B (TGF- β signalling) has shown beneficial effects in preserving muscle mass in different catabolic conditions (see section below 4.2.2.2). Moreover, the stimulation of β 2-adrenoceptors prevents or even reverses muscle wasting and weakness in several

⁸ phosphoinositide 3-kinase

⁹ protein kinase B

¹⁰ wingless/int1-frizzled

¹¹ AMP-activated protein kinase

¹² nuclear factor-kappa B

¹³ janus kinases/signal transducers and activators of transcription

catabolic conditions, including cancer cachexia [102], ageing [103] and muscular dystrophies [104]. Yet, so far, no effective drug has been used in the clinical practice.

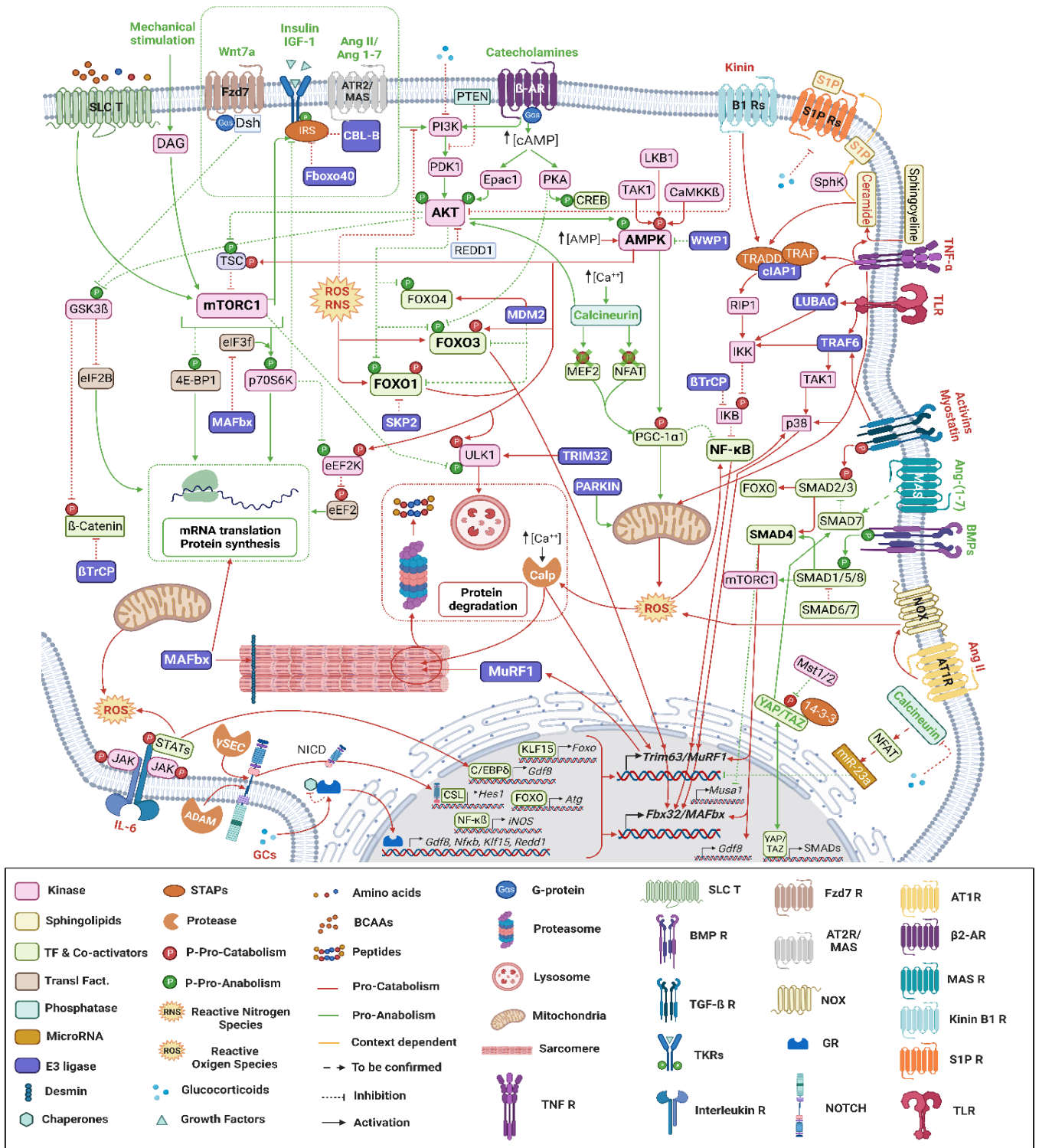


Figure 10. Overview of anabolic and catabolic signalling pathways involved in muscle protein homeostasis (from Peris-Moreno et al., 2021, see Appendix 10.4 [38]).

In this thesis project, we focused on the pivotal role in muscle homeostasis of the TGF- β superfamily (see section below) and the Integrated Stress Response signalling (see section 4.3).

TAKE HOME MESSAGE

Muscle atrophy is a social and economic burden that results from an imbalance in muscle protein synthesis in favour of muscle protein breakdown. However, despite a better understanding of the anabolic and catabolic signalling pathways dysregulated during atrophy, there is still no proven therapeutic or preventive treatment suitable for all patients.

4.2 A pivotal role for the TGF- β superfamily in skeletal muscle homeostasis

4.2.1 Overview

The transforming growth factor- β (TGF- β) superfamily is an ubiquitous family that regulates a multiplicity of biological actions including proliferation, differentiation and apoptosis. This superfamily is divided into two signalling pathways, named TGF- β and bone morphogenetic protein (BMP).

Ligands. More than 30 secretable ligands belong to this family including activins A and B (INHBA and INHBB genes), myostatin (MSTN gene), TGF- β 1-3, growth differentiation factor GDF1/10/11 for TGF- β signalling, and AMH¹⁴, BMP2-7, GDF5/7 for BMP pathway (Figure 11).

Signal transduction. Ligands bind to a type 2 receptor, which subsequently recruits the type 1 receptor to form an heteromeric complex. These receptors pair up in different combinations to mediate the response of each ligand and the subsequent intracellular response [105–107]. Once the receptors are complexed, the adaptor protein SARA¹⁵ recruits the receptor-regulated SMAD family member (R-SMAD), i.e. SMAD2 and 3 for the TGF- β signalling and SMAD1,5 and 8 for the BMP signalling (Figure 11). Thereafter, the receptor complexes phosphorylate the R-SMAD making them recognizable by the common TGF- β and BMP mediator, SMAD4. Subsequently, SMAD4 forms an heteromeric complex with SMAD1/5/8 or SMAD2/3 that translocates into the nucleus and elicits a cell/environment/ligand specific transcriptional program [105–108] (Figure 11).

¹⁴ anti-müllerian hormone

¹⁵ SMAD anchor for receptor activation

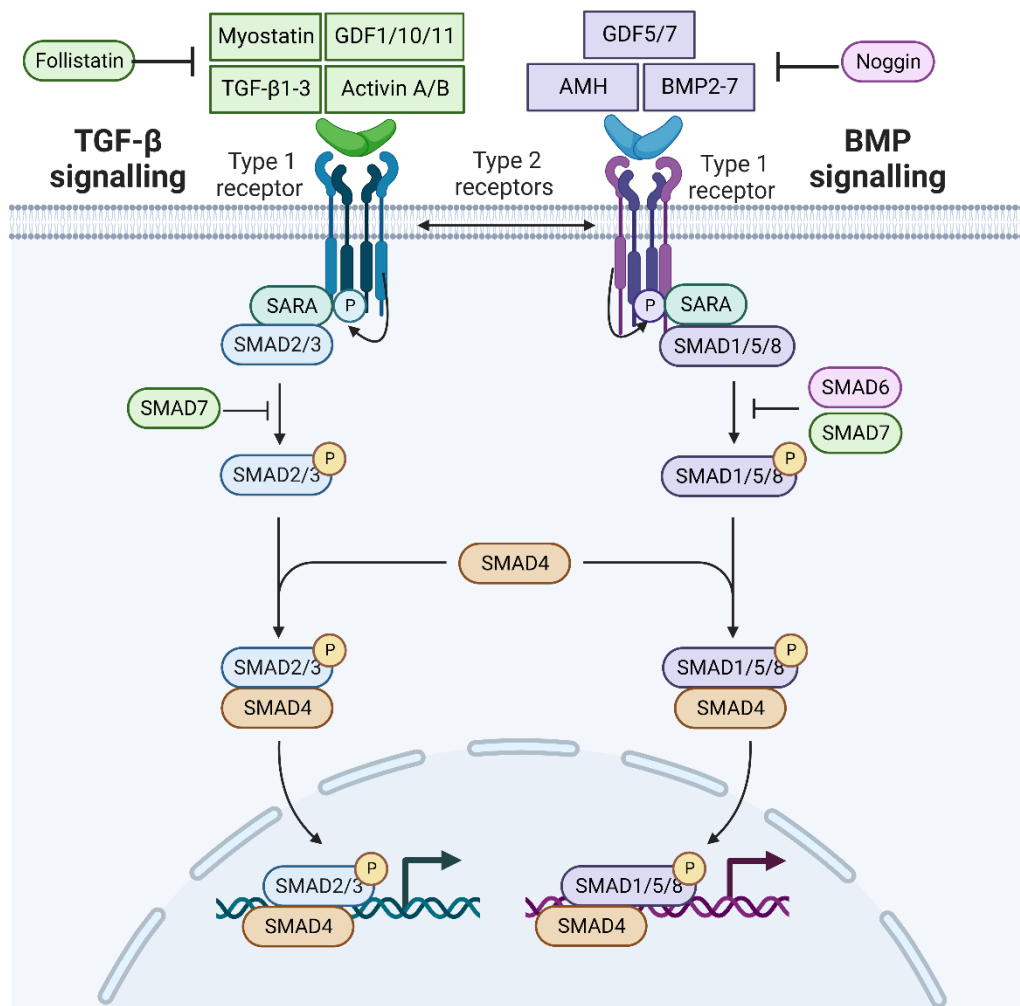


Figure 11. TGF- β superfamily organisation and signal transduction.

Regulation. Regarding the wide range of ubiquitous biological actions, the TGF- β superfamily is tightly regulated at multiple steps. First of all in the ECM, several mechanisms enable the activation of the secreted ligands from their latent inactive state. Second of all, the active ligands can be sequestered by antagonists within the ECM, for instance by follistatin (FST gene) the best described for TGF- β signalling, and noggin (NOG gene) for BMP [109] (Figure 11). Moreover, each ligand can bind to several receptor subtypes which, themselves, can be post-translationally modified, adding layers of complexity [105–107].

In addition, the inhibitory SMADs (I-SMAD), SMAD6 and SMAD7 can antagonize the signal initiated by ligands by competing with R-SMAD for the binding to a given receptor. SMAD6 selectively inhibits BMP signalling whereas SMAD7 inhibits signalling for both TGF- β and BMP signalling (Figure 11). Moreover, both signalling are also tightly regulated by ubiquitination/deubiquitination processes from receptor and R-SMAD activation to induction of the transcriptional program [38,105–107] (Figure 12). Finally,

SMADs are also subject to numerous others post-translational modifications such as acetylation, ADP-ribosylation and linker-domain phosphorylation, all of which changing the fate of the intracellular response [105].

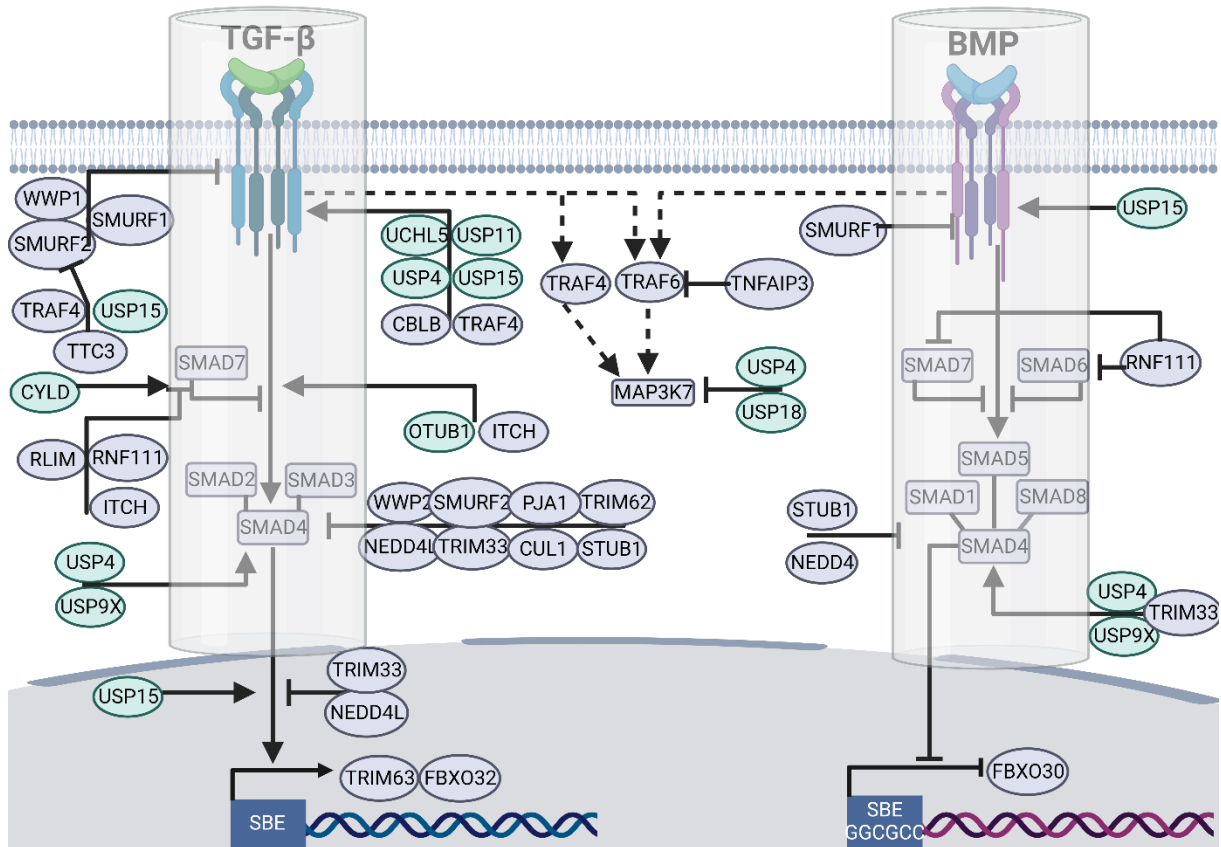


Figure 12. TGF-β superfamily regulation by E3-ubiquitin ligase and deubiquitinase enzymes.

Green and blue circles respectively represent deubiquitinase and E3-ubiquitin ligase enzymes. The schema is adapted from Cussonneau et al., 2021. Full and dotted lines respectively represent the SMAD and non-SMAD signalling. SBE: SMAD Binding Element.

TGF-β superfamily is a master regulator of adult muscle mass with (1) TGF-β signalling as a negative regulator and (2) BMP signalling as a positive regulator [110,111].

4.2.2 TGF-β signalling: The master regulator of skeletal muscle atrophy

Pathophysiological conditions. TGF-β is a catabolic pathway of great interest within the field of skeletal muscle biology. In the late 1990's, the discovery that deletion of the myostatin gene (MSTN), one of its ligands, and inhibition of its receptor, caused a profound hyper-muscularity in mice, cattle, sheep, and dogs sparked the initial interest in its role in atrophy [24,112–114]. Thereafter, MSTN was found to be elevated in muscles or blood in all type of catabolic situations characterised by muscle atrophy, such as in ageing subjects, in response to prolonged bed rest, in patients with acquired

immune deficiency syndrome, renal failure or heart failure [115–119]. Serum levels of other TGF- β ligands such as activin A also rise in response to cancer, kidney failure and heart failure, all associated with muscle wasting [115,120–122]. In addition, TGF- β 1 is remarkably elevated in plasma of patients with muscular dystrophies [123]. Besides, microRNA positively controlling TGF- β signalling are increased in muscles of patients following 10 days of sustained bed rest or in patients in intensive care unit [124,125].

The binding of myostatin or activin A/B to activin receptor type-2B (i.e. to a lesser extent type 2A) ActR-2B/A (ACVR2A/2B genes) leads to the recruitment and phosphorylation of SMAD2/3 and is associated with muscle atrophy in a multiplicity of catabolic situations [110,114,118,126–128].

4.2.2.1 TGF- β underlying mechanisms inducing muscle atrophy

Activation of MPB. TGF- β signalling is involved in the transcription of the atrogenes FBXO32/Atrogin-1 and TRIM63/MuRF1 known to be involved in ubiquitin-proteasome proteolysis. Mice or cultured mice myotubes treated with TGF- β ligands (i.e. activin A/B, myostatin) show muscle atrophy through the activation of SMAD2/3 resulting in overexpression of *Fbxo32/Atrogin-1* and/or *Trim63/MuRF1* atrogenes [127,129] (Figure 13). Similarly, exposing healthy mice to exogenous GDF11 ligand results in muscle wasting through the activation of the SMAD2-ubiquitin-proteasome pathway and autophagy axis [130] (Figure 13). Furthermore, overexpression of the transforming growth factor beta receptor 1 (*Tgfbr1*) in mice muscles also increases the expression of the atrogene *Fbxo32/Atrogin-1* and induces muscle fibre atrophy via a SMAD2/3-dependent mechanism [131] (Figure 13). Conversely, mice with muscle specific deletion of *Smad2* or *3* are resistant to muscle atrophy induced by *Tgfbr1* surepexpression or denervation [131,132]. Additionally, inhibition of TGF- β signalling through muscle-specific KO type 1 receptors (i.e. *Tgfbr1* and *Acvr1b*) or follistatin administration, induces muscle hypertrophy in mice by reducing *Fbxo32/Atrogin-1* and *Trim63/MuRF1* expression [133,134].

Mechanistically, overexpression of *Smad3* in mice muscles is sufficient to induce *Fbxo32/Atrogin-1* expression and ultimately induces muscle fibres atrophy [135]. In cultured mice myotubes, SMAD3 synergises with the transcription factor FOXO3¹⁶ to induce the expression of *Trim63/MuRF1* [136] (Figure 13). Finally, myostatin treatment also inhibits the expression of *MyoD* and *Pax3*¹⁷ myogenic genes in cultured myotubes [129]. Altogether, these data showed that the canonical TGF- β signalling (i.e. SMAD2/3) is required for muscle damage.

¹⁶ forkhead box-O 3

¹⁷ paired box 3

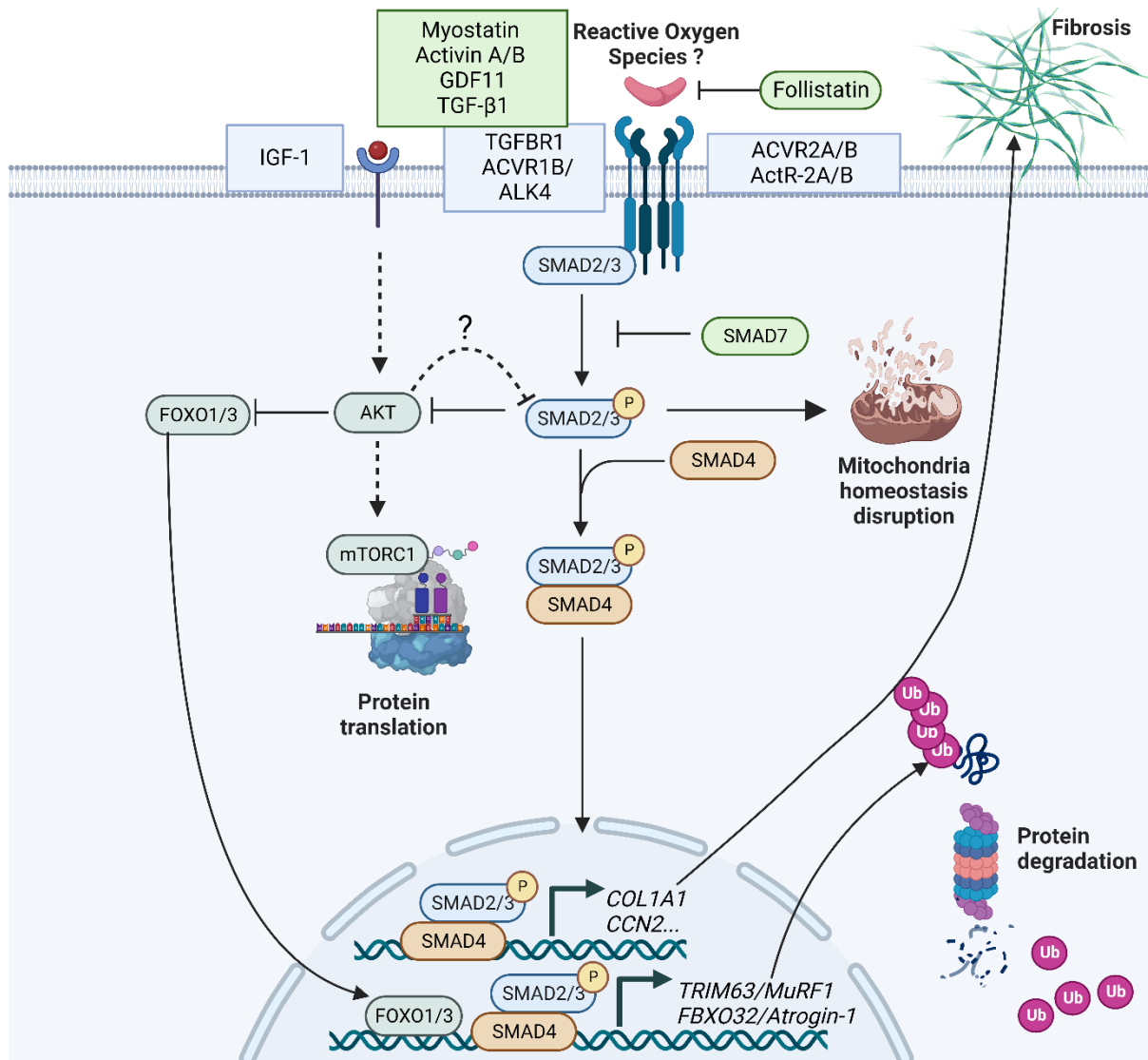


Figure 13. TGF- β signalling involvement in muscle atrophy.

The dotted lines correspond to the signalling impaired in numerous muscle wasting conditions, and the questions marks the unsolved questions.

Inhibition of MPS. TGF- β catabolic action also involves inhibition of protein synthesis. Myostatin or activin A administration are sufficient to inhibit protein synthesis in mice muscles through inhibition of the AKT/mTORC1 signalling [127,131,137,138]. The same phenotype is observed by overexpressing *Smad3* [133,135] (Figure 13). Additionally, inhibition of TGF- β signalling through muscle-specific KO type 1 receptors (i.e *Tgfr1* and *Acvr1b*) or follistatin administration, induces muscle hypertrophy in mice by increasing AKT phosphorylation [133,134]. Moreover, the hypertrophic effect of myostatin blockade is reduced when mTORC1 is genetically or pharmacologically inhibited [131,133,137]. The mechanisms linking SMAD2/3 to AKT/mTORC1 signalling in muscle atrophy conditions remain unclear. Treatment with insulin-like growth factor 1 (IGF-1) activates AKT and increases the interaction between AKT and SMAD3, leading to inhibition of TGF- β signalling in cultured myoblasts [139]. IGF-1/AKT

signalling is altered in many catabolic situations in muscles [140], and impairment of IGF-1 receptor during muscle immobilisation contributes to SMAD2/3 protein accumulation [132]. Accordingly, TGF- β signalling might be further amplified in these situations due to compromised interaction between AKT and SMAD3. In turn, this may reinforce the vicious circle between activation of TGF- β signalling and impairment of AKT-mTORC1 signalling (Figure 13).

Other muscle detrimental actions. A proteomic analysis of mice muscles overexpressing follistatin has uncovered changes in energy metabolism, fibres type, insulin and calcium signalling, providing insight into the intracellular modifications sensitive to TGF- β signalling [141]. In addition, TGF- β signalling in mice represses mitochondrial biogenesis [142,143] and is associated with mitochondrial disruption in cancer cachexia-induced muscle wasting in mice [144] (Figure 13). TGF- β -induced muscle wasting is also linked to reactive species oxygen (ROS). Injection of TGF- β 1 ligand into mice muscles increases ROS content and induces atrophy, both being reversed by administration of an antioxidant treatment, suggesting that TGF- β 1-induced muscle atrophy was ROS-dependent [145]. Finally, the TGF- β pathway is also known to play a major role in fibrosis, promoting muscle mechanical changes and muscle injury in many muscular dystrophies in mice and humans [146,147] (Figure 13).

4.2.2.2 TGF- β -targeted mediation in muscle atrophy: Panacea or smokescreen ?

The establishment of myostatin and activins as robust negative regulators of skeletal muscle has designated these ligands and partners as attractive therapeutic targets for various musculoskeletal disorders.

Promising results in vivo. Follistatin (FST gene) is a potent extracellular inhibitor of myostatin and of several other ligands of the TGF- β superfamily and its overexpression results in muscle hypertrophy in mice. This hypertrophy exceeded that observed in *Mstn* KO mice and was further exacerbated when overexpressing *Fst* in *Mstn* KO mice [133,148]. Inhibition of activin A by a specific antibody leads to muscle hypertrophy in mice and monkeys [128], and codelivery of specific activin A and myostatin inhibitors induces a synergistic response with an increase in muscle mass of up to 150% in mice [149]. Finally, the concomitant neutralization of both ACVR2A and ACVR2B receptors with BYM338 antibody results in a stronger skeletal muscle hypertrophy [150].

These observations led to the utilisation of such strategies during muscle atrophy situations: Pharmacological inhibition of myostatin alleviates muscle wasting in cachectic mice [151]. Inhibition of the receptor TGFBR1 by the LY364947 molecule abolishes diaphragm atrophy in rats undergoing sepsis [152]. Genetic or pharmacological blockade of the myostatin/activin A receptor ACVR2B improves muscle mass and function in mice models of cancer cachexia, spinal muscular atrophy, or microgravity

[153–155]. Overexpression of *Smad7*, the intracellular TGF- β antagonist, prevents cancer-mediated muscle wasting in mice [156,157]. Other effective strategies using muscle-specific microRNAs have also been investigated. For instance, overexpression of *miR-206* attenuates muscle atrophy during denervation in rat by inhibiting TGF- β -SMAD2/3 axis [158]. The system renin-angiotensin is involved in muscle loss. Interestingly, treatment with an angiotensin 2 inhibitor prevents muscle atrophy in mice through a blockade of the TGF- β -induced SMAD2/3 activation [111,145]. Finally, the use of angiotensin 2 inhibitor, extracellular or receptor antagonists shows improvement in muscle function in different muscular dystrophies by inhibiting the TGF- β signalling and hence its consequences as a pro-fibrotic pathway [146].

Disillusion in human clinical trials. Based on the pre-clinical studies, numerous TGF- β -inhibiting pharmacologic agents have progressed in human trials or are still currently under evaluation [119]. Treating elderly patients requiring hip replacement with an anti-myostatin has proven to be safe, although preservation of muscle mass following surgery was minimal [159]. Another anti-myostatin molecule showed promising results with amelioration of muscle locomotor function in spinal muscular dystrophy patients [119]. Other phase 2 clinical trials showed that the use of an antibody blocking the activin type 2 receptor was safe but with little or no functional benefit in patients with muscle wasting (i.e. hip fracture surgery, sporadic inclusion body myositis, sarcopenic elderly, cachexia, chronic obstructive pulmonary disease) [160–163].

Therefore, although these molecules were promising in rodents, they have shown only a minimal effect in humans or have demonstrated important side effects [119,164]. Indeed, most myostatin inhibitors also repress the activities of other closely related TGF- β family members including GDF11, activins, and BMPs, increasing the potential off-targets. Consequently, a careful distinction between targets is required to evaluate the use of these medications in human clinical practice [119,164].

4.2.3 BMP signalling: The silver bullet for muscle atrophy ?

The BMP signalling pathway was originally discovered for its ability to induce bone formation. BMP signalling is important in embryogenesis and development in all organ systems, and also in the maintenance of adult tissue homeostasis [165]. The role of BMP in the regulation of muscle mass was only discovered in 2013 [166,167] (Figure 14). For this reason, much less is known about this pathway and its underlying mechanistic in muscle homeostasis.

Fundamental in healthy adult muscle. BMP signalling controls the mass of healthy adult muscles, since increasing the expression of the ligand *Bmp7* or a constitutively active BMP receptor type 1A

(*caBmpr1a*, ALK3 protein) promotes a SMAD1/5-dependent hypertrophy phenotype in mice [166,167]. Furthermore, inhibition of the BMP pathway by using inhibitors of ligand-receptor interaction (i.e. LDN-193189 or noggin), or invalidation of *Smad1* or *5*, leads to muscle atrophy in healthy adult mice muscles [166]. In addition, the profound increase in muscle mass observed in *Mstn* KO mice is mediated by the activation of BMP signalling via SMAD1/5, whereas overexpressing the selective BMP inhibitor *Smad6*, significantly reduces this hypertrophic phenotype [149].

Regulation in catabolic conditions. SMAD1/5 phosphorylation increased in rodent muscles exhibiting atrophy associated with motor nerve degeneration, intensive care disuse or with amyotrophic lateral sclerosis [166,167]. In addition, the expression of BMP-related components, i.e. BMP ligands *Gdf5* and *Gdf6* and the BMP receptor type 1B (*Bmpr1b*, ALK6 protein), increase in denervated mice muscles. Similarly, the DNA-binding protein inhibitor (ID1)-luciferase reporter, which mirrors BMP transcriptional activity also increases in this situation [166,167]. However, SMAD1/5/8 phosphorylation is down-regulated, whereas gene expression of the BMP inhibitor noggin is up-regulated in muscles of tumour-bearing mice, and in muscles of pre-cachectic and cachectic patients [168]. Additionally, a decreased in gene expression of BMP-related components is also observed in the elderly with muscle atrophy following hip arthroplasty [169].

A central role to counteract muscle atrophy. Administration of tilorone, a molecule capable of inducing BMP signalling, restores BMP-mediated signalling in muscles, limits muscle wasting, and lengthens the survival of tumour-bearing mice [168]. These data showed the necessity of promoting/maintaining BMP signalling to limit cancer-induced muscle atrophy [168]. Overexpression of *caBmpr1a*/ALK3 or *Bmp7* in mice blunts muscle atrophy induced by denervation or cancers [166,167], while *Smad6* or *Nog* overexpression suppresses SMAD1/5 phosphorylation and exacerbates muscle atrophy during denervation and fasting [166,167]. Besides, the role of altered BMP signalling in muscle atrophy was confirmed by Sartori et al. who observed a severe aggravation of denervation-induced muscle atrophy in *Gdf5* KO mice [166]. Moreover, *Mstn* KO mice, which are usually resistant to denervation-induced muscle atrophy, lose this ability when BMP signalling is concomitantly blunted [166]. Finally, a long non-coding RNA, *Chronos*, impairs muscle growth in ageing mice by repressing BMP signalling [170]. Altogether, these data strongly suggest that (1) activation of the BMP pathway in skeletal muscle during catabolic conditions is an adaptive response to counteract atrophy, and (2) a deficiency in this signalling plays a critical role in aggravation of muscle frailty [166,167].

Intracellular actions. In innervated mice muscles, hypertrophy induced by increased expression of *Bmp7* or *caBmpr1a*/ALK3 is associated with increased phosphorylation of AKT and of two mTORC1 substrates (i.e. RPS6 and 4E-BP1), which is blunted by rapamycin treatment. These data provided the

first demonstration that the mTORC1 pathway is indispensable in the regulation of BMP signalling-induced muscle growth [167] (Figure 14). In denervated mice muscles, overexpression of *Nog* significantly enhances the expression of the *Fbxo30*. This gene encodes a protein identified as MUSA1 for muscle ubiquitin ligase of SCF complex in atrophy-1 [166]. The authors proved that BMP signalling acts as a positive regulator of muscle mass by repressing the transcription of *Fbxo30*/MUSA1, whose induction is required for denervation-induced atrophy [166] (Figure 14). Similarly, increased expression of the BMP inhibitor *Smad6* also results in increased *Fbxo30*/MUSA1 expression in denervated muscles [167]. Inhibition of the BMP signalling is also associated with increased expression of *Trim63*/MuRF1 and *Fbxo32*/Atrogin-1 during muscle atrophy associated with denervation [167] and cancer [168] in mice. The repression of the expression of these atrogenes by the BMP pathway is believed to be through the suppression of the HDAC4¹⁸-Myogenin axis, which is involved in the transcription of TRIM63/MuRF1, FBXO32/Atrogin-1, and FBXO30/MUSA1 [167] (Figure 14).

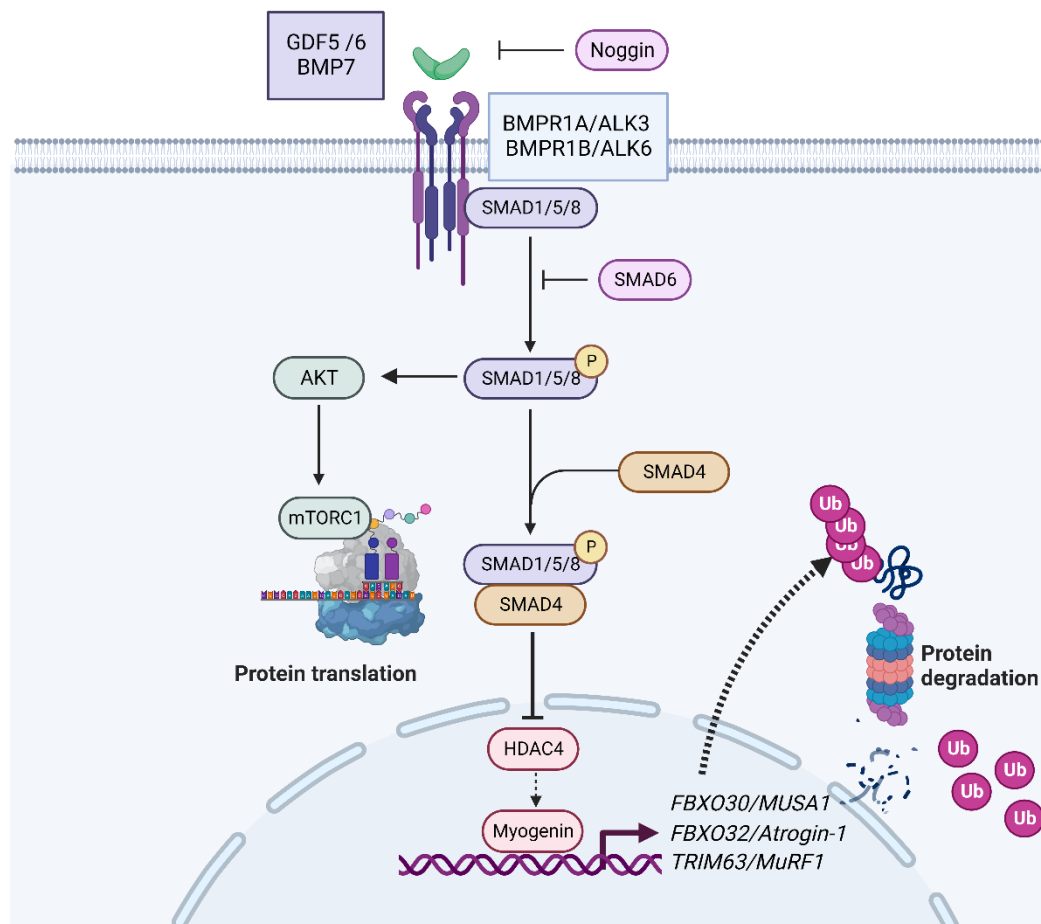


Figure 14. BMP signalling involvement in muscle hypertrophy.

The dotted lines correspond to the signalling impaired when BMP signalling is activated.

¹⁸ histone deacetylase 4

4.2.4 A finely tuned balance between TGF- β and BMP signalling

4.2.4.1 SMAD4 shared custody

SMAD4 is the shared actor between the TGF- β and BMP signalling (Figure 15). *Smad4* KO mice slightly lose muscle mass and are even more susceptible to muscle wasting during denervation or fasting [166]. *Mstn* KO mice exhibit a significant activation of the SMAD1/5/8 transcriptional activity with greater recruitment of SMAD4 on the promoter of BMP target genes. On the contrary, *Gdf5* KO mice lead to an increased binding of the SMAD4-SMAD2/3 complex to the promoter of TGF- β target genes [166].

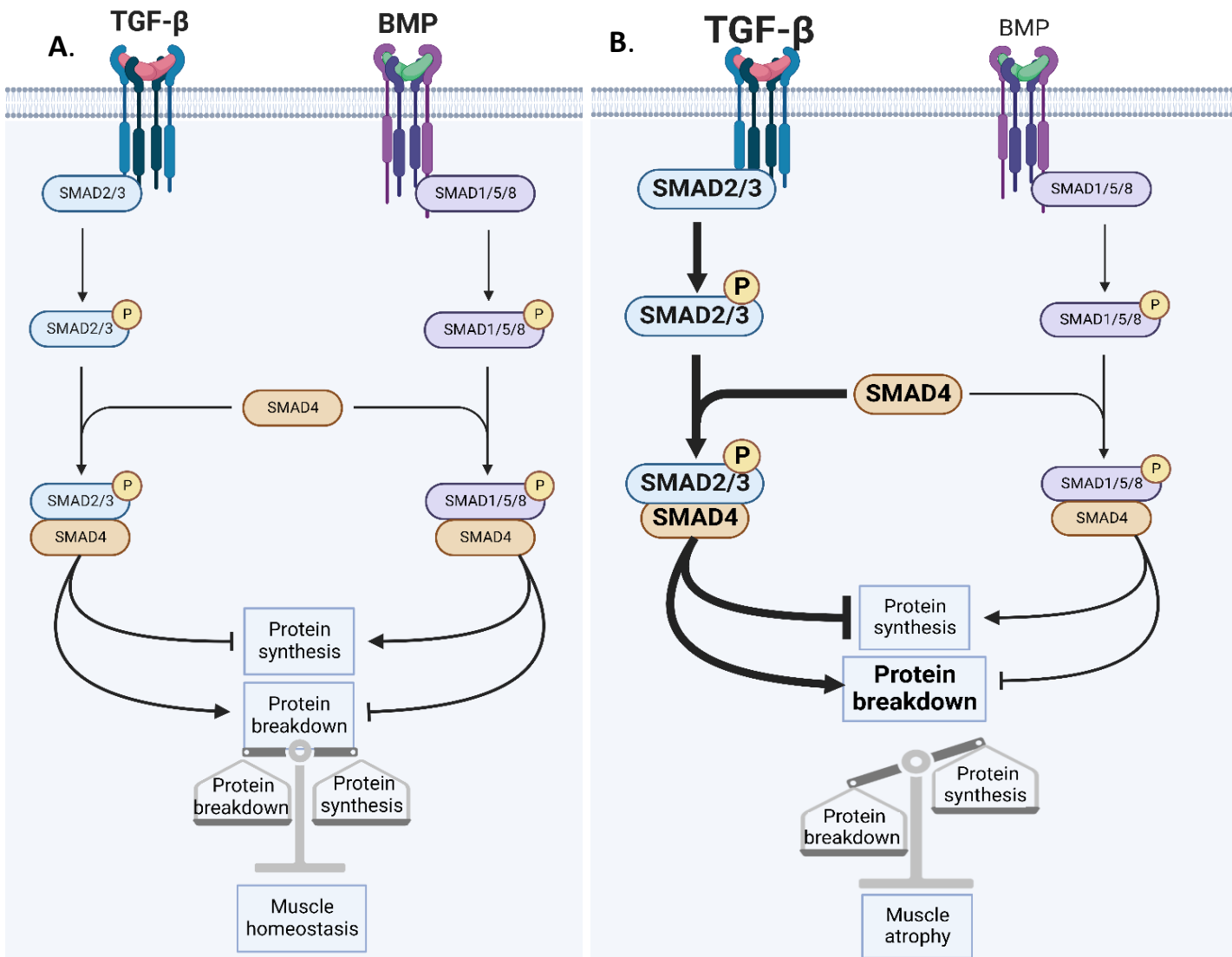


Figure 15. SMAD4 recruitment in muscle in basal (A) or muscle wasting (B) conditions.

This has prompted the concept of a competition between SMAD 2/3 and SMAD 1/5/8 for SMAD4 recruitment. The authors speculated that inhibiting TGF- β signal would release SMAD4 from SMAD2/3 to be more available for SMAD1/5/8. In muscle wasting scenarios, TGF- β over activation is considered

as a factor which reduces the availability of SMAD4 for BMP signalling (Figure 15). This article has strongly highlighted the need for a fine-tuning of the BMP/TGF- β balance to maintain muscle homeostasis [166] (Figure 15). This is consistent with the Myhre syndrome, a human rare autosomal dominant genetic condition characterised by muscle hypertrophy. This syndrome is explained by a missense mutation of *SMAD4*-leading to defects in ubiquitination, and hence Myhre syndrome patients have increased levels of SMAD4 protein rather than SMAD4 loss [171].

4.2.4.2 TGF- β /BMP non-canonical signalling and its dual role in muscle homeostasis

Non-SMAD signalling. In addition to the canonical SMAD-mediated TGF- β superfamily signal transduction, activated receptors also transduce signals through non-SMAD signalling [172] (Figure 16). For example, the TGF- β -activated kinase 1 (TAK1) protein, originally identified as a member of the MAPK¹⁹ family, is a major component of the non-canonical TGF- β superfamily signalling. TAK1 interacts with the TNF Receptor Associated Factor 6 (TRAF6), which is bound to a receptor type 1 of the canonical SMAD signalling [173,174] (Figure 16). Once the receptors type 1 and 2 are complexed, TRAF6 undergoes autoactivation and subsequently activates TAK1. Thereafter, TAK1 phosphorylates MAPK actors leading notably to the activation of the p38 MAPK [173,175] (Figure 16).

TRAF6 a pro-atrophic actor. TRAF6 mediates the activation of p38 and induces the expression of the atrogenes *Trim63*/MuRF1 and *Fbxo32*/Atrogin-1, as well as autophagic-related actors in atrophying muscles during denervation and starvation in mice [176–178] In addition, TRAF6 protein levels increase in muscles of gastric cancer patients [179]. Conversely, *Traf6* deletion suppresses the increase expression of *Fbxo32*/Atrogin-1 and *Trim63*/MuRF1, improves AKT phosphorylation, and limits muscle atrophy in mice during ageing, starvation, denervation, cancer cachexia or dexamethasone treatment [176–179].

A dual role for TAK1. TAK1-p38 signalling is activated under activin A treatment in mice myotubes and *in vivo* ending up by up-regulation of *Fbxo32*/Atrogin-1 and muscle atrophy. Interestingly, the catabolic effect of activin A was abolished by p38 inhibitor administration [180]. Moreover, muscles damages were alleviated through pharmacologic inhibition of TGF- β 1-TAK1 axis by the neuroprotective molecule catalpol in a model of Duchenne muscular dystrophy [181].

In addition to the possible role of TAK1 in muscle atrophy, TAK1 has also been reported to be required for the maintenance of skeletal muscle mass in adult mice. Inducible skeletal muscle-specific *Tak1*-KO mice leads to severe muscle wasting which is accompanied by increased proteasome activity, elevated autophagy, redox imbalance and mitochondrial dysfunctions associated with decreased p38

¹⁹ mitogen-activated protein kinase

phosphorylation [182,183]. Overexpression of *Tak1* in mice induces muscle hypertrophy, increases protein synthesis, and attenuates denervation-induced muscle atrophy, while its genetic inactivation leads to neurogenic atrophy [184]. A very recent study has revealed promising findings. The authors identified a strong physical interaction between TAK1 and SMAD1 in denervated mice muscles. The authors assumed that TAK1 could regulate the spatial distribution of SMADs proteins by promoting (1) the nuclear localisation of SMAD1-SMAD4 to suppress *FBXO30/MUSA1* transcription and (2) the cytosolic retention of the inhibitor SMAD6 in denervated muscles. The underlying mechanisms are however still completely unknown [184]. Whether such an interplay between TAK1 and SMADs also

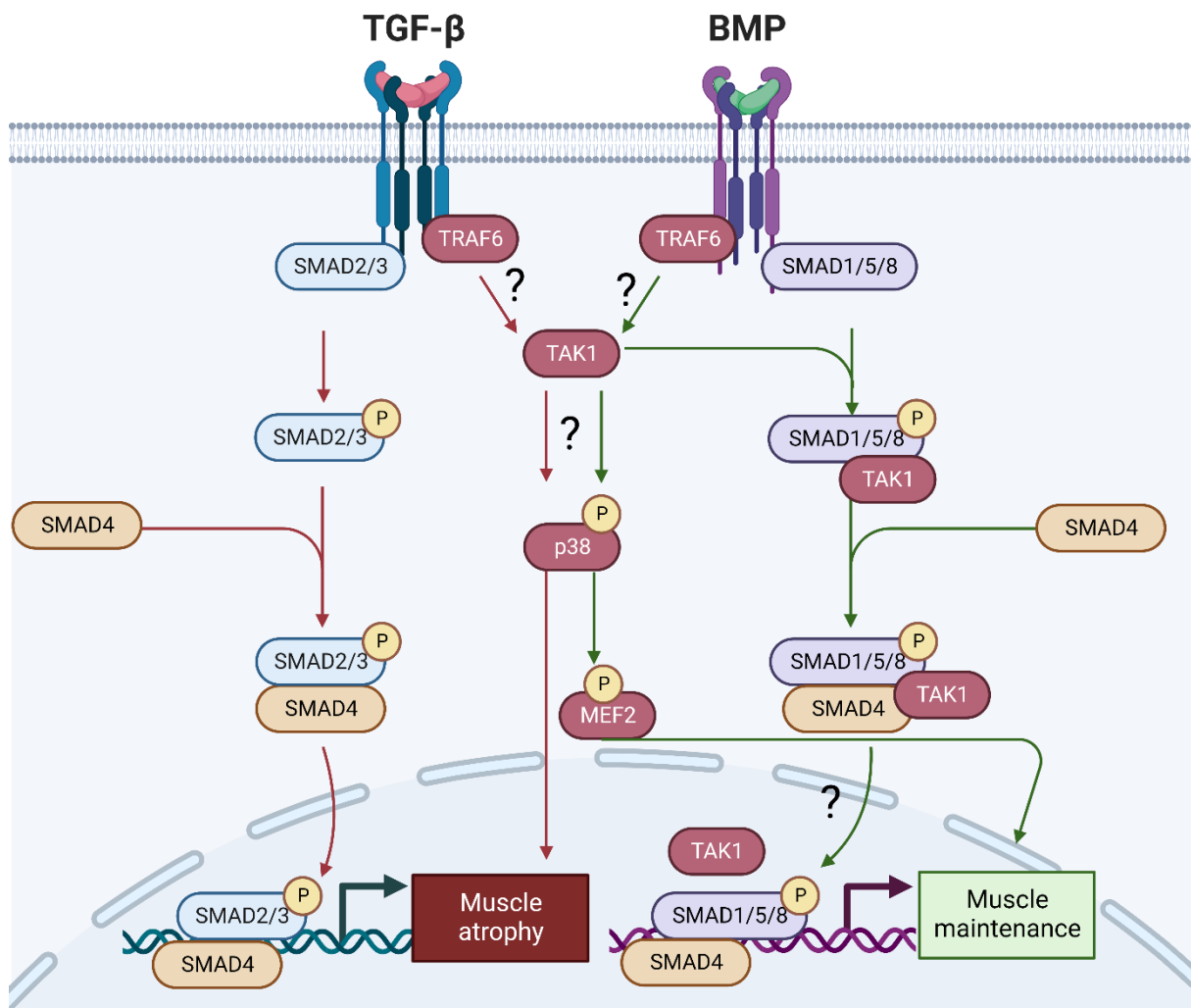


Figure 16. Non-SMAD TGF-β/BMP signalling and its dual involvement in muscle homeostasis.

The red and green lines represent respectively the catabolic and anabolic signalling, and the questions marks the unsolved questions.

exists in other catabolic conditions has never been investigated (Figure 16).

MEF2 a pro-maintenance actor. Myogenic enhancer factor 2 A-D (MEF2A-D) proteins are key transcriptional regulators of skeletal muscle development, sarcomeric gene expression, fibre type control and glucose uptake metabolism [185–187]. p38 MAPK directly phosphorylates MEF2, increases its transcriptional activity in myoblasts from mice or rats, and is required for a proper differentiation process [188,189]. In addition, *Traf6* deletion in mice myotubes inhibits MEF2 transcription [190].

Furthermore, SMAD3 interacts with MEF2C resulting in reducing MEF2C transcriptional activity in mice myoblast cells and thus disrupt differentiation [191]. Finally, activin A treatment in human muscle cells reduces MEF2C expression and activity and leads to myotubes atrophy [192]. To our knowledge, no study has ever explored the TGF- β /BMP-TRAF6-TAK1-p38-MEF2 axis in skeletal muscle *in vitro* or *in vivo* (Figure 16).

The pivotal role for TRAF6-TAK1-p38 in muscle homeostasis beneath TGF- β and BMP signalling is full of unsolved questions. How does TAK1 act as a pro-atrophic actor through TGF- β -p38, and promotes muscle gain through BMP? How does TGF- β /BMP ligand-receptors pair to activate SMAD and non-SMAD signalling? How do these signals interact? These unsolved questions warrant further investigation (Figure 16).

TAKE HOME MESSAGE

A major conceptual insight emerging from these studies is that the balance between TGF- β and BMP signalling pathways plays a key role in determining skeletal muscle fate. Therapies targeting TGF- β induce challenging side effects due to its pleiotropic role. At present, extensive effort should be directed toward further a better understanding of the role of BMP signalling in muscle homeostasis.

4.3 The Integrated Stress Response signalling: Beneficial or harmful for skeletal muscle?

The Integrated Stress Response (ISR) signalling is another pathway involved in muscle homeostasis. First of all, an overview of the signalling organisation will be presented and second of all, a focus will be made on the role of ISR in muscle homeostasis.

4.3.1 Overview

The ISR is a well-conserved signalling present in eukaryotic cells, which is activated in response to a range of physiological stresses [193,194]. Such stresses commonly include extracellular factors such as hypoxia, amino acids deprivation, glucose deprivation, heme deficiency, viral infection, and intracellular stresses such as ER stress. The core event of the ISR activation is the phosphorylation of

the alpha subunit of the eukaryotic translation initiation factor 2 (eIF2 α) on its serine 51 (p-eIF2 α) [193,194] (Figure 17). To date, four kinases have been reported to phosphorylate eIF2 α : PKR-like ER kinase (PERK), double-stranded RNA-dependent protein kinase (PKR), heme-regulated inhibitor (HRI), and general control nonderepressible 2 (GCN2) [193,194] (Figure 17). They all dimerise and auto-phosphorylate to be activated in response to distinct environmental stresses: amino acid deprivation for GCN2, ER stress for PERK, heme deficiency for HRI and viral infection for PKR [193,194] (Figure 17). Phosphorylation of eIF2 α leads to two consequences (1) a general inhibition of the translational machinery and (2) the translation of selected mRNA including ATF4.

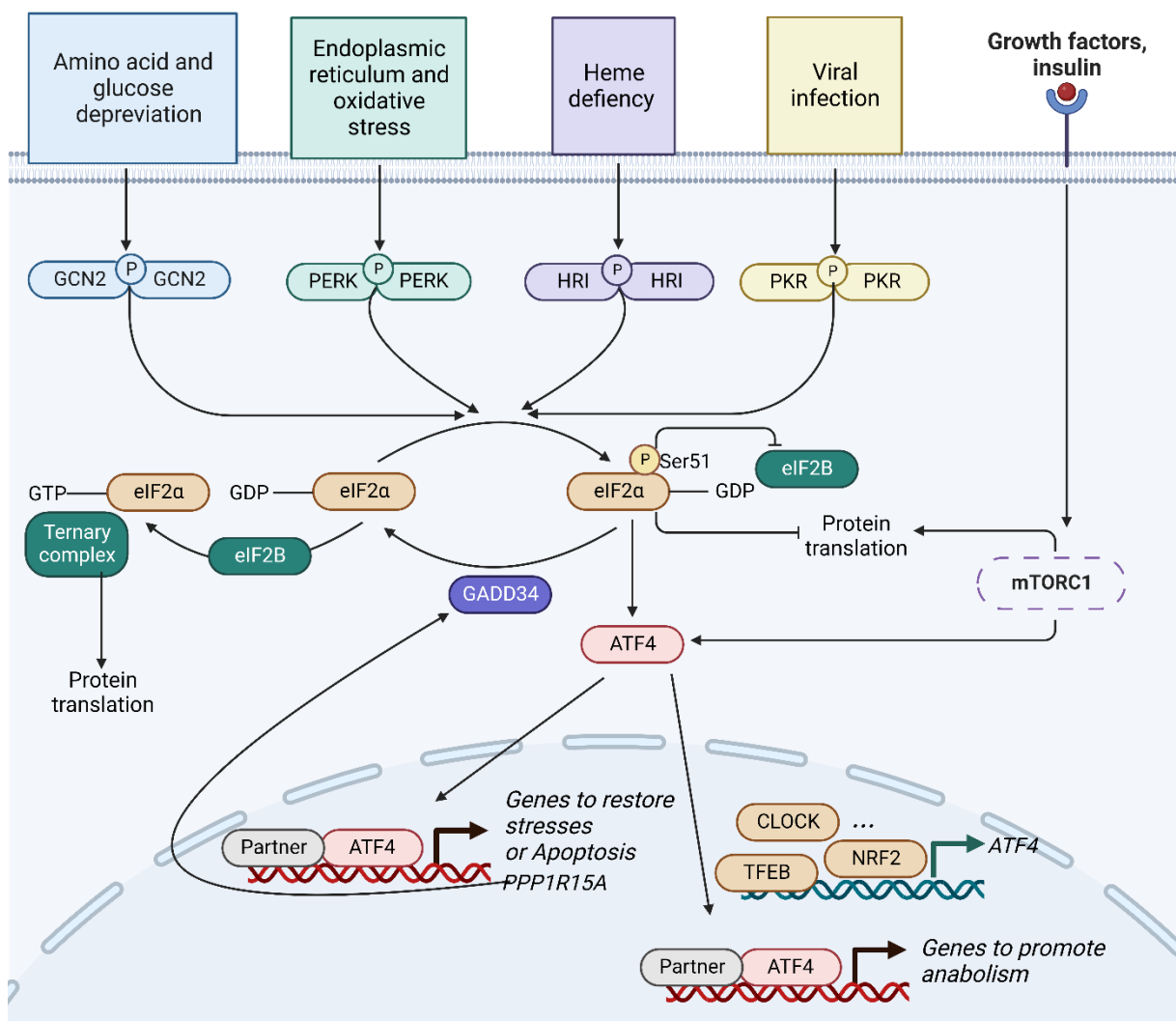


Figure 17. The Integrated Stress Response pathway organisation and signal transduction.

Inhibition of protein translation. In normal conditions, the GDP²⁰-bound form of eIF2 α is exchanged for a GTP²¹-bound form by the action of the guanine nucleotide exchange factor eIF2B (Figure 17). This

²⁰ guanosine diphosphate

²¹ guanosine-5'-triphosphate

event converts eIF2 α to its active form which can recruit the translation initiation ternary complex and subsequently initiates the first step of protein translation. Upon stress conditions, p-eIF2 α inhibits eIF2B action, which thus remains in its GDP-bound form, preventing the formation of the ternary complex and leading to the global inhibition of protein translation [193,194] (Figure 17).

Translation of specific mRNAs. In parallel, p-eIF2 α results in the translation of specific mRNAs, including the activating transcription factor 4 (ATF4) (Figure 18). The mechanism is highly conserved, from yeasts to mammals. The ATF4 transcript is constitutively expressed in many cells and has several small upstream open reading frames (uORF) at its 5' end, being out of frame with the main protein-coding sequence (CDS). These uORFs mediate basal repression of ATF4 translation (Figure 18). Upon normal conditions, when the ternary complex is abundant (i.e. eIF2 α non-phosphorylated), ribosomes initiate scanning at uORF1 and re-initiate at uORF2 overlapping with ATF4 CDS, hence precluding ATF4 translation (Figure 18). Upon stresses conditions (i.e. p-eIF2 α), a limited number of ternary complexes are formed. Ribosomes still initiate scanning at uORF1 but, due to low levels of the ternary complex, ribosomes take longer to re-initiate translation. Hence, they re-initiate scanning at the ATF4 CDS (Figure 18). Therefore, upon p-eIF2 α , this results in approximately fivefold higher ATF4 protein expression [193–195].

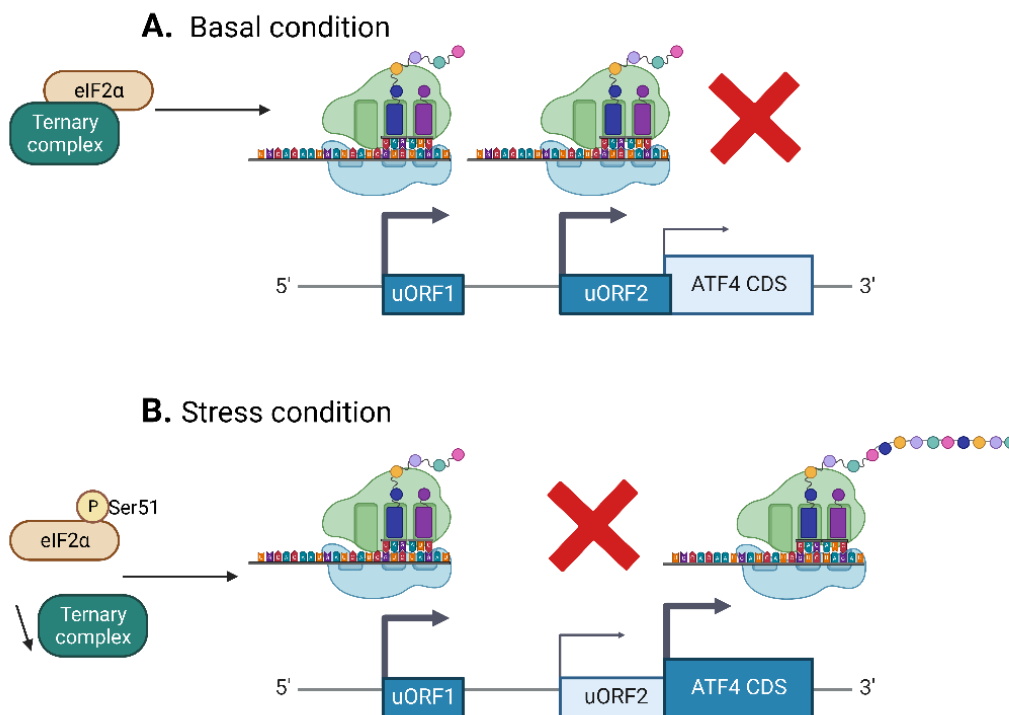


Figure 18. ATF4 mRNA sequence and its translation upon (A) basal condition or (B) stress condition.

uORF: upstream open reading frame; CDS: coding sequence.

Biological role of ATF4. ATF4 is a bZIP²² transcription factor that belongs to the ATF/CREB²³ protein family [196]. ATF4 is a key determinant of cellular fate in response to ISR activation, mainly acting as a transcriptional activator of a cohort of genes involved in cellular stress adaptation (Figure 17). ATF4 has several dimerisation partners that influence its regulation of gene transcription and governs cellular outcome. ATF4 produces distinct tailored responses with the transcription of target genes being highly dependent on the cellular context/stresses [193,194]. For instance, upon nutritional stress, ATF4 stimulates the expression of genes involved in amino acid transport and biosynthesis, and in autophagy, to supply new amino acids for *de novo* protein synthesis [197–199] (see section 4.3.2). Moreover, ATF4 induces the transcription of the protein phosphatase 1 regulatory subunit 15A (PPP1R15A, GADD34²⁴ protein), the main eIF2 α phosphatase, acting as an important negative feedback loop to restore protein synthesis once the stress is overcome [193,194,200] (Figure 17). It has been proposed that the relative duration and intensity of the ISR signalling dictate the cellular outcome. Therefore, ATF4 may also facilitate the execution of a cell death transcriptional program when cellular homeostasis cannot be restored, by activating the transcription of apoptotic genes [201–204] (Figure 17).

Other regulations of ATF4 translation and transcription. ATF4 translation can also be stimulated by anabolic hormones and growth factors, including insulin or IGF-1 (Figure 17), which activate mTORC1 to increase ATF4 translation [205–208]. mTORC1 activation enables ribosomes to bypass short uORF in the 5' of ATF4 mRNA in the same way as ISR activation does [195,207–209]. In contrast to p-eIF2 α , mTORC1 activity increases both ATF4 translation and general protein synthesis [205–208]. In this context, ATF4 heterodimers primarily induce the transcription of genes that promote amino acid uptake and synthesis to facilitate anabolism (Figure 17).

In addition to the translational regulation of ATF4, it can also be regulated at the transcript level. ATF4 mRNA levels are low under normal conditions but are induced in response to different stresses by different transcription factors (Figure 17). For example, ATF4 expression is induced in response to oxidative stress by NRF2²⁵, chemotherapeutic drugs by CLOCK²⁶, or ER stress and starvation by TFEB²⁷ and TFE3²⁸ [193,194]. Interestingly, in a positive feedback loop, ATF4 downstream gene targets, such as NUPR1²⁹, can also elevate ATF4 mRNA levels [210] (Figure 17).

²² basic leucine zipper

²³ cyclic AMP response element binding

²⁴ growth arrest and DNA damage-inducible 34

²⁵ NF-E2-related factor 2

²⁶ clock circadian regulator

²⁷ transcription factor EB

²⁸ transcription factor binding to IGDM enhancer 3

²⁹ nuclear Protein 1, transcriptional regulator

How ATF4 facilitates such diverse cellular adaptations, ranging from anabolism to growth arrest, is an important and unsolved question. One possibility is that different ATF4 heterodimers or different combinations of ATF4 heterodimers mediate the different effects of signalling.

4.3.2 The ISR pathway involvement in autophagy and mitochondrial homeostasis

As written above, autophagy and mitochondrial quality control are cellular processes essential for muscle homeostasis, and deficiency in either is associated with muscle wasting [13,19,66]. The ISR is an important signalling involved in these two processes in a wide range of tissues and cells.

Role in autophagy. During hypoxia, ER stress, amino acid deprivation, lipopolysaccharide treatment, or low protein diet, ATF4 binds to the specific promoter of genes involved in autophagy to promote (1) a pro-survival response *in vitro* or in the liver, heart and skeletal muscle of rodents [197,199,211–217] or (2) a pro-lethal autophagy response in heart and kidney [218,219] (Figure 19). ER stress or hypoxia leads to the upregulation of certain autophagy actors in a PERK-dependent manner *in vitro* and in the heart of mice [197,211,212,214,216,218]. Of note, PERK regulates all stages of autophagy including induction, vesicle nucleation, phagophore elongation, and maturation [220]. GCN2 is also essential for the induction of autophagy-related genes upon amino acid starvation *in vitro* and in the mouse intestine, while a mutant form of eIF2 α suppresses the autophagy process [197,221–223]. Moreover, there are direct interactions between eIF2 α subunits and core autophagy proteins, although it is not yet known whether these interactions are biologically significant [224,225].

Role in mitochondrial quality control. Over the past decades, growing evidence have placed the ISR signalling as essential in mitochondrial quality control, through the mitochondrial unfolded protein response (UPR_{mt}). UPR_{mt} is a mitochondria stress response induced by a loss of mitochondrial homeostasis. UPR_{mt} activates a transcriptional program of mitochondrial chaperone proteins and proteases (i.e. encoded by nuclear DNA) to promote the recovery of mitochondrial proteostasis [226]. Nonetheless, if the UPR_{mt} is unable to repair mitochondrial damages, it promotes the elimination of the entire mitochondrion by mitophagy. Finally, if the damages persist, cells undergo senescence and/or apoptosis [226]. UPR_{mt} is evolutionarily conserved and there are three key regulatory proteins of UPR_{mt}, including ATF4, which is often overexpressed upon mitochondrial damage [227]. Cells lacking a functional gene copy of ATF4 fail to upregulate several mitochondrial enzymes and exhibit a reduction in mitochondrial respiration. A global transcriptomic analysis has validated the presence of ATF4-binding motifs in many UPR_{mt} genes [226–228]. In skeletal muscle, evidence of ATF4 activation by mitochondrial stresses is growing. For instance, ATF4 protein accumulation is linked to HRI or GCN2 activation following the loss of mitochondrial membrane potential *in vitro* [229,230], and is associated

with PERK upon a genetic defect in mitochondrial fission in mice muscles [231,232] (Figure 19). In addition, mitochondrial stresses, induced by a genetic deficiency in mitochondrial fusion or mitophagy in mice muscles, increase p-eIF2 α , ATF4 protein levels and the expression of an ATF4 target gene, the fibroblast growth factor 21 (FGF21) [233]. Of note, although the biological effects of FGF21 are largely unknown, it is massively induced by a defect in mitochondrial homeostasis, and in turn, improves mitochondrial function [233]. There is evidence that the activation of UPRmt-ATF4 following mitochondrial disturbances in muscles can have protective or maladaptive effects. For instance, in a rare children mitochondrial myopathy (i.e. Reversible Infantile Respiratory Chain Deficiency), the induction of ATF4-FGF21 axis and the subsequent induction of mitochondrial biogenesis-related genes precede the complete disease recovery phase in humans [231]. On the contrary, genetic deletion of a mitochondrial fusion protein in muscles leads to an accelerated ageing phenotype with increased muscle atrophy and inflammation through an ATF4-FGF21-dependent mechanism [234].

Taken together, these studies highlight the intricate involvement of the ISR in autophagy and in mitochondrial quality control. These studies support a dual role for ATF4 in mediating survival and cell death responses, depending on the duration and type of stress, the cell type and the pathophysiological context. Moreover, much remain to be explored in understanding ISR-ATF4 involvement in autophagy and mitochondrial quality control in muscle homeostasis.

4.3.3 The ISR pathway implication in muscle atrophy

Some of the ISR members have been associated to muscle weakness and atrophy in different catabolic conditions and will be discussed in the following part (Figure 19).

4.3.3.1 The ISR kinases and eIF2 α

PERK kinase. A ligand-activatable PERK kinase induces p-eIF2 α , expression of ATF4 target genes, and leads to severe muscle atrophy within a few days after injection in mice muscles [235]. However, genetic ablation or pharmacological inhibition of PERK reduces skeletal muscle mass and strength and increases gene expression of UPS and ALS components in healthy mice muscles [236]. In addition, *Perk* is increased in a model of cancer cachexia-induced muscle atrophy in mice, but genetic ablation or pharmacological inhibition of PERK exacerbates muscle atrophy [237]. Of note, in this study, they observed that PERK increased (1) p-eIF2 α and *Atf4* expression and (2) gene expression of the Unfolded Protein Response (UPR) components, which is another PERK downstream signalling [237]. Therefore further studies are needed to decipher by which downstream pathways PERK acts as a negative or positive regulator of muscle mass (Figure 19).

GCN2 kinase. *Gcn2* deficiency protects mice from denervation-induced muscle atrophy while forced *Gcn2* expression worsens denervation-induced atrophy [238]. The authors highlighted that GCN2 could promote FOXO3 nuclear accumulation, and the subsequent transcription of the atrogenes *Trim63*/MuRF1 and *Fbxo32*/Atrogin-1 [238] (Figure 19). Of note, whether the atrophic role of GCN2 is mediated by the downstream p-eIF2 α -ATF4 signalling has not been yet demonstrated.

PKR kinase. Levels of phosphorylated PKR and eIF2 α are increased in muscles of cancer cachectic patients [239] and mice [240]. In addition, the pharmacological inhibition of PKR attenuates muscle atrophy in cancer cachectic mice through a possible inhibition of NF- κ B [240] (Figure 19). Increased levels of intracellular calcium might be the upstream stress activating PKR in skeletal muscle (Figure 19). Currently, as for GCN2 kinase, the atrophic role of PKR has not been demonstrated to be linked to the ATF4 downstream signalling.

eIF2 α . P-eIF2 α is enhanced in muscles during cancer-cachexia and amyotrophic lateral sclerosis in mice or humans [237,239,241]. In addition, fasting-induced muscle atrophy is hampered when mice express a phosphorylation-resistant form of eIF2 α [242]. However, p-eIF2 α is decreased in atrophic mice muscles following food deprivation, while an upregulation of *Atf4* and some of its target genes is observed [243]. In addition, p-eIF2 α is also decreased in atrophying mice muscles during disuse and spinal cord isolation [244,245]. Therefore, p-eIF2 α is definitely not a common feature of muscle atrophy, and its augmentation is likely more a consequence of various extracellular stresses during muscle wasting conditions (Figure 19).

4.3.3.2 The atrogene ATF4

Like other cell types, skeletal muscle fibres do not significantly express the ATF4 protein in the absence of cellular stress, especially as ATF4 is non-essential for the normal development or maintenance of skeletal muscle mass and function [246–248]. Mice with a lifelong absence of ATF4 expression in skeletal muscle fibres undergo normal skeletal muscle development and exhibit normal muscle mass and function until late in life, at which time they begin to exhibit protection from age-related muscle atrophy and weakness [246,247]. ATF4 is considered as an atrogene because its mRNA levels rise in muscle during many catabolic conditions that cause muscle atrophy in mice (i.e. denervation, spinal cord isolation, fasting, ageing, immobilisation, myopathies) [99,242,246,247,249]. In addition, a deletion of *Atf4* in mice muscles limits muscle atrophy during starvation, immobilisation and ageing [242,246–248]. Additionally, a transcriptionally inactive ATF4 does not lead to a reduction of myofiber size during fasting in mice. This suggests that the ATF4-mediated transcriptional program is required to induce atrophy [242]. When ATF4 is expressed in skeletal muscle fibres, it interacts with several

different bZIP family members but only the heterodimerisation with C/EBP β ³⁰ is yet known as required for muscle atrophy caused by immobilisation [250] (Figure 19). The ATF4-C/EBP β heterodimer induces the transcription of the growth arrest and DNA damage inducible alpha (GADD45A) gene in muscle fibres by binding a DNA sequence that is 100% conserved in all mammalian genomes [250] (Figure 19). Of note, in most of the studies, the authors only measured ATF4 mRNA expression and expression of its target genes as evidence of its activity, because endogenous ATF4 protein cannot be reliably detected in skeletal muscle, presumably due to its low abundance, very short half-life, and lack of high-quality antibodies.

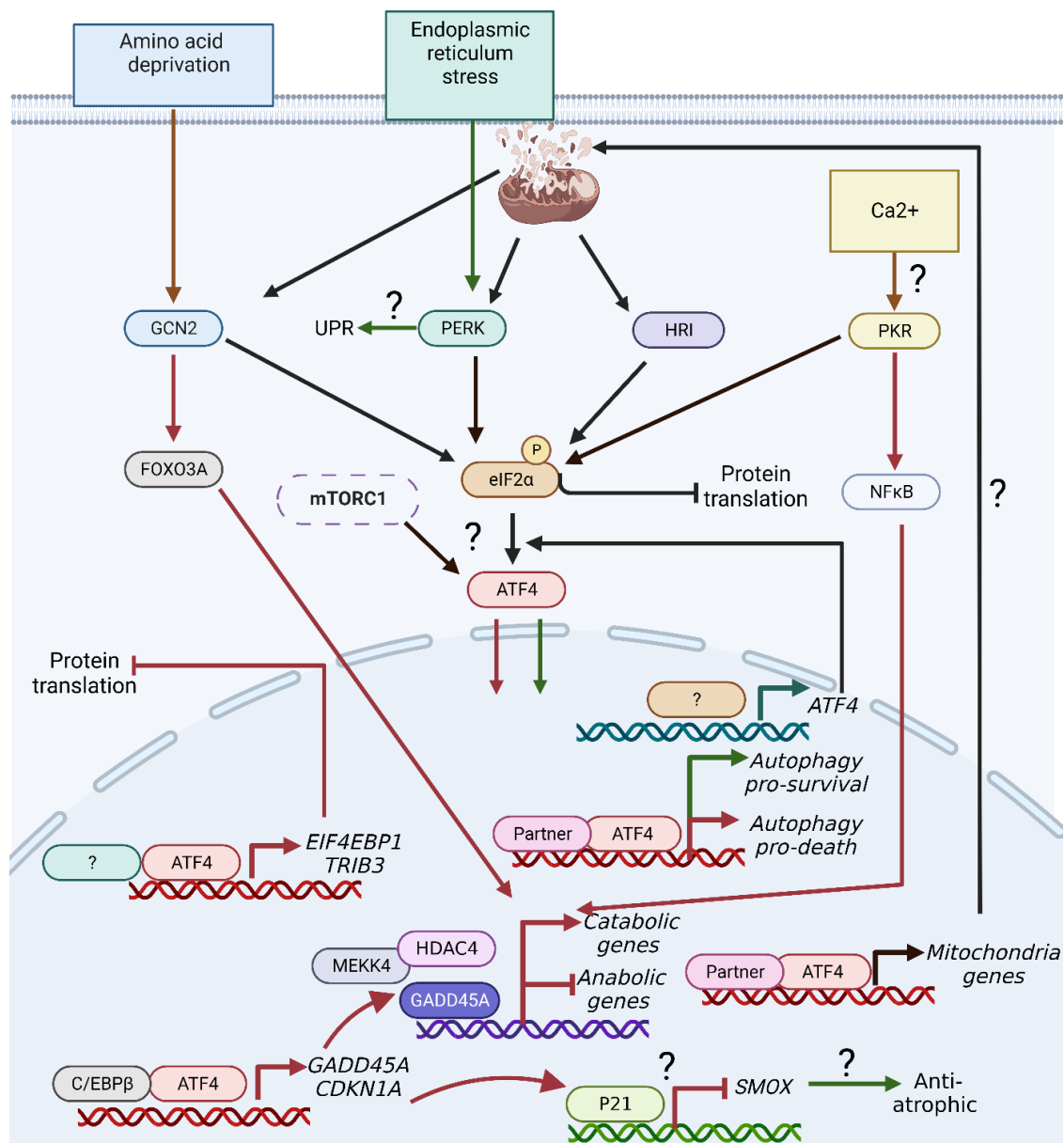


Figure 19. The Integrated Stress Response involvement in muscle homeostasis.

The red and green lines represent respectively the proved pro-atrophic and pro-maintenance signalling, and the questions marks the unsolved questions.

³⁰ CCAAT enhancer binding protein β

At present, the mechanisms by which ATF4 is transcriptionally and translationally activated in catabolic conditions are unclear but may involve different mechanisms or combinations of mechanisms. For example, contrarily to anabolic conditions, mTORC1 activity is increased in muscle during advanced ageing and is thought to contribute to the pathogenesis of age-related skeletal muscle atrophy [207,251,252]. In this context, mTORC1 may be a driver of the ATF4 pathway in skeletal muscle. In contrast, many acute stress conditions repress mTORC1 activity in muscle fibres while inducing eIF2 α kinase signalling [237,239,241,253]. Thus, in some situations, such as starvation, eIF2 α signalling may be the driver of the ATF4 pathway in skeletal muscle fibres (Figure 19). Whether the canonical ISR signalling is always implicated as an atrophic inducer seems unlikely. Further investigation of these issues might uncover new unrelated signalling.

4.3.3.3 ATF4 target genes: the atrogenes GADD45A, CDKN1A and EIF4EBP1

The mechanism by which ATF4 promotes muscle atrophy does not lead to an increase of FBXO32/Atrogin-1 nor TRIM63/MuRF1 gene expression [242]. Much remains to be discovered, but it is currently known that ATF4 contributes to muscle atrophy by modulating the transcription of three genes considered as atrogenes: GADD45A, cyclin-dependent kinase inhibitor 1 (CDKN1A) and eukaryotic translation initiation factor 4E binding protein 1 (EIF4EBP1) [99] (Figure 19).

GADD45A. GADD45A is a myonuclear protein that induces widespread transcriptional changes in muscles. It represses genes involved in anabolic signalling and energy production, and it induces pro-atrophic genes [246]. GADD45A transcript is weakly expressed in non-catabolic conditions in skeletal muscle fibres but strongly induced during muscle atrophy (e.g. ageing, amyotrophic lateral sclerosis, critically ill patients, fasting, immobilisation) in pigs, humans and mice [242,246,248,254–257]. For example, GADD45A is increased by 22-fold in muscle biopsies from critically ill patients with severe generalized skeletal muscle atrophy compared to healthy controls [257]. *Gadd45a* is the earliest and most sustained gene shown to be increased in muscles after denervation in mice [258]. Forced expression of *Gadd45a* in mice muscles or cultured mice myotubes induces atrophy even in the absence of any catabolic stimuli. Additionally, ATF4 is necessary and sufficient to induce *Gadd45a* expression during fasting- and immobilisation-induced muscle atrophy in mice [242,246,259,260]. HDAC4 is required for increasing muscle atrophy induced by *Gadd45a* overexpression during denervation, and forced expression of *Hdac4* is sufficient to induce muscle atrophy in healthy mice muscles [260]. GADD45A by forming a complex with MEKK4³¹ in muscles, increases MEKK4 protein kinase activity, which leads to GADD45A-MEKK4-mediated skeletal muscle atrophy in healthy mice muscles [259]. (Figure 19). Despite the strong evidence that GADD45A is an atrogene, a recent study

³¹ mitogen-activated protein kinase kinase kinase 4

has shown that it is likely induced in the context of denervation for a protective effect because mice lacking *Gadd45a* show accelerated and exacerbated neurogenic muscle atrophy [258].

CDKN1A. Another important ATF4-C/EBP β target gene in muscles is CDKN1A (P21 protein). CDKN1A gene expression is strongly associated with muscle atrophy in pigs, rodents and humans [242,246,248,254–257,261,262]. Increased *Cdkn1a* expression in mice muscles is sufficient to induce muscle fibre atrophy and is required for ATF4-mediated muscle atrophy during immobilisation [248]. However, to date, the cellular mechanisms by which P21 induces muscle atrophy are not defined. Although P21 protein is a well-known cell cycle inhibitor, its mechanistic role in muscle fibres seems likely to be different, essentially because muscle fibres have exited from the cell cycle. Its role in the control of skeletal muscle mass might involve the repression of the spermine oxidase (SMOX) gene expression, a gene suggested as anti-atrophic, even if the mechanisms remain completely unknown [262,263] (Figure 19).

EIF4EBP1. ATF4 heterodimers also induce the expression of the EIF4EBP1 gene, encoding for the well-established inhibitor of global protein synthesis 4E-BP1 [247,250,262] (Figure 5). EIF4EBP1 gene expression rises up in numerous catabolic conditions being as well considered as an atrogene [99,248,249,261,264]. Accordingly, *Eif4ebp1* is often induced alongside *Gadd45a* and *Cdkn1a* during skeletal muscle atrophy in mice [246,247]. However, it remains unclear which ATF4 heterodimers regulate EIF4EBP1 gene expression [264] (Figure 19).

TRIB3. Finally, another ATF4 target gene, the tribbles pseudokinase 3 (TRIB3), has been associated with muscle atrophy in numerous studies. *Trib3* deficient mice show increased muscle mass and MPS rate while decreasing the expression of the atrogenes *Trim63*/MuRF1 and *Fbxo32*/Atrogin-1 in healthy muscles [265]. In addition, *Trib3* deficient mice show attenuation of muscle fibre atrophy and fibrosis during ageing by increasing autophagy flux [266]. Finally, these mice are also partially protected from food deprivation-induced muscle atrophy [267] (Figure 19).

TAKE HOME MESSAGE

A major conceptual insight emerging from these studies is that the ISR pathway is involved (1) in the maintenance of muscle homeostasis likely through autophagy and mitochondrial quality control, but also (2) in the induction of muscle atrophy through ATF4 and its target genes. How such an interplay can occur with two different outcomes on skeletal muscle, remains to be elucidated.

4.4 A natural model of muscle atrophy resistance: the hibernating brown bear

The first three chapters of this review show (1) the need to preserve muscle mass in order to remain healthy, but also (2) that, despite the huge amount of data acquired on the multiple signalling pathways involved in atrophy, there is still no approved treatment that can be used in the clinic. Most, if not all, of the mechanisms have been elucidated using classical laboratory models in rodents and humans. In this thesis project, we have chosen to combine classical and biomimetic approaches.

4.4.1 Getting inspired by the oldest research laboratory: Nature

As noted earlier, global health is being challenged by an ageing population and epidemics of lifestyle diseases such as type 2 diabetes, obesity, atherosclerosis, osteoporosis, or muscle wasting. Rather than destroying and exploiting living beings, we should learn from and emulate ingenious evolutionary adaptations to solve current human challenges. Nature is the oldest of research and development laboratories, where failure becomes fossil and our environment is a secret of survival. Biomimicry or bio-inspiration is an approach that (1) seeks sustainable solutions to human challenges by mimicking nature's patterns and strategies and (2) has enabled significant human biomedical advances and progress [268]. For example, about one-third of the medicines we use today are derived from nature. In addition, marine organisms have inspired polymers for medical adhesives [269] and microscopically small mosquito needles have inspired the development of small, flexible microprobes to be implanted in the brain [270]. A particular species of Namibian desert beetle has a system for collecting water by condensing fog into water droplets in its exoskeleton, and gradually channelling them to its head to drink. Inspired by this ingenious strategy, researchers have replicated this structure with glass and plastic, intending to cover existing objects to turn them into fog collectors, potentially ending the world's water shortage [271] (<https://www.youtube.com/watch?v=lofIT3Uvels>). The examples are vast and endless given the great diversity of the millions of species on Earth, which live in all types of environments from extreme temperatures to total hypoxia, to the driest places on the planet [268]. Therefore, the development of future drugs, technologies, or biomedical advances depends on humans preserving the diversity of nature. Hibernation is a perfect example of seasonal variability that holds clues to diverse solutions for human pathologies.

4.4.2 Hibernation: a bioinspired approach for human challenges

Hibernation comes from the word *hibernare* "the action of overwintering" and may date back 250 million years in the Antarctic Circle [272]. Hibernation is an adaptation used by some animals to cope with an episodic or seasonal lack of energy due to unfavourable environmental conditions (e.g., low food/water availability, high predation pressure) [273]. Torpor is at the heart of hibernation, it

represents a period of metabolic suppression that can last from a few hours to several weeks. Hibernation is a more elaborate behaviour, structured into several long periods of torpor often separated by brief periods of interbout arousals (IBA). IBA last approximately 24 hours and are present in nearly all small hibernators (i.e. <10kg) but not in hibernating bears (see section 4.4.3) [273]. The most typical hibernation season is the cold season (i.e. fall to spring) but is also found in mammals inhabiting temperate and tropical climates [273].

During hibernation, along with the sharp reduction in metabolic rate (MR), there is a strong reduction in respiratory and heart rates, followed by a decrease in body temperature (T_b) [274]. The decrease in T_b can be either extreme, as in small hibernators (e.g. Arctic ground squirrels) where T_b can drop below zero [275], or mild, as in bears, where T_b rarely drops below 30 °C [276–280]. Despite the multiplicity of phenotypes and regulations of hibernation onset, there is likely a single underlying mechanism that reduces MR, although it is still unknown. However, hypotheses are emerging about the role of the hypothalamus, in particular the dorsomedial hypothalamus and a recently discovered set of neurons in the preoptic area [281–283]. A complete understanding of the molecular mechanisms triggering torpor would be of great value in developing a process to induce a hibernation/torpor state in humans, for example for a manned deep space expedition [284].

In the next sections, we will discuss hibernation in bears and how understanding its characteristic could provide insights into human health challenges, particularly muscle atrophy.

4.4.3 Hibernation in bears

4.4.3.1 *Hundred years of myths and legends*

The English word "bear" reflects the long history between bears and humans. Around 500 BC, in Northern Europe, the brown bear was the undisputed predator. In Proto-Germanic, an ancient language spoken by the Nordic tribes, the bear was known by the harsh name of *hrktos*. Hunters were so scared of *hrktos* that they came to believe that the mere mention of the bear was a cause for trouble. Linguists believe that the word became so taboo that tribes began to use the euphemism *bero* "the brown one" instead. In other words, bears were the Voldemort of Northern Europe. As another example, among the Celtic islanders, the bear was more associated with power and sovereignty, as evidenced by the figure of King Arthur, the bear-king. The etymology of the name Arthur comes from the Celtic name of the bear, *artos*, which means both "bear" and "warrior". King Arthur's death occurs on All Saints' Day when the bears begin to hibernate. Like them, Arthur does not die, he goes into dormancy. According to the history books, it is at Candlemas that Arthur takes the sword Excalibur out of the rock, a symbolic day since it corresponds roughly to the end of the hibernation of bears.

Hundreds of myths and legends surround the bears. In recent decades, contemporaries have become interested in the bear for the characteristics of its hibernation characteristics and the opportunity that this represents for medicine.

4.4.3.2 Features of bear hibernation

Ursidae family. Bears are mammals in the diverse family *Ursidae* because (1) they comprise eight species in three subfamilies, (2) they are geographically widespread in North and South America, Europe and Asia and (3) they inhabit a wide range of ecological niches from Arctic ice to tropical rainforests [285]. Bears in warm climates, do not go into hibernation, nor do the giant panda or polar bears. In this manuscript, we will only discuss bears that hibernate, i.e. brown bears (*Ursus arctos*), American black bears (*Ursus americanus*) and Asiatic black bears (*Ursus thibetanus*).

Winter in the dens. Bears enter dens in October-November and remain there until late April or early May (Figure 20); both periods are highly dependent on weather conditions (i.e. snow levels). Unfortunately, researchers have observed a decrease in hibernation duration due to global warming. They estimate that for every 1°C increase in winter temperatures, bears hibernate six days less [286]. As mentioned before, hibernating bears do not exhibit IBA, and not only do they remain physically inactive inside their dens, but they also do not eat, defecate, drink or urinate [276–279,287–289].



Figure 20. Pictures of hibernating brown bear dens in North Sweden.

MR and Tb. Hibernating bears show a 75-85% decline in MR and their Tb only decreases by a few degrees Celsius compared to the values of the active summer season, remaining around 32-33°C [276–280] (Figure 21). Thermoregulatory mechanisms could explain the maintenance of a relatively high Tb, but also body insulation due to high fur coverage, accumulation of subcutaneous fat, and also den

isolation [279,290,291]. Furthermore, in hibernating bears, there is a significant decrease compared to active bears in average heart rate (i.e. from 50-80 to 10-30 beats per minute) [279,292,293] and respiratory rate (i.e. from 10-12 to 5-7 breaths per minute) [294] (Figure 21). At the renal level, the glomerular filtration rate decreases during bear hibernation compared to summer (i.e. from 117 ml to 37 ml per minute) resulting in the production of very small amounts of urine that are reabsorbed by the urothelium of the bladder [295]. MR and Tb are clearly linked. However, bears decrease their activity, heart rate and MR before decreasing their Tb before entering the den (Figure 21). Furthermore, Tb is the first physiological parameter to change before den exit, whereas bears maintain a reduced MR up to 3 weeks after den exit (Figure 21). Therefore, the pronounced reduction and delayed recovery of MR in hibernating bears suggest that the majority of metabolic suppression during hibernation is independent of Tb decline [278,279].

Energy storage. Fat storage is increased before hibernation (i.e. hyperphagia). For example, Swedish brown bears achieve this by eating lots of carbohydrate-rich berries [296]. During the fall, bears more than double their daily energy intake reaching a total weight gain of 40% [297]. During this period of hyperphagia, lipogenesis-related genes are upregulated in white adipose tissue (WAT) to promote fat storage [298]. Energy requirements in winter rely primarily on the mobilisation and oxidation of lipid fuels, with bears experiencing a loss of approximately 22-25% of their body mass during the hibernation season [299,300] and only a moderate loss of muscle protein (see section 4.4.4) [301,302]. The respiratory quotient³² in bears decreases from 0.8 to nearly 0.7 in winter, reflecting pure fat burning [303,304]. In states of negative energy balance such as during hibernation or starvation, triglycerides (TG) stored in the WAT are converted to glycerol and FFA, which are used for gluconeogenesis³³, ketogenesis³⁴ and β -oxidation³⁵ in the liver. Consistently, genes related to these 3 biological processes are upregulated in the liver of hibernating bears [305–307]. This is also consistent with the maintenance of blood glucose levels via gluconeogenesis, and the increase in circulating TG, FFA and ketone bodies during hibernation. Of note, a decrease in circulating glycerol is observed in winter, probably due to greater uptake by the liver and its reaction with ammonia to form amino acids (see section 4.4.4) [298,303,308–312]. Altogether, these data highlight the amazing metabolic flexibility³⁶ of hibernating bears [313,314].

³² the ratio of the volume of carbon dioxide evolved to that of oxygen consumed by an organism or tissue in a given time

³³ glucose production from non-carbohydrate carbon substrates

³⁴ production of ketone bodies by fatty acid breakdown

³⁵ fatty acid catabolism

³⁶ capacity to switch among energy substrates to generate ATP depending on the physiological circumstances

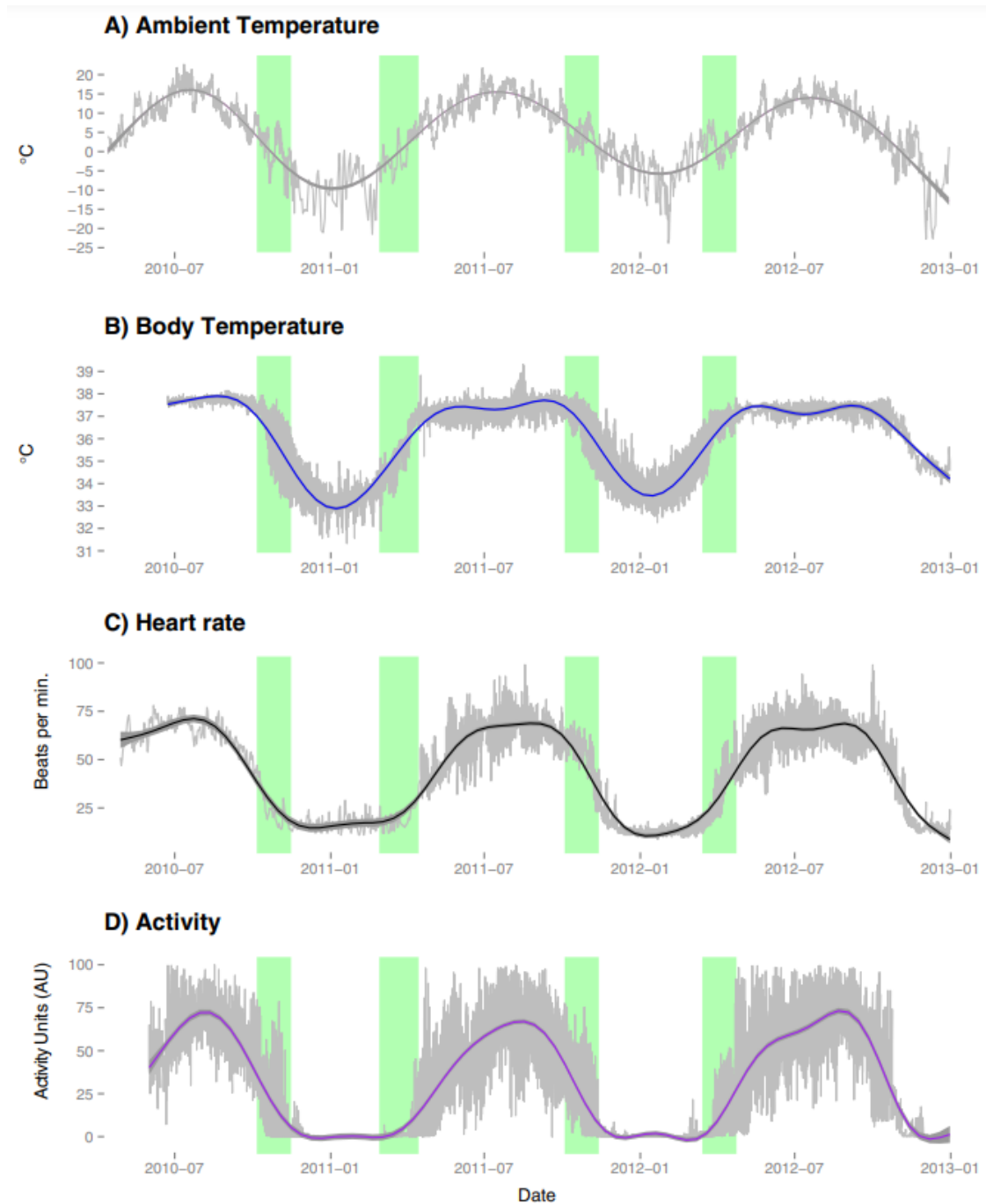


Figure 21. Main physiological characteristics of hibernating bears.

Average of the daily mean values for ambient temperature (A), bear body temperature (B), heart rate (C) and activity level in accelerometry units (D) for 14 individual free-ranging brown bears in central Sweden collected over 3 years. The X-axis indicates the time of year. Green vertical bars indicate the den entry and exit periods (from Evans et al., 2016 [279]).

Model for human pathologies. Hibernating bears appear to be insulin resistant compared to active bears. Insulin resistance is normally observed in hyperinsulinemic diabetic humans [312]. However and surprisingly, hibernating bears do not develop type 2 diabetes. Plasma cholesterol and TG levels are

twice as high in hibernating bears as in healthy humans, but they show no signs of developing atherosclerosis or cardiovascular damage [315]. In brief, bears readily emerge from their dens in spring and show no signs of organ damage [316] (Figure 22). Under similar conditions, humans would develop cardiovascular disease, obesity, muscle loss, osteoporosis and other deleterious health consequences. Dozens of examples could be discussed regarding the extraordinary characteristics of bears during hibernation and the therapeutic possibilities it offers to treat human pathologies (Figure 22). The conservation of muscle mass during a long period of fasting and physical inactivity has attracted our attention and will be discussed in the next section.

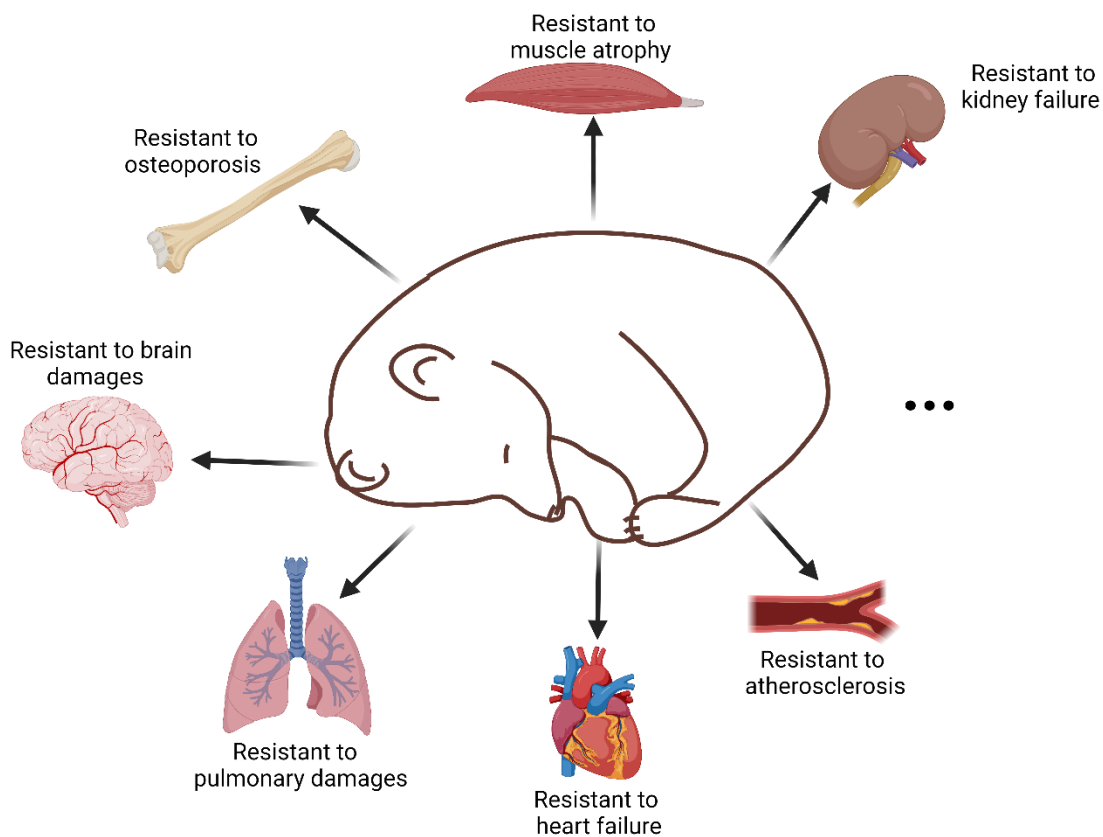


Figure 22. Overview of the spectacular characteristics of bears resistance to physiological damage during hibernation.

4.4.4 Skeletal muscle features in hibernating bears

Over the six months of total physical inactivity and fasting, hibernating bears experience only a moderate loss of muscle protein content. Conversely, over a shorter period of time, this leads to a significant reduction in muscle mass and function in humans [87,90].

4.4.4.1 Histological and functional features

Muscle protein content. The slight decrease in protein content in hibernating bears muscles may differ depending on the muscle considered: it (1) remains stable for the tibialis anterior muscle [317,318], (2) decreases by 4-10% in the gastrocnemius and biceps femoris muscles [302,319], or (3) it decreases by 15% in the vastus lateralis muscle [301]. Interestingly, in the latter study, they found that the 15% muscle loss after 1 month of denning remained the same 4 months later [301] (Figure 23). Furthermore, the nitrogen content of the vastus lateralis muscle remained unchanged in winter compared to summer, indicating a moderate loss of proteins [301]. The limited decrease in muscle protein content is consistent with the slight increase in 3-methylhistidine observed in the serum of hibernating bears [309]. Some researchers have speculated that the small amount of atrophy exhibited by bears may simply be due to muscle dehydration [317]. However, other studies have not observed any change in muscle water composition during winter [302].

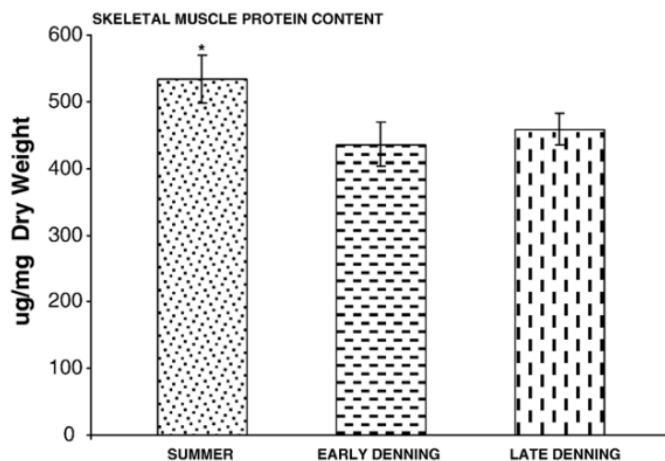


Figure 23. Protein content in bear muscles in summer, early denning and late denning (from Lohuis et al. – 2007 [301]).

Muscle CSA. Remarkably, the number of muscle fibres as well as their CSA remain unchanged in hibernating bears in most studies [302,319,320]. A recent paper showed a 26% decrease in CSA in the sartorius muscle after 5 months of hibernation, but the authors considered that was a minimal loss compared to what would happen in humans [321]. Indeed, under a similar period of disuse, a muscle loss of about 150% would be expected in humans [322,323].

Fibre type composition. It should be noted that the proportion of slow and fast muscle fibre types in active bears is roughly the same as in rodents or humans [320,324], and like humans, bears lack the type 2B fibre isoform [319,324]. Studies have reported conflicting changes in the proportion of fibre types between seasons with (1) an increase in type 1 fibre content and a decrease in type 2A fibre content [324,325], (2) a moderate shift towards more type 2 muscle fibres [302], or even (3) no change

[302,319,320]. These discrepancies can be explained by the biochemical techniques used and the timing of the muscle sampling during hibernation.

Muscle strength and neuromuscular activity. The loss of muscle strength is about 29% after 110 days of anorexia and physical inactivity during hibernation in bears. This is about half of what is observed in humans confined to bed for 90 days, with a 54% loss in muscle strength while on a balanced diet [318,326]. Furthermore, hibernating bears show no or very limited changes in muscle contractile properties (e.g. contraction time, half relaxation time) [302,318,319,326]. Although bears do not exhibit as vigorous shivering thermogenesis as small hibernators, they do make occasional postural adjustments, wake up briefly and shiver. It has been suggested that this mild muscle activity may limit atrophy [278,318,327]. Finally, neural inputs cannot be considered as a mechanism to limit muscle atrophy. Indeed, the denervation-induced decrease in muscle mass in active bears is comparable to that observed in other mammals, whereas hibernating bears are partly resistant to denervation-induced muscle atrophy [328].

4.4.4.2 Regulation of metabolism and signalling pathways

Muscle protein sparing. Lohuis et al., showed that muscle protein synthesis and degradation were lower in bears during hibernation than during the active period [301]. Furthermore, they observed that both phenomena remained unchanged between the beginning and the end of hibernation, indicating that protein balance is maintained throughout the hibernation period (Figure 24). Furthermore, protein synthesis was greater than protein degradation in summer bear muscles, suggesting that they accumulate muscle protein during the season when food is available in abundance [301] (Figure 24). A comprehensive transcriptomic analysis in skeletal muscle also showed that bear hibernation results in (1) increased expression of genes involved in protein biosynthesis (translation) and ribosome biogenesis and (2) decreased expression of genes related to proteolysis in skeletal muscle [304,307,329] (Figure 25). Of note, whole-body protein sparing is also supported by transcriptional downregulation of genes related to amino acid catabolism in the liver of hibernating bears [305–307] (Figure 25).

Unchanged or decreased levels of circulating urea³⁷ and decreased aminotransferase activities reflect low muscle protein mobilisation in bears during winter [289,299,309,330,331]. This is consistent with the coordinated downregulation of genes involved in urea production in skeletal muscle, but also in the liver during hibernation in bears [304,307]. Furthermore, urea recycling is very efficient in hibernating bears, with 99.7% of the urea produced being recycled into protein, which probably limits muscle protein degradation [304,307]. The mechanisms remain to be clarified but urea recycling would

³⁷ the main end product of protein catabolism

include a role for the gut microbiota in the hydrolysis of urea to ammonia, which would subsequently be used for the synthesis of amino acid, in particular glutamine [304,307] (Figure 25). Consistently, an increase in blood glutamine is observed in bears during hibernation [310].

Finally, hibernating bear muscles show an increase in a transcriptomic signalling mediated by MEF2A, contributing to a decrease of the expression of *TRIM63*/MuRF1 and *FBXO32*/Atrogin-1 [332] (Figure 25).

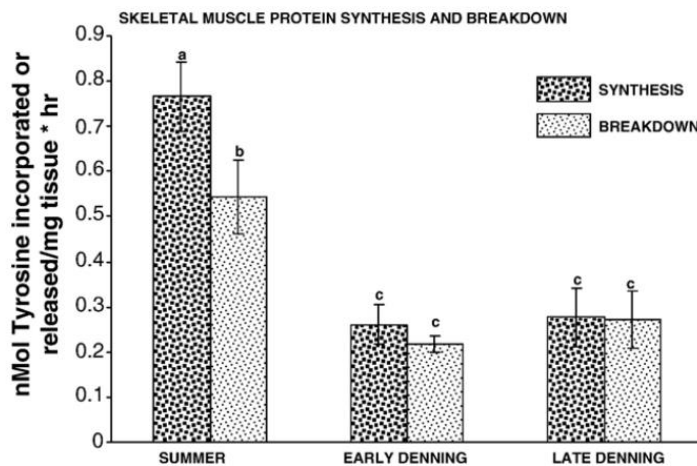


Figure 24. Protein turnover in bear muscles in summer, early denning and late denning (from Lohuis et al. – 2007 [301]).

Muscle energy metabolism. Glycolysis is preserved in the skeletal muscle of hibernating bears, as suggested by (1) an overall increase in protein abundance of all glycolytic enzymes, (2) an increase in muscle lactate dehydrogenase activity and (3) maintenance or reduction of circulating lactate levels [303,310,331] (Figure 25). Bear muscles still oxidise glucose and produce lactate during hibernation. This could help maintain skeletal muscle functionality in unexpected situations, such as an emergency exit from the den that would require a rapid increase in ATP production [308,310]. Glycolysis could be fuelled by hepatic gluconeogenesis and mobilisation of muscle glycogen content, which is higher in bear muscles in winter compared to summer [310,320] (Figure 25). Together, these studies have led some authors to suggest that the Cori cycle³⁸ may be active in bears during hibernation thus contributing to muscle protein sparing [298,310] (Figure 25).

PDK4³⁹ is a switch that enables the use of lipid substrates and thus limits the entry of glycolytic intermediates into the tricarboxylic acid (TCA) cycle. PDK4 protein is increased in hibernating bears muscles [298,310,333], whereas proteins involved in the TCA cycle and β -oxidation are predominantly all downregulated in hibernating bear muscles [310,333] (Figure 25). Although lipids are the preferred

³⁸ degradation of glucose into lactate in muscles, then transformation of lactate into glucose, and finally into glycogen in liver

³⁹ pyruvate dehydrogenase kinase isoenzyme 4

fuels in winter, bear muscles metabolism is mainly characterised by reduced ATP turnover, so that the reduced β -oxidation in muscles during hibernation is due to and/or contributes to the depression of metabolic rate [307,310].

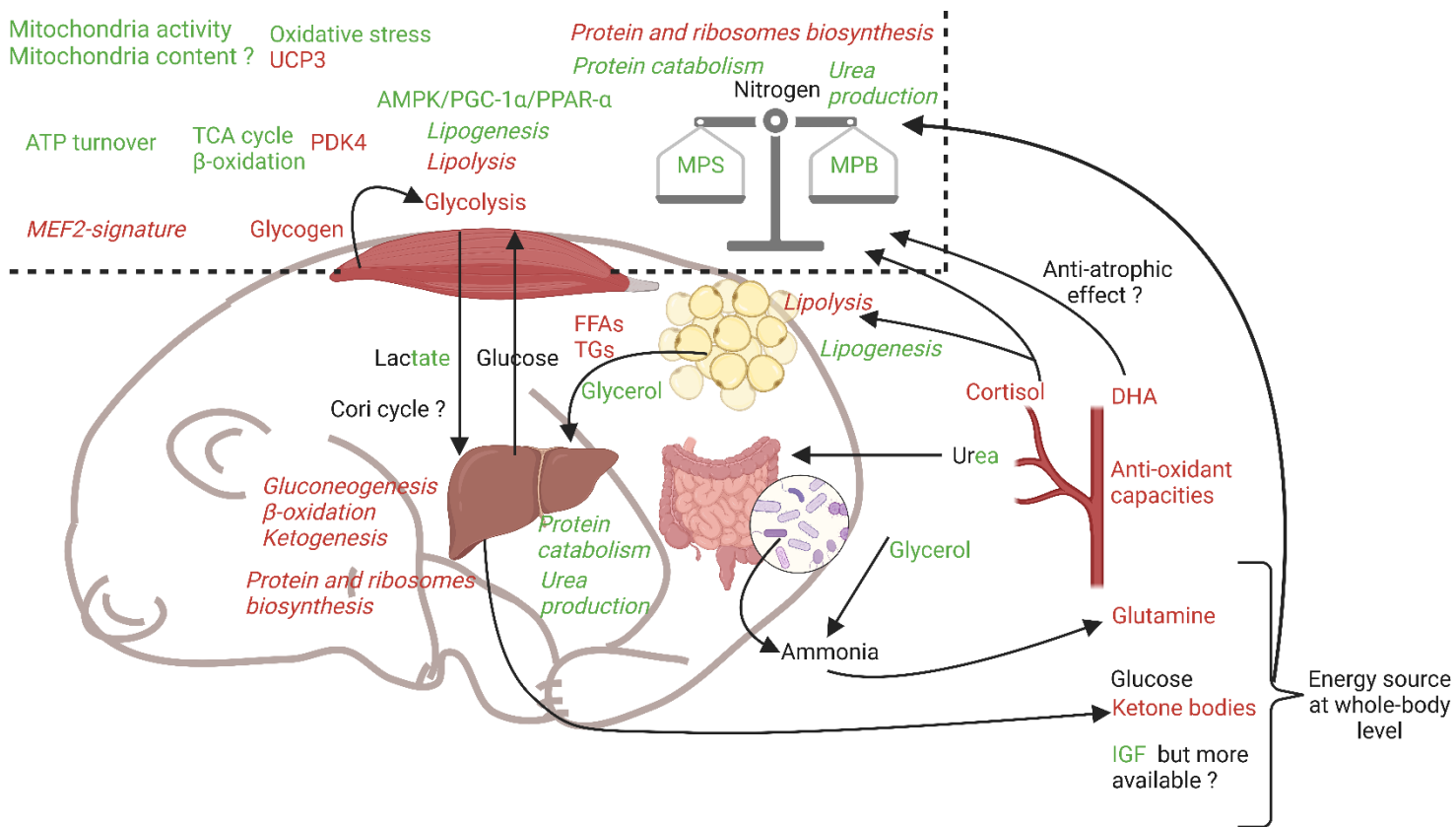


Figure 25. A complex and non-exhaustive overview of the mechanisms identified in bears to save muscle protein content during hibernation.

The words in green, red and black represent respectively the functions/metabolites that are down-regulated, up-regulated or unchanged in winter compared to summer. Two-coloured words (e.g. urea, lactate) represent discrepancies found in the literature. Words in bold represent metabolic processes (e.g. glycolysis). Words in italics represent biological processes regulated at the genetic level. Dashed lines delineate altered intracellular mechanisms and pathways in skeletal muscle in winter versus summer.

Hormonal/growth factor changes.

Cortisol is a glucocorticoid hormone that reduces glucose uptake in peripheral tissues and stimulates lipolysis in adipose tissue and skeletal muscle. Elevated cortisol levels are observed during hibernation and are associated with reduced (1) protein levels of phosphorylated and total AMPK and (2) expression of *PGC-1 α /PPAR- α* ⁴⁰ in skeletal muscle and adipose tissue [308] (Figure 25). Low plasma levels of IGF-1 and IGF-2 are also recorded in hibernating bears, but the authors suggest that they would be present in a different spatial conformation than in summer and therefore more available to tissues such as skeletal muscle [334] (Figure 25). Serum from

⁴⁰ peroxisome proliferator-activated receptor-gamma coactivator 1/ peroxisome proliferator-activator receptor

hibernating bears is also enriched in some specific n-3 polyunsaturated fatty acids, including docosahexaenoic acid (DHA) [310,335] (see Appendix 10.5). DHA has previously been associated with increased muscle glycogen stores and subsequent prevention of muscle atrophy in fasted mice [336]. Interestingly, a 3-fold increase in muscle glycogen content is recorded in hibernating bears muscles compared to active summer bear muscles, while muscle protein is preserved [310] (Figure 25).

Antioxidant defences. Most subunits of mitochondrial complexes are downregulated in hibernating bear muscles [310,337]. This may be due to reduced mitochondrial content in winter compared to summer in bear muscles. In addition, protein levels for UCP3⁴¹, which limits ROS production [338], are increased in bear muscles during hibernation [321,337]. Consistently, increased levels of proteins involved in cytosolic antioxidant systems, higher plasma antioxidant capacities and maintenance of the GSH/GSSG⁴² ratio are recorded in bear muscles during hibernation [337,339] (Figure 25). Overall, this suggests that bear muscles do not undergo significant oxidative damage in winter and/or that antioxidant defence systems remain effective [337].

Overall, metabolic adaptations in skeletal muscle (and other tissues such as liver and adipose tissue) promote (1) lipid catabolism during hibernation, (2) maintenance of glycolysis, and (3) regulation of intracellular pathways that contribute to the preservation of muscle proteins during this period of fasting and physical activity.

4.4.5 Circulating antiproteolytic compounds in hibernating bear serum

The preservation of vital functions of most organs in bears during hibernation, including skeletal muscle, has led researchers to speculate that active circulating factors may be responsible for these characteristics.

Rats muscles incubated *ex vivo* in the presence of hibernating bear serum exhibited a 40% decrease in net proteolytic rate compared to the muscles incubated with active bear serum. This inhibition of proteolysis was accompanied by a decrease in gene expression of the lysosomal (e.g. cathepsin B) and ubiquitin-dependent (e.g. ubiquitin) proteolytic systems. These results showed for the first time that a compound present in bear serum during hibernation had an anti-proteolytic property on skeletal muscle [340]. Subsequently, our team showed that cultivating primary human myotubes with hibernating bear serum favoured an increase in myotubes area compared to summer bear serum [341] (Figure 26). This was the first proof of concept that an active compound in bear serum was transmissible

⁴¹ uncoupling protein 3

⁴² glutathione/oxidized glutathione ratio

to human biological material. We showed that protein turnover in human myotubes was overall reduced when incubated with winter bear serum, with both a dramatic inhibition of proteolysis (i.e. UPS and ALS) and an average reduction in the rate of protein synthesis [341]. Therefore, winter bear serum was able to reproduce in human muscle cells the regulation of protein turnover already described in hibernating bears muscles (i.e. lower rate of protein synthesis and degradation). Recently, another team confirmed our results with an increase in total protein content in myotubes cultured with hibernating bear serum, although they did not observe any alteration in protein anabolism [342]. Overall, these few studies showed similar results, with hibernating circulating compounds being able to induce potent cross-species effects on human or rat muscle cells. It is therefore highly likely that the maintenance of muscle mass during hibernation in bears involves one or more circulating factors. The identification of these factors will undoubtedly open up a new field of study that will lead to new solutions for preventing and/or reversing muscle atrophy in humans.

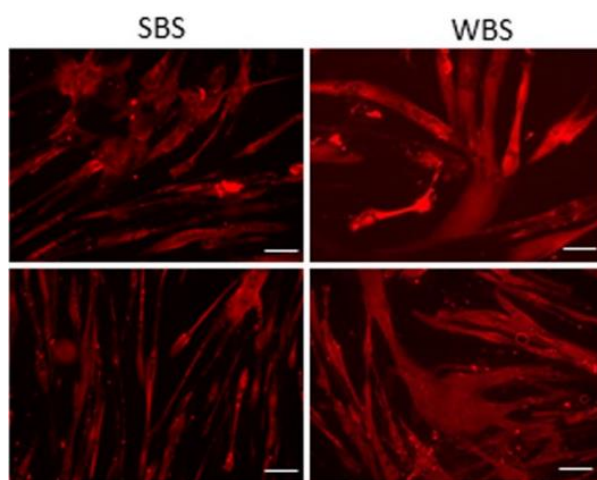


Figure 26. Winter bear serum promotes hypertrophy in human muscle cells.

Illustrative immunodetection and corresponding quantification of myosin heavy chain in cultured myotubes winter bear serum (WBS) or summer bear serum (SBS) treatment (from Chanon et al., 2018 [341]).

4.4.6 The ISR and TGF- β superfamily signalling regulation in hibernating mammal muscles

Very few papers have explored the regulation of ISR or TGF- β /BMP signalling in the skeletal muscle of hibernating mammals and only one in hibernating bears.

TGF/BMP signalling. Studies have shown that (1) myostatin protein expression does not change during early or late torpor in muscles of thirteen-lined ground squirrels (*Spermophilus tridecemlineatus*), but (2) myostatin and phosphorylated SMAD2 protein levels increase as squirrels emerge from torpor [343]. In the latter study, they also observed an increase in phosphorylated SMAD1/5 levels at the beginning of hibernation, which returned to normal levels when the squirrels emerged from torpor [343]. In the muscles of hibernating little brown bats (*Myotis lucifugus*), a decrease in myostatin

protein expression while an increase in the TGF- β inhibitor SMAD7 protein is observed compared to the active animal [344]. Similarly, a decrease in *Mstn* expression is also recorded in the muscles of hibernating ground squirrels (*Spermophilus lateralis*) [345]. To date, only one study has explored the regulation of *Mstn* expression in hibernating bear muscles and shown that it was lower in muscles at den exit compared to summer [321].

ATF4 signalling. In hibernating ground squirrels, ATF4 protein expression is strongly increased in skeletal muscle, and subcellular localisation studies have shown that ATF4 translocates into the nucleus during hibernation, as does its cofactor, the phosphorylated form of CREB-1 [346]. Furthermore, in the torpid muscles of the Daurian ground squirrels (*Spermophilus dauricus*), the levels of phosphorylated PERK and eIF2 α , as well as ATF4 protein are increased during hibernation, and normalised during IBA and the active period [347].

Overall, these few data suggest that upregulation of ATF4 and downregulation of TGF- β signalling may play a role in the coordination of muscle maintenance in small hibernating mammals. However, the ability of hibernating bears to preserve skeletal muscle biochemical and performance characteristics during prolonged hibernation still needs to be explored with respect to these two signalling pathways.

TAKE HOME MESSAGE

(1) Biomimicry is an approach that seeks sustainable solutions to human challenges by mimicking nature's patterns and strategies and has enabled significant human biomedical advances and progress.

(2) Hibernation, particularly in bears, is of great interest for understanding the mechanisms that allow them to cope with prolonged fasting and physical inactivity without deleterious effects on the whole body. The hibernating bear, being resistant to muscle atrophy, is an interesting model for identifying new biomolecular actors that can possibly be translated to human pathophysiology where muscle atrophy is present.

(3) The regulation of TGF- β /BMP and ISR signalling pathway is important for muscle homeostasis in rodents and humans, and interesting clues have been found during hibernation in the muscles of small hibernators. However no studies have yet explored these signalling in the muscles of hibernating bears.

5. Objectives and strategies

KEY POINTS FROM THE LITERATURE:

(1) Muscle atrophy affects millions of people worldwide and despite intensive efforts using laboratory rodents models, there is still no easily used therapeutic or preventive treatments.

(2) TGF- β signalling pathway have been extensively targeted for its pro-atrophic role. However, little is known about the BMP counterpart, which is promising for fighting muscle atrophy.

(3) ISR signalling has a dual and complex role in skeletal muscle homeostasis and needs to be further investigated.

(4) Hibernating bears resist muscle atrophy even when faced with long-term fasting and physical inactivity. Therefore, the hibernating bear is a promising model to find new avenues to fight muscle atrophy in humans.

The main objective of this thesis was to identify new molecular players and their mechanisms that could become therapeutic targets to combat muscle atrophy in humans. For this purpose, , we adopted a biomimetic approach using the brown bear, which is naturally resistant to muscle atrophy, and compared muscle adaptations to those observed in a classical model of sensitivity to atrophy. The project has been subdivided into three studies, as follows.

Study 1 Concurrent BMP Signaling Maintenance and TGF- β Signaling Inhibition Is a Hallmark of Natural Resistance to Muscle Atrophy in the Hibernating Bear (published paper)

The **objectives** were to (1) identify the underlying mechanisms implicated in the resistance of muscle atrophy although prolonged physical inactivity and (2) determine whether these mechanisms were oppositively regulated in a model of susceptibility to atrophy.

We performed a comparative transcriptomic analysis of the atrophy-resistant muscles of the hibernating brown bear and the atrophy-sensitive muscles of the hindlimb-suspended mouse.

Study 2 Induction of ATF4 atrogenes is uncoupled from disuse-induced muscle atrophy in halofuginone-treated mice and in hibernating brown bears (paper under review).

The **objectif** was to further explore the role of ATF4 signalling in skeletal muscle during basal and catabolic conditions.

We first developed an experimental protocol for inducing the ATF4 signalling with the pharmacological molecule halofuginone (HF) in mice. We then (1) investigated the effect of ATF4 induction on mice muscles during basal and hindlimb suspension-induced atrophy conditions and (2) deciphered the HF molecular mechanisms in mice muscles. We also investigated the regulation of this pathway in the atrophy-resistant muscles of the hibernating brown bear.

Study 3 Winter bear serum induces similar characteristics in human muscle cells as those found naturally in hibernating bear muscles (preliminary results).

Our **objective** was to determine whether the molecular characteristics of the atrophy-resistant muscles of hibernating bears can be reproduced in human muscle cells.

We first analysed microarray data from human muscle cells cultivated with winter bear serum to assess whether there is a TGF- β /BMP signalling transcriptomic signature. We then measured TGF- β /BMP signalling transcriptional activity with luciferase reporter assay.

6. Study 1: Concurrent BMP Signaling Maintenance and TGF- β Signaling Inhibition Is a Hallmark of Natural Resistance to Muscle Atrophy in the Hibernating Bear

6.1 Objective and strategy

We sought to compare at the genetic level, the changes occurring in muscles between a natural model of muscle atrophy resistance, the hibernating brown bear, and a model of susceptibility to muscle atrophy, the unloaded mouse. We thus performed muscle RNA sequencing and analysed common and different features in these two models to uncover unexplored intracellular mechanisms (Figure 27).

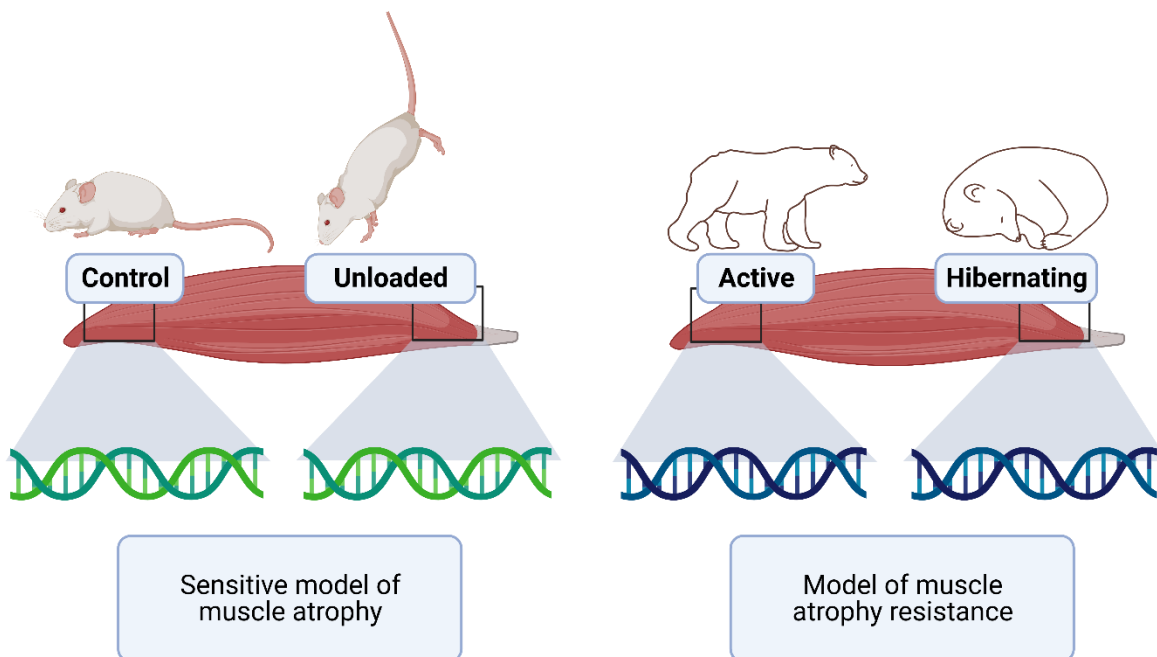


Figure 27. Schema of the experimental strategy of study 1.

6.2 Experimental protocol

Muscle atrophy-sensitive model. We studied disuse atrophy in the hindlimb-suspended (HS) mice model [348]. HS is a method developed in the 1970s, used to mimic space flight and prolonged bed rest in humans. The mouse tail is attached to a device that elevates the hindlimb into an unloaded position (Figure 28). Unlike cast immobilisation-induced muscle atrophy in rodents, the HS procedure does not cause inflammation or fibrosis in muscles [349,350], making it an interesting model to study the role of disuse in the induction of muscle atrophy independently of any other parameters.



Figure 28. Hindlimb suspension model in laboratory mice.

In the cages, there are two rails with wheels connected to the tails of the mice allow them to move. This system leaves the hind legs free to move without being able to grip. The mice can move with their front legs. Their food is underneath the grid.

Muscle atrophy-resistance model. The brown bear, remains resistant to muscle atrophy during hibernation, although confronted with two strong atrophy inducers (i.e. starvation and physical inactivity) (see section 4.4.4). Our laboratory belongs to an international consortium, the Scandinavian Brown Bear Research Project (<http://bearproject.info/>). Our team travels twice a year to Northern Sweden to collect biological samples (e.g. muscle, blood) from bears during the hibernation period (February) and the active period (June). A team of experienced veterinarians care for the bears under anaesthesia and monitor vital signs in the field (Figure 29). Bears are either male or female, from 2 to 3 years old, just before sexual maturity. The same bears are sampled twice a year using GPS collars. One of the disadvantages of using a wild animal is the difficulty of collecting biological samples due to the lack of proximity to their living area. Therefore, some periods during the hibernation or the active seasons remain unexplored in our analysis. Moreover, commercialized biological reagents (e.g. antibodies) do not necessarily react with the cellular components of the bear, and hence, the study of some signalling pathways, for example, is challenging.












Figure 29. Pictures from the collection of free-ranging bears samples in the forest of Northern Sweden as part of the Brown Bear Research Project.

6.3 Paper

Article

Concurrent BMP Signaling Maintenance and TGF- β Signaling Inhibition Is a Hallmark of Natural Resistance to Muscle Atrophy in the Hibernating Bear

Laura Cussonneau ^{1,*} , Christian Boyer ¹, Charlotte Brun ², Christiane Deval ¹, Emmanuelle Loizon ³, Emmanuelle Meugnier ³, Elise Gueret ^{4,5} , Emeric Dubois ^{4,5} , Daniel Taillandier ¹, Cécile Polge ¹ , Daniel Béchet ¹ , Guillemette Gauquelin-Koch ⁶, Alina L. Evans ⁷, Jon M. Arnemo ^{7,8}, Jon E. Swenson ⁹, Stéphane Blanc ², Chantal Simon ³ , Etienne Lefai ¹ , Fabrice Bertile ²  and Lydie Combaret ^{1,*} 

- ¹ INRAE, Unité de Nutrition Humaine, Université Clermont Auvergne, UMR 1019, F-63000 Clermont-Ferrand, France; christian.boyer@inrae.fr (C.B.); christiane.deval@inrae.fr (C.D.); daniel.taillandier@inrae.fr (D.T.); cecile.polge@inrae.fr (C.P.); daniel.bechet@inrae.fr (D.B.); etienne.lefai@inrae.fr (E.L.)
- ² Université de Strasbourg, CNRS, IPHC UMR 7178, F-67000 Strasbourg, France; charlotte.brun@etu.unistra.fr (C.B.); stephane.blanc@iphc.cnrs.fr (S.B.); fberville@unistra.fr (F.B.)
- ³ CarMen Laboratory, INSERM 1060, INRAE 1397, University of Lyon, F-69600 Oullins, France; emmanuelle.loizon@inserm.fr (E.L.); emmanuelle.meugnier@univ-lyon1.fr (E.M.); chantal.simon@univ-lyon1.fr (C.S.)
- ⁴ Institut de Génétique Fonctionnelle (IGF), University Montpellier, CNRS, INSERM, 34094 Montpellier, France; elise.gueret@mgx.cnrs.fr (E.G.); emeric.dubois@mgx.cnrs.fr (E.D.)
- ⁵ Montpellier GenomiX, France Génomique, 34095 Montpellier, France
- ⁶ Centre National d'Etudes Spatiales, CNES, 75001 Paris, France; guillemette.gauquelin Koch@cnes.fr
- ⁷ Department of Forestry and Wildlife Management, Inland Norway University of Applied Sciences, Campus Evenstad, NO-2480 Koppang, Norway; alina.evans@inn.no (A.L.E.); jon.arnemo@inn.no (J.M.A.)
- ⁸ Department of Wildlife, Fish, and Environmental Studies, Swedish University of Agricultural Sciences, SE-901 83 Umeå, Sweden
- ⁹ Faculty of Environmental Sciences and Natural Resource Management, Norwegian University of Life Sciences, NO-1432 Ås, Norway; jon.swenson@nmbu.no
- * Correspondence: Laura.cussonneau@inrae.fr (L.C.); Lydie.combaret@inrae.fr (L.C.); Tel.: +(33)4-7362-4824 (Lydie Combaret)



Citation: Cussonneau, L.; Boyer, C.; Brun, C.; Deval, C.; Loizon, E.; Meugnier, E.; Gueret, E.; Dubois, E.; Taillandier, D.; Polge, C.; et al. Concurrent BMP Signaling Maintenance and TGF- β Signaling Inhibition Is a Hallmark of Natural Resistance to Muscle Atrophy in the Hibernating Bear. *Cells* **2021**, *10*, 1873. <https://doi.org/10.3390/cells10081873>

Academic Editors: Maria Pennuto and Marco Pirazzini

Received: 16 June 2021
Accepted: 20 July 2021
Published: 23 July 2021

Publisher's Note: MDPI stays neutral with regard to jurisdictional claims in published maps and institutional affiliations.



Copyright: © 2021 by the authors. Licensee MDPI, Basel, Switzerland. This article is an open access article distributed under the terms and conditions of the Creative Commons Attribution (CC BY) license (<https://creativecommons.org/licenses/by/4.0/>).

Abstract: Muscle atrophy arises from a multiplicity of physio-pathological situations and has very detrimental consequences for the whole body. Although knowledge of muscle atrophy mechanisms keeps growing, there is still no proven treatment to date. This study aimed at identifying new drivers for muscle atrophy resistance. We selected an innovative approach that compares muscle transcriptome between an original model of natural resistance to muscle atrophy, the hibernating brown bear, and a classical model of induced atrophy, the unloaded mouse. Using RNA sequencing, we identified 4415 differentially expressed genes, including 1746 up- and 2369 down-regulated genes, in bear muscles between the active versus hibernating period. We focused on the Transforming Growth Factor (TGF)- β and the Bone Morphogenetic Protein (BMP) pathways, respectively, involved in muscle mass loss and maintenance. TGF- β - and BMP-related genes were overall down- and up-regulated in the non-atrophied muscles of the hibernating bear, respectively, and the opposite occurred for the atrophied muscles of the unloaded mouse. This was further substantiated at the protein level. Our data suggest TGF- β /BMP balance is crucial for muscle mass maintenance during long-term physical inactivity in the hibernating bear. Thus, concurrent activation of the BMP pathway may potentiate TGF- β inhibiting therapies already targeted to prevent muscle atrophy.

Keywords: brown bear hibernation; mouse unloading; muscle atrophy; physical inactivity; RNA sequencing; TGF- β /BMP signaling

1. Introduction

Muscle atrophy is defined as a loss of muscle mass and strength and is associated with adverse health outcomes, such as an autonomy decline and an increase in morbidity and mortality in many catabolic conditions (e.g., cancer cachexia, heart, and kidney failure, fasting, sepsis, injury, aging, or physical inactivity, etc.) [1–5]. Given the increase in sedentary behavior and improvement in life expectancy, and with to date still no proven therapeutic or preventive treatment to date, muscle atrophy remains a major public health issue (World Health Organization data) [6]. Skeletal muscle tissue represents an important reservoir of amino acids, which are mobilized during catabolic situations to preserve vital functions, resulting in an imbalance of contractile protein turnover (i.e., proteolysis exceeding protein synthesis) [7,8]. Catabolic stimuli (e.g., oxidative stress, endoplasmic reticulum disturbances, nutrient shortage, mitochondrial disruptions, etc.) activate a complex network of intracellular modulators, which in turn lead to the activation of the ubiquitin-proteasome system (UPS) and autophagy [9,10]. These two main proteolytic systems in muscle tissue involve a set of genes, i.e., atrogenes, whose expression at the mRNA levels is commonly altered during atrophy [11]. Cascades of events and players of muscle atrophy are well described and conserved in mammals [12,13] and include the transforming growth factor- β (TGF- β) superfamily, with TGF- β signaling acting as a negative regulator, and Bone Morphogenetic Proteins (BMP) signaling as a positive regulator of muscle mass [14]. The TGF- β pathway mediates muscle atrophy through cytoplasmic and nuclear signaling molecules SMAD2/3, mainly leading to the expression of the atrogenes TRIM63 (MuRF1) and FBXO32 (atrogin-1) [15]. Constitutive expression of SMAD3 triggers muscle wasting, and inhibition of SMAD2 and SMAD3 is sufficient to induce muscle growth in vivo [16–19]. Conversely, the BMP pathway mediates muscle mass maintenance through cytoplasmic and nuclear signaling molecules SMAD1/5/9, promoting a negative transcriptional regulation for a ubiquitin ligase required for muscle wasting, FBXO30 (MUSA1) [20], and increasing the expression of BMP receptors activity in muscles induced hypertrophy through Smad1/5-mediated activation of mTOR signaling [21].

Hibernating bears (Ursidae family) are naturally resistant to muscle atrophy when facing the two major atrophic inducers, prolonged fasting and physical inactivity up to 5–7 months [22,23]. Conversely and during a shorter period, a loss of muscle mass and volume prevails in rodent models [24–29] and humans [4,5]. As in rodent models, the muscles of the active bear are sensitive to disuse after denervation, whereas the muscles of the hibernating brown bear (*Ursus arctos*) are resistant [30]. The hibernating brown bear, therefore, appears as a suitable model to study the underlying mechanisms of muscle mass maintenance [31]. How it withstands muscle loss in conditions where muscle atrophy is expected in non-hibernating mammals remains to be fully elucidated. However, several hypotheses can be raised; our recent analysis of muscle proteome in the hibernating brown bear revealed the maintenance of glycolysis and a turning down of ATP turnover [32]. In addition, we reported (i) a myogenic microRNA signature prone to promoting muscle regeneration and suppressing ubiquitin ligase expression in bear muscle during winter [33], as well as (ii) limited levels of oxidative stress [34]. To unravel the molecular basis of muscle maintenance at the mRNA level, the bear muscle transcriptome has already been explored using cDNA microarrays [35] or RNA sequencing [36,37]. These two transcriptomic studies suggested an overall reduction in energy and protein metabolism, consistent with metabolic suppression and lower energy demand in skeletal muscle during hibernation. Although these studies focused on the changes in bear muscle transcriptome during the hibernating versus active period, our study aimed to compare them with those that occur in the muscle transcriptome of disuse-induced atrophy in a mouse model. The rationale for such a comparative analysis of two contrasted situations of muscle atrophy or maintenance lies in the identification of potential new candidates, beyond already reported metabolic factors [35–37], that may help the hibernating bear resist atrophy, thereby providing new targets for fighting muscle atrophy in humans. Among the transcription factors involved in the regulation of the differentially expressed genes highlighted in bear muscle between

the hibernation and active periods, eight were involved in the regulation of the TGF- β superfamily. We therefore subsequently focused on an in-depth analysis of the TGF- β and BMP intracellular pathways.

2. Materials and Methods

2.1. Animal Experiments

2.1.1. Bear Sample Collection

Biopsies from the vastus lateralis muscle were collected from 17 free-ranging brown bears, 2–3 years old (*Ursus arctos*; 11 females and 6 males), from Dalarna and Gävleborg counties, Sweden, from 2014 to 2019 (Table S6). The samples were immediately frozen on dry ice until storage at -80°C . In a given year, the same bears were captured during winter hibernation (February) and recaptured during their active period (June). The study was approved by the Swedish Ethical Committee on Animal Experiment (applications Dnr C3/2016 and Dnr C18/2015), the Swedish Environmental Protection Agency (NV-0741-18), and the Swedish Board of Agriculture (Dnr 5.2.18–3060/17). All procedures complied with Swedish laws and regulations. Capture, anesthesia, and sampling were carried out according to an established biomedical protocol [38].

2.1.2. Mouse Model of Hindlimb Unloading

Our objective was to compare the muscle transcriptome of the hibernating bear with that in a rodent model of long-term physical inactivity. We chose the 10-day mouse model of unloading as an established disuse-atrophy model, with atrophic pathways still activated [28,39]. All experiments were conducted with the approval of the regional ethics committee (agreement n $^{\circ}$ D6334515) following the European Directive 2010/63/EU on the protection of vertebrate animals used for experimental and scientific purposes. This study was performed with 12 C57BL6/J adult male mice purchased from Janvier Labs (Le Genest-Saint-Isle, France). They were housed by pairs upon arrival in a polycarbonate cage in a controlled room ($22 \pm 2^{\circ}\text{C}$, $60\% \pm 5\%$ humidity, 12 h light/dark cycle, light period starting at 8 h), fed ad libitum, and given free access to water.

After 10 days of acclimatization, the mice were either kept unsuspending (Control, $n = 6$) or subjected to hindlimb unloading through tail suspension (Unloaded, $n = 6$) for 10 days. Custom tail suspension cages were adapted from previous studies [40,41]. The cages ($43 \times 29 \times 24$ cm) have an overhead frame to which two suspension systems are fixed in parallel on the width of the cage. These suspension systems are widely spaced in a cage so that mice can always be housed in pairs without touching each other. Unloaded mice had a metal ring attached near the base of their tails using surgical adhesive tape. This ring was then attached to a swivel that allowed a 360-degree rotation and was attached on a rail that covered the upper width of the cage. The height of the swivel has been adjusted to keep the mouse at an angle of about 30° from the head so that the hindlimbs could not touch the ground or the walls. During the 10 days of unloading, mice showed only a very small body weight loss ($<7\%$) that occurred within the first 3 days, with no change in food intake. At the end of the experiment, soleus muscles were rapidly dissected out and immediately frozen in liquid nitrogen and stored at -80°C until analyses. As for the data used from the RNA sequencing of Zhang et al. [42], the soleus muscle atrophied by 37% (from 7.24 ± 0.27 mg in control mice to 4.58 ± 0.31 mg in unloaded mice, $p < 0.001$ according to the unpaired Student's t -test).

2.2. RNA Sequencing of Brown Bear Muscle

2.2.1. RNA Isolation

Total RNA from bear muscles was isolated as described [43]. Briefly, muscle RNA from six bears (paired samples collected in summer and winter in a given year for the same individual) was extracted using TRIzol reagent (Invitrogen, Courtaboeuf, France).

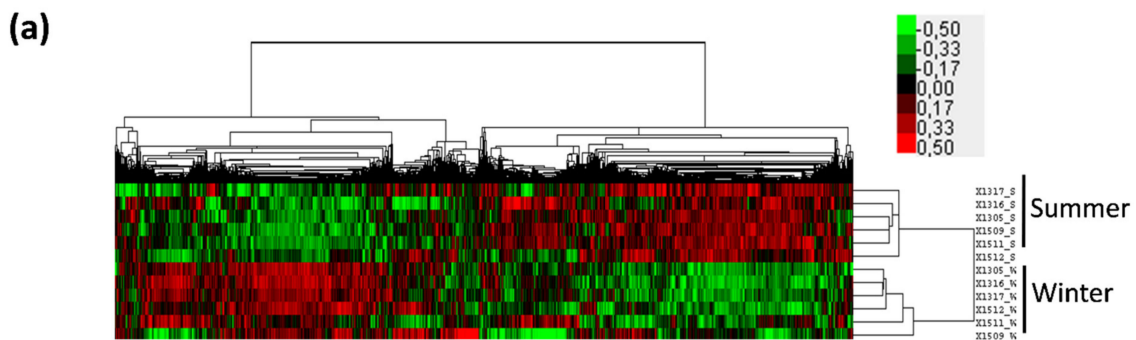
2.2.2. Illumina RNA Sequencing, Data Assembly, Statistical Analysis

We constructed RNA-Seq libraries with the Truseq stranded mRNA sample preparation kit from Illumina and sequenced them in two lanes on an Illumina HiSeq2500 (single-end, 50 bp, six libraries per lane). Image analyses and base calling were performed using the HiSeq Control Software (v2.2.70, Illumina, San Diego, CA, USA) and Real-Time Analysis component (v1.18.66.4, Illumina, San Diego, CA, USA). Demultiplexing was performed using Illumina's conversion software (bcl2fastq 2.20). The quality of the raw data were assessed using FastQC from the Babraham Institute and the Illumina software SAV (Sequencing Analysis Viewer, Illumina, San Diego, CA, USA). A splice junction mapper, TopHat 2.1.1 [44] (using Bowtie 2.3.5.1 [45], Johns Hopkins University, MD, USA), was used to align the RNA-Seq reads to the *Ursus arctos* genome (GCA_003584765.1 ASM358476v1 assembly downloaded from NCBI) with a set of gene model annotations (GCF_003584765.1_ASM358476v1_genomic.gff downloaded on 17 June 2019, from NCBI). Final read alignments having more than three mismatches were discarded. Samtools (v1.9) (<http://samtools.sourceforge.net>) was used to sort the alignment files. Then, the gene quantification was performed with Featurecounts 1.6.2 (<http://subread.sourceforge.net/>) [46]. As the data were from a strand-specific assay, the read had to be mapped to the opposite strand of the gene (-s 2 option). Before statistical analysis, genes with less than 30 reads (cumulating over all the analyzed samples) were filtered out. Differentially expressed genes were identified using the Bioconductor (<https://bioconductor.org/>) [47] package DESeq2 1.26.0 [48] (R version 3.6.1 <https://www.r-project.org/>). Data were normalized using the DESeq2 (<https://bioconductor.org/packages/release/bioc/html/DESeq2.html>, accessed on 16 June 2021) normalization method. Genes with an adjusted *p*-value below 5% (according to the Benjamini–Hochberg procedure that controls the FDR) were declared differentially expressed.

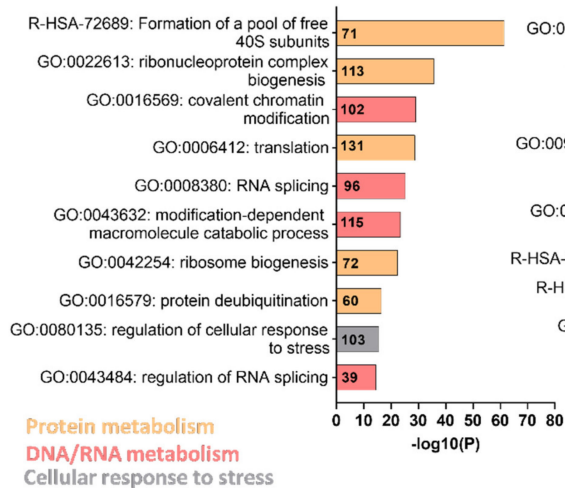
2.2.3. Functional and Pathway Enrichment Analysis

Hierarchical clustering of bear transcriptomic data (log-transformed) was performed using Cluster v3.0 software (University of Tokyo, Tokyo, Japan) from the 13531 reads [49]. Parameters were set as follows: median centering and normalization of genes for adjusting data and centroid linkage clustering for both genes and arrays. Dendrograms were generated and viewed using the Java Treeview v1.3.3 program (Alok Saldanha, Stanford University, Stanford, CA, USA) [50]. To identify the differentially expressed genes (DEGs), we selected a fold change (FC) Winter/Summer $> |1.3|$ or $< |0.77|$ and an adjusted *p*-value $< |0.01|$ as cut-off standards, for the up- and down-regulated genes, respectively. Visualization of functional enrichment was performed using Metascape [51], a web-based portal for visualizing the inference of enriched biological pathways among the DEGs. For the given DEGs gene list, pathway and process enrichment analysis has been carried out with the following ontology sources: KEGG Pathway, GO Biological Processes, Reactome Gene Sets, Canonical Pathways, CORUM, TRRUST, DisGeNET, PaGenBase, Transcription Factor Targets, WikiPathways, PANTHER Pathway, and COVID. All genes in the genome have been used as the enrichment background. Terms with a *p*-value < 0.01 , a minimum count of 3, and an enrichment factor > 1.5 (the enrichment factor is the ratio between the observed counts and the counts expected by chance) are collected and grouped into clusters based on their membership similarities. More specifically, *p*-values are calculated based on the accumulative hypergeometric distribution, and *q*-values are calculated using the Benjamini–Hochberg procedure to account for multiple testings. Kappa scores are used as the similarity metric when performing hierarchical clustering on the enriched terms, and sub-trees with a similarity of > 0.3 are considered a cluster. The most statistically significant term within a cluster is chosen to represent the cluster. The 10 top-score enrichment terms from that analysis are shown in Figure 1b,c, and the 10 top-score enrichment transcription factors regulating the DEGs are shown in Figure 1d. The heat map representing the expression changes of the TGF- β /BMP gene sets in bear versus mouse muscles was made using the Pheatmap package (R 1.4.1106, University of Tartu, Tartu, Estonia). Briefly,

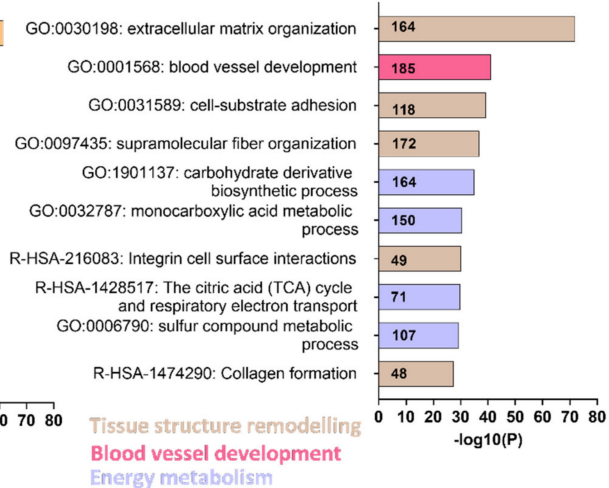
the gene hierarchical clustering is based on Euclidean distance calculated from the log2FC value (Winter/Summer and Unloaded/Control for bear and mouse muscles, respectively).



(b) 10 top-score enriched terms from the 1746 upregulated DEGs



(c) 10 top-score enriched terms from the 2369 downregulated DEGs



(d)

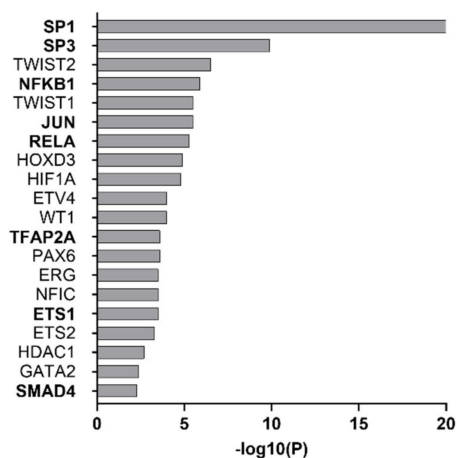


Figure 1. Deep changes in brown bear muscle transcriptome during hibernation. **(a)** Heatmap from brown bear muscle (vastus lateralis) transcripts ($n = 6$ bears/season, the same individuals were sampled and analyzed in summer and winter); red indicates high and green indicates low expression level of the 13531 genes. **(b)** Graph representing the 10 top-score of significantly enriched

terms in winter compared to summer, from the 1746 up-regulated differentially expressed genes (DEGs) ($FC\ W/S > |1.3|$ and $padj < |0.01|$) or (c) from the 2369 down-regulated DEGs ($FC\ W/S < |0.77|$ and $padj < |0.01|$; Table S1). The color code for the functional cluster is indicated in the respective graphs, and the bold numbers in the different bars represent the numbers of DEGs found in the enriched terms. (d) Graph representing the 10 top-score of transcription factors involved in DEGs regulation from “Formation of a pool of free 40S subunits” and “Extracellular matrix organization” enriched terms. The bold TFs are involved in TGF- β superfamily regulation.

2.3. Transcriptomic Data Assembly and Statistical Analysis of Mouse Muscle

We used transcriptomic data from an already published study [42]. Briefly, in this study, C57BL6/J adult male mice were either kept unsuspended (Control, $n = 4$) or subjected to hindlimb unloading through tail suspension (Unloaded, $n = 4$) for 10 days. The fastq files of eight soleus muscles were downloaded from GEO (GSE102284). A splice junction mapper, TopHat 2.1.1 (Johns Hopkins University, MD, USA) [44], was used to align the RNA-Seq reads to the mouse genome (UCSC mm10) with a set of gene model annotations (genes.gtf downloaded from UCSC on 29 October 2019; GeneIDs come from the NCBI gene2refseq file). Final read alignments having more than three mismatches were discarded. Samtools (v1.9, <http://www.htslib.org/>) was used to sort the alignment files. Then, the gene quantification was performed with Featurecounts 2.0.0 (<http://subread.sourceforge.net/>) [46]. As the data were from a strand-specific assay, the read had to be mapped to the opposite strand of the gene ($-s\ 2$ option). Before statistical analysis, genes with less than 20 reads (cumulating all the analyzed samples) were filtered out. Differentially expressed genes were identified using the Bioconductor [47] package DESeq2 1.26.0 [48] as previously described (cf. 2.2.2).

2.4. Western Blot

Vastus lateralis muscles from eleven bears (paired samples collected in summer and winter in a given year for the same individual; Table S6) and soleus muscles from 10-days control or unloaded mice ($n = 6$ /group) (~ 30 mg) were used. Samples were homogenized using a polytron in 1 mL of an ice-cold buffer (10 mM Tris pH 7.5, 150 mM NaCl, 1 mM EDTA, 1 mM EGTA, 1% Triton X-100, 0.5% Igepal CA630) containing inhibitors of proteases (Protease Inhibitor Cocktail) and phosphatases (1 mM Na_3VO_3 , 10 mM NaF) (Sigma, Saint-Quentin-Fallavier, France). The homogenates were stirred for 1 h at 4 °C and then centrifuged at 10,000 g for 15 min at 4 °C. The resulting supernatants were then stored at -80 °C until use. The concentration of proteins was determined using the Bradford Protein Assay Kit (Biorad, Marnes-la-Coquette, France). Proteins were then diluted in Laemmli buffer and stored at -80 °C until use. Protein extracts were subjected to SDS-PAGE (sodium dodecyl sulfate-polyacrylamide gel electrophoresis) using TGX™ FastCast™ 10% Acrylamide gels (Biorad, Marnes-la-Coquette, France) and transferred onto a PVDF membrane (Hybond P, Amersham, England). Blots were blocked for 1 h at room temperature with 5% bovine serum albumin in TBS buffer with 0.1% Tween-20 (TBS-T, pH = 7.8), then washed thrice in TBS-T and incubated (overnight, stirring, 4 °C) with appropriated primary antibodies against SMAD1/5 (PA5-80036, Thermo Fisher, Illkirch, France), SMAD2/3 (#8685, Cell Signaling Technology, Saint-Cyr-L'Ecole, France), SMAD4 (ab230815), CTGF (ab227180), and GDF5 (ab137698) (Abcam, Cambridge, United Kingdom). Blots were then washed and incubated for 1 h with an appropriate secondary horseradish peroxidase-conjugated antibody at room temperature. Signals were detected after incubation with Luminata Crescendo Western HRP substrate (Millipore, Burlington, MA, USA) and visualized using G: BOX ChemiXT4 (XL1) imaging system (Syngene, Frederick, MD, USA). Signals were then quantified using the GeneTools software (Syngene, Cambridge, UK) and normalized against the total amount of proteins determined by TGX signals to correct for uneven loading. Protein data were presented as individual values. The bilateral ratio paired Student's t -test was used to compare the muscles of bears during summer and winter (S and W, respectively). For muscles of control and unloaded mice (C and U, respectively), statistical significance was determined using the bilateral unpaired Student's

t-test. Statistical analysis was performed using Prism 8 (GraphPad Prism 9, San Diego, CA, USA).

3. Results

3.1. Deep Changes in Brown Bear Muscle Transcriptome during Hibernation

The brown bear transcriptome data set revealed that, from 13531 transcripts commonly identified in all individuals, gene expression differed markedly between summer and winter (Figure 1a). We identified 4115 differentially expressed genes (DEGs) between muscles of the active and hibernating bear with mainly down-regulated genes (Table S1). The 10 top-score obtained from an annotation enrichment analysis performed from the down- and up-regulated DEGs highlighted several significant enriched terms regulated differentially in bear muscles between the two seasons (Figure 1b,c). For instance, the protein metabolism functional cluster was the most up-regulated in bear muscles in winter compared to summer, with “Formation of a pool of free 40S subunits”, “Ribonucleoprotein complex biogenesis”, or “Translation” enriched terms (Figure 1b). In addition, the tissue structure remodeling functional cluster was the most down-regulated in muscles of the hibernating versus active bear, with “Extracellular matrix organization”, “Cell-substrate adhesion”, or “Supramolecular fiber organization” enriched terms (Figure 1c). We then run a transcriptional regulatory network analysis to identify transcription factors (TFs) involved in the DEGs regulation from the two most differentially enriched terms between the two seasons (e.g., “Formation of a pool of free 40S subunits” and “Extracellular matrix organization”) (Figure 1d). We found that SP1 was the TF the most involved in the DEGs regulation, as well as others TFs such as SP3, NFKB1, JUN, RELA, TFAP2A, ETS1, or SMAD4. Interestingly, these TFs cited above are all involved in the regulation or signal transduction of the TGF- β superfamily [52–54]. We therefore decided to focus on that superfamily, including (i) TGF- β signaling, which is a master regulator of the extracellular matrix organization and also involved in muscle mass loss, and (ii) BMP signaling, which has recently been discovered to be involved in muscle mass maintenance [20].

3.2. Hibernation Induces a Transcriptional Shift from the TGF- β to the BMP Pathway

From a thorough analysis of the literature [55–57], we have drawn up a list of the actors and regulators of the TGF- β superfamily. We then analyzed precisely how they were regulated at the mRNA level in the muscles of the hibernating bear between the winter and summer seasons.

The expression levels of two main TGF- β ligands, INHBA and MSTN, were dramatically lower (Fold change (FC) = 0.28 and 0.52, respectively) in winter, whereas INHBB expression was higher (FC = 1.85) (Figure 2, Tables S2 and S3). In BMP signaling, the main ligand described in muscle mass maintenance, GDF5, showed higher levels (FC = 2.5) in hibernating bear muscles compared to active muscles. Extracellular actors inhibiting (KCP, DCN, MGP, NOV, or CHRDL) or promoting (CCN2 or BMPER) TGF- β and/or BMP signals were mainly down-regulated in winter compared to summer. Receptors from the TGF- β signaling were differentially expressed during hibernation, with ACVR1C and TGBBR2 levels being considerably lower (FC = 0.28 and 0.80, respectively) in winter compared to summer, whereas TGFBR1 and ACVR1B were higher (FC = 1.42 and 1.47, respectively). The GDF5 receptor, BMPR1B, was higher in winter compared to summer (FC = 1.37). The co-receptors that control intensity and specificity of the downstream TGF- β /BMP signaling were mainly down-regulated or unchanged in winter for both pathways, except for MUSK, an important BMP co-receptor in muscle cells, which was up-regulated (FC = 2.39). Overall, actors involved in the initiation of the TGF- β signal were mainly repressed while those driving the BMP signal were increased.

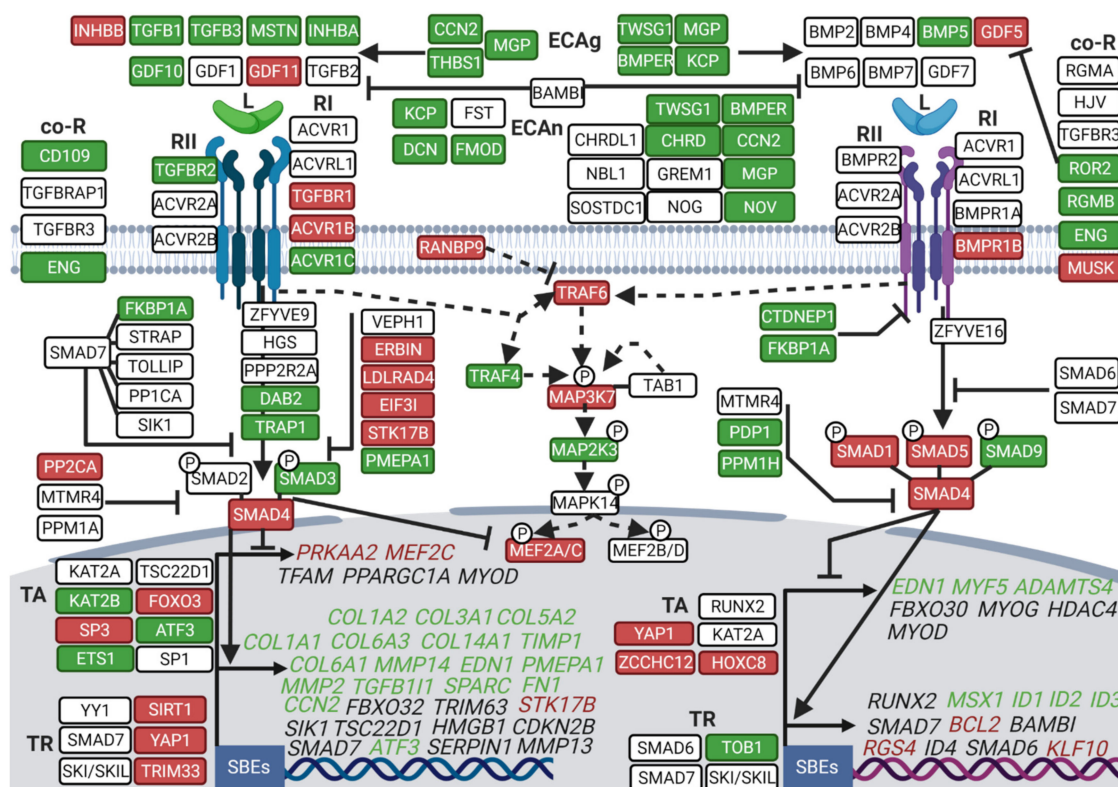


Figure 2. Deep transcriptomic reprogramming of TGF-β and BMP pathways in muscle during brown bear hibernation. Scheme showing brown bear vastus lateralis muscle transcripts involved in TGF-β and BMP signaling and depicting (i) their relationships [55–57] and (ii) the difference in their expression levels between hibernation and activity periods. Red and green boxes indicate, respectively up- and down-regulated genes during hibernation compared to the summer season, and white boxes indicate unchanged genes. Target genes of the TGF and BMP pathways are indicated in italic and are in green when down-regulated, in red when up-regulated, and in black when unchanged. Dashed lines show the SMAD-independent pathway and full lines the canonical signaling pathway. Arrows indicate activation, and ⊥ bars indicate inhibition. (*n* = 6 bears/season, the same individuals were sampled and analyzed in summer and winter, padj < |0.05|; Tables S2 and S3). ECAg: Extracellular Agonist, ECAAn: Extracellular Antagonist, L: Ligand, Co-R: Co-Receptor, RII: Receptor type II, RI: Receptor type I, TA: Transcriptional Activator, TR: Transcriptional Repressor, SBEs: SMAD Binding Element. Created with [BioRender.com](https://www.biorender.com).

For TGF-β signaling, intracellular inhibitors such as ERBIN, LDLRAD4, EIF3I, STK17B, and PP2CA were up-regulated in winter bear muscles (FC = 1.26, 1.50, 1.37, 1.86, and 1.56, respectively), whereas some of the actors promoting the signal were lower expressed, i.e., DAB2 and TRAP1 (FC = 0.50 and 0.63, respectively). By contrast, for BMP signaling, intracellular inhibitors were mainly lower expressed in muscles of the hibernating bear, such as CTDNEP1, FKBP1A (FC = 0.70 and 0.67, respectively). Regarding the intracellular actors triggering TGF-β/BMP signaling, SMAD3 (TGF-β signaling; FC = 0.76) was less expressed, SMAD1 and SMAD5 (BMP signaling; FC = 1.99 and 1.30, respectively), and SMAD4 (common to TGF-β and BMP signaling; FC = 1.34) were more expressed in muscles of the hibernating bear compared to the active one. Thus, expression changes of the intracellular actors again suggest repression of TGF-β signaling but maintenance of the BMP signaling.

For nuclear components, transcriptional activators were either up- (FOXO3 and SP3, FC = 1.68 and 1.70) or down-regulated (e.g., KAT2B, ATF3 and ETS1, FC = 0.55, 0.46, and 0.54) for TGF-β, whereas mainly up-regulated in winter for BMP with YAP1, ZCCHC12, and HOXC8 (FC = 1.63, 2.21, and 2.46, respectively). Conversely, the transcriptional repressors were mainly up-regulated for the TGF-β pathway, i.e., TRIM33, YAP1, and SIRT1 (FC = 1.60, 1.63, and 1.82, respectively), whereas unchanged or lower expressed, i.e.,

TOB1 (FC = 0.78) for BMP during hibernation. Considering TGF- β target genes, an overall down-regulation was observed in winter compared to summer, as highlighted for the different collagen isoforms or the multiple metalloproteinases COL1A1/2 (FC = 0.04 and 0.07), COL3A1 (FC = 0.06), COL5A2 (FC = 0.28), COL6A1/3 (FC = 0.22 and 0.20), COL14A1 (FC = 0.14), and MMP2/14 (FC = 0.33 and 0.46) (Figure 2 and Table S2). For BMP target genes, it was less contrasted, with either an unchanged (e.g., RUNX2 or ID4), down-regulated (e.g., ID1 or ID2, FC = 0.31 and 0.65), or up-regulated expression (RGS4 or KLF10, FC = 1.72 and 1.32) during hibernation, with RGS4 being a muscle-specific gene. Overall, this supports a general down-regulation of the transcriptional activity that drives TGF- β signaling, with possible maintenance of that for BMP signaling.

Finally, TGF- β and BMP signaling also use a shared SMAD-independent pathway, involving a branch of the MAPK (Mitogen-Activated Protein Kinase) pathway [58]. In this pathway, the expression of TRAF6 and its downstream actor MAP3K7 were higher in muscles of the hibernating bear compared to the active one (FC = 1.78 and 1.60, respectively). Some of the TRAF6 downstream actors, including MEF2A and MEF2C, which are key muscle transcription factors, were as well up-regulated (FC = 1.89 and 2.23) in winter compared to summer bear muscles (Figure 2).

TGF- β and BMP signaling pathways are tightly regulated by several UPS members, such as E3 ubiquitin ligases (E3s) and deubiquitinating enzymes (DUB) [55,59]. TGF- β inhibitors localized from the receptors to the nucleus level were up-regulated in winter, such as for CUL1 (FC = 1.85), NEDD4L (FC = 1.63), and TRIM33 (FC = 1.60), the latter being also a positive regulator of BMP signal transduction (Figure 3 and Table S4). SMURF1, an E3 ligase inhibiting both TGF- β and BMP signaling, was also up-regulated (FC = 1.64) in muscles of the hibernating bear. For UPS activators of the TGF- β signaling pathway alone, several DUBs were up-regulated in winter, e.g., UCHL5, USP11, and USP4 (FC = 1.78, 1.77, and 1.37, respectively), the latter also promoting BMP signaling, and others were down-regulated such as for USP15 and TRAF4 (FC = 0.52 and 0.47). The TGF- β and BMP pathways regulate the transcription of some muscle-specific E3s (TRIM63, FBXO32, and FBXO30). None of them were differentially expressed in winter compared to summer (Figure 3 and Table S4).

Overall, this wide transcriptomic analysis highlighted a winter transcriptional pattern in muscles of the brown bear that was prone to shutting down TGF- β signaling while maintaining or even over-activating the BMP pathway.

3.3. Divergent Regulation of TGF- β and BMP Pathways in Atrophy-Resistant Muscles of the Hibernating Brown Bear versus Atrophied Muscles of the Unloaded Mouse

We compared the above-described brown bear muscle transcriptome to published transcriptomic data from a model of long-term physical inactivity in mice induced by 10 days of unloading, where the soleus muscle mass decreased by ~30% [42]. Comparing the two models, the muscle transcriptomic profiles appeared very different for selected gene expression related to TGF- β and BMP signaling pathways (Figure S1 and Tables S2–S4). Of note, gene expressions of TGF- β and BMP ligands were mainly differently regulated, as particularly evidenced for GDF5, which was up-regulated during bear hibernation, but down-regulated during unloading in the mouse model (FC = 0.18), and as well with MSTN strongly down-regulated during bear hibernation but unchanged in unloaded mouse muscles (FC = 1.57) (Figure 4a and Tables S2 and S3). Regarding receptor expressions, the two models responded quite similarly (Figure 4b and Tables S2 and S3), with three notable exceptions. Firstly, the gene expression of ACRV1C did not change in muscles of the unloaded mouse, unlike muscles of the hibernating bear, where a strong down-regulation occurred (FC = 1.11 and 0.28, respectively), what we also observed with the gene expression of TGFBR2 (FC = 1.08 and 0.80, respectively). Secondly, the gene expression of BMPRI1B, GDF5 receptor, was up-regulated in muscles of the hibernating bear but was down-regulated in muscles of the unloaded mouse (FC = 0.66) (Figure 4b). The intracellular actors SMAD3, SMAD4, and SMAD1 were regulated similarly by bear hibernation or mouse unloading, although not to the same extent (FC = 0.73, 1.10, and 1.50, respectively).

However, SMAD2 was up-regulated (FC = 1.24), and SMAD5 and SMAD9 remained unchanged only in the muscles of the unloaded mouse (Figure 4c).

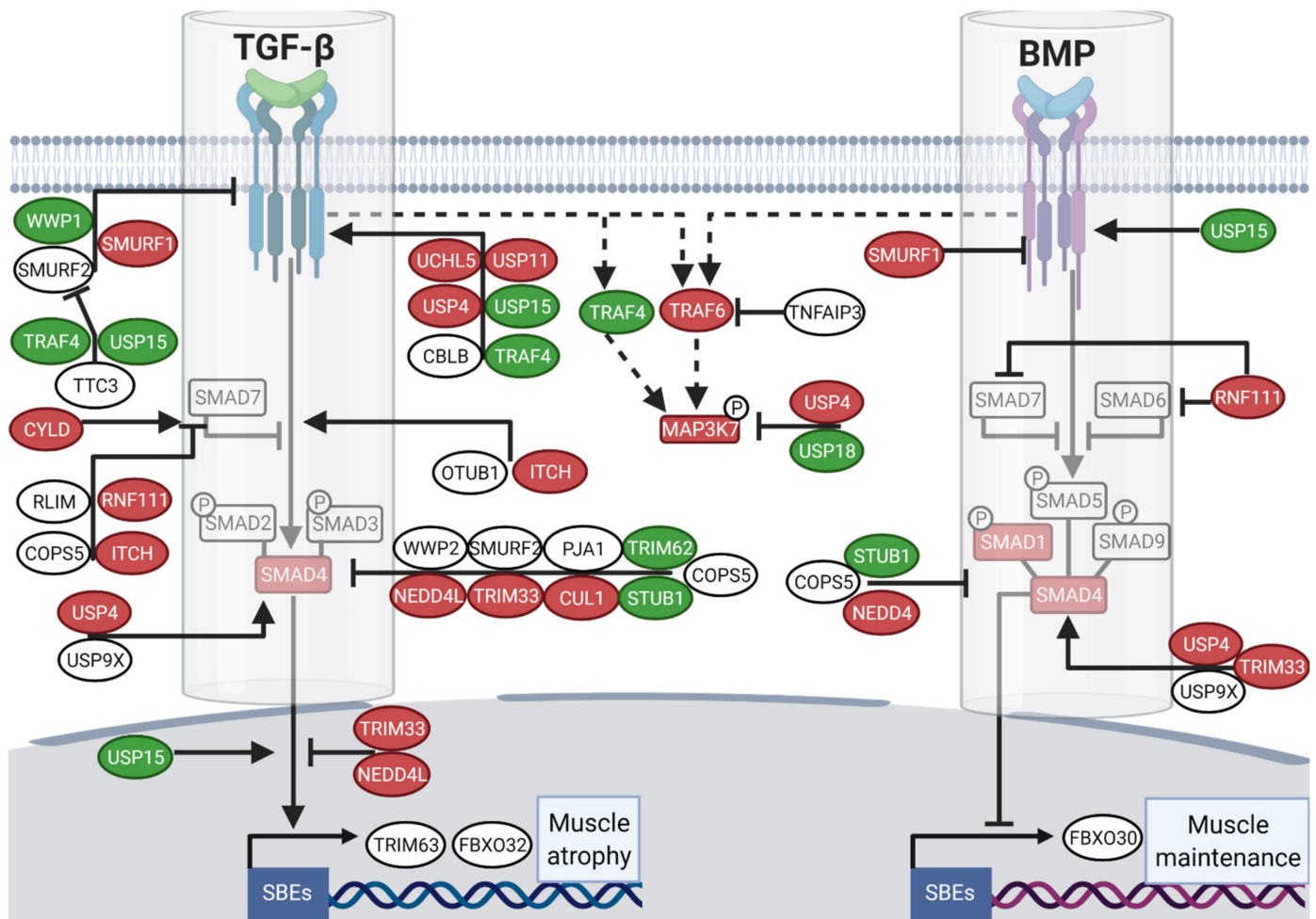


Figure 3. A transcriptomic reprogramming of UPS components involved in TGF- β and BMP regulation prevails in muscle during brown bear hibernation. Scheme showing the E3s/DUBs enzymes regulation of brown bear vastus lateralis muscle transcripts involved in TGF- β and BMP signaling pathways and depicting (i) their relationships [12,60] and (ii) the difference in their expression levels between hibernation and activity periods. Red and green boxes indicate, respectively up- down-regulated genes during hibernation compared to the summer season, and white boxes indicate unchanged genes. Dashed lines show the SMAD-independent pathway and full lines the canonical signaling. Arrows indicate activation and bars inhibition. ($n = 6$ bears/season, the same individuals were sampled and analyzed in summer and winter, $\text{padj} < |0.05|$; Table S4). SBEs: SMAD Binding Elements. Created with [BioRender.com](https://www.biorender.com).

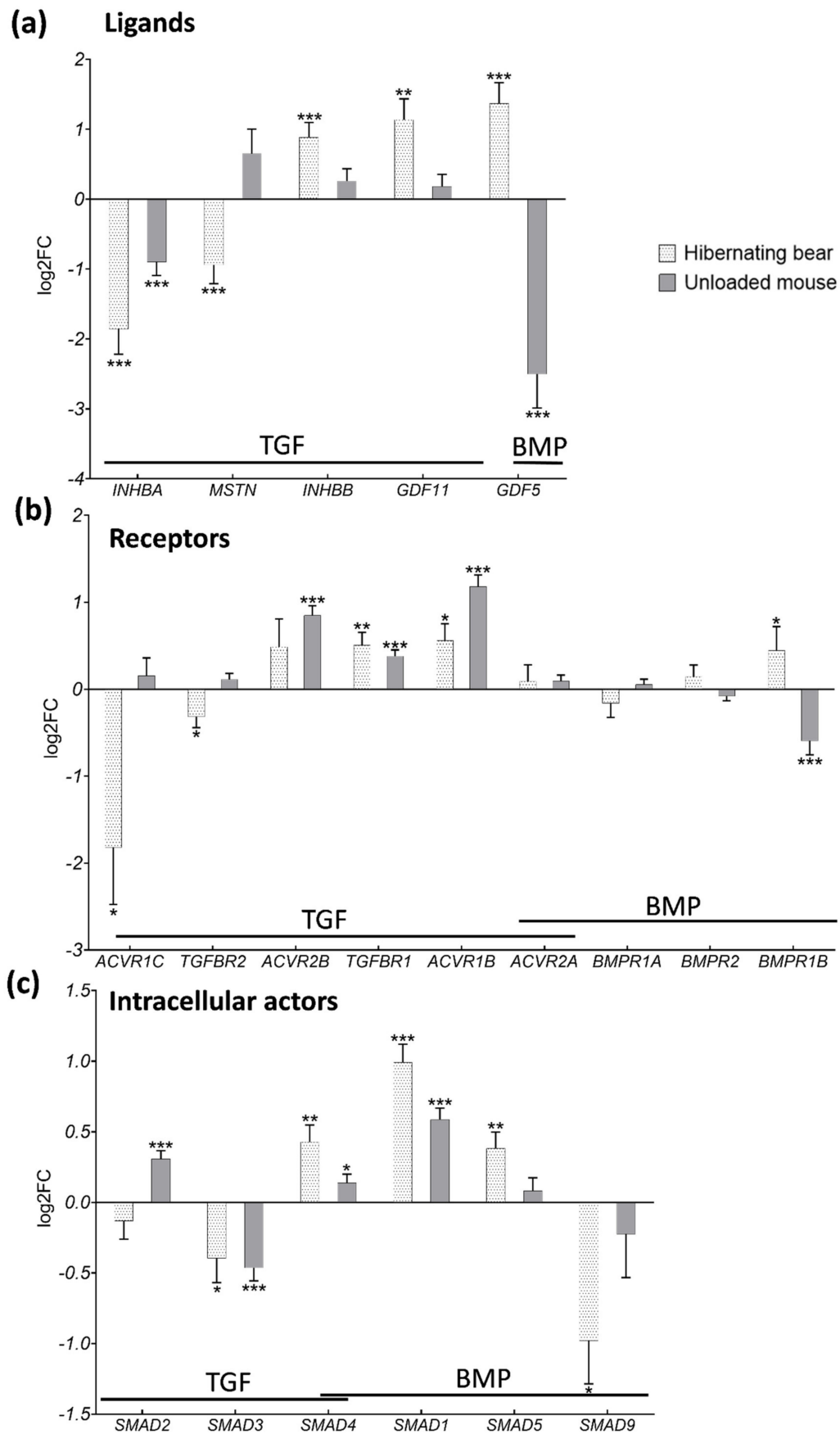


Figure 4. The gene expression pattern of TGF- β and BMP components is different in brown bear muscle resistant to atrophy during hibernation compared to atrophied muscles of the unloaded mouse. Genes expression level in vastus lateralis muscle of

active and hibernating brown bears ($n = 6$ bears/season, the same individuals were sampled and analyzed in summer and winter, \log_2FC Winter/Summer, dotted white bars) and in soleus muscle of control and unloaded mice ($n = 4$ mice per condition, \log_2FC Unloaded/Control, gray bars). The depicted genes were categorized as TGF- β and BMP (a) ligands, (b) receptors, and (c) intracellular actors. Data are expressed as $\log_2FC \pm 1fcSE$. Statistical significance is shown (* $padj < |0.05|$; ** $padj < |0.01|$; *** $padj < |0.001|$).

Regarding the E3s and DUB enzymes involved in the BMP pathway alone (Figure 5 upper panel), NEDD4 was similarly up-regulated in both models (FC = 1.63 and 1.28, respectively in bear and mouse), whereas FBXO30 (FC = 0.82) was down-regulated only in muscles of the unloaded mouse (Figure 5 and Table S4). The enzymes involved in the regulation of both TGF- β /BMP signaling were mainly up- or down-regulated in muscles of the hibernating bear but were mainly unaffected in unloaded mouse muscles (Figure 5 middle panel, Table S4). Finally, the E3s/DUB involved only in TGF- β signaling regulation were for half of them commonly unchanged or up-regulated, e.g., CUL1, UCHL5 or NEDD4L (FC = 1.17, 1.30 or 2.38, respectively), and for the other half oppositely regulated, e.g., SMURF2, CBLB, or TRIM62 (FC = 0.81, 1.50, and 1.97, respectively) in muscles of the unloaded mouse compared to muscles of the hibernating bear (Figure 5 lower panel and Table S4).

Overall, TGF- β and BMP signaling pathways were differentially regulated between atrophy-resistant muscles of the hibernating bear and atrophy-sensitive muscles of the unloaded mouse.

3.4. Hibernation Induces Changes in TGF- β and BMP Pathway Components at the Protein Level

To further compare these models of resistance and vulnerability to atrophy, we explored the protein levels of the SMAD intracellular actors. In the brown bear muscle, we observed a tendency to decrease for SMAD2 protein levels ($p = 0.09$) in winter compared to summer, whereas SMAD3 levels remained quite similar between the two seasons (Figure 6a,c,d). Protein levels of SMAD4 were higher in muscles of the hibernating bear compared to the active one (Figure 6a,e), but the converse was observed for SMAD1/5 (Figure 6a,f). As for mRNA, these SMAD proteins did not follow the same regulation pattern in muscles of the unloaded mouse, where none changed at the protein level (Figure 6b–f). The protein levels of CCN2, a TGF- β target gene that is also an extracellular activator of the TGF- β pathway and an inhibitor of the BMP pathway, were strongly lower in winter bear muscles but were unaffected in unloaded mouse muscles (Figure 6a,b,g). Finally, the protein levels for GDF5, a BMP ligand, remained unchanged in both muscles from the hibernating bear and the unloaded mouse (Figure 6a,b,h).

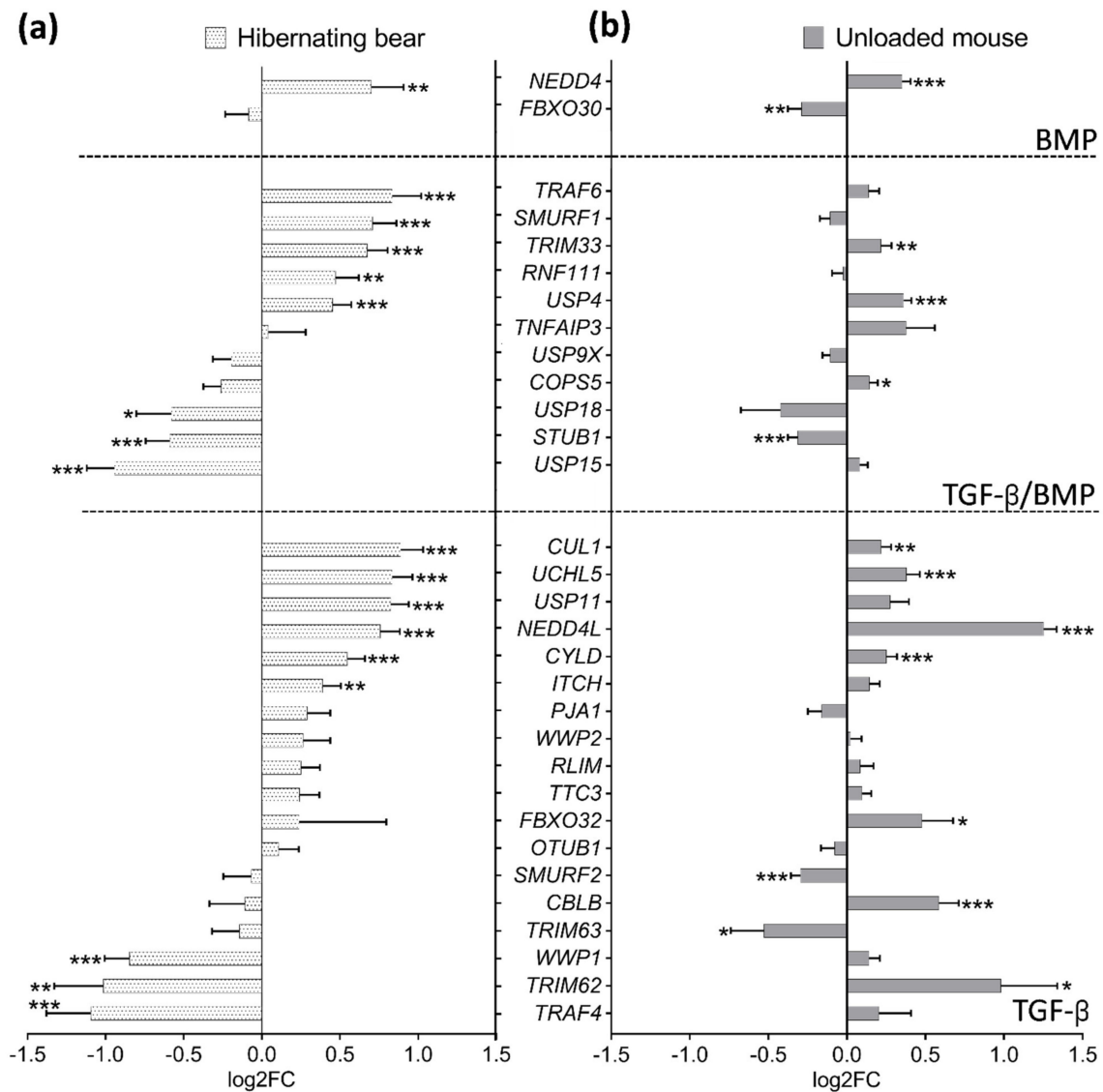


Figure 5. The gene expression pattern of muscle E3s/DUB enzymes involved in TGF-β and BMP pathway regulation differed in the atrophy-resistant brown bear muscle during hibernation compared to the atrophied muscle of the unloaded mouse. Genes expression level (a) in vastus lateralis muscle of active and hibernating brown bears (*n* = 6 bears/season, the same individuals were sampled and analyzed in summer and winter, log₂FC Winter/Summer, dotted white bars), and (b) in soleus muscle of control and unloaded mice (*n* = 4 mice per condition, log₂FC Unloaded/Control, gray bars). Data are expressed as log₂FC ± lfcSE. Statistical significance is shown (* padj < |0.05|; ** padj < |0.01|; *** padj < |0.001|).

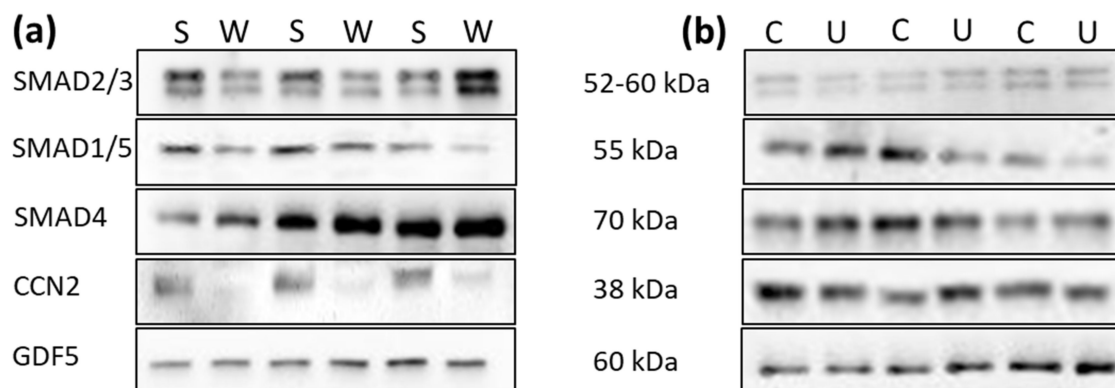


Figure 6. Cont.

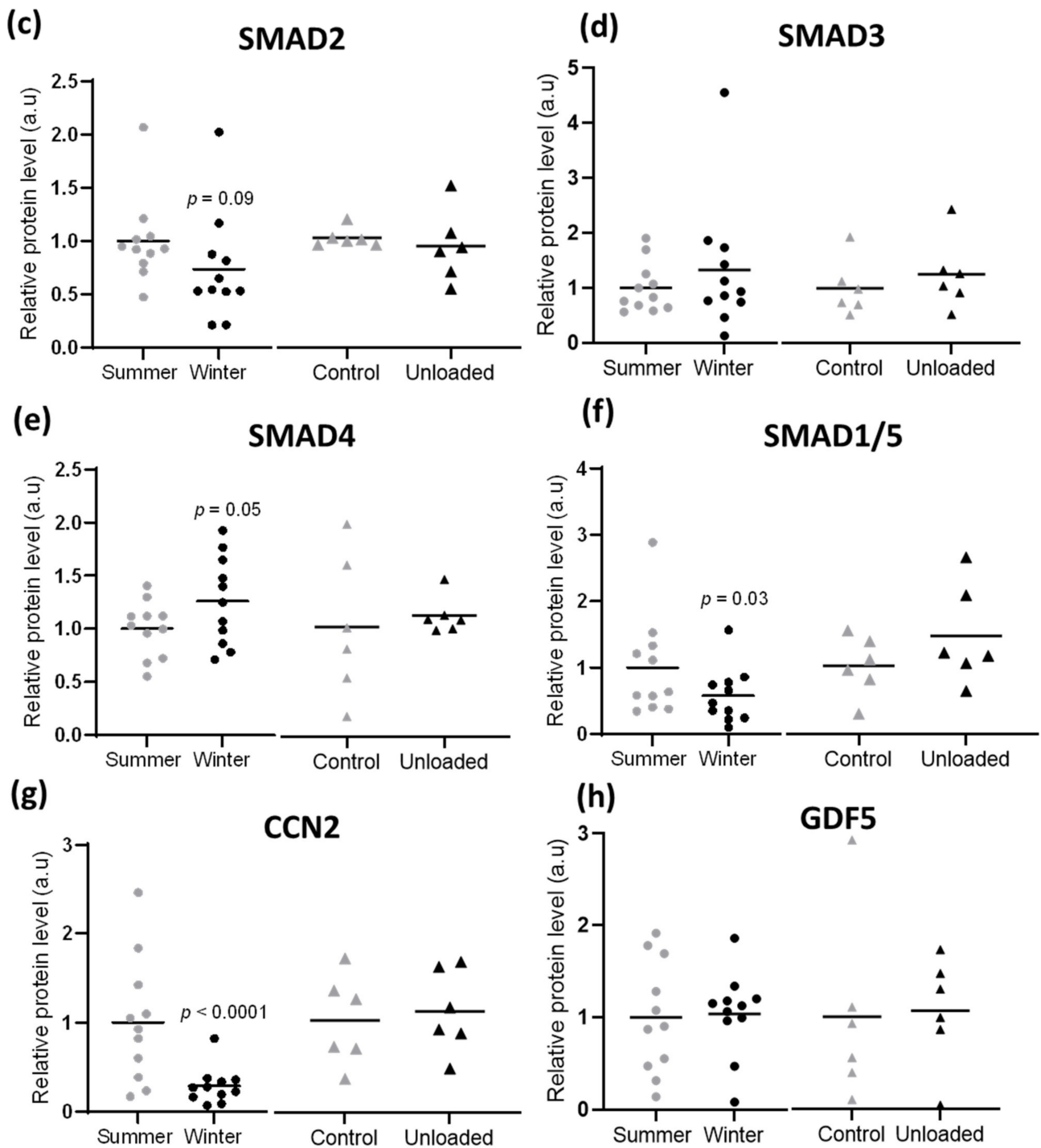


Figure 6. Hibernation induces changes in TGF- β and BMP components at protein level. Protein levels for total SMAD2/3, SMAD1/5, SMAD4, CCN2, and GDF5 were assessed by Western blots (a) in the vastus lateralis muscle of brown bears during summer (S) and winter (W) and (b) in the soleus muscle of control (C) and unloaded mice (U). Representative western blots are shown for three couples of bears and mice. (c–h). Data are presented as individuals' values with mean bars ($n = 11$ bears/season, the same individuals were sampled and analyzed in summer and winter, and $n = 6$ mice per condition). Gray and black dots are for muscles of bears, in summer and winter, respectively, and gray and black triangles are for control and unloaded muscle of mice, respectively.

4. Discussion

Although basic knowledge regarding the underlying mechanisms of muscle atrophy is continuously growing, essentially from rodent models and clinical studies in humans, there are still no efficient therapeutic strategies for its prevention and treatment. To explore new avenues, we compared a model of muscle atrophy resistance, the hibernating brown bear [23], and a mouse model of disuse-induced muscle atrophy [42]. Therefore, we analyzed the bear muscle transcriptome and identified sweeping changes in gene expression between the summer-active period and the winter-hibernating period, and we compared them with transcriptomic data from muscles of the unloaded mouse.

Whereas the loss of muscle mass during inactivity is often associated with a decrease in muscle protein synthesis [42,61–63], we reported here that genes implicated in protein metabolism were mainly up-regulated in muscles of the hibernating bear. This is consistent with previous studies that linked muscle atrophy resistance during hibernation to induction of protein translation [35,36,64]. Under activation of FOXOs transcription factors, atrogenes involved in both autophagy and UPS pathways are enhanced in rodents [65–67]. These atrogenes (e.g., *MAP1LC3A*, *FBXO32*, and *ZFAND5*) were indeed up-regulated or maintained in the unloaded mouse model but down-regulated or unchanged in muscles of the hibernating bear (Table S5). In agreement with previous studies, our data confirmed that proteolytic actors were up-regulated in disuse-induced muscle atrophy in rodents [11] but not in the bear model of muscle atrophy resistance [36]. Despite discrepancies between bear and mouse models (e.g., fed status, torpor vs. hindlimb muscle disuse), both display similar pathways controlling skeletal muscle mass and protein balance. For instance, the TGF- β signaling pathway has been reported to be evolutionarily conserved among several species, from *Caenorhabditis elegans* and *Drosophila melanogaster* to *Mus musculus* [68]. In addition, both models are responsive to denervation-induced atrophy when in active conditions [20,30]. We performed our analyses on the fast-twitch vastus lateralis muscle for the brown bear and the slow-twitch soleus muscle for the mouse. Thus, we cannot exclude the possibility that the differences recorded here between the models may partly have resulted from the specific nature of these muscles concerning their metabolic and contractile properties. However, it is noteworthy that, although fast-twitch muscles are not as sensitive to physical inactivity as slow-twitch muscles, both types of muscles atrophied in classical models of long-term physical inactivity in rodents [25,29,39,69,70] and humans [71–73]. Despite this difference in metabolic and contractile properties, a general down-regulation of genes involved in extracellular matrix (ECM) structure organization was observed in atrophied muscles from the unloaded mouse and atrophy-resistant muscles from the hibernating brown bear (Figure 1 and Table S2). This ECM structure remodeling is a common feature of other atrophic models reported during dystrophic diseases [74] or muscle disuse in rodents or humans [26,69,75–77].

TGF- β is currently of major interest within the field of skeletal muscle biology. Indeed, the gene disruption of two of its ligands Myostatin (*MSTN*) or Activin A (*INHBA*), and the inhibition of their shared receptor ActRIIB (*ACVR2B*) promote a profound muscle hypertrophy phenotype in various conditions and species [78–81]. On the contrary, overexpression of *MSTN* or *INHBA* leads to the recruitment and phosphorylation of SMAD2-3, triggering an atrophic transcriptional program [16,17,82–84]. Here, we reported that the expression levels of both ligands *MSTN* and *INHBA* were lower only in muscles of the hibernating bear. In addition, *ACVR2B* and *SMAD2* mRNA levels were up-regulated in muscles of the unloaded mouse whereas maintained in muscles of the hibernating bear. At the protein level, SMAD2 was maintained in the muscles of the unloaded mouse and showed a tendency to decrease in muscles of the hibernating bear. However, despite extensive efforts and numerous antibodies tested, we could not characterize the SMADs phosphorylation status in bear muscles, which thus remains to be defined.

One TGF- β target gene, *CCN2* (also known as CTGF), is an ECM protein associated with fibrotic activity that is up-regulated in several muscle chronic disorders (i.e., Duchenne muscular dystrophy or the amyotrophic lateral sclerosis) [85]. *CCN2* is one of the main

pro-fibrotic cytokines acting downstream of TGF- β signaling and can amplify its effects through enhancement of TGF- β ligand-receptor binding [85–90]. Inhibition of *CCN2* gene expression reduced fibrosis and improved muscle and locomotor performance in a rodent model of amyotrophic lateral sclerosis [86]. During unloading, mRNA and protein levels of *CCN2* were unchanged in the muscles of the unloaded mouse but were strongly lower in the muscles of the hibernating brown bear. Taken together, our data strongly suggest that TGF- β signaling is overall inhibited only in muscles resistant to atrophy during bear hibernation.

The BMP pathway is a potent inducer of bone and cartilage formation [91]. BMP signaling was also recently discovered as a regulator of muscle mass, as its inhibition abolished the hypertrophic phenotype of the *MSTN*-KO mouse [20], and an increase in its receptor activity induced important muscle hypertrophy [21]. Regarding BMP ligands, GDF5 is essential to muscle mass maintenance, binding preferentially to the type I receptor *BMPRI1B*. GDF5 expression was strongly induced in denervated mouse muscles, and its inhibition worsened muscle atrophy, suggesting a role in counteracting denervation-induced atrophy [20]. We report here that the gene expression for both *GDF5* and *BMPRI1B* was strongly down-regulated in mouse muscles during unloading, whereas up-regulated in muscles of the hibernating bear. However, GDF5 protein levels were stable in the muscles of both the unloaded mouse and the hibernating bear. We recently demonstrated that circulating components of the hibernating bear serum were able to induce trans-species effects on human myotubes, notably inhibition of protein degradation. Therefore, we hypothesized that those components could be involved in the maintenance of muscle mass and strength in the hibernating bear [92]. Along with muscle mass maintenance, bear hibernation is also associated with bone mass maintenance [93], and thus GDF5 may constitute a possible target toward muscle and bone protection during long periods of physical inactivity and/or fasting. Unfortunately, the exploration of GDF5 concentration in bear serum was hampered by species cross-reactivity concerns with commercially available Elisa kits and thus remains to be addressed.

It has been proposed that the BMP and TGF- β common actor SMAD4 mainly engages with the TGF- β pathway, but switches to the BMP pathway when TGF- β transduction is reduced, and thus could be the limiting factor between these two signalings [20]. Moreover, denervation-induced muscle atrophy was exacerbated in the SMAD4 deficient mouse [20], and muscle mass was increased in humans with a mutation-associated gain of function in the SMAD4 gene [94]. We observed here higher mRNA and protein levels for SMAD4 in muscles of the hibernating bear, but only at mRNA levels in muscles of the unloaded mouse. This is concomitant with the overall down-regulation highlighted for the TGF- β signaling in the hibernating bear, which was not observed for the unloaded mouse. Thus, the inhibition of the TGF- β signaling in muscles of the hibernating bear may have released SMAD4 from TGF- β to BMP pathway to maintain muscle mass in a long period of disuse (Graphical abstract).

TGF- β and BMP share a SMAD-independent pathway that activates the E3 ubiquitin ligase TRAF6 [58]. In addition to its pro-atrophic role [95], TRAF6 is also required for myogenic differentiation and muscle regeneration via the MEF2 axis [96]. MEF2 is a conserved family of transcription factors involved in the control of muscle gene expression [97]. A recent muscle transcriptome analysis highlighted an inhibition of MEF2 transcription factors during human bed rest leading to skeletal muscle alterations [98]. Here, only *MEF2A* was up-regulated during unloading in mouse muscles, whereas *TRAF6*, *MEF2A*, and *MEF2C* were up-regulated in the hibernating bear muscles. We already observed a myogenic microRNA signature mediated by MEF2A signaling in the muscles of the hibernating bear, promoting mechanisms of muscle regeneration, suppression of ubiquitin ligases, and resistance to muscle atrophy [33]. Further studies are required to address whether this MEF2 signature could be under the control of the TGF- β and/or the BMP pathway through TRAF6.

5. Conclusions

Resistance to muscle atrophy in hibernating brown bears has so far been linked to a reduction in protein and energy metabolism. Here, we show for the first time that the TGF- β pathway is down-regulated whereas the BMP pathway is concomitantly sustained or even up-regulated in atrophy-resistant muscles of the hibernating brown bear. Thus, beyond strengthening the previous hypothesis of a hypometabolism enabling this natural resistance to muscle atrophy, our study provides new insights regarding the underlying mechanisms.

The originality of the current work lies in the choice to study the mechanisms involved in resistance to atrophy, and not solely, as in many studies, the mechanisms involved in the onset of atrophy. Our comparison of resistance and sensitivity to muscle atrophy animal models suggested the balance between the TGF- β and the BMP pathways as critical for preventing skeletal muscle atrophy over a long period of disuse. Many targeted therapies to counteract muscle atrophy already focus on TGF- β inhibition [99]. Our data open the way for further studies and clinical trials to test the effects of strategies to switch on (or sustain) the BMP pathway in combination with TGF- β inhibition to prevent disuse-induced muscle atrophy.

Supplementary Materials: The following are available online at <https://www.mdpi.com/article/10.3390/cells10081873/s1>, Figure S1, Tables S1–S6, and Blots quantification.

Author Contributions: Individual contributions of authors is as followed: Conceptualization, L.C. (Laura Cussonneau), E.L. (Etienne Lefai), F.B. and L.C. (Lydie Combaret); Methodology, L.C. (Laura Cussonneau), C.B. (Christian Boyer), C.B. (Charlotte Brun), C.D., E.L. (Etienne Lefai), E.M., A.L.E., J.M.A., J.E.S., E.L. (Emmanuelle Loizon), F.B. and L.C. (Lydie Combaret); Analysis, L.C. (Laura Cussonneau), E.G., E.D., E.L. (Etienne Lefai), F.B. and L.C. (Lydie Combaret); Writing—original draft preparation, L.C. (Laura Cussonneau), E.L. (Etienne Lefai), F.B. and L.C. (Lydie Combaret); Writing—review and editing, all authors; Project administration, E.L. (Etienne Lefai), F.B. and L.C. (Lydie Combaret); Funding acquisition, E.L. (Etienne Lefai), F.B. and L.C. (Lydie Combaret). All authors have read and agreed to the published version of the manuscript.

Funding: This work was supported by the Center National d'Etudes Spatiales (CNES, #865, #974, #1006, #1905), the iSITE Challenge 3 Mobility program (Université Clermont Auvergne), and the CNRS and Strasbourg University (H2E project; MyoBears project of the PEPS ExoMod program). MGX acknowledges financial support from France Génomique National infrastructure, funded as part of "Investissement d'Avenir" program managed by the Agence Nationale pour la Recherche (contract ANR-10-INBS-09). L.C. (Laura Cussonneau) was supported by a grant from the Institut National de la Recherche Agronomique et Environnement and Clermont Métropole. C.B. (Christian Boyer) and C.B. (Charlotte Brun) were supported by grants from the Ministère Français de l'Enseignement Supérieur, de la Recherche et de l'Innovation. The long-term funding of Scandinavian Brown Bear Research Project (SBBRP) has come primarily from the Swedish Environmental Protection Agency, the Norwegian Environment Agency, the Austrian Science Fund, and the Swedish Association for Hunting and Wildlife Management.

Institutional Review Board Statement: The study was conducted according to the guidelines of the Declaration of Helsinki and of the European Directive 2010/63/EU and approved by the Institutional Review Board (or Ethics Committee) of (1) the Swedish Ethical Committee on Animal Experiment (applications Dnr C3/2016 and Dnr C18/2015), the Swedish Environmental Protection Agency (NV-0741-18), and the Swedish Board of Agriculture (Dnr 5.2.18–3060/17), and (2) the C2E2A (Comité d'Ethique pour l'Expérimentation Animale Auvergne) (D6334515-08/2018).

Informed Consent Statement: Not applicable.

Data Availability Statement: The analyzed transcriptomic mouse data that support the findings of this study are openly available in the GEO repository database at <https://doi.org/10.1093/gerona/gly051>, accessed on 16 June 2021, reference number (GSE102284). The generated transcriptomic bear data that support the findings of this study are openly available in the GEO repository database at <https://www.ncbi.nlm.nih.gov/geo/query/acc.cgi>, accessed on 16 June 2021, reference number

(GSE144856). Other data that support the findings of this study are available in the supplementary material of this article.

Acknowledgments: The authors thank the field capture team (D. Ahlqvist, A. Friebe, H. Nordin, H. Blomgren, and S. Persson) and the IEN (INRAE Clermont-Ferrand-Theix, France) for excellent assistance with mouse care (A. Cissoire, Y. Delorme, and M. Djelloul-Mazouz), and L. Parry for help during animal slaughtering. The authors are also grateful to T. Brioché (Unité Mixte de Recherche INRAE, Dynamique Musculaire et Métabolisme, Université de Montpellier, France) for his help in implementing the unloading model in mouse and F. Rocher for helpful discussions. This is paper N°317 of the Scandinavian Brown Bear Research Project.

Conflicts of Interest: The authors declare no conflict of interest.

References

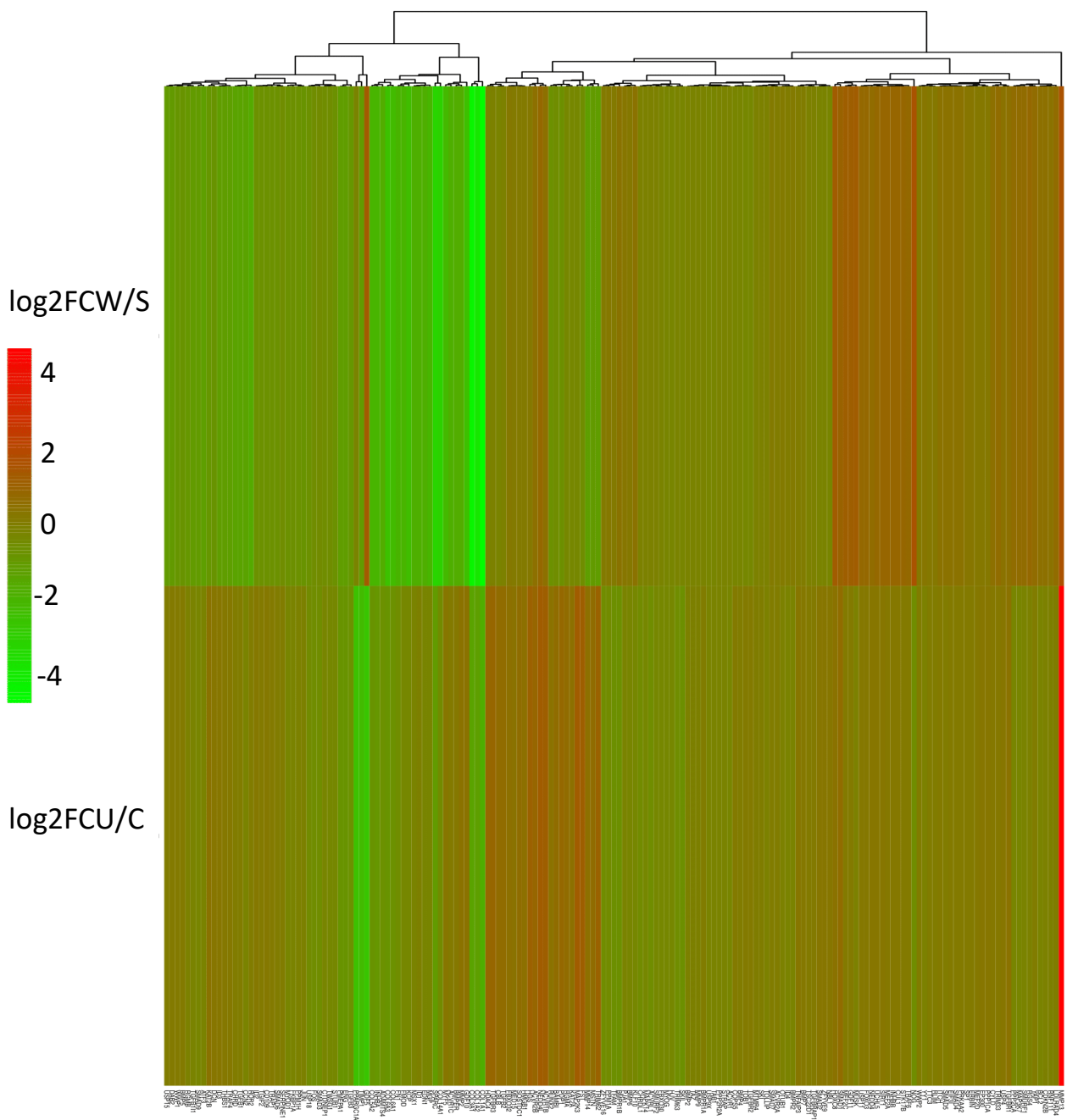
- Jamshidpour, B.; Bahrpeyma, F.; Khatami, M.-R. The Effect of Aerobic and Resistance Exercise Training on the Health Related Quality of Life, Physical Function, and Muscle Strength among Hemodialysis Patients with Type 2 Diabetes. *J. Bodyw. Mov. Ther.* **2019**, *24*, S1360859219303134. [[CrossRef](#)] [[PubMed](#)]
- Leenders, M.; Verdijk, L.B.; van der Hoeven, L.; Adam, J.J.; van Kranenburg, J.; Nilwik, R.; van Loon, L.J.C. Patients With Type 2 Diabetes Show a Greater Decline in Muscle Mass, Muscle Strength, and Functional Capacity With Aging. *J. Am. Med. Dir. Assoc.* **2013**, *14*, 585–592. [[CrossRef](#)]
- DeFronzo, R.A.; Tripathy, D. Skeletal Muscle Insulin Resistance Is the Primary Defect in Type 2 Diabetes. *Diabetes Care* **2009**, *32*, S157–S163. [[CrossRef](#)] [[PubMed](#)]
- Alkner, B.A.; Tesch, P.A. Knee Extensor and Plantar Flexor Muscle Size and Function Following 90 Days of Bed Rest with or without Resistance Exercise. *Eur. J. Appl. Physiol.* **2004**, *93*, 294–305. [[CrossRef](#)] [[PubMed](#)]
- Trappe, S.; Trappe, T.; Gallagher, P.; Harber, M.; Alkner, B.; Tesch, P. Human Single Muscle Fibre Function with 84 Day Bed-Rest and Resistance Exercise. *J. Physiol.* **2004**, *557*, 501–513. [[CrossRef](#)] [[PubMed](#)]
- Thyfault, J.P.; Du, M.; Kraus, W.E.; Levine, J.A.; Booth, F.W. Physiology of Sedentary Behavior and Its Relationship to Health Outcomes. *Med. Sci. Sports Exerc.* **2015**, *47*, 1301–1305. [[CrossRef](#)] [[PubMed](#)]
- Argilés, J.M.; Campos, N.; Lopez-Pedrosa, J.M.; Rueda, R.; Rodriguez-Mañas, L. Skeletal Muscle Regulates Metabolism via Interorgan Crosstalk: Roles in Health and Disease. *J. Am. Med. Dir. Assoc.* **2016**, *17*, 789–796. [[CrossRef](#)] [[PubMed](#)]
- Powers, S.K.; Lynch, G.S.; Murphy, K.T.; Reid, M.B.; Zijdewind, I. Disease-Induced Skeletal Muscle Atrophy and Fatigue. *Med. Sci. Sports Exerc.* **2016**, *48*, 2307–2319. [[CrossRef](#)]
- Bonaldo, P.; Sandri, M. Cellular and Molecular Mechanisms of Muscle Atrophy. *Dis. Model. Mech.* **2013**, *6*, 25–39. [[CrossRef](#)] [[PubMed](#)]
- Lecker, S.H.; Goldberg, A.L.; Mitch, W.E. Protein Degradation by the Ubiquitin–Proteasome Pathway in Normal and Disease States. *J. Am. Soc. Nephrol.* **2006**, *17*, 1807–1819. [[CrossRef](#)]
- Taillandier, D.; Polge, C. Skeletal Muscle Atrogenes: From Rodent Models to Human Pathologies. *Biochimie* **2019**, *166*, 251–269. [[CrossRef](#)] [[PubMed](#)]
- Peris-Moreno, D.; Cussonneau, L.; Combaret, L.; Polge, C.; Taillandier, D. Ubiquitin Ligases at the Heart of Skeletal Muscle Atrophy Control. *Molecules* **2021**, *26*, 407. [[CrossRef](#)]
- Vainshtein, A.; Sandri, M. Signaling Pathways That Control Muscle Mass. *Int. J. Mol. Sci.* **2020**, *21*, 4759. [[CrossRef](#)]
- Sartori, R.; Gregorevic, P.; Sandri, M. TGF β and BMP Signaling in Skeletal Muscle: Potential Significance for Muscle-Related Disease. *Trends Endocrinol. Metab.* **2014**, *25*, 464–471. [[CrossRef](#)] [[PubMed](#)]
- Lokireddy, S.; Mouly, V.; Butler-Browne, G.; Gluckman, P.D.; Sharma, M.; Kambadur, R.; McFarlane, C. Myostatin Promotes the Wasting of Human Myoblast Cultures through Promoting Ubiquitin-Proteasome Pathway-Mediated Loss of Sarcomeric Proteins. *Am. J. Physiol.-Cell Physiol.* **2011**, *301*, C1316–C1324. [[CrossRef](#)] [[PubMed](#)]
- Sartori, R.; Milan, G.; Patron, M.; Mammucari, C.; Blaauw, B.; Abraham, R.; Sandri, M. Smad2 and 3 Transcription Factors Control Muscle Mass in Adulthood. *Am. J. Physiol.-Cell Physiol.* **2009**, *296*, C1248–C1257. [[CrossRef](#)]
- Tando, T.; Hirayama, A.; Furukawa, M.; Sato, Y.; Kobayashi, T.; Funayama, A.; Kanaji, A.; Hao, W.; Watanabe, R.; Morita, M.; et al. Smad2/3 Proteins Are Required for Immobilization-Induced Skeletal Muscle Atrophy. *J. Biol. Chem.* **2016**, *291*, 12184–12194. [[CrossRef](#)]
- Goodman, C.A.; McNally, R.M.; Hoffmann, F.M.; Hornberger, T.A. Smad3 Induces Atrogin-1, Inhibits MTOR and Protein Synthesis, and Promotes Muscle Atrophy In Vivo. *Mol. Endocrinol.* **2013**, *27*, 1946–1957. [[CrossRef](#)]
- Carlson, M.E.; Hsu, M.; Conboy, I.M. Imbalance between PSmad3 and Notch Induces CDK Inhibitors in Old Muscle Stem Cells. *Nature* **2008**, *454*, 528–532. [[CrossRef](#)] [[PubMed](#)]
- Sartori, R.; Schirwis, E.; Blaauw, B.; Bortolanza, S.; Zhao, J.; Enzo, E.; Stantzou, A.; Mouisel, E.; Toniolo, L.; Ferry, A.; et al. BMP Signaling Controls Muscle Mass. *Nat. Genet.* **2013**, *45*, 1309–1318. [[CrossRef](#)]
- Winbanks, C.E.; Chen, J.L.; Qian, H.; Liu, Y.; Bernardo, B.C.; Beyer, C.; Watt, K.I.; Thomson, R.E.; Connor, T.; Turner, B.J.; et al. The Bone Morphogenetic Protein Axis Is a Positive Regulator of Skeletal Muscle Mass. *J. Cell Biol.* **2013**, *203*, 345–357. [[CrossRef](#)] [[PubMed](#)]

22. Tinker, D.B.; Harlow, H.J.; Beck, T.D.I. Protein Use and Muscle-Fiber Changes in Free-Ranging, Hibernating Black Bears. *Physiol. Zool.* **1998**, *71*, 414–424. [[CrossRef](#)]
23. Lohuis, T.D.; Harlow, H.J.; Beck, T.D.I. Hibernating Black Bears (*Ursus Americanus*) Experience Skeletal Muscle Protein Balance during Winter Anorexia. *Comp. Biochem. Physiol. B Biochem. Mol. Biol.* **2007**, *147*, 20–28. [[CrossRef](#)]
24. Deval, C.; Capel, F.; Laillet, B.; Polge, C.; Béchet, D.; Taillandier, D.; Attaix, D.; Combaret, L. Docosahexaenoic Acid-Supplementation Prior to Fasting Prevents Muscle Atrophy in Mice: Docosahexaenoic Acid Limits Muscle Wasting in Fasted Mice. *J. Cachexia Sarcopenia Muscle* **2016**, *7*, 587–603. [[CrossRef](#)] [[PubMed](#)]
25. Vazeille, E.; Codran, A.; Claustre, A.; Averous, J.; Listrat, A.; Béchet, D.; Taillandier, D.; Dardevet, D.; Attaix, D.; Combaret, L. The Ubiquitin-Proteasome and the Mitochondria-Associated Apoptotic Pathways Are Sequentially Downregulated during Recovery after Immobilization-Induced Muscle Atrophy. *Am. J. Physiol. Endocrinol. Metab.* **2008**, *295*, E1181–E1190. [[CrossRef](#)] [[PubMed](#)]
26. Slimani, L.; Vazeille, E.; Deval, C.; Meunier, B.; Polge, C.; Dardevet, D.; Béchet, D.; Taillandier, D.; Micol, D.; Listrat, A.; et al. The Delayed Recovery of the Remobilized Rat Tibialis Anterior Muscle Reflects a Defect in Proliferative and Terminal Differentiation That Impairs Early Regenerative Processes. *J. Cachexia Sarcopenia Muscle* **2015**, *6*, 73–83. [[CrossRef](#)]
27. Gao, Y.; Arfat, Y.; Wang, H.; Goswami, N. Muscle Atrophy Induced by Mechanical Unloading: Mechanisms and Potential Countermeasures. *Front. Physiol.* **2018**, *9*, 235. [[CrossRef](#)] [[PubMed](#)]
28. Cui, Q.; Yang, H.; Gu, Y.; Zong, C.; Chen, X.; Lin, Y.; Sun, H.; Shen, Y.; Zhu, J. RNA Sequencing (RNA-Seq) Analysis of Gene Expression Provides New Insights into Hindlimb Unloading-Induced Skeletal Muscle Atrophy. *Ann. Transl. Med.* **2020**, *8*, 1595. [[CrossRef](#)] [[PubMed](#)]
29. Deval, C.; Calonne, J.; Coudy-Gandilhon, C.; Vazeille, E.; Bechet, D.; Polge, C.; Taillandier, D.; Attaix, D.; Combaret, L. Mitophagy and Mitochondria Biogenesis Are Differentially Induced in Rat Skeletal Muscles during Immobilization and/or Remobilization. *Int. J. Mol. Sci.* **2020**, *21*, 3691. [[CrossRef](#)] [[PubMed](#)]
30. Lin, D.C.; Hershey, J.D.; Mattoon, J.S.; Robbins, C.T. Skeletal Muscles of Hibernating Brown Bears Are Unusually Resistant to Effects of Denervation. *J. Exp. Biol.* **2012**, *215*, 2081–2087. [[CrossRef](#)]
31. Bertile, F.; Habold, C.; Le Maho, Y.; Giroud, S. Body Protein Sparing in Hibernators: A Source for Biomedical Innovation. *Front. Physiol.* **2021**, *12*, 634953. [[CrossRef](#)] [[PubMed](#)]
32. Chazarin, B.; Storey, K.B.; Ziemianin, A.; Chanon, S.; Plumel, M.; Chery, I.; Durand, C.; Evans, A.L.; Arnemo, J.M.; Zedrosser, A.; et al. Metabolic Reprogramming Involving Glycolysis in the Hibernating Brown Bear Skeletal Muscle. *Front. Zool.* **2019**, *16*, 12. [[CrossRef](#)] [[PubMed](#)]
33. Luu, B.E.; Lefai, E.; Giroud, S.; Swenson, J.E.; Chazarin, B.; Gauquelin-Koch, G.; Arnemo, J.M.; Evans, A.L.; Bertile, F.; Storey, K.B. MicroRNAs Facilitate Skeletal Muscle Maintenance and Metabolic Suppression in Hibernating Brown Bears. *J. Cell. Physiol.* **2019**, *235*, 3984–3993. [[CrossRef](#)] [[PubMed](#)]
34. Chazarin, B.; Ziemianin, A.; Evans, A.L.; Meugnier, E.; Loizon, E.; Chery, I.; Arnemo, J.M.; Swenson, J.E.; Gauquelin-Koch, G.; Simon, C.; et al. Limited Oxidative Stress Favors Resistance to Skeletal Muscle Atrophy in Hibernating Brown Bears (*Ursus Arctos*). *Antioxidants* **2019**, *8*, 334. [[CrossRef](#)] [[PubMed](#)]
35. Fedorov, V.B.; Goropashnaya, A.V.; Stewart, N.C.; Tøien, Ø.; Chang, C.; Wang, H.; Yan, J.; Showe, L.C.; Showe, M.K.; Barnes, B.M. Comparative Functional Genomics of Adaptation to Muscular Disuse in Hibernating Mammals. *Mol. Ecol.* **2014**, *23*, 5524–5537. [[CrossRef](#)]
36. Jansen, H.T.; Trojahn, S.; Saxton, M.W.; Quackenbush, C.R.; Evans Hutzenbiler, B.D.; Nelson, O.L.; Cornejo, O.E.; Robbins, C.T.; Kelley, J.L. Hibernation Induces Widespread Transcriptional Remodeling in Metabolic Tissues of the Grizzly Bear. *Commun. Biol.* **2019**, *2*, 336. [[CrossRef](#)]
37. Mugahid, D.A.; Sengul, T.G.; You, X.; Wang, Y.; Steil, L.; Bergmann, N.; Radke, M.H.; Ofenbauer, A.; Gesell-Salazar, M.; Balogh, A.; et al. Proteomic and Transcriptomic Changes in Hibernating Grizzly Bears Reveal Metabolic and Signaling Pathways That Protect against Muscle Atrophy. *Sci. Rep.* **2019**, *9*, 19976. [[CrossRef](#)] [[PubMed](#)]
38. Arnemo, J.M.; Evans, A.L. *Biomedical Protocols for Free-Ranging Brown Bears, Wolves, Wolverines and Lynx*; Inland Norway University of Applied Sciences: Elverum, Norway, 2017.
39. Chacon-Cabrera, A.; Gea, J.; Barreiro, E. Short- and Long-Term Hindlimb Immobilization and Reloading: Profile of Epigenetic Events in Gastrocnemius. *J. Cell. Physiol.* **2017**, *232*, 1415–1427. [[CrossRef](#)]
40. Anderson, M.J.; Diko, S.; Baehr, L.M.; Baar, K.; Bodine, S.C.; Christiansen, B.A. Contribution of Mechanical Unloading to Trabecular Bone Loss Following Non-Invasive Knee Injury in Mice. *J. Orthop. Res.* **2016**, *34*, 1680–1687. [[CrossRef](#)] [[PubMed](#)]
41. Pagano, A.F.; Demangel, R.; Brioché, T.; Jublanc, E.; Bertrand-Gaday, C.; Candau, R.; Dechesne, C.A.; Dani, C.; Bonniou, A.; Py, G.; et al. Muscle Regeneration with Intermuscular Adipose Tissue (IMAT) Accumulation Is Modulated by Mechanical Constraints. *PLOS ONE* **2015**, *10*, e0144230. [[CrossRef](#)] [[PubMed](#)]
42. Zhang, X.; Trevino, M.B.; Wang, M.; Gardell, S.J.; Ayala, J.E.; Han, X.; Kelly, D.P.; Goodpaster, B.H.; Vega, R.B.; Coen, P.M. Impaired Mitochondrial Energetics Characterize Poor Early Recovery of Muscle Mass Following Hind Limb Unloading in Old Mice. *J. Gerontol. Ser. A* **2018**, *73*, 1313–1322. [[CrossRef](#)]
43. Boyer, C.; Cussonneau, L.; Brun, C.; Deval, C.; Pais de Barros, J.-P.; Chanon, S.; Bernoud-Hubac, N.; Daira, P.; Evans, A.L.; Arnemo, J.M.; et al. Specific Shifts in the Endocannabinoid System in Hibernating Brown Bears. *Front. Zool.* **2020**, *17*, 35. [[CrossRef](#)]
44. Kim, D.; Perte, G.; Trapnell, C.; Pimentel, H.; Kelley, R.; Salzberg, S.L. TopHat2: Accurate Alignment of Transcriptomes in the Presence of Insertions, Deletions and Gene Fusions. *Genome Biol.* **2013**, *14*, R36. [[CrossRef](#)] [[PubMed](#)]

45. Langmead, B.; Trapnell, C.; Pop, M.; Salzberg, S.L. Ultrafast and Memory-Efficient Alignment of Short DNA Sequences to the Human Genome. *Genome Biol.* **2009**, *10*, R25. [[CrossRef](#)]
46. Liao, Y.; Smyth, G.K.; Shi, W. FeatureCounts: An Efficient General Purpose Program for Assigning Sequence Reads to Genomic Features. *Bioinformatics* **2014**, *30*, 923–930. [[CrossRef](#)] [[PubMed](#)]
47. Gentleman, R.C.; Carey, V.J.; Bates, D.M.; Bolstad, B.; Dettling, M.; Dudoit, S.; Ellis, B.; Gautier, L.; Ge, Y.; Gentry, J.; et al. Bioconductor: Open Software Development for Computational Biology and Bioinformatics. *Genome Biol.* **2004**, *5*, 16.
48. Love, M.I.; Huber, W.; Anders, S. Moderated Estimation of Fold Change and Dispersion for RNA-Seq Data with DESeq2. *Genome Biol.* **2014**, *15*, 550. [[CrossRef](#)] [[PubMed](#)]
49. De Hoon, M.J.L.; Imoto, S.; Nolan, J.; Miyano, S. Open Source Clustering Software. *Bioinformatics* **2004**, *20*, 1453–1454. [[CrossRef](#)] [[PubMed](#)]
50. Saldanha, A.J. Java Treeview—Extensible Visualization of Microarray Data. *Bioinformatics* **2004**, *20*, 3246–3248. [[CrossRef](#)]
51. Zhou, Y.; Zhou, B.; Pache, L.; Chang, M.; Khodabakhshi, A.H.; Tanaseichuk, O.; Benner, C.; Chanda, S.K. Metascape Provides a Biologist-Oriented Resource for the Analysis of Systems-Level Datasets. *Nat. Commun.* **2019**, *10*, 1523. [[CrossRef](#)]
52. Koinuma, D.; Tsutsumi, S.; Kamimura, N.; Taniguchi, H.; Miyazawa, K.; Sunamura, M.; Imamura, T.; Miyazono, K.; Aburatani, H. Chromatin Immunoprecipitation on Microarray Analysis of Smad2/3 Binding Sites Reveals Roles of ETS1 and TFAP2A in Transforming Growth Factor β Signaling. *Mol. Cell. Biol.* **2009**, *29*, 172–186. [[CrossRef](#)]
53. Luo, K. Signaling Cross Talk between TGF- β /Smad and Other Signaling Pathways. *Cold Spring Harb. Perspect. Biol.* **2017**, *9*, a022137. [[CrossRef](#)]
54. Córdova, G.; Rochard, A.; Riquelme-Guzmán, C.; Cofré, C.; Scherman, D.; Bigey, P.; Brandan, E. SMAD3 and SP1/SP3 Transcription Factors Collaborate to Regulate Connective Tissue Growth Factor Gene Expression in Myoblasts in Response to Transforming Growth Factor β . *J. Cell. Biochem.* **2015**, *116*, 1880–1887. [[CrossRef](#)] [[PubMed](#)]
55. Hata, A.; Chen, Y.-G. TGF- β Signaling from Receptors to Smads. *Cold Spring Harb. Perspect. Biol.* **2016**, *8*, a022061. [[CrossRef](#)] [[PubMed](#)]
56. Itoh, S.; ten Dijke, P. Negative Regulation of TGF- β Receptor/Smad Signal Transduction. *Curr. Opin. Cell Biol.* **2007**, *19*, 176–184. [[CrossRef](#)]
57. Weiss, A.; Attisano, L. The TGFbeta Superfamily Signaling Pathway: TGFbeta Superfamily Signaling Pathway. *Wiley Interdiscip. Rev. Dev. Biol.* **2013**, *2*, 47–63. [[CrossRef](#)] [[PubMed](#)]
58. Zhang, Y.E. Non-Smad Signaling Pathways of the TGF- β Family. *Cold Spring Harb. Perspect. Biol.* **2017**, *9*, a022129. [[CrossRef](#)] [[PubMed](#)]
59. Miyazono, K.; Kamiya, Y.; Morikawa, M. Bone Morphogenetic Protein Receptors and Signal Transduction. *J. Biochem. (Tokyo)* **2010**, *147*, 35–51. [[CrossRef](#)]
60. Inui, N.; Sakai, S.; Kitagawa, M. Molecular Pathogenesis of Pulmonary Fibrosis, with Focus on Pathways Related to TGF- β and the Ubiquitin-Proteasome Pathway. *Int. J. Mol. Sci.* **2021**, *22*, 6107. [[CrossRef](#)]
61. Ferrando, A.A.; Lane, H.W.; Stuart, C.A.; Davis-Street, J.; Wolfe, R.R. Prolonged Bed Rest Decreases Skeletal Muscle and Whole Body Protein Synthesis. *Am. J. Physiol.-Endocrinol. Metab.* **1996**, *270*, E627–E633. [[CrossRef](#)]
62. Ferrando, A.A.; Tipton, K.D.; Bamman, M.M.; Wolfe, R.R. Resistance Exercise Maintains Skeletal Muscle Protein Synthesis during Bed Rest. *J. Appl. Physiol.* **1997**, *82*, 807–810. [[CrossRef](#)]
63. Idris, I.; Atherton, P.J. Human Skeletal Muscle Disuse Atrophy: Effects on Muscle Protein Synthesis, Breakdown, and Insulin Resistance—A Qualitative Review. *Front. Physiol.* **2016**, *7*, 10.
64. Fedorov, V.B.; Goropashnaya, A.V.; Tøien, Ø.; Stewart, N.C.; Gracey, A.Y.; Chang, C.; Qin, S.; Perlea, G.; Quackenbush, J.; Showe, L.C.; et al. Elevated Expression of Protein Biosynthesis Genes in Liver and Muscle of Hibernating Black Bears (*Ursus Americanus*). *Physiol. Genomics* **2009**, *37*, 108–118. [[CrossRef](#)]
65. Zhao, J.; Brault, J.J.; Schild, A.; Cao, P.; Sandri, M.; Schiaffino, S.; Lecker, S.H.; Goldberg, A.L. FoxO3 Coordinately Activates Protein Degradation by the Autophagic/Lysosomal and Proteasomal Pathways in Atrophying Muscle Cells. *Cell Metab.* **2007**, *6*, 472–483. [[CrossRef](#)]
66. Mammucari, C.; Milan, G.; Romanello, V.; Masiero, E.; Rudolf, R.; Del Piccolo, P.; Burden, S.J.; Di Lisi, R.; Sandri, C.; Zhao, J.; et al. FoxO3 Controls Autophagy in Skeletal Muscle In Vivo. *Cell Metab.* **2007**, *6*, 458–471. [[CrossRef](#)] [[PubMed](#)]
67. Sandri, M.; Sandri, C.; Gilbert, A.; Skurk, C.; Calabria, E.; Picard, A.; Walsh, K.; Schiaffino, S.; Lecker, S.H.; Goldberg, A.L. Foxo Transcription Factors Induce the Atrophy-Related Ubiquitin Ligase Atrogin-1 and Cause Skeletal Muscle Atrophy. *Cell* **2004**, *117*, 399–412. [[CrossRef](#)]
68. Fabian, D.K.; Fuentealba, M.; Dönertaş, H.M.; Partridge, L.; Thornton, J.M. Functional Conservation in Genes and Pathways Linking Ageing and Immunity. *Immun. Ageing* **2021**, *18*, 23. [[CrossRef](#)]
69. Slimani, L.; Micol, D.; Amat, J.; Delcros, G.; Meunier, B.; Taillandier, D.; Polge, C.; Béchet, D.; Dardevet, D.; Picard, B.; et al. The Worsening of Tibialis Anterior Muscle Atrophy during Recovery Post-Immobilization Correlates with Enhanced Connective Tissue Area, Proteolysis, and Apoptosis. *Am. J. Physiol.-Endocrinol. Metab.* **2012**, *303*, E1335–E1347. [[CrossRef](#)]
70. Pigna, E.; Renzini, A.; Greco, E.; Simonazzi, E.; Fulle, S.; Mancinelli, R.; Moresi, V.; Adamo, S. HDAC4 Preserves Skeletal Muscle Structure Following Long-Term Denervation by Mediating Distinct Cellular Responses. *Skelet. Muscle* **2018**, *8*, 6. [[CrossRef](#)]

71. Leermakers, P.A.; Kneppers, A.E.M.; Schols, A.M.W.J.; Kelders, M.C.J.M.; Theije, C.C.; Verdijk, L.B.; Loon, L.J.C.; Langen, R.C.J.; Gosker, H.R. Skeletal Muscle Unloading Results in Increased Mitophagy and Decreased Mitochondrial Biogenesis Regulation. *Muscle Nerve* **2019**, *60*, 769–778. [[CrossRef](#)]
72. Dirks, M.L.; Wall, B.T.; van de Valk, B.; Holloway, T.M.; Holloway, G.P.; Chabowski, A.; Goossens, G.H.; van Loon, L.J.C. One Week of Bed Rest Leads to Substantial Muscle Atrophy and Induces Whole-Body Insulin Resistance in the Absence of Skeletal Muscle Lipid Accumulation. *Diabetes* **2016**, *65*, 2862–2875. [[CrossRef](#)] [[PubMed](#)]
73. Brocca, L.; Longa, E.; Cannavino, J.; Seynnes, O.; de Vito, G.; McPhee, J.; Narici, M.; Pellegrino, M.A.; Bottinelli, R. Human Skeletal Muscle Fibre Contractile Properties and Proteomic Profile: Adaptations to 3 Weeks of Unilateral Lower Limb Suspension and Active Recovery: Impact of ULLS and Active Rehabilitation on Human Muscle Fibres. *J. Physiol.* **2015**, *593*, 5361–5385. [[CrossRef](#)] [[PubMed](#)]
74. Gillies, A.R.; Lieber, R.L. Structure and Function of the Skeletal Muscle Extracellular Matrix: Skeletal Muscle ECM. *Muscle Nerve* **2011**, *44*, 318–331. [[CrossRef](#)]
75. Martinez, D.A.; Vailas, A.C.; Vanderby, R.; Grindeland, R.E. Temporal Extracellular Matrix Adaptations in Ligament during Wound Healing and Hindlimb Unloading. *Am. J. Physiol.-Regul. Integr. Comp. Physiol.* **2007**, *293*, R1552–R1560. [[CrossRef](#)]
76. Miller, T.A.; Lesniewski, L.A.; Muller-Delp, J.M.; Majors, A.K.; Scalise, D.; Delp, M.D. Hindlimb Unloading Induces a Collagen Isoform Shift in the Soleus Muscle of the Rat. *Am. J. Physiol.-Regul. Integr. Comp. Physiol.* **2001**, *281*, R1710–R1717. [[CrossRef](#)]
77. Urso, M.L.; Scrimgeour, A.G.; Chen, Y.-W.; Thompson, P.D.; Clarkson, P.M. Analysis of Human Skeletal Muscle after 48 h Immobilization Reveals Alterations in mRNA and Protein for Extracellular Matrix Components. *J. Appl. Physiol.* **2006**, *101*, 13. [[CrossRef](#)]
78. Elkina, Y.; von Haehling, S.; Anker, S.D.; Springer, J. The Role of Myostatin in Muscle Wasting: An Overview. *J. Cachexia Sarcopenia Muscle* **2011**, *2*, 143–151. [[CrossRef](#)]
79. Lee, S.-J.; Reed, L.A.; Davies, M.V.; Girgenrath, S.; Goad, M.E.P.; Tomkinson, K.N.; Wright, J.F.; Barker, C.; Ehrmantraut, G.; Holmstrom, J.; et al. Regulation of Muscle Growth by Multiple Ligands Signaling through Activin Type II Receptors. *Proc. Natl. Acad. Sci. USA* **2005**, *102*, 18117–18122. [[CrossRef](#)]
80. Chen, J.L.; Walton, K.L.; Hagg, A.; Colgan, T.D.; Johnson, K.; Qian, H.; Gregorevic, P.; Harrison, C.A. Specific Targeting of TGF- β Family Ligands Demonstrates Distinct Roles in the Regulation of Muscle Mass in Health and Disease. *Proc. Natl. Acad. Sci. USA* **2017**, *114*, 201620013. [[CrossRef](#)]
81. Latres, E.; Mastaitis, J.; Fury, W.; Miloscio, L.; Trejos, J.; Pangilinan, J.; Okamoto, H.; Cavino, K.; Na, E.; Papatheodorou, A.; et al. Activin A More Prominently Regulates Muscle Mass in Primates than Does GDF8. *Nat. Commun.* **2017**, *8*, 15153. [[CrossRef](#)]
82. Zimmers, T.A. Induction of Cachexia in Mice by Systemically Administered Myostatin. *Science* **2002**, *296*, 1486–1488. [[CrossRef](#)]
83. Langley, B.; Thomas, M.; Bishop, A.; Sharma, M.; Gilmour, S.; Kambadur, R. Myostatin Inhibits Myoblast Differentiation by Down-Regulating MyoD Expression. *J. Biol. Chem.* **2002**, *277*, 49831–49840. [[CrossRef](#)]
84. Ding, H.; Zhang, G.; Sin, K.W.T.; Liu, Z.; Lin, R.-K.; Li, M.; Li, Y.-P. Activin A Induces Skeletal Muscle Catabolism via P38 β Mitogen-Activated Protein Kinase: Activin A Induces Skeletal Muscle Catabolism. *J. Cachexia Sarcopenia Muscle* **2017**, *8*, 202–212. [[CrossRef](#)]
85. Sun, G.; Haginoya, K.; Wu, Y.; Chiba, Y.; Nakanishi, T.; Onuma, A.; Sato, Y.; Takigawa, M.; Iinuma, K.; Tsuchiya, S. Connective Tissue Growth Factor Is Overexpressed in Muscles of Human Muscular Dystrophy. *J. Neurol. Sci.* **2008**, *267*, 48–56. [[CrossRef](#)] [[PubMed](#)]
86. Gonzalez, D.; Rebolledo, D.L.; Correa, L.M.; Court, F.A.; Cerpa, W.; Lipson, K.E.; van Zundert, B.; Brandan, E. The Inhibition of CTGF/CCN2 Activity Improves Muscle and Locomotor Function in a Murine ALS Model. *Hum. Mol. Genet.* **2018**, *27*, 2913–2926. [[CrossRef](#)]
87. Morales, M.G.; Gutierrez, J.; Cabello-Verrugio, C.; Cabrera, D.; Lipson, K.E.; Goldschmeding, R.; Brandan, E. Reducing CTGF/CCN2 Slows down Mdx Muscle Dystrophy and Improves Cell Therapy. *Hum. Mol. Genet.* **2013**, *22*, 4938–4951. [[CrossRef](#)]
88. Abreu, J.G.; Ketpura, N.I.; Reversade, B.; De Robertis, E.M. Connective-Tissue Growth Factor (CTGF) Modulates Cell Signalling by BMP and TGF- β . *Nat. Cell Biol.* **2002**, *4*, 599–604. [[CrossRef](#)]
89. Vial, C.; Zúñiga, L.M.; Cabello-Verrugio, C.; Cañón, P.; Fadic, R.; Brandan, E. Skeletal Muscle Cells Express the Profibrotic Cytokine Connective Tissue Growth Factor (CTGF/CCN2), Which Induces Their Dedifferentiation. *J. Cell. Physiol.* **2008**, *215*, 410–421. [[CrossRef](#)] [[PubMed](#)]
90. Hillege, M.; Galli Caro, R.; Offringa, C.; de Wit, G.; Jaspers, R.; Hoogaars, W. TGF- β Regulates Collagen Type I Expression in Myoblasts and Myotubes via Transient Ctgf and Fgf-2 Expression. *Cells* **2020**, *9*, 375. [[CrossRef](#)] [[PubMed](#)]
91. Salazar, V.S.; Gamer, L.W.; Rosen, V. BMP Signalling in Skeletal Development, Disease and Repair. *Nat. Rev. Endocrinol.* **2016**, *12*, 203–221. [[CrossRef](#)] [[PubMed](#)]
92. Chanon, S.; Chazarin, B.; Touhans, B.; Durand, C.; Chery, I.; Robert, M.; Vieille-Marchiset, A.; Swenson, J.E.; Zedrosser, A.; Evans, A.L.; et al. Proteolysis Inhibition by Hibernating Bear Serum Leads to Increased Protein Content in Human Muscle Cells. *Sci. Rep.* **2018**, *8*, 5525. [[CrossRef](#)] [[PubMed](#)]
93. Donahue, S.W.; McGee, M.E.; Harvey, K.B.; Vaughan, M.R.; Robbins, C.T. Hibernating Bears as a Model for Preventing Disuse Osteoporosis. *J. Biomech.* **2006**, *39*, 1480–1488. [[CrossRef](#)] [[PubMed](#)]

94. Le Goff, C.; Mahaut, C.; Abhyankar, A.; Le Goff, W.; Serre, V.; Afenjar, A.; Destrée, A.; di Rocco, M.; Héron, D.; Jacquemont, S.; et al. Mutations at a Single Codon in Mad Homology 2 Domain of SMAD4 Cause Myhre Syndrome. *Nat. Genet.* **2012**, *44*, 85–88. [[CrossRef](#)]
95. Paul, P.K.; Bhatnagar, S.; Mishra, V.; Srivastava, S.; Darnay, B.G.; Choi, Y.; Kumar, A. The E3 Ubiquitin Ligase TRAF6 Intercedes in Starvation-Induced Skeletal Muscle Atrophy through Multiple Mechanisms. *Mol. Cell. Biol.* **2012**, *32*, 1248–1259. [[CrossRef](#)] [[PubMed](#)]
96. Xiao, F.; Wang, H.; Fu, X.; Li, Y.; Wu, Z. TRAF6 Promotes Myogenic Differentiation via the TAK1/P38 Mitogen-Activated Protein Kinase and Akt Pathways. *PLoS ONE* **2012**, *7*, e34081. [[CrossRef](#)]
97. Taylor, M.V.; Hughes, S.M. Mef2 and the Skeletal Muscle Differentiation Program. *Semin. Cell Dev. Biol.* **2017**, *72*, 33–44. [[CrossRef](#)] [[PubMed](#)]
98. Rullman, E.; Fernandez-Gonzalo, R.; Mekjavić, I.B.; Gustafsson, T.; Eiken, O. MEF2 as Upstream Regulator of the Transcriptome Signature in Human Skeletal Muscle during Unloading. *Am. J. Physiol. Regul. Integr. Comp. Physiol.* **2018**, *315*, R799–R809. [[CrossRef](#)] [[PubMed](#)]
99. Abrigo, J.; Simon, F.; Cabrera, D.; Cordova, G.; Trollet, C.; Cabello-Verrugio, C. Central Role of Transforming Growth Factor Type Beta 1 in Skeletal Muscle Dysfunctions: An Update on Therapeutic Strategies. *Curr. Protein Pept. Sci.* **2018**, *19*, 1189–1200. [[CrossRef](#)]



Supplementary Figure 1

Supplementary Figure 1. The gene expression pattern of TGF- β and BMP components is different in brown bear muscle resistant to atrophy during hibernation compared to atrophied muscles of the unloaded mouse. Heatmap from vastus lateralis muscle of active and hibernating brown bears (n=6 bears/season, the same individuals were sampled and analyzed in summer and winter, $\log_2FC_{Winter/Summer}$), and soleus muscle of control and unloaded mice (n=4 mice per condition, $\log_2FC_{Unloaded/Control}$) of 171 TGF- β /BMP related genes. The green and red colours indicate that the gene expression decreased or increased, respectively, and each line represents one gene.

Supplementary Table 6. Bears features

ID_number	Year of collection	Age (year)	Gender	Experiments
w1305	2014	2	F	RNA sequencing
w1316		2	M	
w1317		2	M	
w1509	2016	2	F	
w1511		2	F	
w1512		2	F	
w1509	2017	3	F	Western Blot
w1610		2	M	
w1709	2018	2	F	
w1710		2	F	
w1707	2019	3	F	
w1802		2	M	
w1803		2	F	
w1806		2	F	
w1812		2	M	
w1813		2	F	
w1814		2	M	
N = 17		2.117647059	Sex ratio : 11F/6M	

6.4 Discussion and perspectives

The main conclusion of our study is that the TGF- β /BMP balance appears to be crucial for the maintenance of muscle mass in hibernating brown bears (Figure 30). In addition to the points raised in the article, there are other issues worth discussing. First of all, we will discuss the transcriptomic regulation of genes related to protein synthesis in hibernating bears muscles. Second of all, we will address in 5 sub-sections the possible reasons why and how the TGF- β and BMP signalling pathways are differentially regulated in the hibernating bears muscles compared to summer.

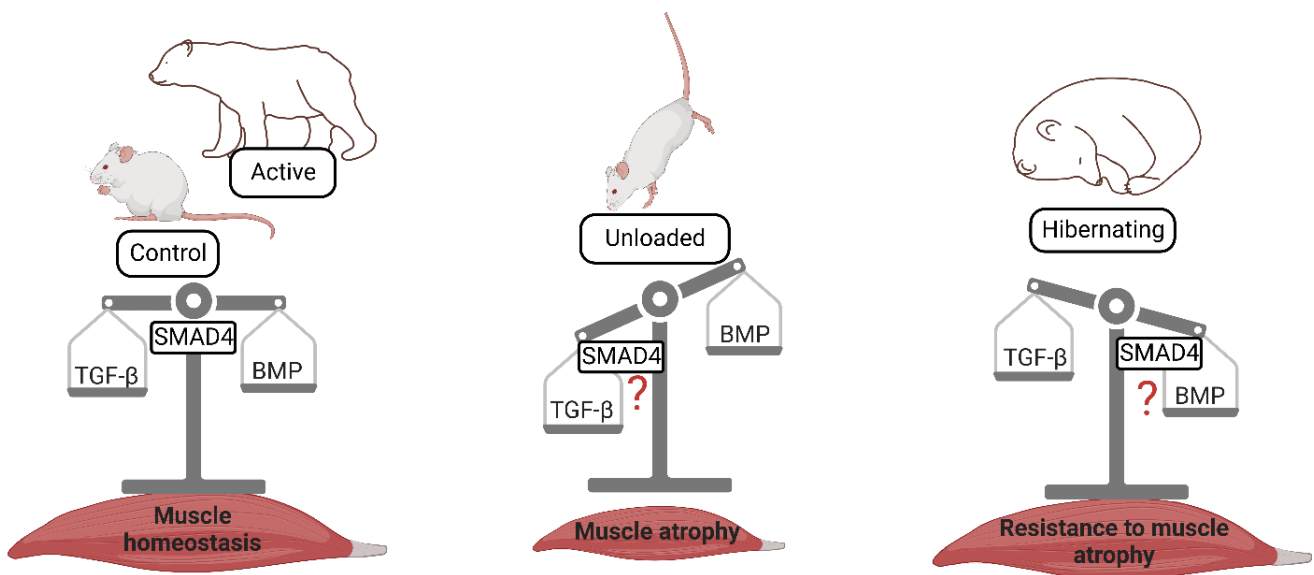


Figure 30. Graphical abstract of the study 1.

6.4.1 Hibernation induces a transcriptomic reprogramming in genes related to protein synthesis and RNA metabolism in bear muscles

Induction of protein synthesis-related genes. As in other transcriptomic studies [304,307,329], we observed (1) an upregulation of genes involved in “protein biosynthesis” (translation) and “ribosome biogenesis” biological processes, and (2) a decrease in genes related to protein degradation pathways in the hibernating brown bear muscles (see Paper 6.3) [351]. Fedorov et al. suggested that the induction of protein translation-related genes provides evidence of an increase in protein synthesis in hibernating bear muscles compared to summer [304,329]. However, using a radioisotope tracer, Lohuis et al. observed a lower rate of protein synthesis in the hibernating bear muscles compare to summer [301] (Figure 24). This was associated with a lower protein degradation rate suggesting that

overall muscle protein turnover was lowered in winter compared to summer in bears [301] (Figure 24). The decrease in the rate of protein degradation is consistent with the downregulation of genes related to protein degradation that we reported in the present transcriptomic study (see Paper 6.3) [351]. However, proteomic data from hibernating bears muscles revealed that proteins involved in the biological processes “protein biosynthesis” and “ribosome biogenesis” were not differentially regulated between winter and summer [310], whereas all were upregulated in winter bear muscles in our transcriptomic analysis (i.e. *RPS2*⁴³, *RPS4X*, *RPS5*, *RPS7* and *RPSA*) (see Paper 6.3) [351].

Induction of RNA metabolism-related genes. We identified RNA binding motif protein 3 (RBM3) as a gene that is highly up-regulated in winter compared to summer in bear muscles (see Paper 6.3) [351]. This appears to be a common feature of many hibernators in almost all tissues (e.g. brain, heart, liver muscle) [304,306,337,352,353]. RBM3 has been described as (1) facilitating the processing of RNA molecules in the cold and protecting mRNA transcripts from degradation in hibernating ground squirrels organs [352,354,355] and (2) playing a role in RNA metabolism and mRNA-related post-transcriptional processes (e.g. trafficking, stability, translation initiation) that ultimately affect protein synthesis [356]. This is consistent with other terms related to RNA metabolism that were found to be enriched in our transcriptomic study (e.g. mRNA 3'-end processing, mRNA splicing, regulation of mRNA stability) (Figure 31) (see Paper 6.3) [351].

What does the muscle translome of the hibernating bear look like? In many cell types, transcript levels do not always predict protein levels [357], hence the emergence of the term translome. For example, synaptic plasticity requires relatively rapid *de novo* protein synthesis and specific mRNAs can be stored in neurons waiting for the precise moment to be translated [358]. To identify the level and type of mRNAs translated in hibernating versus active brown bears muscles, we could combine total RNA sequencing and ribosome profiling (ribosome sequencing). For the time being, many questions remain open, including what factors determine when and in which tissues these mRNAs should be translated? It is possible that elevated mRNAs levels of genes related to protein translation and ribosome biogenesis in winter bear muscles are waiting to be translated when needed. The transcriptional increase in protein biosynthetic-related genes detected in torpid squirrels facilitates the induction of translation in muscle during short bouts of arousal [354,355]. Bears, in contrast, do not undergo periods of arousal but maintain an alertness state during hibernation to potential dangers outside the den [294]. In agreement, we recently reported that hibernating bears have higher plasma levels of the endocannabinoid-like compound N-oleylethanolamide, which has been described to have wakefulness-promoting effects in rodents (see Appendix 10.5) [335]. Therefore, in hibernating

⁴³ ribosomal protein of the small subunit

bear muscles, the increase in protein translation-related mRNAs could serve as a rescue in case of unexpected exit from the den and thus a rapid reactivation of general protein synthesis.

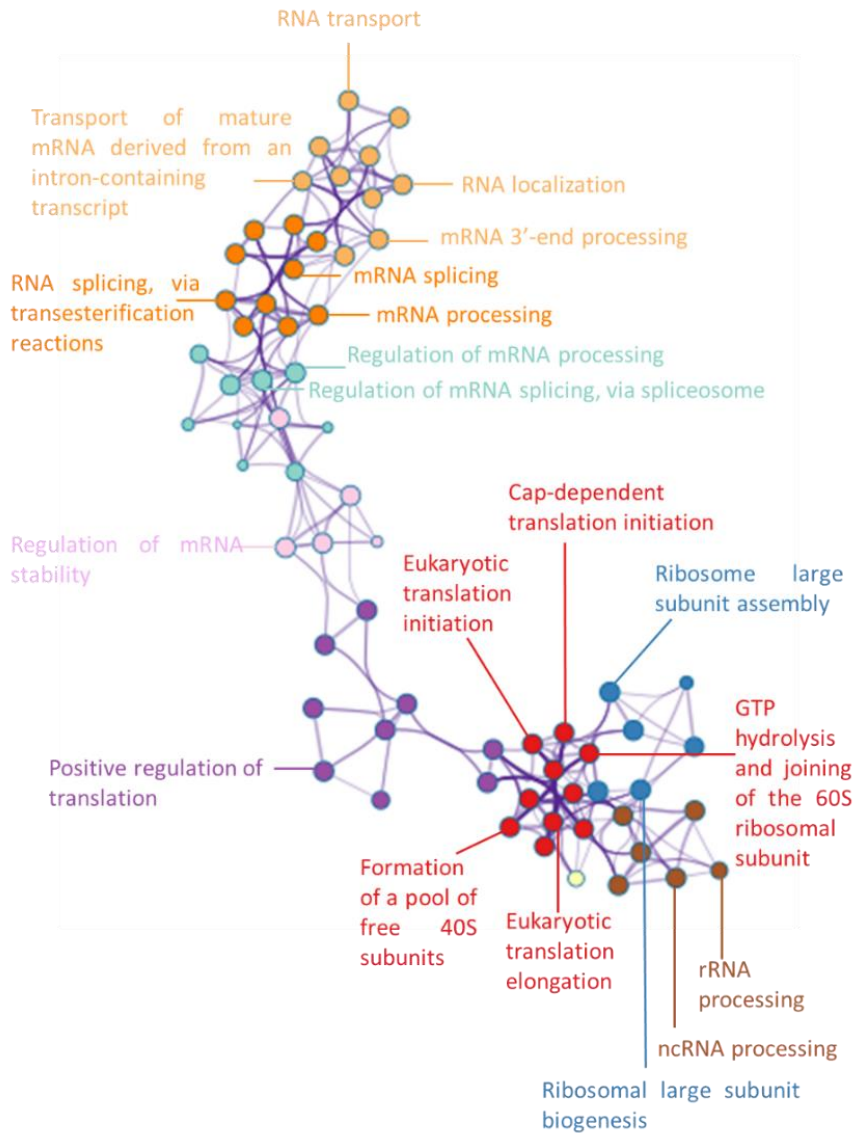


Figure 31. Detailed enriched terms from the biological processes “Protein metabolism” and “RNA metabolism” from the differentially expressed genes in Cussonneau et al., 2021 [351].

Terms written in the same colour represent closely related biological terms.

6.4.2 Hibernation induces a transcriptomic reprogramming in TGF- β superfamily-related genes in bear muscles

The main message from our study is that the TGF- β pathway is down-regulated whereas the BMP pathway is concomitantly maintained or even up-regulated at the transcriptomic level in atrophy-resistant muscles of the hibernating brown bear. Our data suggest that the balance between the TGF- β and the BMP pathways is crucial for preventing skeletal muscle atrophy during a long period of disuse [351] (Figure 30). In the following subsections we will discuss (1) the expression of target genes of BMP

signalling in skeletal muscle, (2) the regulation of the intracellular actor SMAD4, (3) the regulation of the extracellular actor CCN2, (4) the relationship between TGF- β /BMP signalling and changes in lipid membrane composition, (5) the relationship between TGF- β /BMP signalling and neuromuscular junction integrity and (6) muscle-organ crosstalk and connection with TGF- β /BMP signalling.

6.4.2.1 BMP target genes in skeletal muscle, an unresolved question

BMP transcriptional activity in hibernating bear muscles. As mentioned in the state of the art, the involvement of BMP signalling in muscle homeostasis has been only scarcely and recently investigated [166–168]. The list of up-regulated (1746 genes) and down-regulated (2369 genes) genes in the muscles of hibernating bears compared to summer was analysed using BART (Binding Analysis for Regulation of Transcription), a web server for predicting transcription factors and chromatin regulators. 88% of the top 100 transcription factors involved in the regulation of the up-regulated genes were shared with down-regulated genes. One of the common transcription factors detected was SMAD5, which is also upregulated at the mRNA level in hibernating bear muscles (see Paper 6.3) [351]. This result suggests a transcriptional activity of BMP signalling in winter bear muscles. The BMP pathway is thought to suppress the HDAC4-Myogenin axis, and thus the subsequent transcription of the E3 ligase FBXO30/MUSA1 [166,167]. However, although our data indicate that the BMP signalling is maintained and even activated in bear muscles during hibernation, there is no change in *FBXO30*, *Myogenin* or *HDAC4* expression (see Paper 6.3) [351].

Are IDs target genes for BMP signalling in skeletal muscle? The family of DNA binding inhibitor proteins (i.e. ID1-4) are specifically induced by BMP signalling in tissues such as bone and cartilage [359]. A 29 bp GC-rich element located in the 50-enhancer region of the promoter of ID1 and other BMP target genes has been identified as the BMP-responsive element (BRE), which is recognized by the SMAD1/5 and SMAD4 complex [360,361]. Furthermore, TGF- β signalling also causes an increase in *IDs* expression in certain cell types [362,363]. In skeletal muscle, *IDs* proteins are inhibitors of muscle differentiation [360,364]. *ID1* gene expression increases during ageing in human muscles and is involved in denervation-induced muscle atrophy in mice. However, under these catabolic conditions the connection with the BMP signalling has not been established [365,366]. In our transcriptomic study, we showed that *ID1-3* were downregulated whereas *ID4* remained unchanged in winter bear muscles compared to its summer counterpart (see Paper 6.3) [351]. The repression of *IDs* expression involved in muscle atrophy is consistent with the resistance to muscle atrophy in hibernating brown bears. While *IDs* appear to be target genes for BMP signalling in some tissues, our data suggest that

the transcriptional activity of the BMP pathway in muscle during disuse does not necessarily involve the transcription of IDs.

Identification of BMP target genes in skeletal muscle. To our knowledge, no study has explored the transcriptomic signature of BMP signalling in skeletal muscle. Therefore, one of the final objectives of this thesis project was to draw a list of genes induced upon activation of BMP signalling. We first looked for easy-to-use tools for the preliminary experiments and therefore chose the immortalised human muscle cell line CCL136 (rhabdomyosarcoma cell line) as they are undifferentiated cells, which saved time and made the genetic manipulation more efficient. CCL136 were transfected with a dominant negative BMP type 1 receptor (BMPR1A/ALK3) where the kinase is inactivated (K261R) blocking the signal to be transduced [367], and treated with GDF5 ligand to activate BMP signalling (see Appendix 10.1). We observed a lower induction in total and phosphorylated SMAD1/5 and SMAD4 protein contents following GDF5 treatment in CCL136 expressing ALK3-KD compared to non-transfected cells (Figure 32).

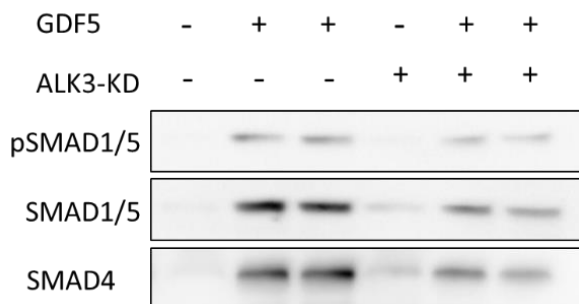


Figure 32. Western blots of total and phosphorylated SMAD1/5, and SMAD4 in CCL136 human muscle cells expressing an inactive BMP receptor.

CCL136 human muscle cells were transfected with the plasmid ALK3-KD (kinase dead) receptor, followed by 6h treatment with GDF5 ligand. BMP intracellular actors SMAD1/5 and SMAD4 were measured by Western blotting (see Appendix 10.1).

The slight decrease in SMADs protein content could be explained by compensatory mechanisms set up by cells with other BMP receptors. Unfortunately, the transfection conditions were not optimal when tested with C2C12 myotubes and human primary myotubes. For these cell lines, the use of viral particles (e.g. lentivirus) to transduce the inactive receptor could improve the transfection efficiency. In addition, other methods can be used to attenuate BMP signalling and overcome the compensatory mechanism of the receptors, for example, the use of siRNAs against SMAD1 and/or SMAD5 or treatment with the BMP inhibitor noggin. Once the optimisation is done, we will perform RNA and chromatin immunoprecipitation (ChIP) sequencing and obtain a list of BMP-dependent genes in muscle. Then, further analysis of the transcriptome of hibernating bear muscles will confirm whether the identified genes are indeed upregulated in this model of natural resistance to muscle atrophy.

6.4.2.2 Is SMAD4 stability the key to TGF- β /BMP balance in hibernating bear muscles?

Is SMAD4 recruited more by TGF- β or BMP signalling? SMAD4 is a shared component between TGF- β and BMP signalling and its recruitment to SMAD2/3 or SMAD1/5 could be a key element that determines the TGF- β /BMP balance and thus muscle homeostasis [166]. In this study, we showed that SMAD4 mRNA and protein levels increased in hibernating bear muscles, and only increased at the mRNA level in the unloaded mice muscles (see Paper 6.3) [351]. We wondered to what extent SMAD4 was recruited to TGF- β versus BMP signalling in hibernating bear muscles. Therefore, we performed co-immunoprecipitation (co-IP) of SMAD4 with SMAD1/5 or SMAD2/3 (see Appendix 10.1). Immunoprecipitation protocols were optimised for SMAD4, SMAD1/5 and SMAD2/3. However, our conditions, unfortunately, did not enable the co-immunodetection of SMAD4 with either SMAD1/5 or SMAD2/3 (Figure 33).

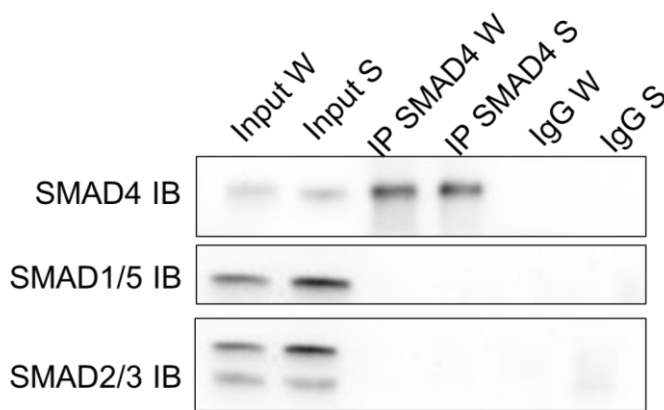


Figure 33. Co-immunoprecipitation of SMAD4 with SMAD1/5 or SMAD2/3 in bear muscles.

SMAD4 immunoprecipitation (IP) in vastus lateralis muscle from hibernating versus active brown bears was followed by immunodetection of SMAD1/5, SMAD4 and SMAD2/3 by Western blotting (IB). IgGs have been used as negative control. W: Winter; S: Summer (see Appendix 10.1).

Co-IP is highly dependent on protein-protein interactions. As bear muscles samples are necessarily frozen when sampling in the field, protein-protein interactions may have been disrupted by a freeze-thaw cycle, which may explain the lack of co-immunodetection. Another antibody against SMAD4 may be used to avoid a possible overlap of the epitope of the SMAD4 antibody with the protein-protein interaction site. Cross-linking the binding partners could also help to stabilize physiological interactions throughout extraction procedures involving mechanical and chemical stresses and thus enhance protein-protein interactions. However, for now, whether the proportion of SMAD4 recruited to TGF- β versus BMP signalling may change in winter versus summer in bear muscles remains unsolved.

SMAD4 stability could be different in bears vs. other mammals. The analysis of the SMAD4 protein sequence revealed two highly conserved domains separated by a proline-rich linker, which is a substrate for kinases and phosphatases. This linker serves as a binding platform for cofactors and ubiquitin ligases, which tag SMAD4 protein for activation or degradation [368,369]. The SMAD4 protein sequence is highly conserved in metazoans. In mammals, the bear or mouse share 98% sequence

homology with the human SMAD4 protein. In the SMAD4 linker region, a Threonine is found at position 272 (Thr272) and is well conserved from drosophila to human (Figure 34). However, in all members of the *Ursidae* family (red box), this Threonine is replaced by a Serine (Figure 34). This characteristic is not shared by other small hibernators (black box) (Figure 34).

Ursus Arctos horribilis :	GSR S APYTPNLPHH
Ursus maritimus :	GSR S APYTPNLPHH
Ursus americanus :	GSR S APYTPNLPHH
Giant panda :	GSR S APYTPNLPHH
13-lined ground squirrel :	GSR T APYTPNLPHH
Hedgehog :	GSR T APYTPNLPHH
Little brown bat :	GSR T APYTPNLPHH
Golden hamster :	GSR T APYTPNLPHH
Human :	GSR T APYTPNLPHH
Mice :	GSR T APYTPNLPHH
Rat :	GSR T APYTPNLPHH
Pig :	GSR T APYPPNLPHH
Bovine :	GSR T APYTPNLPHH
Xenopus :	GSR T AAYTPNMSHH
Zebrafish :	GTV T SP—PSVPHH
Drosophila :	GPNT L TYQSM---

Figure 34. SMAD4 linker protein sequences in different species.

The T bold in black represents the Threonine 272, while the S bold in blue represents the Serine replaced at position 272. The red box represents the *Ursidae* family members, while the black box represents examples of small hibernators.

An *in vitro* study revealed a putative regulatory site consisting of four threonines in the linker region of SMAD4, including Thr272 [370,371]. The authors showed that activation of the MAPK pathway induces phosphorylation of Thr276, which initiates three sequential phosphorylations by GSK3⁴⁴ on Thr272, 268 and 264. This generated the recognition of SMAD4 by the E3 ubiquitin ligase β -TrCP leading to its proteasome-dependent degradation [370,371] (Figure 35).

⁴⁴ glycogen synthase kinase-3

This sequential phosphorylation of SMAD4 may not be possible in the *Ursidae* due to the replacement of this Threonine by a Serine. This could thus stabilise SMAD4, explaining the slight increase in its protein content in hibernating bear muscles [351]. This change in sequence could also allow SMAD4 to interact differently with its partners. Whether this stabilisation and/or interaction with other proteins play a role in regulating the TGF- β /BMP balance in muscles remains to be explored. Myotube culture experiments could be performed by mutating Thr272 within SMAD4 to explore the consequences on TGF- β or BMP transcriptional activities. In addition, using Surface Plasmon Resonance, the real-time association and dissociation rates between wild-type or mutated SMAD4 and SMAD1/5 or SMAD2/3 could be accurately determined.

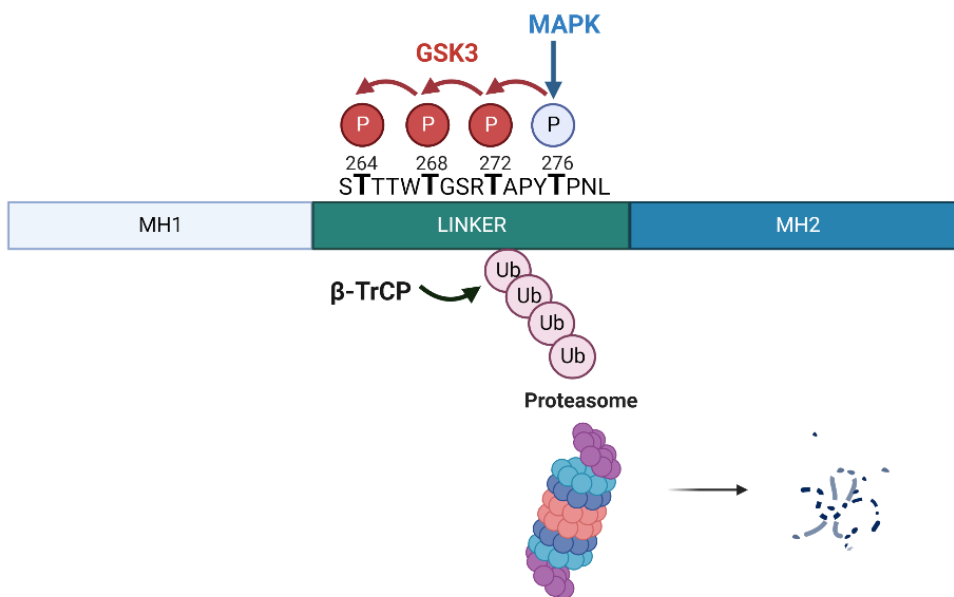


Figure 35. SMAD4 degradation involving MAPK, GSK3 and β -TrCP proteins.

6.4.2.3 CCN2 is strongly reduced in hibernating bear muscles

We showed that the cellular communication network factor 2 (CCN2) mRNA and protein levels were strongly reduced in hibernating bear muscles compared to the summer counterpart (see Paper 6.3) [351]. CCN2 is a secreted matricellular protein predominantly expressed during development in almost all tissues, during numerous pathological conditions that involve enhanced fibrogenesis, and during several cancers [372].

CCN2 and TGF- β signalling. CCN2 expression is regulated by growth factors, cytokines and hormones, including TGF- β 1 [372]. TGF- β 1 induces CCN2 gene expression and plays an important role in fibrosis, especially during dystrophies [372–375]. In turn, once secreted, CCN2 directly interacts with TGF- β ligands and thereby facilitates the signal to transduce [373,376]. Interestingly, CCN2 gene expression

has been reported to be induced by mechanical stretch *in vitro* in a TGF- β signalling-dependent manner [377]. The strong reduction in CCN2 mRNA and protein expression in winter bear muscles is consistent with the very limited mechanical demand in hibernating bear muscles, and the general downregulation of the TGF- β signalling [351]. CCN2 and TGF- β 1 proteins are significantly overexpressed in muscles from Duchenne muscular dystrophy patients and both are positively correlated with the degree of pathology and clinical severity [378]. Furthermore, TGF- β signalling also induces the gene expression of other CCN family members with common biological actions, such as CCN4 (also known as WISP1) [379], which is strongly downregulated in hibernating bear muscles compared to summer in our study (see Paper 6.3) [351]. It remains to be determined whether the downregulation of CCN2 at the transcriptomic and proteomic level in the hibernating bear muscles is a cause and/or a consequence of the TGF- β signalling inhibition. However, CCN2 inhibition is likely to be a consequence of reduced TGF- β signalling given the large number of downregulated TGF- β target genes in winter bear muscles (see Paper 6.3) [351].

CCN2 and BMP signalling. In addition, CCN2 can antagonize the activity of BMP4 and BMP7 ligands by preventing their binding to BMP receptors in *Xenopus* embryos and mice kidneys respectively, resulting in reduced SMAD1/5 signal transduction [376,380]. Moreover, surface plasmon resonance spectroscopy shows that CCN2 and GDF5 protein interacts [381]. Whether CCN2 inhibits the transduction of BMP signalling in muscles remains an open question. However, our data show that CCN2 downregulation is correlated with the maintenance of BMP signalling in winter bear muscles.

From a clinical perspective. CCN2 is considered a therapeutic target in combating fibrosis and related disorders in a variety of organs and tissues. Muscle function is improved by anti-CCN2 antibody in a mouse model of Duchenne muscular dystrophy [382]. In addition, clinical trials in phase 2 and phase 3 are currently testing another fully human monoclonal antibody that interferes with the action of CCN2 during Duchenne muscular dystrophy (ClinicalTrials.gov Identifier: NCT02606136 and NCT04632940). Hibernating bear muscles do not experience fibrosis as shown by the downregulation of most of the extracellular matrix organisation-related genes (see Paper 6.3) [351]. Therefore, our data suggest that in addition to targeting CCN2 to reduce fibrosis in muscular dystrophies, this strategy could also be of interest in other muscle-related diseases without fibrosis likewise the hibernating bear muscles.

6.4.2.4 Is the regulation of TGF- β /BMP balance linked to the modification of the lipid membrane composition?

In hibernating bear serum, we and others published an increase in free circulating fatty acids and triglycerides arising from the lipolysis of the adipose tissue [298,303,309,310,331,335]. These

profound changes in circulating lipids may have altered the composition of membrane lipids and therefore the membrane fluidity of organs, including muscle. The plasma membrane is a critical hub for signalling proteins. Membrane lipids are organised into different microdomains rich in specific lipid species, which attract different types of proteins [383,384]. A change in membrane lipid composition may have altered the heterodimerisation of TGF- β superfamily receptors known to be a dynamic process [107]. TGF- β receptors are distributed in both lipid rafts/caveolae and non-raft membrane microdomains (i.e. clathrin-coated pits). The internalisation of TGF- β receptors via clathrin-coated pits enhances TGF- β signalling, whereas lipid rafts-mediated endocytosis of TGF- β receptors facilitates receptor degradation and thus the turnoff of signalling [385–387]. Cholesterol has been suggested to inhibit SMAD2 activation, promote TGF- β receptor degradation, and therefore inhibit TGF- β signalling. This effect may result from the shifted localisation of TGF- β receptors from non-raft to lipid-raft microdomains in the plasma membrane [386–388]. On the contrary, BMP receptors have been suggested to be distributed in lipid rafts-mediated endocytosis, and a decrease in cholesterol level specifically blocks the BMP receptors-mediated intracellular signalling [389]. To test the dynamics of TGF- β superfamily receptors, we could treat myotubes with winter or summer bear serum and analyse the localisation of the receptors by confocal microscopy. We could also perform lipidomic analysis of membrane phospholipids in myotubes or biopsied bear muscles by functional two-photon microscopy.

6.4.2.5 Is the resistance to denervation-induced muscle atrophy in hibernating bears related to BMP signalling?

BMP signalling in NMJ organisation. BMP signalling is important for the conservation of muscle mass when the neuromuscular junction (NMJ) is compromised, as reported in a model of denervation-induced muscle atrophy in mice [166–168]. In addition, disruption of presynaptic architecture and NMJ degeneration concomitantly to BMP signalling perturbation are observed in muscles of tumour-bearing mice before muscle loss occurred [168]. The same feature was also observed in muscles from pre-cachectic cancer patients [168]. Promoting BMP signalling using genetic or drug-based interventions (tilorone) preserves NMJ function during the development of cachexia and therefore counteract muscle atrophy [168]. On the contrary, overexpression of the BMP inhibitor noggin in muscles of healthy mice induced muscle atrophy, mimicked the loss of presynaptic motor neuron terminals and increased the presence of denervation markers [168]. The BMP pathway regulates peripheral synaptic development and plasticity in *Drosophila* [390,391] and is essential for proper axon elongation in motor neurons during development in mice [392]. However, the role of BMP in controlling postnatal NMJ remodelling in adult mammals, particularly in pathological contexts, remains largely unexplored. TAK1 is involved in non-SMAD TGF- β /BMP signalling (see section 4.2.4.2) and the

receptor tyrosine kinase MuSK (muscle-specific kinase) is a co-receptor of BMP signalling promoting its signalling in muscle cells [393]. Both are up-regulated in muscle of the hibernating brown bears in our study (see Paper 6.3) [351]. Interestingly, (1) activation of TAK1 promotes skeletal muscle growth and mitigates neurogenic atrophy through a SMAD1-dependent mechanism [184] and (2) MuSK is critical for neuromuscular junction formation and maintenance [394].

NMJ in hibernating bear muscles. Amazingly, hibernating bears are partially resistant to denervation-induced muscle atrophy, whereas summer-active bears are susceptible to it like other mammals [328]. Whether the maintenance of BMP signalling in muscles is responsible for this resistance remains to be elucidated (Figure 36). No study has yet explored in detail the structure and characteristics of the NMJ in active versus hibernating bears. For that purpose, histological studies of NMJ markers will be soon initiated in our laboratory.

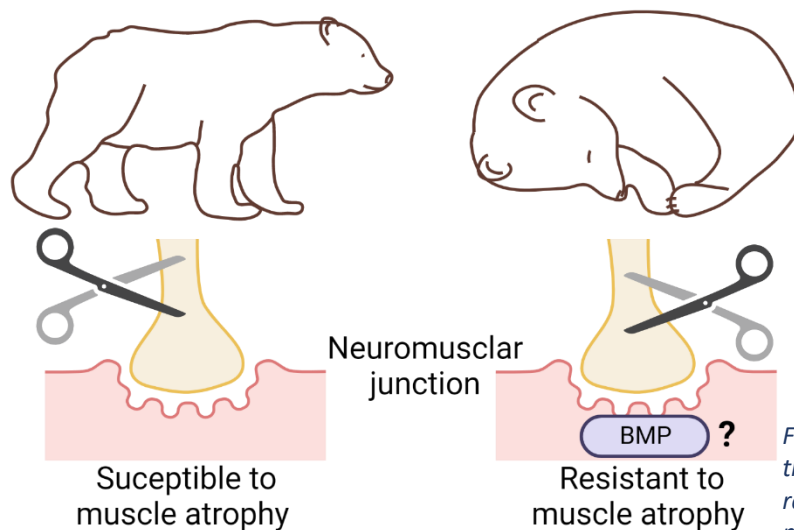


Figure 36. Hypothetical schema to explain the denervation-induced muscle atrophy resistance in the hibernating brown bears muscles.

6.4.2.6 The muscle-organ crosstalk and connection with TGF- β /BMP signalling.

Is GDF5 synthesised and released by adipose tissue? GDF5 and its receptor *BMPRI1B* are strongly upregulated in the hibernating bear muscles relative to its summer counterpart, whereas significantly downregulated in the unloaded mice muscles (see Paper 6.3) [351]. We wondered whether the GDF5 ligand was increased in winter bear serum and could explain the induction of BMP-related gene transcription. Unfortunately, serum GDF5 concentration could not be measured because the only commercially available ELISA⁴⁵ kit did not work in bears (see Appendix 10.1). GDF5 is primarily

⁴⁵ enzyme linked immunosorbent assays

synthesised and secreted by the salivary glands, which is probably not a dynamic tissue during hibernation since bears do not drink or eat for 6 months. GDF5 is also present in adipose tissue (Human Protein Atlas data <https://www.proteinatlas.org/ENSG00000125965-GDF5/tissue>). In mice, GDF5 promotes thermogenesis in subcutaneous white adipose tissue (sWAT) after cold exposure via non-SMAD p38 signalling [395]. In addition, GDF5 facilitates the development of brown fat-like cells in sWAT tissue via SMAD1/5 signalling in mice [396]. However, brown fat in hibernating brown bears has only been described in one study [397], which was subsequently refuted [398]. Shivering plays a role in active thermogenesis in muscles, but there is also non-shivering thermogenesis that occurs primarily through the metabolism of brown fat and, to a lesser degree, white fat [399]. If GDF5 is increased in winter bear serum, it would not only contribute to the maintenance of muscle mass induced by BMP signalling but could also play a role in non-shivering thermogenesis in white adipose tissue (Figure 37). The concentration of GDF5 in bear serum could be assessed by mass spectrometry. Moreover, exploring the gene/protein expression of GDF5 and BMP-related components in adipose tissue could provide valuable information on whether GDF5 is synthesised and released from adipose tissue into the bloodstream during hibernation.

TGF- β signalling and muscle-bone communication. A new concept has emerged that bone also acts as an endocrine tissue targeting other organs such as muscle. Therefore, muscle and bone communicate via soluble factors [400]. Both bone and muscle volumes are sensitive to mechanical loading, which regulates many of their secreted factors. Therefore, muscle and bone mass are both reduced during immobilisation [401]. Bone resorption releases TGF- β 1 into the bloodstream in pediatric burn patients and tumour-bearing mice [402,403]. The use of antiresorptive drugs protects bone and muscle mass, demonstrating that a factor released by bones contributes to muscle wasting in these conditions. TGF- β 1 released from bone suppresses activation of the AKT/mTOR anabolic pathway and promotes expression of UPS players in myoblasts *in vitro* [403]. TGF- β ligands are produced by osteoblasts, stored in the extracellular matrix of bone and released by osteoclastic proteolysis during bone resorption [404,405].

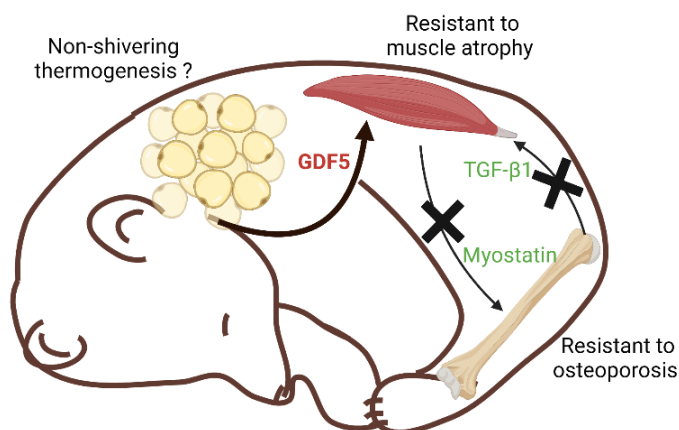


Figure 37. Hypothetical schema of the origin of muscle transcriptomic changes of TGF- β superfamily.

In green and red, the genes down- and upregulated respectively in hibernating bear muscles in Cussonneau et al., 2021 [351].

In addition, myostatin, produced in muscle, stimulates the production and the differentiation of osteoclasts responsible for bone resorption through SMAD-dependent signalling [406–409]. Inhibition of myostatin in muscles can result in either increased bone formation under physiological conditions or decreased bone resorption under pathological conditions [410–412]. Interestingly, *TGFB1* and *MSTN* are downregulated in hibernating bear muscles in our study (see Paper 6.3) [351] and previous studies have clearly shown that bears do not suffer from osteoporosis despite long-term inactivity, lack of food, and cold exposure during hibernation [413]. Furthermore, peripheral blood mononuclear cells collected from hibernating Japanese black bears and cultured with hibernating bear serum do not differentiate into osteoclasts, unlike cells cultured with active bear serum [414]. This study implies the presence of circulating compounds during hibernation that protect bone from resorption. Altogether, these observations raise questions about whether or not soluble bone and muscle factors are secreted during hibernation in bears. Because TGF- β /BMP pathways are ubiquitous throughout the body, their regulation in one place is likely to imply consequences in another place. Is it because bone resorption does not occur in bears during winter that muscle atrophy does not occur either, or is it the other way around (Figure 37)?

7. Study 2: Induction of ATF4 atrogenes is uncoupled from disuse-induced muscle atrophy in halofuginone-treated mice and in hibernating brown bear

7.1 Objective and strategy

In this study, we aimed to explore the impacts of a controlled induction of ATF4 signalling on skeletal muscle. We selected the molecule halofuginone (HF), which (1) induces eIF2 α -ATF4 signalling and (2) is already used and well tolerated in mouse dystrophic models. We designed an experimental protocol, choosing (1) the dose of HF, (2) the mode and frequency of administration, and (3) the duration of treatment (data not shown). Once the protocol was validated, it was tested in mice either in basal conditions or when they were subsequently subjected to muscle atrophy induced by hindlimb suspension (HS) (Figure 38). We also took advantage of a model of muscle atrophy resistance that we previously explored (see Paper 6.3) [351] and studied the regulation of the ATF4 atrogenes in the hibernating brown bear muscles. We showed that induction of ATF4 signalling was not associated with atrophy in muscles from HF-treated mice or hibernating brown bears. We also investigated the molecular mechanisms of HF in skeletal muscle.

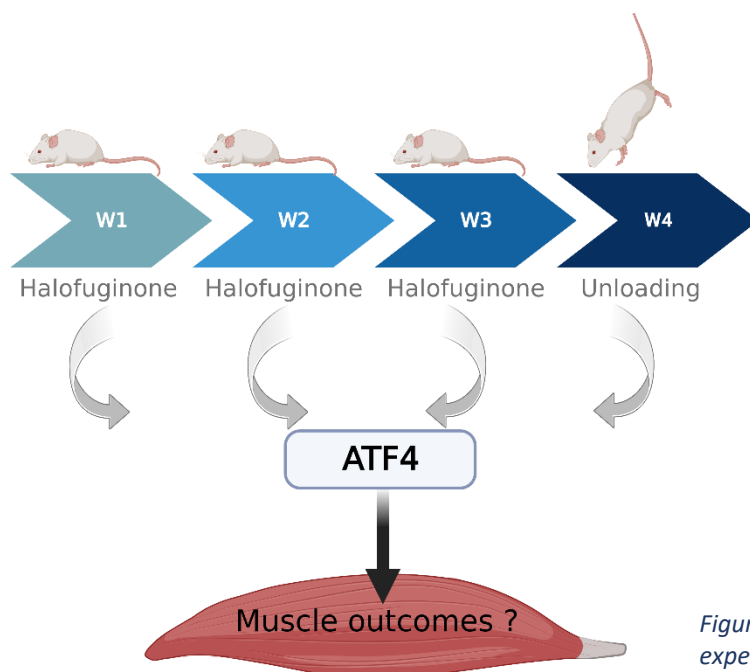


Figure 38. Schema of the experimental strategy of study 2.

7.2 Paper



Article

Induction of ATF4-Regulated Atrogenes Is Uncoupled from Muscle Atrophy during Disuse in Halofuginone-Treated Mice and in Hibernating Brown Bears

Laura Cussonneau ^{1,*} , Cécile Coudy-Gandilhon ¹, Christiane Deval ¹, Ghita Chaouki ¹, Mehdi Djelloul-Mazouz ¹, Yoann Delorme ¹, Julien Hermet ¹, Guillemette Gauquelin-Koch ², Cécile Polge ¹ , Daniel Taillandier ¹, Julien Averous ¹, Alain Bruhat ¹, Céline Jousse ¹, Isabelle Papet ¹ , Fabrice Bertile ³ , Etienne Lefai ¹ , Pierre Fafournoux ¹, Anne-Catherine Maurin ¹ and Lydie Combaret ^{1,*}

¹ Université Clermont Auvergne, INRAE, UNH UMR 1019, CRNH Auvergne, 63000 Clermont-Ferrand, France

² Centre National d'Etudes Spatiales, CNES, 75001 Paris, France

³ Université de Strasbourg, CNRS, IPHC UMR 7178, 67037 Strasbourg, France

* Correspondence: laura.cussonneau@inrae.fr (L.C.); lydie.combaret@inrae.fr (L.C.)

Abstract: Activating transcription factor 4 (ATF4) is involved in muscle atrophy through the overexpression of some atrogenes. However, it also controls the transcription of genes involved in muscle homeostasis maintenance. Here, we explored the effect of ATF4 activation by the pharmacological molecule halofuginone during hindlimb suspension (HS)-induced muscle atrophy. Firstly, we reported that periodic activation of ATF4-regulated atrogenes (*Gadd45a*, *Cdkn1a*, and *Eif4ebp1*) by halofuginone was not associated with muscle atrophy in healthy mice. Secondly, halofuginone-treated mice even showed reduced atrophy during HS, although the induction of the ATF4 pathway was identical to that in untreated HS mice. We further showed that halofuginone inhibited transforming growth factor- β (TGF- β) signalling, while promoting bone morphogenetic protein (BMP) signalling in healthy mice and slightly preserved protein synthesis during HS. Finally, ATF4-regulated atrogenes were also induced in the atrophy-resistant muscles of hibernating brown bears, in which we previously also reported concurrent TGF- β inhibition and BMP activation. Overall, we show that ATF4-induced atrogenes can be uncoupled from muscle atrophy. In addition, our data also indicate that halofuginone can control the TGF- β /BMP balance towards muscle mass maintenance. Whether halofuginone-induced BMP signalling can counteract the effect of ATF4-induced atrogenes needs to be further investigated and may open a new avenue to fight muscle atrophy. Finally, our study opens the way for further studies to identify well-tolerated chemical compounds in humans that are able to fine-tune the TGF- β /BMP balance and could be used to preserve muscle mass during catabolic situations.

Keywords: skeletal muscle; unloading; hindlimb suspension; halofuginone; ATF4; TGF- β /BMP signalling; hibernating bear; atrogenes; muscle atrophy



Citation: Cussonneau, L.; Coudy-Gandilhon, C.; Deval, C.; Chaouki, G.; Djelloul-Mazouz, M.; Delorme, Y.; Hermet, J.; Gauquelin-Koch, G.; Polge, C.; Taillandier, D.; et al. Induction of ATF4-Regulated Atrogenes Is Uncoupled from Muscle Atrophy during Disuse in Halofuginone-Treated Mice and in Hibernating Brown Bears. *Int. J. Mol. Sci.* **2023**, *24*, 621. <https://doi.org/10.3390/ijms24010621>

Academic Editors: Manuela Malatesta and Emerito Carlos Rodriguez-Merchan

Received: 14 October 2022
Revised: 21 December 2022
Accepted: 22 December 2022
Published: 30 December 2022



Copyright: © 2022 by the authors. Licensee MDPI, Basel, Switzerland. This article is an open access article distributed under the terms and conditions of the Creative Commons Attribution (CC BY) license (<https://creativecommons.org/licenses/by/4.0/>).

1. Introduction

Many unloading conditions (e.g., microgravity, bed rest, or physical inactivity) lead to a loss of muscle mass and strength. This muscle atrophy is associated with adverse health effects such as autonomy decline and increased morbidity and mortality [1–3]. Considering the lack of proven, easy-to-use therapeutic or preventive treatment, muscle atrophy remains a major public health issue (World Health Organisation data) [4].

The underlying molecular mechanisms of muscle atrophy involve the dysregulation of a complex network of intracellular pathways leading to an imbalance in protein turnover [5–9]. Activating transcription factor 4 (ATF4) is overexpressed in many conditions of muscle atrophy [10–14] and is, therefore, considered as an atroge, i.e., one of the genes with expression at the mRNA level that is commonly altered during atrophy [14].

ATF4 belongs to the integrated stress response (ISR) pathway, a conserved intracellular network activated in response to various intrinsic and extrinsic stresses (e.g., amino acid (AA) depletion and endoplasmic reticulum (ER) stress) to restore cellular homeostasis [15]. Activation of the ISR involves phosphorylation of eukaryotic translation initiation factor 2 (eIF2 α) by several kinases (i.e., general control nonderepressible 2 (GCN2), protein kinase RNA-like ER kinase (PERK), protein kinase R (PKR), heme-regulated inhibitor (HRI), and microtubule affinity-regulating kinase 2 (MARK2)), resulting in the global inhibition of protein synthesis but the increased translation of certain mRNAs, including ATF4 [15,16]. Inhibition of ATF4 in skeletal muscle limits starvation-, immobilisation-, and ageing-induced atrophy, whereas ATF4 induction results in muscle wasting [11–13,17]. ATF4 target genes include some atrogenes, such as GADD45A and CDKN1A, that are required for ATF4-mediated muscle atrophy [11–13,18], and TRIB3, which is involved in fasting- and ageing-induced muscle atrophy [19,20]. However, ATF4 targets also include genes that may be involved in the maintenance of muscle homeostasis. Indeed, ATF4 contributes to the transcription of autophagy-related genes [21–24] and is activated during mitochondrial perturbations (e.g., oxidative stress) to restore mitochondrial homeostasis [25,26]. In fact, activation of the eIF2 α -ATF4 pathway by the pharmacological molecule halofuginone (HF), prior to stressful events (i.e., ischemia-reperfusion injury models) has shown positive effects on the preservation of kidney and liver function [27]. Moreover, the maintenance of autophagy and mitochondria homeostasis are essential for maintaining muscle mass [28–30]. Altogether, this led to the hypothesis that the ATF4 pathway may have a dual role in skeletal muscle.

Interestingly, halofuginone also improved muscle performance during dystrophies, mainly through its antifibrotic properties [31–34]. Whether these beneficial effects involve a regulation of the ATF4 pathway has never been investigated. However, they mainly involved the inhibition of the transforming growth factor- β (TGF- β) pathway [35–37]. The TGF- β signalling pathway acts as a negative regulator of muscle mass, notably through the transcriptional induction of the atrogenes TRIM63/MuRF1 and FBXO32/Atrogin-1 [38–40]. When inhibited, it promotes a profound muscle hypertrophy phenotype in various conditions and species [41,42]. Members of TGF- β signalling belong to the TGF- β superfamily [38,39], as do the bone morphogenetic protein (BMP) signalling members. The BMP signalling pathway [39,43] instead acts as a positive regulator of muscle mass through the transcriptional repression of the atrogene FBXO30/Musa1, which is required for denervation-induced muscle loss [44,45]. When inhibited, it profoundly exacerbates denervation-induced muscle atrophy [44,45].

This study aimed to explore the impacts of HF-induced ATF4 signalling on skeletal muscle under basal conditions and hindlimb suspension-induced atrophy in mice. We further deciphered the molecular mechanisms of HF by focusing on protein metabolism and TGF- β /BMP signalling. We also took advantage of a model of muscle atrophy resistance that we previously explored [46], and studied the regulation of the ATF4-induced atrogenes in hibernating brown bear muscle.

2. Results

2.1. Induction of ATF4-Regulated Atrogenes Does Not Affect Muscle Mass in Mice

We used halofuginone (HF) to induce ATF4 transcriptional activity in mouse muscles, and we investigated the effect on skeletal muscle mass. For that purpose, mice were treated with HF three times a week for up to 4 weeks. Six hours after the last HF administration at the end of each week, we measured the mRNA levels for some ATF4 target genes, involved in muscle atrophy, i.e., *Trib3*, *Cdkn1a*, *Gadd45a*, and *Eif4ebp1* (Figure 1A–F). Except for *Atf4*, for which mRNA levels were elevated during the first 2 weeks of HF treatment, *Trib3*, *Cdkn1a*, and *Gadd45a* were all overexpressed in muscles after 2 weeks of HF treatment compared to H₂O-treated mice. Of note, *Eif4ebp1* mRNA levels increased in mouse muscles after 4 weeks of HF-treatment compared to H₂O, with a noticeable trend after 3 weeks of treatment (Figure 1F). We also investigated the regulation of other ATF4 target genes and

showed the overexpression of *Asns* over the 4 weeks of HF treatment as well as a trend for *Ddit3* and *Ppp1r15a* (Supplementary Figure S1).

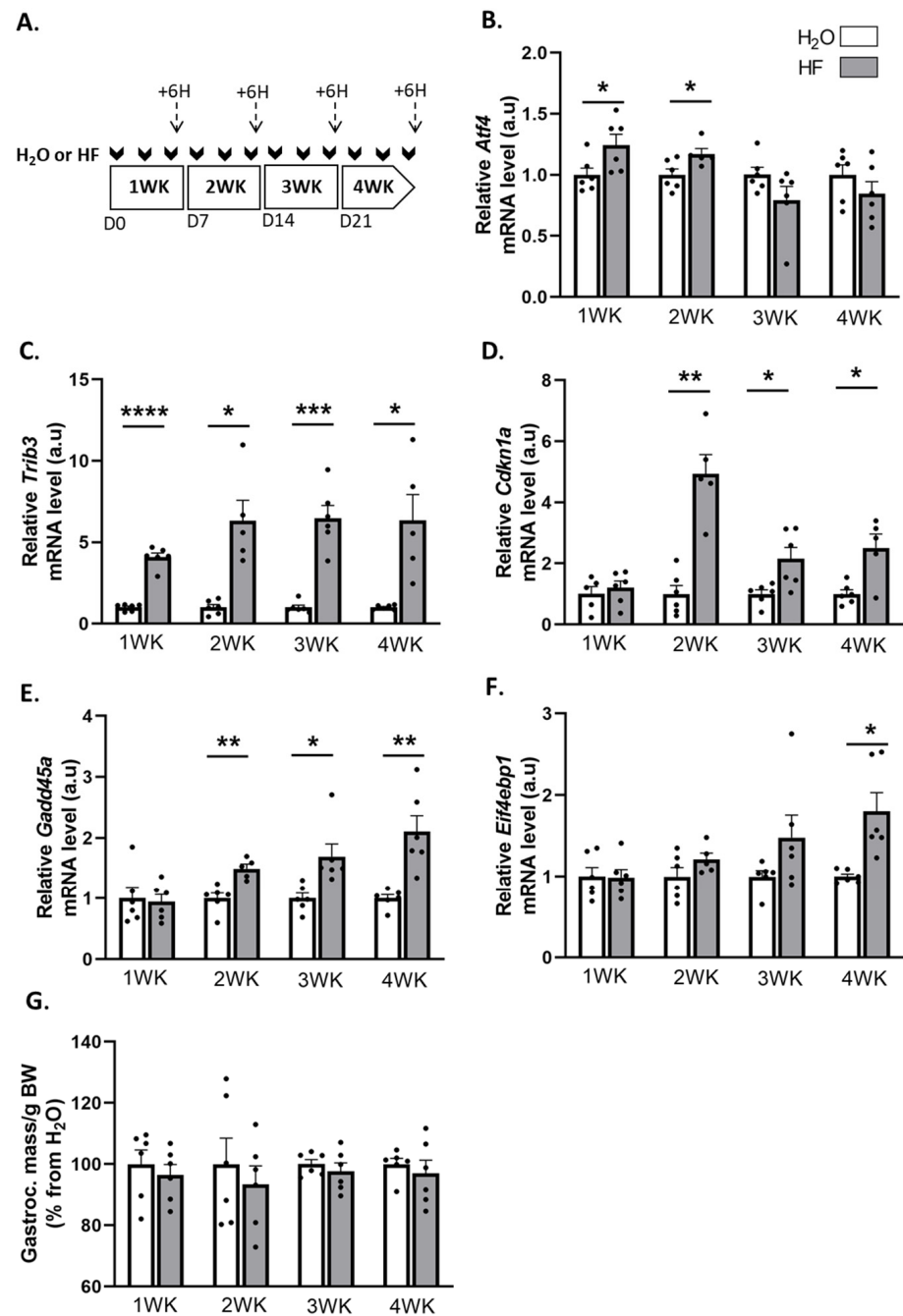


Figure 1. Halofuginone activates the expression of ATF4-regulated atrogenes in muscle without leading to atrophy. (A) Schematic representation of the experimental protocol, where mice received H₂O (white bars) or HF (0.25 μg/g, grey bars) 3 times a week for up to 4 weeks (WK). Muscles were collected 6 h after the last HF administration at the end of each week (dotted arrows). (B–F) Relative mRNA levels in gastrocnemius for *Atf4*, *Trib3*, *Cdkn1a*, *Gadd45a*, and *Eif4ebp1* were measured by RT-qPCR. Data were normalised using *Tbp*. Data are expressed as fold change vs. H₂O within each week and are presented as individual values with mean bars ± SEM. (G) Gastrocnemius muscle mass per gram of body weight (BW). Data are expressed as a percentage from H₂O within each week and presented as individual values with mean bars ± SEM. Statistics are described in Section 4. * $p_{adj} < 0.05$; ** $p_{adj} < 0.01$; *** $p_{adj} < 0.001$; **** $p_{adj} < 0.0001$.

These data underline an activation of the ATF4 transcriptional activity. However, despite the overexpression of the ATF4-regulated atrogenes, the mass of the gastrocnemius, soleus, tibialis anterior, and extensor digitorum longus (EDL) muscles remained unchanged during the 4 weeks of HF treatment (Figure 1G, Supplementary Figure S1). Altogether, these data suggest that a long-term halofuginone administration induced ATF4-regulated atrogenes without leading to muscle atrophy.

2.2. Overexpression of ATF4-Regulated Atrogenes during Hindlimb Suspension Is Uncoupled from Muscle Atrophy in HF-Treated Mice

We then investigated the effect of the induction of the ATF4 pathway by HF treatment during the muscle atrophy induced by hindlimb suspension (HS). Briefly, mice received HF three times a week for 3 weeks and were then, 3 days after the last HF administration, hindlimb-suspended or not for 3 or 7 days (Figure 2A). Measurements were thus performed at least 6 days after the last HF administration. HF induces ATF4 activation through the phosphorylation of eIF2 α [47]. We observed that HF treatment resulted in overall higher phosphorylated and total eIF2 α protein levels compared to H₂O-treated mice (Figure 2B–D). In addition, HS led to an overall decrease in phosphorylated eIF2 α protein levels compared to the controls (Ctrls) (Figure 2B,C). In addition, levels of the mRNA encoding the phosphatase GADD34 (*Ppp1r15a*) were higher at 3 days of hindlimb suspension (HS3) compared to the Ctrls in both H₂O- and HF-treated mice (Supplementary Figure S2). The expression of ATF4-regulated genes was not different between Ctrl-HF and Ctrl-H₂O groups (Figure 2 and Supplementary Figure S2). The mRNA levels of *Atf4* and its target genes involved in muscle atrophy, i.e., *Trib3*, *Cdkn1a*, and *Eif4ebp1*, were higher during HS in both H₂O- and HF-treated mice (Figure 2E–H), while the mRNA levels of the ATF4-regulated atrogenes *Gadd45a* remained unchanged (Figure 2I). Of note, mRNA expression of other ATF4 target genes remained unchanged for *Asns* or slightly decreased upon HS for *Ddit3*. (Supplementary Figure S2). Altogether, Figures 1 and 2 shows that (i) HF administration induced ATF4-regulated atrogenes after 6 h, but no more after 6 days, indicating that this effect was rapid and transient, and (ii) HS induced overexpression of these atrogenes.

We next investigated the outcomes on skeletal muscle. Gastrocnemius muscle had atrophied only in H₂O-treated mice after 3 days of HS (H₂O-HS3) and in both H₂O- and HF-treated mice after 7 days of HS. Surprisingly, the average of the fibre cross-sectional area (CSA) did not change in H₂O-HS3 mice compared to the Ctrls but was lower after HS7 regardless of the treatment (Figure 3B). We further analysed the distribution of gastrocnemius fibre CSA (Supplementary Figure S3A,B). We reported (i) a lower proportion of small fibres and (ii) a higher proportion of large fibres in HF-treated mice compared to the H₂O group (Supplementary Figure S3A). This observation was restricted to fast-twitch fibres (i.e., 2X/2B) (Supplementary Figure S3B). Taken together, our data suggest that induction of ATF4-regulated atrogenes is not associated with muscle atrophy after 3 days of hindlimb suspension in HF-treated mice and, thus, that HF slightly preserves muscle mass during HS.

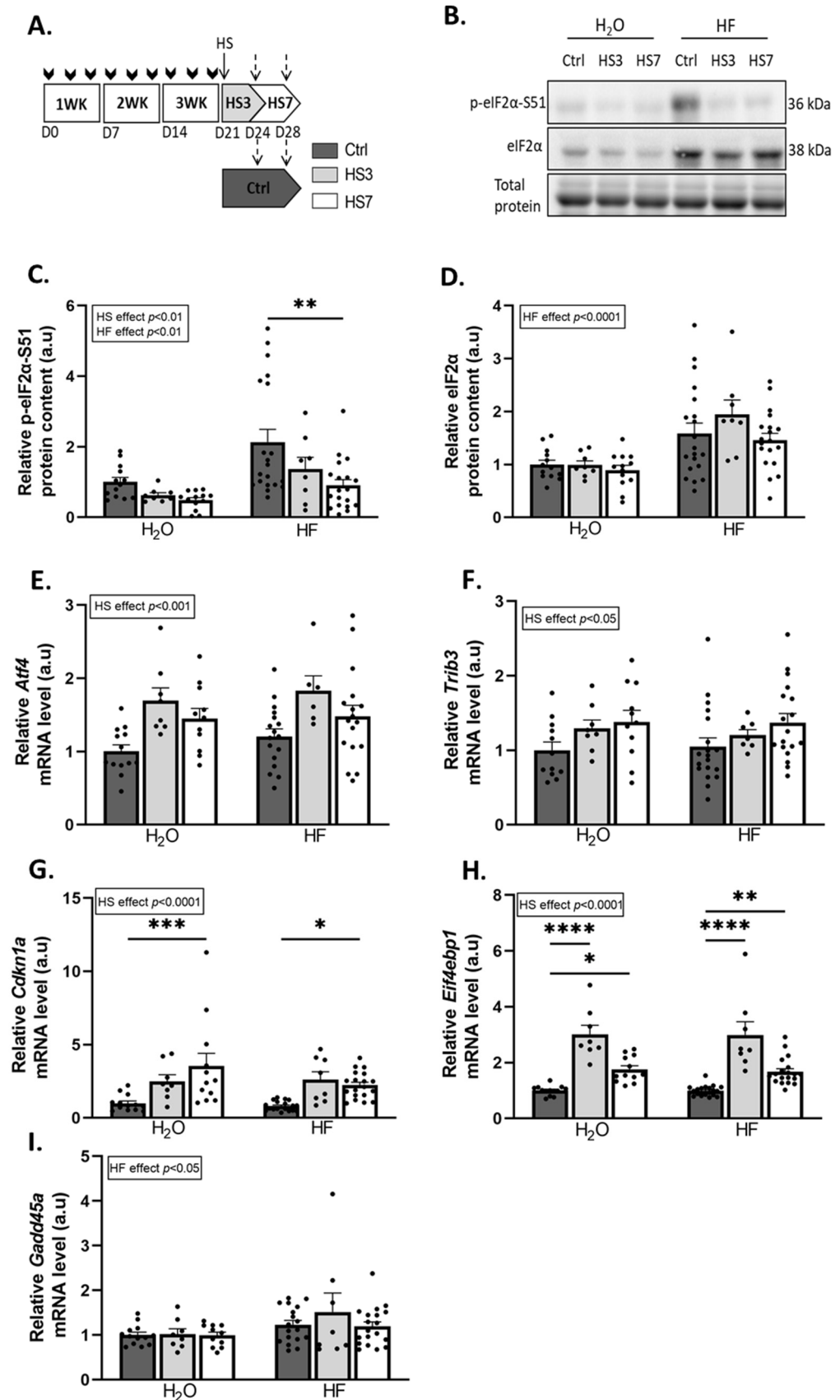


Figure 2. Hindlimb suspension induces ATF4 pathway. (A) Schematic representation of the experimental protocol, where mice received H₂O or halofuginone (HF) oral administration (0.25 μg/g) 3 times a week for 3 weeks (WK) (black arrows) and were then subjected to hindlimb suspension

for 3 (HS3, light grey bars) or 7 (HS7, white bars) days or kept unsuspended (Ctrl, dark grey). The dotted arrows represent the time when the muscles were collected. (B–D) Relative protein levels in gastrocnemius for phosphorylated and total eIF2 α were measured by Western blotting, quantified, and normalised to the total protein content. Representative Western blots are shown. (E–I) Relative mRNA levels in gastrocnemius for *Atf4*, *Trib3*, *Cdkn1a*, *Eif4ebp1*, and *Gadd45a* were measured by RT-qPCR and were normalised using *Tbp*. Data are expressed as fold change vs. H₂O-Ctrl and are presented as individual values normalised mean bars \pm SEM. Statistics are described in Section 4. * $p_{\text{adj}} < 0.05$; ** $p_{\text{adj}} < 0.01$; *** $p_{\text{adj}} < 0.001$; **** $p_{\text{adj}} < 0.0001$.

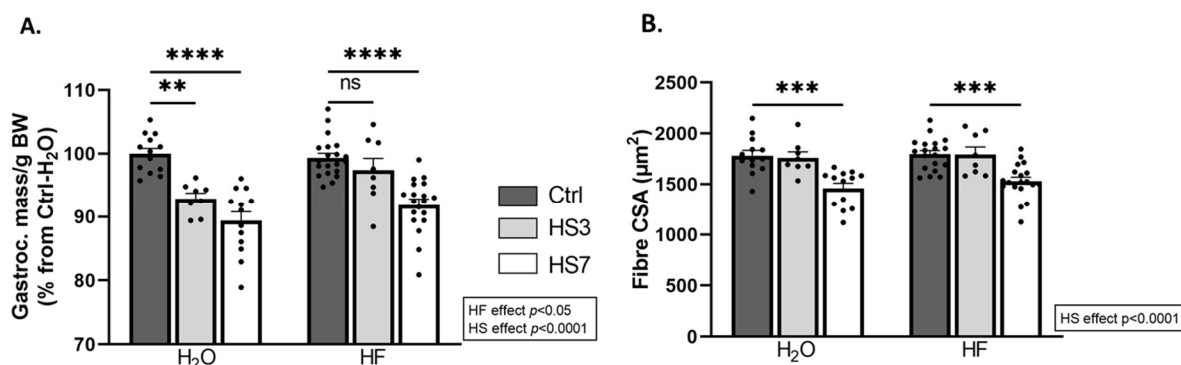


Figure 3. Halofuginone treatment prior to hindlimb suspension mitigates atrophy in gastrocnemius muscle. Mice were treated with H₂O or halofuginone (HF, 0.25 $\mu\text{g/g}$) 3 times a week for 3 weeks and were then subjected to hindlimb suspension for 3 (HS3, light grey bars) or 7 (HS7, white bars) days or kept unsuspended (Ctrl, dark grey bars), as described in Figure 2A. (A) Gastrocnemius muscle mass per gram of body weight (BW). Data are expressed as a percentage from H₂O-Ctrl and presented as individual values with mean bars \pm SEM. (B) Mean fibre cross-sectional area in gastrocnemius muscle. Data are presented as individual values with mean bars \pm SEM. Statistics are described in Section 4. ** $p_{\text{adj}} < 0.01$; *** $p_{\text{adj}} < 0.001$; **** $p_{\text{adj}} < 0.0001$; ns = non-significant.

2.3. Halofuginone Treatment Inhibits TGF- β While Promoting BMP Signalling in Gastrocnemius Muscle

HF inhibits the TGF- β pathway [36,48]. We and others have recently reported that inhibition of the TGF- β signalling is associated with the concomitant activation of BMP signalling [45,46]. Therefore, we investigated how HF treatment and subsequent HS treatment affected these pathways in skeletal muscle. The nuclear localisation of SMADs mirrors the upstream activation of the TGF- β or BMP pathway [49]. We, thus, measured protein levels for the transcription factors SMAD2/3 (TGF- β signalling), SMAD1/5 (BMP signalling), and SMAD4 (TGF- β and BMP signalling) in nuclear and cytosolic fractions (Figure 4A–D and Supplementary Figure S4A–F). The ratio of nuclear SMAD2/3 to total SMAD2/3 was very low in HF-treated mice compared to H₂O-treated mice and decreased upon HS only in H₂O-treated mice (Figure 4A,B). Consistently, the overall mRNA levels of several collagens, which are well-known target genes of TGF- β signalling, decreased upon HS (Supplementary Figure S5). Moreover, the ratio of nuclear SMAD1/5 to total SMAD1/5 was higher in HF-Ctrl mice than in H₂O-Ctrl mice. This ratio was reduced at HS7 compared to the Ctrl in HF-treated mice, while it was increased in H₂O-treated mice (Figure 4A,C). Finally, the ratio of nuclear SMAD4 to total SMAD4 was overall lower in HF- vs. H₂O-treated mice (Figure 4A–D), with a decrease in HF-treated mice at HS7 compared to the Ctrl.

TGF- β catabolic action involves the inhibition of protein synthesis [40,50,51], whereas the anabolic action of BMP involves its promotion [44]. The overall protein-synthesis rates measured by puromycin incorporation were reduced during hindlimb suspension. However, this decrease was only significant in H₂O-HS7 compared to H₂O-Ctrl mice (Figure 5A,B). TGF- β signalling acts also as a negative regulator of muscle mass through the induction of the atrogenes TRIM63/MurF1 and FBXO32/Atrogin-1 [38,39], while BMP

signalling acts as a positive regulator with the transcriptional repression of the atrogene *FBXO30/Musa1* [44,45]. *Trim63* and *Fbxo32* mRNA levels were upregulated only at HS3 in both H₂O and HF-treated mice, while mRNA levels for the atrogene *Fbxo30* remained unchanged (Figure 5C–E). Our data suggest that while HF inhibits TGF- β signalling, it also promotes BMP signalling in the control gastrocnemius muscles. We also showed that HF partially attenuates the drop in protein synthesis during hindlimb suspension.

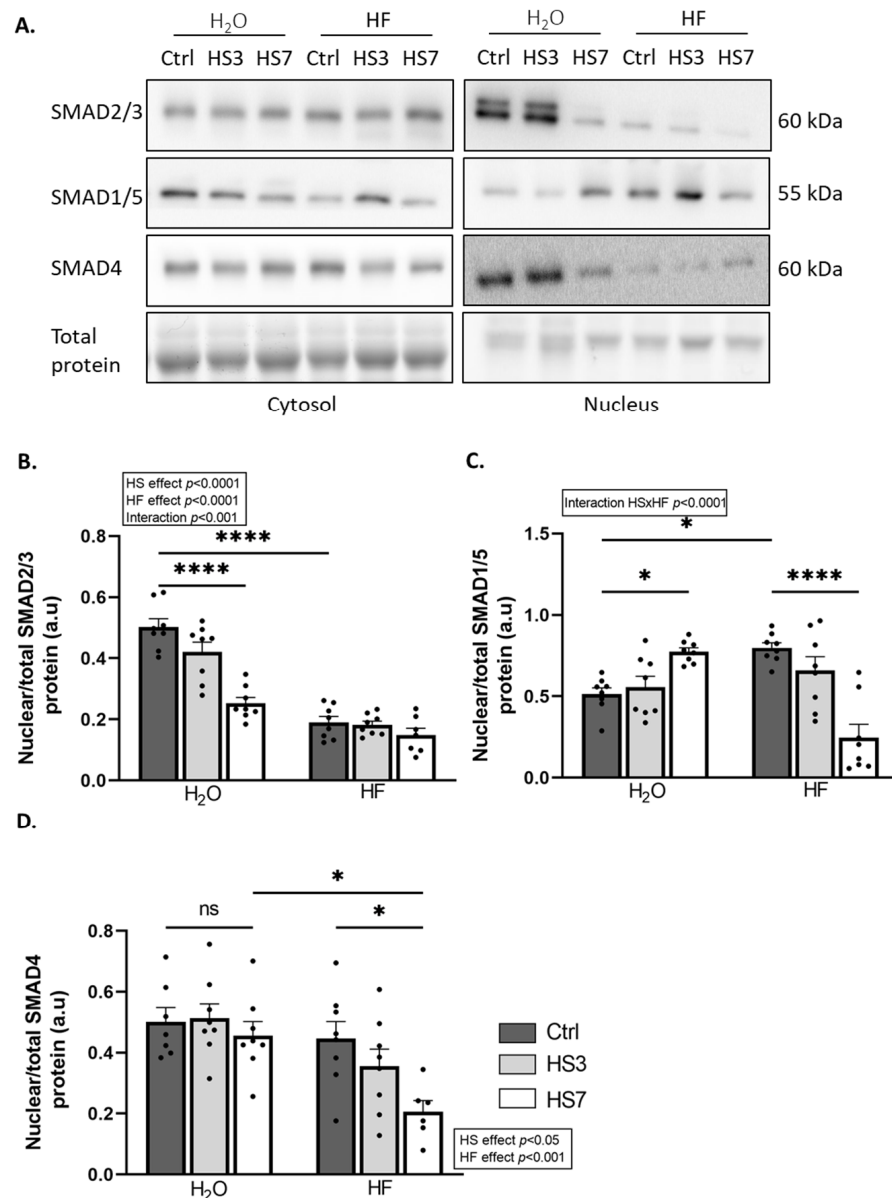


Figure 4. Halofuginone treatment inhibits TGF- β while promoting BMP signalling in gastrocnemius muscle. Mice were treated with H₂O or halofuginone (HF, 0.25 μ g/g) 3 times a week for 3 weeks and were then subjected to hindlimb suspension for 3 (HS3, light grey bars) or 7 (HS7, white bars) days or kept unsuspended (Ctrl, dark grey bars), as described in Figure 2A. (A–D) The ratio of protein levels in gastrocnemius for the transcription factors SMAD2/3 (TGF- β signalling), SMAD1/5 (BMP signalling), and SMAD4 (TGF- β and BMP signalling) have been assessed in the nuclear and cytosolic subcellular fractions, quantified, and normalised to the total protein content. Representative Western blots are shown. The ratio of nuclear SMAD contents on the total (cytosolic and nuclear) SMAD content was calculated. Data are expressed as fold change vs. H₂O-Ctrl and presented as individual values with mean bars \pm SEM. Statistics are described in Section 4. * $p_{\text{adj}} < 0.05$; **** $p_{\text{adj}} < 0.0001$.

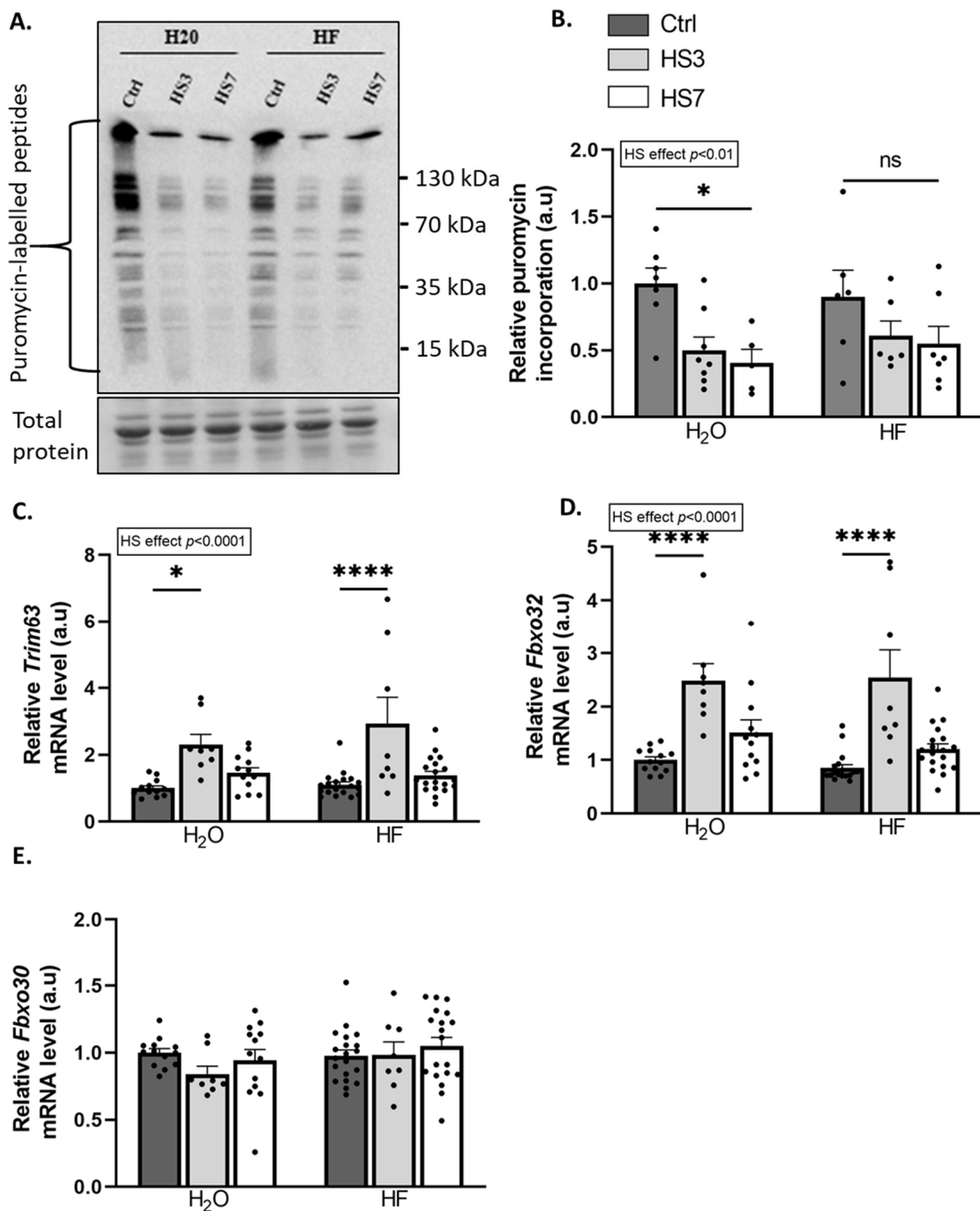


Figure 5. Halofuginone treatment prior to hindlimb suspension partially prevents the decrease in protein synthesis in gastrocnemius muscle. Mice were treated with H₂O or halofuginone (HF, 0.25 μ g/g) 3 times a week for 3 weeks and were then subjected to hindlimb suspension for 3 (HS3, light grey bars) or 7 (HS7, white bars) days or kept unsuspended (Ctrl, dark grey bars), as described in Figure 2A. (A,B) Relative puromycin incorporation into gastrocnemius muscle was assessed by Western blotting, quantified, and normalised to the total protein content. A representative Western blot is shown. (C–E) Relative mRNA levels in gastrocnemius for *Trim63*, *Fbxo32*, and *Fbxo30* were measured by RT-qPCR. Data were normalised using *Tbp*. Data are expressed as fold change vs. H₂O-Ctrl and presented as individual values with mean bars \pm SEM. Statistics are described in Section 4. * $p_{\text{adj}} < 0.05$; **** $p_{\text{adj}} < 0.0001$, or ns = non-significant.

2.4. ATF4-Regulated Atrogenes Are Overexpressed in Atrophy-Resistant Hibernating Brown Bear Muscle

Our data strongly suggest that the induction of ATF4 signalling is not always associated with muscle atrophy, either in basal conditions or in HS-induced muscle atrophy. We took advantage of a natural model, i.e., the hibernating brown bear, which experiences only a moderate loss of muscle protein content while remaining completely inactive for up to 6 months [52–54]. As with HF treatment, we recently reported a concomitant TGF- β pathway inhibition and BMP pathway activation in hibernating brown bear muscle [46]. We, thus, explored whether ATF4-regulated atrogenes may also be induced in this model. Interestingly, as shown in Figure 6, *Atf4* was upregulated in hibernating brown bear muscle compared to the active counterpart. In addition, the two main ATF4-regulated atrogenes (*Gadd45a* and *Cdkn1a*) and *Trib3* were also induced in hibernating brown bear muscle. Other ATF4 target genes were either down- (*Eif4ebp1*, *Ppp1r15a*, and *Asns*) or upregulated (*Ddit3*). These data show that ATF4-regulated atrogenes are induced in hibernating brown bear muscle, even if they are resistant to atrophy.

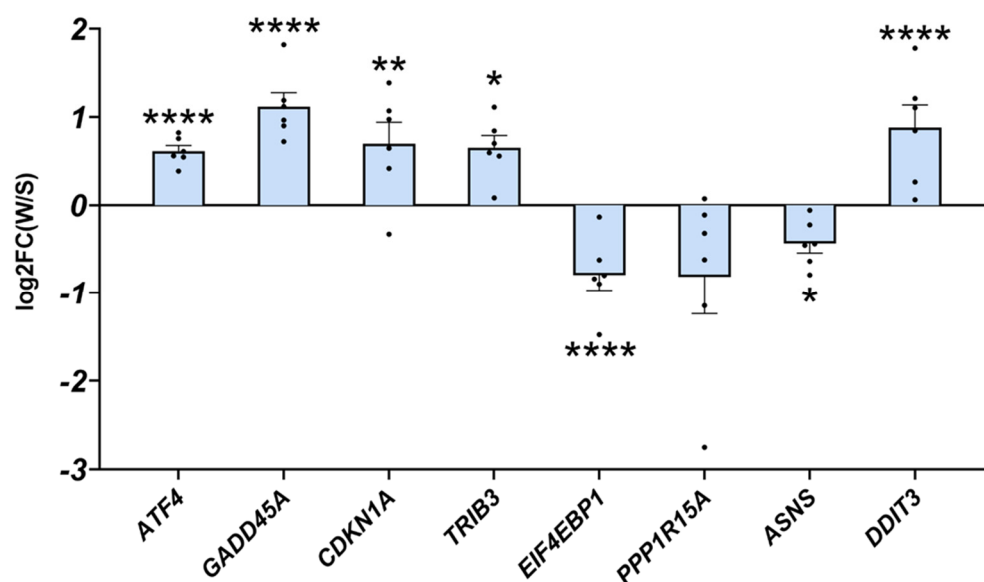


Figure 6. ATF4-regulated atrogenes are induced in atrophy-resistant hibernating brown bear muscles. Gene expression levels for *ATF4*, *GADD45A*, *CDKN1A*, *TRIB3*, *EIF4EBP1*, *PPP1R15A*, *ASNS*, and *DDIT3* in vastus lateralis muscle of active and hibernating brown bears (n = 6 bears/season, the same individuals were sampled and analysed in summer and winter, log₂FC winter/summer). Data are presented as individual values as log₂FC with mean bars \pm lfcSE (log₂ fold change standard error). Statistics are described in [46]. * $p_{\text{adj}} < 0.05$; ** $p_{\text{adj}} < 0.01$; **** $p_{\text{adj}} < 0.0001$. FC: fold change; W: winter (hibernating season); S: summer (active season).

3. Discussion

Several muscle-wasting conditions, including fasting or physical inactivity, are associated with eIF2 α phosphorylation [55,56] and/or ATF4 overexpression, which trigger muscle atrophy [10–13,18,57]. Moreover, muscle atrophy is hampered during fasting or ageing in mice with reduced ATF4 expression or expressing a phosphorylation-resistant form of eIF2 α [11–13]. Both CDKN1A and GADD45A are referred to as atrogenes and are required for ATF4-mediated muscle atrophy [11–13,18], and TRIB3 is another ATF4 target gene involved in fasting- and ageing-induced muscle atrophy [19,20]. We showed here that overexpression of ATF4-regulated atrogenes was dissociated from muscle wasting (1) in a basal condition, (2) during hindlimb suspension, and (3) in a natural model of muscle-atrophy resistance (Figure 7).

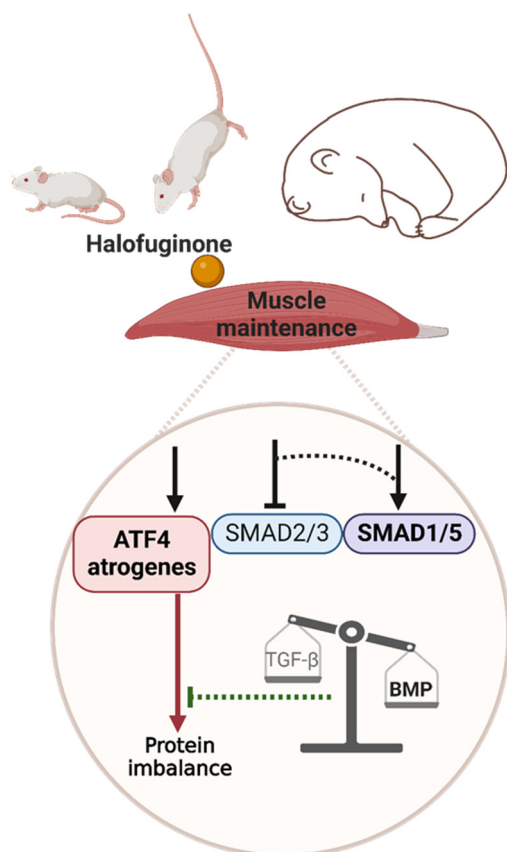


Figure 7. Graphical abstract. The red and green lines represent catabolic and anabolic effects, respectively. Dotted lines represent hypothetical connections. The arrows/T bars above the ATF4 atrogens, SMAD2/3, and SMAD1/5 boxes represent the induction/inhibition by halofuginone or by an as-yet-unknown mechanism in mouse or bear muscle, respectively. Created with BioRender.com.

We first observed that the overexpression of the ATF4-regulated atrogens *Trib3*, *Cdkn1a*, *Gadd45a*, and *Eif4ebp1*, as well as *Atf4* itself, induced by halofuginone treatment for up to 4 weeks, did not coincide with atrophy in all hindlimb muscles, including gastrocnemius. Subsequently, we then reported that pre-treatment with halofuginone mitigated the atrophy of the gastrocnemius muscle during hindlimb suspension. These positive effects of halofuginone treatment are consistent with reports showing that this dose (i.e., 0.25 $\mu\text{g/g}$) and frequency of administration (i) were very well-tolerated in mice for up to 3 months and (ii) improved muscle-cell survival, promoted membrane repair, and improved muscle performances in models of muscular dystrophies [31,33,58–60]. However, none of these studies explored whether the potential effect of HF would involve the ATF4 pathway. Here, we showed that induction of ATF4-regulated atrogens was uncoupled from muscle atrophy during hindlimb suspension. Indeed, although ATF4-regulated atrogens were overexpressed during hindlimb suspension, halofuginone-treated mice displayed a partial preservation of gastrocnemius muscle mass and CSA. In addition, we took advantage of a natural model of resistance to muscle atrophy to examine the expression of ATF4-regulated atrogens. The brown bear remains completely inactive during hibernation for up to 6 months but, surprisingly, is not sensitive to muscle atrophy [52–54], which provides an interesting model for finding new molecular mechanisms to fight muscle atrophy in humans. We showed that the atrogens *CDKN1A*, *GADD45A*, *ATF4* itself, and *TRIB3* were upregulated in atrophy-resistant hibernating brown bear muscle compared to active bear muscle. Of note, ATF4 is mainly regulated at the translational level [15]. However, in most of the previous studies on the topic, the authors only measured *Atf4* mRNA expression and expression of its target genes as evidence of its activity in skeletal muscle. Indeed, endogenous ATF4 protein cannot be reliably detected in skeletal muscle,

presumably due to its low abundance, very short half-life, and lack of a high quality antibody [11–13,17,18,61]. Altogether, these data strongly suggest that the induction of the ATF4 pathway can be dissociated from muscle atrophy. ATF4 target genes are highly dependent on the type and duration of stress stimuli [21,62], and the ability to restore homeostasis may be overwhelmed when the stress is too severe or sustained, resulting in cell death through the transcription of pro-apoptotic genes [63–66]. Therefore, to avoid chronic and acute activation, halofuginone was administered periodically to activate the eIF2 α -ATF4 pathway in mice. In our conditions, the ATF4 transcriptional program may, thus, (i) differ from the transcriptional program induced by a severe and sustained activation and (ii) include genes that might counteract the effect of ATF4-induced atrogenes.

Halofuginone is well-described to also target the TGF- β pathway [35,36]. The nuclear translocation of the TGF- β transcription factors SMAD2/3 requires the formation of a complex with SMAD4 [43]. Halofuginone-induced eIF2 α phosphorylation has been reported to inhibit the nuclear translocation of this complex in intestinal porcine enterocyte cells in vitro [67]. Consistently, we reported here a concomitant overall (i) increase in phosphorylated eIF2 α protein levels and (ii) reduction in SMAD2/3 and SMAD4 nuclear protein levels in HF-treated mice. Thus, this highlights in skeletal muscle, for the first time, the possible role of HF-induced eIF2 α phosphorylation in TGF- β inhibition. Although, the concomitant collagen downregulation and decrease in SMAD2/3 nuclear protein levels during hindlimb suspension in H₂O-treated mice suggest a decrease in TGF- β signalling, we cannot exclude that these events are disconnected. Indeed, the SMAD2/3 nuclear protein levels are consistently low in HF-treated mice and, thus, cannot explain the decreased collagen expression during hindlimb suspension. Much remains to be clarified about the mechanisms of action of HF. Indeed, HF is used for its antifibrotic properties mediated by TGF- β inhibition in situations already characterised by fibrosis [48]. This is, however, not the case in our study. In addition, the inhibition of TGF- β signalling in muscles of HF-treated mice could have led to transcriptional changes that remain to be explored. It is possible that TGF- β signalling is induced later during hindlimb suspension. In fact, the TGF- β signalling pathway has previously been reported to be either unchanged in skeletal muscle after 1–3 days or induced after 7–10 days of unloading [46,68,69]. We also reported an upregulation of *Trim63* and *Fbxo32* during hindlimb suspension. Although these atrogenes are targets of the TGF- β signalling activation, they are also regulated by other signalling pathways [5].

We and others reported that the balance between TGF- β and BMP signalling seems crucial for muscle-mass maintenance during catabolic situations [39,44–46,70]. Indeed, using the hibernating bear model, we recently reported that TGF- β signalling, i.e., a negative regulator of muscle mass, was downregulated at the transcriptomic level in muscles that are resistant to atrophy, while BMP signalling, i.e., a positive regulator of muscle mass, was maintained [46]. Previous data suggested that TGF- β inhibition would release SMAD4, i.e., the common actor in TGF- β and BMP signalling, which could, thus, be recruited to BMP signalling and promote hypertrophy and/or counteract atrophy [45]. Here, we reported an increase in the SMAD1/5 nuclear protein levels in the halofuginone-treated control mice, suggesting there was concomitant BMP signalling activation and TGF- β inhibition. In addition, BMP activation was reported to increase during denervation, intensive care disuse, and amyotrophic lateral sclerosis and was described as essential to counteract excessive muscle wasting [44,45]. In agreement, we reported here that BMP transcription factors SMAD1/5 accumulated in the nucleus in H₂O-treated mice but, surprisingly, declined in HF-treated mice after 7 days of hindlimb suspension. Whether the higher basal pools of nuclear SMAD1/5 and their maintenance after 3 days of hindlimb suspension in HF-treated mice contributed to attenuating skeletal muscle atrophy during hindlimb suspension remains to be explored. Of note, BMP signalling has been reported to promote protein synthesis in muscle [44]. Maintenance of the BMP pathway after 3 days of hindlimb suspension may have contributed to the partial preservation of protein synthesis and muscle mass in HF-treated mice. Nuclear translocation of SMAD1/5 represses the

transcription of *FBXO30/Musa1* [44,45]. However, we did not observe any change in *Fbxo30* expression. Mechanisms by which BMP signalling controls muscle mass are still very poorly understood and will require further studies, particularly with a comprehensive characterisation of the BMP target genes in skeletal muscle. We can also speculate that HF-induced BMP activation has helped to limit muscle atrophy induced by ATF4-regulated atrogenes (Figure 7).

In conclusion, halofuginone treatment reproduced the muscle features of hibernating bears in gastrocnemius mice muscles with (i) the activation of ATF4-regulated atrogenes and (ii) the concurrent inhibition of TGF- β signalling and promotion of BMP signalling, without resulting in muscle atrophy (Figure 7). These characteristics were associated with mitigated muscle atrophy during physical inactivity. To date, clinical trials have all attempted to inhibit the TGF- β pathway, mostly with side effects or minimal efficiency [71]. Our study suggests halofuginone, as a well-tolerated chemical compound, already used in human clinical trials [36], was able to tune the TGF- β /BMP balance in vivo and likely sustained muscle mass. Moreover, our data open new ways to further decipher by which precise mechanisms ATF4 induces atrophy and how BMP activation can interfere.

4. Materials and Methods

Ethics, animals housing, and experimental design. All experiments were conducted with the approval of the regional ethics committee (agreement no. D6334515) following the European Directive 2010/63/EU on the protection of vertebrate animals used for experimental and scientific purposes. This study was performed with 12-week-old C57BL6/J male mice (25–30 g), purchased from Janvier Labs (Le Genest-Saint-Isle, France). They were housed individually upon arrival for 10 days of acclimatisation in a controlled room (22 ± 2 °C, $60 \pm 5\%$ humidity, 12 h light/dark cycle, and light period starting at 8 h), fed ad libitum a standard rodent diet (pellets A03 from Safe, Augy, France), and given free access to water. Two distinct animal experiments were performed. To evaluate the effects of a periodic halofuginone (HF) (#32481, Sigma, Saint-Quentin-Fallavier, France) administration, we performed a first protocol where mice received either HF (0.25 $\mu\text{g/g}$) or water (H_2O) by gavage 3 times a week for 1 to 4 weeks ($n = 6$ animals per group). This dose was reported as well tolerated over longer periods [31,33,60]. Gastrocnemius muscle was sampled 6 h after the last HF/ H_2O administration at the end of each week. Subsequently, we performed a second protocol to test whether HF administration before hindlimb unloading had a positive effect on muscle mass and function. For that purpose, we performed two separate animal experiments. In each experiment, mice received either HF (0.25 $\mu\text{g/g}$) or H_2O by gavage 3 times a week for 3 weeks and were afterwards subjected either to hindlimb unloading through tail suspension (HS) or kept unsuspended (Ctrl) for 3 or 7 days, as previously described [46] ($n = 8$ –19 animals per group). We did not record any difference between Ctrl mice at 3 or 7 days for all the measurements reported in this manuscript. We, therefore, pooled the two groups of Ctrl mice for further analysis and data representation. Food intake and body weight were recorded throughout the different protocols. Unloading in control mice resulted in only a small body weight loss (<10%) that occurred within the first 3 days concomitantly with a decrease in food intake, whereas HF treatment did not modify food intake or body weight (see Supplementary Figures S1 and S2).

Tissue collection. At the end of the experiments, mice were euthanised by cervical dislocation. The soleus, gastrocnemius, tibialis anterior, and extensor digitorum longus (EDL) muscles were carefully collected and weighed prior to immediate freezing in liquid nitrogen and storage at -80 °C until analyses.

Measurement of protein synthesis in gastrocnemius. At the end of protocol 2, mice received an intraperitoneal injection of 0.040 $\mu\text{mol/g}$ puromycin (#P8833, Sigma, Saint-Quentin-Fallavier, France) dissolved in 100 μL of a saline solution before euthanasia, as described previously [72]. At exactly 30 min post-puromycin injection, gastrocnemius muscle was dissected and frozen in liquid nitrogen for Western blot analysis, as follows.

Histology and morphometric measurements. A part of the gastrocnemius muscle was collected at the end of protocol 2 and frozen in isopentane chilled with liquid nitrogen and stored at $-80\text{ }^{\circ}\text{C}$ until use. Serial muscle cross-sections ($10\text{ }\mu\text{m}$ thick) were obtained using a cryostat (HM500M Microm International, Fisher Scientific, Illkirch, France) at $-20\text{ }^{\circ}\text{C}$. Cross-sections were labelled with anti-laminin- α 1 (L9393 Sigma, Saint-Quentin-Fallavier, France) to outline the fibre cross-sectional area (CSA) and BFF3 antibody (#AB_2266724, DSHB, Iowa City, IA, USA) to determine myosin heavy chain type 2B fibre. Both were subsequently hybridised with a corresponding secondary antibody conjugated to Alexa-Fluor (Invitrogen, Cergy-Pontoise, France). Image acquisitions were performed with a high-resolution ORCA-Flash4.0 LT+ Digital CMOS camera coupled to a IX-73 microscope (Olympus, Münster, Germany) and Cell-Sens dimension software (Olympus Soft Imaging Solutions, Münster, Germany). The CSA was determined for 1000–1500 fibres per animal, using ImageJ software 1.53f51 (<http://rsb.info.nih.gov/ij/>, accessed on 3 April 2018).

Protein isolation. Gastrocnemius muscles were pulverised in liquid nitrogen. (1) For all targets, $\sim 30\text{ mg}$ of the resulting powders were homogenised using a polytron in 1 mL of an ice-cold buffer (10 mM Tris pH 7.5, 150 mM NaCl, 1 mM EDTA, 1 mM EGTA, 1% Triton X-100, and 0.5% Igepal CA630) containing inhibitors of proteases (Protease Inhibitor Cocktail) and phosphatases (1 mM Na 3 VO 3 and 10 mM NaF) (Sigma, Saint-Quentin-Fallavier, France). The homogenates were stirred for 1 h at $4\text{ }^{\circ}\text{C}$ and then centrifuged at $10,000\times g$ for 15 min at $4\text{ }^{\circ}\text{C}$. The resulting supernatants containing total soluble proteins were then stored at $-80\text{ }^{\circ}\text{C}$ until use. (2) For SMADs protein level analysis, subcellular fractionation was performed. For that purpose, $\sim 50\text{ mg}$ of gastrocnemius powder samples were homogenised for 1 min on ice using a polytron in $500\text{ }\mu\text{L}$ of ice-cold extraction buffer (10 mM HEPES, pH 7.5, 10 mM MgCl $_2$, 5 mM KCl, 0.1 mM EDTA, pH 8.0, and 0.1% Triton X-100) [73]. The resulting homogenates were subjected to sequential fractionation steps to separate soluble cytosolic and nuclear proteins as described [74]. Pellets containing nuclear proteins were solubilised in nuclear extraction buffer (20 mM HEPES, pH 7.9, 25% glycerol, 500 mM NaCl, 1.5 mM MgCl $_2$, 0.2 mM EDTA, and pH 8.0) [73]. For all protein extracts, protein concentration was determined using the Bradford Protein Assay Kit (Biorad, Marnes-la-Coquette, France). Proteins were then diluted in Laemmli buffer and stored at $-80\text{ }^{\circ}\text{C}$ until use.

Western blots. Protein contents for (i) SMAD family members (anti-SMAD1-5, PA5-80036, Thermofisher, Illkirch, France; anti-SMAD2-3, #8685, Cell Signalling Technology, Saint-Cyr-L'Ecole, France; anti-SMAD4, ab230815, Abcam, Cambridge, UK), (ii) total and phosphorylated eukaryotic initiation factor 2 alpha (anti-eIF2 α , #9722, Cell Signalling Technology; anti-p-Ser51eIF2 α , ab32157, and Abcam), and (iii) incorporation of puromycin (anti-puromycin clone 12D10, MABE343, Millipore, Burlington, MA, USA) were assessed by immunoblotting. Briefly, $20\text{--}40\text{ }\mu\text{g}$ of protein extracts were subjected to SDS-PAGE (sodium dodecyl sulfate-polyacrylamide gel electrophoresis) using TGXTM FastCastTM 10% Acrylamide gels (Biorad, Marnes-la-Coquette, France) and transferred onto a PVDF membrane (Hybond P, Amersham, England) using Trans-Blot[®] TurboTM Transfer System standard protocol (Biorad, Marnes-la-Coquette, France). Western blots were blocked for 1 h at room temperature in TBS (Tris-Buffered Saline) buffer with 0.1% Tween-20 (TBS-T, pH = 7.8) with 5% bovine serum albumin (BSA) for all the targets, in accordance with the instructions of the manufacturer. They were then washed thrice in TBS-T and incubated (overnight, stirring, $4\text{ }^{\circ}\text{C}$) with appropriate primary antibodies diluted at 1:1000, except for anti-puromycin diluted at 1:5000. Western blots were then washed and incubated for 1 h with an appropriate secondary antibody (HRP-conjugated anti-rabbit (#7074) or anti-mouse (#7076) IgGs) (Cell Signalling Technology, Saint-Cyr-L'Ecole, France). For anti-puromycin antibody, an anti-mouse IgG2Ak (115-035-206, Jackson ImmunoResearch Laboratories, West Grove, PA, USA) was used. Signals were detected after incubation with Luminata Crescendo Western HRP substrate (Millipore, Burlington, MA, USA) and visualised using G: BOX ChemiXT4 (XL1) imaging system (Syngene, Frederick, MD, USA). Signals were then quantified using ImageJ 1.53f51 software. Two samples from each group were loaded on each gel. The signal

recorded within each lane of one Western blot was normalised to the overall signal of that blot, and then signals were normalised to the total amount of proteins determined by the Biorad's stain-free system or ponceau S to correct for uneven loading. The normalised values were then averaged by group and expressed as the fold change from the mean of all H₂O-ctrl samples.

RT-qPCR. Total RNA from gastrocnemius muscle samples was extracted with Macherey-Nagel™ NucleoSpin™ 96 RNA Kit and KingFisher™ Duo Prime Purification System, in accordance with the instructions of the manufacturer (Macherey-Nagel, Hoerdet Cedex, France). RNA was quantified by measuring the absorbance at 260 nm on a NanoDrop ND-1000 spectrophotometer (Thermo Scientific, Wilmington, DE, USA). Then, 500 ng of RNA were treated with DNase I (Invitrogen, Cergy-Pontoise, France) prior to reverse transcription using random primers and SuperScript II (Invitrogen, Cergy-Pontoise, France), in accordance with the instructions of the manufacturer. Real-time PCR was carried out using the CFX96 Real-Time PCR detection system (Biorad, Marnes-la-Coquette, France). Primer sequences are provided in Supplementary Table S1. PCR reactions were performed using the IQ SYBR Green Supermix (Biorad, Marnes-la-Coquette, France), in accordance with the instructions of the manufacturer. The comparative threshold cycle ($2\Delta\Delta CT$) method was used to compare the relative mRNA expression between each group, using TBP (TATA binding protein) as a reference gene for muscle. The relative mRNA abundance was arbitrarily set to 1 for the H₂O-Ctrl group.

Statistics. All data are means \pm SEM and were analysed for normality of residuals using the Shapiro-Wilk test. No set of data was transformed for non-normality distribution. For protocol 1 (n = 6/group), we performed a multiple Welch t-test within each week. For protocol 2 (n = 8–19/group), we performed a two-way ANOVA with the factors “Hindlimb suspension” and “Halofuginone” and corrected the data for multiple comparisons using Tukey's test. These analyses were performed using Prism 9 (GraphPad Prism 9, San Diego, CA, USA).

Transcriptomic Data. We used transcriptomic data from already published studies [46]. The transcriptomic bear data supporting Figure 6 of this study are openly available in the GEO repository database (<https://www.ncbi.nlm.nih.gov/geo/query/acc.cgi>, reference no. GSE144856, accessed on 1 September 2021). To identify the differentially expressed genes (DEGs) from this list, we selected a winter/summer (FC) > 1.0 with an adjusted *p*-value < 0.05 as cut-off for the up-regulated genes.

Supplementary Materials: The supporting information can be downloaded at: <https://www.mdpi.com/article/10.3390/ijms24010621/s1>.

Author Contributions: Conceptualisation, L.C. (Laura Cussonneau), A.-C.M. and L.C. (Lydie Combaret); methodology, L.C. (Laura Cussonneau), L.C. (Lydie Combaret), C.D., C.C.-G., G.C., J.H., M.D.-M. and Y.D.; analysis, L.C. (Laura Cussonneau), L.C. (Lydie Combaret), C.D. and C.C.-G.; writing—original draft preparation, L.C. (Laura Cussonneau) and L.C. (Laura Cussonneau); writing—review and editing, all authors; project administration, L.C. (Laura Cussonneau); funding acquisition, E.L., F.B. and L.C. (Laura Cussonneau). All authors have read and agreed to the published version of the manuscript.

Funding: This work was supported by the Center National d'Etudes Spatiales (CNES, #865, #974, #1006, and #1905), the iSITE Challenge 3 Mobility program (Université Clermont Auvergne), and the Agence Nationale de la Recherche (B-STRONG ANR-22-CE14-0018). L.C. (Laura Cussonneau) was supported by a grant from the Institut National de la Recherche Agronomique et Environnement and Clermont Métropole. The long-term funding of the Scandinavian Brown Bear Research Project (SBBRP) comes primarily from the Swedish Environmental Protection Agency, the Norwegian Environment Agency, the Austrian Science Fund, and the Swedish Association for Hunting and Wildlife Management.

Institutional Review Board Statement: The study was conducted according to the guidelines of the Declaration of Helsinki and of the European Directive 2010/63/EU and was approved by the institutional review board (or ethics committee) of (1) the Swedish Ethical Committee on Animal Experiment (application nos. Dnr C3/2016 and Dnr C18/2015), the Swedish Environmental Protection Agency (no. NV0741-18), and the Swedish Board of Agriculture (no. Dnr 5.2.18–3060/17) and (2) the C2E2A (Comité d’Ethique pour l’Expérimentation Animale Auvergne) (no. D6334515).

Data Availability Statement: The analysed transcriptomic bear data that support the findings of Figure 6 are openly available in the GEO repository database at <https://www.ncbi.nlm.nih.gov/geo/query/acc.cgi>, accessed on 16 June 2021, reference no. GSE144856. Other data that support the findings of this study are available in the supplementary materials of this article.

Acknowledgments: The authors thank the IEN (INRA Clermont-Ferrand-Theix, France) for the technical assistance with animal care. We are also grateful to Bogdan Vulpesu (Laboratoire de Physique de Clermont, UMR6533) for the helpful discussions regarding the statistical treatment of fibre CSA distribution.

Conflicts of Interest: The authors declare no conflict of interest.

References

1. Alkner, B.A.; Tesch, P.A. Knee Extensor and Plantar Flexor Muscle Size and Function Following 90 Days of Bed Rest with or without Resistance Exercise. *Eur. J. Appl. Physiol.* **2004**, *93*, 294–305. [[CrossRef](#)] [[PubMed](#)]
2. Cui, Q.; Yang, H.; Gu, Y.; Zong, C.; Chen, X.; Lin, Y.; Sun, H.; Shen, Y.; Zhu, J. RNA Sequencing (RNA-Seq) Analysis of Gene Expression Provides New Insights into Hindlimb Unloading-Induced Skeletal Muscle Atrophy. *Ann. Transl. Med.* **2020**, *8*, 1595. [[CrossRef](#)] [[PubMed](#)]
3. Oliveira, J.R.S.; Mohamed, J.S.; Myers, M.J.; Brooks, M.J.; Alway, S.E. Effects of Hindlimb Suspension and Reloading on Gastrocnemius and Soleus Muscle Mass and Function in Geriatric Mice. *Exp. Gerontol.* **2019**, *115*, 19–31. [[CrossRef](#)] [[PubMed](#)]
4. Thyfault, J.P.; Du, M.; Kraus, W.E.; Levine, J.A.; Booth, F.W. Physiology of Sedentary Behavior and Its Relationship to Health Outcomes. *Med. Sci. Sport. Exerc.* **2015**, *47*, 1301–1305. [[CrossRef](#)] [[PubMed](#)]
5. Peris-Moreno, D.; Cussonneau, L.; Combaret, L.; Polge, C.; Taillandier, D. Ubiquitin Ligases at the Heart of Skeletal Muscle Atrophy Control. *Molecules* **2021**, *26*, 407. [[CrossRef](#)] [[PubMed](#)]
6. Vainshtein, A.; Sandri, M. Signaling Pathways That Control Muscle Mass. *Int. J. Mol. Sci.* **2020**, *21*, 4759. [[CrossRef](#)]
7. Argilés, J.M.; Campos, N.; Lopez-Pedrosa, J.M.; Rueda, R.; Rodriguez-Mañas, L. Skeletal Muscle Regulates Metabolism via Interorgan Crosstalk: Roles in Health and Disease. *J. Am. Med. Dir. Assoc.* **2016**, *17*, 789–796. [[CrossRef](#)]
8. Bonaldo, P.; Sandri, M. Cellular and Molecular Mechanisms of Muscle Atrophy. *Dis. Model. Mech.* **2013**, *6*, 25–39. [[CrossRef](#)]
9. Lecker, S.H.; Goldberg, A.L.; Mitch, W.E. Protein Degradation by the Ubiquitin–Proteasome Pathway in Normal and Disease States. *JASN* **2006**, *17*, 1807–1819. [[CrossRef](#)]
10. Sackey, J.M.; Hyatt, J.K.; Raffaello, A.; Thomas Jagoe, R.; Roy, R.R.; Reggie Edgerton, V.; Lecker, S.H.; Goldberg, A.L. Rapid Disuse and Denervation Atrophy Involve Transcriptional Changes Similar to Those of Muscle Wasting during Systemic Diseases. *FASEB J.* **2007**, *21*, 140–155. [[CrossRef](#)]
11. Ebert, S.M.; Monteys, A.M.; Fox, D.K.; Bongers, K.S.; Shields, B.E.; Malmberg, S.E.; Davidson, B.L.; Suneja, M.; Adams, C.M. The Transcription Factor ATF4 Promotes Skeletal Myofiber Atrophy during Fasting. *Mol. Endocrinol.* **2010**, *24*, 790–799. [[CrossRef](#)] [[PubMed](#)]
12. Ebert, S.M.; Dyle, M.C.; Kunkel, S.D.; Bullard, S.A.; Bongers, K.S.; Fox, D.K.; Dierdorff, J.M.; Foster, E.D.; Adams, C.M. Stress-Induced Skeletal Muscle Gadd45a Expression Reprograms Myonuclei and Causes Muscle Atrophy. *J. Biol. Chem.* **2012**, *287*, 27290–27301. [[CrossRef](#)] [[PubMed](#)]
13. Ebert, S.M.; Dyle, M.C.; Bullard, S.A.; Dierdorff, J.M.; Murry, D.J.; Fox, D.K.; Bongers, K.S.; Lira, V.A.; Meyerholz, D.K.; Talley, J.J.; et al. Identification and Small Molecule Inhibition of an Activating Transcription Factor 4 (ATF4)-Dependent Pathway to Age-Related Skeletal Muscle Weakness and Atrophy. *J. Biol. Chem.* **2015**, *290*, 25497–25511. [[CrossRef](#)]
14. Taillandier, D.; Polge, C. Skeletal Muscle Atrogenes: From Rodent Models to Human Pathologies. *Biochimie* **2019**, *166*, 251–269. [[CrossRef](#)] [[PubMed](#)]
15. Pakos-Zebrucka, K.; Koryga, I.; Mnich, K.; Ljubic, M.; Samali, A.; Gorman, A.M. The Integrated Stress Response. *EMBO Rep.* **2016**, *17*, 1374–1395. [[CrossRef](#)]
16. Lu, Y.-N.; Kaviani, S.; Zhang, T.; Zhang, X.; Nguyen, D.; Thombre, R.; He, L.; Wang, J. MARK2 Phosphorylates EIF2 α in Response to Proteotoxic Stress. *PLoS Biol.* **2021**, *19*, e3001096. [[CrossRef](#)]
17. Fox, D.K.; Ebert, S.M.; Bongers, K.S.; Dyle, M.C.; Bullard, S.A.; Dierdorff, J.M.; Kunkel, S.D.; Adams, C.M. P53 and ATF4 Mediate Distinct and Additive Pathways to Skeletal Muscle Atrophy during Limb Immobilization. *Am. J. Physiol.-Endocrinol. Metab.* **2014**, *307*, E245–E261. [[CrossRef](#)]

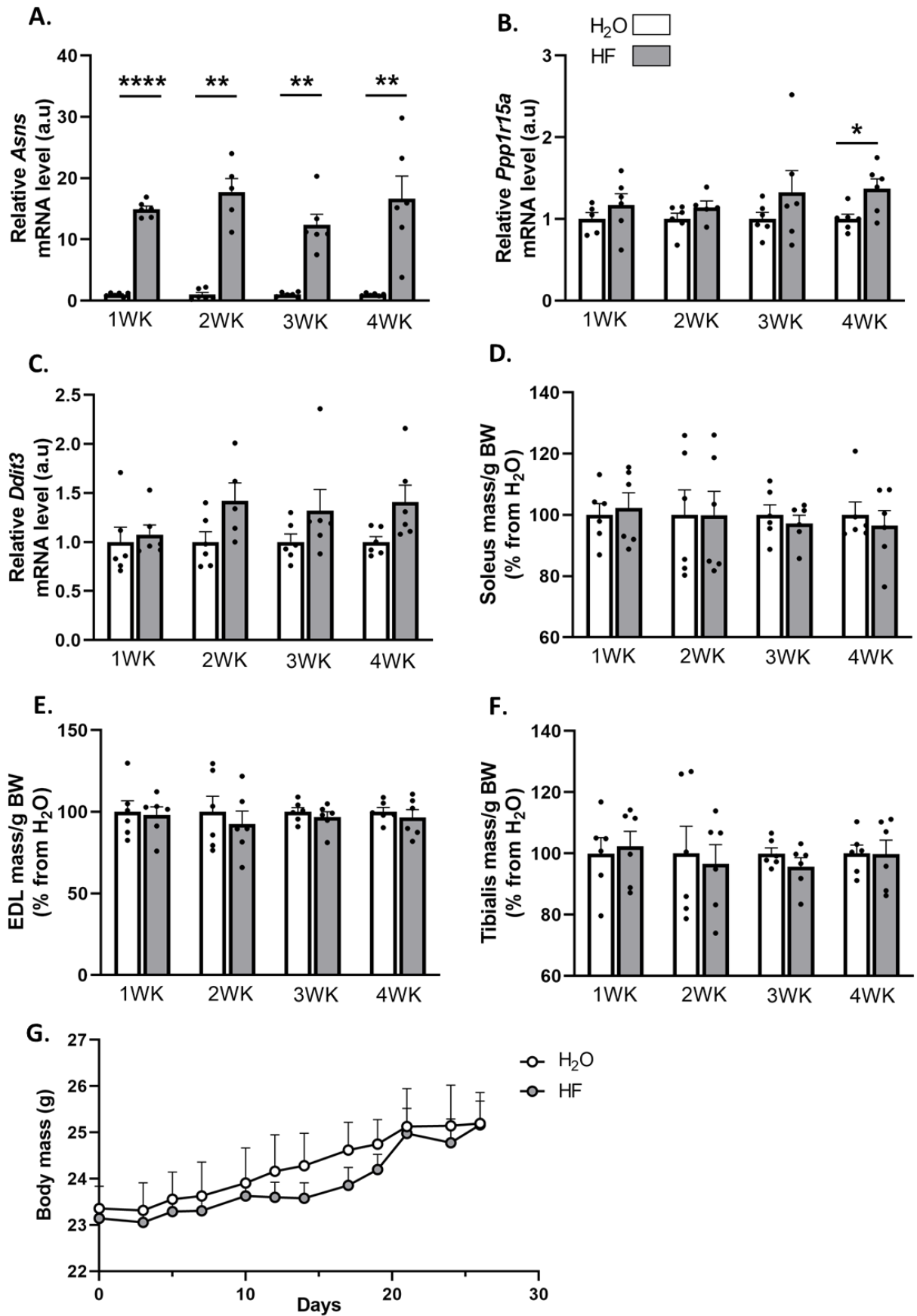
18. Ebert, S.M.; Bullard, S.A.; Basisty, N.; Marcotte, G.R.; Skopec, Z.P.; Dierdorff, J.M.; Al-Zougbi, A.; Tomcheck, K.C.; DeLau, A.D.; Rathmacher, J.A.; et al. Activating Transcription Factor 4 (ATF4) Promotes Skeletal Muscle Atrophy by Forming a Heterodimer with the Transcriptional Regulator C/EBP β . *J. Biol. Chem.* **2020**, *295*, 2787–2803. [[CrossRef](#)] [[PubMed](#)]
19. Choi, R.H.; McConahay, A.; Silvestre, J.G.; Moriscot, A.S.; Carson, J.A.; Koh, H.-J. TRB3 Regulates Skeletal Muscle Mass in Food Deprivation-Induced Atrophy. *FASEB J.* **2019**, *33*, 5654–5666. [[CrossRef](#)]
20. Shang, G.; Han, L.; Wang, Z.; Liu, Y.; Yan, S.; Sai, W.; Wang, D.; Li, Y.; Zhang, W.; Zhong, M. Sarcopenia Is Attenuated by TRB3 Knockout in Aging Mice via the Alleviation of Atrophy and Fibrosis of Skeletal Muscles. *J. Cachexia Sarcopenia Muscle* **2020**, *11*, 1104–1120. [[CrossRef](#)]
21. B'chir, W.; Maurin, A.-C.; Carraro, V.; Averous, J.; Jousse, C.; Muranishi, Y.; Parry, L.; Stepien, G.; Fafournoux, P.; Bruhat, A. The EIF2 α /ATF4 Pathway Is Essential for Stress-Induced Autophagy Gene Expression. *Nucleic Acids Res.* **2013**, *41*, 7683–7699. [[CrossRef](#)] [[PubMed](#)]
22. Han, S.; Zhu, L.; Zhu, Y.; Meng, Y.; Li, J.; Song, P.; Yousafzai, N.A.; Feng, L.; Chen, M.; Wang, Y.; et al. Targeting ATF4-Dependent pro-Survival Autophagy to Synergize Glutaminolysis Inhibition. *Theranostics* **2021**, *11*, 8464–8479. [[CrossRef](#)] [[PubMed](#)]
23. Luhr, M.; Torgersen, M.L.; Szalai, P.; Hashim, A.; Brech, A.; Staerk, J.; Engedal, N. The Kinase PERK and the Transcription Factor ATF4 Play Distinct and Essential Roles in Autophagy Resulting from Tunicamycin-Induced ER Stress. *J. Biol. Chem.* **2019**, *294*, 8197–8217. [[CrossRef](#)] [[PubMed](#)]
24. Rzymiski, T.; Milani, M.; Pike, L.; Buffa, F.; Mellor, H.R.; Winchester, L.; Pires, I.; Hammond, E.; Ragoussis, I.; Harris, A.L. Regulation of Autophagy by ATF4 in Response to Severe Hypoxia. *Oncogene* **2010**, *29*, 4424–4435. [[CrossRef](#)]
25. Kim, K.H.; Jeong, Y.T.; Oh, H.; Kim, S.H.; Cho, J.M.; Kim, Y.-N.; Kim, S.S.; Kim, D.H.; Hur, K.Y.; Kim, H.K.; et al. Autophagy Deficiency Leads to Protection from Obesity and Insulin Resistance by Inducing Fgf21 as a Mitokine. *Nat. Med.* **2013**, *19*, 83–92. [[CrossRef](#)]
26. Kasai, S.; Yamazaki, H.; Tanji, K.; Engler, M.J.; Matsumiya, T.; Itoh, K. Role of the ISR-ATF4 Pathway and Its Cross Talk with Nrf2 in Mitochondrial Quality Control. *J. Clin. Biochem. Nutr.* **2019**, *64*, 1–12. [[CrossRef](#)]
27. Peng, W.; Robertson, L.; Gallinetti, J.; Mejia, P.; Vose, S.; Charlip, A.; Chu, T.; Mitchell, J.R. Surgical Stress Resistance Induced by Single Amino Acid Deprivation Requires *Gcn2* in Mice. *Sci. Transl. Med.* **2012**, *4*, 118ra11. [[CrossRef](#)]
28. Masiero, E.; Agatea, L.; Mammucari, C.; Blaauw, B.; Loro, E.; Komatsu, M.; Metzger, D.; Reggiani, C.; Schiaffino, S.; Sandri, M. Autophagy Is Required to Maintain Muscle Mass. *Cell Metab.* **2009**, *10*, 507–515. [[CrossRef](#)]
29. Rodney, G.G.; Pal, R.; Abo-Zahrah, R. Redox Regulation of Autophagy in Skeletal Muscle. *Free. Radic. Biol. Med.* **2016**, *98*, 103–112. [[CrossRef](#)]
30. Memme, J.M.; Slavin, M.; Moradi, N.; Hood, D.A. Mitochondrial Bioenergetics and Turnover during Chronic Muscle Disuse. *Int. J. Mol. Sci.* **2021**, *22*, 5179. [[CrossRef](#)]
31. Barzilai-Tutsch, H.; Genin, O.; Pines, M.; Halevy, O. Early Pathological Signs in Young Dysf Mice Are Improved by Halofuginone. *Neuromuscul. Disord.* **2020**, *30*, 472–482. [[CrossRef](#)] [[PubMed](#)]
32. Barzilai-Tutsch, H.; Bodanovsky, A.; Maimon, H.; Pines, M.; Halevy, O. Halofuginone Promotes Satellite Cell Activation and Survival in Muscular Dystrophies. *Biochim. Biophys. Acta (BBA) Mol. Basis Dis.* **2016**, *1862*, 1–11. [[CrossRef](#)] [[PubMed](#)]
33. Barzilai-Tutsch, H.; Dewulf, M.; Lamaze, C.; Butler Browne, G.; Pines, M.; Halevy, O. A Promotive Effect for Halofuginone on Membrane Repair and Synaptotagmin-7 Levels in Muscle Cells of Dysferlin-Null Mice. *Hum. Mol. Genet.* **2018**, *27*, 2817–2829. [[CrossRef](#)] [[PubMed](#)]
34. Mordechay, S.; Smullen, S.; Evans, P.; Genin, O.; Pines, M.; Halevy, O. Differential Effects of Halofuginone Enantiomers on Muscle Fibrosis and Histopathology in Duchenne Muscular Dystrophy. *Int. J. Mol. Sci.* **2021**, *22*, 7063. [[CrossRef](#)] [[PubMed](#)]
35. Roffe, S.; Hagai, Y.; Pines, M.; Halevy, O. Halofuginone Inhibits Smad3 Phosphorylation via the PI3K/Akt and MAPK/ERK Pathways in Muscle Cells: Effect on Myotube Fusion. *Exp. Cell Res.* **2010**, *316*, 1061–1069. [[CrossRef](#)] [[PubMed](#)]
36. Pines, M.; Spector, I. Halofuginone—The Multifaceted Molecule. *Molecules* **2015**, *20*, 573–594. [[CrossRef](#)]
37. Gnainsky, Y.; Kushnirsky, Z.; Bilu, G.; Hagai, Y.; Genina, O.; Volpin, H.; Bruck, R.; Spira, G.; Nagler, A.; Kawada, N.; et al. Gene Expression during Chemically Induced Liver Fibrosis: Effect of Halofuginone on TGF- β Signaling. *Cell Tissue Res.* **2007**, *328*, 153–166. [[CrossRef](#)]
38. Lokireddy, S.; Mouly, V.; Butler-Browne, G.; Gluckman, P.D.; Sharma, M.; Kambadur, R.; McFarlane, C. Myostatin Promotes the Wasting of Human Myoblast Cultures through Promoting Ubiquitin-Proteasome Pathway-Mediated Loss of Sarcomeric Proteins. *Am. J. Physiol. Cell Physiol.* **2011**, *301*, C1316–C1324. [[CrossRef](#)]
39. Sartori, R.; Gregorevic, P.; Sandri, M. TGF β and BMP Signaling in Skeletal Muscle: Potential Significance for Muscle-Related Disease. *Trends Endocrinol. Metab.* **2014**, *25*, 464–471. [[CrossRef](#)]
40. Sartori, R.; Milan, G.; Patron, M.; Mammucari, C.; Blaauw, B.; Abraham, R.; Sandri, M. Smad2 and 3 Transcription Factors Control Muscle Mass in Adulthood. *Am. J. Physiol. Cell Physiol.* **2009**, *296*, C1248–C1257. [[CrossRef](#)]
41. Lee, S.-J.; Reed, L.A.; Davies, M.V.; Girgenrath, S.; Goad, M.E.P.; Tomkinson, K.N.; Wright, J.F.; Barker, C.; Ehrmantraut, G.; Holmstrom, J.; et al. Regulation of Muscle Growth by Multiple Ligands Signaling through Activin Type II Receptors. *Proc. Natl. Acad. Sci. USA* **2005**, *102*, 18117–18122. [[CrossRef](#)] [[PubMed](#)]
42. Chen, J.L.; Walton, K.L.; Hagg, A.; Colgan, T.D.; Johnson, K.; Qian, H.; Gregorevic, P.; Harrison, C.A. Specific Targeting of TGF- β Family Ligands Demonstrates Distinct Roles in the Regulation of Muscle Mass in Health and Disease. *Proc. Natl. Acad. Sci. USA* **2017**, *114*, E5266–E5275. [[CrossRef](#)] [[PubMed](#)]

43. Weiss, A.; Attisano, L. The TGFbeta Superfamily Signaling Pathway. *Wiley Interdiscip. Rev. Dev. Biol.* **2013**, *2*, 17. [[CrossRef](#)] [[PubMed](#)]
44. Winbanks, C.E.; Chen, J.L.; Qian, H.; Liu, Y.; Bernardo, B.C.; Beyer, C.; Watt, K.I.; Thomson, R.E.; Connor, T.; Turner, B.J.; et al. The Bone Morphogenetic Protein Axis Is a Positive Regulator of Skeletal Muscle Mass. *J. Cell Biol.* **2013**, *203*, 345–357. [[CrossRef](#)] [[PubMed](#)]
45. Sartori, R.; Schirwis, E.; Blaauw, B.; Bortolanza, S.; Zhao, J.; Enzo, E.; Stantzou, A.; Mouisel, E.; Toniolo, L.; Ferry, A.; et al. BMP Signaling Controls Muscle Mass. *Nat. Genet.* **2013**, *45*, 1309–1318. [[CrossRef](#)]
46. Cussonneau, L.; Boyer, C.; Brun, C.; Deval, C.; Loizon, E.; Meugnier, E.; Gueret, E.; Dubois, E.; Taillandier, D.; Polge, C.; et al. Concurrent BMP Signaling Maintenance and TGF- β Signaling Inhibition Is a Hallmark of Natural Resistance to Muscle Atrophy in the Hibernating Bear. *Cells* **2021**, *10*, 1873. [[CrossRef](#)]
47. Keller, T.L.; Zocco, D.; Sundrud, M.S.; Hendrick, M.; Edenius, M.; Yum, J.; Kim, Y.-J.; Lee, H.-K.; Cortese, J.F.; Wirth, D.F.; et al. Halofuginone and Other Febrifugine Derivatives Inhibit Prolyl-TRNA Synthetase. *Nat. Chem. Biol.* **2012**, *8*, 311–317. [[CrossRef](#)]
48. Luo, Y.; Xie, X.; Luo, D.; Wang, Y.; Gao, Y. The Role of Halofuginone in Fibrosis: More to Be Explored? *J. Leukoc. Biol.* **2017**, *102*, 1333–1345. [[CrossRef](#)] [[PubMed](#)]
49. Hill, C.S. Transcriptional Control by the SMADs. *Cold Spring Harb. Perspect. Biol.* **2016**, *8*, a022079. [[CrossRef](#)]
50. Trendelenburg, A.U.; Meyer, A.; Rohner, D.; Boyle, J.; Hatakeyama, S.; Glass, D.J. Myostatin Reduces Akt/TORC1/P70S6K Signaling, Inhibiting Myoblast Differentiation and Myotube Size. *Am. J. Physiol. Cell Physiol.* **2009**, *296*, C1258–C1270. [[CrossRef](#)]
51. Winbanks, C.E.; Weeks, K.L.; Thomson, R.E.; Sepulveda, P.V.; Beyer, C.; Qian, H.; Chen, J.L.; Allen, J.M.; Lancaster, G.I.; Febbraio, M.A.; et al. Follistatin-Mediated Skeletal Muscle Hypertrophy Is Regulated by Smad3 and MTOR Independently of Myostatin. *J. Cell Biol.* **2012**, *197*, 997–1008. [[CrossRef](#)] [[PubMed](#)]
52. Tinker, D.B.; Harlow, H.J.; Beck, T.D.I. Protein Use and Muscle-Fiber Changes in Free-Ranging, Hibernating Black Bears. *Physiol. Zool.* **1998**, *71*, 414–424. [[CrossRef](#)] [[PubMed](#)]
53. Hershey, J.D.; Robbins, C.T.; Nelson, O.L.; Lin, D.C. Minimal Seasonal Alterations in the Skeletal Muscle of Captive Brown Bears. *Physiol. Biochem. Zool.* **2008**, *81*, 138–147. [[CrossRef](#)] [[PubMed](#)]
54. Lohuis, T.D.; Harlow, H.J.; Beck, T.D.I. Hibernating Black Bears (*Ursus Americanus*) Experience Skeletal Muscle Protein Balance during Winter Anorexia. *Comp. Biochem. Physiol. Part B Biochem. Mol. Biol.* **2007**, *147*, 20–28. [[CrossRef](#)] [[PubMed](#)]
55. Chen, D.; Wang, Y.; Chin, E.R. Activation of the Endoplasmic Reticulum Stress Response in Skeletal Muscle of G93A*SOD1 Amyotrophic Lateral Sclerosis Mice. *Front. Cell. Neurosci.* **2015**, *9*, 170. [[CrossRef](#)]
56. Bohnert, K.R.; Gallot, Y.S.; Sato, S.; Xiong, G.; Hindi, S.M.; Kumar, A. Inhibition of ER Stress and Unfolding Protein Response Pathways Causes Skeletal Muscle Wasting during Cancer Cachexia. *FASEB J.* **2016**, *30*, 3053–3068. [[CrossRef](#)]
57. Ebert, S.M.; Rasmussen, B.B.; Judge, A.R.; Judge, S.M.; Larsson, L.; Wek, R.C.; Anthony, T.G.; Marcotte, G.R.; Miller, M.J.; Yorek, M.A.; et al. Biology of Activating Transcription Factor 4 (ATF4) and Its Role in Skeletal Muscle Atrophy. *J. Nutr.* **2022**, *152*, 926–938. [[CrossRef](#)]
58. Turgeman, T.; Hagai, Y.; Huebner, K.; Jassal, D.S.; Anderson, J.E.; Genin, O.; Nagler, A.; Halevy, O.; Pines, M. Prevention of Muscle Fibrosis and Improvement in Muscle Performance in the Mdx Mouse by Halofuginone. *Neuromuscul. Disord.* **2008**, *18*, 857–868. [[CrossRef](#)]
59. Bodanovsky, A.; Guttman, N.; Barzilai-Tutsch, H.; Genin, O.; Levy, O.; Pines, M.; Halevy, O. Halofuginone Improves Muscle-Cell Survival in Muscular Dystrophies. *Biochim. Biophys. Acta (BBA) Mol. Cell Res.* **2014**, *1843*, 1339–1347. [[CrossRef](#)] [[PubMed](#)]
60. Murphy, A.P.; Grealley, E.; O'Hogain, D.; Blamire, A.; Caravan, P.; Straub, V. Use of EP3533-Enhanced Magnetic Resonance Imaging as a Measure of Disease Progression in Skeletal Muscle of Mdx Mice. *Front. Neurol.* **2021**, *12*, 636719. [[CrossRef](#)]
61. Bongers, K.S.; Fox, D.K.; Ebert, S.M.; Kunkel, S.D.; Dyle, M.C.; Bullard, S.A.; Dierdorff, J.M.; Adams, C.M. Skeletal Muscle Denervation Causes Skeletal Muscle Atrophy through a Pathway That Involves Both Gadd45a and HDAC4. *Am. J. Physiol. Endocrinol. Metab.* **2013**, *305*, E907–E915. [[CrossRef](#)]
62. Harding, H.P.; Zhang, Y.; Zeng, H.; Novoa, I.; Lu, P.D.; Calton, M.; Sadri, N.; Yun, C.; Popko, B.; Paules, R.; et al. An Integrated Stress Response Regulates Amino Acid Metabolism and Resistance to Oxidative Stress. *Mol. Cell* **2003**, *11*, 619–633. [[CrossRef](#)] [[PubMed](#)]
63. Iurlaro, R.; Püschel, F.; León-Annicchiarico, C.L.; O'Connor, H.; Martin, S.J.; Palou-Gramón, D.; Lucendo, E.; Muñoz-Pinedo, C. Glucose Deprivation Induces ATF4-Mediated Apoptosis through TRAIL Death Receptors. *Mol. Cell. Biol.* **2017**, *37*, e00479-16. [[CrossRef](#)] [[PubMed](#)]
64. Qing, G.; Li, B.; Vu, A.; Skuli, N.; Walton, Z.E.; Liu, X.; Mayes, P.A.; Wise, D.R.; Thompson, C.B.; Maris, J.M.; et al. ATF4 Regulates MYC-Mediated Neuroblastoma Cell Death upon Glutamine Deprivation. *Cancer Cell* **2012**, *22*, 631–644. [[CrossRef](#)] [[PubMed](#)]
65. B'chir, W.; Chaveroux, C.; Carraro, V.; Averous, J.; Maurin, A.-C.; Jousse, C.; Muranishi, Y.; Parry, L.; Fafournoux, P.; Bruhat, A. Dual Role for CHOP in the Crosstalk between Autophagy and Apoptosis to Determine Cell Fate in Response to Amino Acid Deprivation. *Cell. Signal.* **2014**, *26*, 1385–1391. [[CrossRef](#)]
66. Lin, J.H.; Li, H.; Zhang, Y.; Ron, D.; Walter, P. Divergent Effects of PERK and IRE1 Signaling on Cell Viability. *PLoS ONE* **2009**, *4*, e4170. [[CrossRef](#)]
67. Duan, M.; Wei, X.; Cheng, Z.; Liu, D.; Fotina, H.; Xia, X.; Hu, J. Involvement of EIF2 α in Halofuginone-Driven Inhibition of TGF- β 1-Induced EMT. *J. Biosci.* **2020**, *45*, 71. [[CrossRef](#)]

68. Yoshihara, T.; Takaragawa, M.; Dobashi, S.; Naito, H. Losartan Treatment Attenuates Hindlimb Unloading-Induced Atrophy in the Soleus Muscle of Female Rats via Canonical TGF- β Signaling. *J. Physiol. Sci.* **2022**, *72*, 6. [[CrossRef](#)]
69. Hirose, T.; Nakazato, K.; Song, H.; Ishii, N. TGF- β 1 and TNF- α Are Involved in the Transcription of Type I Collagen α 2 Gene in Soleus Muscle Atrophied by Mechanical Unloading. *J. Appl. Physiol.* **2008**, *104*, 170–177. [[CrossRef](#)]
70. Sartori, R.; Hagg, A.; Zampieri, S.; Armani, A.; Winbanks, C.E.; Viana, L.R.; Haidar, M.; Watt, K.I.; Qian, H.; Pezzini, C.; et al. Perturbed BMP Signaling and Denervation Promote Muscle Wasting in Cancer Cachexia. *Sci. Transl. Med.* **2021**, *13*, eaay9592. [[CrossRef](#)]
71. Suh, J.; Lee, Y.-S. Myostatin Inhibitors: Panacea or Predicament for Musculoskeletal Disorders? *J. Bone Metab.* **2020**, *27*, 151–165. [[CrossRef](#)] [[PubMed](#)]
72. Goodman, C.A.; Hornberger, T.A. Measuring Protein Synthesis With SUNSET: A Valid Alternative to Traditional Techniques? *Exerc. Sport Sci. Rev.* **2013**, *41*, 107–115. [[CrossRef](#)] [[PubMed](#)]
73. Blough, E.; Dineen, B.; Esser, K. Extraction of Nuclear Proteins from Striated Muscle Tissue. *BioTechniques* **1999**, *26*, 202–206. [[CrossRef](#)] [[PubMed](#)]
74. Dimauro, I.; Pearson, T.; Caporossi, D.; Jackson, M.J. A Simple Protocol for the Subcellular Fractionation of Skeletal Muscle Cells and Tissue. *BMC Res. Notes* **2012**, *5*, 513. [[CrossRef](#)]

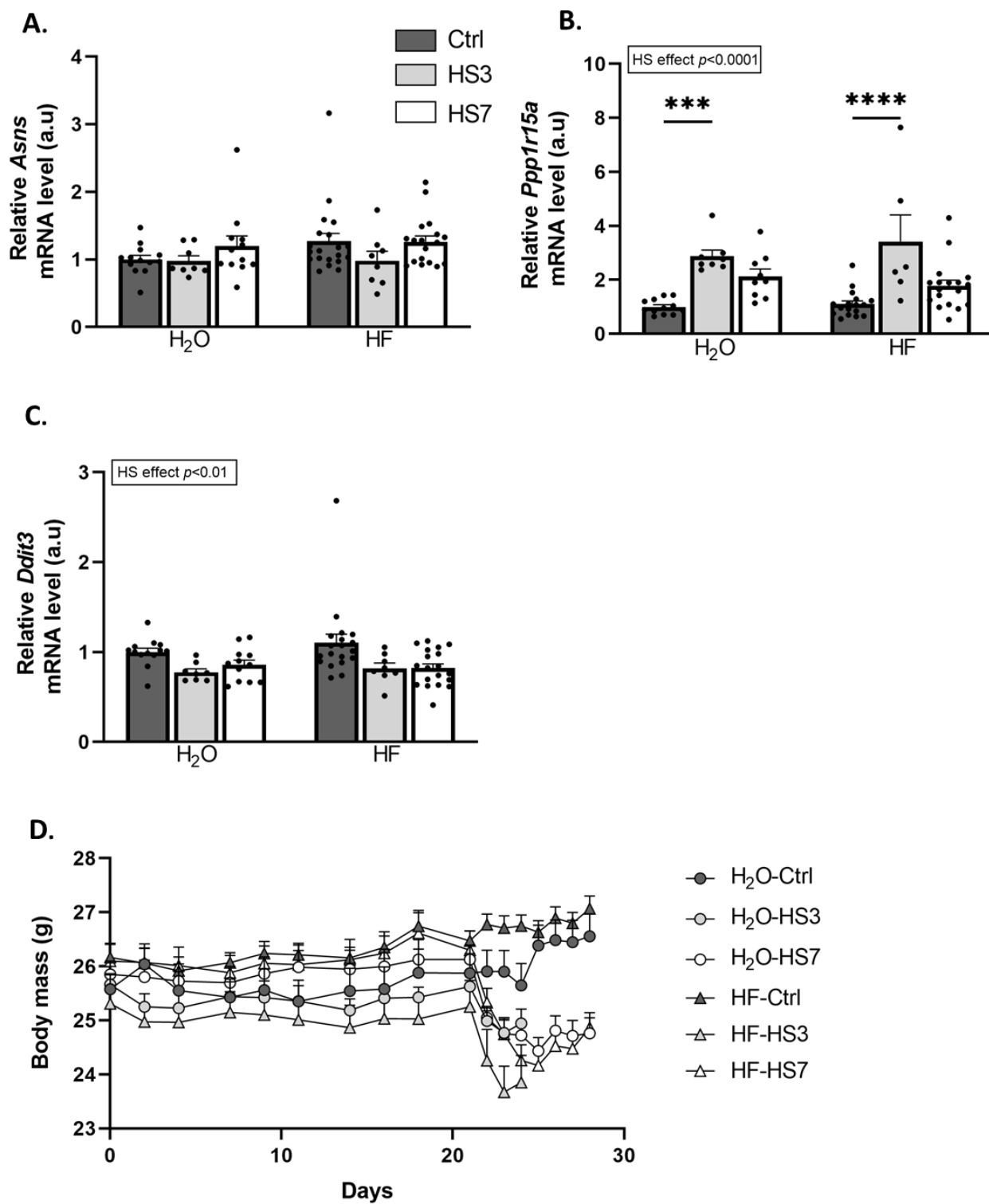
Disclaimer/Publisher’s Note: The statements, opinions and data contained in all publications are solely those of the individual author(s) and contributor(s) and not of MDPI and/or the editor(s). MDPI and/or the editor(s) disclaim responsibility for any injury to people or property resulting from any ideas, methods, instructions or products referred to in the content.

Supplementary Figure S1



Supplementary Figure S1. Effect of halofuginone treatment on muscle mass. Mice were treated with H₂O (white bars) or HF (0.25 µg/g, grey bars) 3 times a week up to 4 weeks (WK) as described in Figure 1A. Muscles were collected 6h after the last HF administration at the end of each week. (A-C) Relative mRNA levels in gastrocnemius for *Asns*, *Ppp1r15a* and *Ddit3* were measured by RT-qPCR. Data were normalized using *Tbp*. Data are expressed as fold change vs. H₂O within each week and presented as individual values with mean bars ± SEM. (D-F) Soleus, Tibialis anterior and Extensor digitorum longus (EDL) mass per gram of body weight (BW). Data are expressed as a percentage from H₂O0 within each week and presented as individual values with mean bars ± SEM. (G) Body mass in grams (g) of H₂O (white circles) or HF (grey circles) treated mice. Data are presented as means ± SEM. Statistics are described in Methods. * $p_{adj} < 0.05$; ** $p_{adj} < 0.01$; **** $p_{adj} < 0.0001$.

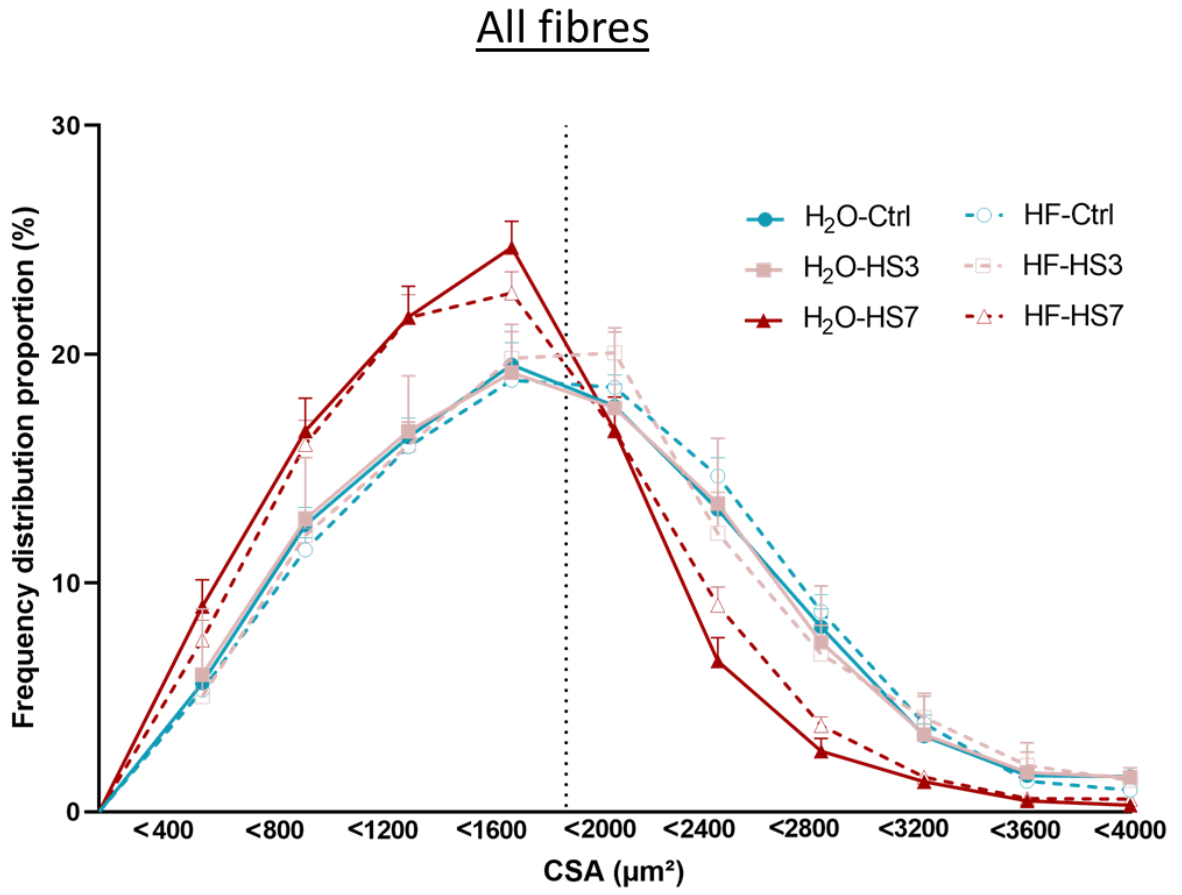
Supplementary Figure S2



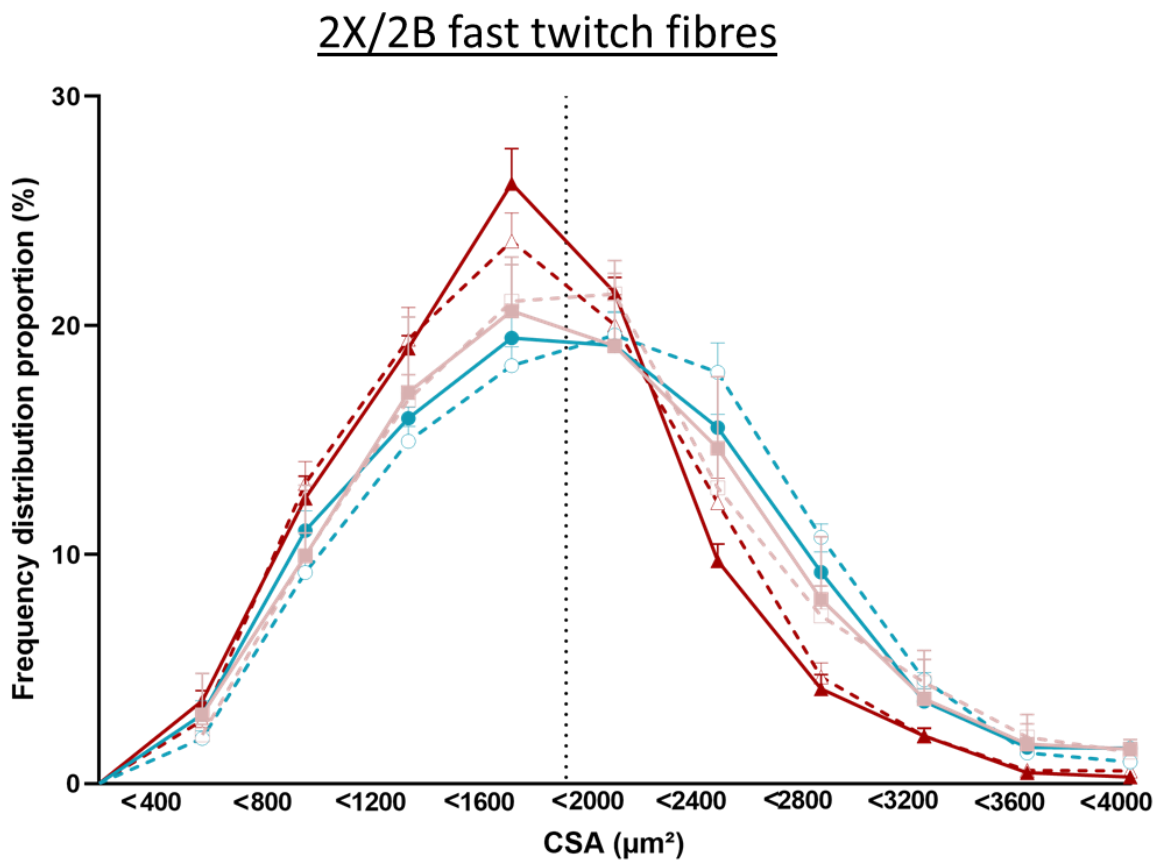
Supplementary Figure S2. ATF4-regulated alternative target genes expression in muscle during hindlimb suspension. Mice were treated with H₂O or halofuginone (HF) oral administration (0.25µg/g) 3 times a week for 3 weeks and were then subjected to hindlimb suspension for 3 or 7 days (HS3 and HS7, light grey and white bars, respectively) or kept unsuspended (Ctrl, dark grey bars). (A-C) Relative mRNA levels in gastrocnemius for *Asns*, *Ppp1r15a* and *Ddit3* were measured by RT-qPCR. Data were normalized using *Tbp*. Data are expressed as fold change vs. H₂O-Ctrl and presented as individual values with mean bars ± SEM. Statistics are described in Methods. *** $p_{adj} < 0.001$; **** $p_{adj} < 0.0001$. (D) Body mass in grams (g) of H₂O (circles) or HF (triangles) treated mice unsuspended (Ctrl, dark grey) or suspended for 3 or 7 days (HS3 and HS7, light grey and white, respectively). Data are presented as mean ± SEM.

Supplementary Figure S3

A.

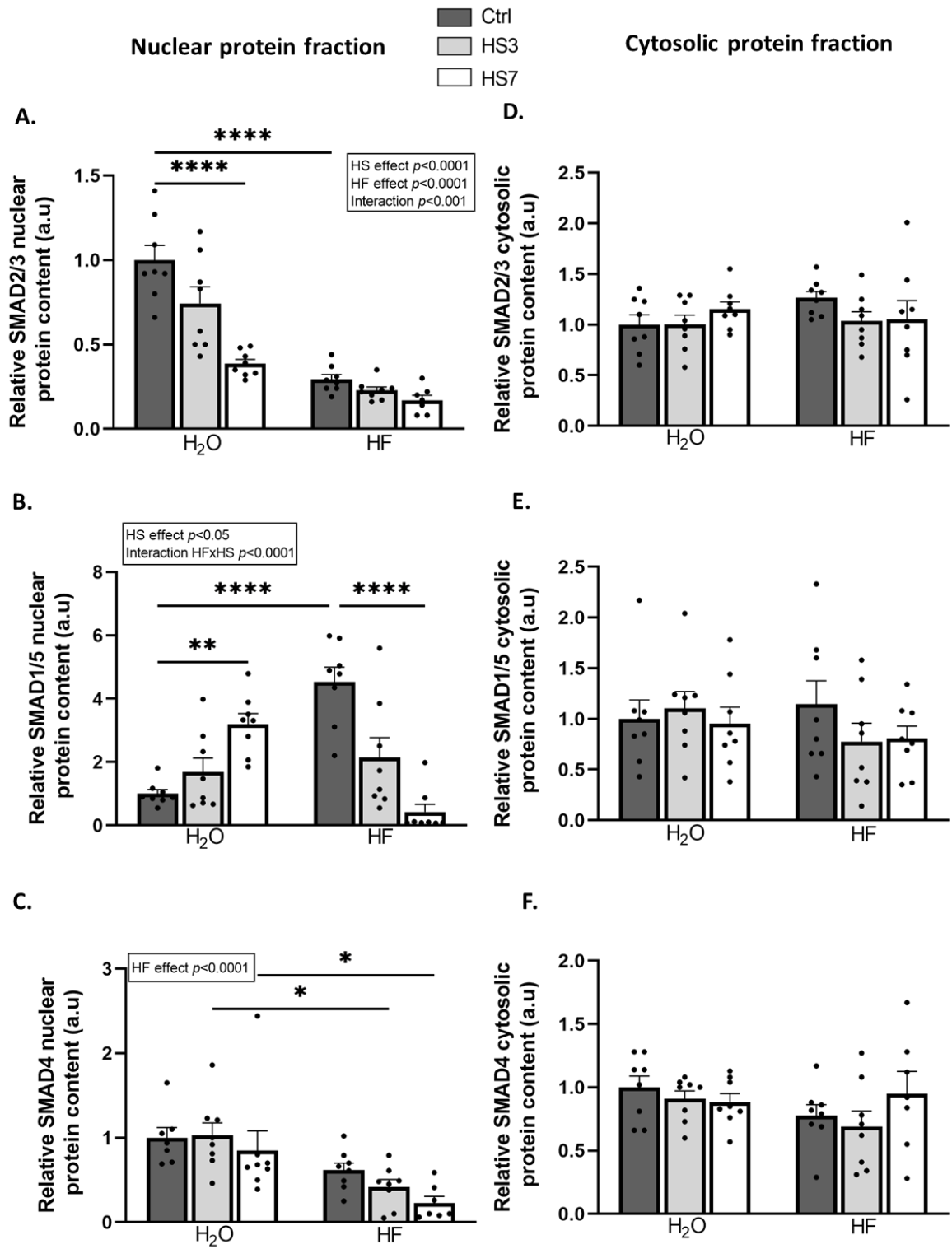


B.



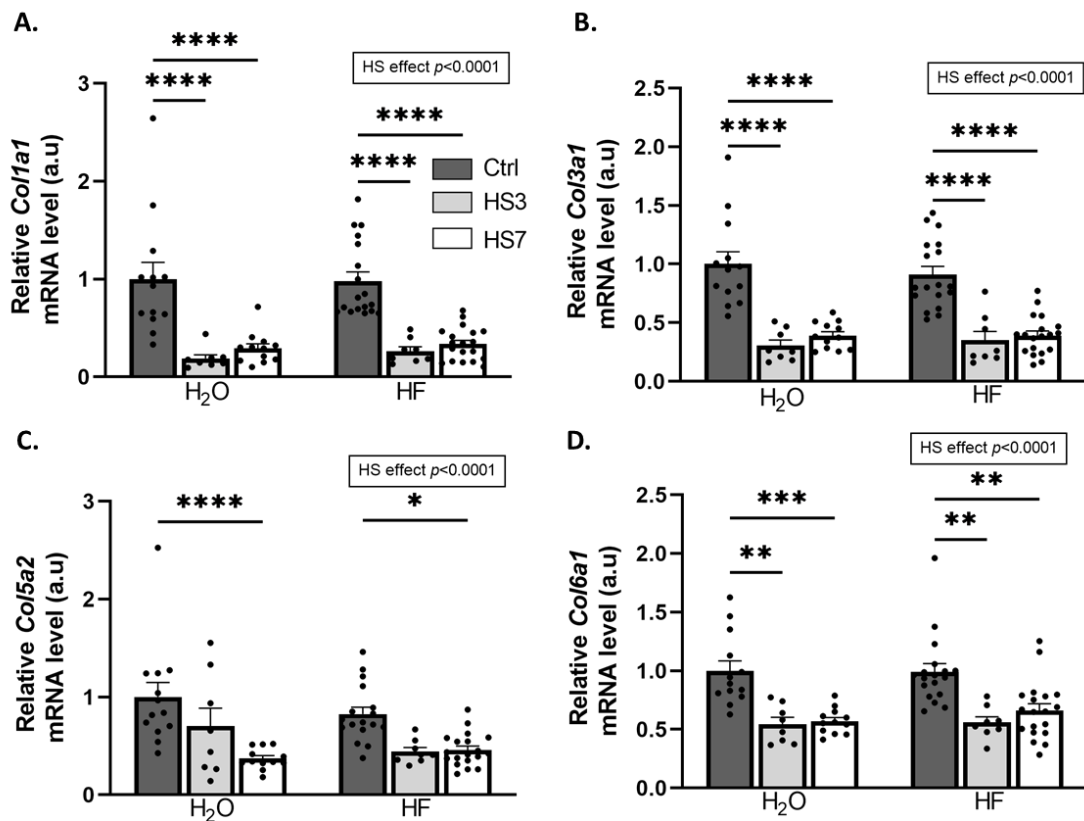
Supplementary Figure S3. Effects of halofuginone treatment prior to hindlimb suspension on skeletal muscle. Mice were treated with H₂O or halofuginone (HF, 0.25µg/g) 3 times a week for 3 weeks and were then subjected to hindlimb suspension for 3 or 7 days (HS3 and HS7, respectively) or kept unsuspended (Ctrl) as described in Figure 2A. (A-B) Frequency distribution proportion of fibres cross-sectional area (CSA) in Ctrl (blue circle), HS3 (pink square) or HS7 (red triangle) of mice treated with H₂O (filled forms and lines) or HF (empty forms and dotted lines), for all fibres type (A) or 2X/2B fast twitch fibres (B). Data are means ± SEM.

Supplementary Figure S4



Supplementary Figure S4. Effect of halofuginone treatment prior to hindlimb suspension on SMADs protein content in gastrocnemius muscle. Mice were treated with H₂O or halofuginone (HF, 0.25µg/g) 3 times a week for 3 weeks and were then subjected for 3 or 7 days (HS3 and HS7, light grey and white bars, respectively) or kept unsuspended (Ctrl, dark grey bars) as described in Figure 2A. (A-F) Relative SMAD2/3, SMAD1/5 and SMAD4 protein levels in gastrocnemius muscle were assessed by Western blotting in the nuclear (A-C) and the cytosolic (D-F) protein fractions;. They were then quantified and normalized to the total protein content. Data are expressed as fold change vs. H₂O-Ctrl and presented as individual values with mean bars ± SEM. Statistics are described in Methods. * p_{adj} <0.05; ** p_{adj} <0.01; **** p_{adj} <0.0001.

Supplementary Figure S5



Supplementary Figure S5. Effect of halofuginone treatment prior to hindlimb suspension on collagens expression in gastrocnemius muscle. Mice were treated with H₂O or halofuginone (HF) oral administration (0.25µg/g) 3 times a week for 3 weeks and were then subjected to hindlimb suspension for 3 or 7 days (HS3 and HS7, light grey and white bars, respectively) or kept unsuspended (Ctrl, dark grey bars). (A-D) Relative mRNA levels in gastrocnemius for *Col1a1*, *Col3a1*, *Col5a2* and *Col6a1* were measured by RT-qPCR. Data were normalized using *Tbp*. Data are expressed as fold change vs. H₂O-Ctrl and presented as individual values with mean bars ± SEM. Statistics are described in Methods. * $p_{\text{adj}} < 0.05$; ** $p_{\text{adj}} < 0.01$; *** $p_{\text{adj}} < 0.001$; **** $p_{\text{adj}} < 0.0001$.

Supplementary Table S1: Primers

Gene	Forward	Reverse
Atf4	TCGATGCTCTGTTTCGAATG	AGAATGTAAGGGGGCAACC
Asns	TACAACCACAAGGCGCTACA	AAGGGCCTGACTCCATAGGT
Cdkn1a	GTCTTGCACTCTGGTGTC	CTTGGAGTGATAGAAATCTG
Col1a1	CGTGGTGACAAGGGTGAGAC	AACCAGGAGAACCAGGAGGA
Col3a1	CTGCTGGTCCTTCTGGTGCT	AGCCACGTTACCAGTTTCA
Col5a2	CCTGGTCCAATGGTGAACA	CCAGGGTTTCCTTCTTTCC
Col6a1	CCACAACCAGATGCAAGAGC	CACCAGCCATCCATTGTAGC
Ddit3	GCATGAAGGAGAAGGAGCAG	CTCCGGAGAGACAGACAGG
Eif4ebp1	CAGGCGGTGAAGAGTCACAA	CCTTGGGGGACATAGAAGCA
Fbxo30	GTTGGGATTGCGTAGTGACC	CCCTCATTAGCCGGGATACA
Fbxo32	AGTGAGGACCGGCTACTGTG	GATCAAACGCTTGCGAATCT
Gadd45a	AGTCAACTTATTTGTTTTTGC	GCAATTTGGTTCAGTTATTT
Ppp1r15a	GACTCAAGCCAGAGTCCCTG	TAGAGGAATCTCGGGTCTCT
Tbp	TGGTGTGCACAGGAGCCAAG	TTCACATCACAGCTCCCCAC
Trib3	CCAGAGATACTCAGCTCCCG	GAGGAGACAGCGGATCAGAC
Trim63	ATGGAGAACCTGGAGAAGCA	AACGACCTCCAGACATGGAC

Atf4: activating transcription factor 4; Asns: asparagine synthetase; Cdkn1a: cyclin dependent kinase inhibitor 1a; Col1a1: collagen type I alpha 1; Col3a1: collagen type III alpha 1; Col5a2: collagen type V alpha 2; Col6a1: collagen type VI alpha 1; Ddit3: DNA damage inducible transcript 3; Eif4ebp1: eukaryotic translation initiation factor 4E binding protein 1; Fbxo 30/32: F-Box protein 30/32; Gadd45a: growth arrest and DNA damage inducible alpha; Ppp1r15a: protein phosphatase 1 regulatory subunit 15a; Tbp: tata binding protein; Trib3: tribbles pseudokinase 3; Trim63: tripartite motif containing 63

7.3 Discussion and perspectives

In our study, we found that the induction of ATF4 atrogenes in skeletal muscle was not associated with atrophy (1) in healthy and (2) catabolic conditions in halofuginone-treated mice, and also (3) in hibernating brown bears. Even more, we found benefits on gastrocnemius muscle mass in halofuginone-treated mice when subjected to hindlimb suspension (HS) compared to the untreated mice. Furthermore, we demonstrated that the molecular mechanisms of halofuginone involve the inhibition of TGF- β signalling while concomitantly promoting BMP signalling (Figure 39). In addition to the points discussed in the article, other points deserve to be discussed. First, we will discuss the halofuginone mechanisms of actions, its biological effects on muscle mass, and finally the dual role of ATF4 signalling in skeletal muscle.

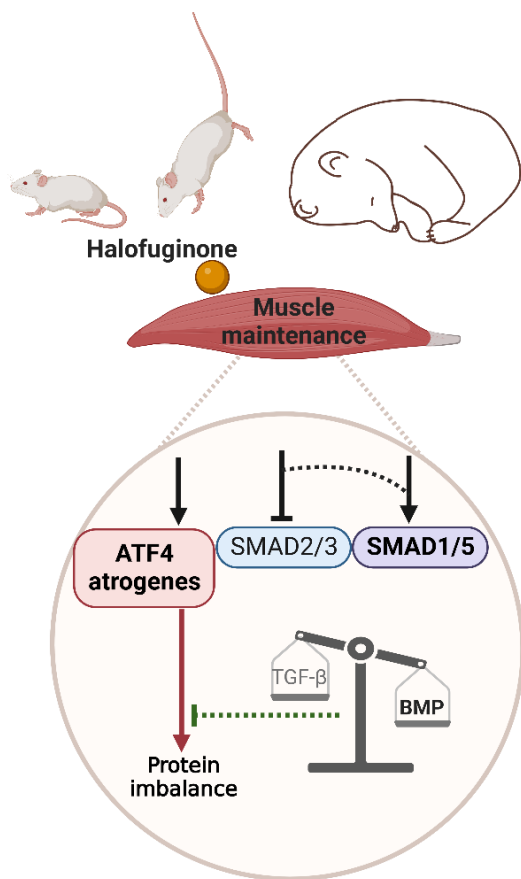


Figure 39. Graphical abstract of the study 2.

7.3.1 Halofuginone mechanism of action in skeletal muscle

Halofuginone (HF) is a synthetic derivative of febrifugine that has been isolated from the roots and leaves of *Dichroa febrifuga* and also from *Hydrangea* [415] (Figure 40). Febrifugine, and subsequently HF, have been used in traditional Chinese medicine for many years for their therapeutic benefit against malaria, cancer, fibrosis and inflammatory diseases [416]. Currently, two modes of action of HF have

been described: (1) inhibition of the prolyl-tRNA synthetase (ProRS) activity leading to ISR activation and (2) inhibition of type 1 collagen production via SMAD3 inhibition [416]. In addition, expression profiling of HF targets in epithelial cells revealed that this molecule can induce the expression of ATF4 target genes, including TRIB3, GADD45A and ATF4 itself [417]. Consistently, in our study, we found that *Atf4* and its target genes were upregulated following HF treatment in mice muscles.

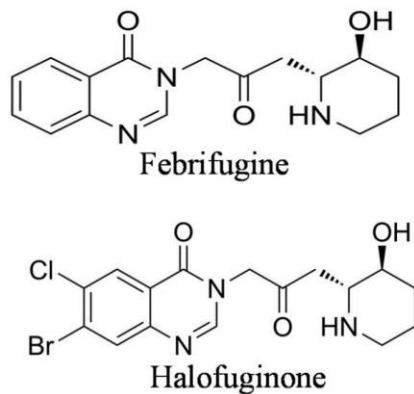


Figure 40. Chemical structures of febrifugine and halofuginone (from Pines et Spector 2015 [416]).

7.3.1.1 Does halofuginone induce GCN2 phosphorylation in skeletal muscle ?

HF binds and inhibits the activity of prolyl-tRNA synthetase (ProRS) [418]. This mimics the response to amino acid starvation by increasing GCN2 and subsequently eIF2 α phosphorylation, and thus ATF4 translation [418]. Unfortunately, examining GCN2 phosphorylation in skeletal muscle is impossible given the commercially available antibodies. Therefore, it is unclear in our study whether the increased transcriptional activity of ATF4 following HF treatment was mediated by HF canonical activation of GCN2. ATF4 binds to specific CCAAT/enhancer binding protein (C/EBP)-ATF response elements (CAREs) located in the promoters of its target genes. Our team has developed a CARE-driven luciferase mouse model (CARE-LUC) that enables the study of the activity of the eIF2 α -ATF4 pathway in the whole organism, and at tissue and cellular levels, by combining imaging, luciferase assays and immunochemistry [419]. We could use wild-type CARE-LUC mice and CARE-LUC *Gcn2* KO mice available in our laboratory to compare the intensity of luciferase in muscles during HF treatment and subsequent hindlimb suspension. This will enable determination of whether ATF4 transcriptional activity induced by HF treatment is GCN2 dependent.

7.3.1.2 Halofuginone inhibits TGF- β signalling while concomitantly promoting BMP signalling in skeletal muscle

HF, which binds to receptor tyrosine kinases and/or enters the cell directly, activates the PI3K and MAPK signalling pathways thereby inhibiting SMAD3 phosphorylation in muscle cells [420]. In addition, phosphorylation of eIF2 α by HF would prevent SMAD2/3 from translocating to the nucleus in intestinal cells [421]. TGF- β is a major cytokine that drives tissue fibrosis [146]. Through inhibition of the TGF- β pathway, HF reduces collagen production and then improves the histopathology and function of fibrotic tissues, including dystrophic muscles [146,422]. In our study, we confirmed that HF inhibited TGF- β signalling (see Paper 7.2) [423]. However, muscles from mice subjected to HS, whether treated with H2O or HF, did not show fibrotic features with, instead, a decrease in collagen expression (Figure 41) (see Appendix 10.2). This indicates that the beneficial effect of HF pre-treatment on muscle mass and CSA did not involve its anti-fibrotic properties.

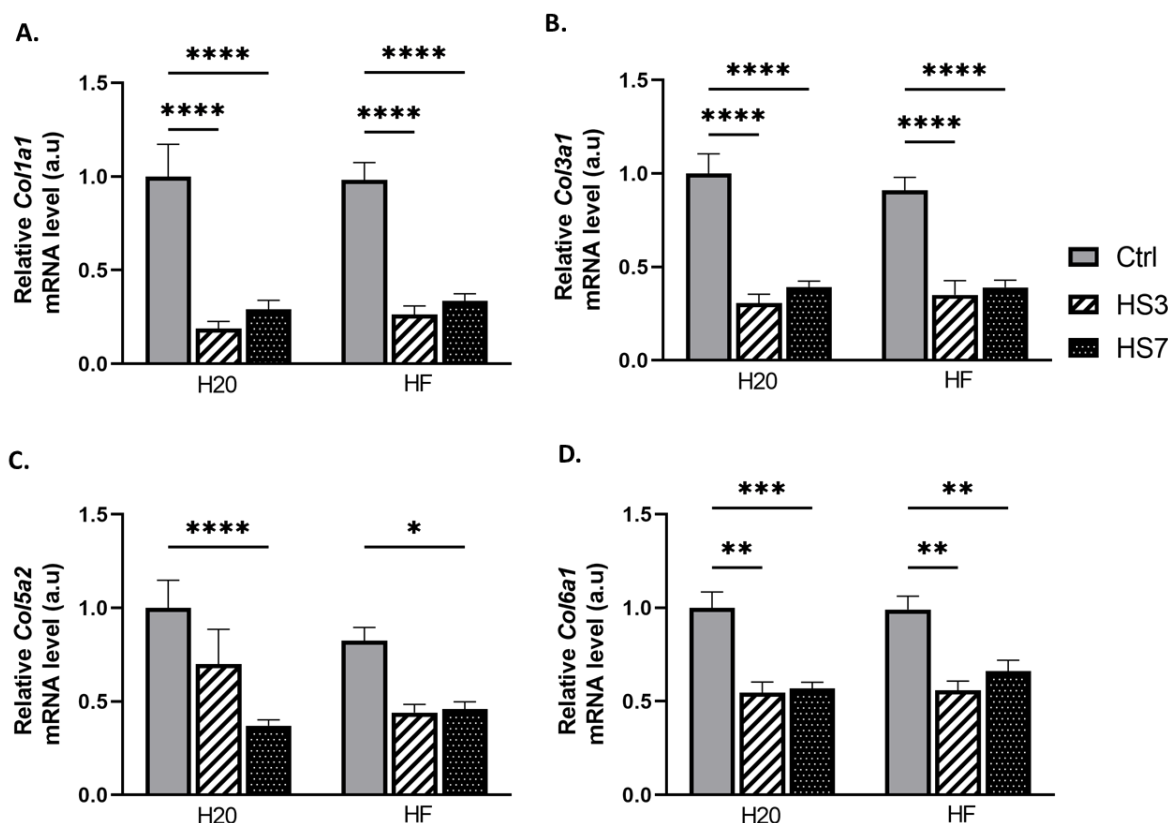


Figure 41. Effect of halofuginone treatment prior to hindlimb suspension on extracellular matrix components expression in gastrocnemius muscle in mice.

Mice were treated with H2O or halofuginone (HF, 0.25 μ g/g) 3 times a week for 3 weeks and were then subjected to hindlimb suspension for 3 (HS3) or 7 (HS7) days or kept unsuspended (Ctrl). (A-D) Gastrocnemius relative mRNA levels for *Col1a1*, *Col3a1*, *Col5a2* and *Col6a1* by RT-qPCR (see Appendix 10.2). Data were normalised using *Tbp* gene. Data are means \pm SEM (expressed as fold change vs. H2O-Ctrl). Two-way ANOVA: * p_{adj} < 0.05; ** p_{adj} < 0.01; *** p_{adj} < 0.001; **** p_{adj} < 0.0001.

Furthermore, we showed for the first time that TGF- β inhibition by HF was concomitant with a promotion of BMP signalling with nuclear translocation of SMAD1/5 (see Paper 7.2) [423]. We suggested that this promotion and the resulting transcriptional program, might be in favour of neutralising the atrophic actions of ATF4 in muscles subjected to HS but also in muscles of the hibernating bears. A study showed that BMP2 treatment induced an increase in ATF4 protein levels and its phosphorylation in chondrocyte cells [424]. Several post-translational modifications of ATF4, including phosphorylation, regulate its stability or enhance its transcriptional activity [194]. Whether BMP signalling in muscles can induce ATF4 phosphorylation and whether this post-translational modification can alter its stability and/or transcriptional activity has never been studied. As it is not possible to analyse ATF4 at the protein level in muscles *in vivo*, *in vitro* experiments will be needed to explore this hypothesis.

7.3.2 Biological effects of halofuginone on skeletal muscle

Duration of HF pre-treatment. In this study, we reported that 3-weeks of HF pre-treatment slightly preserved the mass and CSA of the gastrocnemius muscle during hindlimb suspension in mice (HS) (see Paper 7.2) [423]. We also recorded slight preservation of muscle mass during HS in mice that were pre-treated with HF for a shorter period (i.e. 2 weeks) (Figure 42). This slight preservation of muscle mass occurred even if ATF4 atrogenes were overexpressed during HS both in mice pre-treated for 2 or 3 weeks with HF (see Paper 7.2 and data not shown) [423].

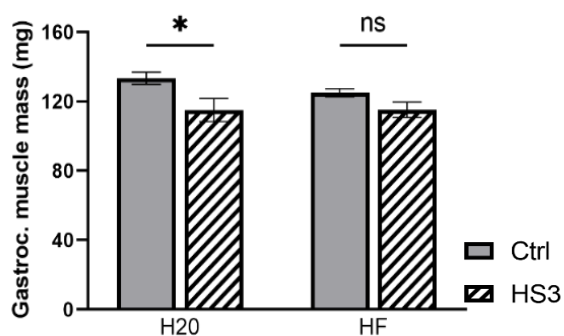


Figure 42. Halofuginone treatment for 2 weeks prior to hindlimb suspension mitigates atrophy in gastrocnemius muscle in mice.

Mice were treated with H₂O or halofuginone (HF, 0.25 μ g/g) 3 times a week for 2 weeks and were then subjected to hindlimb suspension for 3 (HS3) days or kept unsuspended (Ctrl). Gastrocnemius muscle mass (mg) represented with means \pm SEM. Two-way ANOVA * $p_{adj} < 0.05$; ns= non-significant.

The effect of HF may depend on the nature of the muscle. The slight preservation of gastrocnemius CSA observed in HF-treated mice subjected to HS was mainly observed in glycolytic fibres (i.e. type 2X/2B) (see Paper 7.2) [423]. Oxidative fibres (i.e. type 1/2A) are well-documented to be more susceptible to disuse-induced atrophy than glycolytic fibres [425]. Unlike the glycolytic gastrocnemius muscle, the mass of the oxidative soleus muscle was not protected after 3 days of HS when mice were

pre-treated with HF for 2 (Figure 43) or 3 weeks (data not shown). Consistently, the average CSA of soleus muscle fibres was similarly reduced in both untreated and HF-treated mice (Figure 43). We then analysed the distribution of fibre CSA in the soleus and compared it to the gastrocnemius muscle (Figure 43). Overall, HF reduced the proportion of small fibres and increase the proportion of large fibres in both the soleus and the gastrocnemius muscle in control mice (see Paper 7.2 and Figure 43) [423]. However, contrarily to the gastrocnemius muscle (see Paper 7.2) [423], this difference in CSA fibre distribution was not maintained during hindlimb suspension in the soleus muscle (Figure 43). This suggests that muscle fibre type may influence the effect of HF on skeletal muscle and could be specific to the pathophysiological condition and/or the nature of the muscle. It is therefore conceivable that HF treatment is even more successful in preserving muscle mass in glycolytic muscles under catabolic conditions where glycolytic fibres are more likely to atrophy, such as ageing, cancer or glucocorticoid treatment.

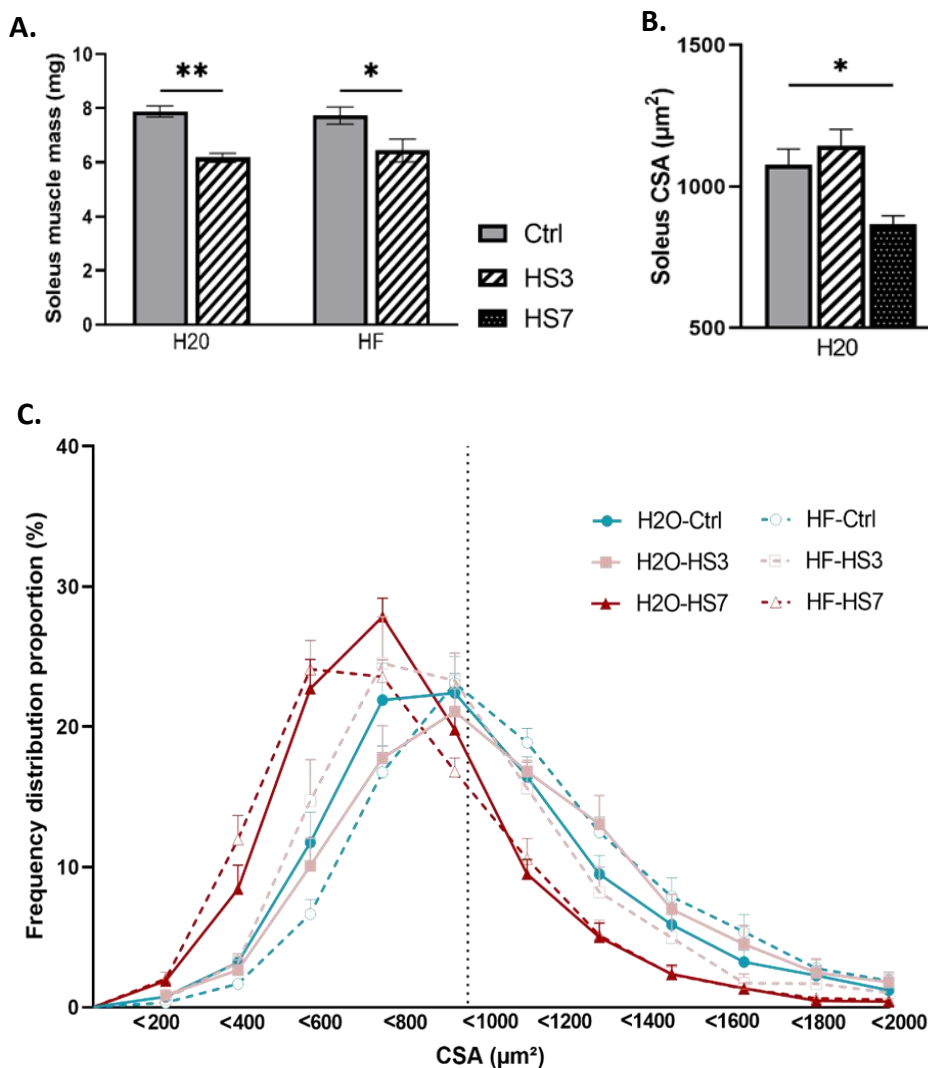


Figure 43. Effect of halofuginone treatment prior to hindlimb suspension in soleus muscle.

Mice were treated with H2O or halofuginone (HF, 0.25µg/g) 3 times a week for 3 weeks and were then subjected to hindlimb suspension for 3 (HS3) or 7 (HS7) days or kept unsuspended (Ctrl). (A) Soleus muscle mass (mg) represented with means ± SEM. (B) Mean fibre cross-sectional area (CSA) of soleus muscle in Ctrl, HS3 and HS7. Data are means ± SEM. Two-way ANOVA. * padj<0.05; ** padj <0.01; **** padj <0.0001. (C) Frequency distribution proportion of fibres CSA of soleus muscle in Ctrl, HS3 or HS7 of mice treated with H2O or HF, for all fibres type. Data are means ± SEM.

Finally, to examine whether this slight preservation of gastrocnemius mass and CSA might have had functional muscle benefits, we performed locomotor experiments using the Rotarod and Catwalk devices. The Rotarod test is widely used to assess the effects of drugs on motor coordination and balance, while the Catwalk is used for the quantitative assessment of stepping and motor performance in rodents. These functional measures did not show much difference between control and HS mice with or without HF treatment. Other functional measures could be considered, such as electromyography.

7.3.3 The dual role of ATF4 signalling in skeletal muscle

As mentioned in the state of the art (see section 4.3.2), ATF4 target genes comprise atrogenes, but also genes that may be involved in muscle homeostasis including autophagy. In our study, we showed that the induction of ATF4 atrogenes was not associated with muscle atrophy during disuse in halofuginone-treated mice and in hibernating bears. For these reasons, we hypothesised that ATF4 may play a dual role in skeletal muscle, either pro-atrophic or pro-homeostatic, and that this may depend on the frequency and duration of its activation.

7.3.3.1 Does halofuginone-induced ATF4 signalling lead to the expression of autophagy-related genes?

ATF4 is a transcription factor involved in the transcription of autophagy-related genes in response to various stresses (e.g. amino acid starvation, ER stress) [197,211–214,216,217]. We thus examined the expression of some autophagy-related genes known to be targets of ATF4 [217]. We observed no change in the muscle expression of *Atg5*, *Atg12* nor *Atg16*, whether the mice were treated with HF or hindlimb suspended (Figure 44) (see Appendix 10.2). However, mRNA and/or protein levels for microtubule associated protein 1 light chain 3 alpha (LC3) and BCL2-interacting protein 3 (BNIP3), involved in autophagosome formation were increased during HS in both H₂O- and HF-treated mice [426,427] (Figure 44). Therefore, the uncoupling of ATF4 from atrophy observed in our study in halofuginone-treated mice does not seem to be dependent on autophagy induction. Interestingly, BNIP3, with the help of LC3, can sequester ATF4 into mitophagosomes leading to ATF4 degradation by mitophagy in response to nutrient deprivation in cancer cells [428]. It would therefore be very interesting to study the cellular localisation of ATF4 upon HF treatment. In addition, RNA sequencing analysis of muscles from HF-treated mice would provide insight into the signalling pathways that may explain the uncoupling between ATF4 atrogenes induction and muscle atrophy.

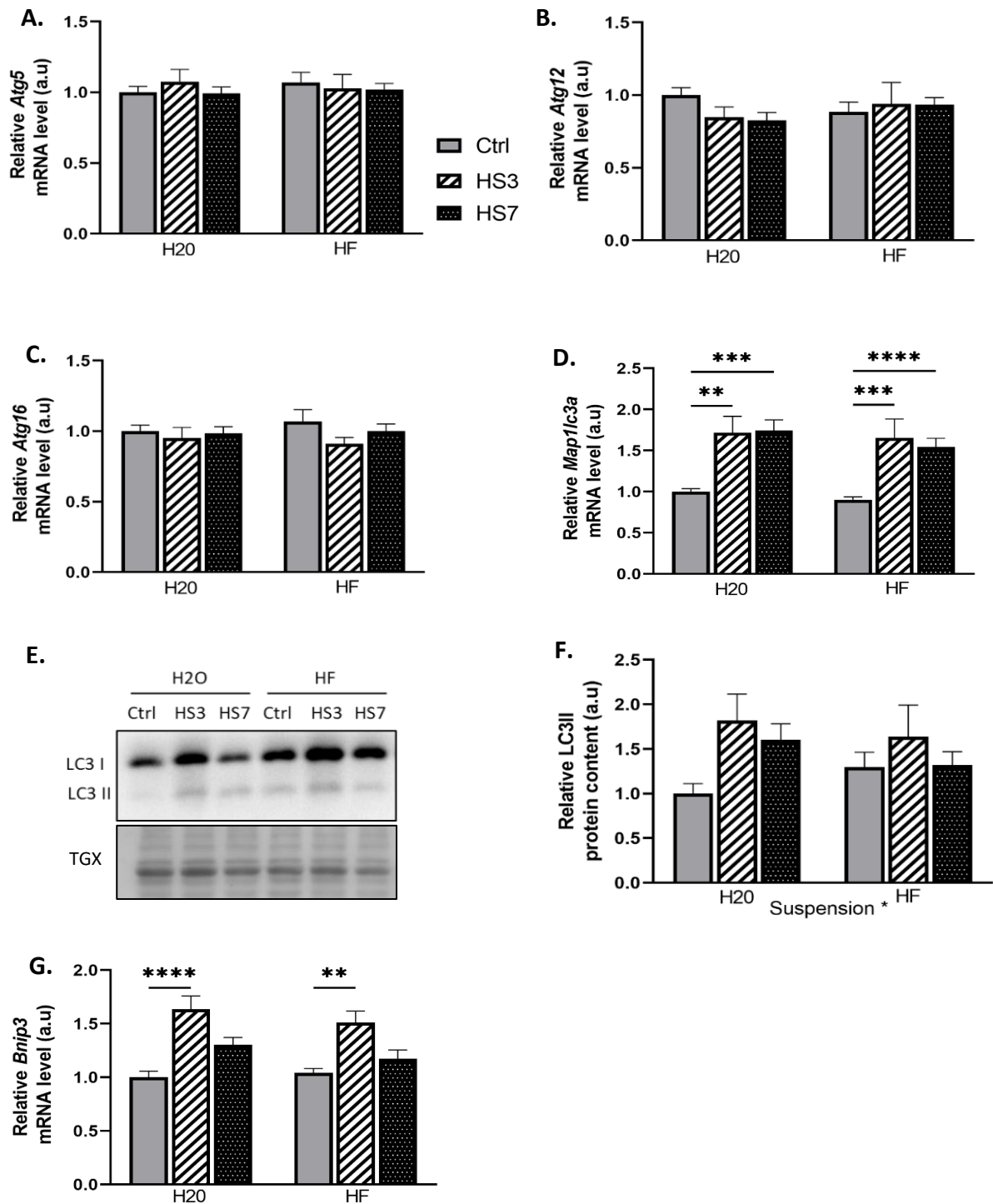


Figure 44. Effect of halofuginone treatment prior to hindlimb suspension on autophagy-lysosomal system in gastrocnemius muscle.

Mice were treated with H2O or halofuginone (HF, 0.25 μ g/g) 3 times a week for 3 weeks and were then subjected to hindlimb suspension for 3 (HS3) or 7 (HS7) days or kept unsuspended (Ctrl). (A-D) and (G) Gastrocnemius relative mRNA levels for *Atg5*, *Atg12*, *Atg16*, *Map1lc3a* and *Bnip3* were assessed by RT-qPCR. Data were normalised using *Tbp*. (E-F) Gastrocnemius relative protein levels for LC3II were assessed by Western blotting quantified and normalised using TGX signal for uneven loading, and a representative western blot is shown (see Appendix 10.2). Data are means \pm SEM (expressed as fold change vs. H2O-Ctrl). Two-way ANOVA: **padj*<0.05; ** *padj*<0.01; *** *padj*<0.001; **** *padj*< 0.0001.

7.3.3.2 ATF4 signalling in hibernating bear muscles

Induction of ATF4 atrogens is associated with moderate muscle atrophy in hindlimb suspended mice when treated with HF or in hibernating brown bears muscles (see Paper 7.2) [423]. We further explored the transcriptome of the muscle of the hibernating brown bear from study 1 [351] to analyse the ATF4 gene signature. Based on an extensive literature review and the use of databases (i.e. GeneCards), we have established a list of ATF4-related genes (see Appendix 10.2). Using the same strategy as in study 1, we performed an enrichment analysis from the down-(161) and up-regulated (105) ATF4-related genes.

A. ATF4-related genes in hibernating bear muscles

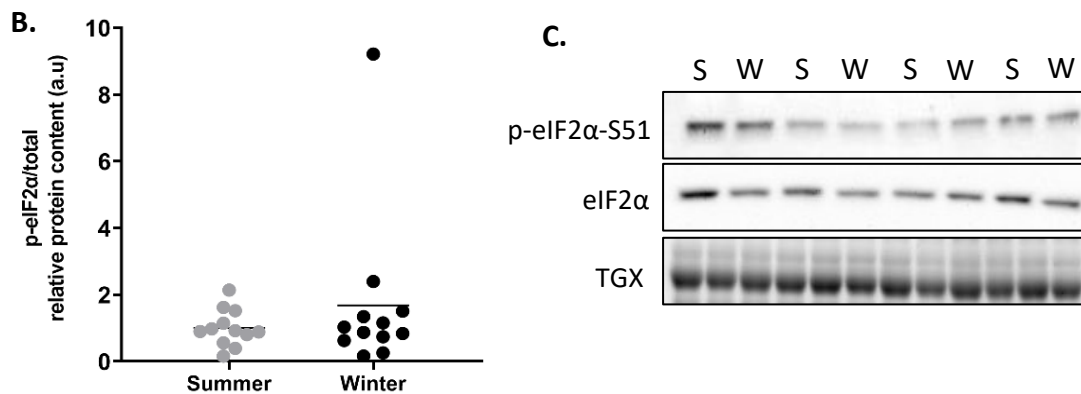
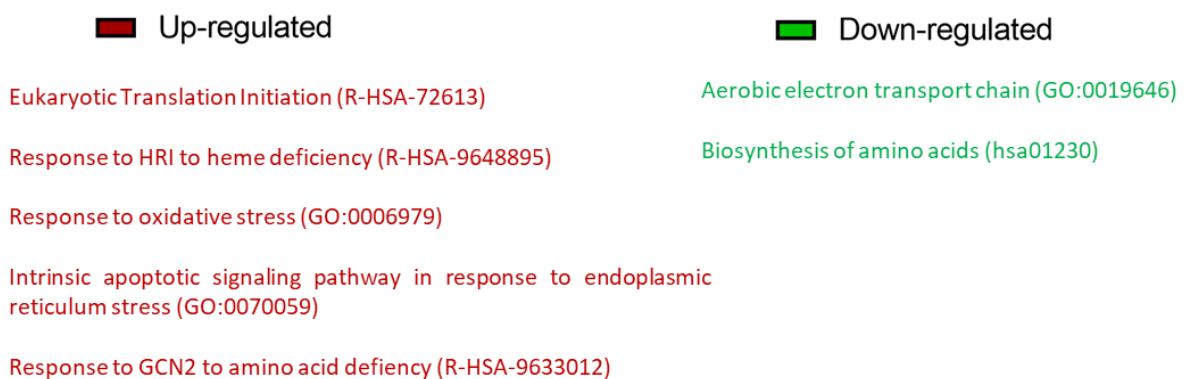


Figure 45. ATF4 signalling regulation in atrophy-resistant muscle of the hibernating bear.

(A) A list of 614 ATF4-related genes has been drawn up from the Genecards web-based portal. Their expression has been analysed in a model of atrophy resistance (the hibernating brown bear) as described before (Cussonneau et al., 2021 [351]). Biological processes represents the protein-protein enrichment analysis performed on Metascape from the respective down-(green) or up-(red) regulated genes. (B-C) Vastus lateralis relative protein levels were assessed by Western blotting and the ratio phosphorylated/total form for eIF2 α was calculated after quantification and normalisation using TGX signal for uneven loading. A representative western blot is shown (see Appendix 10.2). Data are presented as individuals values with mean bars (n=12 bears/season, the same individuals were sampled and analysed in summer and winter). S: summer; W: winter.

Enrichment analysis revealed that ATF4-related genes in the biological processes such as heme deficiency response, oxidative stress, endoplasmic reticulum stress and amino acid deficiency were upregulated in atrophy-resistant muscles of the hibernating bear (Figure 45). In contrast, ATF4-related genes in the biological processes of the aerobic electron transport chain and amino acid biosynthesis were predominantly downregulated (Figure 45). These data suggest that the ATF4 transcription factor is transcriptionally active in hibernating bear muscles. We also observed that the ratio of phosphorylated eIF2 α to total eIF2 α remains unchanged between hibernating and active bear muscles (Figure 45) (see Appendix 10.2). ATF4 target genes are highly dependent on the intensity and duration of the stress [197,204,429]. When the stress is too severe and sustained, eIF2 α is phosphorylated leading to the induction by ATF4 of a pro-apoptotic transcriptional program [202–204]. The maintenance of a low level of phosphorylated eIF2 α may avoid any death-like transcriptional response in bear muscles during hibernation, but also suggest an uncoupling between eIF2 α phosphorylation and ATF4 transcriptional activity. This is consistent with the decrease in phosphorylated eIF2 α protein levels that occurs alongside an increase in the expression of ATF4 target genes during HS in mice (see Paper 7.2) [423]. Therefore, the transcriptional activity of ATF4 may be independent of the level of phosphorylated eIF2 and may depend on other signals in certain situations such as disuse.

7.3.4 Halofuginone-like compound enriched in bear food

As mentioned above, HF is a synthetic derivative of febrifugine that has been isolated from the roots and leaves of *Dichroa febrifuga* and also from *Hydrangea* [415]. *Dichroa febrifuga* is mainly found in Asia. However, a certain type of *Hydrangea*, named *Hydrangea macrophylla* occurs in northern and southern Europe, as well as in southern China. Thus, the geographical distribution of this plant overlaps with some of the brown bear habitat areas (Figure 46). Interestingly, the fruiting of this plant occurs from April to September, and hyperphagia of the brown bear occurs before den entry in late October [296]. Regarding the biological similarity between the muscles of HF-treated mice and hibernating bears (i.e. ATF4 and BMP signalling induction and TGF- β inhibition), it could be envisaged that a halofuginone-like molecule is present in the brown bear food before it enters hibernation. This molecule/compound could be stored in the adipose tissue and released into the bloodstream during the hibernation period. This hypothesis is part of a larger hypothesis that active circulating compounds may be present in the serum of the hibernating bear, which could explain the general hypometabolism present during hibernation and the consequent preservation of organ functions such as skeletal muscle.

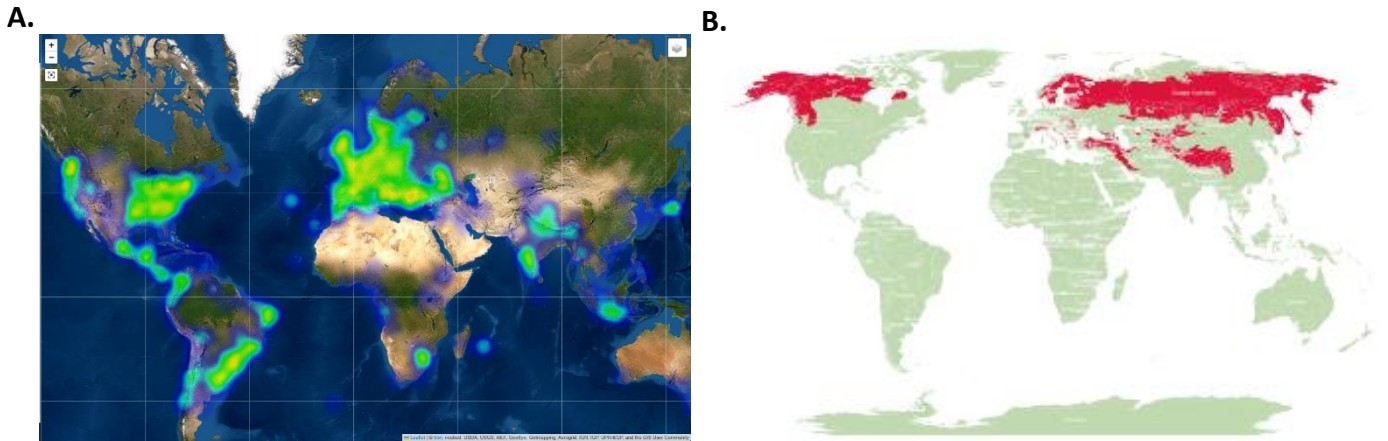


Figure 46. Worldwide geographic repartition of (A) *Hydrangea macrophylla* and (B) brown bear living area (*Ursus arctos*).

(A) Map of *Hydrangea macrophylla* geographic repartition found on <https://identify.plantnet.org/fr/the-plant-list/species>. (B) Map of brown bear living area repartition found on <https://databayou.com/bear/habitat.html>.

Altogether, the various points discussed above have enabled us to draw an hypothetical schema of the molecular mechanisms of halofuginone and halofuginone-like compound in skeletal muscle (Figure 47).

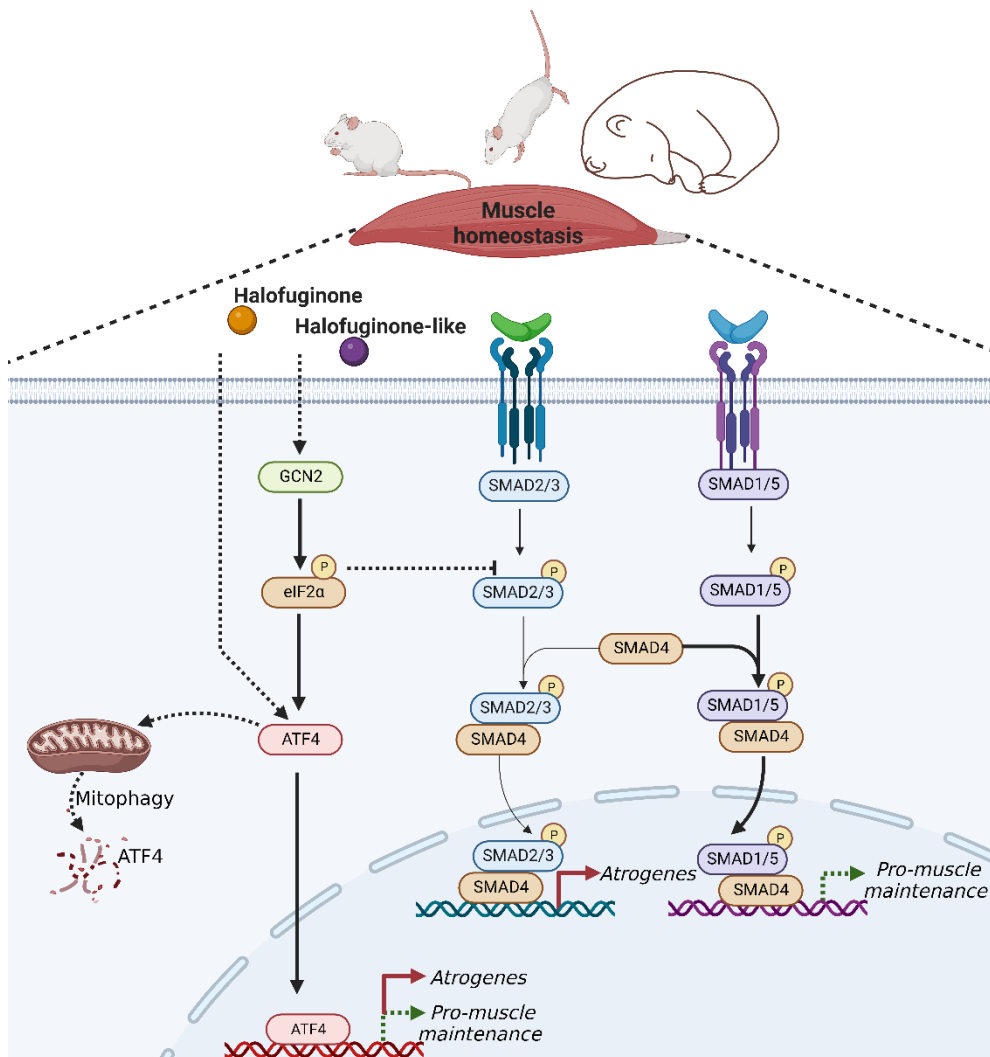


Figure 47. Hypothetical halofuginone and halofuginone-like molecular mechanisms in skeletal muscle.

The dotted lines correspond to the unknown/hypothetic mechanisms in our study.

8. Study 3: Winter bear serum induces similar characteristics in human muscle cells as those found naturally in hibernating bear muscle

8.1 Objective and strategy

This last part contains preliminary results. We sought to replicate the molecular characteristics of atrophy-resistant muscles of hibernating bears in human muscle cells. Our team previously reported an increase in total protein content in human myotubes (HM) cultured with hibernating bear serum. This result proved for the first time that a circulating compound in bear serum could transfer biological properties to human muscle cells [341]. In this thesis project, we showed concurrent TGF- β inhibition and BMP activation in atrophy-resistant muscles of the hibernating brown bear (see Paper 6.3) [351] that we replicated in muscles of hindlimb-suspended mice treated with HF (see Paper 7.2) [423]. We aimed at determining whether a compound in bear serum during hibernation could reproduce these changes in TGF- β /BMP balance in human muscle cells. Our strategy was first to analyse microarray data from human muscle cells cultivated with winter bear serum (WBS) or summer bear serum (SBS) to assess whether there is a transcriptomic signature of TGF- β /BMP signalling. Subsequently, we optimised tools to measure TGF- β /BMP signalling transcriptional activity through their canonical or non-canonical signalling, using luciferase reporter assays in human muscle cells cultivated with SBS or WBS (Figure 48).

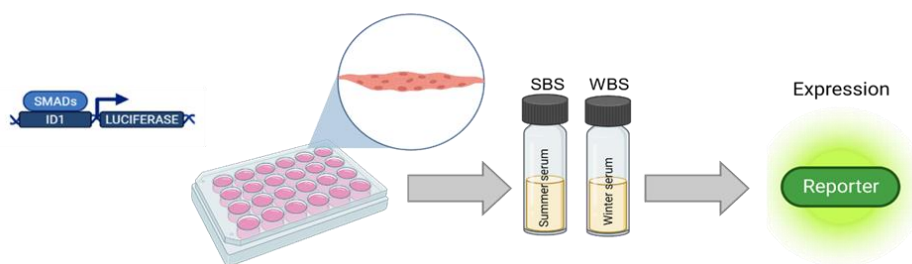


Figure 48. Schema of the experimental strategy of study 3.

8.2 Results, discussion and perspectives

8.2.1 Analysis of microarrays in human muscle cells cultivated with WBS

Prior to the start of this thesis project, human primary myotubes (HM) were cultured with SBS or WBS and a microarray sequencing experiment was performed. We analysed these data focusing on the TGF- β /BMP-related genes. Interestingly, we observed common features with hibernating bear muscles, with down-regulation of *CCN2*, *ID1,3* and *4*, and up-regulation of *MEF2A* expression when HM were treated with WBS compared to SBS (Figure 49). Furthermore, we found that *NOG* (noggin protein), a

well-known antagonist of BMP signalling, was also downregulated in HM after WBS treatment (Figure 49), although this was not the case in the hibernating bear muscles (see Paper 6.3) [351]. The downregulation of NOG and CCN2 are key features of TGF- β inhibition and promotion of BMP signalling. These data indicate that WBS can induce transcriptional changes in the TGF- β /BMP balance in HM similar to those occurring in hibernating bear muscles, supporting the existence of circulating active compounds in the winter bear serum.

8.2.2 Optimisation of tools for the screening active compounds in WBS

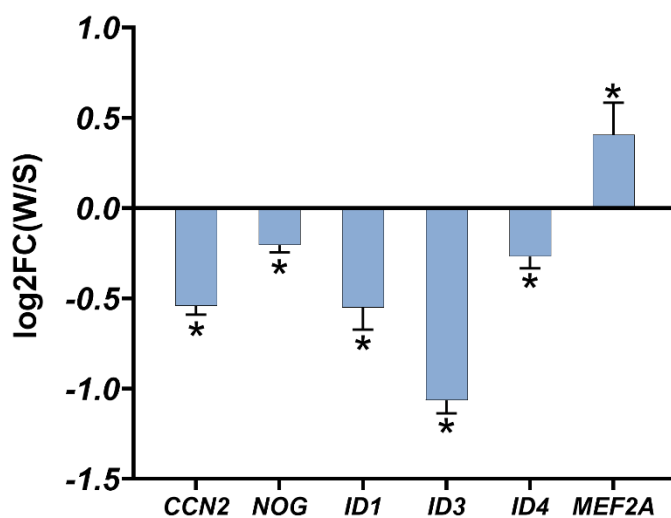


Figure 49. Human myotubes cultivated with winter bear serum induces similar transcriptional changes than those occurring in hibernating bears muscles.

Human myotubes cultured upon winter bear serum (W) or summer bear serum (S) treatment for 48 hours. Gene expression assessed by DNA microarrays was analysed focusing on TGF- β and BMP signalling components. Data are expressed as log₂FoldChange (FC) W/S \pm lfcSE of 3 independent experiments (different cell preparations and bear serum mixes). Statistical significance is shown * padj < 0.05.

We used luciferase reporters to visualise the induction/inhibition of BMP or TGF- β transcriptional activity in muscle cells cultivated with bear serum (see Appendix 10.3). To minimise the need for bear serum, we miniaturised the protocol using the immortalised CCL136 human muscle cell line (rhabdomyosarcoma cell line).

BMP signalling. We first used a BMP response element (BRE) luciferase reporter containing the mouse ID1 promoter responsive region for BMP [430]. We first validated that this pathway is active and that the machinery to transduce the BMP signal from the ligand to the target genes is operational in CCL136 cells (data not shown). Thereafter, we observed a decrease in luciferase intensity when CCL136 were treated with WBS for 6 to 24h compared to SBS (Figure 50). This was confirmed on HM after 24h WBS treatment (Figure 50). These data suggest that the downregulation of *ID1* observed in hibernating bear muscles *in vivo* is the result of a compound present in WBS. Furthermore, this effect of WBS could be direct since it occurred after only 6h of treatment (Figure 50).

TGF- β signalling. We also used a SMAD binding element (SBE) luciferase reporter containing four copies of the SMAD binding site GTCTAGAC corresponding to the main TGF- β responsive element

[431]. We did not observe any change in luciferase intensity in CCL136 cultivated with WBS or SBS after 24h treatment (Figure 50). This experiment will be (1) complemented by a kinetic study of bear serum treatment, with notably shorter time points of treatment, and (2) performed on HM.

MEF2 non-canonical signalling. Finally, we used luciferase reporter for MEF2 transcription factors. As mentioned in the state of the art (see section 4.2.4.2) MEF2 transcription factors may be linked to the BMP pathway through the non-canonical signalling TRAF6-TAK1-p38, although no studies have ever explored this connection in muscle.

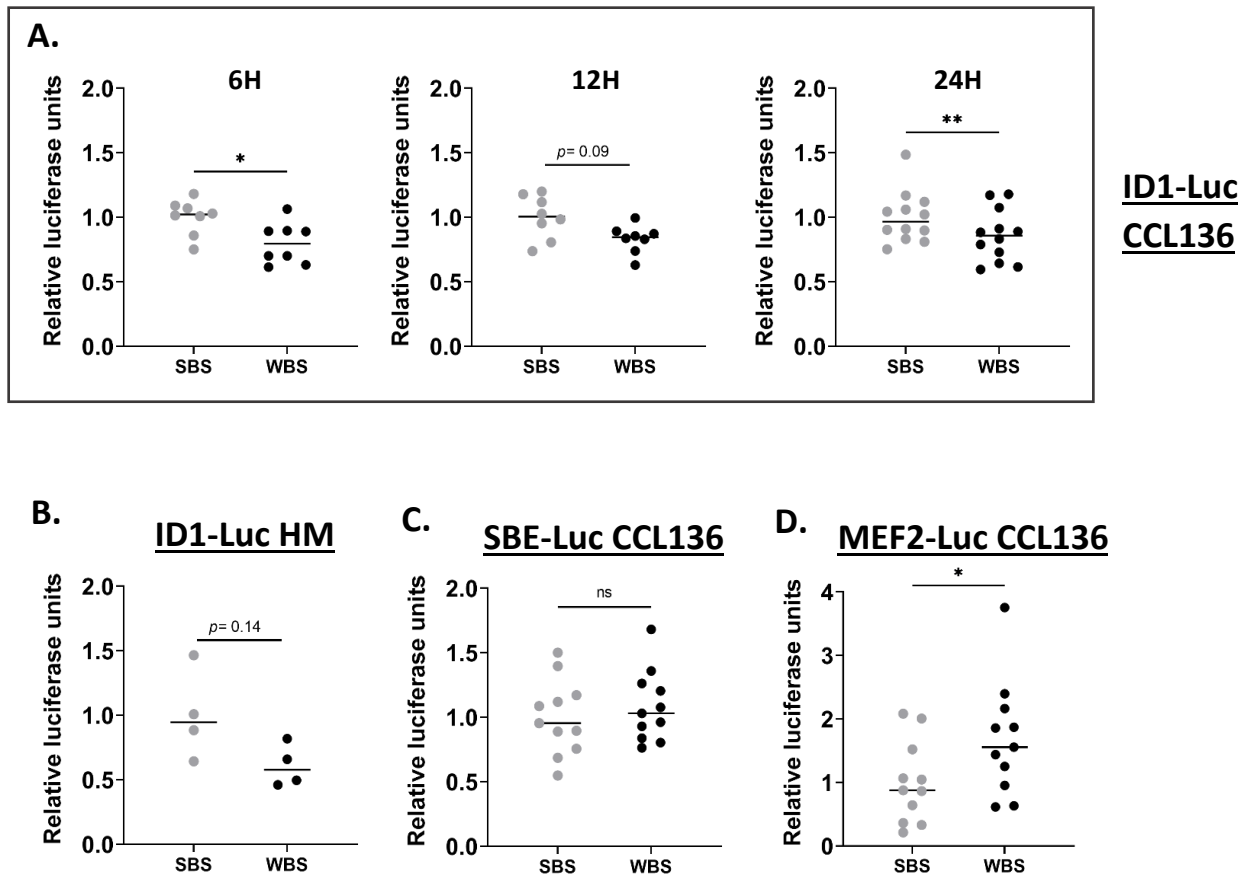


Figure 50. Winter bear serum mimics in human muscle cells what occurs naturally in the muscles of hibernating bears.

CCL136 cells were transfected with (A) ID1-Luc, (C) SBE-Luc and (D) MEF2-Luc and cultivated with summer bear serum (SBS) or winter bear serum (WBS) for (A) 6, 12 or 24 hours or (B and C) 24 hours. Cells were then lysed and luciferase activity was measured. Data are presented as individuals values with mean bars ($n = 8-12$ bear serum/season the same individuals were sampled and analysed in summer and winter). (B) Human primary myotubes (HM) were transfected with ID1-Luc, cultivated with SBS or WBS for 24 hours, and then lysed before measuring luciferase activity (see Appendix 10.3). Data are presented as individuals values with mean bars ($n = 4$ bear serum/season). Statistical significance is shown (Ratio paired t test) * p value<0.05; ** p value<0.01; ns: non-significant.

Moreover, our team has previously shown a MEF2A signature in hibernating bear muscles compared to its active counterpart [332], and we observed that *MEF2A* and *MEF2C* were also upregulated in hibernating bear muscles compared to active bear muscles in study 1 (see Paper 6.3) [351]. We observed that CCL136 cells cultivated for 24h with WBS increased the luciferase intensity compared to

the cells treated with SBS (Figure 50). This preliminary result is very promising as this is the second proof of concept that a compound in the WBS can mimic what happens naturally in winter bear muscles *in vivo*. Further studies are needed to determine whether this MEF2 signature observed in hibernating bear muscle, *in vivo* and in human muscle cells cultured with WBS, could be under the control of the TGF- β and/or BMP pathway via a circulating compound.

8.2.3 Perspective on identifying the circulating active compound in WBS

The identification of compounds in hibernating bear serum that have the potential to control the TGF- β /BMP balance is the core of a project recently granted by the ANR⁴⁶ with a PhD student just starting. The prospects are promising. They will include confirmation of the results with the MEF2-Luc reporter in HM, and repetition with more individuals for the ID1-Luc reporter.

Is ID1 disconnected from BMP signalling in skeletal muscle? The decrease in the luminescence of ID1-Luc reporter observed in HM cultivated with WBS is coherent with what we showed in hibernating bear muscles (see Paper 6.3) [351]. However, ID1 is a well-known BMP target gene in bone and cartilage (see Discussion 6.4.2.1), therefore its reduction raises questions about the disconnection of ID1 transcription and BMP transcriptional activity in skeletal muscle. Moreover, ID1 expression is under the control of other signalling pathways, including TGF- β [362,363]. Whether the decrease in *ID1* expression in hibernating bear muscles or HM cultivated with WBS reflects inhibition of TGF- β signalling remains to be explored. Therefore, we will examine the SMADs nuclear translocation, as performed in study 2, in HM cultivated with either WBS or SBS. Then, once the genetic signature of BMP signalling in muscle cells will be identified (see Discussion 6.4.2.1), we will design a BMP-Luc reporter with a BMP-dependent gene in muscle to address whether a circulating compound can activate the transcriptional activity of BMP signalling when HM are cultivated with WBS.

Is BMP canonical signalling involved? Subsequently, we will decipher the molecular mechanisms capable of inducing BMP signalling when human muscle cells are exposed to winter bear serum. For example, we can examine whether BMP inhibition with silencing RNAs (e.g. siSMAD1) or pharmacological treatments (e.g. noggin) abolish/limit ID1 down-regulation or MEF2A up-regulation in cells treated with SBS or WBS. This will allow us to find out whether the biological effect observed on muscle cells treated with WBS is mediated by BMP canonical signalling.

What is the nature of the active compound in WBS? The project also includes serum fractionation processes (e.g. delipidation, dealbumination, heat denaturation) to determine the nature of the compounds that may be involved in the regulation of the TGF- β /BMP balance in muscle cells. Serum

⁴⁶ agence nationale de la recherche

fractionation is already performed by one of our collaborators, Dr Bertile Fabrice at the IPHC in Strasbourg. This is also why we have miniaturised the reporter assay experiments in 96-well plates using CCL136 cells to test the different fractions and easily read the luminescence of the TGF- β /BMP reporters. Therefore, we will be able to investigate the nature of the compound (e.g. lipid, protein, ...) leading to transcriptional modifications of the TGF- β /BMP signalling *in vitro*.

Finally, the aim is also to reproduce *in vitro* and then *in vivo* the atrophy resistance phenotype of hibernating bear muscles, using active fractions and/or compounds of bear serum to prevent or reverse atrophy under catabolic conditions (e.g. dexamethasone-induced atrophy on myotubes *in vitro*).

9. General conclusion

Some therapies to combat muscle wasting have been developed, including exercise, nutritional interventions and certain medications. However, no effective treatment has been found to completely and safely prevent muscle wasting. Furthermore, despite all its preclinical success, modulation of TGF- β signalling has not translated into the desired effects in humans. The promotion of BMP signalling has received very little attention to date, and the concept that simultaneous fine-tuning of the BMP and TGF- β pathways might be of interest against the development of muscle atrophy has been mentioned in very few papers. The use of a model of natural resistance to muscle atrophy, the hibernating brown bear, has great potential for the discovery of new therapeutic targets for the human clinic. In addition, our comparative physiology strategy between an induced atrophy model and an atrophy-resistant model unveiled new and promising avenues for new future treatments. In this thesis project, we (1) performed a transcriptomic analysis comparing hibernating versus active bear muscles to unloaded versus control mouse muscles, (2) studied the impact of controlled ATF4 induction by halofuginone in mice subjected to hind limb suspension and (3) explored the effect of winter bear serum on human muscle cells. This work (1) demonstrated that the BMP/TGF- β balance is important in the muscle atrophy resistance phenotype and (2) suggested that it could be replicated in human muscle cells by the presence of circulating compounds in hibernating bear serum. The identification of new relevant targets within the BMP and TGF- β pathways that could be modulated by compounds in the hibernating bear serum and the identification of these compounds would therefore allow the development of innovative strategies against muscle atrophy. The continuation of this project is therefore the first step in the future development of new therapeutic solutions to confer resistance to muscle atrophy in humans.

10. Appendix

10.1 Materials and Methods discussion 1

10.1.1 Identification of BMP target genes in skeletal muscle

Cell culture. The CCL136 human rhabdomyosarcoma cell line (ATCC, USA) was maintained in dulbecco's modified eagle medium (DMEM) 4,5g/L glucose medium (Gibco, USA) containing 1% penicillin-streptomycin (Gibco, USA) and 10% fetal bovine serum (FBS) (Gibco, USA). The cells were seeded in 12-wells plates at a density of 1.5×10^5 cells/well, cultured at 37 °C under 5% CO₂, and transfected the day after.

Plasmid. Plasmid cloning (pc)DNA3-ALK3 K261R was a gift from Aristidis Moustakas (Addgene plasmid # 80875; <http://n2t.net/addgene:80875>; RRID: Addgene_80875) [367]. This pcDNA3 back bone contains the DNA sequence of the BMP receptor BMPR1A/ALK3 carrying a K261R mutation leading to an inactive kinase.

Transfection. CCL136 cells were transfected using the ViaFect Transfection Reagent (Promega, E4981). The ratio of ViaFect™ Transfection Reagent volume (μL) to DNA amount (μg) was optimised with green fluorescent protein (GFP) transfection assays prior to the actual experiments. We chose the 3:1 ratio (3 μl reagent: 1 μg DNA) as increasing the quantity of DNA or reagent did not increase the efficacy of the transfection. On the day of transfection, DNA and Viafect transfection reagent were mixed at the 1:3 ratio described above in a serum-free medium and incubated for 15 minutes at room temperature to form the ViaFect™ Transfection Reagent:DNA complex. Cells were transfected with 1 μg of DNA/well by adding 100 μl of the transfection mixture to the wells.

GDF5 treatment. After one night of transfection, the media have been replaced by fresh media. Half of the wells were treated with recombinant human GDF5 protein (Accession # P43026, BioLegend) at 0.1 μg /mL for 6 hours. Cells were then washed with phosphate-buffered saline (PBS), harvested for protein extraction in the same protein extraction buffer as described in study 2 (see Paper 7.2) [423], and then stored at -80 until use. Western blots experiments have been performed as described in study 2 (see Paper 7.2) [423] with the same SMAD4 and SMAD1/5 antibodies, and Phospho-SMAD1/5 (Ser463/465) (#9516, Cell Signalling Technology, Saint-Cyr-L'Ecole, France) diluted 1:1000 in 5% bovine serum albumin (BSA).

10.1.2 Is SMAD4 recruited more by TGF- β or BMP signalling: Co-immunoprecipitation

Protein extraction. 5 mg of bear muscle powder were lysed on ice using a polytron with 500 μ L NP-40 buffer (10mM Tris pH 7.5, 150 mM NaCl, 1 mM EDTA, 1.0% Nonidet P-40, 20mM beta-glycerophosphate) containing inhibitors of proteases (Protease Inhibitor Cocktail) and phosphatases (1 mM Na₃VO₃, 10 mM NaF) (Sigma, Saint-Quentin-Fallavier, France). The homogenates were then centrifuged at 10,000 g for 10min at 4°C and the concentration was determined using the Bradford Protein Assay Kit (Biorad, Marnes-la-Coquette, France). An aliquot was taken for protein expression analyses.

Immunoprecipitation. The remaining lysates, containing equivalent amounts of 1 mg of total protein, were pre-cleaned for 1 h with 40 μ L of Protein A-Agarose beads (sc-2001, Santa Cruz Biotechnology) and 1 μ g of IgG isotype control antibody (sc-2027, Santa Cruz Biotechnology, Nanterre, France) with gentle rotation at 4°C. The samples were then centrifuged at 3200g for 30 seconds at 4°C, and the supernatants were stored. Immunoprecipitation was performed by the addition of 1.8 μ g of SMAD4 antibody (ab230815, Abcam, Cambridge, UK) and protein A-Agarose, followed by incubation at 4°C overnight with gentle rotation. The immune complex was isolated by centrifugation at 3500g for 5 minutes. The resulting pellet was then washed with 350 μ l of wash buffer (PBS pH 7.4, 5mM EDTA, 10mM NaF) and centrifuged at 3500g for 5 minutes without vortexing. This last step was repeated twice.

Immunodetection. The resulting pellet was eluted in 80 μ L Laemmli 1X. Proteins were then denatured at 95°C for 5min, and 25 μ L of the eluate was separated by sodium dodecyl sulfate–polyacrylamide gel electrophoresis (SDS-PAGE) using tris-glycine eXtended (TGX)[™] FastCast[™] 7,5% Acrylamide gels (Biorad, Marnes-la-Coquette, France) and transferred onto a polyvinylidene difluoride (PVDF) membrane (Hybond P, Amersham, England) using Trans-Blot[®] Turbo[™] Transfer System standard protocol (Biorad, Marnes-la-Coquette, France). Blots were blocked for 1 h at room temperature in Tris-Buffered Saline (TBS) buffer with 0.1% Tween-20 (TBS-T, pH = 7.8) and 5% BSA for all the targets according to the manufacturer's instructions. They were then washed thrice in TBS-T and incubated (overnight, stirring, 4°C) with appropriate primary antibodies: (1) for validating the immunoprecipitation, SMAD4 (ab230815, Abcam, Cambridge, United Kingdom) antibody was used diluted 1:1000 in 5% BSA and (2) for checking the protein partners, membranes were hybridised with either SMAD1/5 (PA5-80036, Thermo Fisher, Illkirch, France) or SMAD2/3 (#8685, Cell Signalling Technology, Saint-Cyr-L'Ecole, France) both diluted 1:1000 in 5% BSA overnight at 4°C. Blots were then washed and incubated for 1 h at room temperature with VeriBlot for IP Detection Reagent (HRP) (ab131366, Abcam) diluted 1:2000 in 5% non-fat dried milk. Signals were detected after incubation

with Luminata Crescendo Western HRP substrate (Millipore, Burlington, MA, USA) and visualized using G: BOX ChemiXT4 (XL1) imaging system (Syngene, Frederick, MD, USA).

10.1.3 Is GDF5 synthesised and released by adipose tissue: GDF5 ELISA

We used the only commercially available GDF5 ELISA kit (Catalog Number: DY853-05 and DuoSet Ancillary Reagent Kit2 Catalog number: DY008; R&D Systems Europe) and performed GDF5 immunodetection in serum from hibernating and active bears following the supplier protocol.

10.2 Materials and Methods discussion 2

10.2.1 Complementary RT-qPCR and Western blots of study 2

RT-qPCR. Reverse transcription and quantitative polymerase chain reaction (RT-qPCR) of gastrocnemius muscle have been performed as previously described in study 2 (see Paper 7.2) [423] and the primers used are described in the following table :

Gene	Forward	Reverse
<i>Atg5</i>	TCAACCGGAAACTCATGGAA	CGGAACAGCTTCTGGATGAA
<i>Atg12</i>	TAAACTGGTGGCCTCGGAAC	CCATCACTGCCAAAACACTCA
<i>Atg16</i>	TCCCGTGATGACCTGCTAAA	CAGTCAGAGCCGCATTTGAA
<i>Map1lc3a</i>	GAGCGAGTTGGTCAAGATCA	GGAGGCGTAGACCATGTAG
<i>Bnip3</i>	TCACTGTGACAGCCACCTC	GCTGTTTTTCTCGCCAAAGC
<i>Col1a1</i>	CGTGGTGACAAGGGTGAGAC	AACCAGGAGAACCAGGAGGA
<i>Col3a1</i>	CTGCTGGTCCTTCTGGTGCT	AGCCACGTTCAACCAGTTTCA
<i>Col5a2</i>	CCTGGTCCAAATGGTGAACA	CCAGGGTTTCCTTCCTTTCC
<i>Col6a1</i>	CCACAACCAGATGCAAGAGC	CACCAGCCATCCATTGTAGC

Immunodetection of LC3 protein. The lipidation of the LC3 protein has been assessed by Western blots in gastrocnemius muscle, as previously described in study 2 (see Paper 7.2) [423]. As LC3 protein has a pHi > 8.0, a CAPS (3-(cyclohexylamino)-1-propanesulfonic acid)-ethanol buffer (10 mM CAPS, 10% ethanol, pH = 11) was used to optimise protein transfer. Blots were blocked for 1 h at room temperature in TBS buffer with 0.1% Tween-20 (TBS-T, pH = 7.8) with 5% non-fat dried milk according to the manufacturer's instructions. They were then washed thrice in TBS-T and incubated (overnight, stirring, 4°C) with LC3 antibody (#ab48394, Abcam) diluted 1:1000 with 5% non-fat dried milk.

10.2.2 ATF4 signalling in hibernating bear muscles

Transcriptomic Data and Functional Pathway Enrichment Analysis for ATF4 pathway. Transcriptomic data from the already published study 1 (see Paper 6.3) [351] are openly available in the GEO repository databases (bear: <https://www.ncbi.nlm.nih.gov/geo/query/acc.cgi>, reference number (GSE144856)). Genecards web-based portal was used to draw up an ATF4 gene set list, selecting genes with a score > 1.3. To identify the differentially expressed genes (DEGs) from this list, we selected a Winter/Summer fold change (FC) >|1.0| or <|1.0| with an adjusted p-value < |0.05| as cut-off standards, for the up- and down-regulated genes, respectively. Visualization of functional enrichment was performed using Metascape [432], a web-based portal for visualizing the inference of enriched biological pathways and protein-protein interaction among the DEGs as described in study 1 (see Paper 6.3) [351].

Immunodetection of total and phosphorylated eIF2 α protein. The total and phosphorylated eIF2 α protein content has been assessed by Western blots in vastus lateralis muscle of bears, as previously described in study 1 (see Paper 6.3) [351] using eIF2 α (#9722S, Cell Signalling) and p-Ser51eIF2 α (#ab32157) antibodies diluted 1:1000 in 5% BSA.

10.3 Materials and Methods discussion 3

10.3.1 Optimisation of tools for screening active compounds in WBS

Cell culture. CCL136 cells were cultured as described in Materials and Methods discussion 1, and seeded in 96-wells plates at a density of 2.0×10^4 cells/well.

Human myotubes (HM) were derived from vastus lateralis muscle biopsies obtained from healthy control donors (Diomedee experimental protocol). All procedures were approved by the French Ethical Committee SUD EST IV (Agreement #12/111A 13-02) and performed according to French legislation (Huriet's law). All patients gave their written consent after being informed of the nature, purpose, and possible risks of the study. The myoblasts were thawed from liquid nitrogen, directly plated into 6-well plates coated with collagen (Corning® BioCoat® Collagen I 6-well Clear Flat Bottom TC-treated Multiwell Plate, Product Number 356400), and maintained in medium Ham's F10 (1g/L glucose, Dutscher) containing 1% penicillin-streptomycin (Gibco, USA) and 10% FBS (Gibco, USA). The cells were seeded in 12-wells plates at a density of 4×10^4 cells/well and cultured at 37 °C under 5% CO₂. After reaching 80% confluence, differentiation was triggered by replacing the previous medium with DMEM 1g/L glucose containing 2% FBS for 5 days. The differentiation media were changed every other day.

Plasmid. pGL3 BRE Luciferase was a gift from Martine Roussel & Peter ten Dijke (Addgene plasmid # 45126; <http://n2t.net/addgene:45126>; RRID: Addgene_45126) [430]. Two copies of the SMAD binding element present in the ID1 promoter are cloned into pGL3-MLP-luc minimal promoter vector.

SBE4-Luc was a gift from Bert Vogelstein (Addgene plasmid # 16495; <http://n2t.net/addgene:16495>; RRID: Addgene_16495) [431]. This vector contains four copies of the SMAD binding site (GTCTAGAC) which are cloned into pBV-Luc.

3XMEF2-luc was a gift from Ron Prywes (Addgene plasmid # 32967 ; <http://n2t.net/addgene:32967> ; RRID:Addgene_32967). This plasmid was cloned from pFOS WT-GL3 (Addgene #11983), where the human c-fos promoter was removed and replaced with 4 MEF2 sites.

Transfection. CCL136 were transfected with 50 ng of DNA/well the day after seeding and HM cells with 1 µg of DNA/well at the end of the differentiation process, by adding respectively 5 or 100 µl of the transfection mixture described above (see Appendix 10.1). We added a renilla luciferase plasmid (i.e. 0,25 ng for CCL136 and 5 ng for HM) in the transfection mixture for intra-well luminescence normalisation

Bear serum treatment. After one night of transfection, the media have been replaced by fresh media containing 5% winter or summer bear serum instead of 5% FBS for 6, 12 or 24 hours. CCL136 cells were treated with the serum of 12 individuals bears for each season. HM cells were treated with 3 mixes of bear serum for each season. Bears characteristics for individuals sera or for pools of sera are described in the table below. Cells were then washed with PBS and lysed with the passive lysis buffer from Dual-Luciferase® Reporter Assay System 100 assays E1910 (Promega, Charbonnières-les-Bains, France) by adding 20 µl for CCL136 or 250 µl for HM cells.

Bear ID_number	Year of collection	Age (year)	Gender	Experiments
w1601	2017	2	M	CCL136 cell line, BRE, SBE or MEF2 plasmid transfection
w1610		2	M	
w1604	2018	3	F	
w1701		2	F	
w1707	2019	3	F	
w1709		3	F	
w1803		2	F	
w1806		2	F	
w1812		2	M	
w1814	2020	2	M	
w1813		3	F	
w1909		2	F	

Pools	Bear ID_number	Year of collection	Age (year)	Gender	Experiments
P1	1813	2020	3	F	HM cell line, BRE plasmid transfection
	1509	2017	2	F	
	1701	2018	2	F	
	1814	2019	2	M	
P2	1604	2018	3	F	
	1610	2017	2	M	
	1710	2018	2	F	
	1803	2019	2	F	
P4	1707	2019	3	F	
	1608	2017	2	F	
	1806	2019	2	F	
	1812	2019	2	M	

Luminescence reading. In the Dual-Luciferase® Reporter (DLR™) Assay System, the activities of firefly (from BRE-Luc, SBE-Luc or MEF2-Luc plasmids) and renilla luciferases are measured sequentially from a single sample. 10 µl of the lysed cells were added in each well of a 96-well flat-white plate. Thereafter, the plate was placed into the plate-reading Synergy™ 2 luminometer (Biotek, Colmar, France) equipped with two reagent injectors. The firefly luciferase reporter was measured first by adding 50 µl of Luciferase Assay Reagent II (LAR II) in each well. After quantifying the firefly luminescence for 12 seconds, this reaction was quenched, and the renilla luciferase reaction was simultaneously initiated by adding 50 µl of Stop & Glo® Reagent to the same well. The Stop & Glo® Reagent also produces a stabilized signal from the renilla luciferase, which decays slowly over the course of the measurement. The signal was measured for 12 seconds. The firefly values were then normalised by the renilla luciferase values.

10.4 Review

Review

Ubiquitin Ligases at the Heart of Skeletal Muscle Atrophy Control

Dulce Peris-Moreno , Laura Cussonneau, Lydie Combaret , Cécile Polge [†]  and Daniel Taillandier ^{*,†}

Unité de Nutrition Humaine (UNH), Institut National de Recherche pour l'Agriculture, l'Alimentation et l'Environnement (INRAE), Université Clermont Auvergne, F-63000 Clermont-Ferrand, France; dulce.peris-moreno@inrae.fr (D.P.-M.); laura.cussonneau@inrae.fr (L.C.); lydie.combaret@inrae.fr (L.C.); cecile.polge@inrae.fr (C.P.)

* Correspondence: daniel.taillandier@inrae.fr

† These authors contributed equally to the work.

Abstract: Skeletal muscle loss is a detrimental side-effect of numerous chronic diseases that dramatically increases mortality and morbidity. The alteration of protein homeostasis is generally due to increased protein breakdown while, protein synthesis may also be down-regulated. The ubiquitin proteasome system (UPS) is a master regulator of skeletal muscle that impacts muscle contractile properties and metabolism through multiple levers like signaling pathways, contractile apparatus degradation, etc. Among the different actors of the UPS, the E3 ubiquitin ligases specifically target key proteins for either degradation or activity modulation, thus controlling both pro-anabolic or pro-catabolic factors. The atrogenes MuRF1/TRIM63 and MAFbx/Atrogin-1 encode for key E3 ligases that target contractile proteins and key actors of protein synthesis respectively. However, several other E3 ligases are involved upstream in the atrophy program, from signal transduction control to modulation of energy balance. Controlling E3 ligases activity is thus a tempting approach for preserving muscle mass. While indirect modulation of E3 ligases may prove beneficial in some situations of muscle atrophy, some drugs directly inhibiting their activity have started to appear. This review summarizes the main signaling pathways involved in muscle atrophy and the E3 ligases implicated, but also the molecules potentially usable for future therapies.

Keywords: skeletal muscle atrophy; hypertrophy; E3 ubiquitin ligase; MuRF1; MAFbx; anabolism; catabolism; signaling; therapy; treatment



Citation: Peris-Moreno, D.; Cussonneau, L.; Combaret, L.; Polge, C.; Taillandier, D. Ubiquitin Ligases at the Heart of Skeletal Muscle Atrophy Control. *Molecules* **2021**, *26*, 407. <https://doi.org/10.3390/molecules26020407>

Academic Editor: Jorge A. R. Salvador
Received: 8 December 2020
Accepted: 10 January 2021
Published: 14 January 2021

Publisher's Note: MDPI stays neutral with regard to jurisdictional claims in published maps and institutional affiliations.



Copyright: © 2021 by the authors. Licensee MDPI, Basel, Switzerland. This article is an open access article distributed under the terms and conditions of the Creative Commons Attribution (CC BY) license (<https://creativecommons.org/licenses/by/4.0/>).

1. Introduction

Cachexia is a multifactorial syndrome leading to serious clinical complications with high mortality rates and is present in almost all chronic diseases [1]. Besides inflammation and metabolic modifications, skeletal muscle loss is an important factor of cachexia and limiting muscle wasting is a major challenge for maintaining well-being of patients, the capacity of the organism to fight against diseases and the tolerance of the patients towards challenging therapies like cancer chemotherapies [2].

Muscle homeostasis is mainly driven by the ubiquitin-proteasome system (UPS) that controls signaling pathways, contractile structure, cellular architecture, energy metabolism, protein translation, etc., thus allowing a fine-tuning of skeletal muscle metabolism [3–6]. The UPS is composed by hundreds of proteins and controls protein fate by ubiquitination, a post-translational modification carried out by the E1, E2, E3 enzymatic cascade (see [7] for a review). Ubiquitin (Ub) is covalently attached to the target proteins thanks to the interactions between Ub conjugating E2 enzymes (35–40 members according to species) and E3 Ub ligases (>600 in human). Another complexity of the UPS resides in the multitude of Ub signals that can be synthesized on the target proteins, from mono-Ub, multiple mono-Ub, or poly-Ub chains with at least eight different topologies. Each type of Ub modification is dedicated to a specific fate for the target protein, the role of some Ub linkages being

still obscure. This Ub code can send the target protein for either proteasome or autophagy degradation or for non-proteolytic purposes (addressing, stabilization, activation, etc.) [7]. Furthermore, the multiple possible combinations between a given E3 and several E2s (and vice versa) further increase the potential of the UPS for controlling cellular metabolism.

E3 ligases can be either monomeric or multi-protein complexes and are classified into three families according to their structure and mode of action (recently reviewed [8]). The first class contains 28 members that contain a C-terminal Homologous to E6-Associated Protein C Terminus (HECT) domain that is necessary and sufficient to accept Ub from an E2 enzyme and to transfer it to the substrate, HECT E3 ligases having their own catalytic activity. Their N-terminal domain is involved in the recognition of the substrate. The second class comprises $\approx 90\%$ of the E3 Ub ligases and are known as Really Interesting New Gene-finger (RING) type. RING domains are defined by eight cysteine and/or histidine residues coordinating four zinc atoms that allow interaction with E2 enzymes. RING-type E3s do not bind Ub, but they serve as a platform for the E2 and the substrate and promote the Ub transfer from the E2 to the substrate. Within multi-protein RING-E3 complexes, also named cullin-containing RING Ligase E3s (CRLs), several families of proteins with motifs involved in protein-protein interactions (e.g., F-box pattern) are responsible for substrate recognition [9]. The third class of E3 ubiquitin ligases are the RING-in-Between-RING (RBR)-type that combine properties of RING- and HECT-type E3s. They utilize an E2-binding RING domain and a second domain (called RING2) that binds Ub before transferring it to substrate [10,11].

Within muscle atrophy, numerous ubiquitinating enzymes are now identified for their involvement in the regulation of both anabolic and catabolic pathways during the atrophy process, notably by being responsible for the degradation of the contractile proteins [12]. The E3 Ub ligases appear to be at the heart of these regulations and some of them may prove to be efficient therapeutic drug strategies with roughly two main approaches: (i) indirect modulation of an E3 ligase by targeting the signals involved in its regulation [13–16] or (ii) direct inhibition of the E3 ligase [17–19]. However, the intertwinement between anabolic and catabolic processes (including the signaling pathways) often renders difficult an indirect modulation of E3 ligases, while direct inhibition strategies is limited by the somehow limited data available on E3 ligases.

This review summarizes the signaling pathways implicated in muscle homeostasis, and highlights the E3 ligases playing a role in the regulation of skeletal muscle mass and function, excluding the muscle regeneration process where numerous E3 Ub ligases are also involved. We more specifically focus on the strategies that have already been used for modulating E3 ligase activity, including pharmaceutical drugs or natural compound-based approaches.

2. Signaling Pathways Regulating Skeletal Muscle Mass and Function

Skeletal muscle homeostasis is controlled by numerous signaling pathways (Figure 1) that act either as anabolic or catabolic factors. Depicting in detail their regulation is beyond the scope of this review and we just briefly summarize their implication in muscle mass control.

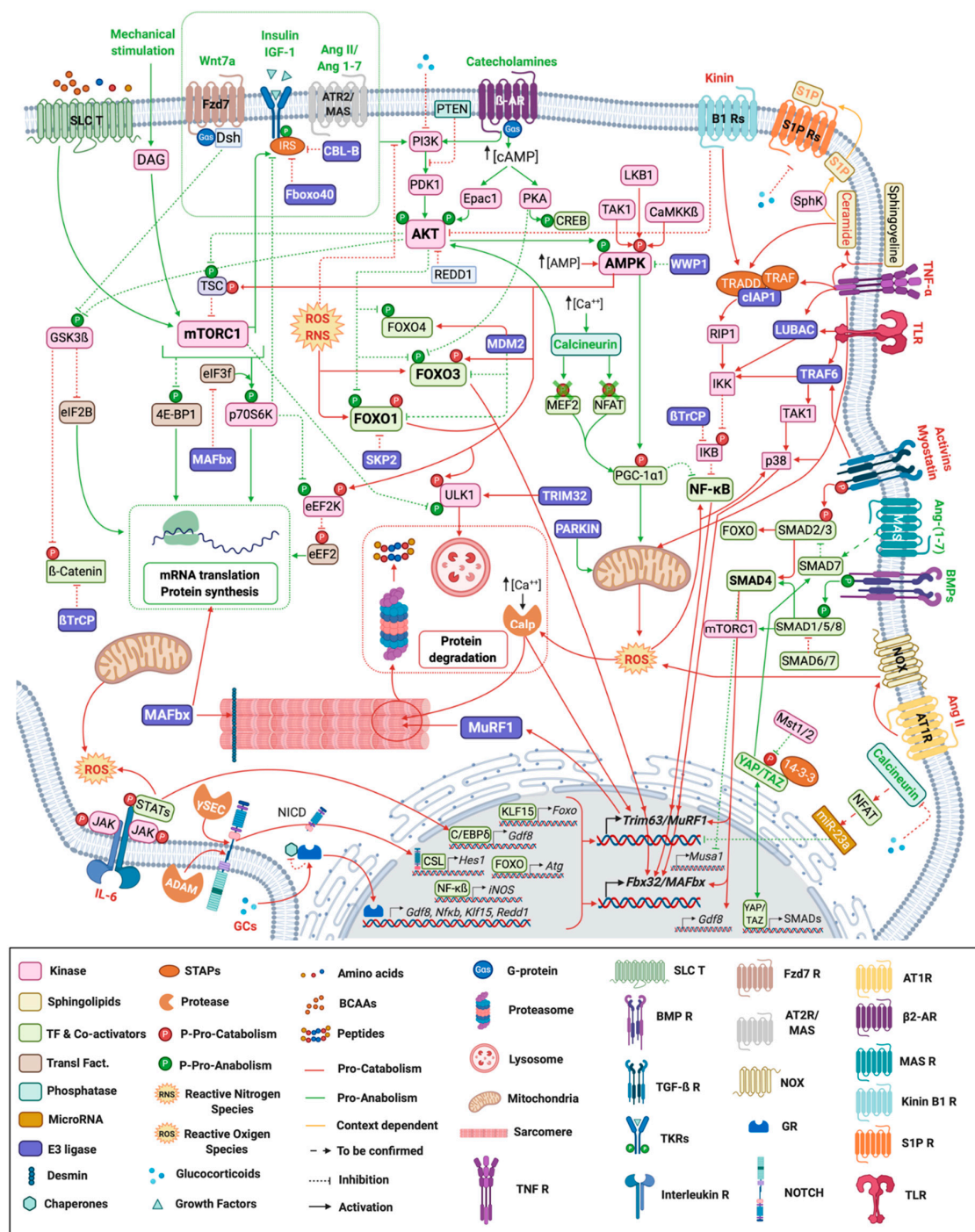


Figure 1. Signaling pathways regulating skeletal muscle mass and function. Myofiber representation of the different signaling pathways controlling skeletal muscle mass and function during atrophy conditions. Ligands and arrows (both with head or perpendicular line) in green denote those signaling pathways and interactions with an anabolic effect whereas the red ones represent catabolic signaling. Orange ligands and arrows stand for pathways with a dual role (context-dependent). β2-AR: β-2 Adrenergic Receptor; γ-sec: γ-secretase; Ang: Angiotensin; AT1R: Angiotensin II Type 1 Receptor; AT2R: Angiotensin II Type 2 Receptor; BCAAs: Branched-chain amino acids; BMP R: Bone Morphogenetic Receptor; Calp: Calpain; CSL: CBF1, Suppressor of Hairless, Lag-1; Dsh: Dishevelled; Fzd: Frizzled; GR: Glucocorticoid Receptor; IL-6: Interleukin-6; NICD: Notch Intracellular domain; NOX: NADPH oxidase activator; P: Phosphorylation; S1P: Sphingosine-1-phosphate; SLC T: Solute Carrier Transporter; STAPs: Signal Transducing Adaptor Proteins; TF: Transcription Factors; TGF-β R: Transforming Growth Factor β Receptor; TKR: Tyrosine-protein Kinase Receptor; TLR: Toll-like Receptor; TNF R: Tumor Necrosis Factor Receptor; Transl. Fact.: Translational Factors.

2.1. Anabolic Pathways

2.1.1. PI3K/AKT Signaling Pathway

Skeletal muscle hypertrophy via the PI3K/AKT (phosphatidylinositol 3-kinase/protein kinase B) pathway can be induced by nutrients (amino acids, glucose and fatty acids) [20], hormones (insulin) [20,21] growth factors (Insulin Growth Factor-1 (IGF-1)) [22,23], and mechanical stimuli (e.g., exercise) [24]. Upon ligand binding, the PI3K/AKT pathway activates mTORC1 that phosphorylates numerous substrates [25,26], which regulate the activation of translation, transcription, ribosome biogenesis, and autophagy [27,28]. AKT also phosphorylates and inactivates GSK3 β (a negative regulator of protein translation) [29] and the pro-catabolic FOXOs transcription factors (TF), the latter being crucial inducers of muscle loss upon catabolic situations via the expression of numerous atrophy-related genes [30–33]. Moreover, mTORC1 also inhibits the autophagy induction complex [34]. Intriguingly, mTORC1 can also exhibit adverse effects on skeletal muscle homeostasis upon denervation [35] or ageing [36,37]. In these situations, a negative feedback loop from mTORC1 to AKT was involved, thus favoring FOXOs activation and the subsequent expression of proteolytic genes like the atrophy-related E3 ligases *MuRF1/TRIM63* and *MAFbx/Atrogin-1*.

2.1.2. G Protein-Coupled Receptors (GPCRs) and cAMP Signaling

1. β 2-Adrenergic Receptors Signaling Pathway

Upon stimulation by endogenous catecholamines or synthetic agonists, β 2-Adrenergic Receptors (β 2-ARs) lead to skeletal muscle hypertrophy (Figure 1) through: (i) PKA-mediated expression of genes containing cAMP response elements (follistatin, NR4A3, calpastatin) via CREB [38] (ii) PKA-mediated inhibition of FOXO activity in vivo [39] or (iii) the activation of PI3K/AKT/mTORC1 [40,41], or both AKT and CaMKII/HDAC4 signaling [42].

2. WNT/FZD Signaling Pathway

The Wingless-type mouse mammary tumor virus integration site (Wnt) family of proteins induce hypertrophy via Wnt/ β -catenin and PI3K/AKT/mTORC1 cascades [43,44] (Figure 1). The former one controls the transcriptional regulation of growth-related genes (e.g., *C-myc* and *Cyclin 1*) via β -catenin and T-cell factor/lymphoid enhancer factor (TCF/LEF) transcription factors [45,46] whereas the latter regulates the protein synthesis process. The PI3K/AKT/mTORC1 pathway is induced via the specific interaction of WNT7a (ligand) and FZD7 (receptor) proteins [47–50]. Under mechanical stimulation, WNT is the only pathway able to stabilize β -catenin and therefore to promote growth-related gene expression [51,52]. Accordingly, therapeutic stimulation of WNT7a/FZD7 by injection of recombinant Wnt7a resulted in a significant increase in muscle strength and a reduce contractile damages in mdx mice (Duchenne Muscular Dystrophy (DMD) model) [49]. By contrast, in dystrophic muscles WNT7a increased fibrosis by inducing transforming growth factor- β 2 (TGF β 2) [53], and Wnt activation enhanced the fibrotic response in aged mice [54]. These data suggest WNT7a to have a context-dependent effect in skeletal muscle, thus complicating future therapeutic strategies.

2.1.3. Calcineurin Signaling Pathway

Different downstream effectors have been proposed for calcineurin (Cn) during skeletal muscle hypertrophy, such as NFAT [55], GAT-2 [55] and MEF-2 [56], which seem to be activated during skeletal muscle hypertrophy in a fiber-specific manner [57]. Cn can modulate these TFs and downstream effectors (including the E3 ligases *MuRF1/TRIM63* and *MAFbx/atrogin-1*) upon several conditions (dexamethasone [58], diabetes [56], exercise [59] or starvation [60] (Figure 1).

2.1.4. Hippo Signaling Pathway

The Hippo signaling pathway consists of a cascade of kinases that inhibits the transcriptional co-activators YAP and TAZ (Figure 1) (for a review, see [61]). Upon exercise and myostatin/activin inhibition in *mdx* mice [62], mechanical overloading [63] and following injury or degeneration of motor nerves [64], the expression and phosphorylation of YAP increased [62,63] along with those of other pro-hypertrophy proteins [40]. Furthermore, YAP negatively regulated the myostatin/activins signaling pathway by inhibiting SMAD2/3 transduction and consequently blunted the SMAD-mediated MuRF1/TRIM63 E3-ligase expression [63].

2.2. Transforming Growth Factor (TGFs), Pro-Anabolic and Pro-Catabolic Pathways

The transforming growth factor (TGF) multifunctional cytokine family is divided in two subfamilies with opposite outcomes on muscle mass: myostatin/activin/TGF- β are negative regulators of muscle mass and BMPs (Bone Morphogenic Proteins)/GDF (Growth and Differentiation Factors) are positive regulators [65]. Myostatin/activin/TGF- β activate the pro-catabolic SMADs 2–3 whereas BMP ligands recruit pro-anabolic Smads 1-5-8 and elicit an anabolic transcriptional program (Figure 1). SMAD4 is shared by both pro-anabolic and pro-catabolic SMADs and can be a limiting factor for SMADs downstream effects [45].

Upon myostatin binding, Mafbx/Atrogin-1 and genes involved in the degradation of several anabolic factors (ribosomal proteins, translation initiation factors, MyoD, desmin and vimentin) are up-regulated [49,66] and the AKT/mTORC1 pathway is inhibited [67]. TGF- β signaling also regulates *MuRF1/Trim63* expression through the synergistic action of FOXO3a and SMAD3 [68,69] (see [12] for a recent review). Similarly, Activin A ligand negatively regulates muscle mass by binding to the same receptor than myostatin and by activating the same intracellular pathway [70–72]. Interestingly, the non-canonical TGF- β pathway involving TAK1-p38 MAP kinase can also be activated under Activin A treatment in cellulo and in vivo, with MAFbx-mediated myotube atrophy [73]. Moreover, TGF- β induces skeletal muscle atrophy through a mechanism dependent on NOX-derived ROS production, in vivo [69]. The TGF- β pathway is also known for its master role in fibrosis, which promotes muscle mechanical constraints and injuries [74,75]. Recent reports showed that the canonical NF- κ B and angiotensin pathways mediate the TGF- β effects in cellulo and in vivo [76].

Conversely, the BMP pathway regulates hypertrophy by repressing the E3 ligases MUSA1/Fbxo30 [77] MAFbx/Atrogin-1, MuRF1/Trim63 [78,79] and through the positive modulation of mTORC1 and consequently protein synthesis [80]. Additionally, the long non-coding RNAs Myoparr and Chronos negatively modulate the BMP pathway (and muscle mass) by repressing *Gdf5* [81] and *Bmp7* [82] respectively. Altogether, a major conceptual idea is that a net balance between TGF- β /BMP pathways plays a major role in determining skeletal muscle mass.

2.3. Catabolic Pathways

2.3.1. AMPK Signaling Pathway

The adenosine 5'-monophosphate-activated (AMP)-activated protein kinase (AMPK) is an energy sensor that preserves energy by turning on catabolic pathways and turning off ATP-consuming anabolic pathways [83–85]. In skeletal muscle, AMPK inhibits protein synthesis through the reduction of the mTORC1 signaling and favors contractile protein breakdown via the activation of FOXO1 and FOXO3a TFs (Figure 1) [86]. Consequently, MuRF1/TRIM63 and MAFbx/Atrogin-1 E3 ligases target different proteins involved in muscle contraction and protein synthesis initiation for UPS-dependent degradation [86,87]. Additionally, AMPK also promotes skeletal muscle autophagy [88].

2.3.2. The NF- κ B Signaling Pathway

NF- κ B, a major pro-inflammatory transcription factor, is considered one of the main effectors of muscle atrophy via the regulation of UPS-related proteins expression [89–96].

Indeed, the NF- κ B pathway is consistently upregulated upon catabolic conditions in both mouse models [89,97,98] and patients suffering from chronic obstructive pulmonary disease (COPD) [99] or chronic heart failure (CHF) [100] patients. A hypertrophic response is also observed in myotubes when blunting NF- κ B activation upon catabolic TNF α exposure [93]. In addition to TNF α induction of NF- κ B signaling, other proinflammatory cytokines (such as IL6 and TWEAK), bacterial products, growth factors, ROS, genotoxic stress, and viruses can activate this pathway [101]. Interestingly, for controlling the proper signaling, the NF- κ B pathway comprises several E3 ubiquitin ligases, TRAF6 [95,102,103], cIAP1 [19,104], LUBAC [95,105], SCF $^{\beta}$ -TRCP [105,106] that represent several opportunities for future potential therapies (Figure 2).

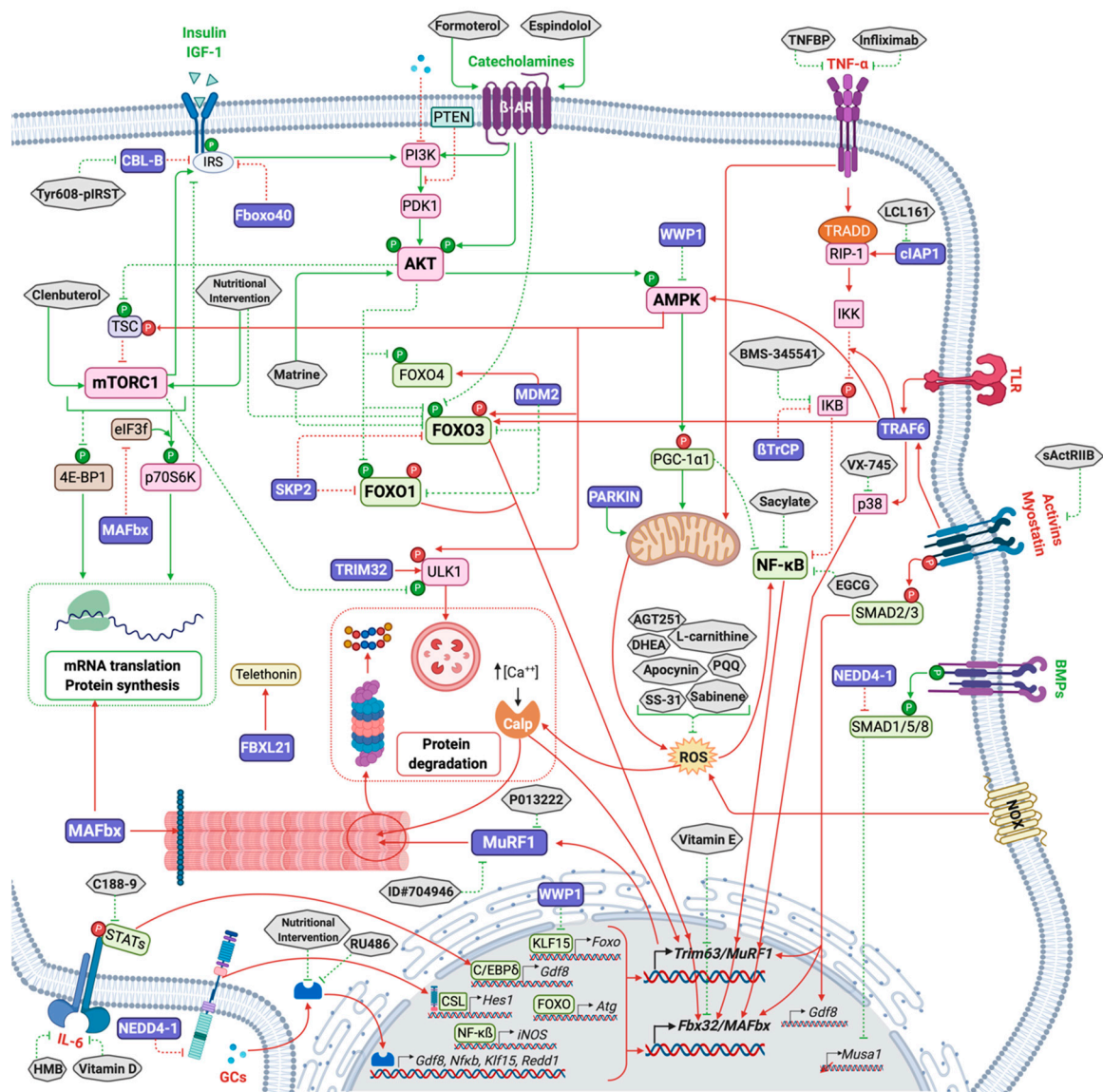


Figure 2. Cont.

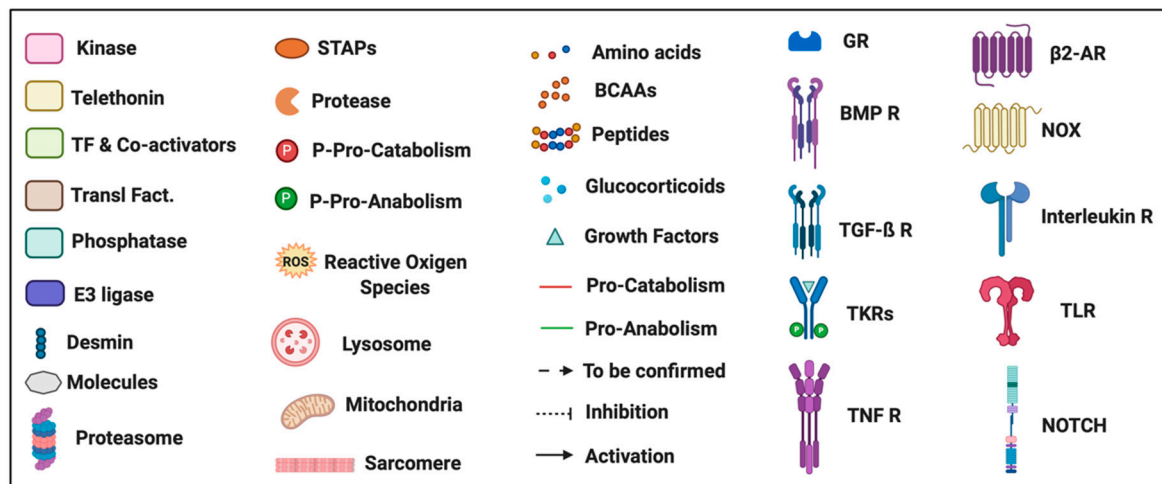


Figure 2. E3 ubiquitin ligases regulating skeletal muscle mass and molecules developed to modulate their activity and expression. Myofiber representation of the different E3-ligases and molecules targeting the signaling pathways controlling skeletal muscle mass and function during atrophy conditions. Ligands and arrows (both with head or perpendicular line) in green denote those signaling pathways and interactions with an anabolic effect whereas the red ones indicate catabolic signaling. β 2-AR: β -2 Adrenergic Receptor; BCAAs: Branched-chain amino acids; BMP R: Bone Morphogenetic Receptor; Calp: Calpain; CSL: CBF1, Suppressor of Hairless, Lag-1; GR: Glucocorticoid Receptor; IL-6: Interleukin-6; NCID: Notch Intracellular domain; NOX: NADPH oxidase activator; P: Phosphorylation; STAPs: Signal Transducing Adaptor Proteins; TF: Transcription Factors; TGF- β R: Transforming Growth Factor β Receptor; TKR: Tyrosine-protein Kinase Receptor; TLR: Toll-like Receptor; TNF R: Tumor Necrosis Factor Receptor; Transl. Fact.: Translational Factors.

2.3.3. Glucocorticoid Receptor Signaling Pathway

Glucocorticoids (GCs) are endogenous stress hormones involved in modulating inflammation [107]. GCs are well known for their catabolic effects on skeletal muscle [108] and can exert their action via different mechanisms (Figure 1). In skeletal muscles, GCs mainly operate through the glucocorticoid receptor (GR), that interacts with specific DNA sequences, DNA-bound TFs as well as transcriptional co-regulatory proteins, which modulate the transcription of numerous genes [108–110] like *MuRF1/Trim63*, *MAFbx/Atrogin-1*, *Foxo* transcription factors, the myokine *Gdf8*, *Klf15*, *Redd1* and *Sesn1* [110]. Intriguingly, the effect of GCs on muscle mass is dependent on the type of GC, fiber type composition, muscle type, sex and dose, but also on the type of catabolic situation (e.g., starvation, diabetes, sepsis, cancer cachexia, etc.) (for details, refer to [110,111]). Recent works at least partly explained these differential effects by the capacity of GCs to use different signaling pathways, such as IGF-1/PI3K/AKT, MEK/ERK, Myostatin [112], NF- κ B [113], NOTCH [114] or to depend on co-factors such as connexin-based hemichannels [115], high-fat diet [116], oxidative stress [111] or mechanical load [51,52,117].

2.3.4. Angiotensin Signaling Pathway

Angiotensin (Ang) is a peptide hormone that upon enzymatic processing [118] renders different variants like Ang-II and Ang-(1–7) (Figure 1) that can either be linked to catabolic conditions (Ang-II) [118–123] or counteract muscle atrophy (Ang-(1–7)) [124–128]. However, Ang-II can also exhibit anticatabolic properties, but only in some circumstances [127,129]). High levels of Ang-II have been associated with skeletal muscle atrophy in CHF, CKD, and SARS-CoV-2 pathologies [120,130]. Ang-II induced atrophy was also linked to increased proteasome activity [131], elevated polyubiquitinated protein conjugates [132], and early and transient accumulation of *MuRF1/Trim63* and *MAFbx/Atrogin-1* mRNA [119,123]. Therefore, the differential modulation of the enzymes processing Ang may be a promising approach for improving skeletal muscle atrophy.

2.3.5. JAK/STAT Signaling Pathway

In skeletal muscle, the Janus Kinase/Signal Transducers and Activators of Transcription (JAK/STAT) pathway has been reported to be essential for transducing signals from growth factors and IL-6 among others (For a recent review, see [133,134]). STAT3, one of its effectors (Figure 1), is particularly implicated in skeletal muscle atrophy upon disease [recently reviewed elsewhere [135], notably through the development of skeletal muscle insulin resistance in Type 2 diabetes mellitus [136,137], the induction of myostatin [138], caspase-3 [139] and UPS [14], and increased mitochondrial ROS [140].

2.3.6. Kinin Signaling Pathway

Kinins are a group of peptides that act via inducible (B1) or constitutive (B2) receptors [141]. Using B1 receptors, kinins participate to muscle atrophy by blunting the PI3K/AKT/mTORC1 axis and by stimulating the IKK/NF- κ B pathway (Figure 1) [142]. Both genetic or pharmacologic ablation of B1 receptor protect skeletal muscles from atrophy in androgen-sensitive mice, mainly by blunting *MuRF1/Trim63* expression [142]. The role of kinin B2 receptors is more controversial as they may either be pro-catabolic via activation of myostatin signaling [143] or pro-anabolic [144]. Therefore, kinin receptors may regulate muscle mass but more studies are clearly needed before they become potential targets to modulate muscle atrophy.

2.3.7. Sphingolipids Signaling Pathway

The sphingomyelin pathway plays a role in skeletal muscle mass through the hydrolysis of plasma membrane sphingomyelin (SM) and the subsequent formation of ceramide and sphingosine-1-phosphate (S1P) (Figure 1). Ceramide, is linked to muscle atrophy through (i) the reduction of protein synthesis [145–148] and (ii) the activation of NF- κ B [149–151]. Oppositely, S1P can promote skeletal muscle mass in denervated mice [152] although the downstream signaling depends on the context and the S1P-receptor type [153].

2.3.8. NOTCH Signaling Pathway

Hyperactivation of NOTCH leads to atrophy during cancer cachexia [154], denervation [155–157], chronic alcohol consumption [158], hypovitaminosis D [159], and glucocorticoid treatment [114]. Upon cleavage of the NOTCH receptor by secretases [160], the Notch Intracellular Domain (NICD) translocates to the nucleus (Figure 1) and binds directly to the *MuRF1/Trim63* promoter to activate its transcription, thereby establishing NOTCH signaling as a proteolysis inducer [161].

2.3.9. Oxidative Stress Is an Inducer of Skeletal Muscle Atrophy

Oxidative stress is characterized by increased levels of reactive oxygen species (ROS) and/or reactive nitrogen species (RNS) and is a well-known mechanism of atrophy induction in skeletal muscle under several conditions and proteolytic mechanisms (reviewed elsewhere [162,163]) (Figure 1). Both ROS and RNS negatively impact muscle mass during COPD [164,165]. ROS induce a FOXO1-dependent *MuRF1/Trim63* and *MAFbx/Atrogin-1* overexpression in COPD peripheral muscle cells in cellulo [166]. NOS activation was suggested to occur through inflammation and hypoxia in COPD patients with low body weight via an activation of NF- κ B and iNOS-generated RNS [99]. Besides increased protein breakdown, a decrease in protein synthesis via AKT/mTORC1 also contributes to muscle mass loss by ROS [162]. Importantly, depending on the type, duration and intensity of the imposed stress, specific signaling mechanisms are activated [162,163,166–169] indicating that the underlying mechanisms by which oxidative stress contributes to muscle wasting is context-dependent.

3. E3 Ligases Involved in the Regulation of Muscle Atrophy

3.1. E3 Ligases Involved in the Regulation of Anabolic Pathways

3.1.1. The CBL-B and FBXO40 E3 Ubiquitin Ligases Target IRS1 to Degradation in Skeletal Muscle

One strategy to fight against atrophy may be to stimulate the anabolic pathways leading to skeletal muscle hypertrophy. Insulin-like growth factor 1 (IGF1) induces skeletal muscle hypertrophy by activating the IGF1R/PI3K/AKT pathway, a critical mediator and checkpoint being IRS1. Indeed, the effect of IGF1 is time-limited by the phosphorylation of IRS1 by IGF1R and its subsequent ubiquitination and proteasome-mediated degradation.

Different E3 ligases can target IRS1 in different tissues. For example, in embryonic fibroblasts, the CUL7 E3 ligase, containing FBXW8, has been shown to target IRS1 for ubiquitin-dependent degradation [170]. In skeletal muscle, Casitas B-lineage lymphoma-b (CBL-B), a RING E3 ligase, targets IRS1 for degradation and thus impairs muscular trophic signals in response to unloading conditions [171–173], which inhibits downstream IGF1 signaling [173] (Figure 2 and Table 1). Accordingly, mice deficient for CBL-B were partly resistant to unloading-induced skeletal muscle atrophy and dysfunction [173]. These results highlight the importance of CBL-B in the process of muscle atrophy in response to unloading.

FBXO40 is a muscle-specific F-box protein [174], component of an SCF (Skp1-Cullin1-F-box protein) E3 ligase complex. Following IRS1 activation, IGF1R phosphorylates IRS1 leading to its ubiquitination by FBXO40 and its degradation by the 26S proteasome, in cultured myotube and in mice [22,175]. FBXO40 expression is decreased in muscles from Limb-girdle muscular dystrophy (LGMD) patients, and up-regulated in mice skeletal muscle following denervation and in chronic kidney disease (CKD) mice model, but not during starvation [174,175]. Accordingly, the knock-down of *Fbxo40* resulted in thicker myotubes (20% to 50% increase in diameter) [22] and its deletion in mice also induced muscle hypertrophy during the growth phase, a phase associated with high IGF1 levels [22] (Figure 2 and Table 1).

Table 1. Phenotypes of transgenic mice for genes encoding ubiquitin ligases involved in the control of muscle mass and function.

Gene Product	E3 Family	Mouse Model	Phenotype	References
E3 ligases regulating the anabolic pathways				
CBL-B	RING	KO	Protection from unloading-induced muscle atrophy and dysfunction	[171]
FBXO40	RING	KD	Myofibers hypertrophy	[22]
NEDD4-1	HECT	OX	Muscle hypertrophy	[176,177]
		KO	Myocardial activation of AKT during I/R	[178]
		KO	Partially resistant to denervation-induced skeletal muscle atrophy	[178]
E3 ligases regulating the catabolic pathways				
TRAF6	RING	m.KO	Resistance to starvation induced muscle atrophy	[179]
		m.KO	Resistance to denervation-induced loss of muscle mass and function	[180]
cIAP1	RING	KO	Limitation of denervation-induced muscle atrophy	[19]
		OX	Myotube atrophy	
WWP1	HECT	KD	Muscle fiber atrophy	[181]
TRIM32	RING	KO	Muscular dystrophy	[182]
		DN	Muscular dystrophy	[183]
Other E3 ligases involved in the control of muscle mass and function				
MuRF1	RING	KO	Resistance to catabolic-induced muscle atrophy	[4]
MAFbx	RING	KO	Resistance to catabolic-induced muscle atrophy	[4]
PARKIN	RBR	KO	Impaired mitochondrial function and muscle atrophy	[184]
		OX	Increased muscle mass and function in young and old mice	[185]
		OX	Prevention of sepsis-induced muscle atrophy	[186]
SMART/FBXO21	RING	KD	Resistance to denervation-induced muscle atrophy	[187]
MUSA1/FBXO30	RING	KD	Resistance to denervation-induced muscle atrophy	[77]
FBXL21	RING	HM	Impaired muscle functions	[188]
UBR4	HECT	KD	Muscle hypertrophy	[189]
UBR5	HECT	KD	Muscle atrophy	[190]

DN, Dominant Negative mutation; HM, Hypomorphic Mutation; I/R, Ischemia/Reperfusion; KD, knock-down mutant; KO, Knock-out mutant; m.KO, skeletal muscle-specific KO mice; OX, overexpressing mutant; PTEN, Phosphatase and tensin homologue.

IRS1 is thus an important checkpoint of the IGF1/PI3K/AKT pathway controlled by at least 2 E3 ligases (CBL-B and FBXO40). Although being an attractive target for fighting against muscle atrophy, the multiple ways for degrading IRS1 may complicate the development of drugs.

3.1.2. NEDD4-1 E3 Ubiquitin Ligase, Friend or Foe?

In muscles undergoing atrophy, NEDD4-1 mRNA levels are elevated upon severe sepsis [191], denervation or unloading [178,192,193]. On the one hand, NEDD4-1 E3 Ub ligase targets phosphatase and tensin homologue (PTEN). PTEN is a redox sensitive phosphatase that negatively regulates the PI3K-AKT signaling pathway, thereby affecting metabolic and cell survival processes. The deletion of PTEN improves muscle mass and function in a mouse model of Duchenne muscular dystrophy [194]. PTEN inhibition may thus also represent a potential therapeutic strategy to maintain muscle function during catabolic situations. The over-expression of NEDD4-1 is sufficient for activating the PI3K/AKT signaling in cardiac muscle, following myocardial ischemia/reperfusion (I/R) [176]. However, the negative regulation of PTEN by NEDD4-1 remains to be confirmed in skeletal muscle, especially since NEDD4-1 has also been shown to promote skeletal muscle atrophy in a denervation model. Indeed, NEDD4-1-KO mice exhibited increased weights and type II muscle fiber cross-sectional areas in denervated gastrocnemius muscle [178]. Moreover, NEDD4-1 also negatively regulates the hypertrophic BMP signaling (Figures 1 and 2). Indeed, NEDD4-1 ubiquitinates phosphorylated-SMAD1 leading to its proteasomal degradation, thereby silencing BMP signaling in C2C12 myoblasts, and conversely the knock-down of *Nedd4-1* potentiates BMP signal through upregulation of phospho-SMAD1 [195]. Altogether, the exact function of NEDD4-1 in skeletal muscle is still obscure and needs more work.

3.2. E3 Ubiquitin Ligases Involved in the Regulation of Catabolic Pathways

3.2.1. Regulating the Canonical NF- κ B Pathway via the Manipulation of cIAP and TRAF6 E3 Ligases

Among the E3s involved in the regulation of the NF- κ B pathway, two promising candidates may be manipulated to limit muscle atrophy, namely cIAP and TRAF6 (Figures 1 and 2). cIAP1 is up-regulated in denervated gastrocnemius muscle, paralleling the upregulation of *MAFbx/atrogen-1* and *MuRF1/Trim63* mRNA [19]. Mice with genetic ablation of cIAP1 (cIAP1-KO mice) displayed limited denervation-induced atrophy in TA, gastrocnemius and EDL muscles. This was correlated with the blunting of the denervation-induced upregulation of *MAFbx/Atrogen-1* and *MuRF1/Trim63* [19]. The authors further demonstrated that cIAP1 induced atrophy through the up-regulation of the canonical NF- κ B signaling. Conversely, cIAP1 overexpression in myotubes induced atrophy and the strong up-regulation of *MAFbx/Atrogen-1* and *MuRF1/Trim63* protein expression [19]. The E3 Ub ligase cIAP1 represents thus a potential therapeutic target at least for fighting against denervation-induced muscle atrophy.

TRAF6 is a RING-type Ub ligase that plays an important role during skeletal muscle atrophy. TRAF6 expression is enhanced during starvation or within aged-induced muscle atrophy [179,196,197]. *Traf6*-KO mice are resistant to skeletal muscle loss (rescue of myofibril degradation, preservation of myofiber size and strength) induced by denervation, cancer cachexia, starvation or Dex and a concomitant suppression of the expression of key regulators of muscle atrophy was observed, including *MAFBx/Atrogen-1*, *MuRF1/TRIM63*, p62, Lc3b, Beclin1, Atg12, and Fn14 [179,180,196–198]. Moreover, inhibition of *Traf6* expression through miR-351 administration in C2C12 myotubes or in denervated mice attenuated Dex-induced muscle atrophy and concomitantly decreased the expression of *MAFBx/Atrogen-1* and *MuRF1/Trim63* [199,200]. Overexpression of miR-125b targeted *Traf6* for degradation and protected skeletal muscle samples from atrophy in starved myotubes or in denervated rat tibialis muscle [201]. The implicated mechanisms involved both direct and indirect effects of TRAF6 on protein breakdown with TRAF6-mediated ubiquitination being re-

quired for the optimal activation of JNK, AMPK, FOXO3, and NF- κ B catabolic pathway in muscle [202].

In human, gastric cancer patients suffering from cachexia exhibited an upregulation of TRAF6 associated with an upregulation of ubiquitination in the rectus abdominis muscle [203]. Altogether, this highlights the importance for targeting TRAF6 inhibition to counteract muscle atrophy.

3.2.2. WWP1 in the Regulation of Muscle Atrophy

WWP1 is a HECT E3 ligase that is involved in chicken muscular dystrophy. Indeed, a missense mutation in the gene coding WWP1 was identified as the most promising candidate responsible for chicken muscular dystrophy (MD), potentially affecting the E3 function of WWP1 protein [204]. WWP1 was also shown to target the transcription factor KLF15 [181]. In response to glucocorticoids, KLF15 is up-regulated at the mRNA levels [205]. This induction leads to the up-regulation of the E3 ligases *MAFbx/Atrogin-1* and *MuRF1/Trim63* expression, likely in cooperation with a FOXO transcription factor, while inhibiting the anabolic mTORC1 [205]. Likewise, exogenous KLF15 expression in myotubes and in TA muscle leads to myofiber atrophy [205]. It has recently been shown that KLF15 protein expression was upregulated in skeletal muscle of diabetic mice, without any change in its mRNA expression [181]. This increase correlated with an increase in *MAFbx/Atrogin-1*, *Murf1/Trim63* and *Foxo3* genes expression and accordingly, the muscle-specific deletion of *Klf15* in this model prevented from diabetes-induced muscle atrophy [181]. The authors identified WWP1 as an E3 ligase targeting KLF15 and showed that knocking-down WWP1 in both C2C12 myotubes and in tibialis anterior muscles increased *MuRF1/Trim63* and *MAFbx/Atrogin-1* expression and induced atrophy [181] (Figure 2). WWP1 E3 ligase is indeed induced by high glucose conditions in myotubes [206]. Conversely, in high glucose conditions, WWP1 has also been implicated in the down-regulation of AMPK α 2 protein levels [206]. The authors have shown that WWP1 interacted with AMPK α 2 leading to a proteasome-dependent decrease of AMPK α 2 in myotubes; however, direct ubiquitination was not addressed [206]. WWP1 may thus control muscle mass through a direct action on AMPK, a known modulator of FOXO3a, MuRF1/TRIM63 and MAFbx/Atrogin-1 [88].

3.2.3. TRIM32 in the Regulation of Autophagy

TRIM32 is a RING E3 Ub ligase whose mutation is responsible for the development of limb girdle dystrophy 2H (LGMD2H) [207]. Several substrates have been identified for TRIM32 in non-muscle cells, including cell cycle regulators (c-Myc, MYCN, p53), the cell growth and transformation factor ABI2 and PIASY (a SUMO E3 ligase). TRIM32 is also involved in the targeting of factors influencing myogenesis (NDRG2 and TRIM72) that regulate muscle satellite cells renewal and differentiation [208]. While initially postulated to promote muscle atrophy, TRIM32 is in fact a master regulator of myogenesis during recovery situations [208]. Indeed, the dystrophic phenotype of TRIM32 mutations appeared to be largely due to impaired myogenesis [208–210].

More recently, TRIM32 was implicated in the early events leading to autophagy. Indeed, TRIM32 targets ULK1, a Ser/Thr protein kinase (Figures 1 and 2). ULK1 is an upstream regulator of autophagy rapidly activated to ensure a rapid response to stress conditions [211]. The authors showed that TRIM32 deficiency was directly responsible for autophagy defects both in cultured cells and in mice treated with Dex. The mechanisms by which TRIM32 controls the activation of autophagy through ULK1 involves its binding to AMBRA1, a positive regulator of autophagy [211]. AMBRA1 is a pivotal factor able to bind several E3 ligases during the course of the autophagy process. In presence of AMBRA1, TRIM32 binds to ULK1, synthesizes unanchored K63 Ub chains that activate ULK1 kinase activity, thus promoting autophagy. The role of TRIM32 during the autophagy process is not limited to ULK1 as p62, an important autophagy receptor [212], is also a TRIM32 substrate. p62 activity is modulated by multi mono-Ub catalyzed by TRIM32 and loss of

function of TRIM32 largely abolished autophagy [213]. Altogether, TRIM32 appears as a master regulator of muscle renewal through the initiation of autophagy.

3.2.4. FOXO Transcription Factors Are Regulated by MDM2 and SKP2 E3 Ubiquitin Ligases

Alternatively to phosphorylation, FOXO can be regulated by acetylation/deacetylation, methylation and ubiquitination to modulate its activity, localization as well as degradation [214–216].

Ubiquitination modulate FOXO activity by either mono- or polyubiquitination through MDM2 and SKP2 E3 Ub ligases (Figures 1 and 2). MDM2 is the enzyme responsible of a single addition of an ubiquitin moiety to FOXOs, specifically to FOXO4, thus allowing its nuclear localization and transcriptional activation [217,218]. Mono-Ub of FOXO4 is observed under oxidative stress conditions and can be counteracted by deubiquitinating enzymes such as ubiquitin-specific protease (USP7). Importantly, ubiquitination mediated by MDM2 is context specific and upon growth factor stimulation can induce FOXO1 and 3 degradation [217]. In addition, interaction between FOXOs and SKP2, a subunit of the SKP/cullin 1/F-box protein E3 ligase leads to proteasomal degradation of FOXO1 in the cytosol [218].

Combined with the other posttranslational modifications, ubiquitination allows FOXOs to integrate information arising from insulin, growth factors, cytokines, and oxidative stress and to control downstream signaling. Interestingly, FOXO TFs have systematically been envisioned as crucial drivers of catabolic pathways during muscle wasting. Nonetheless, recent work showed that FOXO1 and 3a participate to skeletal muscle adaptation upon exercise thus adding a new of FOXOs in the control of muscle cell homeostasis [219–222].

3.3. E3 Ubiquitin Ligases Involved in the Regulation of Muscle Mass and Function

3.3.1. MuRF1/TRIM63

Muscle-specific RING finger protein 1 (MuRF1), also named TRIM63, is a RING-type E3 ligase and a founding member of the so-called “atrogenes” (see [6] for a recent review). MuRF1/TRIM63 is a master regulator of skeletal muscle atrophy development occurring in numerous catabolic conditions and *MuRF1/Trim63* mRNA appeared to be upregulated in more than 25 atrophying situations [6] (Figures 1 and 2). Mice deleted for MuRF1/TRIM63 (MuRF1-KO mice) were partially resistant (preservation of muscle mass and structure) to skeletal muscle atrophy induced by denervation [4], hindlimb suspension [4,223], glucocorticoid [224], amino acid deprivation [225], and acute lung injury [226]. MuRF1/TRIM63 is responsible for the coordinated breakdown of both thick and thin filaments occurring during catabolic states in skeletal muscle, targeting to degradation the main proteins of the contractile apparatus: myosin heavy chains (MHC) [227], alpha-actin [228], troponin I [229], TCAP/telethonin [230]. During denervation and starvation, MuRF1/TRIM63 has also been involved in the degradation of acetylcholine receptor (CHRN), the major postsynaptic ion channel of the neuromuscular junction. This degradation is mediated by the activation of selective autophagy and degradation of CHRN, likely via the degradation of BIF-1 (Bax interacting factor 1)/EndoB1 (EndophilinB1) and/or SQTm1/p62 (sequestosome-1) [231,232].

While numerous studies have promoted a major role of MuRF1/TRIM63 in the development of skeletal muscle atrophy during catabolic states, in the heart, the analyses of MuRF1 mutants have highlighted a beneficial cardioprotective role [233]. These opposites roles in both kind of muscles imply the development of skeletal muscle-specific drugs to inhibit MuRF1/TRIM63. Moreover, one should also take into account that MuRF1/TRIM63 has two homologs, MuRF2 and MuRF3 that share some redundant functions and could replace its role [12].

3.3.2. MAFbx/Atrogin-1/FBXO32

The multimeric E3 ligase MAFbx/atrogin-1/FBXO32 is another founding member of the atrogin family ([6] for a recent review) crucial for the development of muscle atrophy. Interestingly, nearly all catabolic situations induce an overexpression of both MAFbx/Atrogin-1 and MuRF1/TRIM63, which are controlled by the same TFs (FOXO1/FOXO3a, NF- κ B, C/EBP β , Smad 3, etc.) and the same signaling pathways [234] (Figures 1 and 2).

In contrast with MuRF1/TRIM63 that targets directly the contractile proteins for their degradation (α -actin, MHC, etc. [227–230], MAFbx appeared to target pro-anabolic factors like MyoD, myogenin or eIF3f [235–237]. MyoD is a muscle-specific transcription factor that plays crucial roles during cell cycle and muscle differentiation [238]. The eukaryotic initiation factor 3 subunit f (eIF3f) is a pivotal element of protein synthesis and its control by MAFbx allows the latter to master the anabolic processes [235]. While a putative role of MAFbx/Atrogin-1 on sarcomeric proteins was hypothesized using an indirect approach, this has never been confirmed [239]. By contrast, the authors found that desmin, a main component of the intermediate filaments, physically interacted with MAFbx and was degraded in myostatin-treated cultured C2C12 myotubes.

As MAFbx/Atrogin-1 and MuRF1/TRIM63 are controlled by similar signaling pathways, the strategies for the upstream control of *MuRF1/Trim63* expression are generally also valid for MAFbx/Atrogin-1 (Table 2). By contrast with MuRF1/TRIM63, no direct inhibitor of MAFbx/Atrogin-1 has been described so far but general strategies, like targeting the interface responsible for substrate recognition or impeding the assembly of the F-box (i.e., the subunit recognizing the substrates) into the SCF complex, may prove to be efficient.

Altogether, controlling concomitantly MAFbx/Atrogin-1 and MuRF1/TRIM63 E3 ligases allows skeletal muscle cells to both increase the degradation of the contractile apparatus and to depress the protein synthesis machinery, which allows a tight regulation of protein homeostasis.

3.3.3. PARKIN Controls Muscle Mass through the Maintenance of Mitochondrial Homeostasis

PARKIN is an E3 ubiquitin ligase implicated in the regulation of mitophagy, a quality control process in which defective mitochondria are degraded. Mitochondrial quality control through both mitochondria turnover and dynamic plays an essential role in the maintenance of muscle mass (see [240] for a review). During mitophagy, PARKIN ubiquitinates several outer mitochondrial membrane proteins leading to subsequent autophagosomal engulfment and lysosomal degradation (Figures 1 and 2).

This role of PARKIN has been emphasized in rodent models or in humans where a deregulation of PARKIN mRNA and/or protein expression prevailed in response to catabolic or anabolic situations. An accumulation of PARKIN protein prevailed during: (i) muscle wasting situations such as chronic kidney disease [241], chronic obstructive pulmonary disease (COPD) [242], physical inactivity [243,244] and (ii) upon exercise training [245,246]. Conversely, PARKIN mRNA or protein levels decreases in skeletal muscles from some elderly populations, perhaps related to the loss of muscle mass and poor physical function, e.g., physically inactive frail older women [247,248] or gastric cancer patients with cachexia [249].

In the last two years many studies using loss/gain of function models have provided insight on the role of PARKIN in skeletal muscle. Loss of function mouse models pointed out the essential role of PARKIN in basal conditions for the maintenance of (i) mitochondrial function [250,251] and (ii) skeletal muscle mass and normal contractile function [184,251]. Such studies also reported that PARKIN helps to resist to some drug-induced muscle damages [252] and is required for exercise-induced mitophagy flux and for the accumulation of functional mitochondria following muscle adaptations to training [250]. In addition, these loss-of-function studies also highlighted that PARKIN-mediated mitochondrial clearance contributes to proteasome activation during denervation in atrophied slow-twitch mus-

cles [253]. On the flip side, gain-of-function studies showed that PARKIN overexpression in mice: (i) attenuates the ageing-related and the sepsis-induced muscle wasting and causes hypertrophy in adult skeletal muscle, (ii) increases mitochondrial content and enzymatic activities and (iii) protects from ageing-related increases of oxidative stress markers, fibrosis and apoptosis [185,186]. It is very likely that this role of PARKIN in controlling muscle mass has been evolutionary conserved. Indeed, similar observations were also reported in the fruit fly model: *Parkin* deficiency in *Drosophila* leads to severe degeneration of the flight muscles with accumulation of swollen mitochondria [254] whereas *Parkin* overexpression promotes mitophagy in older muscles and extend lifespan.

Together, these studies clearly indicate that PARKIN is an important player in the control of muscle mass through its role in the maintenance of mitochondrial homeostasis. This makes it a potential therapeutic target of interest for preserving muscle mass or fighting against atrophy. Nevertheless, the regulation of PARKIN can be very different according to the physiological or pathological situation or during ageing. Further investigations should enable defining how this actor could be a target of interest according to the population considered.

3.3.4. MUSA1/FBXO30

FBXO30, also called muscle ubiquitin ligase of the SCF complex in atrophy-1 (MUSA1), is a FBOX protein forming an SCF complex with SKP1, Cullin1 and ROC1 [77]. Proteins targeted by MUSA1 remain undefined, but its inhibition in denervated muscles reduces remarkably muscle atrophy, and reverts almost completely the strong atrophic phenotype of *Smad4*-KO mice [77] (Figures 1 and 2). In muscle, *Musa1* expression is upregulated in atrophic mice muscle undergoing CKD [255] or sepsis [256].

3.3.5. FBXL21

Very recently, a new E3 ubiquitin ligase involved in muscle function control has emerged, FBXL21 [188]. FBXL21 forms an SCF E3 ligase complex and was first identified as clock-controlled E3 ligase modulating circadian periodicity via subcellular cryptochrome degradation [257]. Accordingly, in mice, the *Psttm* mutation, corresponding to a hypomorphic mutation of FBXL21 with reduced FBXL21 activity, caused circadian period shortening [257]. Further studies of these mice revealed that they also displayed skeletal muscle deficiencies with a decrease in fiber CSA (gastrocnemius) and impaired exercise tolerance and grip strength for both forelimbs and hindlimbs [188]. The authors nicely demonstrated the circadian degradation of the cytosolic TCAP/Telethonin by FBXL21 (Figure 2), under the control of GSK-3 β . They reported that GSK-3 β phosphorylated both FBXL21 and TCAP leading to FBXL21-CULLIN1 complex formation and phosphodegron-dependent TCAP turnover.

3.3.6. Ubiquitin Ring-Type E3 Ligases (UBR)

Ubiquitin Ring-type (UBR, also referred to as E3 α) proteins are RING finger E3 ligases that compose a 7-member family and that mainly recognize their substrate through the N-end rule pathway [258]. A first member, UBR2/E3 α -II, has been shown to be significantly induced in skeletal muscle, in two different animal models of cancer cachexia, at the onset and during the progression of muscle wasting [259]. However, its exact function and importance in skeletal muscle maintain during catabolic states have not been further studied. UBR4 is overexpressed in the skeletal from fasted mice and genetic ablation of UBR4 preserves muscle mass in tumor-bearing mice [189] (Table 1). Intriguingly, the protection of UBR4 knockout against tumor-induced atrophy was limited to type IIA fibers. In contrast, UBR5 has been implicated in muscle hypertrophy [260] and reported to be at least partially associated to the proteasome [261]. Recently several members of the UPS have been described as UBR5 substrates, which included an E2 (UBE2B, an abundant muscle E2), several E3 ligases, proteins involved in chromatin remodeling, etc. [189]. As

the main UBR4 targets are positive regulators of muscle growth, the authors concluded that UBR4 acts as a negative regulator of muscle hypertrophy.

3.3.7. FBXO21/SMART

FBXO21/SMART forms an SCF complex with Skp1, Cullin1 and Roc1, in skeletal muscle and has been shown to promote atrophy during denervation [187]. Indeed, the authors showed that FBXO21/SMART upregulation was required for atrophy while, knock-down in TA muscle protected denervated muscles from atrophy (Table 1), probably due to a global reduction of protein ubiquitination [187]. FBXO21/SMART might therefore be a new critical E3 to target to limit skeletal muscle atrophy. Further work should determine whether this E3 is crucial for the development of atrophy in other catabolic conditions and what are the mechanisms involved.

3.4. Promising E3 Ubiquitin Ligases Regulating Muscle Mass and Function

Other E3 ubiquitin ligases are also promising putative targets for maintaining muscle mass and function, if we rely on what has been published in other organs or organisms. For example, the SIAH-1 RING E3 ligase has been identified in the same RNAi screen that UBR4, performed to identify ubiquitin-related enzymes that regulate myofiber size, using the fruit fly *Drosophila* [189]. In *Drosophila*, SIAH1 knock-down led to muscular hypertrophy while its overexpression led to atrophy [189]. It is noteworthy that, in space flown rats, *SIAH1* mRNA expression has been shown upregulated suggesting also a putative role during this process in mammals [172]. However, in mammals two isoforms, SIAH1 and SIAH2, are expressed in muscle and could share redundant functions [189].

SMURF1, an HECT ubiquitin ligase interacts with SMAD1 and SMAD5 (BMP pathway) and SMAD4 in a certain context, leading them all to proteasomal degradation in vitro [262]. Moreover, it can degrade the main TGF- β receptor through an indirect recruitment to the receptor by SMAD7, leading to the receptor degradation [263]. In COPD leading to muscle atrophy, TGF- β signaling is abnormally up-regulated and this, is negatively correlated to SMURF1 expression. This highlights that the inhibitory effect of SMURF1 over TGF- β is needed for muscle homeostasis [264].

The C terminus of Hsc70-interacting protein (STUB1/CHIP) serves as an E3 ubiquitin ligase. This E3 plays a dual role in BMP/TGF signaling. Overexpression of CHIP inhibits TGF- β luciferase reporter through the ubiquitination and degradation of SMAD3, and conversely silencing it leads to increase the signal transduction in HEK293T cells [265]. In cellulo experiments showed that CHIP mediates as well SMAD1-5 poly-ubiquitination, and subsequent degradation to terminate BMP signaling [266]. In muscle, CHIP is highly expressed. For instance, *Chip*^{-/-} mice at 6 months shows muscle morphological changes consistent with increased sarcoplasmic reticulum compartments in quadriceps muscle and gastrocnemius, resulting in damages and fiber switch composition [267]. From our knowledge, no studies have shown the implication of CHIP in TGF/BMP signaling-mediated muscle atrophy.

TRIM62 belongs to the TRIM/RBCC family. This enzyme acts as a negative regulator of TGF- β signaling by binding to SMAD3 and promoting its ubiquitination and degradation, resulting in a decrease of TGF- β /SMAD3 target genes in HEK and human mammary epithelial cells [268]. TRIM62 is increased in the skeletal muscle of ICUAW patients (Intensive care unit-acquired weakness), a devastating illness characterized by loss of muscle mass [269]. In this context, the authors proposed TRIM62 contribution in inflammation-induced muscle atrophy through IL-6 pathway. Indeed, *Trim62-KD* inhibited LPS-induced IL-6 expression in C2C12 cells [269].

TRIM72/MG53 is a muscle-specific E3 ligase, also called mitsugumin 53, specifically expressed in the plasma membrane of skeletal muscle, and has a critical role in membrane repair. Membrane repair deficiency causes muscle cell death, injury, and dystrophy. Accordingly, the overexpression of human TRIM72 in a hamster model of genetic muscular dystrophy protects skeletal muscle damage through enhancement of membrane

repair [270]. Similarly, short-term TRIM72 injection ameliorates the underlying defects in dysferlin-deficient muscle by increasing sarcolemma membrane integrity [271] while *Trim72*^{-/-} mice develop significant skeletal muscle myopathy and cardiovascular defects due to defective sarcolemma repair [272].

4. Current Treatments/Potential Modes of Action

The importance of maintaining muscle mass together with the discovery of several E3 ligases implicated in muscle homeostasis has rapidly end up with multiple approaches to chemically alter the expression of these enzymes. This includes chemical drugs but also several natural molecules that have been tested for their ability to modulate the UPS and more particularly the E3 ligases (Table 2).

4.1. Indirect Action on E3 Ligases

4.1.1. PI3K-AKT-mTORC1

As E3 ligases are controlled by several signaling pathways, one possibility that was first addressed was to block these signals. The PI3K-AKT-mTORC1 axis is known to control muscle mass by directly acting on FOXO transcription factors, the latter being master regulators of several E3 ligases, like *MAFbx/Atrogin-1*, *MuRF1/TRIM63*, *MUSA1*, *SMART* and *FBXO31*, during several atrophy situations [187]. As such, clenbuterol (Table 2 and Figure 2), an activator of the AKT-mTORC1 pathway, is able to decrease *MuRF1/Trim63* and *MAFbx/Atrogin-1* expression in denervated or hindlimb suspend rats and to partially preserve muscle mass [273].

4.1.2. Glucocorticoids

Glucocorticoids are potent manipulators of muscle mass and the glucocorticoid receptor antagonist RU486 proved to be efficient in rats for blocking dexamethasone (Dex)-induced induction of *MuRF1/Trim63* of *MAFbx/Atrogin-1*, the main regulators of muscle mass [13] (Table 2 and Figure 2). Similarly, the authors demonstrated that blocking TNF α by the TNF-binding protein (TNFBP) was efficient for blunting LPS-induced expression of *MuRF1/Trim63* and *MAFbx/Atrogin-1*. However, when sepsis was induced by cecal ligation and puncture, neither RU486 nor TNFBP were able to counteract the overexpression of *MuRF1/Trim63* and *MAFbx/Atrogin-1*, indicating that multiple signals were activated by sepsis. This points out the difficulty of treating complex catabolic signals in vivo. Infliximab is an anti-TNF- α agent able to lower the downstream NF- κ B signaling. In patient's suffering from Crohn disease, treatment with infliximab was able to ameliorate muscle atrophy but, although hypothesized by the authors, the expression of *MuRF1/Trim63* or any other E3 ligase was not addressed [274].

4.1.3. Il-6

Il-6 is another inflammatory cytokine that can be implicated during muscle wasting conditions like muscle disuse [275]. Increased IL-6 in tail-suspended mice paralleled skeletal muscle atrophy and was accompanied by increased levels of *MuRF1/Trim63* and *MAFbx/Atrogin-1*. The inhibition of the IL-6 receptor by hydroxymethyl butyrate (HMB, a metabolite of leucine) or vitamin D tended to decrease IL-6 levels and when combined, HMB and vitamin D exhibited better efficiency for blunting IL-6 production [275] (Table 2 and Figure 2). By contrast, each molecule was sufficient for decreasing *MuRF1/TRIM63* and *MAFbx/atrogin-1* levels and to attenuate muscle atrophy. While the authors attributed the beneficial effects of HMB and vitamin D on IL-6 receptor, using a monoclonal antibody directed against IL-6 receptor (MR16-1) proved to be inefficient as only *MuRF1/Trim63* expression was decreased with no amelioration on muscle mass. As for the TNF- α , this work underscores the multiplicity of signaling during atrophy situations and the difficulty of blunting efficiently receptor-linked signaling. STAT-3 is a downstream effector of IL-6 signaling and a specific inhibitor of STAT-3 (C188-9) was investigated for its capacity to block muscle atrophy in a model of mice deficient for the vitamin D receptor (VDR) [14].

In these conditions, $VDR^{-/-}$ mice exhibited exacerbated *MuRF1/Trim63* expression and increased muscle atrophy. While C188-9 was able to partially preserve muscle mass, its efficacy against MuRF1/TRIM63 was not addressed.

4.1.4. NF- κ B

Inhibition of the NF- κ B signaling pathway was also efficiently performed using high doses of salicylate (Table 2 and Figure 2), which allowed the reversion of MuRF1-induced muscle atrophy in tumor bearing or denervated mice [89]. However, the high doses used for achieving a potent inhibitor would be toxic when administered to humans.

4.1.5. β 2 Adrenergic Receptor (β 2-AR)

β 2-AR agonists can exert both anabolic and anti-catabolic effects on skeletal muscles either by decreasing catabolic signals or by promoting anabolic ones or both. Formoterol (Table 2 and Figure 2), a β 2-AR agonist, was shown to reverse *MuRF1/Trim63* and *MAFbx/Atrogin-1* overexpression with a concomitant muscle sparing in tumor-bearing mice [276]. Intriguingly, neither a repression of FOXO1 and FOXO3a transcription factors nor an activation of AKT-mTORC1 pathway explained the positive effect of formoterol. By contrast, formoterol was able to blunt *MuRF1/Trim63* and *MAFbx/Atrogin-1* expression in LPS-induced muscle atrophy through restoration of the AKT-mTORC1 pathway and reversal of P-FOXO/FOXO1 ratio [277].

Table 2. Treatments influencing E3 ligases expression and/or activity.

E3 Ligases Inhibited	Molecule	Mode of Inhibition	Signal inhibited/Activated	Efficiency on E3 Ligases	Efficiency on Muscle Mass	References
Indirect inhibition of E3 ligases						
MuRF1/MAFbx Expression	4-aminopyridine (4-AP)	K ⁺ -channels blockade	K ⁺ -channels blocking	Yes	Yes	[278]
MuRF1 Expression	AGT251	<i>Notch1</i> , <i>Notch3</i> expression inhibition	NOTCH	Yes	Yes	[161]
MuRF1/MAFbx/MuSA1 Expression	Anti-TLR2	IKK2 (NF- κ B)	TLRs Serum Amyloib A1	Yes	Yes	[256]
MuRF1 Expression	Anti-TLR4	IKK2 (NF- κ B)	TLRs Serum Amyloib A1	Yes	Yes	[256]
MuRF1/MAFbx/MuSA1 Expression	BMS-345541	IKK2 (NF- κ B)	TLRs Serum Amyloib A1	Yes	Yes	[256]
MuRF1 expression	C188-9	STAT3 inhibition	STAT3 signaling	ND	Partially	[14]
MuRF1/MAFbx Expression	Clenbuterol	AKT-FOXO axis	Activation of PI3K-AKT	Yes	Yes	[15]
MuRF1 not MAFbx	Dehydroepiandrosterone (DHEA)	ND	ND	Yes	Yes	[168]
MuRF1 Expression	Epigallocatechin-3-gallate/EGCG	ND	NF- κ B	Yes	Yes	[279]
MuRF1 Expression	Espindolol	ND	Myostatin and NF- κ B	Yes	Yes	[280]
MuRF1/MAFbx Expression	Formoterol	ND	ND	Yes	Yes	[276]
MuRF1/MAFbx Expression	Formoterol	AKT/mTORC1/FOXO1	β 2 Adrenergic receptor?	Yes	Yes	[277]
MuRF1/MAFbx Expression	Formoterol	ND	AKT and NF- κ B	Yes	Yes	[281]
MuRF1/MAFbx Expression	HMB	IL-6 receptor inhibition	NF- κ B	Yes	Partially	[275]
MuRF1 expression	HMB or Leucine	FOXO1 nuclear translocation	Glucocorticoid	Yes	No	[282]

Table 2. Cont.

E3 Ligases Inhibited	Molecule	Mode of Inhibition	Signal inhibited/Activated	Efficiency on E3 Ligases	Efficiency on Muscle Mass	References
Cbl-b activity	IRS1 peptide mimetic	Cbl-b targeting	Activation of PI3K-AKT	Yes	Yes	[171]
MuRF1/MAFbx Expression	Leucine	ND	FOXO3a and VPS34 nuclear translocation	Yes	Yes, myotube diameter	[283]
MuRF1/MAFbx Expression	Matrine	AKT/mTORC1/FOXO3 α	FOXO3a and VPS34 nuclear translocation	Yes	Yes	[284]
MuRF1 expression	MR16-1	Anti-IL-6 receptor	NF- κ B	Mitigated	No	[275]
MuRF1 expression	<i>N</i> -acetyl cysteine	ROS	TGF- β	Yes	Yes	[69]
MuRF1/MAFbx Expression	Pyrroloquinoline quinone (PQQ)	ROS	ND	Yes	Yes	[285]
MuRF1/MAFbx Expression	RU486	GR	Glucocorticoid	Yes	ND	[13]
MuRF1 Expression	Sabinene	ROS	ERK, p38 MAPK	Yes	Yes	[286]
MuRF1/MAFbx Expression	sActRIIB	ActRIIB antagonist	SMADs	Yes	Yes	[16]
MuRF1/MAFbx/MuSA1 Expression	Salicylate	IKK2 (NF- κ B)	NF- κ B	Yes	Yes but toxic	[89]
MuRF1/MAFbx Expression	SS-31	ROS	No	Yes	Yes	[287]
MuRF1/MAFbx Expression	Teaghrelin	ND	Myogenin	Yes	Moderate	[288–290]
MuRF1/MAFbx Expression	TNF-BP	TNF binding	TNF	Yes	ND	[13]
MuRF1/MAFbx/MuSA1 Expression	Ursolic acid	ND	Myostatin and inflammatory cytokines	Yes	Moderate	[255]
MuRF1/MAFbx Expression	Vitamin E	ND but seems ROS independent	Unknown	Yes	Moderate	[291]
MuRF1/MAFbx Expression	Vitamin-D	IL-6 receptor inhibition	NF- κ B	Yes	Partially	[275]
MuRF1 expression	VX-745/Neflamapimod	p38 α MAPK	p38 α MAPK	Partially	Moderate	[292]
Direct inhibition of E3 ligases						
MuRF1 expression	ID#704946/MyoMed-946	ND	MuRF1 Expression	Yes	Partially	[293]
MuRF1 Expression	ID#704946/MyoMed-946	ND	MuRF1 and MuRF2 Expression	Yes	Partially	[17,18]
MuRF1 and MuRF2 Expression	MyoMed-205	ND	MuRF1 expression			[17]
MuRF1 activity	P013222	MuRF1 targeting	–	Yes	ND	[294]
cIAP1 (<i>activity??</i>)	LCL161	cIAP1	NF- κ B	Yes	Very moderate	[19]

β 2-AR reversion of E3 ligases expression and muscle sparing was also observed in a rat rheumatoid arthritis model and was attributed to modulation of both the AKT and the NF- κ B pathways [293]. Other 2-AR agonists like espidolol have also been shown to ameliorate muscle loss and to blunt E3 ligase expression in aged rats. The authors found that both NF- κ B and myostatin expression was reduced with no effect on AKT and FOXO3a [292]. Altogether, this strongly suggests that the positive effects of 2-AR agonists on muscle mass are mediated through the modulation of different signaling pathways depending on the catabolic stimuli, which complicates future therapeutical strategies.

4.1.6. p38 α Mitogen-Activated Protein Kinase (p38 α MAPK)

p38 α MAPK is known to play an important role in the development of muscle atrophy [295]. Inhibition of the p38 α MAPK receptor by the selective inhibitor VX-745 (Table 2 and Figure 2) partially improved muscle weight in hindlimb suspended rats with a modest inhibition of MuRF1 expression but no modification of MAFbx [292].

4.1.7. NOTCH

The NOTCH pathway is mainly known for its implication in muscle development and regeneration upon injury. However, it has been also implicated in muscle atrophy linked to either cancer or amyotrophic lateral sclerosis (ALS) mice models [161]. Using a tocopherol derivative (AGT251) (Table 2 and Figure 2), the authors found that this antioxidant molecule was protective against muscle atrophy and *MuRF1/Trim63* expression, and that the effects may be mediated through NOTCH1 and 3 expression.

4.1.8. Ion Channels

Electrical stimulation is an important signal that controls muscle mass and ion exchange through specific channels, e.g., K⁺-channels, [296]. Following nerve injury, improvement of muscle mass was observed by blocking K⁺ channels with 4-aminopyridine (4-AP) [278]. 4-AP (Table 2) was able to partially restore muscle fiber diameter with a concomitant decrease of *MuRF1/Trim63* expression accompanied by decreased *Foxo1* and *Foxo3a* expression.

4.1.9. Acute-Phase Protein Serum Amyloid A1 (SAA1)

Skeletal muscle loss in intensive care unit patients has been at least partially attributed to the acute-phase protein serum amyloid A1 (SAA1) [256] (Table 2). Recent work performed in cultured C2C12 myotubes and septic mice showed that SAA1 effects were mediated through TLR-dependent IL-6 expression and recruitment of the NF- κ B pathway. This leads with muscle atrophy and an overactivation of MuRF1/TRIM63, MAFbx/Atrogin-1 and MUSA1 E3 ligases. Using BMS-345541, an inhibitor of the I κ B kinase, the authors found that the expression of the E3 ligases returned to basal levels and muscle sparing was observed, indicating that blocking the NF- κ B pathway may be an efficient way for indirectly modulating E3 ligases [266].

4.1.10. TGF- β

TGF- β family ligands, including myostatin and activin, are potential effectors of muscle atrophy in several situations of muscle atrophy like cancer [16]. The injection of a truncated form (aa 7-100) of the TGF- β ligands ActRIIB (Table 2 and Figure 2) in mice subjected to several models of cancer cachexia was sufficient for blocking *MuRF1/Trim63* and *MAFbx/Atrogin-1* expression together with complete sparing of both skeletal muscle and heart mass [16].

4.1.11. Reactive oxygen species (ROS)

ROS are downstream modulators of muscle wasting and may be also potential levers for preserving muscle mass [162]. Several molecules have been tested for their potency to modulate E3 ligase expression and thus to preserve muscle mass. Dehydroepiandrosterone (DHEA) (Table 2 and Figure 2), a multifunctional steroid with antioxidant properties was shown to decrease *MuRF1/Trim63* expression (but not *MAFbx/Atrogin-1*) in tumor-bearing rats, which helped moderately preserving muscle mass [168]. Transforming growth factor type beta 1 (TGF- β 1) regulates the function and pathological status of skeletal muscle and was found to modulate muscle mass by increasing the activity of NADPH oxidase (NOX), a major ROS producer [69]. This was accompanied by an increased expression of MuRF1. Interestingly, N-acetylcysteine (NAC, a clinically used anti-oxidant) and apocynin (NOX inhibitor) were able to reverse both MuRF1 overexpression and muscle mass loss in cultured myotubes treated with TGF- β 1. Similarly, NAC or pyrroloquinoline

quinone (PQQ, a naturally occurring antioxidant) were able to decrease *MuRF1/Trim63* and *MAFbx/Atrogin-1* expression and to preserve muscle mass in denervated mice or in starved cultured myotubes [285]. SS-31 is a cell-permeable mitochondria-targeted antioxidant tetrapeptide undergoing clinical trials [297]. This peptide is efficient for lowering ROS production, improving muscle atrophy and decreasing *MuRF1/Trim63* and *MAFbx/Atrogin-1* expression [287]. While ROS modulation seems to be efficient for protecting muscle mass, the mechanisms involved in the decrease of E3 ligases expression is far from being understood. Vitamin E is another antioxidant that has been used in a rat model of muscle disuse (hindlimb suspension) [291]. Vitamin E supplementation was able to largely prevent the overexpression of several proteolytic enzymes including *MuRF1/TRIM63* and *MAFbx/atrogin-1* but the impact on muscle mass fiber cross section was moderate. Interestingly, the authors attributed the protective role of vitamin E to a direct action on gene expression and not to its antioxidant properties [291].

4.1.12. Leucine and Its Derivative β -Hydroxy- β -Methylbutyrate (HMB)

The essential amino acid leucine and its derivative HMB were described as modulators of protein synthesis through an action on the mTORC1 pathway [298,299]. The efficiency of HMB and Leucine on *MuRF1/Trim63* expression was addressed in Dex-treated rats [282] (Table 2). However, while HMB and leucine ameliorated muscle function and decreased *MuRF1* expression, no effect of both HMB and leucine was observed on muscle weight. This might be due to partial effect of the treatment on muscles. Interestingly, the modulation of FOXO1 nuclear translocation was the putative mechanism for *MuRF1/Trim63* down-regulation. Leucine was also implicated in the modulation of both *MuRF1/TRIM63* and *MAFbx/atrogin-1* with an improvement of myotube diameter in Dex-treated primary muscle cells [283,300]. The authors found that the effect of leucine on E3 ligase expression was mediated by FOXO3a cytoplasmic sequestration and concomitant vacuolar protein sorting 34 (VPS34) nuclear accumulation. Alternatively, a supplementation with Vital01 (composed by high levels of BCAAs, increased ratio of whey and casein proteins, vitamin D, and ursolic acid) in calorically restricted mouse model of muscle atrophy preserved muscle mass both during and after the atrophic conditions were established. The catabolic phenotype was ameliorated by Vital01, notably through the modulation of the UPS (decreased expression of *MuRF1/Trim63* and *MAFbx/Atrogin-1*) and the autophagy-lysosome pathways, [301]. However, Leu and HMB exhibit no effect on E3 ligase expression (*MuRF1/Trim63* and *MAFbx/Atrogin-1*) in human during fasting [210] and the beneficial muscle sparing was attributed to a stimulation of the mTORC1 pathway [298]. On the whole, the potential beneficial effect of Leu and HMB is still controversial for both its action on E3 ligases and for muscle preservation effect.

4.1.13. Plant Derivatives

Plant derivatives were also tested for their potency to protect skeletal muscle atrophy. Ursolic acid (Table 2), was able to partially decrease muscle atrophy in mice subjected to chronic kidney disease and a moderate effect on *MuRF1/TRIM63*, *MAFbx/Atrogin-1* and *MUSA1* expression was observed, that was attributed to decreased expression of myostatin and inflammatory cytokines [255]. However, ursolic acid was unable to modify E3 ligases expression in cultured myotubes treated with Dex, and ursolic acid was able to directly induce the expression of *MuRF1/Trim63* and *MAFbx/Atrogin-1* in C2C12 myotubes. More investigation is clearly needed before concluding of any potential therapy using ursolic acid. A polyphenol from green tea, epigallocatechin-3-gallate (EGCG), was also used as a countermeasure for fighting against cancer cachexia [279]. EGCG was able to reduce NF- κ B expression and the downstream E3 ligases *MuRF1/TRIM63* and *MAFbx/Atrogin-1* (only a trend for *MuRF1/TRIM63*). However, the decrease of the tumor volume renders difficult the interpretation of the effect of EGCG as its protective role on muscles might be indirect. Teaghrelin, an analog of the human ghrelin, was efficient for decreasing the catabolic effect of Dex in cultured C2C12 myotubes, with depressed expression of *MuRF1/Trim63* and

MAFbx/Atrogin-1 [289]. The authors suggested that increased myogenin expression might be implicated in the beneficial effect of teaghrelin. In rats submitted to thermal injury, ghrelin blunted the expression of *MuRF1/Trim63* and *MAFbx/Atrogin-1* [302]. While the exact mechanism was not addressed, the authors found that TNF α and IL-6 mRNA levels were normalized upon ghrelin infusion. Interestingly, mice knocked out for ghrelin exhibit an increased expression of *MuRF1/Trim63* and are less protected from fasting atrophy [290]. Sabinene is a terpene present in plant essential oil and was found to decrease muscle atrophy in starved rats through reversal of the increased *MuRF1/Trim63* overexpression that is commonly observed upon fasting [286]. The mechanism proposed by the authors was the repression of ROS-mediated activation of ERK and p38 MAKp.

Matrine (Table 2 and Figure 2) is a natural compound used in traditional medicine and approved for cancer therapy in China [284]. The authors demonstrated that this compound was able to partially reverse muscle atrophy in mice subjected to Colon 26 adenocarcinoma with a concomitant decrease of *MuRF1/Trim63* and *MAFbx/Atrogin-1* expression. Using cultured C2C12 myotubes, the authors found that the effect of matrine was mainly driven by the AKT/mTORC1/FOXO3a signaling pathway with both a repression of the catalytic axis and an up regulation of the anabolic one.

4.2. E3 Ligases Inhibitors

The main E3 ligase that has been investigated so far for the design of inhibitors is MuRF1/TRIM63. This can be explained by the fact it is also the only E3 ligase known to target contractile proteins from both the thin and the thick filament [227,228,230,303].

In a first attempt, the screening of a small molecule library for finding MuRF1/TRIM63 inhibitors identified a compound (P013222) (Table 2 and Figure 2) that was able to decrease MuRF1/TRIM63 autoubiquitylation [294]. The selectivity was within the μ M range with a 10 times preference for MuRF1/TRIM63 compared to other E3 ligases and P013222 was able to inhibit the degradation of MHC in Dex-treated C2C12 myotubes.

More recently, the screening of a library identified another small molecule compound (ID#704946/MyoMed-946) able to alter MuRF1-titin interaction (IC₅₀ around 25 μ M), thus targeting the coiled-coil region of MuRF1/TRIM63 [293]. Compound ID#704946/MyoMed-946 was able to decrease in vitro MuRF1/TRIM63 self-ubiquitination and surprisingly was also able to decrease the mRNA levels of *MuRF1/Trim63* in catabolic C2C12 myotubes [293]. This suggests that this compound may be interfering on several mechanisms modulating MuRF1/TRIM63 action. This compound was at least partially effective for preserving muscle mass in catabolic mice. The mechanism by which compound ID#704946/MyoMed-946 preserve muscle function needs further investigations as the same laboratory found that it was also able to modulate MuRF2 expression [17,18].

The cellular inhibitor of apoptosis 1 (cIAP1) E3 ligase is a negative regulator of muscle mass by acting on TNF α -mediated NF- κ B signaling. cIAP1 is in fact an E3 ligase whose role is to blunt the non-canonical NF- κ B signaling and its genetical ablation was reported to improve muscle mass in *mdx* mice [91]. Recently, an inhibitor of cIAP1 (LCL161) was addressed for its capacity to improve skeletal muscle mass in denervated mice [19]. While genetic ablation of cIAP1 was able to preserve muscle mass in denervated mice, its inhibition by LC161 was only moderately efficient as only the EDL muscle was preserved, indicating either a poor inhibition efficiency of LCL161 or a compensation by other E3 ligases and/or signaling pathways.

CBL-B is an E3 ligase involved in the targeting of the Insulin Receptor Substrate 1 (IRS1) that mediates IGF1 signaling, notably by activating the AKT-mTORC1 pathway. CBL-B is involved in spaceflight-induced muscle atrophy and genetic ablation of CBL-B protects skeletal muscle from disuse atrophy [171]. CBL-B can be inhibited by a small pentapeptide mimetic of tyrosine608-phosphorylated IRS-1 that restores IGF1 signaling and protects from atrophy. Interestingly, IGF1 signaling restoration induced a concomitant decrease of *MAFbx* expression while no variation on *MuRF1/Trim63* mRNA levels was

observed [171]. Another peptide, called cblin, was also reported to exhibit some protective action on skeletal muscle through the inhibition of Cbl-b [304].

5. Conclusions and Future Directions

The discovery of molecules able to lower muscle loss during catabolic situations is a promising field of investigation and numerous possibilities can be envisaged, from directly blunting the signals arriving at the cellular membrane levels to more specifically inhibiting the E3 ligase(s) involved in the degradation of the muscle contractile apparatus. Each strategy has advantages and disadvantages. The first approaches are not specific and alter numerous metabolic pathways, which may end up with side effects both at the short- and long-term levels. For example, suppressing the general protein breakdown by acting on the PI3K/AKT/FOXO pathway might be deleterious by accumulating misfolded proteins. On the other side, receptor or metabolic pathways have been studied for decades and several inhibitors have been well characterized, which allows more straightforward investigations dedicated to muscle atrophy.

The drugs targeting directly the E3 ligases, so far mostly focused on MuRF1/TRIM63, have the advantage of being more selective and should prove to be better tolerated by the muscle cells and the whole organism. Indeed, MuRF1/TRIM63 (and some other ligases) is muscle-specific, which means that drugs will only affect muscles. This is an important advantage over metabolic pathways that are shared by several organs. More investigations are clearly needed for ameliorating the first generation of molecules or for finding new ones, which includes new strategies for modulating E3 ligases activity.

Author Contributions: Conceptualization, C.P., D.T. and D.P.-M.; writing, review: D.P.-M., L.C. (Laura Cussonneau), D.T., C.P., L.C. (Lydie Combaret) and editing, D.P.-M. All authors have read and agreed to the published version of the manuscript.

Funding: Our laboratory is supported by grants from the AFM/Telethon (grant #19521), from the French government IDEX-ISITE initiative 16-IDEX-0001 (CAP 20e25) and from the Fondation pour la Recherche Médicale (labelling FRM, labelling FRM, DEQ20180339180 and from CNES (Centre national d'études spatiales; DAR 4800001057). This work has received funding from the European Union's Horizon 2020 research and innovation programme under the Marie Skłodowska-Curie grant agreement No. 813599.

Institutional Review Board Statement: Not applicable.

Informed Consent Statement: Not applicable.

Data Availability Statement: No new data were created or analyzed in this study. Data sharing is not applicable to this article.

Acknowledgments: This work was supported by the French *Institut National de Recherche pour l'Agriculture, l'Alimentation et l'Environnement* (INRAE). Laura Cussonneau is supported by Clermont-Auvergne-Métropole and Dulce Peris-Moreno by the European Union's Horizon 2020 research and innovation programme under the Marie Skłodowska-Curie grant agreement No. 813599.

Conflicts of Interest: The authors declare no conflict of interest. The funders had no role in the writing of the manuscript.

Abbreviations

AMPK	Adenosine 5'-monophosphate-activated (AMP)-activated protein kinase
ATG9	Autophagy related gene 9
BMP	Bone Morphogenic Protein
CaMKK β	Ca ²⁺ /calmodulin-dependent protein kinase kinase β
cAMP	cyclic Adenosine Monophosphate
CHF	Congestive Heart Failure
CKD	Chronic Kidney Disease
Cn	Calcineurin

CSL	CBF1, Suppressor of Hairless, Lag-1
DMD	Duchenne Muscle Dystrophy
Dsh	Dishevelled
EDL	Extensor digitorum longus
ERK	Extracellular signal-regulated kinases
Fd	Frizzled
FOXO	Forkhead box protein O
GC	Glucocorticoids
GR	Glucocorticoids Receptor
GDF	Growth Differentiation Factor
GPCR	G-protein coupled receptors
HBM	β -hydroxy- β -methylbutyrate
HDAC4	Histone deacetylase 4
HECT	Homologous to E6-Associated Protein C Terminus
IGF1	Insulin-like growth factor 1
IKK	I κ B Kinase
KD	Knock Down
KO	Knock-Out
LKB1	Liver kinase B1
MAFbx/Atrogin-1	Muscle atrophy F-box
MAPK	Mitogen Activated Protein Kinase
Mdx	The mdx mouse has a point mutation in its DMD gene (coding for Dystrophin)
MSTN	Myostatin
mTORC	Mechanistic (or mammalian) target of rapamycin complex
MuRF1	Muscle Ring-Finger 1 Protein
MyoD	Myogenic regulatory factor
NAC	N-acetyl cysteine
NFAT	Nuclear factor of activated T-cells
NICD	Notch Intracellular Domain
NOX	NADPH oxidase
PTEN	Phosphatase and tensin homologue
PDK1	3-phosphoinositide-dependent protein kinase 1
PGC-1 α	Peroxisome proliferator-activated receptor gamma coactivator 1-alpha
PI3K	Phosphoinositide 3-kinase
PKA	cAMP-dependent protein kinase
PQQ	pyrroloquinoline quinone
RBR	RING-in-Between-RING
RING	Really Interesting New Gene-finger
RNS	Reactive Nitrogen Species
ROS	Reactive Oxygen Species
SDEN	Surgical sympathetic denervation
SMAD	Small Mothers Against Decapentaplegic
TA	Tibialis Anterior
TAK-1	transforming growth factor β -activated kinase 1
TAZ/WWTR1	WW domain containing protein 1
TFs	Transcription factors
TGF	Transforming Growth Factor
TRADD	TNF receptor associated via death domain
TRAF6	TNF receptor-associated factor 6
TSC	Tuberous Sclerosis Complex
ULK1	uncoordinated 51-like kinase 1
UPS	Ubiquitin-Proteasome System
Wnt	Wingless-type mouse mammary tumor virus integration site
YAP	Yes-Associated Protein

References

1. Von Haehling, S.; Anker, M.S.; Anker, S.D. Prevalence and clinical impact of cachexia in chronic illness in Europe, USA, and Japan: Facts and numbers update 2016. *J. Cachexia Sarcopenia Muscle* **2016**, *7*, 507–509. [[CrossRef](#)]
2. Penna, F.; Ballarò, R.; Beltrà, M.; De Lucia, S.; García Castillo, L.; Costelli, P. The Skeletal Muscle as an Active Player against Cancer Cachexia. *Front. Physiol.* **2019**, *10*, 41. [[CrossRef](#)]
3. Blondelle, J.; Biju, A.; Lange, S. The Role of Cullin-RING Ligases in Striated Muscle Development, Function, and Disease. *Int. J. Mol. Sci.* **2020**, *21*, 7936. [[CrossRef](#)]
4. Bodine, S.C.; Latres, E.; Baumhueter, S.; Lai, V.K.; Nunez, L.; Clarke, B.A.; Poueymirou, W.T.; Panaro, F.J.; Na, E.; Dharmarajan, K.; et al. Identification of ubiquitin ligases required for skeletal muscle atrophy. *Science* **2001**, *294*, 1704–1708. [[CrossRef](#)]
5. Polge, C.; Attaix, D.; Taillandier, D. Role of E2-Ub-conjugating enzymes during skeletal muscle atrophy. *Front. Physiol.* **2015**, *6*, 59. [[CrossRef](#)]
6. Taillandier, D.; Polge, C. Skeletal muscle atrogenes: From rodent models to human pathologies. *Biochimie* **2019**, *166*, 251–269. [[CrossRef](#)]
7. Kwon, Y.T.; Ciechanover, A. The Ubiquitin Code in the Ubiquitin-Proteasome System and Autophagy. *Trends. Biochem. Sci.* **2017**, *42*, 873–886. [[CrossRef](#)]
8. Zheng, N.; Shabek, N. Ubiquitin Ligases: Structure, Function, and Regulation. *Annu. Rev. Biochem.* **2017**, *86*, 129–157. [[CrossRef](#)]
9. Weissman, A.M. Themes and variations on ubiquitylation. *Nat. Rev. Mol. Cell. Biol.* **2001**, *2*, 169–178. [[CrossRef](#)]
10. Walden, H.; Rittinger, K. RBR ligase-mediated ubiquitin transfer: A tale with many twists and turns. *Nat. Struct. Mol. Cell. Biol.* **2018**, *25*, 440–445. [[CrossRef](#)]
11. Dove, K.K.; Klevit, R.E. RING-between-RING E3 Ligases: Emerging Themes amid the Variations. *J. Mol. Biol.* **2017**, *429*, 3363–3375. [[CrossRef](#)]
12. Peris-Moreno, D.; Taillandier, D.; Polge, C. MuRF1/TRIM63, Master Regulator of Muscle Mass. *Int. J. Mol. Sci.* **2020**, *21*, 6663. [[CrossRef](#)]
13. Frost, R.A.; Nystrom, G.J.; Jefferson, L.S.; Lang, C.H. Hormone, cytokine, and nutritional regulation of sepsis-induced increases in atrogin-1 and MuRF1 in skeletal muscle. *Am. J. Physiol.-Endocrinol. Metab.* **2007**, *292*, E501–E512. [[CrossRef](#)]
14. Gopinath, S.D. Inhibition of stat3 signaling ameliorates atrophy of the soleus muscles in mice lacking the vitamin D receptor. *Skelet. Muscle* **2017**, *7*, 1–17. [[CrossRef](#)] [[PubMed](#)]
15. Kline, W.O.; Panaro, F.J.; Yang, H.; Bodine, S.C. Rapamycin inhibits the growth and muscle-sparing effects of clenbuterol. *J. Appl. Physiol.* **2007**, *102*, 740–747. [[CrossRef](#)] [[PubMed](#)]
16. Zhou, X.; Wang, J.L.; Lu, J.; Song, Y.; Kwak, K.S.; Jiao, Q.; Rosenfeld, R.; Chen, Q.; Boone, T.; Simonet, W.S.; et al. Reversal of Cancer Cachexia and Muscle Wasting by ActRIIB Antagonism Leads to Prolonged Survival. *Cell* **2010**, *142*, 531–543. [[CrossRef](#)] [[PubMed](#)]
17. Adams, V.; Gußen, V.; Zozulya, S.; Cruz, A.; Moriscot, A.; Linke, A.; Labeit, S. Small-Molecule Chemical Knockdown of MuRF1 in Melanoma Bearing Mice Attenuates Tumor Cachexia Associated Myopathy. *Cells* **2020**, *9*, 2272. [[CrossRef](#)]
18. Adams, V.; Bowen, T.S.; Werner, S.; Barthel, P.; Amberger, C.; Konzer, A.; Graumann, J.; Sehr, P.; Lewis, J.; Provaznik, J.; et al. Small-molecule-mediated chemical knock-down of MuRF1/MuRF2 and attenuation of diaphragm dysfunction in chronic heart failure. *J. Cachexia Sarcopenia Muscle* **2019**, *10*, 1102–1115. [[CrossRef](#)]
19. Lala-Tabbert, N.; Lejmi-Mrad, R.; Timusk, K.; Fukano, M.; Holbrook, J.; St-Jean, M.; LaCasse, E.C.; Korneluk, R.G. Targeted ablation of the cellular inhibitor of apoptosis 1 (cIAP1) attenuates denervation-induced skeletal muscle atrophy. *Skelet. Muscle* **2019**, *9*, 1–13. [[CrossRef](#)]
20. Saha, A.K.; Xu, X.J.; Lawson, E.; Deoliveira, R.; Brandon, A.E.; Kraegen, E.W.; Ruderman, N.B. Downregulation of AMPK accompanies leucine- and glucose-induced increases in protein synthesis and insulin resistance in rat skeletal muscle. *Diabetes* **2010**, *59*, 2426–2434. [[CrossRef](#)]
21. Haar, E.V.; Lee, S.; Bandhakavi, S.; Griffin, T.J.; Kim, D.-H. Insulin signalling to mTOR mediated by the Akt/PKB substrate PRAS40. *Nat. Cell Biol.* **2007**, *9*, 316–323. [[CrossRef](#)] [[PubMed](#)]
22. Shi, J.; Luo, L.; Eash, J.; Ibebunjo, C.; Glass, D.J. The SCF-Fbxo40 Complex Induces IRS1 Ubiquitination in Skeletal Muscle, Limiting IGF1 Signaling. *Dev. Cell.* **2011**, *21*, 835–847. [[CrossRef](#)] [[PubMed](#)]
23. Stitt, T.N.; Drujan, D.; Clarke, B.A.; Panaro, F.; Timofeyeva, Y.; Kline, W.O.; Gonzalez, M.; Yancopoulos, G.D.; Glass, D.J. The IGF-1/PI3K/Akt pathway prevents expression of muscle atrophy-induced ubiquitin ligases by inhibiting FOXO transcription factors. *Mol. Cell.* **2004**, *14*, 395–403. [[CrossRef](#)]
24. Tremblay, F.; Marette, A. Amino acid and insulin signaling via the mTOR/p70 S6 kinase pathway. A negative feedback mechanism leading to insulin resistance in skeletal muscle cells. *J. Biol. Chem.* **2001**, *276*, 38052–38060.
25. Huang, J.; Dibble, C.C.; Matsuzaki, M.; Manning, B.D. The TSC1-TSC2 Complex Is Required for Proper Activation of mTOR Complex 2. *Mol. Cell. Biol.* **2008**, *28*, 4104–4115. [[CrossRef](#)]
26. Glasgow, C.G.; Steagall, W.K.; Taveira-Dasilva, A.; Pacheco-Rodriguez, G.; Cai, X.; El-Chemaly, S.; Moses, M.; Darling, T.; Moss, J. Lymphangiomyomatosis (LAM): Molecular Insights into mTOR Regulation Lead to Targeted Therapies. *Respir. Med.* **2010**, *104*, S45–S58. [[CrossRef](#)]
27. Polak, P.; Hall, M.N. mTOR and the control of whole body metabolism. *Curr. Opin. Cell Biol.* **2009**, *21*, 209–218. [[CrossRef](#)]
28. Chantranupong, L.; Sabatini, D.M. The TORC1 pathway to protein destruction. *Nature* **2016**, *536*, 155–156. [[CrossRef](#)]

29. Verhees, K.J.P.; JSchols, A.M.W.; Kelders, M.C.J.M.; Op den Kamp, C.M.H.; van der Velden, J.L.J.; Langen, R.C.J. Glycogen synthase kinase-3 β is required for the induction of skeletal muscle atrophy. *Am. J. Physiol.-Cell Physiol.* **2011**, *301*, 13. [[CrossRef](#)]
30. Brunet, A.; Bonni, A.; Zigmond, M.J.; Lin, M.Z.; Juo, P.; Hu, L.S.; Anderson, M.J.; Arden, K.C.; Blenis, J.; Greenberg, M.E. Akt Promotes Cell Survival by Phosphorylating and Inhibiting a Forkhead Transcription Factor. *Cell* **1999**, *96*, 857–868. [[CrossRef](#)]
31. Kops, G.J.P.L.; Ruiter ND de De Vries-Smits, A.M.M.; Powell, D.R.; Bos, J.L. Burgering BMTh. Direct control of the Forkhead transcription factor AFX by protein kinase B. *Nature* **1999**, *398*, 630–634. [[CrossRef](#)]
32. Rena, G.; Guo, S.; Cichy, S.C.; Unterman, T.G.; Cohen, P. Phosphorylation of the Transcription Factor Forkhead Family Member FKHR by Protein Kinase B. *J. Biol. Chem.* **1999**, *274*, 17179–17183. [[CrossRef](#)] [[PubMed](#)]
33. Takaishi, H.; Konishi, H.; Matsuzaki, H.; Ono, Y.; Shirai, Y.; Saito, N.; Kitamura, T.; Ogawa, W.; Kasuga, M.; Kikkawa, U. Regulation of nuclear translocation of Forkhead transcription factor AFX by protein kinase B. *Proc. Natl. Acad. Sci. USA* **1999**, *96*, 11836–11841. [[CrossRef](#)] [[PubMed](#)]
34. Kim, J.; Kundu, M.; Viollet, B.; Guan, K.L. AMPK and mTOR regulate autophagy through direct phosphorylation of Ulk1. *Nat. Cell Biol.* **2011**, *13*, 132–141. [[CrossRef](#)] [[PubMed](#)]
35. Tang, H.; Inoki, K.; Lee, M.; Wright, E.; Khuong, A.; Khuong, A.; Sugiarto, S.; Garner, M.; Paik, J.; DePinho, R.A.; et al. mTORC1 promotes denervation-induced muscle atrophy through a mechanism involving the activation of FoxO and E3 ubiquitin ligases. *Sci. Signal.* **2014**, *7*, 1–11. [[CrossRef](#)]
36. Tang, H.; Inoki, K.; Brooks, S.V.; Okazawa, H.; Lee, M.; Wang, J.; Michael Kim, M.; Catherine L Kennedy, C.L.; Macpherson, P.C.D.; Ji, X.; et al. mTORC1 underlies age-related muscle fiber damage and loss by inducing oxidative stress and catabolism. *Aging Cell.* **2019**, *18*, 1–20. [[CrossRef](#)] [[PubMed](#)]
37. Ham, A.S.; Chojnowska, K.; Tintignac, L.A.; Lin, S.; Schmidt, A.; Ham, D.J.; Sinnreich, M.; Rüegg, M.A. mTORC1 signalling is not essential for the maintenance of muscle mass and function in adult sedentary mice. *J. Cachexia Sarcopenia Muscle* **2020**, *11*, 259–273. [[CrossRef](#)] [[PubMed](#)]
38. Joassard, O.R.; Durieux, A.C.; Freyssenet, D.G. β 2-Adrenergic agonists and the treatment of skeletal muscle wasting disorders. *Int. J. Biochem. Cell Biol.* **2013**, *45*, 2309–2321. [[CrossRef](#)]
39. Silveira, W.A.; Gonçalves, D.A.; Machado, J.; Lautherbach, N.; Lustrino, D.; Paula-Gomes, S.; Pereira, M.G.; Miyabara, E.H.; Sandri, M.; Isis C Kettelhut, I.C.; et al. cAMP-dependent protein kinase inhibits FoxO activity and regulates skeletal muscle plasticity in mice. *FASEB J.* **2020**, *34*, 12946–12962. [[CrossRef](#)]
40. Arcaro, C.A.; Assis, R.P.; Zanon, N.M.; Paula-Gomes, S.; Navegantes, L.C.C.; Kettelhut, I.C.; Brunetti, I.L.; Baviera, A.M. Involvement of cAMP/EPAC/Akt signaling in the antiproteolytic effects of pentoxifylline on skeletal muscles of diabetic rats. *J. App. Physiol.* **2018**, *124*, 704–716. [[CrossRef](#)]
41. Baviera, A.M.; Zanon, N.M.; Navegantes, L.C.C.; Kettelhut, I.C. Involvement of cAMP/Epac/PI3K-dependent pathway in the antiproteolytic effect of epinephrine on rat skeletal muscle. *Mol. Cell Endocrinol.* **2010**, *315*, 104–112. [[CrossRef](#)] [[PubMed](#)]
42. Ohnuki, Y.; Umeki, D.; Mototani, Y.; Jin, H.; Cai, W.; Shiozawa, K.; Suita, K.; Saeki, Y.; Fujita, T.; Ishikawa, Y.; et al. Role of cyclic AMP sensor Epac1 in masseter muscle hypertrophy and myosin heavy chain transition induced by β 2-adrenoceptor stimulation. *J. Physiol.* **2014**, *592*, 5461–5475. [[CrossRef](#)] [[PubMed](#)]
43. Fedon, Y.; Bonnieu, A.; Gay, S.; Vernus, B.; Bacou, F.; Bernardi, H. Role and Function of Wnts in the Regulation of Myogenesis: When Wnt Meets Myostatin. In *Skeletal Muscle-From Myogenesis to Clinical Relations*; InTech: London, UK, 2012; p. 13. [[CrossRef](#)]
44. von Maltzahn, J.; Chang, N.C.; Bentzinger, C.F.; Rudnicki, M.A. Wnt signaling in myogenesis. *Trends Cell Biol.* **2012**, *22*, 602–609. [[CrossRef](#)] [[PubMed](#)]
45. Armstrong, D.D.; Wong, V.L.; Esser, K.A. Expression of β -catenin is necessary for physiological growth of adult skeletal muscle. *Am. J. Physiol.-Cell Physiol.* **2006**, *291*, 185–188. [[CrossRef](#)] [[PubMed](#)]
46. Armstrong, D.D.; Esser, K.A. Wnt/ β -catenin signaling activates growth-control genes during overload-induced skeletal muscle hypertrophy. *Am. J. Physiol.-Cell Physiol.* **2005**, *289*, 853–859. [[CrossRef](#)]
47. Von Maltzahn, J.; Bentzinger, C.F.; Rudnicki, M.A. Wnt7a-Fzd7 signalling directly activates the Akt/mTOR anabolic growth pathway in skeletal muscle. *Nat. Cell Biol.* **2012**, *14*, 186–191. [[CrossRef](#)] [[PubMed](#)]
48. Schmidt, M.; Poser, C.; von Maltzahn, J. Wnt7a Counteracts Cancer Cachexia. *Mol. Ther. Oncolytics* **2020**, *16*, 134–146. [[CrossRef](#)]
49. von Maltzahn, J.; Renaud, J.M.; Parise, G.; Rudnicki, M.A. Wnt7a treatment ameliorates muscular dystrophy. *Proc. Natl. Acad. Sci. USA* **2012**, *109*, 20614–20619. [[CrossRef](#)]
50. Bentzinger, C.F.; von Maltzahn, J.; Dumont, N.A.; Stark, D.A.; Wang, Y.X.; Nhan, K.; Frenette, J.; Cornelison, D.D.W.; Rudnicki, M.A. Wnt7a stimulates myogenic stem cell motility and engraftment resulting in improved muscle strength. *J. Cell Biol.* **2014**, *205*, 97–111. [[CrossRef](#)]
51. Fischer, M.; Rikeit, P.; Knaus, P.; Coirault, C. YAP-Mediated Mechanotransduction in Skeletal. *Muscle Front. Physiol.* **2016**, *7*. [[CrossRef](#)]
52. Kirby, T.J. Mechanosensitive pathways controlling translation regulatory processes in skeletal muscle and implications for adaptation. *J. Appl. Physiol.* **2019**, *127*, 608–618. [[CrossRef](#)] [[PubMed](#)]
53. Biressi, S.; Miyabara, E.H.; Gopinath, S.D.; MCarlig, P.M.; Rando, T.A. A Wnt-TGF 2 axis induces a fibrogenic program in muscle stem cells from dystrophic mice. *Sci. Transl. Med.* **2014**, *6*, 176–267. [[CrossRef](#)]
54. Brack, A.S.; Conboy, M.J.; Roy, S.; Lee, M.; Kuo, C.J.; Keller, C.; Rando, T.A. Increased Wnt Signaling During Aging Alters Muscle Stem Cell Fate and Increases Fibrosis. *Science* **2007**, *317*, 807–810. [[CrossRef](#)] [[PubMed](#)]

55. Musarò, A.; McCullagh, K.J.A.; Naya, F.J.; Olson, E.N.; Rosenthal, N. IGF-1 induces skeletal myocyte hypertrophy through calcineurin in association with GATA-2 and NF-ATc1. *Nature* **1999**, *400*, 581–585. [[CrossRef](#)] [[PubMed](#)]
56. Roberts-Wilson, T.K.; Reddy, R.N.; Bailey, J.L.; Zheng, B.; Ordas, R.; Gooch, J.L.; Price, S.R. Calcineurin signaling and PGC-1 α expression are suppressed during muscle atrophy due to diabetes. *Biochim. Biophys. Acta-Mol. Cell Res.* **2010**, *1803*, 960–967. [[CrossRef](#)] [[PubMed](#)]
57. Sakuma, K.; Yamaguchi, A. The functional role of calcineurin in hypertrophy, regeneration, and disorders of skeletal muscle. *J. Biomed. Biotechnol.* **2010**, *2010*, 721219. [[CrossRef](#)] [[PubMed](#)]
58. Hudson, M.B.; Woodworth-Hobbs, M.E.; Zheng, B.; Rahnert, J.A.; Blount, M.A.; Gooch, J.L.; Searles, C.D.; Price, S.R. miR-23a is decreased during muscle atrophy by a mechanism that includes calcineurin signaling and exosome-mediated export. *Am. J. Physiol.-Cell Physiol.* **2014**, *306*, C551–C558. [[CrossRef](#)]
59. Delacroix, C.; Hyzewicz, J.; Lemaitre, M.; Friguet, B.; Li, Z.; Klein, A.; Furling, D.; Agbulut, O.; Ferry, A. Improvement of Dystrophic Muscle Fragility by Short-Term Voluntary Exercise through Activation of Calcineurin Pathway in mdx Mice. *Am. J. Pathol.* **2018**, *188*, 2662–2673. [[CrossRef](#)]
60. Lara-Pezzi, E.; Winn, N.; Paul, A.; McCullagh, K.; Slominsky, E.; Santini, M.P.; Mourkioti, F.; Sarathchandra, P.; Fukushima, S.; Suzuki, K.; et al. A naturally occurring calcineurin variant inhibits FoxO activity and enhances skeletal muscle regeneration. *J. Cell Biol.* **2007**, *179*, 1205–1218. [[CrossRef](#)]
61. Watt, K.I.; Goodman, C.A.; Hornberger, T.A.; Gregorevic, P. The Hippo Signaling Pathway in the Regulation of Skeletal Muscle Mass and Function. *Exerc Sport. Sci. Rev.* **2018**, *46*, 92–96. [[CrossRef](#)]
62. Hulmi, J.J.; Oliveira, B.M.; Silvennoinen, M.; Hoogaars, W.M.H.; Ma, H.; Pierre, P.; Pasternack, A.; Kainulainen, H.; Ritvos, O. Muscle protein synthesis, mTORC1/MAPK/Hippo signaling, and capillary density are altered by blocking of myostatin and activins. *Am. J. Physiol.-Endocrinol. Metab.* **2013**, *304*, E41–E50. [[CrossRef](#)] [[PubMed](#)]
63. Goodman, C.A.; Dietz, J.M.; Jacobs, B.L.; McNally, R.M.; You, J.S.; Hornberger, T.A. Yes-Associated Protein is up-regulated by mechanical overload and is sufficient to induce skeletal muscle hypertrophy. *FEBS Lett.* **2015**, *589*, 1491–1497. [[CrossRef](#)] [[PubMed](#)]
64. Watt, K.I.; Turner, B.J.; Hagg, A.; Zhang, X.; Davey, J.R.; Qian, H.; Beyer, C.; Winbanks, C.E.; Harvey, K.F.; Gregorevic, P. The Hippo pathway effector YAP is a critical regulator of skeletal muscle fibre size. *Nat Commun.* **2015**, *6*, 6048. [[CrossRef](#)] [[PubMed](#)]
65. Weiss, A.; Attisano, L. The TGF β superfamily signaling pathway. *Wiley Interdiscip. Rev. Dev. Biol.* **2013**, *2*, 47–63. [[CrossRef](#)]
66. Qin, H.; Chan, M.W.; Liyanarachchi, S.; Balch, C.; Potter, D.; Souriraj, I.J.; Cheng, A.S.L.; Agosto-Perez, F.J.; Nikonova, E.V.; Yan, P.S. An integrative ChIP-chip and gene expression profiling to model SMAD regulatory modules. *BMC Syst. Biol.* **2009**, *3*, 73. [[CrossRef](#)]
67. Amirouche, A.; Durieux, A.-C.; Banzet, S.; Koulmann, N.; Bonnefoy, R.; Mouret, C.; Bigard, X.; Peinnequin, A.; Freyssenet, D. Down-regulation of Akt/mammalian target of rapamycin signaling pathway in response to myostatin overexpression in skeletal muscle. *Endocrinology* **2009**, *150*, 286–294. [[CrossRef](#)]
68. Bollinger, L.M.; Witezak, C.A.; Houmard, J.A.; Brault, J.J. SMAD3 augments FoxO3-induced MuRF-1 promoter activity in a DNA-binding-dependent manner. *Am. J. Physiol.-Cell Physiol.* **2014**, *307*, 278–287. [[CrossRef](#)]
69. Abrigo, J.; Rivera, J.C.; Simon, F.; Cabrera, D.; Cabello-Verrugio, C. Transforming growth factor type beta (TGF- β) requires reactive oxygen species to induce skeletal muscle atrophy. *Cell Signal.* **2016**, *28*, 366–376. [[CrossRef](#)]
70. Latres, E.; Mastaitis, J.; Fury, W.; Miloscio, L.; Trejos, J.; Pangilinan, J.; Okamoto, H.; Cavino, K.; Na, E.; Papatheodorou, A.; et al. Activin A more prominently regulates muscle mass in primates than does GDF8. *Nat. Commun.* **2017**, *8*, 15153. [[CrossRef](#)]
71. Chen, J.L.; Walton, K.L.; Qian, H.; Colgan, T.D.; Hagg, A.; Watt, M.J.; Harrison, C.A.; Gregorevic, P. Differential Effects of IL6 and Activin A in the Development of Cancer-Associated Cachexia. *Cancer Res.* **2016**, *76*, 5372–5382. [[CrossRef](#)]
72. Chen, J.L.; Walton, K.; Winbanks, C.E.; Murphy, K.T.; Thomson, R.E.; Makanji, Y.; Qian, H.; Lynch, G.S.; Harrison, C.A.; Gregorevic, P. Elevated expression of activins promotes muscle wasting and cachexia. *FASEB J.* **2014**, *28*, 1711–1723. [[CrossRef](#)] [[PubMed](#)]
73. Ding, H.; Zhang, G.; Sin, K.W.T.; Liu, Z.; Lin, R.-K.; Li, M.; Li, Y.-P. Activin A induces skeletal muscle catabolism via p38 β mitogen-activated protein kinase. *J. Cachexia Sarcopenia Muscle* **2017**, *8*, 202–212. [[CrossRef](#)] [[PubMed](#)]
74. Garg, K.; Corona, B.T.; Walters, T.J. Therapeutic strategies for preventing skeletal muscle fibrosis after injury. *Front. Pharmacol.* **2015**, *6*. [[CrossRef](#)] [[PubMed](#)]
75. Walton, K.L.; Johnson, K.E.; Harrison, C.A. Targeting TGF- β Mediated SMAD Signaling for the Prevention of Fibrosis. *Front. Pharmacol.* **2017**, *8*. [[CrossRef](#)]
76. Ma, Z.-Y.; Zhong, Z.-G.; Qiu, M.-Y.; Zhong, Y.-H.; Zhang, W.-X. TGF- β 1 activates the canonical NF- κ B signaling to promote cell survival and proliferation in dystrophic muscle fibroblasts in vitro. *Biochem. Biophys. Res. Commun.* **2016**, *471*, 576–581. [[CrossRef](#)]
77. Sartori, R.; Schirwis, E.; Blaauw, B.; Bortolanza, S.; Zhao, J.; Enzo, E.; Stantzou, A.; Mouisel, E.; Toniolo, L.; Ferry, A.; et al. BMP signaling controls muscle mass. *Nat. Genet.* **2013**, *45*, 1309–1321. [[CrossRef](#)]
78. Sartori, R.; Gregorevic, P.; Sandri, M. TGF β and BMP signaling in skeletal muscle: Potential significance for muscle-related disease. *Trends Endocrinol. Metab.* **2014**, *25*, 464–471. [[CrossRef](#)]
79. Winbanks, C.E.; Chen, J.L.; Qian, H.; Liu, Y.; Bernardo, B.C.; Beyer, C.; Watt, K.I.; Thomson, R.E.; Connor, T.; Turner, B.J.; et al. The bone morphogenetic protein axis is a positive regulator of skeletal muscle mass. *J. Cell Biol.* **2013**, *203*, 345–357. [[CrossRef](#)]
80. Saxton, R.A.; Sabatini, D.M. mTOR Signaling in Growth, Metabolism, and Disease. *Cell* **2017**, *168*, 960–976. [[CrossRef](#)]

81. Hitachi, K.; Nakatani, M.; Tsuchida, K. Long Non-Coding RNA Myoparr Regulates GDF5 Expression in Denervated Mouse Skeletal Muscle. *Non-Coding RNA* **2019**, *5*, 33. [[CrossRef](#)]
82. Neppel, R.L.; Wu, C.-L.; Walsh, K. IncRNA Chronos is an aging-induced inhibitor of muscle hypertrophy. *J. Cell Biol.* **2017**, *216*, 3497–3507. [[CrossRef](#)]
83. McCarthy, J.J.; Murach, K.A. Anabolic and Catabolic Signaling Pathways That Regulate Skeletal Muscle Mass. In *Nutrition and Enhanced Sports Performance: Muscle Building, Endurance, and Strength*; Academic Press: Cambridge, MA, USA, 2018. [[CrossRef](#)]
84. Sanchez, A.M.J.; Candau, R.B.; Csibi, A.; Pagano, A.F.; Raibon, A.; Bernardi, H. The role of AMP-activated protein kinase in the coordination of skeletal muscle turnover and energy homeostasis. *Am. J. Physiol.-Cell Physiol.* **2012**, *303*, C475–C485. [[CrossRef](#)]
85. Zungu, M.; Schisler, J.C.; Essop, M.F.; McCudden, C.; Patterson, C.; Willis, M.S. Regulation of AMPK by the ubiquitin proteasome system. *Am. J. Pathol.* **2011**, *178*, 4–11. [[CrossRef](#)] [[PubMed](#)]
86. Sanchez, A.; Candau, R.; Bernardi, H. Recent Data on Cellular Component Turnover: Focus on Adaptations to Physical Exercise. *Cells* **2019**, *8*, 542. [[CrossRef](#)] [[PubMed](#)]
87. Egawa, T.; Goto, A.; Ohno, Y.; Yokoyama, S.; Ikuta, A.; Suzuki, M.; Sugiura, T.; Ohira, Y.; Yoshioka, T.; Hayashi, T.; et al. Involvement of AMPK in regulating slow-twitch muscle atrophy during hindlimb unloading in mice. *Am. J. Physiol.-Endocrinol. Metab.* **2015**, *309*, E651–E662. [[CrossRef](#)] [[PubMed](#)]
88. Thomson, D.M. The Role of AMPK in the Regulation of Skeletal Muscle Size, Hypertrophy, and Regeneration. *Int. J. Mol. Sci.* **2018**, *19*, 3125. [[CrossRef](#)]
89. Cai, D.; Frantz, J.D.; Tawa, N.E.; Melendez, P.A.; Oh, B.C.; Lidov, H.G.W.; Hasselgren, P.-O.; Frontera, W.R.; Lee, J.; Glass, D.J.; et al. IKK β /NF- κ B activation causes severe muscle wasting in mice. *Cell* **2004**, *119*, 285–298. [[CrossRef](#)]
90. Enwere, E.K.; Boudreault, L.; Holbrook, J.; Timusk, K.; Earl, N.; LaCasse, E.; Renaud, J.-M.; Korneluk, R.G. Loss of cIAP1 attenuates soleus muscle pathology and improves diaphragm function in mdx mice. *Hum. Mol. Genet.* **2013**, *22*, 867–878. [[CrossRef](#)]
91. Enwere, E.K.; Holbrook, J.; Lejmi-Mrad, R.; Vineham, J.; Timusk, K.; Sivaraj, B.; Isaac, M.; Uehling, D.; Al-awar, R.; LaCasse, E.; et al. TWEAK and cIAP1 Regulate Myoblast Fusion Through the Noncanonical NF- κ B Signaling Pathway. *Sci. Signal.* **2012**, *5*, ra75. [[CrossRef](#)]
92. Li, H.; Malhotra, S.; Kumar, A. Nuclear factor-kappa B signaling in skeletal muscle atrophy. *J. Mol. Med.* **2008**, *86*, 1113–1126. [[CrossRef](#)]
93. Li, Y.P.; Reid, M.B. NF- κ B mediates the protein loss induced by TNF- α in differentiated skeletal muscle myotubes. *Am. J. Physiol.-Regul. Integr. Comp. Physiol.* **2000**, *279*, 1165–1170. [[CrossRef](#)] [[PubMed](#)]
94. Sato, S.; Ogura, Y.; Kumar, A. TWEAK/Fn14 Signaling Axis Mediates Skeletal Muscle Atrophy and Metabolic Dysfunction. *Front. Immunol.* **2014**, *5*. [[CrossRef](#)] [[PubMed](#)]
95. Shih, V.F.S.; Tsui, R.; Caldwell, A.; Hoffmann, A. A single NF κ B system for both canonical and non-canonical signaling. *Cell Res.* **2011**, *21*, 86–102. [[CrossRef](#)] [[PubMed](#)]
96. Sun, S.C. The non-canonical NF- κ B pathway in immunity and inflammation. *Nat. Rev. Immunol.* **2017**, *17*, 545–558. [[CrossRef](#)]
97. Mourkioti, F.; Kratsios, P.; Luedde, T.; Song, Y.H.; Delafontaine, P.; Adami, R.; Parente, V.; Bottinelli, R.; Pasparakis, M.; Rosenthal, N. Targeted ablation of IKK2 improves skeletal muscle strength, maintains mass, and promotes regeneration. *J. Clin. Investig.* **2006**, *116*, 2945–2954. [[CrossRef](#)]
98. Hunter, R.B.; Kandarian, S.C. Disruption of either the Nfkb1 or the Bcl3 gene inhibits skeletal muscle atrophy. *J. Clin. Investig.* **2004**, *114*, 1504–1511. [[CrossRef](#)]
99. Agustí, A.; Morlá, M.; Sauleda, J.; Saus, C.; Busquets, X. NF- κ B activation and iNOS upregulation in skeletal muscle of patients with COPD and low body weight. *Thorax* **2004**, *59*, 483–487. [[CrossRef](#)]
100. Adams, V.; Späte, U.; Kränkel, N.; Schulze, P.C.; Linke, A.; Schuler, G.; Hambrecht, R. Nuclear factor-kappa B activation in skeletal muscle of patients with chronic heart failure: Correlation with the expression of inducible nitric oxide synthase. *Eur. J. Cardiovasc. Prev. Rehabil.* **2003**, *10*, 273–277. [[CrossRef](#)]
101. Liu, T.; Zhang, L.; Joo, D.; Sun, S.-C. NF- κ B signaling in inflammation. *Signal Transduct. Target. Ther.* **2017**, *2*, 1–9. [[CrossRef](#)]
102. Lamothe, B.; Besse, A.; Campos, A.D.; Webster, W.K.; Wu, H.; Darnay, B.G. Site-specific Lys-63-linked tumor necrosis factor receptor-associated factor 6 auto-ubiquitination is a critical determinant of I κ B kinase activation. *J. Biol. Chem.* **2007**, *282*, 4102–4112. [[CrossRef](#)] [[PubMed](#)]
103. Hindi, S.M.; Sato, S.; Choi, Y.; Kumar, A. Distinct roles of TRAF6 at early and late stages of muscle pathology in the mdx model of duchenne muscular dystrophy. *Hum. Mol. Genet.* **2014**, *23*, 1492–1505. [[CrossRef](#)] [[PubMed](#)]
104. Enwere, E.K.; Lacasse, E.C.; Adam, N.J.; Korneluk, R.G. Role of the TWEAK-Fn14-cIAP1-NF- κ B Signaling Axis in the Regulation of Myogenesis and Muscle Homeostasis. *Front. Immunol.* **2014**, *5*, 34. [[CrossRef](#)] [[PubMed](#)]
105. Cohen, P.; Strickson, S. The role of hybrid ubiquitin chains in the MyD88 and other innate immune signalling pathways. *Cell Death Differ.* **2017**, *24*, 1153–1159. [[CrossRef](#)] [[PubMed](#)]
106. Hayden, M.S.; Ghosh, S. Shared Principles in NF- κ B Signaling. *Cell* **2008**, *132*, 344–362. [[CrossRef](#)]
107. Gensler, L.S. Glucocorticoids: Complications to Anticipate and Prevent. *Neurohospitalist* **2013**, *3*, 92–97. [[CrossRef](#)]
108. Hardy, R.S.; Raza, K.; Cooper, M.S. Therapeutic glucocorticoids: Mechanisms of actions in rheumatic diseases. *Nat. Rev. Rheumatol.* **2020**, *16*, 133–144. [[CrossRef](#)]

109. Revollo, J.R.; Cidlowski, J.A. Mechanisms generating diversity in glucocorticoid receptor signaling. *Ann. N. Y. Acad. Sci.* **2009**, *1179*, 167–178. [[CrossRef](#)]
110. Bodine, S.C.; Furlow, J.D. Glucocorticoids and Skeletal Muscle. *Adv. Exp. Med. Biol.* **2015**, *872*, 145–176.
111. Braun, T.P.; Marks, D.L. The regulation of muscle mass by endogenous glucocorticoids. *Front. Physiol.* **2015**, *6*, 1–12. [[CrossRef](#)]
112. Fappi, A.; Neves, J.D.; Sanches, L.N.; Massaroto e Silva, P.V.; Sikusawa, G.Y.; Brandão, T.P.; Chadi, G.; Zanoteli, E. Skeletal Muscle Response to Deflazacort, Dexamethasone and Methylprednisolone. *Cells* **2019**, *8*, 406. [[CrossRef](#)]
113. Fry, C.S.; Nayeem, S.Z.; Dillon, E.L.; Sarkar, P.S.; Tumurbaatar, B.; Urban, R.J.; Wright, T.J.; Sheffield-Moore, S.; Tilton, R.G.; Choudhary, S. Glucocorticoids increase skeletal muscle NF- κ B inducing kinase (NIK): Links to muscle atrophy. *Physiol. Rep.* **2016**, *4*, 1–13. [[CrossRef](#)] [[PubMed](#)]
114. Sato, A.Y.; Richardson, D.; Cregor, M.; Davis, H.M.; Au, E.D.; McAndrews, K.; Zimmers, T.A.; Organ, J.M.; Peacock, M.; Plotkin, L.I.; et al. Glucocorticoids induce bone and muscle atrophy by tissue-specific mechanisms upstream of E3 ubiquitin ligases. *Endocrinology* **2017**, *158*, 664–677. [[PubMed](#)]
115. Cea, L.A.; Balboa, E.; Puebla, C.; Vargas, A.A.; Cisterna, B.A.; Escamilla, R.; Regueira, T.; Sáez, J.C. Dexamethasone-induced muscular atrophy is mediated by functional expression of connexin-based hemichannels. *Biochim. Biophys. Acta-Mol. Basis Dis.* **2016**, *1862*, 1891–1899. [[CrossRef](#)]
116. Adhikary, S.; Kothari, P.; Choudhary, D.; Tripathi, A.K.; Trivedi, R. Glucocorticoid aggravates bone micro-architecture deterioration and skeletal muscle atrophy in mice fed on high-fat diet. *Steroids* **2019**, *149*, 108416. [[CrossRef](#)] [[PubMed](#)]
117. Aguilar-Agon, K.W.; Capel, A.J.; Fleming, J.W.; Player, D.J.; Martin, N.R.W.; Lewis, M.P. Mechanical loading of tissue engineered skeletal muscle prevents dexamethasone induced myotube atrophy. *J. Muscle Res. Cell Motil.* **2020**. [[CrossRef](#)]
118. Powers, S.K.; Morton, A.B.; Hyatt, H.; Hinkley, M.J. The Renin-Angiotensin System and Skeletal Muscle Exerc. *Sport Sci. Rev.* **2018**, *46*, 205–214.
119. Du Bois, P.; Tortola, C.P.; Lodka, D.; Kny, M.; Schmidt, F.; Song, K.; Schmidt, S.; Bassel-Duby, R.; Olson, E.N.; Fielitz, J. Angiotensin II Induces Skeletal Muscle Atrophy by Activating TFEB-Mediated MuRF1 Expression. *Circ. Res.* **2015**, *117*, 424–436. [[CrossRef](#)]
120. Rezk, B.M.; Yoshida, T.; Semprun-Prieto, L.; Higashi, Y.; Sukhanov, S.; Delafontaine, P. Angiotensin II infusion induces marked diaphragmatic skeletal muscle atrophy. *PLoS ONE* **2012**, *7*, e30276. [[CrossRef](#)]
121. Sugiyama, M.; Yamaki, A.; Furuya, M.; Inomata, N.; Minamitake, Y.; Ohsuye, K.; Kangawa, K. Ghrelin improves body weight loss and skeletal muscle catabolism associated with angiotensin II-induced cachexia in mice. *Regul. Pept.* **2012**, *178*, 21–28. [[CrossRef](#)]
122. Tabony, A.M.; Yoshida, T.; Galvez, S.; Higashi, Y.; Sukhanov, S.; Chandrasekar, B.; Mitch, W.E.; Delafontaine, P. Angiotensin II Upregulates Protein Phosphatase 2C α and Inhibits AMP-Activated Protein Kinase Signaling and Energy Balance Leading to Skeletal Muscle Wasting. *Hypertension* **2011**, *58*, 643–649. [[CrossRef](#)]
123. Yoshida, T.; Semprun-Prieto, L.; Sukhanov, S.; Delafontaine, P. IGF-1 prevents ANG II-induced skeletal muscle atrophy via Akt- and Foxo-dependent inhibition of the ubiquitin ligase atrogin-1 expression. *Am. J. Physiol.-Heart Circ. Physiol.* **2010**, *298*, H1565–H1570. [[CrossRef](#)] [[PubMed](#)]
124. Aravena, J.; Abrigo, J.; Gonzalez, F.; Aguirre, F.; Gonzalez, A.; Simon, F.; Cabello-Verrugio, C. Angiotensin (1-7) decreases myostatin-induced NF- κ b signaling and skeletal muscle atrophy. *Int. J. Mol. Sci.* **2020**, *21*, 1167. [[CrossRef](#)] [[PubMed](#)]
125. Meneses, C.; Morales, M.G.; Abrigo, J.; Simon, F.; Brandan, E.; Cabello-Verrugio, C. The angiotensin-(1-7)/Mas axis reduces myonuclear apoptosis during recovery from angiotensin II-induced skeletal muscle atrophy in mice. *Pflug. Arch.-Eur. J. Physiol.* **2015**, *467*, 1975–1984. [[CrossRef](#)] [[PubMed](#)]
126. Morales, M.G.; Abrigo, J.; Acuña, M.J.; Santos, R.A.; Bader, M.; Brandan, E.; Simon, F.; Olguin, H.; Cabrera, D.; Cabello-Verrugio, C. Angiotensin-(1-7) attenuates disuse skeletal muscle atrophy in mice via its receptor. *Mas. Dis. Model. Mech.* **2016**, *9*, 441–449. [[CrossRef](#)] [[PubMed](#)]
127. Echeverría-Rodríguez, O.; Gallardo-Ortiz, I.A.; Valle-Mondragón, L.D.; Villalobos-Molina, R. Angiotensin-(1-7) participates in enhanced skeletal muscle insulin sensitivity after a bout of exercise. *J. Endocr. Soc.* **2020**, *4*, 1–11. [[CrossRef](#)]
128. Ábrigo, J.; Simon, F.; Cabrera, D.; Cabello-Verrugio, C. Angiotensin-(1-7) Prevents Skeletal Muscle Atrophy Induced by Transforming Growth Factor Type Beta (TGF- β) via Mas Receptor Activation. *Cell. Physiol. Biochem.* **2016**, *40*, 27–38. [[CrossRef](#)]
129. Yan, F.; Yuan, Z.; Wang, N.; Carey, R.M.; Aylor, K.W.; Chen, L.; Zhou, X.; Liu, Z. Direct activation of angiotensin II type 2 receptors enhances muscle microvascular perfusion, oxygenation, and insulin delivery in male rats. *Endocrinology* **2018**, *159*, 685–695. [[CrossRef](#)]
130. Bahat, G. Covid-19 and the Renin Angiotensin System: Implications for the Older Adults. *J. Nutr. Health Aging* **2020**, *24*, 699–704. [[CrossRef](#)]
131. Sanders, P.M.; Russell, S.T.; Tisdale, M.J. Angiotensin II directly induces muscle protein catabolism through the ubiquitin-proteasome proteolytic pathway and may play a role in cancer cachexia. *Br. J. Cancer* **2005**, *93*, 425–434. [[CrossRef](#)]
132. Song, Y.-H.; Li, Y.; Du, J.; Mitch, W.E.; Rosenthal, N.; Delafontaine, P. Muscle-specific expression of IGF-1 blocks angiotensin II-induced skeletal muscle wasting. *J. Clin. Investig.* **2005**, *115*, 451–458. [[CrossRef](#)]
133. Belizário, J.E.; Fontes-Oliveira, C.C.; Borges, J.P.; Kashiabara, J.A.; Vannier, E. Skeletal muscle wasting and renewal: A pivotal role of myokine IL-6. *SpringerPlus* **2016**, *5*, 619. [[CrossRef](#)] [[PubMed](#)]
134. Moresi, V.; Adamo, S.; Berghella, L. The JAK/STAT pathway in skeletal muscle pathophysiology. *Front. Physiol.* **2019**, *30*, 500. [[CrossRef](#)]

135. Guadagnin, E.; Mázala, D.; Chen, Y.W. STAT3 in skeletal muscle function and disorders. *Int. J. Mol. Sci.* **2018**, *19*, 2265. [[CrossRef](#)] [[PubMed](#)]
136. Mashili, F.; Chibalin, A.V.; Krook, A.; Zierath, J.R. Constitutive STAT3 phosphorylation contributes to skeletal muscle insulin resistance in type 2 diabetes. *Diabetes* **2013**, *62*, 457–465. [[CrossRef](#)] [[PubMed](#)]
137. Kim, T.H.; Choi, S.E.; Ha, E.S.; Jung, J.G.; Han, S.J.; Kim, H.J.; Kim, D.J.; Kang, Y.; Lee, K.W. IL-6 induction of TLR-4 gene expression via STAT3 has an effect on insulin resistance in human skeletal muscle. *Acta Diabetol.* **2013**, *50*, 189–200. [[CrossRef](#)]
138. Zhang, L.; Pan, J.; Dong, Y.; Twardy, D.J.; Dong, Y.; Garibotto, G.; Mitch, W.E. Stat3 activation links a C/EBP δ to myostatin pathway to stimulate loss of muscle mass. *Cell Metab.* **2013**, *18*, 368–379. [[CrossRef](#)]
139. Silva, K.A.S.; Dong, J.; Dong, Y.; Dong, Y.; Schor, N.; Twardy, D.J.; Zhang, L.; Mitch, W.E. Inhibition of Stat3 activation suppresses caspase-3 and the ubiquitin-proteasome system, leading to preservation of muscle mass in cancer cachexia. *J. Biol. Chem.* **2015**, *290*, 11177–11187. [[CrossRef](#)]
140. Abid, H.; Ryan, Z.C.; Delmotte, P.; Sieck, G.C.; Lanza, I.R. Extramyocellular interleukin-6 influences skeletal muscle mitochondrial physiology through canonical JAK/STAT signaling pathways. *FASEB J.* **2020**, *34*, 14458–14472. [[CrossRef](#)]
141. Calixto, J.B.; Medeiros, R.; Fernandes, E.S.; Ferreira, J.; Cabrini, D.A.; Campos, M.M. Kinin B 1 receptors: Key G-protein-coupled receptors and their role in inflammatory and painful processes. *Br. J. Pharmacol.* **2004**, *143*, 803–818. [[CrossRef](#)]
142. Parreiras-e-Silva, L.T.; Reis, R.I.; Santos, G.A.; Pires-Oliveira, M.; Pesquero, J.B.; Gomes, M.D.; Godinho, R.O.; Costa-Neto, C.M. The kinin B1 receptor regulates muscle-specific E3 ligases expression and is involved in skeletal muscle mass control. *Clin. Sci.* **2014**, *127*, 185–194. [[CrossRef](#)]
143. de Picoli Souza, K.; Batista, E.C.; Silva, E.D.; Reis, F.C.; Silva, S.M.A.; Araujo, R.C.; Luz, J.; Santos, E.L.; Pesquero, J.B. Effect of kinin B2 receptor ablation on skeletal muscle development and myostatin gene expression. *Neuropeptides* **2010**, *44*, 209–214. [[CrossRef](#)]
144. Popadic Gacesa, J.Z.; Momcilovic, M.; Veselinovic, I.; Brodie, D.A.; Grujic, N.G. Bradykinin type 2 receptor -9/-9 genotype is associated with triceps brachii muscle hypertrophy following strength training in young healthy men. *BMC Musculoskelet. Disord.* **2012**, *13*, 1–7. [[CrossRef](#)] [[PubMed](#)]
145. Chavez, J.A.; Knotts, T.A.; Wang, L.P.; Li, G.; Dobrowsky, R.T.; Florant, G.L.; Summers, S.A. A role for ceramide, but not diacylglycerol, in the antagonism of insulin signal transduction by saturated fatty acids. *J. Biol. Chem.* **2003**, *278*, 10297–10303. [[CrossRef](#)]
146. Hyde, R.; Hajduch, E.; Powell, D.J.; Taylor, P.M.; Hundal, H.S. Ceramide down-regulates System A amino acid transport and protein synthesis in rat skeletal muscle cells. *FASEB J.* **2005**, *19*, 1–24. [[CrossRef](#)] [[PubMed](#)]
147. Orsini, M.; Chateauvieux, S.; Rhim, J.; Gaigneaux, A.; Cheillan, D.; Christov, C.; Dicato, M.; Morceau, F.; Diederich, M. Sphingolipid-mediated inflammatory signaling leading to autophagy inhibition converts erythropoiesis to myelopoiesis in human hematopoietic stem/progenitor cells. *Cell Death Diff.* **2019**, *26*, 1796–1812. [[CrossRef](#)] [[PubMed](#)]
148. Tardif, N.; Salles, J.; Guillet, C.; Tordjman, J.; Reggio, S.; Landrier, J.; Giraudet, C.; Patrac, V.; Bertrand-Michel, J.; Migne, C. Muscle ectopic fat deposition contributes to anabolic resistance in obese sarcopenic old rats through e IF 2 α activation. *Aging Cell* **2014**, *13*, 1001–1011. [[CrossRef](#)]
149. De Larichaudy, J.; Zufferli, A.; Serra, F.; Isidori, A.M.; Naro, F.; Dessalle, K.; Desgeorges, M.; Piraud, M.; Cheillan, D.; Vidal, H.; et al. TNF- α - and tumor-induced skeletal muscle atrophy involves sphingolipid metabolism. *Skelet. Muscle* **2012**, *2*, 1–19. [[CrossRef](#)]
150. Rivas, D.A.; McDonald, D.J.; Rice, N.P.; Haran, P.H.; Dolnikowski, G.G.; Fielding, R.A. Diminished anabolic signaling response to insulin induced by intramuscular lipid accumulation is associated with inflammation in aging but not obesity. *Am. J. Physiol.-Regul. Integr. Comp. Physiol.* **2016**, *310*, R561–R569. [[CrossRef](#)]
151. Rivas, D.A.; Morris, E.P.; Haran, P.H.; Pasha, E.P.; Da Silva Morais, M.; Dolnikowski, G.G.; Phillips, E.M.; Fielding, R.A. Increased ceramide content and NF κ B signaling may contribute to the attenuation of anabolic signaling after resistance exercise in aged males. *J. Appl. Physiol.* **2012**, *113*, 1727–1736. [[CrossRef](#)]
152. Zanin, M.; Germinario, E.; Dalla Libera, L.; Sandonà, D.; Sabbadini, R.A.; Betto, R.; Danieli-Betto, D. Trophic action of sphingosine 1-phosphate in denervated rat soleus muscle. *Am. J. Physiol.-Cell Physiol.* **2008**, *294*, 36–46. [[CrossRef](#)]
153. Pierucci, F.; Frati, A.; Battistini, C.; Matteini, F.; Iachini, M.C.; Vestri, A.; Penna, F.; Costelli, P.; Meacci, E. Involvement of released sphingosine 1-phosphate/sphingosine 1-phosphate receptor axis in skeletal muscle atrophy. *Biochim. Biophys. Acta-Mol. Basis Dis.* **2018**, *1864*, 3598–3614. [[CrossRef](#)] [[PubMed](#)]
154. Mu, X.; Agarwal, R.; March, D.; Rothenberg, A.; Voigt, C.; Tebbets, J.; Huard, J.; Weiss, K. Notch Signaling Mediates Skeletal Muscle Atrophy in Cancer Cachexia Caused by Osteosarcoma. *Sarcoma* **2016**, 3758162. [[CrossRef](#)] [[PubMed](#)]
155. Feng, F.; Shan, L.; Deng, J.X.; Luo, L.L.; Huang, Q.S. Role of the Notch Signaling Pathway in Fibrosis of Denervated Skeletal Muscle. *Curr. Med. Sci.* **2019**, *39*, 419–425. [[CrossRef](#)] [[PubMed](#)]
156. Liu, X.H.; Yao, S.; Qiao, R.F.; Levine, A.C.; Kirschenbaum, A.; Pan, J.; Wu, Y.; Qin, W.; Bauman, W.A.; Cardozo, C.P. Nandrolone reduces activation of Notch signaling in denervated muscle associated with increased Numb expression. *Biochem. Biophys. Res. Commun.* **2011**, *414*, 165–169. [[CrossRef](#)] [[PubMed](#)]
157. Zhao, J.; Zhang, Y.; Zhao, W.; Wu, Y.; Pan, J.; Bauman, W.A.; Cardozo, C. Effects of nandrolone on denervation atrophy depend upon time after nerve transection. *Muscle Nerve* **2008**, *37*, 42–49. [[CrossRef](#)]

158. Khayrullin, A.; Smith, L.; Mistry, D.; Dukes, A.; Pan, Y.A.; Hamrick, M.W. Chronic alcohol exposure induces muscle atrophy (myopathy) in zebrafish and alters the expression of microRNAs targeting the Notch pathway in skeletal muscle. *Biochem. Biophys. Res. Commun.* **2016**, *479*, 590–595. [[CrossRef](#)]
159. Domingues-Faria, C.; Chanet, A.; Salles, J.; Berry, A.; Giraudet, C.; Patrac, V.; Denis, P.; Bouton, K.; Goncalves-Mendes, N.; Vasson, M.-P.; et al. Vitamin D deficiency down-regulates Notch pathway contributing to skeletal muscle atrophy in old wistar rats. *Nutr. Metab.* **2014**, *11*, 1–13. [[CrossRef](#)]
160. Hori, K.; Sen, A.; Artavanis-Tsakonas, S. Notch signaling at a glance. *J. Cell Sci.* **2013**, *126*, 2135–2140. [[CrossRef](#)]
161. von Grabowiecki, Y.; Licon, C.; Palamiuc, L.; Abreu, P.; Vidimar, V.; Coowar, D.; Mellitzer, G.; Gaiddon, C. Regulation of a Notch3-Hes1 pathway and protective effect by a tocopherol-omega alkanol chain derivative in muscle atrophy. *J. Pharmacol. Exp. Therap.* **2015**, *352*, 23–32. [[CrossRef](#)]
162. Powers, S.K.; Morton, A.B.; Ahn, B.; Smuder, A.J. Redox control of skeletal muscle atrophy. *Free Radic. Biol. Med.* **2016**, *98*, 208–217. [[CrossRef](#)]
163. Abrigo, J.; Elorza, A.A.; Riedel, C.A.; Vilos, C.; Simon, F.; Cabrera, D.; Estrada, L.; Cabello-Verrugio, C. Role of oxidative stress as key regulator of muscle wasting during cachexia. *Oxid Med. Cell. Longev.* **2018**, *28*, 2063179. [[CrossRef](#)]
164. Passey, S.L.; Hansen, M.J.; Bozinovski, S.; McDonald, C.F.; Holland, A.E.; Vlahos, R. Emerging therapies for the treatment of skeletal muscle wasting in chronic obstructive pulmonary disease. *Pharmacol. Therapeut.* **2016**, *166*, 56–70. [[CrossRef](#)] [[PubMed](#)]
165. Leitner, L.M.; Wilson, R.J.; Yan, Z.; Gödecke, A. Reactive Oxygen Species/Nitric Oxide Mediated Inter-Organ Communication in Skeletal Muscle Wasting Diseases. *Antioxid. Redox Signal.* **2017**, *26*, 700–717. [[CrossRef](#)] [[PubMed](#)]
166. Pomiès, P.; Blaquièrre, M.; Maury, J.; Mercier, J.; Gouzi, F.; Hayot, M. Involvement of the FoxO1/MuRF1/Atrogin-1 Signaling Pathway in the Oxidative Stress-Induced Atrophy of Cultured Chronic Obstructive Pulmonary Disease Myotubes. *PLoS ONE* **2016**, *11*, e0160092. [[CrossRef](#)]
167. Beyfuss, K.; Hood, D.A. A systematic review of p53 regulation of oxidative stress in skeletal muscle. *Redox Rep.* **2018**, *23*, 100–117. [[CrossRef](#)]
168. Mastrocola, R.; Reffo, P.; Penna, F.; Tomasinelli, C.E.; Boccuzzi, G.; Baccino, F.M.; Aragno, M.; Costelli, P. Muscle wasting in diabetic and in tumor-bearing rats: Role of oxidative stress. *Free Radic. Biol. Med.* **2008**, *44*, 584–593. [[CrossRef](#)]
169. Rosa-Caldwell, M.E.; Greene, N.P. Muscle metabolism and atrophy: Let's talk about sex. *Biol. Sex Differ.* **2019**, *10*, 1–14. [[CrossRef](#)]
170. Xu, X.; Sarikas, A.; Dias-Santagata, D.C.; Dolios, G.; Lafontant, P.J.; Tsai, S.-C.; Zhu, W.; Nakajima, H.; Nakajima, H.-O.; Field, L.J.; et al. The CUL7 E3 Ubiquitin Ligase Targets Insulin Receptor Substrate 1 for Ubiquitin-Dependent Degradation. *Mol. Cell.* **2008**, *30*, 403–414. [[CrossRef](#)]
171. Nakao, R.; Hirasaka, K.; Goto, J.; Ishidoh, K.; Yamada, C.; Ohno, A.; Okumura, Y.; Nonaka, I.; Yasutomo, K.; Baldwin, K.M.; et al. Ubiquitin Ligase Cbl-b Is a Negative Regulator for Insulin-Like Growth Factor 1 Signaling during Muscle Atrophy Caused by Unloading. *Mol. Cell. Biol.* **2009**, *29*, 4798–4811. [[CrossRef](#)]
172. Nikawa, T.; Ishidoh, K.; Hirasaka, K.; Ishihara, I.; Ikemoto, M.; Kano, M.; Kominami, E.; Nonaka, I.; Ogawa, T.; Adams, G.R.; et al. Skeletal muscle gene expression in space-flown rats. *FASEB J.* **2004**, *18*, 522–524. [[CrossRef](#)]
173. Uchida, T.; Sakashita, Y.; Kitahata, K.; Yamashita, Y.; Tomida, C.; Kimori, Y.; Komatsu, A.; Hirasaka, K.; Ohno, A.; Nakao, R.; et al. Reactive oxygen species upregulate expression of muscle atrophy-associated ubiquitin ligase Cbl-b in rat L6 skeletal muscle cells. *Am. J. Physiol.-Cell Physiol.* **2018**, *314*, C721–C731. [[CrossRef](#)] [[PubMed](#)]
174. Ye, J.; Zhang, Y.; Xu, J.; Zhang, Q.; Zhu, D. FBXO40, a gene encoding a novel muscle-specific F-box protein, is upregulated in denervation-related muscle atrophy. *Gene* **2007**, *404*, 53–60. [[CrossRef](#)]
175. Zhang, L.; Chen, Z.; Wang, Y.; Tweardy, D.J.; Mitch, W.E. Stat3 activation induces insulin resistance via a muscle-specific E3 ubiquitin ligase Fbxo40. *Am. J. Physiol.-Endocrinol. Metab.* **2020**, *318*, E625–E635. [[CrossRef](#)] [[PubMed](#)]
176. Hu, W.; Zhang, P.; Gu, J.; Yu, Q.; Zhang, D. NEDD4-1 protects against ischaemia/reperfusion-induced cardiomyocyte apoptosis via the PI3K/Akt pathway. *Apoptosis* **2017**, *22*, 437–448. [[CrossRef](#)] [[PubMed](#)]
177. Wang, X.; Trotman, L.C.; Koppie, T.; Alimonti, A.; Chen, Z.; Gao, Z.; Wang, J.; Erdjument-Bromage, H.; Tempst, P.; Cordon-Cardo, C.; et al. NEDD4-1 Is a Proto-Oncogenic Ubiquitin Ligase for PTEN. *Cell* **2007**, *128*, 129–139. [[CrossRef](#)] [[PubMed](#)]
178. Nagpal, P.; Plant, P.J.; Correa, J.; Bain, A.; Takeda, M.; Kawabe, H.; Rotin, D.; Bain, J.R.; Batt, J.A.E. The Ubiquitin Ligase Nedd4-1 Participates in Denervation-Induced Skeletal Muscle Atrophy in Mice. *PLoS ONE* **2012**, *7*, e46427. [[CrossRef](#)]
179. Paul, P.K.; Bhatnagar, S.; Mishra, V.; Srivastava, S.; Darnay, B.G.; Choi, Y.; Kumar, A. The E3 Ubiquitin Ligase TRAF6 Intercedes in Starvation-Induced Skeletal Muscle Atrophy through Multiple Mechanisms. *Mol. Cell. Biol.* **2012**, *32*, 1248–1259. [[CrossRef](#)]
180. Paul, P.K.; Gupta, S.K.; Bhatnagar, S.; Panguluri, S.K.; Darnay, B.G.; Choi, Y.; Kumar, A. Targeted ablation of TRAF6 inhibits skeletal muscle wasting in mice. *J. Cell Biol.* **2010**, *191*, 1395–1411. [[CrossRef](#)]
181. Hirata, Y.; Nomura, K.; Senga, Y.; Okada, Y.; Kobayashi, K.; Okamoto, S.; Minokoshi, Y.; Imamura, M.; Takeda, S.; Hosooka, T.; et al. Hyperglycemia induces skeletal muscle atrophy via a WWP1/KLF15 axis. *JCI Insight* **2019**, *4*, e124952. [[CrossRef](#)]
182. Kudryashova, E.; Wu, J.; Havton, L.A.; Spencer, M.J. Deficiency of the E3 ubiquitin ligase TRIM32 in mice leads to a myopathy with a neurogenic component. *Hum. Mol. Genet.* **2009**, *18*, 1353–1367. [[CrossRef](#)]
183. Kudryashova, E.; Struyk, A.; Mokhonova, E.; Cannon, S.C.; Spencer, M.J. The common missense mutation D489N in TRIM32 causing limb girdle muscular dystrophy 2H leads to loss of the mutated protein in knock-in mice resulting in a Trim32-null phenotype. *Hum. Mol. Genet.* **2011**, *20*, 3925–3932. [[CrossRef](#)]

184. Peker, N.; Donipadi, V.; Sharma, M.; McFarlane, C.; Kambadur, R. Loss of Parkin impairs mitochondrial function and leads to muscle atrophy. *Am. J. Physiol.-Cell Physiol.* **2018**, *315*, C164–C185. [[CrossRef](#)] [[PubMed](#)]
185. Leduc-Gaudet, J.P.; Reynaud, O.; Hussain, S.N.; Gouspillou, G. Parkin overexpression protects from ageing-related loss of muscle mass and strength. *J. Physiol.* **2019**, *597*, 1975–1991. [[CrossRef](#)] [[PubMed](#)]
186. Leduc-Gaudet, J.-P.; Mayaki, D.; Reynaud, O.; Broering, F.E.; Chaffer, T.J.; Hussain, S.N.A.; Gouspillou, G. Parkin Overexpression Attenuates Sepsis-Induced Muscle Wasting. *Cells* **2020**, *9*, 1454. [[CrossRef](#)]
187. Milan, G.; Romanello, V.; Pescatore, F.; Armani, A.; Paik, J.-H.; Frasson, L.; Seydel, A.; Zhao, J.; Abraham, R.; Goldberg, A.L.; et al. Regulation of autophagy and the ubiquitin–proteasome system by the FoxO transcriptional network during muscle atrophy. *Nat. Commun.* **2015**, *6*, 6670. [[CrossRef](#)] [[PubMed](#)]
188. Wirianto, M.; Yang, J.; Kim, E.; Gao, S.; Paudel, K.R.; Choi, J.M.; Choe, J.; Gloston, G.F.; Ademoji, P.; Parakramaweera, R.; et al. The GSK-3 β -FBXL21 Axis Contributes to Circadian TCAP Degradation and Skeletal Muscle Function. *Cell Rep.* **2020**, *32*, 108140. [[CrossRef](#)]
189. Hunt, L.C.; Stover, J.; Haugen, B.; Shaw, T.I.; Li, Y.; Pagala, V.R.; Finkelstein, D.; Berton, E.R.; Fan, Y.; Labelle, M.; et al. A Key Role for the Ubiquitin Ligase UBR4 in Myofiber Hypertrophy in Drosophila and Mice. *Cell Rep.* **2019**, *28*, 1268–1281.e6. [[CrossRef](#)]
190. Hughes, D.C.; Turner, D.C.; Baehr, L.M.; Seaborne, R.A.; Viggars, M.; Jarvis, J.C.; Gorski, P.P.; Stewart, C.E.; Owens, D.J.; Bodine, S.C.; et al. Knockdown of the E3 Ubiquitin ligase UBR5 and its role in skeletal muscle anabolism. *Am. J. Physiol.-Cell Physiol.* **2020**, *320*, C45–C56. [[CrossRef](#)]
191. Stana, F.; Vujovic, M.; Mayaki, D.; Leduc-Gaudet, J.P.; Leblanc, P.; Huck, L.; Hussain, S.N.A. Differential Regulation of the Autophagy and Proteasome Pathways in Skeletal Muscles in Sepsis. *Crit. Care Med.* **2017**, *45*, e971–e979. [[CrossRef](#)]
192. Batt, J.; Bain, J.; Goncalves, J.; Michalski, B.; Plant, P.; Fahnstock, M.; Woodgett, J. Differential gene expression profiling of short and long term denervated muscle. *FASEB J.* **2006**, *20*, 115–117. [[CrossRef](#)] [[PubMed](#)]
193. Koncarevic, A.; Jackman, R.W.; Kandarian, S.C. The ubiquitin-protein ligase Nedd4 targets Notch1 in skeletal muscle and distinguishes the subset of atrophies caused by reduced muscle tension. *FASEB J.* **2007**, *21*, 427–437. [[CrossRef](#)]
194. Yue, F.; Song, C.; Huang, D.; Narayanan, N.; Qiu, J.; Jia, Z.; Yuan, Z.; Oprescus, S.N.; Roseguini, B.T.; Deng, M.; et al. PTEN Inhibition Ameliorates Muscle Degeneration and Improves Muscle Function in a Mouse Model of Duchenne Muscular Dystrophy. *Mol. Therap.* **2020**. [[CrossRef](#)]
195. Kim, B.G.; Lee, J.H.; Yasuda, J.; Ryoo, H.M.; Cho, J.Y. Phospho-Smad1 modulation by nedd4 e3 ligase in BMP/TGF- β signaling. *J. Bone Min. Res.* **2011**, *26*, 1411–1424. [[CrossRef](#)]
196. Li, J.; Yi, X.; Yao, Z.; Chakkalakal, J.V.; Xing, L.; Boyce, B.F. TNF Receptor-Associated Factor 6 Mediates TNF α -Induced Skeletal Muscle Atrophy in Mice During Aging. *J. Bone Min. Res.* **2020**, *35*, 1535–1548. [[CrossRef](#)] [[PubMed](#)]
197. Sun, H.; Gong, Y.; Qiu, J.; Chen, Y.; Ding, F.; Zhao, Q. TRAF6 inhibition rescues dexamethasone-induced muscle atrophy. *Int. J. Mol. Sci.* **2014**, *15*, 11126–11141. [[CrossRef](#)]
198. Sun, H.; Qiu, J.; Chen, Y.; Yu, M.; Ding, F.; Gu, X. Proteomic and bioinformatic analysis of differentially expressed proteins in denervated skeletal muscle. *Int. J. Mol. Med.* **2014**, *33*, 1586–1596. [[CrossRef](#)]
199. He, Q.; Qiu, J.; Dai, M.; Fang, Q.; Sun, X.; Gong, Y.; Ding, F.; Sun, H. MicroRNA-351 inhibits denervation-induced muscle atrophy by targeting TRAF6. *Exp. Therap. Med.* **2016**, *12*, 4029–4034. [[CrossRef](#)]
200. Qiu, J.; Wang, L.; Wang, Y.; Zhang, Q.; Ma, W.; Fang, Q.; Sun, H.; Ding, F. MicroRNA351 targeting TRAF6 alleviates dexamethasone-induced myotube atrophy. *J. Thorac. Dis.* **2018**, *10*, 6238–6246. [[CrossRef](#)]
201. Qiu, J.; Zhu, J.; Zhang, R.; Liang, W.; Ma, W.; Zhang, Q.; Huang, Z.; Ding, F.; Sun, H. miR-125b-5p targeting TRAF6 relieves skeletal muscle atrophy induced by fasting or denervation. *Ann. Transl. Med.* **2019**, *7*, 456. [[CrossRef](#)] [[PubMed](#)]
202. Paul, P.K.; Kumar, A. TRAF6 coordinates the activation of autophagy and ubiquitin-proteasome systems in atrophying skeletal muscle. *Autophagy* **2011**, *7*, 555–556. [[CrossRef](#)]
203. Sun, Y.S.; Ye, Z.Y.; Qian, Z.Y.; Xu, X.D.; Hu, J.F. Expression of TRAF6 and ubiquitin mRNA in skeletal muscle of gastric cancer patients. *J. Exp. Clin. Cancer Res.* **2012**, *31*, 1–5. [[CrossRef](#)]
204. Imamura, M.; Nakamura, A.; Mannen, H.; Takeda, S. Characterization of WWP1 protein expression in skeletal muscle of muscular dystrophy chickens. *J. Biochem.* **2016**, *159*, 171–179. [[CrossRef](#)]
205. Shimizu, N.; Yoshikawa, N.; Ito, N.; Maruyama, T.; Suzuki, Y.; Takeda, S.I.; Nakae, J.; Tagata, Y.; Nishitani, S.; Takehana, K.; et al. Crosstalk between glucocorticoid receptor and nutritional sensor mTOR in skeletal muscle. *Cell Metab.* **2011**, *13*, 170–182. [[CrossRef](#)]
206. Lee, J.O.; Lee, S.K.; Kim, N.; Kim, J.H.; You, G.Y.; Moon, J.W.; Jie, S.; Kim, S.J.; Lee, Y.W.; Kang, H.J.; et al. E3 ubiquitin ligase, WWP1, interacts with AMPK α 2 and down-regulates its expression in skeletal muscle C2C12 cells. *J. Biol. Chem.* **2013**, *288*, 4673–4680. [[CrossRef](#)] [[PubMed](#)]
207. Frosk, P.; Weiler, T.; Nysten, E.; Sudha, T.; Greenberg, C.R.; Morgan, K.; Fujiwara, T.M.; Wrogemann, K. Limb-Girdle Muscular Dystrophy Type 2H Associated with Mutation in TRIM32, a Putative E3-Ubiquitin–Ligase Gene. *Am. J. Hum. Genet.* **2002**, *70*, 663–672. [[CrossRef](#)] [[PubMed](#)]
208. Mokhonova, E.I.; Avliyakov, N.K.; Kramerova, I.; Kudryashova, E.; Haykinson, M.J.; Spencer, M.J. The E3 ubiquitin ligase TRIM32 regulates myoblast proliferation by controlling turnover of NDRG2. *Hum. Mol. Genet.* **2015**, *24*, 2873–2883. [[CrossRef](#)]
209. Kudryashova, E.; Kramerova, I.; Spencer, M.J. Satellite cell senescence underlies myopathy in a mouse model of limb-girdle muscular dystrophy 2H. *J. Clin. Investig.* **2012**, *122*, 1764–1776. [[CrossRef](#)] [[PubMed](#)]

210. Servián-Morilla, E.; Cabrera-Serrano, M.; Rivas-Infante, E.; Carvajal, A.; Lamont, P.J.; Pelayo-Negro, A.L.; Ravenscroft, G.; Junckerstorff, R.; Dyke, J.M.; Fletcher, S.; et al. Altered myogenesis and premature senescence underlie human TRIM32-related myopathy. *Acta Neuropathol. Commun.* **2019**, *7*, 30. [[CrossRef](#)] [[PubMed](#)]
211. Di Rienzo, M.; Antonioli, M.; Fusco, C.; Liu, Y.; Mari, M.; Orhon, I.; Refolo, G.; Germani, F.; Corazzari, M.; Romagnoli, A.; et al. Autophagy induction in atrophic muscle cells requires ULK1 activation by TRIM32 through unanchored K63-linked polyubiquitin chains. *Sci. Adv.* **2019**. [[CrossRef](#)] [[PubMed](#)]
212. Peng, H.; Yang, J.; Li, G.; You, Q.; Han, W.; Li, T.; Gao, D.; Xie, X.; Lee, B.-H.; Du, J.; et al. Ubiquitylation of p62/sequestosome1 activates its autophagy receptor function and controls selective autophagy upon ubiquitin stress. *Cell Res.* **2017**, *27*, 657–674. [[CrossRef](#)]
213. Overå, K.S.; Garcia-Garcia, J.; Bhujabal, Z.; Jain, A.; Øvervatn, A.; Larsen, K.B.; Johansen, T.; Lamark, T.; Sjøttem, E. TRIM32, but not its muscular dystrophy-associated mutant, positively regulates and is targeted to autophagic degradation by p62/SQSTM1. *J. Cell Sci.* **2019**, *132*. [[CrossRef](#)] [[PubMed](#)]
214. Alamdari, N.; Aversa, Z.; Castellero, E.; Hasselgren, P.-O. Acetylation and deacetylation—Novel factors in muscle wasting. *Metabolism* **2013**, *62*, 1–11. [[CrossRef](#)] [[PubMed](#)]
215. Bertaglia, E.; Coletto, L.; Sandri, M. Posttranslational modifications control FoxO3 activity during denervation. *Am. J. Physiol.-Cell Physiol.* **2012**, *302*, C587–C596. [[CrossRef](#)] [[PubMed](#)]
216. Kim, H.; Kang, J.-S.; Jeong, H.-J. Arginine methylation as a key post-translational modification in skeletal muscle homeostasis: A review. *Precis. Future Med.* **2019**, *3*, 139–145. [[CrossRef](#)]
217. Brown, A.K.; Webb, A.E. Regulation of FOXO Factors in Mammalian Cells. *Curr. Top. Dev. Biol.* **2018**, *127*, 165–192.
218. Eijkelenboom, A.; Burgering, B.M.T. FOXOs: Signalling integrators for homeostasis maintenance. *Nat. Rev. Mol. Cell. Biol.* **2013**, *14*, 83–97. [[CrossRef](#)]
219. Jamart, C.; Naslain, D.; Gilson, H.; Francaux, M. Higher activation of autophagy in skeletal muscle of mice during endurance exercise in the fasted state. *Am. J. Physiol.-Endocrinol. Metab.* **2013**, *305*, 964–974. [[CrossRef](#)]
220. Louis, E.; Raue, U.; Yang, Y.; Jemiolo, B.; Trappe, S. Time course of proteolytic, cytokine, and myostatin gene expression after acute exercise in human skeletal muscle. *J. Appl. Physiol.* **2007**, *103*, 1744–1751. [[CrossRef](#)]
221. Pasiakos, S.M.; McClung, H.L.; McClung, J.P.; Urso, M.L.; Pikosky, M.A.; Cloutier, G.J.; Fielding, R.A.; Young, A.J. Molecular responses to moderate endurance exercise in skeletal muscle. *Int. J. Sport Nutr. Exerc. Metab.* **2010**, *20*, 282–290. [[CrossRef](#)]
222. Sanchez, A.M.J.; Candau, R.B.; Bernardi, H. FoxO transcription factors: Their roles in the maintenance of skeletal muscle homeostasis. *Cell. Mol. Life Sci.* **2014**, *71*, 1657–1671. [[CrossRef](#)]
223. Labeit, S.; Kohl, C.H.; Witt, C.C.; Labeit, D.; Jung, J.; Granzier, H. Modulation of muscle atrophy, fatigue and MLC phosphorylation by MuRF1 as indicated by hindlimb suspension studies on MuRF1-KO mice. *J. Biomed. Biotechnol.* **2010**, 693741. [[CrossRef](#)]
224. Baehr, L.M.; Furlow, J.D.; Bodine, S.C. Muscle sparing in muscle RING finger 1 null mice: Response to synthetic glucocorticoids. *J. Physiol.* **2011**, *589*, 4759–4776. [[CrossRef](#)] [[PubMed](#)]
225. Koyama, S.; Hata, S.; Witt, C.C.; Ono, Y.; Lerche, S.; Ojima, K.; Chiba, T.; Doi, N.; Kitamura, F.; Tanaka, K.; et al. Muscle RING-Finger Protein-1 (MuRF1) as a Connector of Muscle Energy Metabolism and Protein Synthesis. *J. Mol. Biol.* **2008**, *376*, 1224–1236. [[CrossRef](#)]
226. Files, D.C.; D’Alessio, F.R.; Johnston, L.F.; Kesari, P.; Aggarwal, N.R.; Garibaldi, B.T.; Mock, J.R.; Simmers, J.L.; DeGorordo, A.; Murdoch, J.; et al. A Critical Role for Muscle Ring Finger-1 in Acute Lung Injury–associated Skeletal Muscle Wasting. *Am. J. Respir. Crit. Care Med.* **2012**, *185*, 825–834. [[CrossRef](#)]
227. Fielitz, J.; Kim, M.-S.; Shelton, J.M.; Latif, S.; Spencer, J.A.; Glass, D.J.; Richardson, J.A.; Bassel-Duby, R.; Olson, R.N. Myosin accumulation and striated muscle myopathy result from the loss of muscle RING finger 1 and 3. *J. Clin. Investig.* **2007**, *117*, 2486–2495. [[CrossRef](#)] [[PubMed](#)]
228. Polge, C.; Heng, A.; Jarzaguat, M.; Ventadour, S.; Claustre, A.; Combaret, L.; Béchet, D.; Matondo, M.; Uttenweiler-Joseph, S.; Monsarrat, B.; et al. Muscle actin is polyubiquitinated in vitro and in vivo and targeted for breakdown by the E3 ligase MuRF1. *FASEB J.* **2011**, *25*, 3790–3802. [[CrossRef](#)] [[PubMed](#)]
229. Kedar, V.; McDonough, H.; Arya, R.; Li, H.-H.; Rockman, H.A.; Patterson, C. Muscle-specific RING finger 1 is a bona fide ubiquitin ligase that degrades cardiac troponin I. *Proc. Natl. Acad. Sci. USA* **2004**, *101*, 18135–18140. [[CrossRef](#)]
230. Polge, C.; Cabantous, S.; Deval, C.; Claustre, A.; Hauvette, A.; Bouchenot, C.; Anjort, J.; Béchet, D.; Combaret, L.; Attaix, D.; et al. A muscle-specific MuRF1-E2 network requires stabilization of MuRF1-E2 complexes by telethonin, a newly identified substrate. *J. Cachexia Sarcopenia Muscle* **2018**, *9*, 129–145. [[CrossRef](#)]
231. Rudolf, R.; Bogomolovas, J.; Strack, S.; Choi, K.R.; Khan, M.M.; Wagner, A.; Brohm, K.; Hanashima, A.; Gasch, A.; Labeit, D.; et al. Regulation of nicotinic acetylcholine receptor turnover by MuRF1 connects muscle activity to endo/lysosomal and atrophy pathways. *Age* **2013**, *35*, 1663–1674. [[CrossRef](#)]
232. Khan, M.M.; Strack, S.; Wild, F.; Hanashima, A.; Gasch, A.; Brohm, K.; Reischl, M.; Carnio, S.; Labeit, D.; Sandri, M.; et al. Role of autophagy, SQSTM1, SH3GLB1, and TRIM63 in the turnover of nicotinic acetylcholine receptors. *Autophagy* **2014**, *10*, 123–136. [[CrossRef](#)]
233. Li, H.-H.; Du, J.; Fan, Y.-N.; Zhang, M.-L.; Liu, D.-P.; Li, L.; Lockyer, P.; Kang, E.Y.; Patterson, C.; Willis, M.S. The Ubiquitin Ligase MuRF1 Protects Against Cardiac Ischemia/Reperfusion Injury by Its Proteasome-Dependent Degradation of Phospho-c-Jun. *Am. J. Pathol.* **2011**, *178*, 1043–1058. [[CrossRef](#)] [[PubMed](#)]

234. Bodine, S.C.; Baehr, L.M. Skeletal muscle atrophy and the E3 ubiquitin ligases MuRF1 and MAFbx/atrogin-1. *Am. J. Physiol.-Endocrinol. Metab.* **2014**, *307*, E469–E484. [[CrossRef](#)] [[PubMed](#)]
235. Csibi, A.; Leibovitch, M.P.; Cornille, K.; Tintignac, L.A.; Leibovitch, S.A. MAFbx/Atrogin-1 Controls the Activity of the Initiation Factor eIF3-f in Skeletal Muscle Atrophy by Targeting Multiple C-terminal Lysines. *J. Biol. Chem.* **2009**, *284*, 4413–4421. [[CrossRef](#)] [[PubMed](#)]
236. Jogo, M.; Shiraishi, S.; Tamura, T.A. Identification of MAFbx as a myogenin-engaged F-box protein in SCF ubiquitin ligase. *FEBS Lett.* **2009**, *583*, 2715–2719. [[CrossRef](#)]
237. Lagirand-Cantaloube, J.; Cornille, K.; Csibi, A.; Batonnet-Pinchon, S.; Leibovitch, M.P.; Leibovitch, S.A. Inhibition of atrogin-1/MAFbx mediated MyoD proteolysis prevents skeletal muscle atrophy in vivo. *PLoS ONE* **2009**, *4*, e4973. [[CrossRef](#)] [[PubMed](#)]
238. Wardle, F.C. Master control: Transcriptional regulation of mammalian Myod. *J. Muscle Res. Cell Motil.* **2019**, *40*, 211–226. [[CrossRef](#)]
239. Lokireddy, S.; Wijesoma, I.W.; Sze, S.K.; McFarlane, C.; Kambadur, R.; Sharma, M. Identification of atrogin-1-targeted proteins during the myostatin-induced skeletal muscle wasting. *Am. J. Physiol.-Cell Physiol.* **2012**, *303*, C512–C529. [[CrossRef](#)]
240. Romanello, V.; Sandri, M. Mitochondrial quality control and muscle mass maintenance. *Front. Physiol.* **2016**, *2*, 422. [[CrossRef](#)]
241. Zhang, J.; Xie, J.J.; Zhou, S.J.; Chen, J.; Hu, Q.; Pu, J.X.; Lu, J.-L. Diosgenin inhibits the expression of nedd4 in prostate cancer cells. *Am. J. Transl. Res.* **2019**, *11*, 3461–3471.
242. Leermakers, P.A.; Schols, A.M.W.J.; Kneppers, A.E.M.; Kelders, M.C.J.M.; de Theije, C.C.; Lainscak, M.; Gosker, H.R. Molecular signalling towards mitochondrial breakdown is enhanced in skeletal muscle of patients with chronic obstructive pulmonary disease (COPD). *Sci. Rep.* **2018**, *8*, 1–13. [[CrossRef](#)]
243. Deval, C.; Calonne, J.; Coudy-Gandilhon, C.; Vazeille, E.; Bechet, D.; Polge, C.; Taillandier, D.; Attaix, D.; Combaret, L. Mitophagy and Mitochondria Biogenesis Are Differentially Induced in Rat Skeletal Muscles during Immobilization and/or Remobilization. *Int. J. Mol. Sci.* **2020**, *21*, 3691. [[CrossRef](#)] [[PubMed](#)]
244. Kang, C.; Yeo, D.; Ji, L.L. Muscle immobilization activates mitophagy and disrupts mitochondrial dynamics in mice. *Acta Physiol.* **2016**, *218*, 188–197. [[CrossRef](#)] [[PubMed](#)]
245. Balan, E.; Schwalm, C.; Naslain, D.; Nielens, H.; Francaux, M.; Deldicque, L. Regular Endurance Exercise Promotes Fission, Mitophagy, and Oxidative Phosphorylation in Human Skeletal Muscle Independently of Age. *Front. Physiol.* **2019**, *10*, 1088. [[CrossRef](#)] [[PubMed](#)]
246. Ehrlicher, S.E.; Stierwalt, H.D.; Miller, B.F.; Newsom, S.A.; Robinson, M.M. Mitochondrial adaptations to exercise do not require Bcl2-mediated autophagy but occur with BNIP3/Parkin activation. *FASEB J.* **2020**, *34*, 4602–4618. [[CrossRef](#)]
247. Drummond, M.J.; Addison, O.; Brunker, L.; Hopkins, P.N.; McClain, D.A.; LaStayo, P.C.; Marcus, R.L. Downregulation of E3 Ubiquitin Ligases and Mitophagy-Related Genes in Skeletal Muscle of Physically Inactive, Frail Older Women: A Cross-Sectional Comparison. *J. Gerontol. A Biol. Sci. Med. Sci.* **2014**, *69*, 1040–1048. [[CrossRef](#)]
248. Russ, D.W.; Wills, A.M.; Boyd, I.M.; Krause JWeakness, S.R. function and stress in gastrocnemius muscles of aged male rats. *Exp. Gerontol.* **2014**, *50*, 40–44. [[CrossRef](#)]
249. Marzetti, E.; Lorenzi, M.; Landi, F.; Picca, A.; Rosa, F.; Tanganelli, F.; Galli, M.; Doglietto, G.B.; Pacelli, F.; Cesari, M.; et al. Altered mitochondrial quality control signaling in muscle of old gastric cancer patients with cachexia. *Exp. Gerontol.* **2017**, *87*, 92–99. [[CrossRef](#)]
250. Chen, C.C.W.; Erlich, A.T.; Crilly, M.J.; Hood, D.A. Parkin is required for exercise-induced mitophagy in muscle: Impact of aging. *Am. J. Physiol.-Endocrinol. Metab.* **2018**, *315*, E404–E415. [[CrossRef](#)]
251. Gousspillou, G.; Godin, R.; Piquereau, J.; Picard, M.; Mofarrahi, M.; Mathew, J.; Purves-Smith, F.M.; Sgarioni, N.; Hepple, R.T.; Burelle, Y.; et al. Protective role of Parkin in skeletal muscle contractile and mitochondrial function: Parkin is essential for optimal muscle and mitochondrial functions. *J. Physiol.* **2018**, *596*, 2565–2579. [[CrossRef](#)]
252. Ramesh, M.; Campos, J.C.; Lee, P.; Song, Y.; Hernandez, G.; Sin, J.; Tucker, K.C.; Saadaejahromi, H.; Gurney, M.; Ferreira, J.C.B.; et al. Mitophagy protects against statin-mediated skeletal muscle toxicity. *FASEB J.* **2019**, *33*, 11857–11869. [[CrossRef](#)]
253. Furuya, N.; Ikeda, S.-I.; Sato, S.; Soma, S.; Ezaki, J.; Trejo, J.A.O.; Takeda-Ezaki, M.; Fujimura, T.; Arikawa-Hirasawa, E.; Tada, N.; et al. PARK2/Parkin-mediated mitochondrial clearance contributes to proteasome activation during slow-twitch muscle atrophy via NFE2L1 nuclear translocation. *Autophagy* **2014**, *10*, 631–641. [[CrossRef](#)] [[PubMed](#)]
254. Greene, J.C.; Whitworth, A.J.; Kuo, I.; Andrews, L.A.; Feany, M.B.; Pallanck, L.J. Mitochondrial pathology and apoptotic muscle degeneration in *Drosophila* parkin mutants. *Proc. Natl. Acad. Sci. USA* **2003**, *100*, 4078–4083. [[CrossRef](#)] [[PubMed](#)]
255. Yu, R.; Chen, J.A.; Xu, J.; Cao, J.; Wang, Y.; Thomas, S.S.; Hu, Z. Suppression of muscle wasting by the plant-derived compound ursolic acid in a model of chronic kidney disease. *J. Cachexia Sarcopenia Muscle* **2017**, *8*, 327–341. [[CrossRef](#)] [[PubMed](#)]
256. Hahn, A.; Kny, M.; Pablo-Tortola, C.; Todiras, M.; Willenbrock, M.; Schmidt, S.; Schmoekkel, K.; Jorde, I.; Nowak, M.; Jarosch, E.; et al. Serum amyloid A1 mediates myotube atrophy via Toll-like receptors. *J. Cachexia Sarcopenia Muscle* **2020**, *11*, 103–119. [[CrossRef](#)] [[PubMed](#)]
257. Yoo, S.-H.; Mohawk, J.A.; Siepka, S.M.; Shan, Y.; Huh, S.K.; Hong, H.-K.; Kornblum, I.; Kumar, V.; Koike, N.; Xu, M.; et al. Competing E3 Ubiquitin Ligases Govern Circadian Periodicity by Degradation of CRY in Nucleus and Cytoplasm. *Cell* **2013**, *152*, 1091–1105. [[CrossRef](#)]
258. Lucas, X.; Ciulli, A. Recognition of substrate degrons by E3 ubiquitin ligases and modulation by small-molecule mimicry strategies. *Curr. Opin. Struct. Biol.* **2017**, *44*, 101–110. [[CrossRef](#)]

259. Kwak, K.S.; Zhou, X.; Solomon, V.; Baracos, V.E.; Davis, J.; Bannon, A.W.; Boyle, W.J.; Lacey, D.L.; Han, H.Q. Regulation of protein catabolism by muscle-specific and cytokine-inducible ubiquitin ligase E3 α -II during cancer cachexia. *Cancer Res.* **2004**, *64*, 8193–8198. [[CrossRef](#)]
260. Seaborne, R.A.; Hughes, D.C.; Turner, D.C.; Owens, D.J.; Baehr, L.M.; Gorski, P.; Semenova, E.A.; Borisov, O.V.; Larin, A.K.; Popov, D.V.; et al. UBR5 is a novel E3 ubiquitin ligase involved in skeletal muscle hypertrophy and recovery from atrophy. *J. Physiol.* **2019**, *597*, 3727–3749. [[CrossRef](#)]
261. Besche, H.C.; Haas, W.; Gygi, S.P.; Goldberg, A.L. Isolation of Mammalian 26S Proteasomes and p97/VCP Complexes Using the Ubiquitin-like Domain from HHR23B Reveals Novel Proteasome-Associated Proteins. *Biochemistry* **2009**, *48*, 2538–2549. [[CrossRef](#)]
262. Morén, A.; Imamura, T.; Miyazono, K.; Heldin, C.H.; Moustakas, A. Degradation of the tumor suppressor Smad4 by WW and HECT domain ubiquitin ligases. *J. Biol. Chem.* **2005**, *280*, 22115–22123. [[CrossRef](#)]
263. Ebisawa, T.; Fukuchi, M.; Murakami, G.; Chiba, T.; Tanaka, K.; Imamura, T.; Miyazono, K. Smurf1 interacts with transforming growth factor- β type I receptor through Smad7 and induces receptor degradation. *J. Biol. Chem.* **2001**, *276*, 12477–12480. [[CrossRef](#)] [[PubMed](#)]
264. Tényi, Á.; Cano, I.; Marabita, F.; Kiani, N.; Kalko, S.G.; Barreiro, E.; de Atauri, P.; Cascante, M.; Gomez-Cabrero, D.; Roca, J. Network modules uncover mechanisms of skeletal muscle dysfunction in COPD patients. *J. Transl. Med.* **2018**, *16*, 1–12. [[CrossRef](#)] [[PubMed](#)]
265. Xin, H.; Xu, X.; Li, L.; Ning, H.; Rong, Y.; Shang, Y.; Wang, Y.; Fu, X.-Y.; Chang, Z. CHIP controls the sensitivity of transforming growth factor- β signaling by modulating the basal level of Smad3 through ubiquitin-mediated degradation. *J. Biol. Chem.* **2005**, *280*, 20842–20850. [[CrossRef](#)] [[PubMed](#)]
266. Li, R.F.; Shang, Y.; Liu, D.; Ren, Z.S.; Chang, Z.; Sui, S.F. Differential Ubiquitination of Smad1 Mediated by CHIP: Implications in the Regulation of the Bone Morphogenetic Protein Signaling Pathway. *J. Mol. Biol.* **2007**, *374*, 777–790. [[CrossRef](#)]
267. Schisler, J.C.; Patterson, C.; Willis, M.S. Skeletal Muscle Mitochondrial Alterations in Carboxyl Terminus of HSC70 Interacting Protein (CHIP)^{-/-} Mice. *Afr. J. Cell. Pathol.* **2016**, *6*, 28–36.
268. Chen, N.; Balasenthil, S.; Reuther, J.; Frayna, A.; Wang, Y.; Chandler, D.S.; Abruzzo, L.V.; Rashid, A.; Rodriguez, J.; Lozano, G.; et al. DEAR1 is a chromosome 1p35 tumor suppressor and master regulator of TGF- β -driven epithelial-mesenchymal transition. *Cancer Discov.* **2013**, *3*, 1172–1189. [[CrossRef](#)]
269. Schmidt, F.; Kny, M.; Zhu, X.; Wollersheim, T.; Persicke, K.; Langhans, C.; Lodka, D.; Kleber, C.; Weber-Carstens, S.; Fielitz, J. The E3 ubiquitin ligase TRIM62 and inflammation-induced skeletal muscle atrophy. *Crit. Care* **2014**, *18*, 1–12. [[CrossRef](#)]
270. He, B.; Tang, R.H.; Weisleder, N.; Xiao, B.; Yuan, Z.; Cai, C.; Zhu, H.; Lin, P.; Qiao, C.; Li, J.; et al. Enhancing muscle membrane repair by gene delivery of MG53 ameliorates muscular dystrophy and heart failure in δ -sarcoglycan-deficient hamsters. *Mol. Ther.* **2012**, *20*, 727–735. [[CrossRef](#)]
271. Gushchina, L.V.; Bhattacharya, S.; McElhanon, K.E.; Choi, J.H.; Manring, H.; Beck, E.X.; Alloush, J.; Weisleder, N. Treatment with Recombinant Human MG53 Protein Increases Membrane Integrity in a Mouse Model of Limb Girdle Muscular Dystrophy 2B. *Mol. Ther.* **2017**, *25*, 2360–2371. [[CrossRef](#)]
272. Cao, C.M.; Zhang, Y.; Weisleder, N.; Ferrante, C.; Wang, X.; Lv, F.; Zhang, Y.; Song, R.; Hwang, M.; Jin, L.; et al. MG53 constitutes a primary determinant of cardiac ischemic preconditioning. *Circulation* **2010**, *121*, 2565–2574. [[CrossRef](#)]
273. Gonçalves, D.A.P.; Silveira, W.A.; Lira, E.C.; Graça, F.A.; Paula-Gomes, S.; Zanon, N.M.; Kettelhut, I.C.; Navegantes, L.C.C. Clenbuterol suppresses proteasomal and lysosomal proteolysis and atrophy-related genes in denervated rat soleus muscles independently of Akt. *Am. J. Physiol.-Endocrinol. Metab.* **2012**, *302*, E123–E133. [[CrossRef](#)] [[PubMed](#)]
274. Subramaniam, K.; Fallon, K.; Ruut, T.; Lane, D.; McKay, R.; Shadbolt, B.; Ang, S.; Cook, M.; Platten, J.; Pavli, P.; et al. Infliximab reverses inflammatory muscle wasting (sarcopenia) in Crohn's disease. *Aliment. Pharmacol. Ther.* **2015**, *41*, 419–428. [[CrossRef](#)] [[PubMed](#)]
275. Yakabe, M.; Ogawa, S.; Ota, H.; Iijima, K.; Eto, M.; Ouchi, Y.; Akishita, M. Inhibition of interleukin-6 decreases atrogenes expression and ameliorates tail suspension-induced skeletal muscle atrophy. *PLoS ONE* **2018**, *13*, e0191318. [[CrossRef](#)]
276. Salazar-Degracia, A.; Busquets, S.; Argilés, J.M.; Bargalló-Gispert, N.; López-Soriano, F.J.; Barreiro, E. Effects of the beta2 agonist formoterol on atrophy signaling, autophagy, and muscle phenotype in respiratory and limb muscles of rats with cancer-induced cachexia. *Biochimie* **2018**, *149*, 79–91. [[CrossRef](#)] [[PubMed](#)]
277. Martín, A.I.; Gómez-SanMiguel, A.B.; Priego, T.; López-Calderón, A. Formoterol treatment prevents the effects of endotoxin on muscle TNF/NF- κ B, Akt/mTOR, and proteolytic pathways in a rat model. Role of IGF-I and miRNA 29b. *Am. J. Physiol.-Endocrinol. Metab.* **2018**, *315*, E705–E714. [[CrossRef](#)] [[PubMed](#)]
278. Yue, L.; Talukder, M.A.H.; Gurjar, A.; Lee, J.I.; Noble, M.; Dirksen, R.T.; Chakkalakal, J.; Elfar, J.C. 4-Aminopyridine attenuates muscle atrophy after sciatic nerve crush injury in mice. *Muscle Nerve* **2019**, *60*, 192–201. [[CrossRef](#)]
279. Wang, H.; Lai, Y.-J.; Chan, Y.-L.; Li, T.-L.; Wu, C.-J. Epigallocatechin-3-gallate effectively attenuates skeletal muscle atrophy caused by cancer cachexia. *Cancer Lett.* **2011**, *305*, 40–49. [[CrossRef](#)] [[PubMed](#)]
280. Pötsch, M.S.; Tschirner, A.; Palus, S.; Haehling, S.; von Doehner, W.; Beadle, J.; Coats, A.J.S.; Anker, S.D.; Springer, J. The anabolic catabolic transforming agent (ACTA) espidolol increases muscle mass and decreases fat mass in old rats. *J. Cachexia Sarcopenia Muscle* **2014**, *5*, 149–158. [[CrossRef](#)]

281. Gómez-SanMiguel, A.B.; Gomez-Moreira, C.; Nieto-Bona, M.P.; Fernández-Galaz, C.; Villanúa, M.Á.; Martín, A.I.; López-Calderón, A. Formoterol decreases muscle wasting as well as inflammation in the rat model of rheumatoid arthritis. *Am. J. Physiol.-Endocrinol. Metab.* **2016**, *310*, E925–E937. [[CrossRef](#)]
282. Noh, K.K.; Chung, K.W.; Choi, Y.J.; Park, M.H.; Jang, E.J.; Park, C.H.; Yoon, C.; Kim, N.D.; Kim, M.K.; Chung, H.Y. β -Hydroxy β -Methylbutyrate Improves Dexamethasone-Induced Muscle Atrophy by Modulating the Muscle Degradation Pathway in SD Rat. *PLoS ONE* **2014**, *9*, e102947. [[CrossRef](#)] [[PubMed](#)]
283. Baptista, I.L.; Leal, M.L.; Artioli, G.G.; Aoki, M.S.; Fiamoncini, J.; Turri, A.O.; Curi, R.; Miyabara, E.H.; Moriscot, A.S. Leucine attenuates skeletal muscle wasting via inhibition of ubiquitin ligases. *Muscle Nerve* **2010**, *41*, 800–808. [[CrossRef](#)] [[PubMed](#)]
284. Chen, L.; Chen, L.; Wan, L.; Huo, Y.; Huang, J.; Li, J.; Lu, J.; Xin, B.; Yang, Q.; Guo, C. Matrine improves skeletal muscle atrophy by inhibiting E3 ubiquitin ligases and activating the Akt/mTOR/FoxO3 α signaling pathway in C2C12 myotubes and mice. *Oncol. Rep.* **2019**, *42*, 479–494. [[CrossRef](#)] [[PubMed](#)]
285. Qiu, J.; Fang, Q.; Xu, T.; Wu, C.; Xu, L.; Wang, L.; Yang, X.; Yu, S.; Zhang, Q.; Ding, F.; et al. Mechanistic role of reactive oxygen species and therapeutic potential of antioxidants in denervation-or fasting-induced skeletal muscle atrophy. *Front. Physiol.* **2018**, *9*, 215. [[CrossRef](#)]
286. Ryu, Y.; Lee, D.; Jung, S.H.; Lee, K.-J.; Jin, H.; Kim, S.J.; Lee, H.M.; Kim, B.; Won, K.-J. Sabinene Prevents Skeletal Muscle Atrophy by Inhibiting the MAPK-MuRF-1 Pathway in Rats. *Int. J. Mol. Sci.* **2019**, *20*, 4955. [[CrossRef](#)]
287. Powers, S.K.; Hudson, M.B.; Nelson, W.B.; Talbert, E.E.; Min, K.; Szeto, H.H.; Kavazis, A.N.; Smuder, A.J. Mitochondria-targeted antioxidants protect against mechanical ventilation-induced diaphragm weakness. *Crit. Care Med.* **2011**, *39*, 1749–1759. [[CrossRef](#)]
288. Guillory, B.; Chen, J.; Patel, S.; Luo, J.; Splenser, A.; Mody, A.; Ding, M.; Baghaie, S.; Anderson, B.; Iankova, B.; et al. Deletion of ghrelin prevents aging-associated obesity and muscle dysfunction without affecting longevity. *Aging Cell.* **2017**, *16*, 859–869. [[CrossRef](#)]
289. Hsieh, S.K.; Lin, H.Y.; Chen, C.J.; Jhuo, C.F.; Liao, K.Y.; Chen, W.Y.; Tzen, J.T.C. Promotion of myotube differentiation and attenuation of muscle atrophy in murine C2C12 myoblast cells treated with teaghrelin. *Chem. Biol. Interact.* **2020**, *315*, 108893. [[CrossRef](#)]
290. Wu, C.-S.; Wei, Q.; Wang, H.; Kim, D.M.; Balderas, M.; Wu, G.; Lawler, J.; Safe, S.; Guo, S.; Devaraj, S.; et al. Protective Effects of Ghrelin on Fasting-Induced Muscle Atrophy in Aging Mice. *J. Gerontol. A Biol. Sci. Med. Sci.* **2020**, *75*, 621–630. [[CrossRef](#)]
291. Servais, S.; Letexier, D.; Favier, R.; Duchamp, C.; Desplanches, D. Prevention of unloading-induced atrophy by vitamin E supplementation: Links between oxidative stress and soleus muscle proteolysis? *Free Radic. Biol. Med.* **2007**, *42*, 627–635. [[CrossRef](#)]
292. Belova, S.P.; Mochalova, E.P.; Kostrominova, T.Y.; Shenkman, B.S.; Nemirovskaya, T.L. P38 α -MAPK Signaling Inhibition Attenuates Soleus Atrophy during Early Stages of Muscle Unloading. *Int. J. Mol. Sci.* **2020**, *21*, 2756. [[CrossRef](#)]
293. Bowen, T.S.; Adams, V.; Werner, S.; Fischer, T.; Vinke, P.; Brogger, M.; Mangner, N.; Linke, A.; Sehr, P.; Lewis, J.; et al. Small-molecule inhibition of MuRF1 attenuates skeletal muscle atrophy and dysfunction in cardiac cachexia: Inhibition of MuRF1 prevents skeletal muscle wasting. *J. Cachexia Sarcopenia Muscle* **2017**, *8*, 939–953. [[CrossRef](#)] [[PubMed](#)]
294. Eddins, M.J.; Marblestone, J.G.; Suresh Kumar, K.G.; Leach, C.A.; Sterner, D.E.; Mattern, M.R.; Nicholson, B. Targeting the ubiquitin E3 ligase MuRF1 to inhibit muscle atrophy. *Cell Biochem. Biophys.* **2011**, *60*, 113–118. [[CrossRef](#)] [[PubMed](#)]
295. Yuasa, K.; Okubo, K.; Yoda, M.; Otsu, K.; Ishii, Y.; Nakamura, M.; Itoh, Y.; Horiuchi, K. Targeted ablation of p38 α MAPK suppresses denervation-induced muscle atrophy. *Sci. Rep.* **2018**, *8*, 1–9. [[CrossRef](#)]
296. Tricarico, D.; Selvaggi, M.; Passantino, G.; De Palo, P.; Dario, C.; Centoducati, P.; Tateo, A.; Curci, A.; Maquod, F.; Mele, A.; et al. ATP Sensitive Potassium Channels in the Skeletal Muscle Function: Involvement of the KCNJ11(Kir6.2) Gene in the Determination of Mechanical Warner Bratzer Shear Force. *Front. Physiol.* **2016**, *7*, 167. [[CrossRef](#)] [[PubMed](#)]
297. Chavez, J.D.; Tang, X.; Campbell, M.D.; Reyes, G.; Kramer, P.A.; Stuppard, R.; Keller, A.; Zhang, H.; Rabinovitch, P.S.; Marcinek, D.J.; et al. Mitochondrial protein interaction landscape of SS-31. *Proc. Natl. Acad. Sci. USA* **2020**, *117*, 15363–15373. [[CrossRef](#)]
298. Rittig, N.; Bach, E.; Thomsen, H.H.; Møller, A.B.; Hansen, J.; Johannsen, M.; Jensen, E.; Serena, A.; Jørgensen, J.O.; Richelsen, B.; et al. Anabolic effects of leucine-rich whey protein, carbohydrate, and soy protein with and without β -hydroxy- β -methylbutyrate (HMB) during fasting-induced catabolism: A human randomized crossover trial. *Clin. Nutr.* **2017**, *36*, 697–705. [[CrossRef](#)]
299. Girón, M.D.; Vilchez, J.D.; Salto, R.; Manzano, M.; Sevillano, N.; Campos, N.; Argilés, J.M.; Rueda, R.; López-Pedrosa, J.M. Conversion of leucine to β -hydroxy- β -methylbutyrate by α -keto isocaproate dioxygenase is required for a potent stimulation of protein synthesis in L6 rat myotubes. *J. Cachexia Sarcopenia Muscle* **2016**, *7*, 68–78. [[CrossRef](#)]
300. Baptista, I.L.; Silvestre, J.G.; Silva, W.J.; Labeit, S.; Moriscot, A.S. FoxO3a suppression and VPS34 activity are essential to anti-atrophic effects of leucine in skeletal muscle. *Cell Tissue Res.* **2017**, *369*, 381–394. [[CrossRef](#)]
301. van den Hoek, A.M.; Zondag, G.C.M.; Verschuren, L.; de Ruiter, C.; Attema, J.; de Wit, E.C.; Schwerk, A.M.K.; Guigas, B.; Lek, S.; Rietman, A.; et al. A novel nutritional supplement prevents muscle loss and accelerates muscle mass recovery in caloric-restricted mice. *Metabolism* **2019**, *97*, 57–67. [[CrossRef](#)]
302. Balasubramaniam, A.; Joshi, R.; Su, C.; Friend, L.A.; Sheriff, S.; Kagan, R.J.; James, J.H. Ghrelin inhibits skeletal muscle protein breakdown in rats with thermal injury through normalizing elevated expression of E3 ubiquitin ligases MuRF1 and MAFbx. *Am. J. Physiol.-Regul. Integr. Comp. Physiol.* **2009**, *296*, R893–R901. [[CrossRef](#)]

-
303. Clarke, B.A.; Drujan, D.; Willis, M.S.; Murphy, L.O.; Corpina, R.A.; Burova, E.; Rakhilin, S.V.; Stitt, T.N.; Patterson, C.; Latres, E.; et al. The E3 Ligase MuRF1 Degrades Myosin Heavy Chain Protein in Dexamethasone-Treated Skeletal Muscle. *Cell Metab.* **2007**, *6*, 376–385. [[CrossRef](#)]
304. Ochi, A.; Abe, T.; Nakao, R.; Yamamoto, Y.; Kitahata, K.; Takagi, M.; Hirasaka, K.; Ohno, A.; Teshima-Kondo, S.; Taesik, G.; et al. N-myristoylated ubiquitin ligase Cbl-b inhibitor prevents on glucocorticoid-induced atrophy in mouse skeletal muscle. *Arch. Biochem. Biophys.* **2015**, *570*, 23–31. [[CrossRef](#)]


10.5 Paper

RESEARCH

Open Access



Specific shifts in the endocannabinoid system in hibernating brown bears

Christian Boyer¹, Laura Cussonneau¹, Charlotte Brun², Christiane Deval¹, Jean-Paul Pais de Barros³, Stéphanie Chanon⁴, Nathalie Bernoud-Hubac⁴, Patricia Daira⁴, Alina L. Evans⁵, Jon M. Arnemo^{5,6}, Jon E. Swenson⁷, Guillemette Gauquelin-Koch⁸, Chantal Simon⁴, Stéphane Blanc², Lydie Combaret¹, Fabrice Bertile^{2†} and Etienne Lefai^{1*†} 

Abstract

In small hibernators, global downregulation of the endocannabinoid system (ECS), which is involved in modulating neuronal signaling, feeding behavior, energy metabolism, and circannual rhythms, has been reported to possibly drive physiological adaptation to the hibernating state. In hibernating brown bears (*Ursus arctos*), we hypothesized that beyond an overall suppression of the ECS, seasonal shift in endocannabinoids compounds could be linked to bear's peculiar features that include hibernation without arousal episodes and capacity to react to external disturbance. We explored circulating lipids in serum and the ECS in plasma and metabolically active tissues in free-ranging subadult Scandinavian brown bears when both active and hibernating. In winter bear serum, in addition to a 2-fold increase in total fatty acid concentration, we found significant changes in relative proportions of circulating fatty acids, such as a 2-fold increase in docosahexaenoic acid C22:6 n-3 and a decrease in arachidonic acid C20:4 n-6. In adipose and muscle tissues of hibernating bears, we found significant lower concentrations of 2-arachidonoylglycerol (2-AG), a major ligand of cannabinoid receptors 1 (CB1) and 2 (CB2). Lower mRNA level for genes encoding CB1 and CB2 were also found in winter muscle and adipose tissue, respectively. The observed reduction in ECS tone may promote fatty acid mobilization from body fat stores, and favor carbohydrate metabolism in skeletal muscle of hibernating bears. Additionally, high circulating level of the endocannabinoid-like compound N-oleoylethanolamide (OEA) in winter could favor lipolysis and fatty acid oxidation in peripheral tissues. We also speculated on a role of OEA in the conservation of an anorexigenic signal and in the maintenance of torpor during hibernation, while sustaining the capacity of bears to sense stimuli from the environment.

Keywords: Hibernation, Brown bear, Metabolism, Lipidomic, Docosahexaenoic acid, Endocannabinoid system, Cannabinoid receptor 1, Cannabinoid receptor 2, 2-arachidonoylglycerol, Anandamide, N-oleoylethanolamide

Background

To deal with seasonal cold and food shortage during winter, hibernating mammals show a combination of behavioral and physiological changes. To save energy during hibernation, hibernating animals use periods of torpor characterized by decreased metabolic rate and body

temperature, reduction in respiratory and heart rates, and physical inactivity [1, 2]. Brown bears (*Ursus arctos*) exhibit unique features, as they hibernate at mild hypothermia (32–35 °C) and can stay inside their dens for up to 7 months, without drinking, eating, defecating or urinating, and with no arousal episodes [3–6]. While denning, they reduce their metabolic rate by about 75% [7], and rely primarily on mobilization of fat stores, which is reflected by increased circulating fatty acid concentration and body fat store depletion during winter [8–10].

* Correspondence: etienne.lefai@inrae.fr

†Fabrice Bertile and Etienne Lefai contributed equally to this work.

¹Université Clermont Auvergne, INRAE, UNH, Clermont-Ferrand, France

Full list of author information is available at the end of the article



© The Author(s). 2020 **Open Access** This article is licensed under a Creative Commons Attribution 4.0 International License, which permits use, sharing, adaptation, distribution and reproduction in any medium or format, as long as you give appropriate credit to the original author(s) and the source, provide a link to the Creative Commons licence, and indicate if changes were made. The images or other third party material in this article are included in the article's Creative Commons licence, unless indicated otherwise in a credit line to the material. If material is not included in the article's Creative Commons licence and your intended use is not permitted by statutory regulation or exceeds the permitted use, you will need to obtain permission directly from the copyright holder. To view a copy of this licence, visit <http://creativecommons.org/licenses/by/4.0/>. The Creative Commons Public Domain Dedication waiver (<http://creativecommons.org/publicdomain/zero/1.0/>) applies to the data made available in this article, unless otherwise stated in a credit line to the data.

Beyond energy substrates, lipids also have pleiotropic actions in the regulation of metabolism, and changes in membrane fatty acid composition have already been described in hibernating animals [11–14], including the brown bear [9]. Membrane phospholipids can also provide long-chain fatty acids for the synthesis of bioactive lipid mediators, such as endocannabinoids [15–17]. The endocannabinoid system (ECS) was originally described as being composed of G-protein coupled receptors (CB1 and CB2) and their endogenous ligands, of which the main ones are derived from arachidonic acid 20:4n-6 (AA) esterified into phospholipids, and called 2-arachidonoyl glycerol (2-AG) and anandamide (AEA) [15–20]. These two well-characterized compounds clearly show varying affinity for CB1 and CB2 receptors. Indeed, AEA is considered as a high affinity CB1-partial agonist (and weak CB2 agonist), whereas 2-AG is described as a low-to-moderate affinity CB1 and CB2 full agonist [21, 22]. 2-AG and AEA belong to the large family of 2-acylglycerols (2-AcGs) and N-acylethanolamines (NAEs), respectively [17, 19]. N-acylphosphatidylethanolamine-hydrolyzing phospholipase D (NAPEPLD) and sn-1-specific diacylglycerol lipase- α and β (DAGLA and DAGLB) are the main enzymes involved in the biosynthesis of NAEs and 2-AcGs, respectively [17, 19]. Fatty acid amide hydrolase (FAAH) is responsible for NAEs catabolism (and to a lesser extent for 2-AG) [23], and monoacylglycerol lipase (MGLL) specifically catabolizes 2-AcGs [17, 19]. eCBs can also be metabolized by lipoxygenases (LOXs) and by cyclooxygenase-2 (COX-2), an alternative pathway for eCBs catabolism [17].

The ECS includes structurally related compounds like N-oleylethanolamine (OEA), called «endocannabinoids-like compounds» (eCBs-like). The latter are metabolized by the same biosynthetic and catabolic enzymes as eCBs [17]. Although eCBs-like compounds are not able to bind to CB1 and CB2 receptors, they can bind to other G-protein coupled receptors (e.g. GPR119 and GPR55) or nuclear receptors, like peroxisome proliferator-activated receptor α (PPARA) [17].

Endogenous cannabinoids are involved in the regulation of many physiological processes, including neuronal signaling [24], stress response [25], metabolism [25–27], feeding behavior and energy storage [25, 28]. Evidences support the fact that the ECS could be involved in sleep cycles [29], circadian and potentially circannual rhythms [30]. At the central level (e.g. hypothalamus), CB1 is able to promote food intake and reduce energy expenditure [25, 31]. In addition, CB1 activation in adipose tissue leads to fatty acid and glucose uptake, and to upregulation of lipogenesis [25]. In liver, CB1 signaling leads to increased expression of genes involved in the synthesis of fatty acids [32], and in skeletal muscle tissue, CB1 activation triggers a decrease in glucose uptake and insulin sensitivity [25]. The CB2 receptor is well known to be widespread over immune cells and

to have numerous immunomodulatory roles [33]. CB2 has also been detected in metabolic tissues, like adipose tissue and skeletal muscle [34, 35] and CB2 pharmacological or genetic inactivation in murine obesity models promote insulin-mediated glucose uptake in skeletal muscles, reduce adipose tissue inflammation, and thus improves insulin sensitivity [36, 37]. Finally, the eCB-like OEA promotes lipolysis, fatty acid oxidation in skeletal muscle and liver, and triggers an anorexigenic signal, notably through the nuclear receptor PPARA [38, 39]. Considering the pleiotropic roles of ECS in neuronal signaling, regulation of feeding behavior, energy metabolism and circannual rhythms, important changes are expected during hibernation. Several ECS circulating compounds have been quantified in hibernating black bears, during and around the torpor phase [40], with no major changes observed except a slight increase in 2-AG in the period of metabolic drop before torpor. Although a decrease in ECS tone has been observed in hibernating marmots (*Marmota monax and flaviventris*) and ground squirrels (*Spermophilus richardsonii*) [30, 41, 42], we hypothesize that a similar decrease should occur in hibernating bears, not excluding specific changes due to their unique features during hibernation (mild hypothermia, no periodic arousal, and maintenance of alertness). Therefore, we explored here seasonal variations in fatty acid composition and ECS tone, in both circulating compartment and in muscle and adipose tissues, in winter-hibernating and summer-active brown bears.

Results

Seasonal differences in serum lipids

We explored the fatty acid (FA) composition of winter-hibernating (WBS) and summer-active (SBS) bear serum (see supplementary Table S1). From the lipidomic data, we compared both the summer and winter concentrations and proportions of fatty acids (see supplementary Table S2 and S3 for detailed lipidomic results). As shown in Fig. 1a, the total concentration of FAs was about twofold higher in WBS relative to SBS (28.82 ± 1.71 vs. 15.99 ± 1.09 mmol/L). All but two quantified lipid species were higher in concentration in hibernating bears, i.e. saturated fatty acids (SFAs), monounsaturated fatty acids (MUFAs), and n-6 polyunsaturated fatty acids (PUFAs) (Supplementary Table S2). Only concentrations of alpha-linolenic acid C18:3 n-3 (ALA) (0.49 -fold, non-significant) and eicosa-pentaenoic acid C20:5 n-3 (EPA) (0.26-fold) were lower in WBS (Supplementary Table S2).

Meanwhile, the molar percent of total n-6 species were found to be lower in WBS compared to SBS (Fig. 1b). Lipid species with the highest molar percent are presented in Fig. 1c (see Supplementary Table S3). Among SFAs, palmitic acid C16:0 (PA) was found in higher proportion, whereas stearic acid C18:0 (SA) was in lower proportion in winter serum. Similar proportions of oleic acid 18:1n-9 (OA),

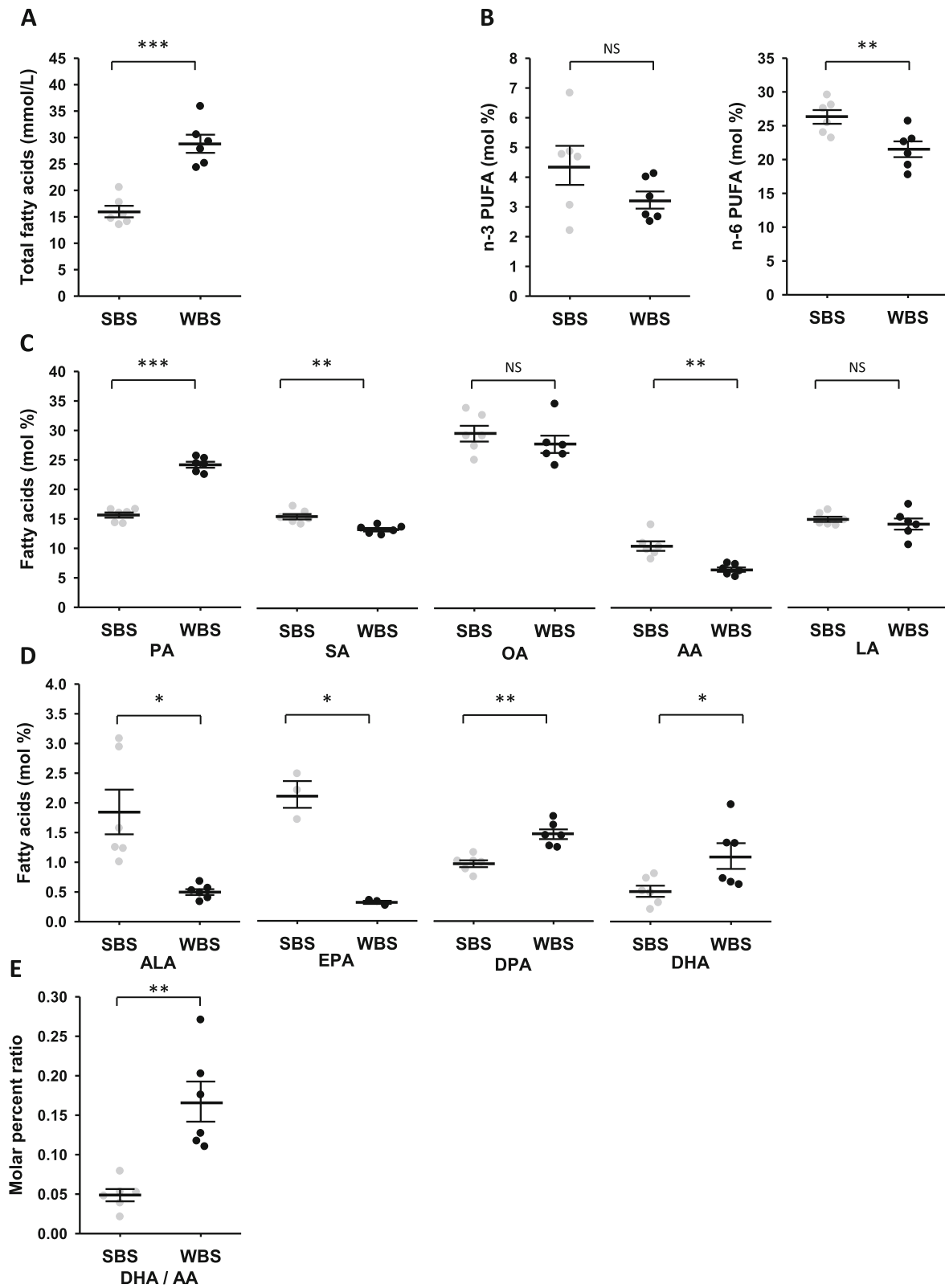


Fig. 1 (See legend on next page.)

(See figure on previous page.)

Fig. 1 Lipidomic from summer and winter brown bear serum. The winter and summer bear serum mixes were prepared as described (Supplementary Table S1). **a:** Total fatty acid (FA) concentration. **b:** Total n-6 and n-3 FA relative proportions of total lipids. **c:** Highest molar percent lipid species D: Molar percent of the n-3 family lipid species. **e:** Molar ratios of DHA/AA in summer and winter serum. Detailed lipidomic results are presented in Supplementary Tables S2 and S3. Data are expressed in mmol/L for total FAs concentration, or molar percentage of total lipids and are represented as mean \pm SEM of separate extractions and quantifications from the twelve mixes (six summer and six winter serum mixes, except for EPA with data from only three summer and three winter mixes). Paired Student t-test were used to compare wummer and winter data and Benjamini-Hochberg correction was applied for multiple comparisons. * indicates BH adjusted p value < 0.05 when comparing seasons, ** for $p < 0.01$, *** for $p < 0.001$, NS: non significant. AA: arachidonic acid, ALA: alpha-linolenic acid, DHA: docosahexaenoic acid, DPA: docosapentaenoic acid, EPA: eicosapentaenoic acid, LA: linoleic acid, OA: oleic acid, PA: palmitic acid, SA: stearic acid, SBS: summer bear serum, WBS: winter bear serum

belonging to the n-9 MUFAs, were found in winter and summer bear serum. Concerning n-6 PUFAs, the proportion of arachidonic acid C20:4 n-6 (AA) was lower during winter, whereas proportion of linoleic acid C18:2 n-6 (LA) remained unchanged (Fig. 1c). For individual species of the n-3 family (Fig. 1d and Supplementary Table S3), docosapentaenoic acid C22:5 n-3 (DPA, 1.5-fold) and docosahexaenoic acid C22:6 n-3 (DHA, 2.2-fold) were found in higher proportions.

The proportion of C20:5 n-3 (EPA) was found much lower (0.15-fold) in winter serum, as well as the alpha-linolenic acid C18:3 n-3 (ALA, 0.27-fold), a precursor of the EPA, DPA and DHA species.

From molar percent values, the DHA/AA ratio was 3.2-fold higher in winter (Fig. 1e).

Changes in plasma endocannabinoids and endocannabinoids-like compounds

We next assessed circulating eCBs and eCBs-like in bear plasma. Paired samples were collected in winter and in summer from eight bears (Supplementary Table S1) and quantification of AEA, 2-AG and OEA are presented in Fig. 2 and supplementary Table S5. Lower concentrations were observed for AEA (0.63-fold) in winter compared to summer, whereas the reverse was observed for OEA (3.3-fold). No difference was found for 2-AG plasma concentration.

Changes in endocannabinoid concentrations in muscle and adipose tissues

Quantification of endocannabinoids was then performed in bear muscle and adipose tissues. Paired tissues samples were collected from bears in winter and in summer (Supplementary Table S1) and quantification of AEA, 2-AG and OEA are presented in Fig. 3 and supplementary Table S5. AEA concentration was lower in both muscle and adipose tissues during winter versus summer, close to the statistical threshold ($p = 0.064$ and $p = 0.069$, respectively). 2-AG concentration was significantly lower in muscle and adipose tissues samples during winter, by about 1.6- and 9-fold, respectively. By contrast, no seasonal changes were found in OEA concentrations in both muscle and adipose tissues.

Changes in endocannabinoid pathway-related gene expressions in muscle and adipose tissues

To explore tissue metabolism of endocannabinoids, we quantified gene expression in muscle and adipose tissue of the eCBs membrane receptors CB1 and CB2, and several enzymes involved in the synthesis and catabolism of eCBs. For muscle tissue, paired samples were from 8 bears at the two time points, while for adipose tissue, data are coming from 5 bears in summer and 13 bears

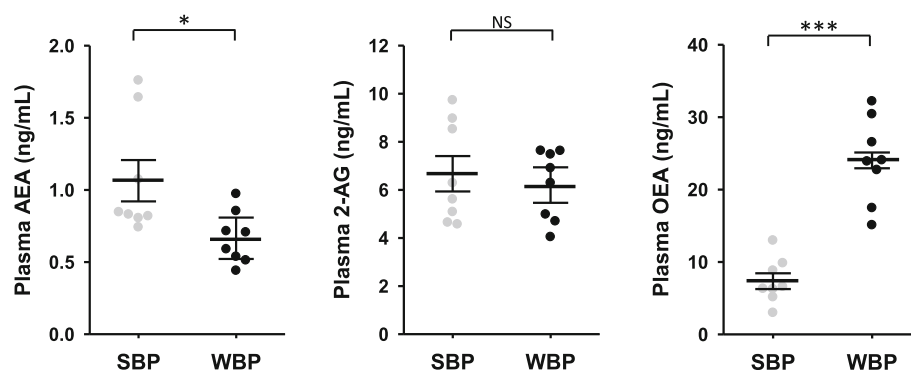
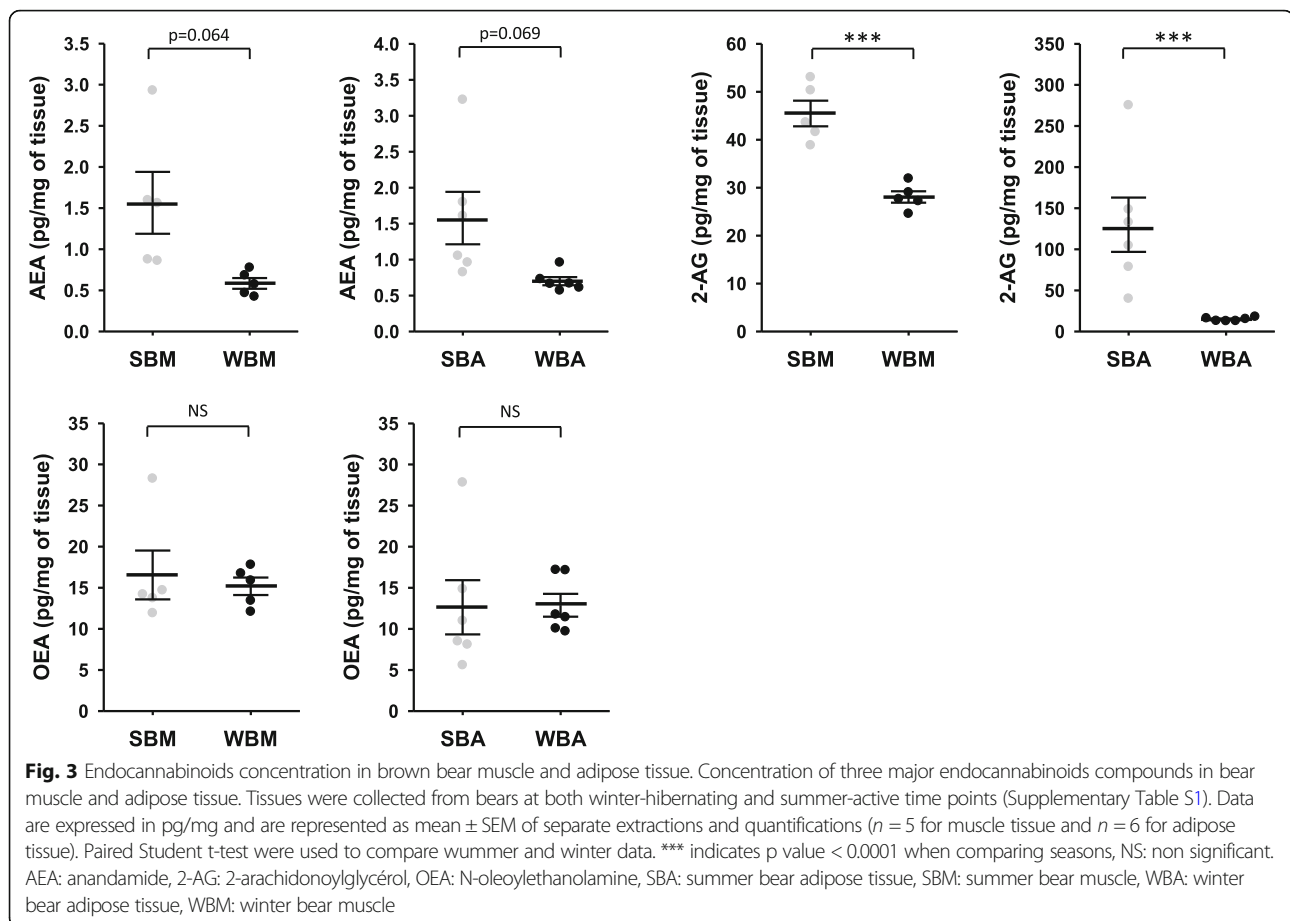


Fig. 2 Circulating endocannabinoids concentration in brown bear plasma. Concentration of three major endocannabinoids compounds in bear plasma. Plasma were collected from bears at both winter-hibernating and summer-active time points (Supplementary Table S1). Data are expressed in ng/mL and are represented as mean \pm SEM of separate extractions and quantifications ($n = 8$). Paired Student t-test were used to compare wummer and winter data. * indicates p value < 0.05 when comparing seasons, *** for $p < 0.001$, NS: non significant. AEA: anandamide, 2-AG: 2-arachidonoylglycérol, eCBs: endocannabinoids, OEA: N-oleoylethanolamine, SBP: summer bear plasma, WBP: winter bear plasma



in winter (Supplementary Table S1). Data are presented in Fig. 4 and Supplementary Table S5.

For genes that encode the membrane receptors CB1 and CB2 in muscle tissue, CNR1 mRNA level, but not CNR2, was decreased (0.63-fold) in winter (Fig. 4). Concerning enzymes that catabolize AEA and 2-AG, mRNA level of FAAH was induced (2.3-fold) in winter, but MGLL gene expression did not change. For genes encoding enzymes of the biosynthetic pathway, DAGLA mRNA level was strongly reduced in muscle tissue during winter (0.40-fold), whereas DAGLB mRNA level was increased (1.53-fold). Finally, gene expression of NAPEPLD did not change in muscle (Fig. 4).

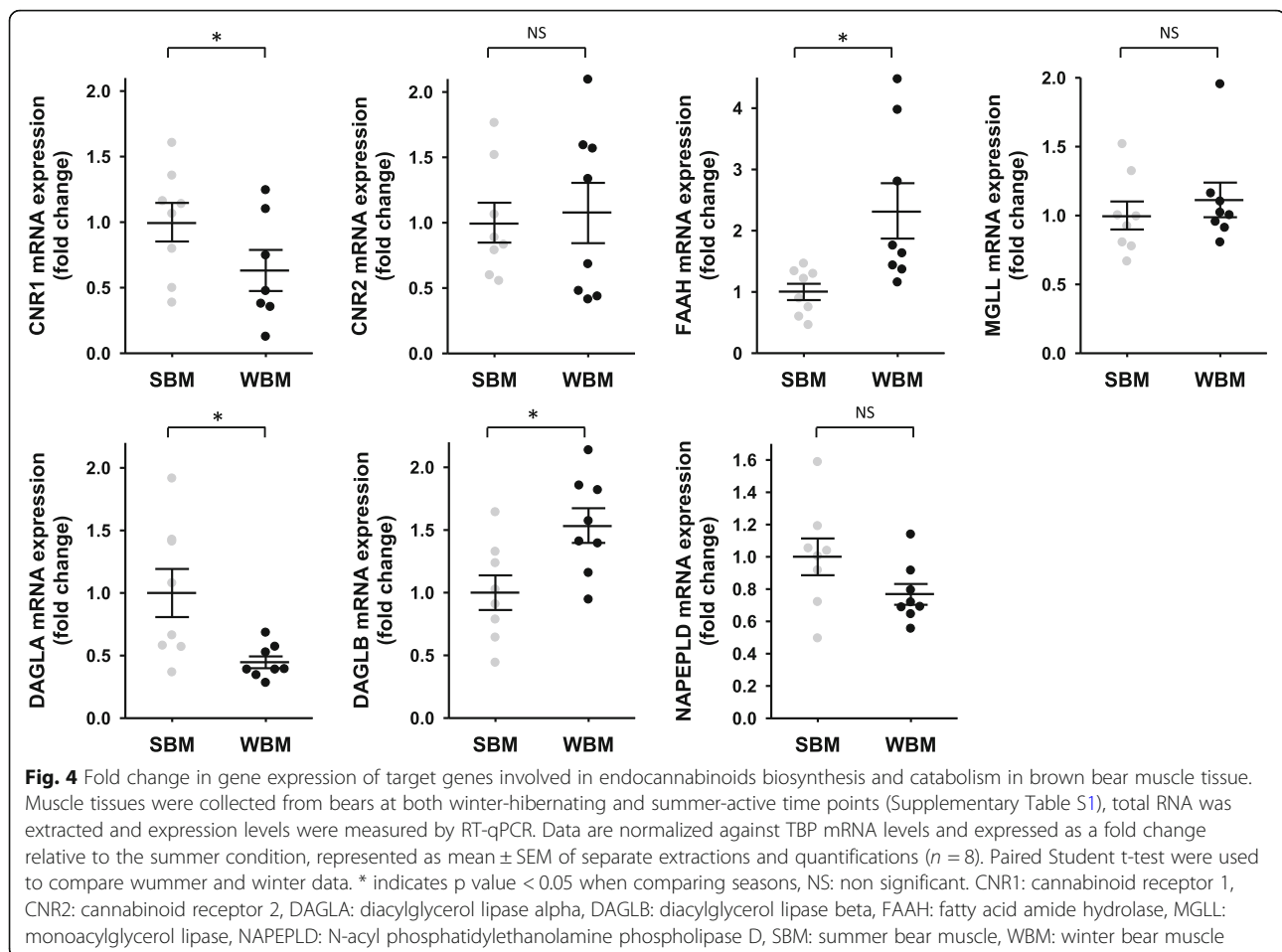
Conversely, in adipose tissue (Fig. 5), no significant changes in CNR1 gene expression were reported whereas CNR2 expression was strongly decreased in winter (0.42-fold). For gene expression of catabolic enzymes (FAAH and MGLL), did not change in adipose tissue between seasons. Finally, for genes encoding biosynthetic enzymes, mRNA levels of DAGLB and NAPELD were respectively found higher (1.44-fold) and lower (0.75-fold) in winter.

Discussion

Thanks to repeated capture sessions, we were able to gather samples of serum, plasma and tissues from high number of

free-living brown bears (*Ursus arctos*). From the 28 bears included in this study, samples were collected both in February during winter hibernation and in June during summer active period. Due to limited amount of available biological material, the analyses were performed on samples coming from different subsets of the 28 bears. In all but adipose tissue, analyses were performed on winter and summer paired samples (Supplementary Table S1). We examined circulating lipid and ECS compounds in both summer-active and winter-hibernating brown bears to explore the extent to which regulation of the ECS reflects bear hibernation peculiarities, including survival due to lipid oxidation, maintenance of muscle glycolysis, and maintained alertness during dormancy. The seasonal shift we highlighted in serum FAS composition, together with a decrease in tissue AEA and 2-AG, and a three-fold increase in circulating OEA during winter, could contribute to the behavioral and metabolic changes that occur in hibernating bears.

Hibernators experience extended periods of food shortage during hibernation and primarily rely on mobilization of fat stores from white adipose tissue [1]. Accordingly, we found that the concentration of total circulating fatty acids was elevated in hibernating bears, a finding in line with previous studies [5, 43]. Considering both the amount and

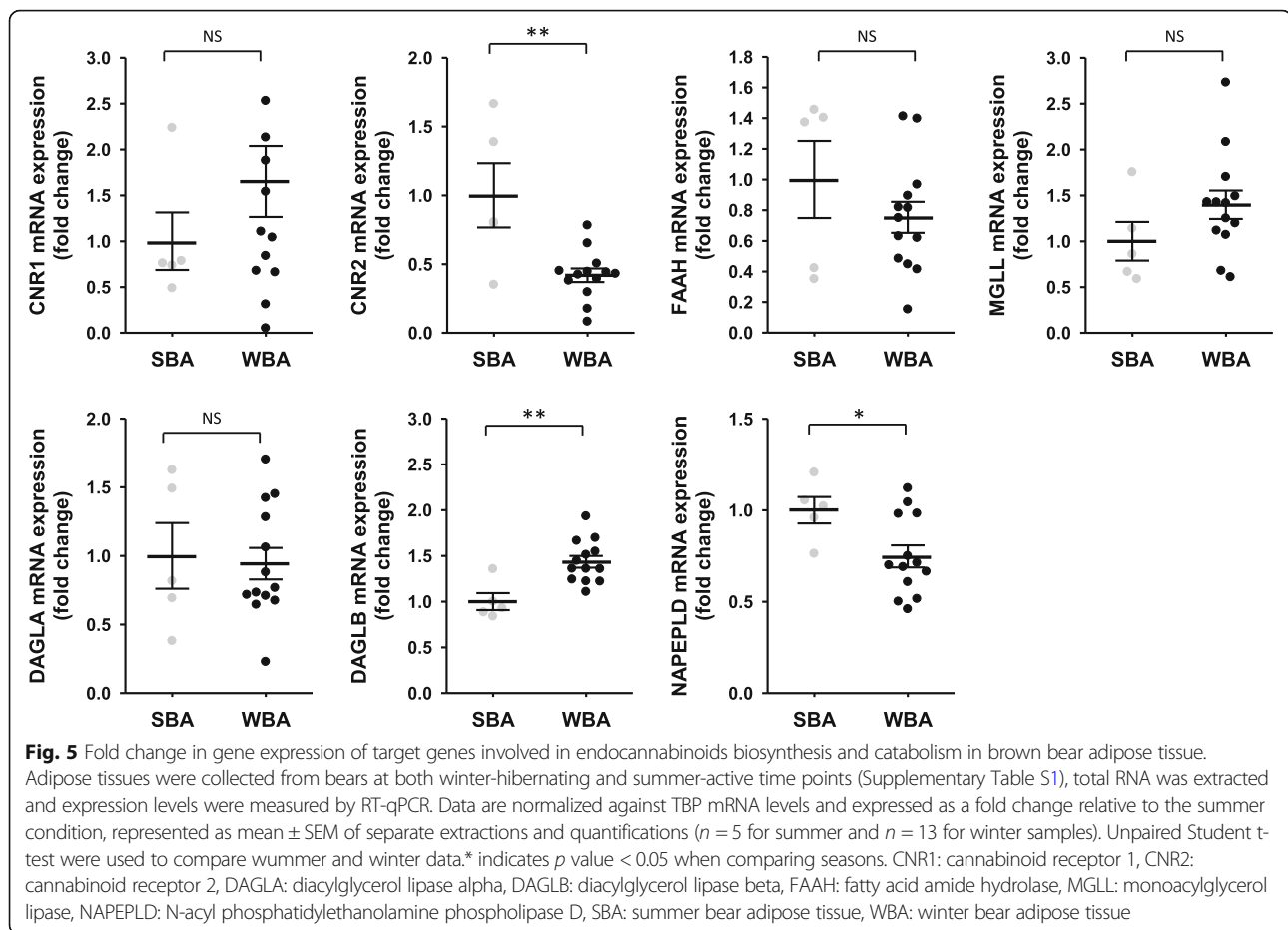


relative proportions of circulating lipids, our results are consistent with changes in serum and plasma lipid profiles during hibernation that have been previously published [5, 9, 10], notably an enrichment in DHA C22:6 n-3 and depletions in ALA C18:3 n-3 and EPA C20:5 n-3, during winter compared to summer. Whether the depletion in the ALA and EPA precursor species could be directly linked to the observed DHA increase remains to be elucidated.

Here, the DHA serum enrichment that we observed in hibernating bears is actually not coming from dietary FAs intake but rather due to lipid stores mobilization. The health benefits that have been attributed to n-3 PUFAs (e.g. DHA), essentially triggered by DHA dietary intervention studies, could potentially be transposed in the context of hibernation. Indeed, it has already been hypothesized that DHA could be involved in the bear's resistance to muscle atrophy during hibernation [10]. DHA appears to prevent muscle atrophy in fasting mice, and increases muscle glycogen stores [44]. Strikingly, in parallel to DHA serum enrichment, hibernating bears have more than a 3-fold higher glycogen muscle content compared to summer-active animals [10]. In addition to its anti-inflammatory effects, DHA

is also known to exert a positive effect on protein balance by decreasing expression of factors involved in protein breakdown [45] and enhancing protein synthesis, notably by promoting mammalian Target Of Rapamycin (mTOR) activation [46].

Concomitantly to serum DHA enrichment, we observed a drop in AA proportion, thus leading to a sharp increase in the DHA/AA ratio. Omega-3/omega-6 ratio is known to have an impact on global health [47], and the balance of this ratio could also impact the endocannabinoid system [48], notably because AA is a precursor of the two main eCBs 2-AG and AEA. Indeed, n-6 PUFAs-enriched diets have been shown to increase the level of 2-AG or AEA in the brain, plasma, and peripheral tissues in non-hibernating animal models [49–52]. It is noteworthy to mention that, in response to DHA supplementation, an enrichment of this fatty acid in phospholipids of cell membranes occurs in parallel with a decrease in AA content [38, 49, 53, 54]. By remodeling the amount of AA-containing phospholipids, DHA is able to reduce the synthesis of AEA and 2-AG [49, 54]. Further studies on bears, focusing on fatty acid membrane composition in tissues at different time points, will be helpful to characterize the



remodeling of membrane lipids that could affect the availability of FAs precursors for eCBs biosynthesis. Data on eCBs compounds from experimental short fasting in non-hibernating mammals are very divergent, depending on the tissue considered (e.g. brain or peripheral tissues) and the duration of food deprivation, but tissue levels of eCBs are mainly regulated by the availability of their membrane phospholipid precursors and by the activity of biosynthetic and catabolic enzymes [28, 49, 55, 56].

We hypothesized that drastic reduction in metabolic activity, lack of intake of dietary PUFAs, significant increase in the serum DHA/AA ratio, and perhaps reduction in tissue AA-phospholipids concentration, could lead to a global reduction in ECS tone during the hibernation period. The reduction in ECS tone has already been documented in hibernating marmots [30, 41], but not confirmed in large-bodied hibernators.

Comparing active and hibernation states in brown bears, we reported here a decrease in plasma concentration of AEA, and an unexpected 3-fold increase in OEA circulating levels in hibernating bears. In both muscle and adipose tissues, 2-AG and AEA (close to statistical threshold) were found lower in winter, while OEA did not change. Quantification of winter serum eCBs was

previously reported in black bears during and around the topor phase, but summer active bears were not investigated [40]. Nutritional status of the captured animals and diet were not specified. These elements strongly limit comparison between the two studies.

Taken together, our data allowed us to make several hypotheses about possible mechanisms by which ECS could contribute to the metabolic and behavioral changes that occur in bears during hibernation. First, considering that AEA and 2-AG CB1 agonists favor food intake and stimulate lipogenesis [25], CB1 signaling is expected to be upregulated during the active summer period in order to promote energy storage, and downregulated during winter hibernation to stimulate lipolysis and FAs oxidation. The tissue concentration drops in 2-AG and AEA observed during winter could be due to a decrease in tissue AA-phospholipids concentration, as we hypothesized above. The degradation of AEA could also be increased in muscle tissue during hibernation, as reflected in the higher mRNA levels of FAAH, the main hydrolase that degrades AEA [19, 23]. In adipose tissue, lower NAPEPLD mRNA level content during hibernation may support a decrease in AEA synthesis, and ultimately content. The tissue content in 2-AG is decreased in winter with no changes in mRNA levels

of the catabolic enzyme MGLL. Furthermore, opposite changes in DAGLA and DAGLB gene expression do not allow to speculate on the biosynthetic/degradation balance. One limitation of our study is that gene expression could not reflect biological activity. Moreover, we only focused on main biosynthetic and catabolic enzymes involved in eCBs metabolism, and investigation on alternative degradation route as endocannabinoid oxygenation by cyclooxygenases and lipoxygenases would bring new insights.

During hibernation, lower 2-AG (and AEA close to statistical threshold) tissue content and the reduction of CNR1 and CNR2 mRNA levels in muscle and adipose tissue, respectively, strongly support reduced ECS tone in both tissues. In non-hibernating mammals, pharmacological inhibition of CB1 leads to a decrease in PDK4 expression [25, 57]. PDK4 is a major negative regulator of PDH activity, that in turn regulates the whole body oxidative carbohydrate metabolism. In hibernating bear muscle, recent studies have shown that PDK4 is upregulated compared to summer active state [10, 58] and expression of PDK4 during hibernation appear thus to be disconnected from direct regulation by CB1. CB1 receptor antagonism also leads to an increased uptake of glucose in muscle via PI3K signaling [59], and glycolysis appears preserved in bear skeletal muscle during hibernation, as suggested by an overall increase in the protein abundance of all glycolytic enzymes [10]. As proposed by Chazarin et al. and Vella et al., bears still oxidize glucose and produce lactate in skeletal muscle during hibernation [10, 60].

Overactivation of the ECS is a hallmark of obesity [61, 62], and 2-AG is predominantly found in higher concentration in tissues of obese people [61, 63]. Interestingly, in murine models of obesity, gain of adipose tissue often leads to increased fat inflammation [36, 37]. Genetic or pharmacological inactivation of CB2 receptor contribute to reduce adipose tissue inflammation, increase insulin sensitivity and skeletal muscle glucose uptake [36, 37]. Strikingly, insulin resistance has been described in hibernating bears adipocytes [64]. As bears don't experience health consequences of circannual high body fat storage [65], a reduced CB2 signaling in adipose tissue could dampen adipose tissue inflammation. Lower amounts of 2-AG and AEA could also reduced CB1 signaling in adipose tissue, thus limiting lipogenesis and promoting lipolysis during hibernation in bears, as also suggested for hibernating marmots [30].

OEA is a high-affinity agonist for peroxisome proliferator-activated receptor α (PPARA), regulating food intake and stimulating fat catabolism [38, 39, 53, 66, 67]. The eCB-like OEA is generally synthesized in response to dietary oleic acid intake by enterocytes of the small intestine [49, 54], and inhibits food intake. It has already been shown in rodents that food deprivation inhibits OEA synthesis in the small intestine, but stimulates its synthesis in

liver [38, 53, 68, 69]. Therefore, during bear hibernation, circulating OEA could originate from tissue synthesis (probably hepatic) and be released in the blood flow. The high OEA level that we found in hibernating bears, not triggered by food intake, could participate in a sustained anorexigenic signal during the hibernation state.

Consequences of high levels of circulating OEA have been studied in non-hibernating rodents. Intraperitoneal OEA administration in rats notably impairs locomotor activity, which is supported by a decrease in ambulation, an increase of the time spent in inactivity, and the presence of signs of catalepsy [66, 70]. We thus can hypothesize that a higher amount of plasma OEA during bear hibernation can participate in the maintenance of prolonged physical inactivity. It has also been shown that intracerebroventricular injections of OEA promote alertness, with the observation of enhanced dopamine and c-Fos expressions in wake-related brain areas [71]. Bears are known to stay sensitive to disturbance during hibernation [72–74]. High circulating amounts of OEA might thus participate in alertness to external stimuli from the environment in hibernating bears. OEA during winter possibly also favors body fat mobilization for energy needs, with stimulation of FA and glycerol release from adipocytes [38, 39]. Finally, a potential role for OEA in the promotion of fasting-induced ketogenesis during hibernation could also be considered, as OEA has been demonstrated to increase 3-hydroxybutyrate production in in vivo rodent models [38, 39].

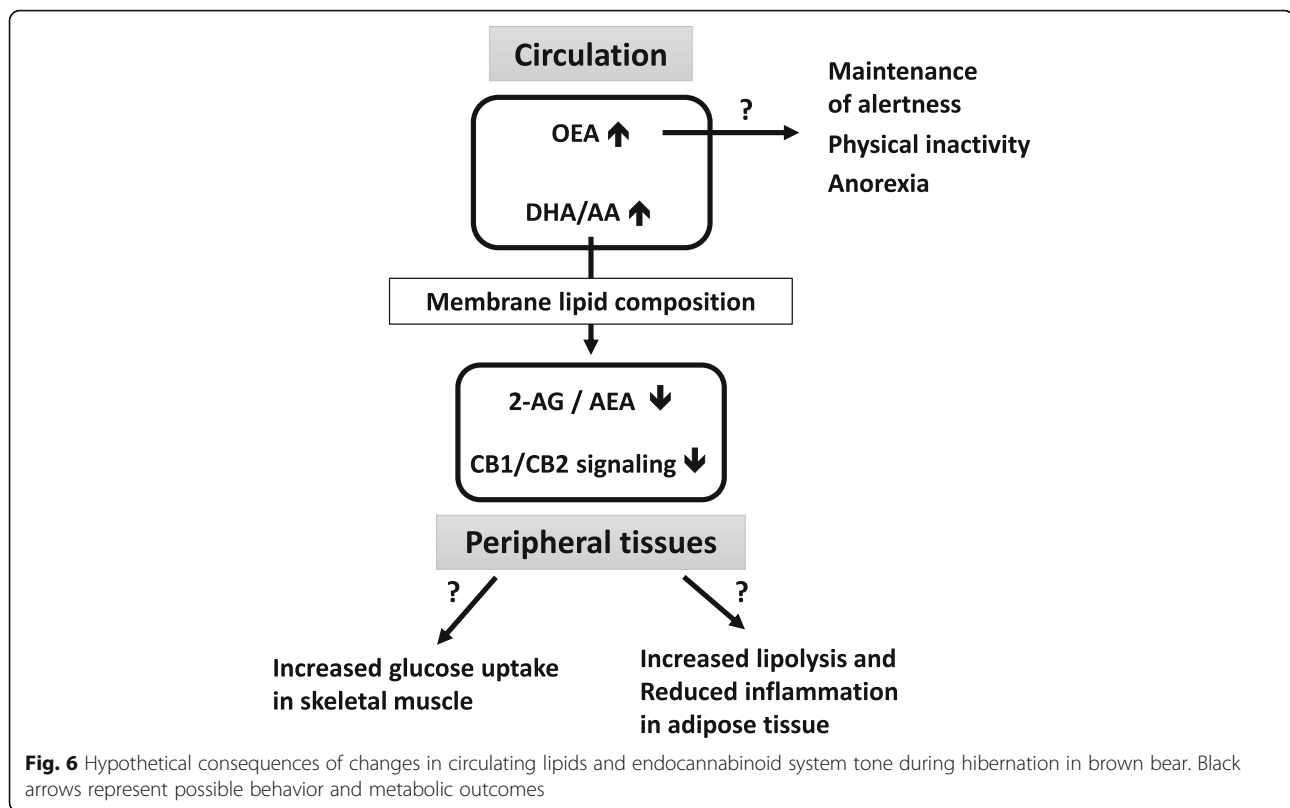
Conclusions

In conclusion, our results show a reduction in ECS tone in hibernating bears and suggest a coordinated downregulation of CB1 and CB2 signaling in skeletal muscle and adipose tissue. As summarized in Fig. 6, these features could favor energy mobilization through lipolysis, and optimization of glucose uptake by skeletal muscles. Despite high fat stores in winter, bears do not exhibit features of ECS overactivation, and decrease in CB2 signaling could dampen adipose tissue inflammation. The observed increase in circulating OEA level may participate in the behavioral and physiological adaptations during bear hibernation state, like maintenance of an anorexigenic signaling pathway, and promotion of lipolysis and fatty acid β -oxidation. We also speculated about OEA involvement in torpor maintenance and in motor activity reduction, as well as a role in conservation of alertness at the level of central nervous system.

Methods

Bear sample collection

A total of 28 free ranging subadult brown bears (*Ursus arctos*) from Dalarna and Gävleborg counties, Sweden, were included in this study, including 4 bears captured two consecutive years. All samples and data were collected



under protocols approved by the Swedish Ethical Committee on Animal Experiment (applications Dnr C3/2016 and Dnr C18/2015), the Swedish Environmental Protection Agency (NV-00741-18), and the Swedish Board of Agriculture (Dnr 5.2.18–3060/17). All procedures complied with Swedish laws and regulations.

As described previously [10, 75], blood, subcutaneous adipose tissue, and muscle tissue (vastus lateralis) samples were collected at two time points, in February during winter hibernation (W) and in June during summer-active period (S). Blood samples were collected from the jugular vein into 8 ml dry tubes for serum (Vacuette® Z serum Sep Clot Activator, Greiner Bio-One GmbH, Kremsmünster, Austria) or into 10 ml EDTA-coated tubes (BD Vacutainer®, FisherScientific, Illkirch, France) for plasma.

The analyses were performed on samples coming from different subsets of bears as described in Supplementary Table S1.

Lipid extraction and analysis

To perform serum lipidomic analysis, serum mixes were prepared as followed: for a given year, 50 µl of summer serum from each bear of the year was pooled to obtain the summer mix. In parallel, 50 µl of winter serum from the same bears was pooled to obtain the winter mix. A total of 6 summer and winter paired mixes were obtained (Supplementary Table S1). Lipids were extracted and analyzed

as previously described [76]. After addition of an internal standard (tri-17:0 triacylglycerol), total lipids were extracted twice from bear serum mixes with ethanol/chloroform (1:2, v/v). The organic phases were dried under nitrogen and lipids were transmethylated. Briefly, samples were treated with toluene-methanol (1:1, v/v) and boron trifluoride in methanol (14%). Transmethylation was carried out at 100 °C for 90 min in screw-capped tubes. Then 1.5 mL K₂CO₃ in 10% water was added and the resulting fatty acid methyl esters were extracted by 2 mL of isooctane and analyzed by gas chromatography (GC) with a HP6890 instrument equipped with a fused silica capillary BPX70 SGE column (60 × 0.25 mm). The vector gas was hydrogen. Temperatures of the Ross injector and the flame ionization detector were set to 230 °C and 250 °C, respectively. Data were expressed in mmol/L for total or individual fatty acids (FAs) concentration or molar percentage of total lipids for individual FAs. Detailed lipidomic results are presented in supplementary Table S2 (serum fatty acid concentrations) and S3 (serum fatty acid relative proportions).

Endocannabinoid quantification

For quantification of circulating endocannabinoids, analysis was performed on 500 µl of plasma collected at the two time points (S and W) from 8 individual animals (see supplementary Table S1). Standard endocannabinoids

(eCBs), i.e.- PEA, PEA-d5, OEA, OEA-d4, AEA, AEA-d4, 2AG, and 2AG-d5, were purchased from Cayman (Bertin BioReagent, Saint-Quentin en Yvelines, France). Mass spectrometry quality grade solvents were purchased from Fischer Scientific (Illkirch, France). Tissue samples (adipose and muscle tissues); c.a 100 mg) were crushed in an Omni Bead Ruptor 24 apparatus (Omni International, Kennesaw, USA) with circa twenty 1.4 mm OD zirconium oxide beads ($S = 6.95$ m/s, $T = 30$ s, $C = 3$; $D = 10$ s) and 900 μ l of methanol/Tris-buffer (50 mM, pH = 8) 1/1 containing 20 ng of PEA-d5, 2 ng OEA-d4, 10 ng AEA-d4, and 20 ng 2AG-d5. Then, each homogenate was added with 2 mL of $\text{CHCl}_3/\text{MeOH}$ (1:1, v/v) and 500 μ L of Tris (50 mM, pH = 8), vortexed and centrifuged 10 min at 3000 g. The organic layer was recovered and the upper aqueous phase was extracted twice with chloroform (1 mL). Finally, organic phases were pooled and evaporated under vacuum.

Plasma (500 μ L) were mixed with 500 μ L cold methanol containing 11 ng AEA. After protein precipitation at -20°C for 2 h, endocannabinoids were extracted with methanol/chloroform (1:1, v/v) (5 ml) and saline (1.25 mL). The organic phase was recovered and the aqueous phase was extracted twice with chloroform (3 mL). Organic phases were finally pooled and evaporated under vacuum.

Dried extracts were solubilized with methanol (200 μ L) and centrifuged for 5 min at 20,000 g. Four microliters of the supernatant were injected into a 1200 LC system coupled to a 6460-QqQ MS/MS system equipped with an ESI source (Agilent technologies). Separation was achieved on Zorbax SB-C18 2.1×50 mm, 1.8 μ m column (Agilent technologies) at a flow rate of 0.4 mL/min, 40°C , with a linear gradient of (solvent A) water containing 0.1% formic acid and (solvent B) methanol containing 0.1% formic acid as follows: 10% of B for 1 min, up to 85% of B in 8 min, and then 100% B for 4.5 min. Acquisition was performed in positive Selected Reaction Monitoring (SRM) mode (source temperature: 350°C , nebulizer gas flow rate: 10 L/min, 40 psi, sheath gas flow 10 L/min, sheath gas temperature 350°C , capillary 4000 V, nozzle 1000 V).

Transitions used were: 2AG-d5 384.3 \rightarrow 91.1 (frag 120 V, CE 62 V), 2AG 379.1 \rightarrow 91 (frag 120 V, CE 62 V), AEA-d4 352.2 \rightarrow 66.1 (frag 115 V, CE 14 V), AEA 348.2 \rightarrow 62 (frag 120 V, CE 14 V), OEA-d4 330.2 \rightarrow 66.1 (frag 120 V, CE 14 V), OEA 326.2 \rightarrow 62 (frag 115 V, CE 14 V), PEA-d5 305.2 \rightarrow 62 (frag 124 V, CE 14 V), and PEA 300.2 \rightarrow 62 (frag 124 V, CE 14 V).

Endocannabinoids quantification in tissues was performed on tissue samples collected at the two time points (S and W) from 5 (muscle tissue) and 6 (adipose tissue) bears (Supplementary Table S1). eCBs from tissues were quantitated according to the isotope dilution method. Results are expressed as pg per mg of wet weight of tissue. eCBs from plasma were quantitated using calibration curves obtained with authentic standards extracted by the

same method used for plasma samples. Linear regression was applied for calculations. Results are expressed as ng of endocannabinoid per mL of plasma.

Quantification of mRNAs by real-time RT-PCR

For mRNA quantification using RT-qPCR, total RNAs were obtained from muscle and adipose tissues collected at the two time points (S and W). For the muscle tissue, RNAs were extracted from 8 bears in summer and winter, while for adipose tissue, RNAs were extracted from 5 bears in summer and 13 bears in winter (Supplementary Table S1).

Muscle and adipose tissue total RNA was isolated using the TRIzol reagent (Invitrogen, Courtaboeuf, France) according to the manufacturer's instructions. First-strand cDNAs were synthesized from 1 μ g of total RNA using the PrimeScript RT kit (Ozyme, saint Quentin en Yveline, France) with a mixture of random hexamers and oligo(dT) primers, and treated with 60 units of RnaseH (Ozyme). Real-time PCR assays were performed with Rotor-Gene 6000 (Qiagen, Courtaboeuf, France). The primers and real-time PCR assay conditions are listed in supplementary Table S4. The results were normalized by using TBP (TATA box binding protein) mRNA concentration, measured as reference gene in each sample.

Statistical analysis

Statistical analysis was performed using the R software environment v3.0.2 [77]. For each set of values, distribution of the data was tested using the Shapiro-Wilk normality test, and using the $p = 0.01$ threshold normal distribution was considered in all cases. Differences between summer and winter data were tested using paired Student t-test for lipidomic, endocannabinoid quantification in plasma and tissues, and mRNA level in muscle tissue. For mRNA level in adipose tissue, differences between summer and winter data were tested using unpaired Student t-test. For multiple comparison (lipidomic data), the Benjamini-Hochberg correction using the p.adjust function (Package *stats* version 4.0.0 of R studio) was applied. Data are presented as means \pm SEM and individual values are plotted as grey and black dots for respectively summer and winter values. Means, SEM, fold change and associated p -values are reported in supplementary Tables S2 to S5. Statistical significance was considered with p values or adjusted p values lower than 0.05.

Supplementary Information

The online version contains supplementary material available at <https://doi.org/10.1186/s12983-020-00380-y>.

Additional file 1 Table S1. Characteristics of brown bears included in the study. **Table S2.** Serum fatty acid concentrations (mmol/L) in winter hibernating (WBS) and summer active (SBS) bears. **Table S3.** Serum fatty acid relative proportions (mol %) in winter hibernating (WBS) and summer active (SBS) bears. **Table S4.** List of primers used for RT-qPCR.

Table S5: Endocannabinoids (eCBs) and mRNA quantification in plasma and tissues in winter hibernating (W) and summer active (S) bears.**Abbreviations**

AA: Arachidonic acid; 2-AcG: 2-acylglycerol; AEA: Anandamide; 2-AG: 2-arachidonoylglycerol; ALA: Alpha-linolenic acid; AMPK: AMP-activated protein kinase; CNR1: Cannabinoid receptor 1 (gene); CB1: Cannabinoid receptor 1; CNR2: Cannabinoid receptor 2 (gene); CB2: Cannabinoid receptor 2; DAGLA: Diacylglycerol lipase α ; DAGLB: Diacylglycerol lipase β ; DPA: Docosapentaenoic acid; DHA: Docosahexaenoic acid; eCB: Endocannabinoid; eCB-like: Endocannabinoid-like compound; ECS: Endocannabinoid system; EPA: Eicosapentaenoic acid; FA: Fatty acid; FAAH: Fatty acid amide hydrolase; GPR55: G protein-coupled receptor 55; GPR119: G protein-coupled receptor 119; LA: Linoleic acid; MGLL: Monoacylglycerol lipase; mTOR: Mammalian target of rapamycin; MUFA: Monounsaturated fatty acid; NAE: N-acyl-phosphatidylethanolamine; NAPEPLD: N-acyl-phosphatidylethanolamine-hydrolyzing phospholipase D; OA: Oleic acid; OEA: N-oleoylethanolamide; PA: Palmitic acid; PDH: Pyruvate dehydrogenase; PDK4: Pyruvate dehydrogenase kinase 4; PPARA: Peroxisome proliferator-activated receptor α ; PUFA: Polyunsaturated fatty acid; SA: Stearic acid; SBA: Summer bear adipose tissue; SBM: Summer bear muscle; SBP: Summer bear plasma; SBS: Summer bear serum; SFA: Saturated fatty acid; WBA: Winter bear adipose tissue; WBM: Winter bear muscle; WBP: Winter bear plasma; WBS: Winter bear serum

Acknowledgments

The authors wish to thank the field capture team (D Ahlqvist, A Friebe, H Nordin, H Blomgren, S Persson), and are grateful to H el ene Choubley and Victoria Bergas from the lipidomic platform of the university of Bourgogne-Franche-Comt e for their valuable technical assistance. This is scientific paper no. 296 from the SBBRP.

Authors' contributions

EL, and FB conceived the study; CBo, CBr, LCu, CD, JPB, IC, NBH, PD, AE, JMA, SB, EL, and FB performed the experiments and analyzed the data; CBr, FB and EL wrote the original draft; LCo, GG-K, CS, JS, FB, and EL reviewed and edited the manuscript. All authors read and approved the final manuscript.

Funding

This work was supported by the French Space Agency (CNES), iSITE Challenge 3 Mobility program (UCA), CNRS and Strasbourg University (H2E project; MyoBears project of the PEPS ExoMod program), French Proteomic Infrastructure (ProFI; ANR-10-INBS-08-03, and MetaHUB (French infrastructure in metabolomics & fluxomics; ANR-11-INBS-0010). CBo was supported by a grant from the MESRI, LCu by grants from the INRAE and Clermont M etropole and CBr by a grant from French space agency (CNES). The long-term funding of Scandinavian Brown Bear Research Project (SBBRP) has come primarily from the Swedish Environmental Protection Agency, the Norwegian Environment Agency, the Austrian Science Fund, and the Swedish Association for Hunting and Wildlife Management.

Availability of data and materials

The datasets generated during and/or analyzed during the current study available from the corresponding author on reasonable request.

Ethics approval

All samples and data were collected under protocols approved by the Swedish Ethical Committee on Animal Experiment (applications Dnr C3/2016 and Dnr C18/2015), the Swedish Environmental Protection Agency (NV-00741-18), and the Swedish Board of Agriculture (Dnr 5.2.18-3060/17). All procedures complied with Swedish laws and regulations.

Competing interests

The authors declare no competing interests.

Author details

¹Universit e Clermont Auvergne, INRAE, UNH, Clermont-Ferrand, France.

²Universit e de Strasbourg, CNRS, IPHC UMR 7178, Strasbourg, France.

³Plateforme de Lipidomique, INSERM UMR1231, Universit e de Bourgogne, Dijon, France. ⁴Universit e de Lyon, INSERM, INRAE, INSA, Functional Lipidomic

Platform, Lyon, France. ⁵Department of Forestry and Wildlife Management, Inland Norway University of Applied Sciences, Campus Evenstad, NO-2480 Koppang, Norway. ⁶Department of Wildlife, Fish, and Environmental Studies, Swedish University of Agricultural Sciences, SE-901 83 Ume a, Sweden. ⁷Faculty of Environmental Sciences and Natural Resource Management, Norwegian University of Life Sciences, NO-1432  s, Norway. ⁸Centre National d'Etudes Spatiales, CNES, F-75001 Paris, France.

Received: 16 May 2020 Accepted: 20 October 2020

Published online: 23 November 2020

References

- Carey HV, Andrews MT, Martin SL. Mammalian hibernation: cellular and molecular responses to depressed metabolism and low temperature. *Physiol Rev.* 2003;83:1153–81.
- Geiser F. Hibernation. *Curr Biol.* 2013;23:R188–93.
- Folk GE, Hunt JM, Folk MA. Further evidence for hibernation of bears. *Bears Their Biol Manag.* 1980;4:43.
- Hellgren EC. Physiology of hibernation in bears. *Ursus.* 1998;10:467–77.
- Hissa R, Hohtola E, Tuomala-Saramaki T, Laine T, Kallio H. Seasonal changes in fatty acids and leptin contents in the plasma of the European brown bear (*Ursus arctos arctos*). *Ann Zool Fenn.* 1998;35:215–24.
- Manchi S, Swenson JE. Denning behaviour of Scandinavian brown bears *Ursus arctos*. *Wildl Biol.* 2005;11:123–32.
- Toien O, Blake J, Edgar DM, Grahn DA, Heller HC, Barnes BM. Hibernation in black bears: independence of metabolic suppression from body temperature. *Science.* 2011;331:906–9.
- LeBlanc PJ, Obbard M, Battersby BJ, Felskie AK, Brown L, Wright PA, et al. Correlations of plasma lipid metabolites with hibernation and lactation in wild black bears *Ursus americanus*. *J Comp Physiol B.* 2001;171:327–34.
- Giroud S, Chery I, Bertile F, Bertrand-Michel J, Tascher G, Gauquelin-Koch G, et al. Lipidomics reveal seasonal shifts in large-bodied hibernator, the brown bear. *Front Physiol.* 2019;10:389.
- Chazarin B, Storey KB, Ziemianin A, Chanon S, Plumel M, Chery I, et al. Metabolic reprogramming involving glycolysis in the hibernating brown bear skeletal muscle. *Front Zool.* 2019;16:12.
- Aloia RC, Raison JK. Membrane function in mammalian hibernation. *Biochim Biophys Acta BBA - Rev Biomembr.* 1989;988:123–46.
- Munro D, Thomas DW. The role of polyunsaturated fatty acids in the expression of torpor by mammals: a review. *Zool Jena.* 2004;107:29–48.
- Ruf T, Arnold W. Effects of polyunsaturated fatty acids on hibernation and torpor: a review and hypothesis. *Am J Physiol-Regul Integr comp Physiol.* American Physiological Society. 2008;294:R1044–52.
- Arnold W, Ruf T, Frey-Roos F, Bruns U. Diet-Independent Remodeling of Cellular Membranes Precedes Seasonally Changing Body Temperature in a Hibernator. *PLOS ONE. Public Libr Sci.* 2011;6:e18641.
- Battista N, Di Tommaso M, Bari M, Maccarrone M. The endocannabinoid system: an overview. *Front Behav Neurosci.* 2012;14:6–9.
- De Petrocellis L, Di Marzo V. An introduction to the endocannabinoid system: from the early to the latest concepts. *Best Pract Res Clin Endocrinol Metab.* 2009;23:1–15.
- Fezza F, Bari M, Florio R, Talamonti E, Feole M, Maccarrone M. Endocannabinoids, related compounds and their metabolic routes. *Mol Basel Switz.* 2014;19:17078–106.
- Aizpurua-Olaizola O, Elezgarai I, Rico-Barrio I, Zarandona I, Etxebarria N, Usobiaga A. Targeting the endocannabinoid system: future therapeutic strategies. *Drug Discov Today.* 2017;22:105–10.
- Di Marzo V. New approaches and challenges to targeting the endocannabinoid system. *Nat Rev Drug Discov.* 2018;17:623–39.
- Ligresti A, Petrosino S, Di Marzo V. From endocannabinoid profiling to 'endocannabinoid therapeutics'. *Curr Opin Chem Biol.* 2009;13:321–331.
- Zou S, Kumar U. Cannabinoid receptors and the Endocannabinoid system: signaling and function in the central nervous system. *Int J Mol Sci.* 2018;19:833.
- Di Marzo V, De Petrocellis L. Why do cannabinoid receptors have more than one endogenous ligand? *Philos Trans R Soc B Biol Sci.* 2012;367:3216–28.
- Di Marzo V, Maccarrone M. FAAH and anandamide: is 2-AG really the odd one out? *Trends Pharmacol Sci.* 2008;29:229–33.
- Wilson RI, Nicoll RA. Endocannabinoid signaling in the brain. *Science.* 2002;296:678–82.
- Piazza PV, Cota D, Marsicano G. The CB1 receptor as the cornerstone of exostasis. *Neuron.* 2017;93:1252–74.

26. Shrestha N, Cuffe JSM, Hutchinson DS, Headrick JP, Perkins AV, McAinch AJ, et al. Peripheral modulation of the endocannabinoid system in metabolic disease. *Drug Discov Today*. 2018;23:592–604.
27. Silvestri C, Di Marzo V. The Endocannabinoid system in energy homeostasis and the Etiopathology of metabolic disorders. *Cell Metab*. 2013;17:475–90.
28. Matias I, Bisogno T, Marzo VD. Endogenous cannabinoids in the brain and peripheral tissues: regulation of their levels and control of food intake. *Int J Obes Nature Publishing Group*. 2006;30:57–12.
29. Prospéro-García O, Amancio-Belmont O, Becerril Meléndez AL, Ruiz-Contreras AE, Méndez-Díaz M. Endocannabinoids and sleep. *Neurosci Biobehav Rev*. 2016;71:671–9.
30. Vaughn LK, Denning G, Stuhr KL, de Wit H, Hill MN, Hillard CJ. Endocannabinoid signalling: has it got rhythm? *Br J Pharmacol*. 2010;160:530–43.
31. Cardinal P, Bellocchio L, Clark S, Cannich A, Klugmann M, Lutz B, et al. Hypothalamic CB1 cannabinoid receptors regulate energy balance in mice. *Endocrinology*. 2012;153:4136–43.
32. Osei-Hyiaman D, DePetrillo M, Pachec P, Liu J, Radaeva S, Bátkai S, et al. Endocannabinoid activation at hepatic CB1 receptors stimulates fatty acid synthesis and contributes to diet-induced obesity. *J Clin Invest*. 2005;115:1298–305.
33. Turcotte C, Blanchet M-R, Laviolette M, Flamand N. The CB2 receptor and its role as a regulator of inflammation. *Cell Mol Life Sci*. 2016;73:4449–70.
34. Cavuoto P, McAinch AJ, Hatzinikolas G, Janovská A, Game P, Wittert GA. The expression of receptors for endocannabinoids in human and rodent skeletal muscle. *Biochem Biophys Res Commun*. 2007;364:105–10.
35. Starowicz KM, Cristino L, Matias I, Capasso R, Racioppi A, Izzo AA, et al. Endocannabinoid Dysregulation in the pancreas and adipose tissue of mice fed with a high-fat diet. *Obesity*. 2008;16:553–65.
36. Agudo J, Martin M, Roca C, Molas M, Bura AS, Zimmer A, et al. Deficiency of CB2 cannabinoid receptor in mice improves insulin sensitivity but increases food intake and obesity with age. *Diabetologia*. 2010;53:2629–40.
37. Deveaux V, Cadoudal T, Ichigotani Y, Teixeira-Clerc F, Louvet A, Manin S, et al. Cannabinoid CB2 Receptor Potentiates Obesity-Associated Inflammation, Insulin Resistance and Hepatic Steatosis. *PLOS ONE*. *Public Libr Sci*. 2009;4:e5844.
38. Bowen KJ, Kris-Etherton PM, Shearer GC, West SG, Reddivari L, Jones PJH. Oleic acid-derived oleoylethanolamide: a nutritional science perspective. *Prog Lipid Res*. 2017;67:1–15.
39. Guzmán M, Verme JL, Fu J, Oveisi F, Blázquez C, Piomelli D. Oleoylethanolamide stimulates lipolysis by activating the nuclear receptor peroxisome proliferator-activated receptor α (PPAR- α). *J Biol Chem*. 2004;279:27849–54.
40. Kirkwood JS, Broeckling CD, Donahue S, Prenni JE. A novel microflow LC-MS method for the quantitation of endocannabinoids in serum. *J Chromatogr B Analyt Technol Biomed Life Sci*. 2016;1033–1034:271–7.
41. Mulawa EA, Kirkwood JS, Wolfe LM, Wojda SJ, Prenni JE, Florant GL, et al. Seasonal changes in Endocannabinoid concentrations between active and hibernating marmots (*Marmota flaviventris*). *J Biol Rhythm*. 2018;33:388–401.
42. Stewart JM, Boudreau NM, Blakely JA, Storey KB. A comparison of oleamide in the brains of hibernating and non-hibernating Richardson's ground squirrel (*Spermophilus richardsonii*) and its inability to bind to brain fatty acid binding protein. *J Therm Biol*. 2002;27:309–15.
43. Græsli AR, Evans AL, Fahlman Å, Bertelsen MF, Blanc S, Arnemo JM. Seasonal variation in haematological and biochemical variables in free-ranging subadult brown bears (*Ursus arctos*) in Sweden. *BMC Vet Res*. 2015;11:301.
44. Deval C, Capel F, Laillet B, Polge C, Béchet D, Taillandier D, et al. Docosahexaenoic acid-supplementation prior to fasting prevents muscle atrophy in mice. *J Cachexia Sarcopenia Muscle*. 2016;7:587–603.
45. McGlory C, Calder PC, Nunes EA. The influence of Omega-3 fatty acids on skeletal muscle protein turnover in health, disuse, and disease. *Front Nutr*. 2019;6:144.
46. Wei H-K, Zhou Y, Jiang S, Tao Y-X, Sun H, Peng J, et al. Feeding a DHA-enriched diet increases skeletal muscle protein synthesis in growing pigs: association with increased skeletal muscle insulin action and local mRNA expression of insulin-like growth factor 1. *Br J Nutr*. 2013;110:671–80.
47. Simopoulos AP. The importance of the ratio of omega-6/omega-3 essential fatty acids. *Biomed Pharmacother*. 2002;56:365–79.
48. Bosch-Bouju C, Layé S. Dietary Omega-6/Omega-3 and Endocannabinoids: implications for brain health and diseases. 2016; in "cannabinoids in health and disease", (Meccariello R. and Chianese R. eds). IntechOpen (Rijeka).
49. Naughton SS, Mathai ML, Hryciw DH, McAinch AJ. Fatty acid modulation of the Endocannabinoid system and the effect on food intake and metabolism. *Int J Endocrinol*. 2013;2013:361895.
50. Alveim AR, Torstensen BE, Lin YH, Lillefosse HH, Lock E-J, Madsen L, et al. Dietary linoleic acid elevates the Endocannabinoids 2-AG and Anandamide and promotes weight gain in mice fed a low fat diet. *Lipids*. 2014;49:59–69.
51. Alveim AR, Malde MK, Osei-Hyiaman D, Lin YH, Pawlosky RJ, Madsen L, et al. Dietary linoleic acid elevates endogenous 2-AG and anandamide and induces obesity. *Obes Silver Spring Md*. 2012;20:1984–94.
52. Ghosh S, O'Connell JF, Carlson OD, González-Mariscal I, Kim Y, Moaddel R, et al. Linoleic acid in diets of mice increases total endocannabinoid levels in bowel and liver: modification by dietary glucose. *Obes Sci Pract*. 2019;5:383–94.
53. Schwartz GJ, Fu J, Astarita G, Li X, Gaetani S, Campolongo P, et al. The lipid messenger OEA links dietary fat intake to satiety. *Cell Metab*. 2008;8:281–8.
54. Walker C, West A, Browning L, Madden J, Gambell J, Jebb S, et al. The pattern of fatty acids displaced by EPA and DHA following 12 months supplementation varies between blood cell and plasma fractions. *Nutrients*. 2015;7:6281–93.
55. Matias I, Carta G, Murru E, Petrosino S, Banni S, Di Marzo V. Effect of polyunsaturated fatty acids on endocannabinoid and N-acyl-ethanolamine levels in mouse adipocytes. *Biochim Biophys Acta BBA - Mol Cell Biol Lipids*. 1781;2008:52–60.
56. DiPatrizio NV, Igarashi M, Narayanaswami V, Murray C, Gancayco J, Russell A, et al. Fasting stimulates 2-AG biosynthesis in the small intestine: role of cholinergic pathways. *Am J Physiol - Regul Integr Comp Physiol*. 2015;309:R805–13.
57. Cavuoto P, McAinch AJ, Hatzinikolas G, Cameron-Smith D, Wittert GA. Effects of cannabinoid receptors on skeletal muscle oxidative pathways. *Mol Cell Endocrinol*. 2007;267:63–9.
58. Mughaid DA, Sengul TG, You X, Wang Y, Steil L, Bergmann N, et al. Proteomic and Transcriptomic changes in hibernating grizzly bears reveal metabolic and signaling pathways that protect against muscle atrophy. *Sci Rep*. 2019;9:19976.
59. Esposito I, Proto MC, Gazzerò P, Laezza C, Miele C, Alberobello AT, et al. The cannabinoid CB1 receptor antagonist Rimonabant stimulates 2-Deoxyglucose uptake in skeletal muscle cells by regulating the expression of Phosphatidylinositol-3-kinase. *Mol Pharmacol*. 2008;74:1678–86.
60. Vella CA, Nelson OL, Jansen HT, Robbins CT, Jensen AE, Constantinescu S, et al. Regulation of metabolism during hibernation in brown bears (*Ursus arctos*): involvement of cortisol, PGC-1 α and AMPK in adipose tissue and skeletal muscle. *Comp Biochem Physiol A Mol Integr Physiol*. 2019;240:110591.
61. Engeli S. Dysregulation of the endocannabinoid system in obesity. *J Neuroendocrinol*. 2008;20(Suppl 1):110–5.
62. Nesto RW, Mackie K. Endocannabinoid system and its implications for obesity and cardiometabolic risk. *Eur Heart J Suppl Oxford Academic*. 2008;10:B34–41.
63. Di Marzo V. The endocannabinoid system in obesity and type 2 diabetes. *Diabetologia*. 2008;51:1356–67.
64. Rigano KS, Gehring JL, Evans Hutzenbiler BD, Chen AV, Nelson OL, Vella CA, et al. Life in the fat lane: seasonal regulation of insulin sensitivity, food intake, and adipose biology in brown bears. *J Comp Physiol B*. 2017;187:649–76.
65. Frøbert O, Frøbert AM, Kindberg J, Arnemo JM, Overgaard MT. The brown bear as a translational model for sedentary lifestyle-related diseases. *J Intern Med*. 2019;join.12983.
66. Proulx K, Cota D, Castañeda TR, Tschöp MH, D'Alessio DA, Tso P, et al. Mechanisms of oleoylethanolamide-induced changes in feeding behavior and motor activity. *Am J Physiol-Regul Integr Comp Physiol*. 2005;289:R729–37.
67. Sarro-Ramirez A, Sanchez-Lopez D, Tejada-Padron A, Frias C, Zaldivar- Rae J, Murillo-Rodriguez E. Brain Molecules and Appetite: The Case of Oleoylethanolamide. *Cent Nerv Syst Agents Med Chem*. 2013;13:88–91.
68. Fu J, Astarita G, Gaetani S, Kim J, Cravatt BF, Mackie K, et al. Food Intake Regulates Oleoylethanolamide Formation and Degradation in the Proximal Small Intestine. *J Biol Chem*. 2007;282:1518–28.
69. Izzo AA, Piscitelli F, Capasso R, Marini P, Cristino L, Petrosino S, et al. Basal and fasting/refeeding-regulated tissue levels of endogenous PPAR-alpha ligands in Zucker rats. *Obes Silver Spring Md*. 2010;18:55–62.
70. Fedele S, Arnold M, Krieger J-P, Wolfstädter B, Meyer U, Langhans W, et al. Oleoylethanolamide-induced anorexia in rats is associated with locomotor impairment. *Physiol Rep*. 2018;6:e13517.
71. Murillo-Rodríguez E, Palomero-Rivero M, Millán-Aldaco D, Arias-Carrión O, Drucker-Colín R. Administration of URB597, Oleoylethanolamide or

Palmitoylethanolamide Increases Waking and Dopamine in Rats. *PLOS ONE*. 2011;6:e20766.

72. Swenson JE, Sandegren F, Brunberg S, Wabakken P. Winter den abandonment by brown bears *Ursus arctos*: causes and consequences. *Wildl Biol. Nordic Board for Wildlife Research*; 1997;3:35–8.
73. Linnell JDC, Swenson JE, Andersen R, Barnes B. How Vulnerable Are Denning Bears to Disturbance? *Wildl Soc Bull.* 2000;28:400–13.
74. Evans AL, Singh NJ, Fuchs B, Blanc S, Friebe A, Laske TG, et al. Physiological reactions to capture in hibernating brown bears. *Conserv Physiol.* 2016;4: cow61.
75. Chanon S, Chazarin B, Toubhans B, Durand C, Chery I, Robert M, et al. Proteolysis inhibition by hibernating bear serum leads to increased protein content in human muscle cells. *Sci Rep.* 2018;8:5525.
76. Lefils J, Gélœn A, Vidal H, Lagarde M, Bernoud-Hubac N. Dietary DHA: time course of tissue uptake and effects on cytokine secretion in mice. *Br J Nutr.* 2010;104:1304–12.
77. R Development Core Team. R: a language and environment for statistical computing. R Foundation for Statistical Computing, Vienna. 2008; ISBN 3–900051–07-0. Available from: <https://www.r-project.org/>.

Publisher's Note

Springer Nature remains neutral with regard to jurisdictional claims in published maps and institutional affiliations.

Ready to submit your research? Choose BMC and benefit from:

- fast, convenient online submission
- thorough peer review by experienced researchers in your field
- rapid publication on acceptance
- support for research data, including large and complex data types
- gold Open Access which fosters wider collaboration and increased citations
- maximum visibility for your research: over 100M website views per year

At BMC, research is always in progress.

Learn more biomedcentral.com/submissions



10.6 Résumé de la thèse en français

10.6.1 Introduction bibliographique

10.6.1.1 Le muscle squelettique

Physiologie. Il existe 3 différents types de muscle, et dans ce projet de thèse nous nous sommes intéressés au muscle squelettique. Les muscles squelettiques recouvrent notre squelette et sont essentiellement responsables des mouvements volontaires et de la posture. Il s'agit également d'un tissu très dynamique et plastique qui agit comme principal tissu du métabolisme énergétique avec la production de chaleur, l'absorption, l'utilisation et le stockage de substrats énergétiques tels que le glucose et les acides aminés (AA). Le muscle est essentiellement composé d'eau (75%) et de protéines (20%) [1]. C'est un tissu hautement organisé contenant plusieurs faisceaux de myofibrilles dont chaque couche est successivement encapsulée par la matrice extracellulaire. Les myofibrilles sont des cellules multinucléées et post-mitotiques. Chaque myofibrille contient des milliers de myofibrilles qui sont composées de l'unité cellulaire de base du muscle, le sarcomère. Le sarcomère lui-même est composé de milliards de myofilaments, à la fois épais (myosine) et fins (actine) qui sont essentiels à la contraction musculaire nécessitant une forte consommation d'ATP. Les myofilaments représentent le principal contenu protéique du muscle (c'est-à-dire 70-80% du contenu protéique total d'une seule fibre) [1].

Mitochondries. Les muscles sont hautement vascularisés et innervés. Les besoins énergétiques pendant une contraction multiplient par 100 la consommation normale d'ATP dans le muscle. Pour répondre à cette demande énergétique élevée, le muscle dépend en partie de la phosphorylation oxydative mitochondriale (OXPHOS) pour la production d'ATP. Deux populations distinctes de mitochondries sont présentes dans les myofibrilles, subsarcolemmales et les intermyofibrillaires [10]. Le maintien d'un réseau mitochondrial fonctionnel dans le muscle est fondamental pour soutenir les demandes métaboliques imposées par la contraction. L'intégrité et la fonction mitochondriale sont hautement régulées par des systèmes de contrôle qualité (la biogenèse, la dynamique et la dégradation mitochondriales) afin de maintenir l'homéostasie. Cependant, un dysfonctionnement mitochondrial peut résulter en plusieurs maladies musculaires humaines appelées myopathies mitochondriales [19].

Réservoir d'acide aminés. Un des rôles majeurs du muscle squelettique est d'être le principal réservoir d'acides aminés (AA) du corps. Les AA musculaires peuvent être mobilisés en l'absence d'un apport nutritionnel adéquat pour assurer de nombreuses fonctions au niveau corps entier [30]. Par exemple, les AA libérés par les muscles servent de précurseurs pour le maintien du niveau de glucose sanguin grâce à la gluconéogenèse hépatique pendant le jeûne. Cependant, la réduction de la masse

musculaire compromet la capacité de l'organisme à répondre à différents stress en raison d'une altération des interactions entre les muscles et les organes.

Balance protéique musculaire. Chez les organismes adultes, la régulation de la masse musculaire résulte de la croissance des myofibrilles existantes par le biais de signalisations intracellulaires qui contrôlent la balance protéique [38]. L'équilibre entre les taux de synthèse des protéines musculaires (SPM) et de dégradation des protéines musculaires (DPM) détermine le contenu en protéines et donc l'homéostasie musculaire. La SPM et la DPM sont sensibles à de nombreux facteurs, notamment l'état nutritionnel, l'équilibre hormonal, l'activité physique ou les maladies. La diminution de la taille des muscles chez l'adulte, c'est-à-dire l'atrophie musculaire, résulte d'une balance protéique négative, tandis que l'augmentation de la taille des muscles, c'est-à-dire l'hypertrophie, résulte d'une balance positive.

Les AA apportés par une alimentation adaptée agissent comme des substrats et des signaux et sont essentiels pour induire la SPM. L'un des acteurs les plus reconnus de la SPM est le complexe mTORC1 qui joue un rôle central dans la régulation de la synthèse des protéines et de la biogenèse ribosomale [48]. Par exemple, la délétion spécifique de mTOR (la kinase du complexe) dans les muscles de souris induit une myopathie sévère entraînant une mort prématurée.

Concernant la DPM, les principaux systèmes qui y contribuent sont les systèmes autophagie-lysosome (ALS) et ubiquitine-protéasome (UPS). L'ALS implique la formation du phagosome, qui englobe des composés intracellulaires environnants, tels que des protéines endommagées, et qui fusionne avec les lysosomes pour entraîner la dégradation du contenu protéique et le recyclage des AA [55]. Dans des conditions normales, l'ALS empêche principalement l'accumulation d'organites endommagés et de protéines mal repliées. En réponse au stress, comme le jeûne, l'ALS agit principalement comme un mécanisme pro-survie dans le muscle, fournissant des substrats métaboliques [55]. Alors qu'un flux d'autophagie trop important contribue à l'atrophie musculaire, l'inhibition de l'ALS entraîne également une atrophie musculaire [62]. Dans les muscles sains, les mitochondries endommagées et dépolarisées sont sélectivement éliminées par le processus de mitophagie, une forme spécifique d'autophagie. Des études ont démontré que la mitophagie est essentielle au maintien de l'homéostasie du muscle squelettique [10]. Il existe de nombreuses preuves que des altérations de la mitophagie sont présentes dans le muscle au cours de nombreuses conditions cataboliques conduisant à l'atrophie musculaire [10]. Le système UPS joue également un rôle fondamental dans la physiologie du muscle, notamment en dégradant les protéines myofibrillaires [70]. La plupart des protéines subissent une dégradation en étant ciblées par le protéasome 26S grâce à la fixation covalente d'une chaîne d'ubiquitine. Ces protéines marquées sont ensuite reconnues par le protéasome 26S, qui initie un processus de

dégradation dépendant de l'ATP. Grâce à ce mécanisme, l'UPS dégrade spécifiquement le substrat. L'inhibition de l'activité du protéasome dans le muscle est associée à un défaut de croissance musculaire et à une diminution de la durée de vie chez les rongeurs [70].

10.6.1.2 L'atrophie musculaire

Causes. La perte de masse et de force musculaire est appelée atrophie musculaire. Les causes peuvent être diverses, par exemple congénitales ou génétiques, ou acquises suite à certaines conditions physiopathologiques [75] (Figure 51). Les conditions pathologiques qui conduisent à l'atrophie musculaire comprennent la cachexie cancéreuse, les troubles pulmonaires obstructifs chroniques, le diabète et l'obésité, ou encore des conditions associées à l'anorexie ou à la malnutrition [75] (Figure 51). L'inactivité physique entraîne également une fonte musculaire, comme dans le cas de fractures, d'immobilisation et d'alitement prolongé et même chez les personnes ayant un mode de vie sédentaire, comme observé lors du confinement de la COVID-19 [75] (Figure 51). L'atrophie musculaire résulte d'un déséquilibre entre la SPM et la DPM, en faveur de la DPM [75] (Figure 51). Au cours de ma thèse, je me suis principalement intéressée à l'atrophie musculaire induite par l'inactivité physique.

Conséquences. Le muscle est un organe majeur du métabolisme du glucose, de fait l'atrophie musculaire est étroitement liée à la résistance à l'insuline et au syndrome métabolique. De plus, l'atrophie musculaire limite les activités quotidiennes, réduit la qualité de vie et prolonge les temps de convalescence après une maladie tout en augmentant la morbidité et la mortalité (Figure 51). Compte tenu de ses conséquences néfastes, de l'augmentation de la sédentarité et de l'allongement de l'espérance de vie dans le monde, la fonte musculaire touche des millions de personnes et reste un fardeau social et économique majeur. Actuellement, les stratégies thérapeutiques pour limiter l'atrophie musculaire comprennent essentiellement l'exercice physique et des stratégies nutritionnelles, qui ne sont cependant pas applicables à tous (par exemple aux patients immobilisés ou en unité de soins intensifs) [75]. A ce jour, aucun médicament n'a été approuvé pour un usage clinique et aucun remède efficace contre l'atrophie musculaire n'a été découvert. Il est donc nécessaire de mieux comprendre les mécanismes sous-jacents et de découvrir de nouvelles cibles thérapeutiques potentielles. Notre compréhension s'est considérablement améliorée au cours des dernières décennies, principalement grâce à l'utilisation de modèles de rongeurs de laboratoire.

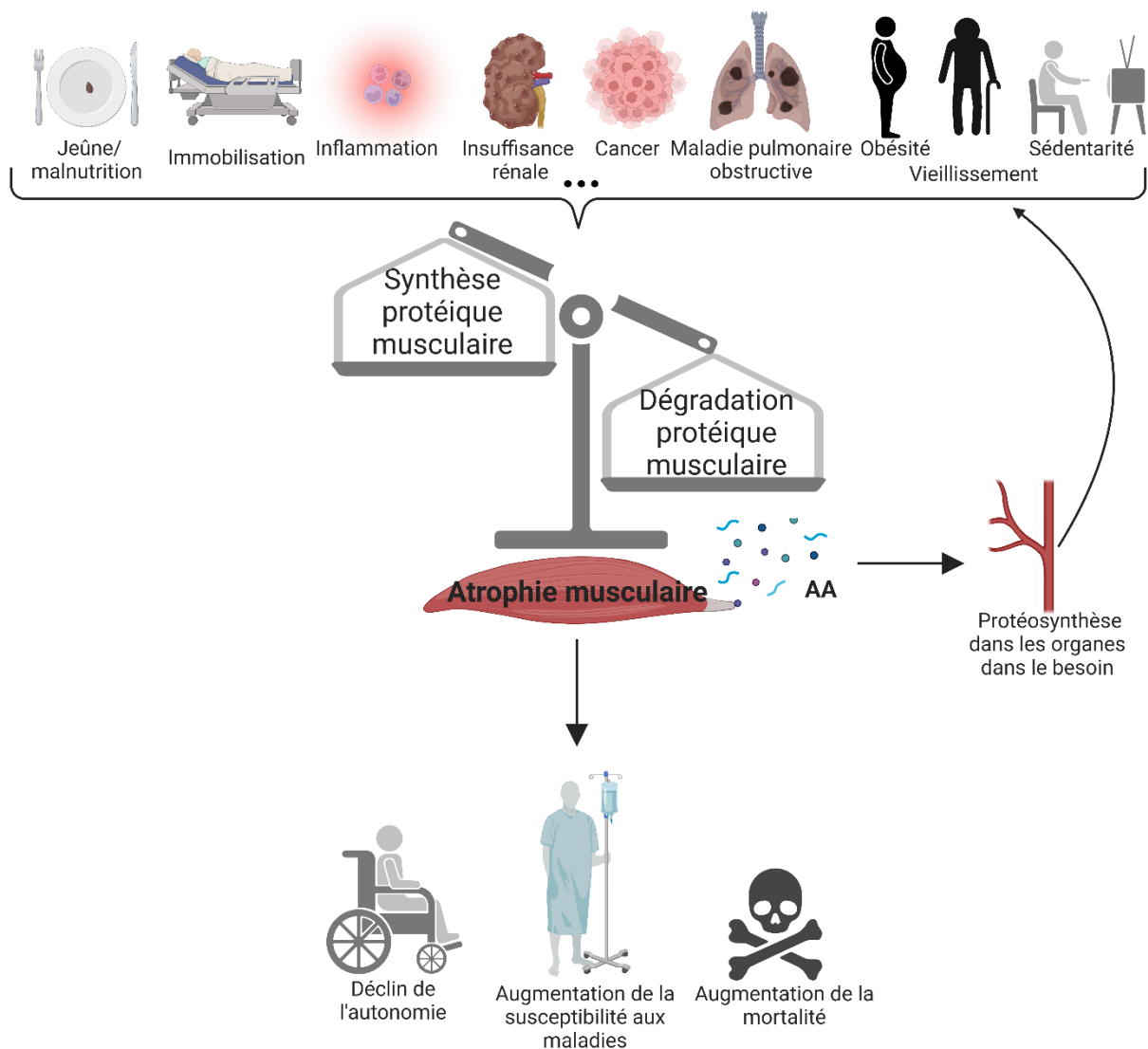


Figure 51. Déséquilibre dans la balance protéique dans des conditions physiopathologiques conduisant à l'atrophie musculaire.

AA : acides aminé

Les acteurs moléculaires. La SPM et la DPM sont influencés par un large éventail d'acteurs moléculaires extra et intracellulaires. Les stimuli extracellulaires comprennent des facteurs inflammatoires tels que des cytokines ou des facteurs endocriniens tels que des facteurs de croissance, qui activent diverses voies intracellulaires. Ces acteurs intracellulaires interconnectés contribuent à la régulation de l'équilibre protéique musculaire en travaillant en synergie ou en opposition, favorisant soit l'anabolisme, soit le catabolisme [38]. Dans le contexte de l'atrophie musculaire, le dérèglement d'un ou de plusieurs de ces acteurs entraîne une atténuation de la signalisation anabolique en faveur du catabolisme, ce qui conduit soit à l'inhibition de la SPM, soit à la suractivation des systèmes UPS et ALS, soit aux deux [38]. Les atrogènes sont désignés comme un ensemble de gènes dont l'expression

au niveau transcriptomique est modifiée de manière quasi systématique dans de nombreuses situations cataboliques associées à une atrophie musculaire [99]. Les atrogènes appartiennent à différentes voies cellulaires, principalement aux systèmes protéolytiques UPS et ALS, et incluent notamment les ligases E3-ubiquitine TRIM63⁴⁷/MuRF1⁴⁸ et FBXO32⁴⁹/Atrogin-1 [99]. Par exemple, TRIM63/MuRF1 cible les protéines myofibrillaires et FBXO32/Atrogin-1 est impliqué dans la dégradation des protéines ribosomales et des facteurs d'initiation de la traduction.

Plusieurs acteurs de ce réseau interconnecté se sont avérés efficaces lorsqu'ils ont été ciblés pour limiter ou contrecarrer l'atrophie des muscles dans des modèles expérimentaux. Pourtant, jusqu'à présent, aucun médicament efficace n'a été utilisé dans la pratique clinique.

Dans mon projet de thèse, je me suis concentrée sur le rôle central de la superfamille du TGF- β et de la signalisation d'ATF4 dans l'homéostasie musculaire.

10.6.1.3 La superfamille du TGF- β et son implication dans l'homéostasie musculaire

Généralités. La superfamille du TGF- β ⁵⁰, est une famille ubiquitaire qui régule une multiplicité d'actions biologiques dont la prolifération, la différenciation et l'apoptose. Cette superfamille est divisée en deux signalisations, nommées TGF- β et BMP⁵¹ [105]. Plus de 30 ligands appartiennent à cette famille, par exemple les activines A et B et la myostatine pour la signalisation du TGF- β , et BMP7 et GDF5 pour la signalisation du BMP (Figure 52). Les ligands se lient à un complexe hétéromérique de récepteurs qui recrutent et phosphorylent les R-SMAD⁵²s, c'est-à-dire SMAD2 et 3 pour la signalisation du TGF- β et SMAD1,5 et 8 pour la signalisation du BMP [105] (Figure 52). Les R-SMADs phosphorylés sont reconnus par le médiateur commun des signalisations TGF- β et BMP, SMAD4. SMAD4 forme un complexe hétéromérique avec SMAD1/5/8 ou SMAD2/3 puis transloque dans le noyau et déclenche un programme transcriptionnel spécifique à la cellule, à l'environnement et au ligand [105] (Figure 52).

⁴⁷ tripartite motif 63

⁴⁸ muscle ring finger-1

⁴⁹ F-Box 32 protein

⁵⁰ transforming growth factor- β

⁵¹ bone morphogenetic protein

⁵² receptor-regulated SMAD family member

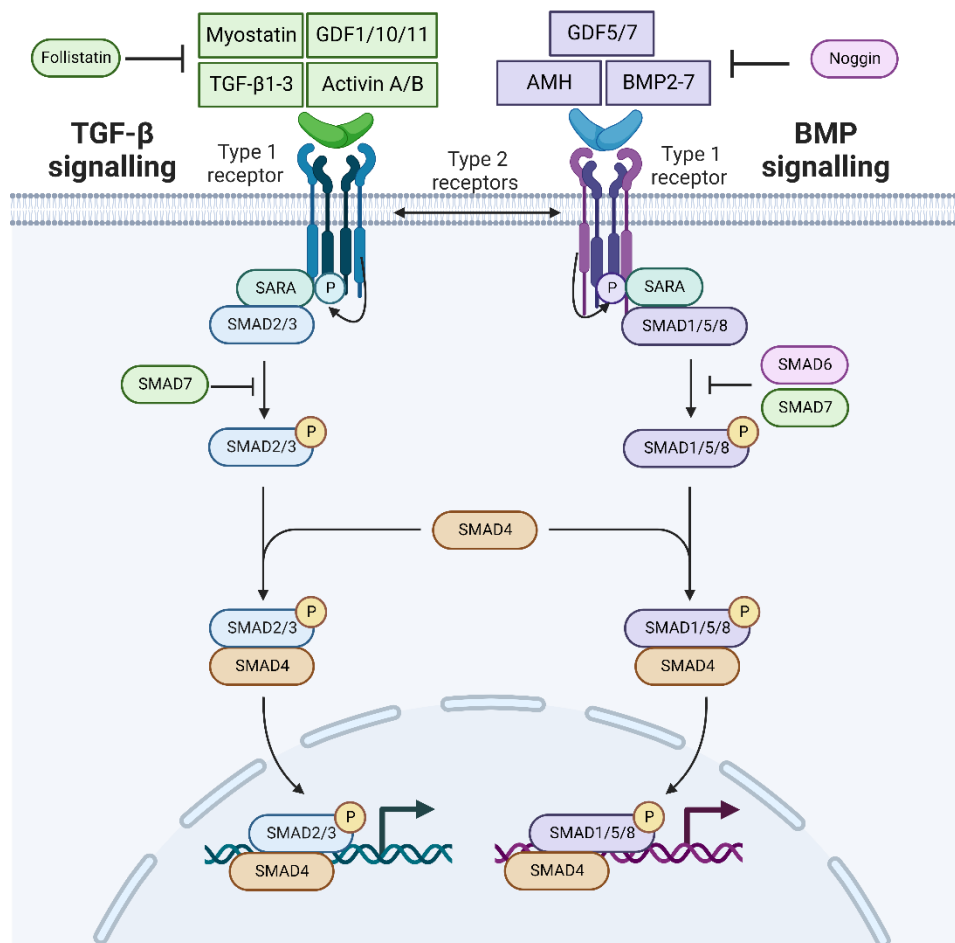


Figure 52. Organisation et transduction du signal de la superfamille du TGF- β .

La superfamille du TGF- β est un des régulateurs principaux de l'homéostasie musculaire avec (1) la signalisation TGF- β , étant un régulateur négatif de la masse musculaire et (2) la signalisation BMP étant un régulateur positif de la masse musculaire [110].

La signalisation pro-atrophique du TGF- β . L'intérêt initial est venu de la découverte que la perturbation de la myostatine, l'un de ses ligands, et l'inhibition du récepteur à la myostatine, produisaient une hyper-musculature chez les souris, les bovins, les moutons ou encore les chiens [110]. Par la suite, il a été constaté que les niveaux protéiques de la myostatine étaient élevés dans le muscle ou dans le sang lors de nombreuses situations cataboliques caractérisées par une atrophie musculaire, comme chez les sujets vieillissants, suite à un alitement prolongé ou lors d'insuffisance cardiaque. Les taux sériques d'autres ligands du TGF- β , comme l'activine A, augmentent également en réponse à la cachexie cancéreuse, à l'insuffisance rénale ou encore à l'insuffisance cardiaque associée à la fonte musculaire.

La mécanistique de la signalisation TGF- β . La surexpression de la signalisation du TGF- β dans les muscles de souris induit la transcription des atrogènes *Fbxo32/Atrogin-1* et *Trim63/MuRF1* via un mécanisme SMAD2/3-dépendant et donc à la protéolyse musculaire [110] (Figure 53). Inversement, les muscles de souris déficients pour *Smad3* sont résistants à l'atrophie musculaire induite par la dénervation [110]. En parallèle, l'action catabolique du TGF- β implique également l'inhibition de la protéosynthèse [110] (Figure 53). L'administration de myostatine ou d'activine A est suffisante pour inhiber la synthèse protéique dans les muscles de souris par l'inhibition de la signalisation mTORC1 et le même phénotype est observé en surexprimant *Smad3*. De plus, l'inhibition de la signalisation du TGF- β induit une hypertrophie musculaire chez la souris en augmentant la signalisation mTORC1, et l'inhibition génétique ou pharmacologique de mTORC1 réduit cet effet hypertrophique [110]. De plus, la signalisation du TGF- β chez la souris réprime la biogenèse mitochondriale. Enfin, la signalisation du TGF- β est également connue pour son rôle majeur dans la fibrose, favorisant les changements mécaniques et donc les lésions musculaires dans de nombreuses dystrophies musculaires chez la souris et l'Homme.

Les essais pré-cliniques et cliniques anti-TGF- β . De nombreuses études pré-cliniques ont ainsi montré qu'inhiber la voie du TGF- β , de manière génétique ou pharmacologique, limitait ou prévenait la survenue de l'atrophie musculaire dans de nombreuses situations cataboliques [119]. Cependant, sur les nombreux agents pharmacologiques testés dans des essais cliniques chez l'humain, un très grand nombre n'a montré qu'un effet minime ou a démontré des effets secondaires importants. En effet, la plupart des inhibiteurs de la myostatine répriment également les activités d'autres membres de la famille du TGF- β , notamment la voie du BMP. Par conséquent, une distinction entre les cibles est nécessaire pour évaluer l'utilisation de ces médicaments dans la pratique clinique humaine [119].

La signalisation hypertrophique du BMP. Le rôle de la voie BMP dans la régulation de la masse musculaire n'a été découverte qu'en 2013 et par conséquent beaucoup moins de choses sont connues sur sa mécanistique sous-jacente dans l'homéostasie musculaire [119]. La signalisation BMP contrôle la masse des muscles adultes dans des conditions physiologiques puisque (1) l'augmentation de l'expression de son ligand *Bmp7* entraîne une hypertrophie dépendante de SMAD1/5 et (2) l'inhibition pharmacologique ou génétique de la voie BMP conduit à une atrophie musculaire dans les muscles adultes sains. De même, chez la souris adulte, l'augmentation profonde de la masse musculaire observée dans les souris déficientes pour la myostatine (*Mstn*) est médiée par l'activation de la signalisation BMP via SMAD1/5 [110]. De façon surprenante, (1) la phosphorylation de SMAD1/5 est augmentée dans les muscles de rongeurs présentant une atrophie suite à une dénervation et (2) l'inhibition génétique de la signalisation BMP exacerbe l'atrophie musculaire pendant la dénervation et le jeûne. Par ailleurs, une aggravation sévère de l'atrophie musculaire induite par la dénervation est

observée chez les souris déficientes pour *Gdf5*, un autre ligand de la signalisation BMP. Pour finir, les souris déficientes pour le gène *Mstn*, qui sont habituellement résistantes à l'atrophie musculaire induite par la dénervation, perdent cette capacité lorsque la signalisation BMP est inhibée. Dans l'ensemble, ces données suggèrent fortement que (1) l'activation de la voie BMP dans le muscle lors de conditions cataboliques est une réponse adaptative pour contrer l'atrophie, et (2) une déficience de cette signalisation joue un rôle critique dans l'aggravation de la fonte musculaire [110]. L'hypertrophie induite par la signalisation BMP est associée à une induction de la signalisation mTORC1, et cette hypertrophie est atténuée par un traitement à la rapamycine [110] (Figure 53). De plus, la signalisation BMP agit comme un régulateur positif de la masse musculaire en réprimant la transcription de l'atrogène *Fbxo30/MUSA1*, dont l'induction est requise pour l'induction de l'atrophie par la dénervation [110] (Figure 53).

SMAD4 le facteur contrôlant la balance protéique. SMAD4 est l'acteur commun entre la signalisation du TGF- β et du BMP (Figure 53). Les muscles des souris déficients pour *Smad4* s'atrophient fortement et présentent une protéolyse excessive après un mois de dénervation chez la souris. Les souris déficientes pour la *Mstn* présentent un recrutement plus important de SMAD4 sur le promoteur des gènes cibles de la signalisation BMP. Au contraire, les souris déficientes pour *Gdf5* présentent une augmentation de la liaison du complexe SMAD4-SMAD2/3 sur le promoteur des gènes cibles du TGF- β . De ces résultats a émergé le concept d'une compétition entre SMAD2/3 et SMAD 1/5/8 pour le recrutement de SMAD4. L'inhibition du signal TGF- β libérerait SMAD4 de SMAD2/3 pour être plus disponible pour SMAD1/5/8. Ainsi, la suractivation du TGF- β lors de situations cataboliques est considérée comme un facteur qui réduit la disponibilité de SMAD4 pour la signalisation BMP. Il y a donc une vraie nécessité d'un équilibre finement régulé de la balance BMP/TGF- β afin de maintenir l'homéostasie musculaire [110] (Figure 53).

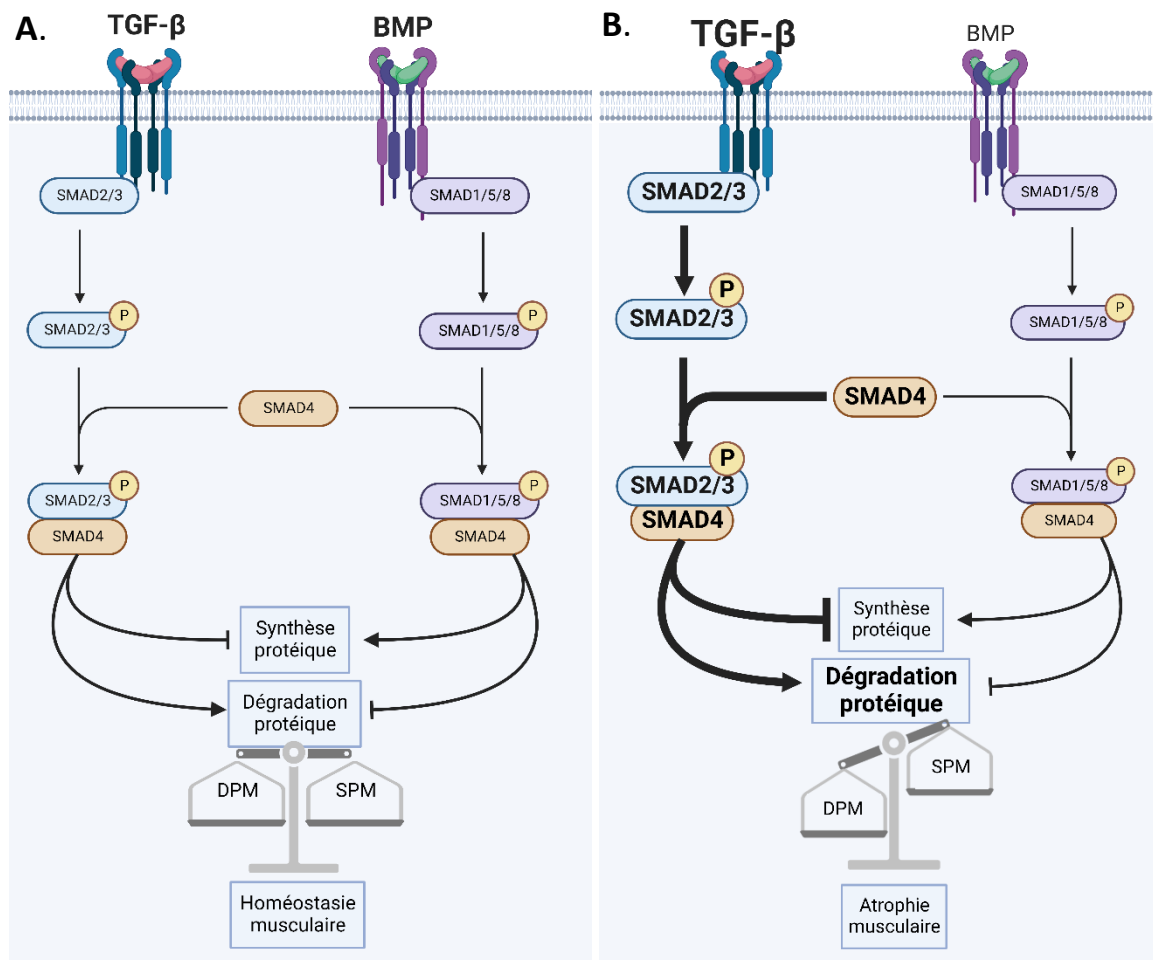


Figure 53. Compétition pour le recrutement de SMAD4 en conditions physiologiques (A) ou cataboliques (B).

DPM : dégradation protéique musculaire ; SPM : synthèse protéique musculaire.

10.6.1.4 La signalisation de l'ISR et son implication dans l'homéostasie musculaire

Généralités. L'ISR⁵³ est une autre voie de signalisation impliquée dans l'homéostasie musculaire. L'ISR est une signalisation bien conservée présente dans toutes les cellules eucaryotes et qui est activée en réponse à une série de stress physiologiques [193]. Ces stress incluent des facteurs extracellulaires tels que l'hypoxie, une déplétion en AA ou glucose, ou des stress intracellulaires tels que le stress du réticulum endoplasmique (RE). L'événement central de l'activation de l'ISR est la phosphorylation de la sous-unité alpha du facteur d'initiation de la traduction eucaryote 2 (eIF2 α) sur sa sérine 51 (p-eIF2 α) [193] (Figure 54). A ce jour, quatre kinases sont connues pour phosphoryler eIF2 α , à savoir PERK⁵⁴,

⁵³ integrated stress response

⁵⁴ PKR-like ER kinase

PKR⁵⁵, HRI⁵⁶, et GCN2⁵⁷ [193] (Figure 54). P-eIF2 α conduit à deux conséquences : (1) une inhibition générale de la machinerie traductionnelle et (2) la traduction d'ARNm spécifiques dont ATF4⁵⁸ [193] (Figure 54). ATF4 est un facteur de transcription qui agit principalement comme un activateur transcriptionnel d'une cohorte de gènes impliqués dans l'adaptation au stress cellulaire en réponse à l'activation de l'ISR [193] (Figure 54). ATF4 produit des réponses distinctes en fonction du stress cellulaire. Par exemple, lors d'un stress nutritionnel, ATF4 stimule l'expression de gènes impliqués dans le transport et la biosynthèse des AA, et l'autophagie pour fournir de nouveaux AA pour la synthèse *de novo* des protéines. De plus, ATF4 induit la transcription de PPP1R15A⁵⁹ (la protéine GADD34), la principale phosphatase d'eIF2 α , agissant comme une importante boucle de rétrocontrôle négatif pour restaurer la synthèse protéique une fois le stress résolu [193] (Figure 54). Il a été proposé que la durée et l'intensité de la signalisation de l'ISR dicteraient la résultante biologique cellulaire. Par conséquent, ATF4 peut également faciliter l'exécution d'un programme transcriptionnel de mort cellulaire par apoptose lorsque l'homéostasie cellulaire ne peut être restaurée, en induisant la transcription de gènes apoptotiques [193] (Figure 54).

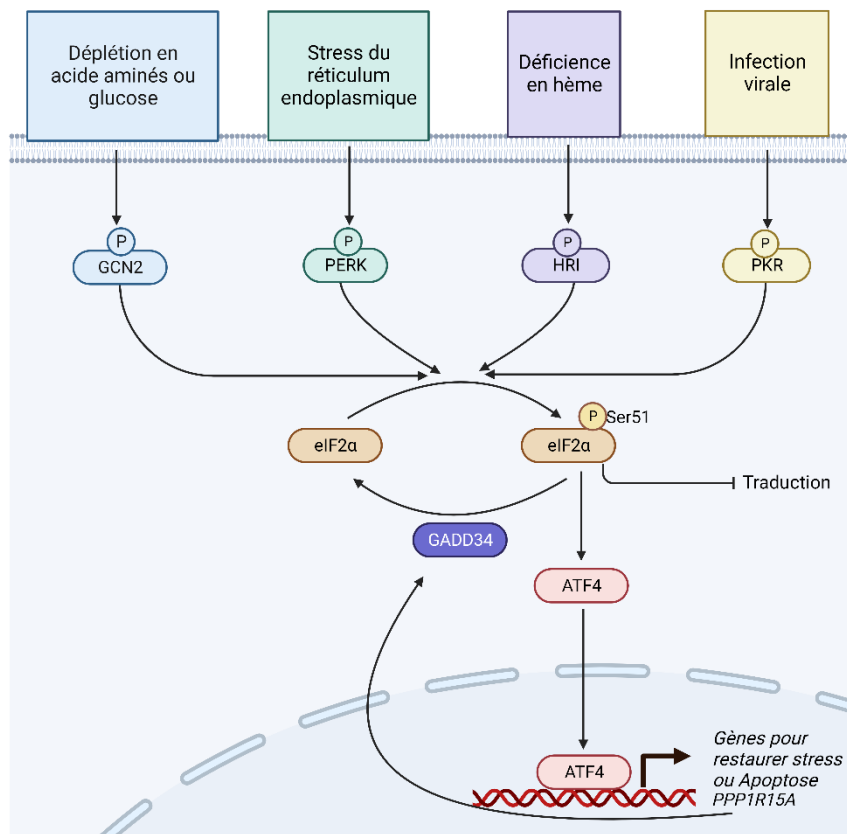


Figure 54. Organisation et transduction du signal de la signalisation de l'ISR.

⁵⁵ double-stranded RNA-dependent protein kinase

⁵⁶ heme-regulated inhibitor

⁵⁷ general control nonderepressible 2

⁵⁸ activating transcription factor 4

⁵⁹ protein phosphatase 1 regulatory subunit 15A

La manière dont ATF4 facilite des adaptations cellulaires aussi diverses, allant de l'anabolisme à l'arrêt de la croissance, est une question importante et non résolue. Une des possibilités pourrait venir des différents hétérodimères d'ATF4 ou différentes combinaisons d'hétérodimères qui médieraient les différents effets de la signalisation.

Le rôle de l'ISR dans l'autophagie et l'homéostasie mitochondriale. Comme indiqué plus haut, l'autophagie et le contrôle de la qualité mitochondriale sont des processus cellulaires essentiels à l'homéostasie musculaire, et une déficience de l'un ou l'autre est associée à la l'atrophie musculaire [13]. L'ISR est impliquée dans ces deux processus dans un large éventail de tissus et de cellules. Lors de divers stress, ATF4 se lie au promoteur spécifique de gènes impliqués dans l'autophagie pour promouvoir une réponse pro-survie ou une réponse pro-létale, de manière PERK- ou GCN2-dépendante (Figure 55). La signalisation de l'ISR est également essentielle au contrôle de la qualité des mitochondries, par le biais de UPRmt⁶⁰. L'UPRmt est une réponse à divers stress mitochondriaux. Il active un programme transcriptionnel codé par l'ADN nucléaire pour favoriser le retour à une homéostasie mitochondriale [226]. Néanmoins, si l'UPRmt est incapable de réparer les dommages mitochondriaux, l'élimination de la mitochondrie entière par mitophagie est favorisée. Il existe trois protéines régulatrices clés de l'UPRmt, dont la protéine ATF4 qui est souvent surexprimée suite à des dommages mitochondriaux. Une analyse transcriptomique globale a validé la présence de motifs de liaison d'ATF4 dans de nombreux gènes UPRmt [226] (Figure 55). Dans les muscles de souris, des stress mitochondriaux causés par une mauvaise fusion mitochondriale ou mitophagie, augmentent p-eIF2 α et les niveaux protéiques d'ATF4. Cependant, des preuves montrent que l'activation de l'UPRmt-ATF4 suite à des perturbations mitochondriales dans les muscles peuvent avoir à la fois des effets protecteurs ou néfastes pour le muscle [226]. Ainsi, ces études mettent en évidence l'implication complexe de l'ISR dans l'autophagie et dans le contrôle de la qualité mitochondriale. En outre, il reste beaucoup à explorer pour comprendre l'implication de l'ISR-ATF4 dans l'autophagie et le contrôle de la qualité mitochondriale dans l'homéostasie musculaire.

⁶⁰ mitochondrial unfolded protein response

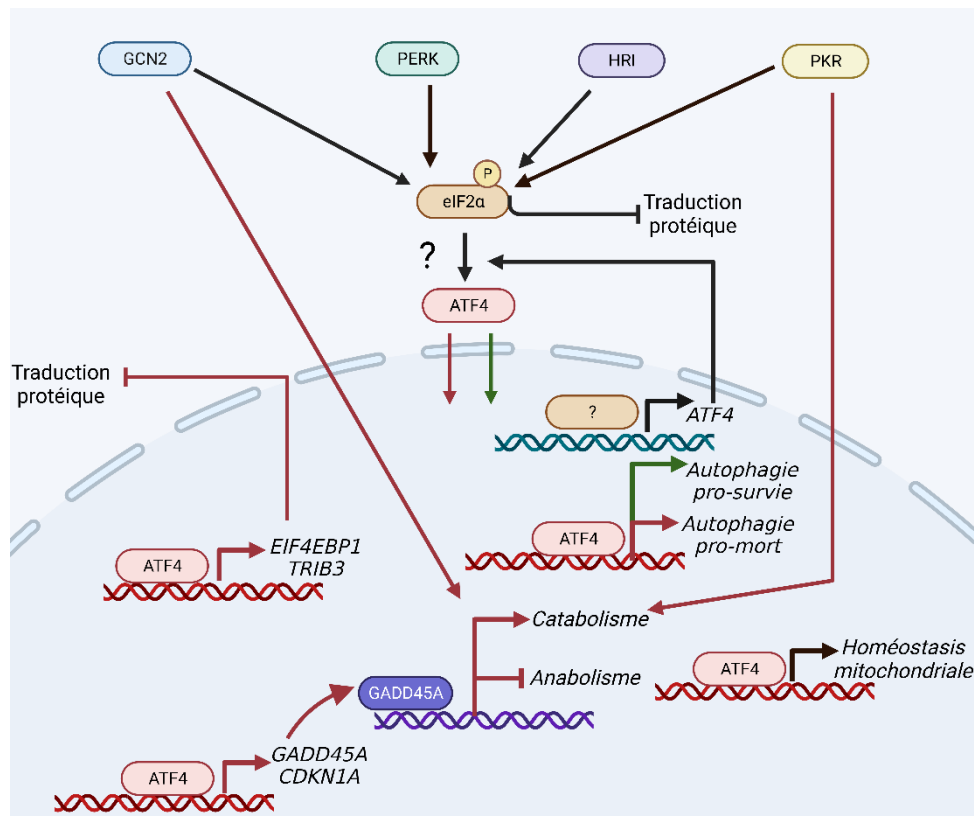


Figure 55. Le rôle double de l'ISR dans l'homéostasie musculaire.

Les flèches vertes représentent des conséquences cellulaires anaboliques, les flèches rouges des effets cataboliques, et noires des conséquences encore mal comprises.

Le rôle de l'ISR dans l'atrophie musculaire. Certains membres de l'ISR ont été associés de près ou de loin à l'atrophie musculaire dans différentes conditions cataboliques. Pour la kinase PERK et p-eIF2 α , certaines études les associent à l'atrophie musculaire, pendant que d'autres leur confèrent une action anti-atrophique. Pour les kinases GCN2 et PKR, il semblerait que leurs activations soient associées à l'atrophie musculaire, bien qu'aucune connection avec ATF4 n'ait été faite. Le gène ATF4 est quant à lui considéré comme un atrogène car ses niveaux d'ARNm augmentent dans de nombreuses conditions cataboliques induisant l'atrophie musculaire [99,207]. Les souris déficientes pour *Atf4* dans les fibres musculaires se développent normalement et présentent une masse et une fonction musculaire normale jusqu'à un âge avancé. Par la suite, elles commencent à présenter une protection contre l'atrophie musculaire liée à l'âge [207]. Une délétion d'*Atf4* dans les muscles de souris limite l'atrophie musculaire induite par le jeûne, l'immobilisation ou encore le vieillissement [207]. Le rôle catabolique d'ATF4 passe par la transcription des atrogènes *Gadd45a*⁶¹, *Cdkn1a*⁶² and *Eif4ebp1*⁶³ dans les muscles

⁶¹ growth arrest and DNA damage inducible alpha

⁶² cyclin-dependent kinase inhibitor 1

⁶³ eukaryotic translation initiation factor 4E binding protein 1

de souris [99,207] (Figure 55). GADD45A est une protéine myonucléaire qui réprime des gènes impliqués dans l'anabolisme et induit des gènes impliqués dans le catabolisme (Figure 55). ATF4 est nécessaire et suffisante pour induire l'expression de *Gadd45a* en condition d'atrophie musculaire induite par le jeûne et l'immobilisation [207]. L'augmentation de *Cdkn1a* (protéine P21) dans les muscles de souris, est nécessaire et suffisante pour induire une atrophie par immobilisation médiée par ATF4 [207]. ATF4 induit également l'expression du gène *Eif4ebp1*, codant pour l'inhibiteur de la synthèse protéique 4E-BP1 [207] (Figure 55). Enfin, un autre gène cible d'ATF4, TRIB3⁶⁴, a été associé à l'atrophie musculaire dans de nombreuses études. Par exemple, les souris déficientes pour *Trib3* sont en partie résistante à l'induction de l'atrophie par le jeûne.

À l'heure actuelle, les mécanismes par lesquels ATF4 est activé sur le plan transcriptionnel et traductionnel dans des conditions cataboliques ne sont pas clairs, mais peuvent impliquer différents mécanismes ou combinaisons de mécanismes.

10.6.1.5 Le modèle de résistance naturelle à l'atrophie musculaire de l'ours brun hibernant

Le biomimétisme est une approche qui cherche des solutions durables aux défis humains en imitant les modèles et les stratégies de la nature, ce qui a déjà permis des avancées et des progrès biomédicaux humains significatifs. L'hibernation est un parfait exemple de variabilité saisonnière pouvant receler des indices et solutions diverses pour les pathologies humaines.

Généralités de l'hibernation chez les ours. L'hibernation est une adaptation utilisée par certains animaux pour faire face à un manque épisodique ou saisonnier d'énergie dû à des conditions environnementales défavorables (par exemple, faible disponibilité de nourriture/eau, forte pression de prédation) [273]. La torpeur est au cœur de l'hibernation, elle représente une période de suppression métabolique qui peut durer de quelques heures à plusieurs semaines. L'hibernation est un comportement plus élaboré, structuré en plusieurs longues périodes de torpeur souvent séparées par de brèves périodes d'éveil (IBA⁶⁵). Les IBA durent environ 24 heures et sont présents chez presque tous les petits hibernants (c'est-à-dire <10kg) mais pas chez les ours hibernants [273].

Les ours sont des mammifères de la famille des *Ursidae*. Les ours des climats chauds n'entrent pas en hibernation, pas plus que le panda géant ou l'ours polaire. Dans ce projet de thèse, nous nous sommes concentrés sur les ours hibernants, c'est-à-dire les ours bruns (*Ursus arctos*), les ours noirs américains

⁶⁴ tribbles pseudokinase 3

⁶⁵ Interbout arousal

(*Ursus americanus*) et les ours noirs asiatiques (*Ursus thibetanus*). Les ours entrent dans leur tanière en octobre-novembre et y restent jusqu'à la fin avril-début mai. Les ours hibernants restent physiquement inactifs à l'intérieur de leur tanière, ne mangent pas, ne défèquent pas, ne boivent pas et n'urinent pas pendant 5 à 7 mois [279]. Les ours hibernants montrent une baisse de 75-85% de leur taux métabolique (MR), une réduction du rythme respiratoire et cardiaque, suivie d'une diminution modérée de la température corporelle (Tb), qui descend rarement en dessous des 30 °C [279]. Le stockage des graisses est augmenté avant l'hibernation, notamment par un comportement hyperphagique, où les ours font plus que doubler leur apport énergétique quotidien. Les besoins énergétiques en hiver reposent principalement sur la mobilisation et l'oxydation des lipides, les ours subissant une perte d'environ 22-25% de leur masse corporelle pendant la saison d'hibernation et seulement une perte modérée de protéines musculaires [301]. Malgré le stockage important de graisses, les ours hibernants ne montrent aucun signe de développement d'athérosclérose ou de dommages cardiovasculaires. De plus, malgré leur inactivité physique prolongée, ils ne subissent pas l'ostéoporose ni l'atrophie musculaire. En bref, les ours sortent de leur tanière au printemps et ne montrent aucun signe de dommages physiologiques [316] (Figure 56). Dans des conditions similaires, les humains développeraient des maladies cardiovasculaires, de l'obésité, de la perte musculaire, de l'ostéoporose et d'autres conséquences délétères sur la santé. La conservation de la masse musculaire pendant une longue période de jeûne et d'inactivité physique a attiré notre attention et a été centrale dans ce projet de thèse.

La résistance à l'atrophie musculaire de l'ours brun hibernant. Au cours des six mois d'inactivité physique totale, les ours hibernants ne subissent qu'une perte modérée de la teneur en protéines musculaires, entre 5 à 15% en fonction des études. Il est intéressant de noter que la perte musculaire constatée après 1 mois d'hibernation reste la même 4 mois plus tard [301]. De plus, la teneur en azote du muscle reste inchangée en hiver par rapport à l'été, indiquant une perte modérée de protéines [301]. La perte de force musculaire est d'environ 29 % après 110 jours d'inactivité physique pendant l'hibernation chez l'ours. C'est environ la moitié de ce qui est observé chez les humains confinés au lit pendant 90 jours. En outre, les ours en hibernation ne montrent aucun changement ou des changements très limités dans les propriétés contractiles des muscles [301]. Bien que les ours ne présentent pas une thermogénèse par frissonnements, ils effectuent tout de même des ajustements posturaux occasionnels, se réveillent brièvement et frissonnent. Il a été suggéré que cette activité musculaire pourrait limiter l'atrophie. Enfin, les influx nerveux ne peuvent pas être considérés comme un mécanisme permettant de limiter l'atrophie musculaire. En effet, la diminution de la masse musculaire induite par la dénervation chez les ours actifs est comparable à celle observée chez d'autres

mammifères, alors que les ours hibernants résistent en partie à l'atrophie musculaire induite par la dénervation.

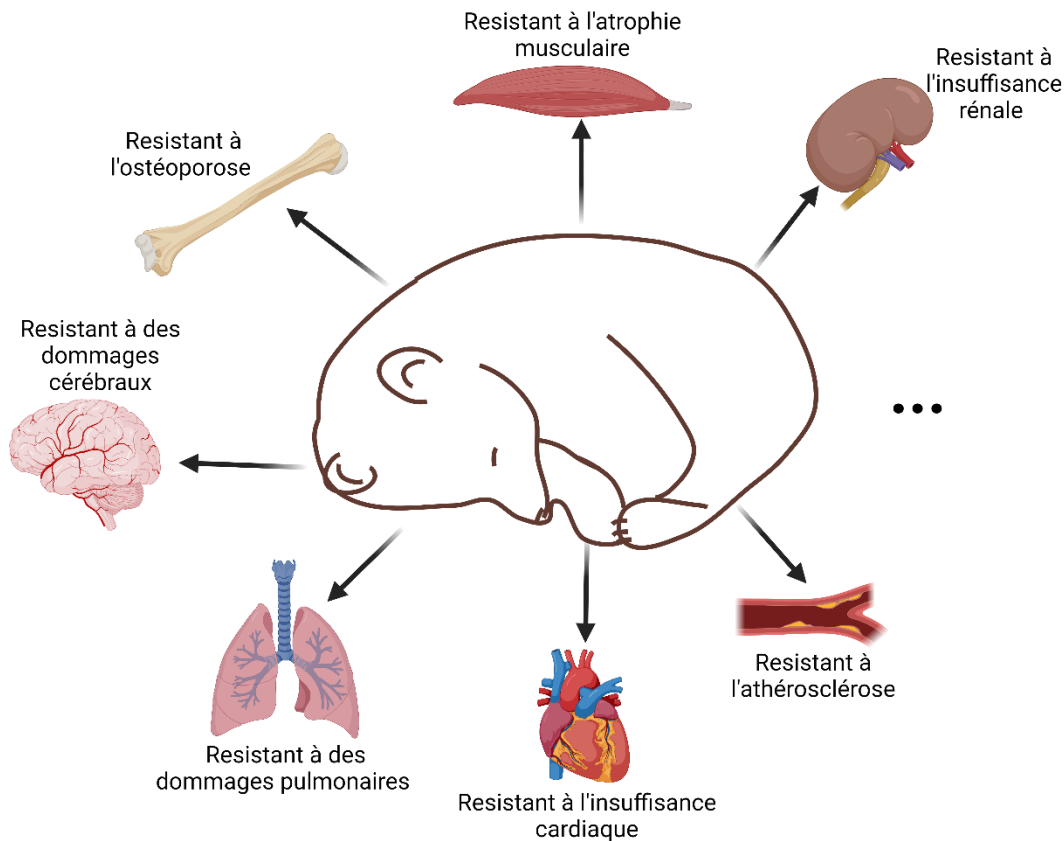


Figure 56. Caractéristiques physiologiques fascinantes de l'ours brun hibernant.

Épargne des protéines musculaires. Lohuis et al. ont montré que la synthèse et la dégradation des protéines musculaires étaient plus faibles chez les ours pendant l'hibernation par rapport à la période active. De plus, ils ont observé que ces deux phénomènes restaient inchangés entre le début et la fin de l'hibernation, ce qui indique que l'équilibre protéique est maintenu tout au long de la période d'hibernation [301]. Une analyse transcriptomique a également montré que pendant l'hibernation des ours, il y a une induction de l'expression de gènes impliqués dans la biosynthèse des protéines et la biogenèse des ribosomes, et une diminution des gènes liés à la protéolyse dans les muscles squelettiques [307]. De plus, le recyclage de l'urée est très efficace chez l'ours hibernant, 99,7% de l'urée produite étant recyclée en protéines, ce qui limite probablement la dégradation des protéines musculaires.

Métabolisme énergétique musculaire. La glycolyse est préservée dans les muscles des ours hibernants [310]. Cela pourrait aider à maintenir la fonctionnalité des muscles dans des situations inattendues, comme une sortie urgente de la tanière qui nécessiterait une augmentation rapide de la production

d'ATP. La glycolyse pourrait être alimentée par la néoglucogenèse hépatique et la mobilisation du contenu en glycogène musculaire, qui est plus important dans les muscles de l'ours en hiver par rapport à l'été [310].

Composés circulants anti-protéolytiques dans le sérum des ours en hibernation. Des chercheurs ont émis l'hypothèse que des facteurs circulants pendant l'hibernation pourrait expliquer le phénotype de résistance à l'atrophie musculaire de l'ours. Notre équipe a montré que la culture primaire de myotubes humains avec du sérum d'ours hibernant entraînait une augmentation du contenu protéique par rapport au sérum d'ours d'été [341]. Il s'agit de la première preuve de concept qu'un composé actif du sérum d'ours est transmissible à du matériel biologique humain. De plus, la régulation de renouvellement des protéines observé dans le muscle de l'ours en hibernation (c'est-à-dire un taux de synthèse et de dégradation plus faible) a été reproduite dans des myotubes humains traités par le sérum d'ours hibernant [341].

Il est donc fort probable que le maintien de la masse musculaire pendant l'hibernation des ours fasse intervenir un ou plusieurs facteurs circulants. L'identification de ces facteurs ouvrira sans aucun doute un nouveau champ d'étude qui conduira à de nouvelles solutions pour prévenir et/ou inverser l'atrophie musculaire chez l'homme.

10.6.2 Objectifs et stratégies

L'objectif principal de cette thèse était d'identifier de nouveaux acteurs moléculaires et leurs mécanismes qui pourraient devenir des cibles thérapeutiques pour combattre l'atrophie musculaire chez l'homme. Pour cela, nous avons adopté une approche biomimétique en utilisant l'ours brun, qui est naturellement résistant à l'atrophie musculaire, et nous avons comparé les adaptations musculaires à celles observées dans un modèle classique de sensibilité à l'atrophie. Le projet a été subdivisé en trois études, comme suit.

Etude 1 Le maintien concomitant de la signalisation BMP et l'inhibition de la signalisation TGF- β est une caractéristique de la résistance naturelle à l'atrophie musculaire chez l'ours hibernant (article publié).

Les objectifs étaient (1) d'identifier les mécanismes sous-jacents impliqués dans la résistance de l'atrophie musculaire lors d'une inactivité physique prolongée et (2) de déterminer si ces mécanismes étaient régulés de manière opposée dans un modèle de susceptibilité à l'atrophie. Nous avons réalisé une analyse transcriptomique comparative des muscles résistants à l'atrophie de l'ours brun en hibernation et des muscles sensibles à l'atrophie de la souris suspendue par les membres postérieurs (Figure 57).

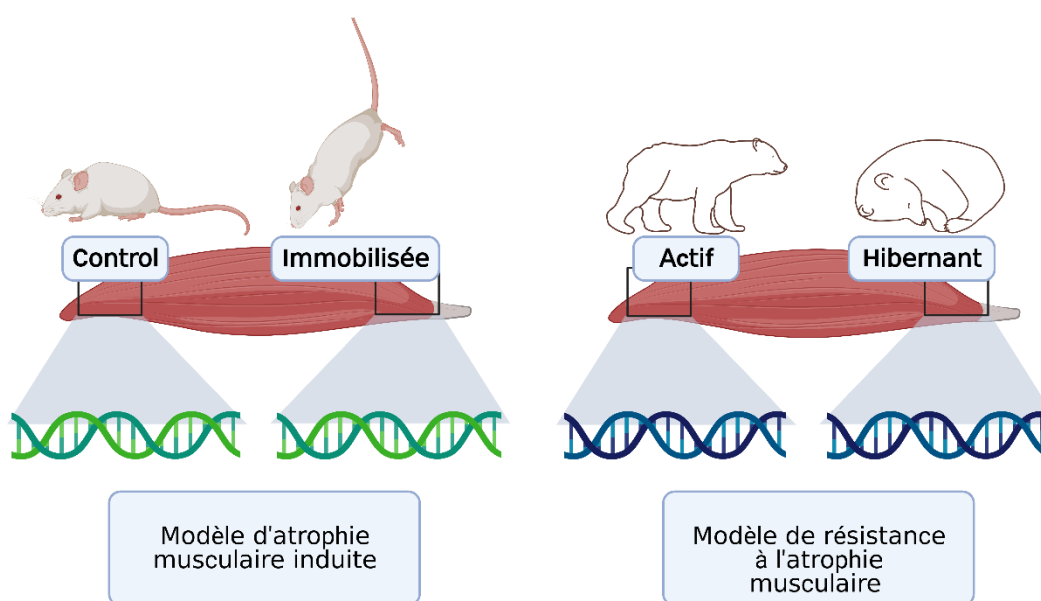


Figure 57. Schéma expérimental de l'étude 1.

Etude 2 L'induction d'ATF4 est découplée de l'atrophie musculaire lors de l'inactivité physique chez les souris traitées à l'halofuginone et chez les ours bruns hibernants (article en révision).

L'objectif était d'explorer le rôle de la signalisation d'ATF4 dans le muscle squelettique dans des conditions basales et cataboliques. Nous avons d'abord développé un protocole expérimental pour induire la signalisation ATF4 avec la molécule pharmacologique halofuginone (HF) chez la souris. Nous avons ensuite (1) étudié l'effet de l'induction d'ATF4 sur les muscles de souris dans des conditions basales et d'atrophie induite par la suspension du train arrière et (2) décrypté les mécanismes moléculaires de l'HF dans les muscles de souris (Figure 58). Nous avons également étudié la régulation de cette voie dans les muscles résistants à l'atrophie de l'ours brun hibernant.

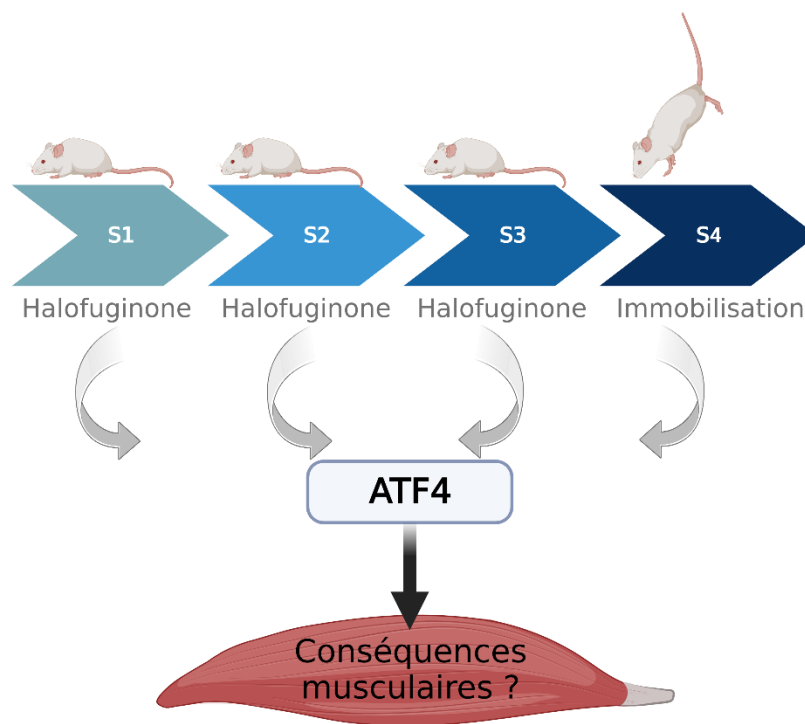


Figure 58. Schéma expérimental de l'étude 2.

Etude 3 Le sérum d'ours d'hiver induit dans les cellules musculaires humaines des caractéristiques similaires à celles que l'on trouve naturellement dans les muscles d'ours en hibernation (résultats préliminaires).

Notre objectif était de déterminer si les caractéristiques moléculaires des muscles résistants à l'atrophie des ours hibernants pouvaient être reproduites dans les cellules musculaires humaines. Nous avons d'abord analysé les données de microarray de cellules musculaires humaines cultivées avec du sérum d'ours d'hiver pour évaluer s'il existait une signature transcriptomique des signalisations TGF- β /BMP. Nous avons ensuite mesuré l'activité transcriptionnelle de la signalisation TGF- β /BMP à l'aide de plasmides rapporteurs luciférase (Figure 59).

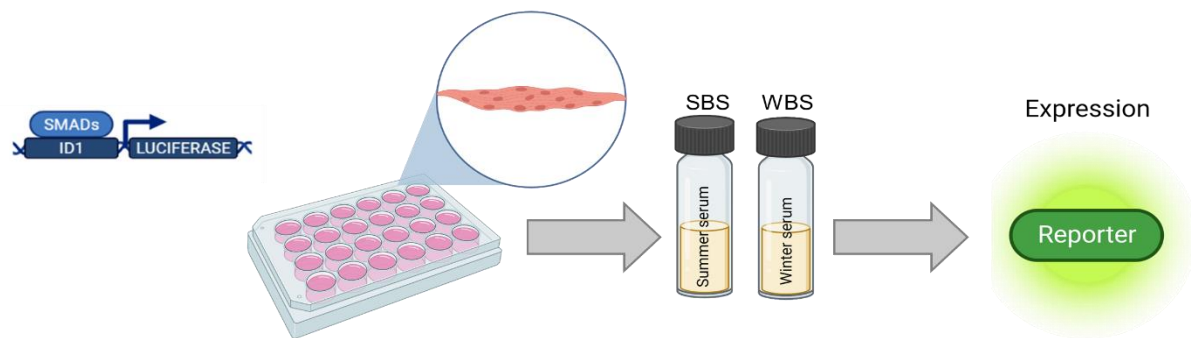


Figure 59. Schéma expérimental de l'étude 3.

Les cellules musculaires humaines sont transfectées avec un plasmide rapporteur luciférase pour le gène ID1 avant d'être traitées par du sérum d'ours d'été (SBS) ou d'hiver (WBS), avant de lire la luminescence.

10.6.3 Résultats

10.6.3.1 Étude 1

Cette étude visait à identifier de nouveaux facteurs de résistance à l'atrophie musculaire. Nous avons choisi une approche innovante qui compare le transcriptome musculaire entre un modèle original de résistance naturelle à l'atrophie musculaire, l'ours brun hibernant, et un modèle classique d'atrophie induite, la souris suspendue par le train arrière. En utilisant le séquençage de l'ARN, nous avons identifié 4415 gènes différentiellement exprimés, dont 1746 gènes régulés à la hausse et 2369 gènes régulés à la baisse, dans les muscles de l'ours entre la période active et la période d'hibernation [351]. Nous nous sommes concentrés sur les signalisations du TGF- β et du BMP, respectivement impliquées dans la perte et le maintien de la masse musculaire. Les gènes liés à la signalisation du TGF- β et du BMP étaient respectivement, globalement régulés à la baisse et à la hausse dans les muscles non atrophiés de l'ours en hibernation, et le contraire était observable pour les muscles atrophiés de la souris immobilisée [351] (Figure 61). Ces résultats ont été confirmés au niveau protéique. Nos données suggèrent que l'équilibre TGF- β /BMP est crucial pour le maintien de la masse musculaire pendant une longue période d'inactivité physique. Cet équilibre pourrait venir d'un meilleur recrutement de SMAD4, l'acteur commun aux deux voies, du côté de la signalisation BMP, qui voit à la fois ses niveaux d'ARN messenger et de protéine augmentés pendant la période d'hibernation par rapport à la période active [351] (Figure 60). Nous avons également trouvé que la séquence protéique de SMAD4 était différente dans la famille des *Ursidae* par rapport aux autres mammifères ce qui pourrait induire une meilleure stabilité. De nombreuses interrogations restent en suspens quant à la mécanistique d'activation/inhibition de la balance TGF- β /BMP. Une première hypothèse serait qu'un des ligands de la signalisation BMP, GDF5, proviendrait du tissu adipeux qui subit une forte lipolyse pendant la période d'hibernation. En parallèle, les ligands de la signalisation TGF- β , qui proviennent habituellement de la résorption osseuse avec un impact direct sur la protéolyse musculaire, ne seraient pas présents en hiver considérant que l'ours hibernant résiste également à l'ostéoporose. Cette étude suggère que l'activation simultanée de la signalisation BMP pourrait potentialiser les thérapies inhibant la signalisation du TGF- β qui est déjà ciblée dans certains essais cliniques pour prévenir l'atrophie musculaire chez l'humain.

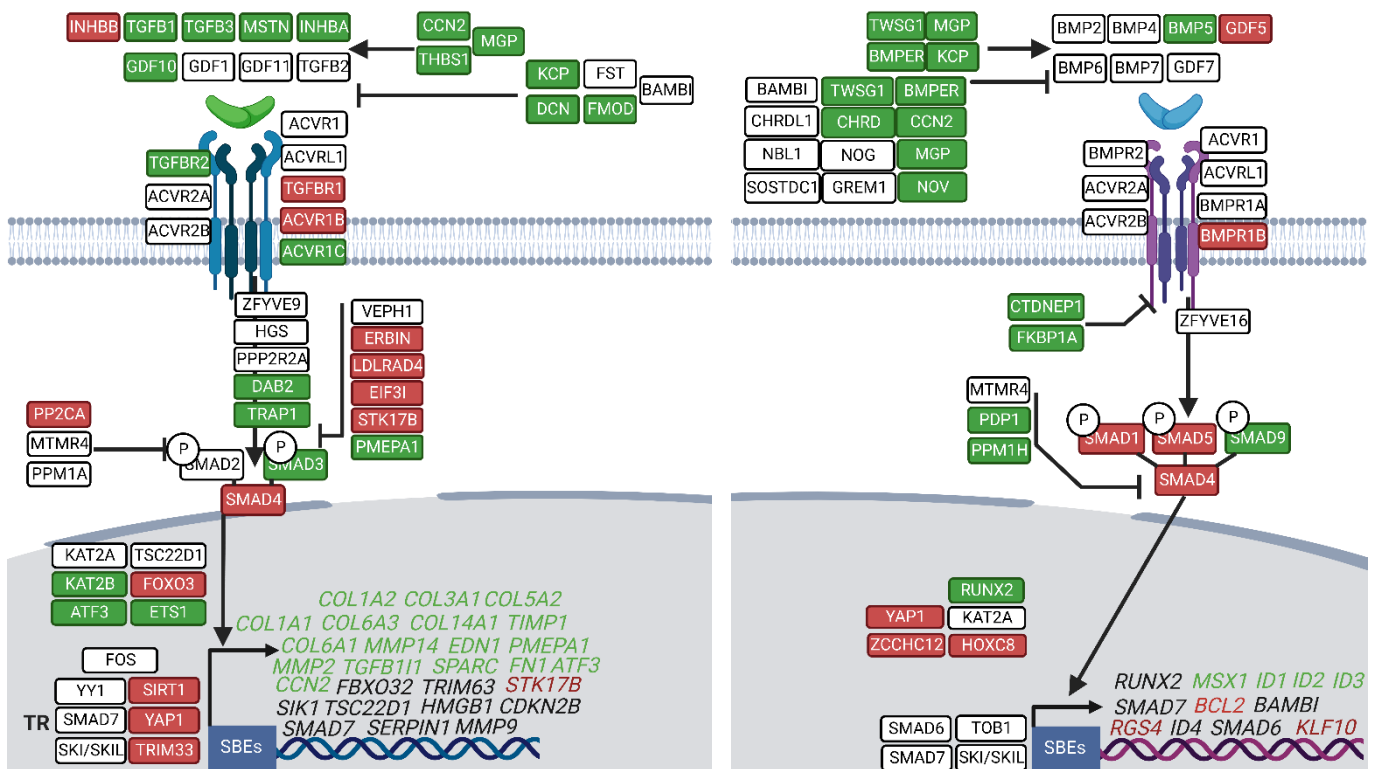


Figure 61. Expression des gènes associés aux signalisations TGF-β (à gauche) et BMP (à droite) dans les muscles de l'ours hibernants.

Figure simplifiée extraite de la publication Cussonneau et al., 2021 [351]. Schéma montrant les transcriptions des gènes impliqués dans les signalisations TGF-β et BMP du muscle vastus lateralis de l'ours brun et décrivant (1) leurs relations et (2) la différence de leurs niveaux d'expression entre les périodes d'hibernation et d'activité. Les cases rouges et vertes indiquent, respectivement, les gènes régulés à la hausse et à la baisse pendant l'hibernation par rapport à la saison d'été, et les cases blanches indiquent les gènes inchangés. Les gènes cibles des signalisations TGF-β et BMP sont indiqués en italique et sont en vert lorsqu'ils sont régulés à la baisse, en rouge lorsqu'ils sont régulés à la hausse, et en noir lorsqu'ils sont inchangés. Les flèches indiquent l'activation, et les barres ⊥ l'inhibition (n = 6 ours/saison, les mêmes individus ont été échantillonnés et analysés en été et en hiver). SBEs : SMAD Binding Element. Créé avec BioRender.com.

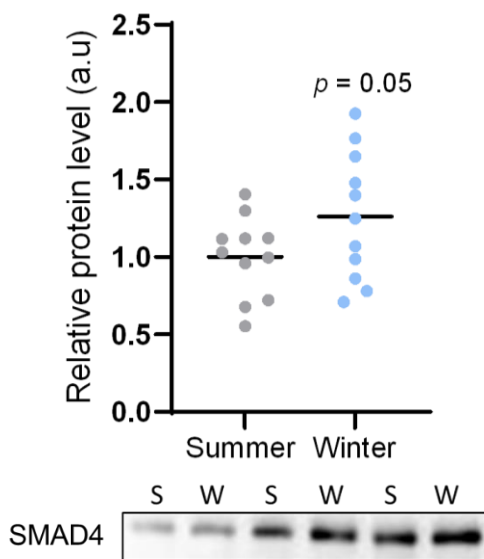


Figure 60. Les niveaux protéiques de SMAD4 sont augmentés dans le muscle de l'ours brun hibernant.

Les niveaux de la protéine SMAD4 ont été évalués par Western blots dans le muscle vastus latéralis des ours bruns pendant l'été (S) et l'hiver (W), et des Westerns blots représentatifs sont présentés pour trois couples d'ours. Les données sont représentées sous forme de valeurs individuelles avec des barres moyennes (n=11 ours/saison, les mêmes individus ont été échantillonnés et analysés en été et en hiver). Les points gris et bleus représentent les muscles des ours en été et en hiver respectivement.

10.6.3.2 Étude 2

Dans cette étude, nous avons exploré les conséquences musculaires de l'activation de la signalisation d'ATF4 par la molécule pharmacologique halofuginone au cours de l'atrophie musculaire induite par la suspension du train arrière chez la souris (HS). Premièrement, nous avons rapporté que l'activation des atrogènes d'ATF4 (*Gadd45a*, *Cdkn1a*) par l'halofuginone n'était pas associée à l'atrophie musculaire chez les souris en condition basale. De plus, les souris traitées à l'halofuginone ont montré une atrophie réduite par rapport aux souris non traitées au cours de l'HS, bien que l'induction de la signalisation d'ATF4 ait été identique à celle des souris HS non traitées (Figure 62). Nous avons également montré que l'halofuginone inhibait la signalisation du TGF- β tout en favorisant la signalisation du BMP chez les souris saines et préservait légèrement la synthèse protéique pendant l'HS (Figure 63). Enfin, nous avons montré que les atrogènes d'ATF4 étaient induits dans les muscles résistants à l'atrophie de l'ours brun hibernant, où nous avons précédemment également montré une inhibition de la signalisation du TGF- β simultanément à une activation de la signalisation BMP simultanées (étude 1). Globalement, nous avons montré dans cette étude que l'induction des atrogènes d'ATF4 pouvait être dissociée de l'atrophie musculaire. En outre, nos données indiquent également que l'halofuginone peut contrôler l'équilibre TGF- β /BMP vers le maintien de la masse musculaire. Une des questions qui reste en suspens est de savoir si la signalisation hypertrophique de BMP induite par l'halofuginone a pu contrecarrer les conséquences délétères supposées de l'induction des atrogènes d'ATF4. De plus, nous hypothésons que le programme transcriptionnel induit par ATF4 est également composé de gènes bénéfiques pour le maintien de l'homéostasie musculaire. Nous allons réaliser un séquençage d'ARN des muscles et des foies des souris traitées afin d'analyser plus en profondeur la signature transcriptomique du traitement à l'halofuginone.

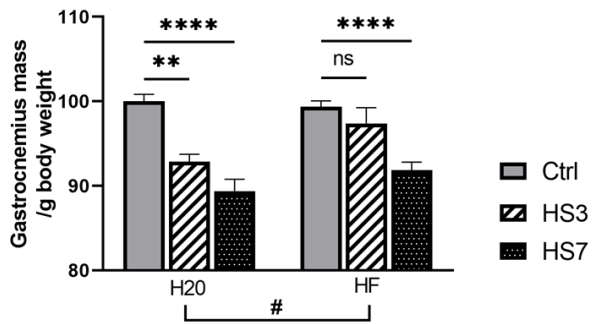


Figure 62. Le traitement à l'halofuginone avant la suspension par le train arrière atténué l'atrophie du muscle gastrocnémien chez les souris.

Les souris ont été traitées avec de l'H2O ou de l'halofuginone (HF, 0.25µg/g) 3 fois par semaine pendant 3 semaines et ont ensuite été soumises à une suspension du train arrière pendant 3 (HS3, barres hachurées) ou 7 (HS7, barres noires pointillées) jours ou non suspendues (Ctrl, barres grises). Masse du muscle gastrocnémien par gramme de poids corporel, les données sont des moyennes ± SEM (exprimées par rapport aux souris H2O-Ctrl). Test statistique d'ANOVA à deux facteurs : ** p_{adj} < 0.01; **** p_{adj} < 0.0001; ns= non-significatif ; # p_{adj} (effet de l'HF) < 0.05.

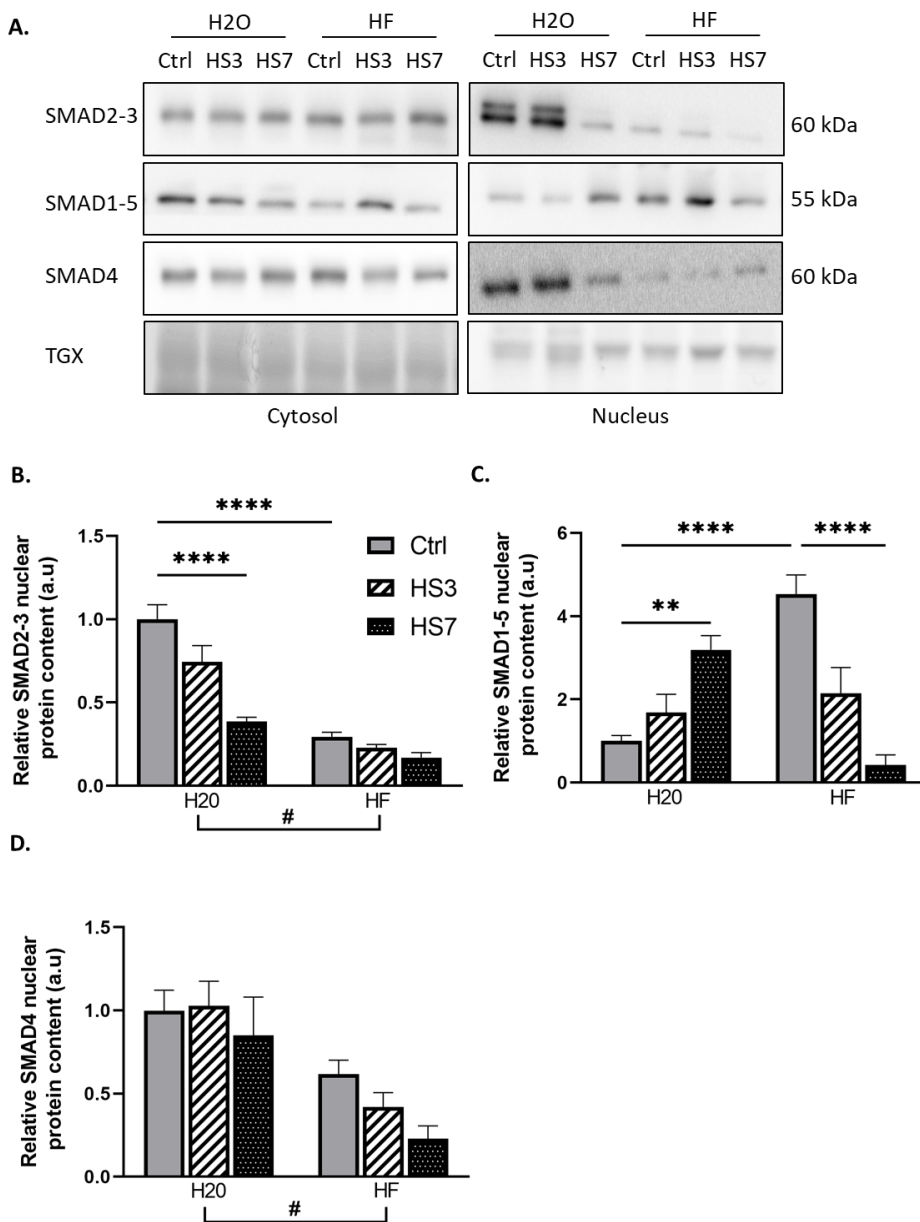


Figure 63. Le traitement à l'halofuginone inhibe la signalisation du TGF-β tout en favorisant la signalisation du BMP dans le muscle gastrocnémien chez les souris.

Le même protocole expérimental qu'expliqué dans la légende de la figure 63 a été réalisé. Les niveaux protéiques relatifs du gastrocnémien pour les facteurs de transcription (B) SMAD2-3 (TGF-β), (A) SMAD1-5 (BMP) et (C) SMAD4 (TGF-/BMP) ont été évalués dans la fraction subcellulaire nucléaire, quantifiés et normalisés en utilisant le signal TGX. Des Western blots représentatifs pour les fractions subcellulaires nucléaires et cytosoliques sont présentés. Les données sont des moyennes ± SEM (exprimées par rapport aux souris H2O-Ctrl). Test statistique d'ANOVA à deux facteurs : ** p_{adj} < 0,01 ; **** p_{adj} < 0,0001. # p_{adj} (effet de l'HF) < 0,05.

10.6.3.3 Étude 3

Cette dernière partie contient des résultats préliminaires. Nous avons cherché à reproduire les caractéristiques moléculaires du muscle résistant à l'atrophie des ours hibernants dans des cellules musculaires humaines. Notre équipe a précédemment publié des données montrant une augmentation de la teneur en protéines totales dans des cellules humaines musculaires cultivées avec du sérum d'ours hibernant (WBS), prouvant pour la première fois qu'un composé circulant était transmissible au matériel biologique humain et que ce composé avait un effet biologique sur les cellules [341]. En outre, dans l'étude 2, nous avons reproduit certaines des caractéristiques biomoléculaires des muscles d'ours bruns en hibernation dans des muscles de souris en utilisant la molécule halofuginone. Nous avons d'abord décidé d'examiner si le traitement au WBS pouvait reproduire, dans les cellules musculaires humaines *in vitro*, les modifications de l'équilibre TGF- β /BMP que nous avons observé dans les muscles d'ours hibernants *in vivo*. De 6h à 24h de traitement au WBS, nous avons observé une réduction de la luminescence du rapporteur ID1 dans les cellules musculaires humaines (Figure 64). La transcription de ce gène est également réprimée dans les muscles d'ours hibernants [351]. Ce résultat a été une autre preuve de concept qu'un ou plusieurs composés présents dans le sérum de l'ours hibernant avaient la faculté d'induire les mêmes modifications transcriptomiques observées *in vivo* en hiver.

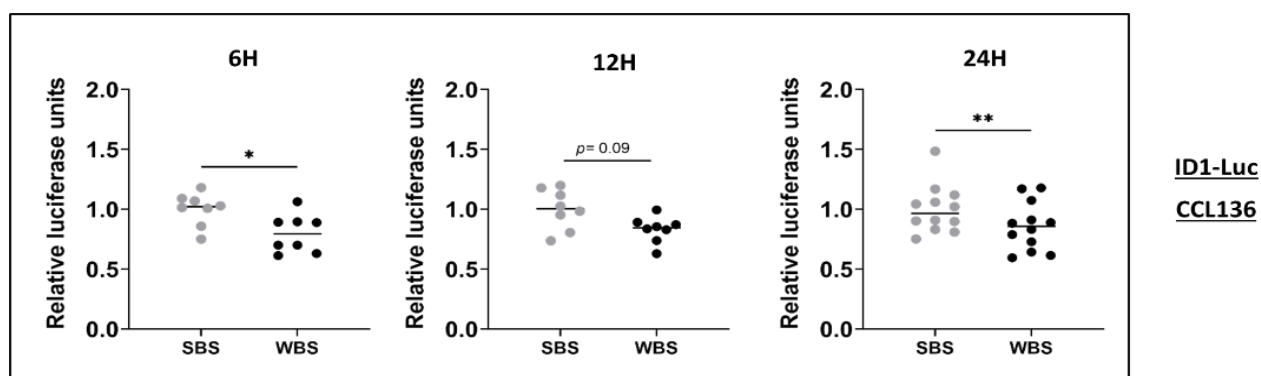


Figure 64. Le sérum d'ours d'hiver réprime la transcription du gène ID1 dans les cellules musculaires humaines.

Des cellules CCL136 ont été transfectées avec le plasmide ID1-Luc et cultivées avec du sérum d'ours d'été (SBS, points gris) ou du sérum d'ours d'hiver (WBS, points noirs) pendant 6, 12 ou 24 heures, puis les cellules ont été lysées et l'activité de la luciférase a été mesurée. Les données sont présentées sous forme de valeurs individuelles avec des barres moyennes (n = 12 sérum d'ours/saison, les mêmes individus ont été échantillonnés et analysés en été et en hiver). La signification statistique est indiquée (test t apparié de ratio) * pvalue<0,05 ; ** pvalue<0,01 ; ns : non significatif.

10.6.4 Conclusion générale

Certaines thérapies pour combattre l'atrophie musculaire ont été développées, notamment l'exercice physique, les interventions nutritionnelles et certains médicaments. Cependant, aucun traitement efficace n'a été trouvé pour prévenir complètement et en toute sécurité la fonte musculaire. En outre, malgré tous ses succès précliniques, la modulation de la signalisation du TGF- β ne s'est pas traduite par les effets souhaités chez l'Homme. La promotion de la signalisation BMP a reçu très peu d'attention à ce jour, et le concept selon lequel une régulation fine et simultanée des voies BMP et TGF- β pourrait être intéressante pour lutter contre l'atrophie musculaire a été mentionné dans très peu d'articles. L'utilisation d'un modèle de résistance naturelle à l'atrophie musculaire, l'ours brun en hibernation, présente un grand potentiel pour la découverte de nouvelles cibles thérapeutiques pour la clinique humaine. De plus, notre stratégie de physiologie comparative entre un modèle d'atrophie induite et un modèle résistant à l'atrophie a révélé de nouvelles pistes prometteuses pour de futurs traitements. Dans ce projet de thèse, nous avons (1) réalisé une analyse transcriptomique comparant des muscles d'ours en hibernation versus actifs à des muscles de souris suspendues versus contrôles, (2) étudié l'impact de l'induction contrôlée d'ATF4 par l'halofuginone chez des souris soumises à une suspension du train arrière et (3) exploré l'effet du sérum d'ours d'hiver sur des cellules musculaires humaines. Ces travaux ont (1) démontré que l'équilibre BMP/TGF- β est important dans le phénotype de résistance à l'atrophie musculaire et (2) suggéré qu'il pourrait être reproduit dans les cellules musculaires humaines par la présence de composés actifs circulants dans le sérum d'ours hibernant. L'identification de nouvelles cibles pertinentes au sein des signalisations BMP et TGF- β qui pourraient être modulées par les composés du sérum d'ours hibernant et l'identification de ces composés permettraient donc de développer des stratégies innovantes contre l'atrophie musculaire. La poursuite de ce projet est donc la première étape du développement futur de nouvelles solutions thérapeutiques pour conférer une résistance à l'atrophie musculaire chez l'homme.

11. References

1. Frontera, W.R.; Ochala, J. Skeletal Muscle: A Brief Review of Structure and Function. *Calcif Tissue Int* **2015**, *96*, 183–195, doi:10.1007/s00223-014-9915-y.
2. Zumbaugh, M.D.; Johnson, S.E.; Shi, T.H.; Gerrard, D.E. Molecular and Biochemical Regulation of Skeletal Muscle Metabolism. *Journal of Animal Science* **2022**, *100*, skac035, doi:10.1093/jas/skac035.
3. Schiaffino, S.; Reggiani, C. Fiber Types in Mammalian Skeletal Muscles. *Physiological Reviews* **2011**, *91*, 1447–1531, doi:10.1152/physrev.00031.2010.
4. Needham, D.M. RED AND WHITE MUSCLE. *Physiological Reviews* **1926**, doi:10.1152/physrev.1926.6.1.1.
5. Bloemberg, D.; Quadrilatero, J. Rapid Determination of Myosin Heavy Chain Expression in Rat, Mouse, and Human Skeletal Muscle Using Multicolor Immunofluorescence Analysis. *PLoS ONE* **2012**, *7*, e35273, doi:10.1371/journal.pone.0035273.
6. Brooke, M.H.; Kaiser, K.K. Muscle Fiber Types: How Many and What Kind? *Archives of Neurology* **1970**, *23*, 369–379, doi:10.1001/archneur.1970.00480280083010.
7. Gaitanos, G.C.; Williams, C.; Boobis, L.H.; Brooks, S. Human Muscle Metabolism during Intermittent Maximal Exercise. *Journal of Applied Physiology* **1993**, doi:10.1152/jappl.1993.75.2.712.
8. Vincent, A.E.; White, K.; Davey, T.; Philips, J.; Ogden, R.T.; Lawless, C.; Warren, C.; Hall, M.G.; Ng, Y.S.; Falkous, G.; et al. Quantitative 3D Mapping of the Human Skeletal Muscle Mitochondrial Network. *Cell Reports* **2019**, *26*, 996-1009.e4, doi:10.1016/j.celrep.2019.01.010.
9. Ferreira, R.; Vitorino, R.; Alves, R.M.P.; Appell, H.J.; Powers, S.K.; Duarte, J.A.; Amado, F. Subsarcolemmal and Intermyo-fibrillar Mitochondria Proteome Differences Disclose Functional Specializations in Skeletal Muscle. *Proteomics* **2010**, *10*, 3142–3154, doi:10.1002/pmic.201000173.
10. Romanello, V.; Sandri, M. Mitochondrial Biogenesis and Fragmentation as Regulators of Protein Degradation in Striated Muscles. *Journal of Molecular and Cellular Cardiology* **2013**, *55*, 64–72, doi:10.1016/j.yjmcc.2012.08.001.
11. Dahl, R.; Larsen, S.; Dohmann, T.L.; Qvortrup, K.; Helge, J.W.; Dela, F.; Prats, C. Three-Dimensional Reconstruction of the Human Skeletal Muscle Mitochondrial Network as a Tool to Assess Mitochondrial Content and Structural Organization. *Acta Physiol* **2015**, *213*, 145–155, doi:10.1111/apha.12289.
12. Mishra, P.; Varuzhanyan, G.; Pham, A.H.; Chan, D.C. Mitochondrial Dynamics Is a Distinguishing Feature of Skeletal Muscle Fiber Types and Regulates Organellar Compartmentalization. *Cell Metabolism* **2015**, *22*, 1033–1044, doi:10.1016/j.cmet.2015.09.027.
13. Romanello, V.; Sandri, M. The Connection between the Dynamic Remodeling of the Mitochondrial Network and the Regulation of Muscle Mass. *Cell. Mol. Life Sci.* **2021**, *78*, 1305–1328, doi:10.1007/s00018-020-03662-0.
14. Lewis-Smith, D.; Kamer, K.J.; Griffin, H.; Childs, A.-M.; Pysden, K.; Titov, D.; Duff, J.; Pyle, A.; Taylor, R.W.; Yu-Wai-Man, P.; et al. Homozygous Deletion in *MICU1* Presenting with Fatigue and Lethargy in Childhood. *Neurol Genet* **2016**, *2*, e59, doi:10.1212/NXG.000000000000059.

15. Pitceathly, R.D.S.; McFarland, R. Mitochondrial Myopathies in Adults and Children: Management and Therapy Development. *Current Opinion in Neurology* **2014**, *27*, 576–582, doi:10.1097/WCO.0000000000000126.
16. Riley, L.G.; Cooper, S.; Hickey, P.; Rudinger-Thirion, J.; McKenzie, M.; Compton, A.; Lim, S.C.; Thorburn, D.; Ryan, M.T.; Giegé, R.; et al. Mutation of the Mitochondrial Tyrosyl-TRNA Synthetase Gene, YARS2, Causes Myopathy, Lactic Acidosis, and Sideroblastic Anemia—MLASA Syndrome. *The American Journal of Human Genetics* **2010**, *87*, 52–59, doi:10.1016/j.ajhg.2010.06.001.
17. Vincent, A.E.; Ng, Y.S.; White, K.; Davey, T.; Mannella, C.; Falkous, G.; Feeney, C.; Schaefer, A.M.; McFarland, R.; Gorman, G.S.; et al. The Spectrum of Mitochondrial Ultrastructural Defects in Mitochondrial Myopathy. *Sci Rep* **2016**, *6*, 30610, doi:10.1038/srep30610.
18. Gehrig, S.M.; Mihaylova, V.; Frese, S.; Mueller, S.M.; Ligon-Auer, M.; Spengler, C.M.; Petersen, J.A.; Lundby, C.; Jung, H.H. Altered Skeletal Muscle (Mitochondrial) Properties in Patients with Mitochondrial DNA Single Deletion Myopathy. *Orphanet J Rare Dis* **2016**, *11*, 105, doi:10.1186/s13023-016-0488-x.
19. De Mario, A.; Gherardi, G.; Rizzuto, R.; Mammucari, C. Skeletal Muscle Mitochondria in Health and Disease. *Cell Calcium* **2021**, *94*, 102357, doi:10.1016/j.ceca.2021.102357.
20. Severinsen, M.C.K.; Pedersen, B.K. Muscle–Organ Crosstalk: The Emerging Roles of Myokines. *Endocr Rev* **2020**, *41*, 594–609, doi:10.1210/endrev/bnaa016.
21. Chen, W.; Wang, L.; You, W.; Shan, T. Myokines Mediate the Cross Talk between Skeletal Muscle and Other Organs. *J Cell Physiol* **2021**, *236*, 2393–2412, doi:10.1002/jcp.30033.
22. Thyfault, J.P.; Bergouignan, A. Exercise and Metabolic Health: Beyond Skeletal Muscle. *Diabetologia* **2020**, *63*, 1464–1474, doi:10.1007/s00125-020-05177-6.
23. Laurens, C.; Bergouignan, A.; Moro, C. Exercise-Released Myokines in the Control of Energy Metabolism. *Front. Physiol.* **2020**, *11*, 91, doi:10.3389/fphys.2020.00091.
24. McPherron, A.C.; Lawler, A.M.; Lee, S.-J. Regulation of Skeletal Muscle Mass in Mice by a New TGF- β Superfamily Member. **1997**, *8*.
25. Steensberg, A.; Hall, G.; Osada, T.; Sacchetti, M.; Saltin, B.; Pedersen, B.K. Production of Interleukin-6 in Contracting Human Skeletal Muscles Can Account for the Exercise-induced Increase in Plasma Interleukin-6. *The Journal of Physiology* **2000**, *529*, 237–242, doi:10.1111/j.1469-7793.2000.00237.x.
26. Pedersen, B.K.; Febbraio, M.A. Muscle as an Endocrine Organ: Focus on Muscle-Derived Interleukin-6. *Physiological Reviews* **2008**, *88*, 1379–1406, doi:10.1152/physrev.90100.2007.
27. Pedersen, B.K.; Steensberg, A.; Fischer, C.; Keller, C.; Keller, P.; Plomgaard, P.; Febbraio, M.; Saltin, B. Searching for the Exercise Factor: Is IL-6 a Candidate? *J Muscle Res Cell Motil* **2003**, *24*, 113–119, doi:10.1023/a:1026070911202.
28. Pedersen, B.K.; Febbraio, M.A. Muscles, Exercise and Obesity: Skeletal Muscle as a Secretory Organ. *Nat Rev Endocrinol* **2012**, *8*, 457–465, doi:10.1038/nrendo.2012.49.
29. Pang, B.P.S.; Chan, W.S.; Chan, C.B. Mitochondria Homeostasis and Oxidant/Antioxidant Balance in Skeletal Muscle—Do Myokines Play a Role? *Antioxidants* **2021**, *10*, 179, doi:10.3390/antiox10020179.

30. Wolfe, R.R. The Underappreciated Role of Muscle in Health and Disease. *Cell* **2013**, *153*, 8.
31. Felig, P.; Owen, O.E.; Wahren, J.; Cahill, G.F. Amino Acid Metabolism during Prolonged Starvation. *J. Clin. Invest.* **1969**, *48*, 584–594, doi:10.1172/JCI106017.
32. Biolo, G.; Zhang, X.-J.; Wolfe, R.R. Role of Membrane Transport in Interorgan Amino Acid Flow between Muscle and Small Intestine. *Metabolism* **1995**, *44*, 719–724, doi:10.1016/0026-0495(95)90183-3.
33. Drenick, E.J.; Swendseid, M.E.; Blahd, W.H.; Tuttle, S.G. Prolonged Starvation as Treatment for Severe Obesity. *JAMA* **1964**, *187*, doi:10.1001/jama.1964.03060150024006.
34. Felig, P. The Glucose-Alanine Cycle. *Metabolism* **1973**, *22*, 179–207, doi:10.1016/0026-0495(73)90269-2.
35. Chal, J.; Pourquié, O. Making Muscle: Skeletal Myogenesis *in Vivo* and *in Vitro*. *Development* **2017**, *144*, 2104–2122, doi:10.1242/dev.151035.
36. White, R.B.; Biérinx, A.-S.; Gnocchi, V.F.; Zammit, P.S. Dynamics of Muscle Fibre Growth during Postnatal Mouse Development. *BMC Dev Biol* **2010**, *10*, 21, doi:10.1186/1471-213X-10-21.
37. Vainshtein, A.; Sandri, M. Signaling Pathways That Control Muscle Mass. *IJMS* **2020**, *21*, 4759, doi:10.3390/ijms21134759.
38. Peris-Moreno, D.; Cussonneau, L.; Combaret, L.; Polge, C.; Taillandier, D. Ubiquitin Ligases at the Heart of Skeletal Muscle Atrophy Control. *Molecules* **2021**, *26*, 407, doi:10.3390/molecules26020407.
39. van Vliet, S.; Burd, N.A.; van Loon, L.J. The Skeletal Muscle Anabolic Response to Plant- versus Animal-Based Protein Consumption. *The Journal of Nutrition* **2015**, *145*, 1981–1991, doi:10.3945/jn.114.204305.
40. Witard, O.; Wardle, S.; Macnaughton, L.; Hodgson, A.; Tipton, K. Protein Considerations for Optimising Skeletal Muscle Mass in Healthy Young and Older Adults. *Nutrients* **2016**, *8*, 181, doi:10.3390/nu8040181.
41. Dideriksen, K.; Reitelseder, S.; Holm, L. Influence of Amino Acids, Dietary Protein, and Physical Activity on Muscle Mass Development in Humans. *Nutrients* **2013**, *5*, 852–876, doi:10.3390/nu5030852.
42. Gao, Y.; Arfat, Y.; Wang, H.; Goswami, N. Muscle Atrophy Induced by Mechanical Unloading: Mechanisms and Potential Countermeasures. *Front. Physiol.* **2018**, *9*, 235, doi:10.3389/fphys.2018.00235.
43. Kirby, T.J. Mechanosensitive Pathways Controlling Translation Regulatory Processes in Skeletal Muscle and Implications for Adaptation. *Journal of Applied Physiology* **2019**, *127*, 608–618, doi:10.1152/jappphysiol.01031.2018.
44. Wackerhage, H.; Schoenfeld, B.J.; Hamilton, D.L.; Lehti, M.; Hulmi, J.J. Stimuli and Sensors That Initiate Skeletal Muscle Hypertrophy Following Resistance Exercise. *Journal of Applied Physiology* **2019**, *126*, 30–43, doi:10.1152/jappphysiol.00685.2018.
45. Burkholder, T., J. Mechanotransduction in Skeletal Muscle. *Front Biosci* **2007**, *12*, 174, doi:10.2741/2057.

46. Miller, B.F. Human Muscle Protein Synthesis After Physical Activity and Feeding. *Exercise and Sport Sciences Reviews* **2007**, *35*, 50–55, doi:10.1097/jes.0b013e31803eac78.
47. Tipton, K.D.; Ferrando, A.A.; Phillips, S.M.; Doyle, D.; Wolfe, R.R. Postexercise Net Protein Synthesis in Human Muscle from Orally Administered Amino Acids. *American Journal of Physiology-Endocrinology and Metabolism* **1999**, *276*, E628–E634, doi:10.1152/ajpendo.1999.276.4.E628.
48. Yoon, M.-S. mTOR as a Key Regulator in Maintaining Skeletal Muscle Mass. *Front Physiol* **2017**, *8*, doi:10.3389/fphys.2017.00788.
49. Schiaffino, S.; Reggiani, C.; Akimoto, T.; Blaauw, B. Molecular Mechanisms of Skeletal Muscle Hypertrophy. *JND* **2021**, *8*, 169–183, doi:10.3233/JND-200568.
50. Drummond, M.J.; Fry, C.S.; Glynn, E.L.; Dreyer, H.C.; Dhanani, S.; Timmerman, K.L.; Volpi, E.; Rasmussen, B.B. Rapamycin Administration in Humans Blocks the Contraction-Induced Increase in Skeletal Muscle Protein Synthesis. *J Physiol* **2009**, *12*.
51. Risson, V.; Mazelin, L.; Roceri, M.; Sanchez, H.; Moncollin, V.; Corneloup, C.; Richard-Bulteau, H.; Vignaud, A.; Baas, D.; Defour, A.; et al. Muscle Inactivation of mTOR Causes Metabolic and Dystrophin Defects Leading to Severe Myopathy. *Journal of Cell Biology* **2009**, *187*, 859–874, doi:10.1083/jcb.200903131.
52. Laplante, M.; Sabatini, D.M. mTOR Signaling in Growth Control and Disease. *Cell* **2012**, *149*, 274–293, doi:10.1016/j.cell.2012.03.017.
53. Pasiakos, S.M.; Carbone, J.W. Assessment of Skeletal Muscle Proteolysis and the Regulatory Response to Nutrition and Exercise: Protein Degradation in Healthy Muscle. *IUBMB Life* **2014**, *66*, 478–484, doi:10.1002/iub.1291.
54. Tipton, K.D.; Hamilton, D.L.; Gallagher, I.J. Assessing the Role of Muscle Protein Breakdown in Response to Nutrition and Exercise in Humans. *Sports Med* **2018**, *48*, 53–64, doi:10.1007/s40279-017-0845-5.
55. Rabinowitz, J.D.; White, E. Autophagy and Metabolism. *Science* **2010**, *330*, 1344–1348, doi:10.1126/science.1193497.
56. Solomon, V.; Goldberg, A.L. Importance of the ATP-Ubiquitin-Proteasome Pathway in the Degradation of Soluble and Myofibrillar Proteins in Rabbit Muscle Extracts. *Journal of Biological Chemistry* **1996**, *271*, 26690–26697, doi:10.1074/jbc.271.43.26690.
57. Du, J.; Wang, X.; Miereles, C.; Bailey, J.L.; Debigare, R.; Zheng, B.; Price, S.R.; Mitch, W.E. Activation of Caspase-3 Is an Initial Step Triggering Accelerated Muscle Proteolysis in Catabolic Conditions. *J. Clin. Invest.* **2004**, *113*, 115–123, doi:10.1172/JCI18330.
58. Ju, J.-S.; Varadhachary, A.S.; Miller, S.E.; Wehl, C.C. Quantitation of “Autophagic Flux” in Mature Skeletal Muscle. *Autophagy* **2010**, *6*, 929–935, doi:10.4161/auto.6.7.12785.
59. Paré, M.F.; Baechler, B.L.; Fajardo, V.A.; Earl, E.; Wong, E.; Campbell, T.L.; Tupling, A.R.; Quadrilatero, J. Effect of Acute and Chronic Autophagy Deficiency on Skeletal Muscle Apoptotic Signaling, Morphology, and Function. *Biochimica et Biophysica Acta (BBA) - Molecular Cell Research* **2017**, *1864*, 708–718, doi:10.1016/j.bbamcr.2016.12.015.

60. Sylow, L.; Tokarz, V.L.; Richter, E.A.; Klip, A. The Many Actions of Insulin in Skeletal Muscle, the Paramount Tissue Determining Glycemia. *Cell Metabolism* **2021**, *33*, 758–780, doi:10.1016/j.cmet.2021.03.020.
61. Frendo-Cumbo, S.; Tokarz, V.L.; Bilan, P.J.; Brumell, J.H.; Klip, A. Communication Between Autophagy and Insulin Action: At the Crux of Insulin Action-Insulin Resistance? *Front. Cell Dev. Biol.* **2021**, *9*, 708431, doi:10.3389/fcell.2021.708431.
62. Franco-Romero, A.; Sandri, M. Role of Autophagy in Muscle Disease. *Molecular Aspects of Medicine* **2021**, *82*, 101041, doi:10.1016/j.mam.2021.101041.
63. Sandri, M. Protein Breakdown in Muscle Wasting: Role of Autophagy-Lysosome and Ubiquitin-Proteasome. *Int J Biochem Cell Biol* **2013**, *45*, 2121–2129, doi:10.1016/j.biocel.2013.04.023.
64. Masiero, E.; Agatea, L.; Mammucari, C.; Blaauw, B.; Loro, E.; Komatsu, M.; Metzger, D.; Reggiani, C.; Schiaffino, S.; Sandri, M. Autophagy Is Required to Maintain Muscle Mass. *Cell Metabolism* **2009**, *10*, 507–515, doi:10.1016/j.cmet.2009.10.008.
65. Carnio, S.; LoVerso, F.; Baraibar, M.A.; Longa, E.; Khan, M.M.; Maffei, M.; Reischl, M.; Canepari, M.; Loeffler, S.; Kern, H.; et al. Autophagy Impairment in Muscle Induces Neuromuscular Junction Degeneration and Precocious Aging. *Cell Rep* **2014**, *8*, 1509–1521, doi:10.1016/j.celrep.2014.07.061.
66. Leduc-Gaudet, J.-P.; Hussain, S.N.A.; Barreiro, E.; Gousspillou, G. Mitochondrial Dynamics and Mitophagy in Skeletal Muscle Health and Aging. *IJMS* **2021**, *22*, 8179, doi:10.3390/ijms22158179.
67. Romanello, V.; Guadagnin, E.; Gomes, L.; Roder, I.; Sandri, C.; Petersen, Y.; Milan, G.; Masiero, E.; Del Piccolo, P.; Foretz, M.; et al. Mitochondrial Fission and Remodelling Contributes to Muscle Atrophy. *EMBO J* **2010**, *29*, 1774–1785, doi:10.1038/emboj.2010.60.
68. Brown, J.L.; Rosa-Caldwell, M.E.; Lee, D.E.; Blackwell, T.A.; Brown, L.A.; Perry, R.A.; Haynie, W.S.; Hardee, J.P.; Carson, J.A.; Wiggs, M.P.; et al. Mitochondrial Degeneration Precedes the Development of Muscle Atrophy in Progression of Cancer Cachexia in Tumour-Bearing Mice: Mitochondrial Degeneration Precedes Cancer Cachexia. *Journal of Cachexia, Sarcopenia and Muscle* **2017**, *8*, 926–938, doi:10.1002/jcsm.12232.
69. Kee, A.J.; Combaret, L.; Talignac, T.; Souweine, B.; Arousseau, E.; Dalle, M.; Taillandier, D.; Attaix, D. Ubiquitin-proteasome-dependent Muscle Proteolysis Responds Slowly to Insulin Release and Refeeding in Starved Rats. *The Journal of Physiology* **2003**, *546*, 765–776, doi:10.1113/jphysiol.2002.032367.
70. Kitajima, Y.; Yoshioka, K.; Suzuki, N. The Ubiquitin–Proteasome System in Regulation of the Skeletal Muscle Homeostasis and Atrophy: From Basic Science to Disorders. *J Physiol Sci* **2020**, *70*, 40, doi:10.1186/s12576-020-00768-9.
71. Glickman, M.H.; Ciechanover, A. The Ubiquitin-Proteasome Proteolytic Pathway: Destruction for the Sake of Construction. *Physiological Reviews* **2002**, *82*, 373–428, doi:10.1152/physrev.00027.2001.
72. Ferrington, D.A.; Husom, A.D.; Thompson, L.V. Altered Proteasome Structure, Function, and Oxidation in Aged Muscle. *FASEB j.* **2005**, *19*, 1–24, doi:10.1096/fj.04-2578fje.

73. Kitajima, Y.; Tashiro, Y.; Suzuki, N.; Warita, H.; Kato, M.; Tateyama, M.; Ando, R.; Izumi, R.; Yamazaki, M.; Abe, M.; et al. Proteasome Dysfunction Induces Muscle Growth Defects and Protein Aggregation. *Journal of Cell Science* **2014**, jcs.150961, doi:10.1242/jcs.150961.
74. Pankiv, S.; Clausen, T.H.; Lamark, T.; Brech, A.; Bruun, J.-A.; Outzen, H.; Øvervatn, A.; Bjørkøy, G.; Johansen, T. P62/SQSTM1 Binds Directly to Atg8/LC3 to Facilitate Degradation of Ubiquitinated Protein Aggregates by Autophagy. *Journal of Biological Chemistry* **2007**, *282*, 24131–24145, doi:10.1074/jbc.M702824200.
75. Yin, L.; Li, N.; Jia, W.; Wang, N.; Liang, M.; Yang, X.; Du, G. Skeletal Muscle Atrophy: From Mechanisms to Treatments. *Pharmacological Research* **2021**, *172*, 105807, doi:10.1016/j.phrs.2021.105807.
76. Dao, T.; Green, A.E.; Kim, Y.A.; Bae, S.-J.; Ha, K.-T.; Gariani, K.; Lee, M.; Menzies, K.J.; Ryu, D. Sarcopenia and Muscle Aging: A Brief Overview. *Endocrinol Metab* **2020**, *35*, 716–732, doi:10.3803/EnM.2020.405.
77. Yang, W.; Huang, J.; Wu, H.; Wang, Y.; Du, Z.; Ling, Y.; Wang, W.; Wu, Q.; Gao, W. Molecular Mechanisms of Cancer Cachexia-induced Muscle Atrophy (Review). *Mol Med Rep* **2020**, *22*, 4967–4980, doi:10.3892/mmr.2020.11608.
78. Taivassalo, T.; Hepple, R.T. Integrating Mechanisms of Exacerbated Atrophy and Other Adverse Skeletal Muscle Impact in COPD. *Front. Physiol.* **2022**, *13*, 861617, doi:10.3389/fphys.2022.861617.
79. Wang, M.; Tan, Y.; Shi, Y.; Wang, X.; Liao, Z.; Wei, P. Diabetes and Sarcopenic Obesity: Pathogenesis, Diagnosis, and Treatments. *Front. Endocrinol.* **2020**, *11*, 568, doi:10.3389/fendo.2020.00568.
80. Sabatino, A.; Cuppari, L.; Stenvinkel, P.; Lindholm, B.; Avesani, C.M. Sarcopenia in Chronic Kidney Disease: What Have We Learned so Far? *J Nephrol* **2021**, *34*, 1347–1372, doi:10.1007/s40620-020-00840-y.
81. Curcio, F.; Testa, G.; Liguori, I.; Papillo, M.; Flocco, V.; Panicara, V.; Galizia, G.; Della-Morte, D.; Gargiulo, G.; Cacciatore, F.; et al. Sarcopenia and Heart Failure. *Nutrients* **2020**, *12*, 211, doi:10.3390/nu12010211.
82. Mankowski, R.T.; Laitano, O.; Clanton, T.L.; Brakenridge, S.C. Pathophysiology and Treatment Strategies of Acute Myopathy and Muscle Wasting after Sepsis. *JCM* **2021**, *10*, 1874, doi:10.3390/jcm10091874.
83. Knuth, C.M.; Auger, C.; Jeschke, M.G. Burn-Induced Hypermetabolism and Skeletal Muscle Dysfunction. *Am J Physiol Cell Physiol* **2021**, *321*, C58–C71, doi:10.1152/ajpcell.00106.2021.
84. Sieber, C.C. Malnutrition and Sarcopenia. *Aging Clin Exp Res* **2019**, *31*, 793–798, doi:10.1007/s40520-019-01170-1.
85. Howard, E.E.; Pasiakos, S.M.; Fussell, M.A.; Rodriguez, N.R. Skeletal Muscle Disuse Atrophy and the Rehabilitative Role of Protein in Recovery from Musculoskeletal Injury. *Advances in Nutrition* **2020**, *11*, 989–1001, doi:10.1093/advances/nmaa015.
86. Nunes, E.A.; Stokes, T.; McKendry, J.; Currier, B.S.; Phillips, S.M. Disuse-Induced Skeletal Muscle Atrophy in Disease and Nondisease States in Humans: Mechanisms, Prevention, and Recovery

- Strategies. *American Journal of Physiology-Cell Physiology* **2022**, *322*, C1068–C1084, doi:10.1152/ajpcell.00425.2021.
87. Alkner, B.A.; Tesch, P.A. Knee Extensor and Plantar Flexor Muscle Size and Function Following 90 Days of Bed Rest with or without Resistance Exercise. *Eur J Appl Physiol* **2004**, *93*, 294–305, doi:10.1007/s00421-004-1172-8.
88. Dirks, M.L.; Wall, B.T.; van de Valk, B.; Holloway, T.M.; Holloway, G.P.; Chabowski, A.; Goossens, G.H.; van Loon, L.J.C. One Week of Bed Rest Leads to Substantial Muscle Atrophy and Induces Whole-Body Insulin Resistance in the Absence of Skeletal Muscle Lipid Accumulation. *Diabetes* **2016**, *65*, 2862–2875, doi:10.2337/db15-1661.
89. Ferrando, A.A.; Lane, H.W.; Stuart, C.A.; Davis-Street, J.; Wolfe, R.R. Prolonged Bed Rest Decreases Skeletal Muscle and Whole Body Protein Synthesis. *American Journal of Physiology-Endocrinology and Metabolism* **1996**, *270*, E627–E633, doi:10.1152/ajpendo.1996.270.4.E627.
90. Trappe, S.; Trappe, T.; Gallagher, P.; Harber, M.; Alkner, B.; Tesch, P. Human Single Muscle Fibre Function with 84 Day Bed-Rest and Resistance Exercise. *J Physiol* **2004**, *557*, 501–513, doi:10.1113/jphysiol.2004.062166.
91. Narici, M.; Vito, G.D.; Franchi, M.; Paoli, A.; Moro, T.; Marcolin, G.; Grassi, B.; Baldassarre, G.; Zuccarelli, L.; Biolo, G.; et al. Impact of Sedentarism Due to the COVID-19 Home Confinement on Neuromuscular, Cardiovascular and Metabolic Health: Physiological and Pathophysiological Implications and Recommendations for Physical and Nutritional Countermeasures. *European Journal of Sport Science* **2021**, *21*, 614–635, doi:10.1080/17461391.2020.1761076.
92. Arnold, J.; Campbell, I.T.; Samuels, T.A.; Devlin, J.C.; Green, C.J.; Hipkin, L.J.; MacDonald, I.A.; Scrimgeour, C.M.; Smith, K.; Rennie, M.J. Increased Whole Body Protein Breakdown Predominates over Increased Whole Body Protein Synthesis in Multiple Organ Failure. *Clinical Science* **1993**, *84*, 655–661, doi:10.1042/cs0840655.
93. Goldberg, A.L. Protein Turnover in Skeletal Muscle. *Journal of Biological Chemistry* **1969**, *244*, 3223–3229, doi:10.1016/S0021-9258(18)93117-0.
94. Rennie, M.J.; Edwards, R.H.T.; Emery, P.W.; Halliday, D.; Lundholm, K.; Millward, D.J. Depressed Protein Synthesis Is the Dominant Characteristic of Muscle Wasting and Cachexia. *Clin Physiol* **1983**, *3*, 387–398, doi:10.1111/j.1475-097X.1983.tb00847.x.
95. Pedersen, B.K. The Physiology of Optimizing Health with a Focus on Exercise as Medicine. *Annu. Rev. Physiol.* **2019**, *81*, 607–627, doi:10.1146/annurev-physiol-020518-114339.
96. Nishikawa, H.; Asai, A.; Fukunishi, S.; Nishiguchi, S.; Higuchi, K. Metabolic Syndrome and Sarcopenia. *Nutrients* **2021**, *13*, 3519, doi:10.3390/nu13103519.
97. Yadav, A.; Yadav, S.S.; Singh, S.; Dabur, R. Natural Products: Potential Therapeutic Agents to Prevent Skeletal Muscle Atrophy. *European Journal of Pharmacology* **2022**, *925*, 174995, doi:10.1016/j.ejphar.2022.174995.
98. Lecker, S.H.; Jagoe, R.T.; Gilbert, A.; Gomes, M.; Baracos, V.; Bailey, J.; Price, S.R.; Mitch, W.E.; Goldberg, A.L. Multiple Types of Skeletal Muscle Atrophy Involve a Common Program of Changes in Gene Expression. *FASEB j.* **2004**, *18*, 39–51, doi:10.1096/fj.03-0610com.
99. Taillandier, D.; Polge, C. Skeletal Muscle Atrogenes: From Rodent Models to Human Pathologies. *Biochimie* **2019**, *166*, 251–269, doi:10.1016/j.biochi.2019.07.014.

100. Peris-Moreno, D.; Taillandier, D.; Polge, C. MuRF1/TRIM63, Master Regulator of Muscle Mass. *IJMS* **2020**, *21*, 6663, doi:10.3390/ijms21186663.
101. Lokireddy, S.; Wijesoma, I.W.; Sze, S.K.; McFarlane, C.; Kambadur, R.; Sharma, M. Identification of Atrogin-1-Targeted Proteins during the Myostatin-Induced Skeletal Muscle Wasting. *American Journal of Physiology-Cell Physiology* **2012**, *303*, C512–C529, doi:10.1152/ajpcell.00402.2011.
102. Toledo, M.; Penna, F.; Oliva, F.; Luque, M.; Betancourt, A.; Marmonti, E.; López-Soriano, F.J.; Argilés, J.M.; Busquets, S. A Multifactorial Anti-Cachectic Approach for Cancer Cachexia in a Rat Model Undergoing Chemotherapy: Chemotherapy and Cachexia. *Journal of Cachexia, Sarcopenia and Muscle* **2016**, *7*, 48–59, doi:10.1002/jcsm.12035.
103. Nadon, N.L. Of Mice and Monkeys: National Institute on Aging Resources Supporting the Use of Animal Models in Biogerontology Research. *The Journals of Gerontology Series A: Biological Sciences and Medical Sciences* **2006**, *61*, 813–815, doi:10.1093/gerona/61.8.813.
104. Dufresne, S.S.; Boulanger-Piette, A.; Frenette, J. Osteoprotegerin and B2-Agonists Mitigate Muscular Dystrophy in Slow- and Fast-Twitch Skeletal Muscles. *The American Journal of Pathology* **2017**, *187*, 498–504, doi:10.1016/j.ajpath.2016.11.006.
105. Weiss, A.; Attisano, L. The TGFbeta Superfamily Signaling Pathway. **2013**, *2*, 17.
106. Hata, A.; Chen, Y.-G. TGF- β Signaling from Receptors to Smads. *Cold Spring Harb Perspect Biol* **2016**, *8*, a022061, doi:10.1101/cshperspect.a022061.
107. Budi, E.H.; Duan, D.; Derynck, R. Transforming Growth Factor- β Receptors and Smads: Regulatory Complexity and Functional Versatility. *Trends in Cell Biology* **2017**, *27*, 658–672, doi:10.1016/j.tcb.2017.04.005.
108. Hill, C.S. Transcriptional Control by the SMADs. *Cold Spring Harb Perspect Biol* **2016**, *8*, doi:10.1101/cshperspect.a022079.
109. Robertson, I.B.; Rifkin, D.B. Regulation of the Bioavailability of TGF- β and TGF- β -Related Proteins. *Cold Spring Harb Perspect Biol* **2016**, *8*, a021907, doi:10.1101/cshperspect.a021907.
110. Sartori, R.; Gregorevic, P.; Sandri, M. TGF β and BMP Signaling in Skeletal Muscle: Potential Significance for Muscle-Related Disease. *Trends in Endocrinology & Metabolism* **2014**, *25*, 464–471, doi:10.1016/j.tem.2014.06.002.
111. Klein, G.L. Transforming Growth Factor-Beta in Skeletal Muscle Wasting. *IJMS* **2022**, *23*, 1167, doi:10.3390/ijms23031167.
112. Lee, S.-J.; McPherron, A.C. Regulation of Myostatin Activity and Muscle Growth. *Proc. Natl. Acad. Sci. U.S.A.* **2001**, *98*, 9306–9311, doi:10.1073/pnas.151270098.
113. Mosher, D.S.; Quignon, P.; Bustamante, C.D.; Sutter, N.B.; Mellersh, C.S.; Parker, H.G.; Ostrander, E.A. A Mutation in the Myostatin Gene Increases Muscle Mass and Enhances Racing Performance in Heterozygote Dogs. *PLoS Genet* **2007**, *3*, e79, doi:10.1371/journal.pgen.0030079.
114. Kollias, H.D.; McDermott, J.C. Transforming Growth Factor- β and Myostatin Signaling in Skeletal Muscle. *Journal of Applied Physiology* **2008**, *104*, 579–587, doi:10.1152/jappphysiol.01091.2007.

115. Han, H.Q.; Mitch, W.E. Targeting the Myostatin Signaling Pathway to Treat Muscle Wasting Diseases. *Current Opinion in Supportive & Palliative Care* **2011**, *5*, 334–341, doi:10.1097/SPC.0b013e32834bddf9.
116. Bataille, S.; Chauveau, P.; Fouque, D.; Aparicio, M.; Koppe, L. Myostatin and Muscle Atrophy during Chronic Kidney Disease. *Nephrology Dialysis Transplantation* **2021**, *36*, 1986–1993, doi:10.1093/ndt/gfaa129.
117. Fife, E.; Kostka, J.; Kroc, Ł.; Guligowska, A.; Pięłowska, M.; Sołtysik, B.; Kaufman-Szymczyk, A.; Fabianowska-Majewska, K.; Kostka, T. Relationship of Muscle Function to Circulating Myostatin, Follistatin and GDF11 in Older Women and Men. *BMC Geriatr* **2018**, *18*, 200, doi:10.1186/s12877-018-0888-y.
118. Elkina, Y.; von Haehling, S.; Anker, S.D.; Springer, J. The Role of Myostatin in Muscle Wasting: An Overview. *J Cachexia Sarcopenia Muscle* **2011**, *2*, 143–151, doi:10.1007/s13539-011-0035-5.
119. Suh, J.; Lee, Y.-S. Myostatin Inhibitors: Panacea or Predicament for Musculoskeletal Disorders? *J Bone Metab* **2020**, *27*, 151–165, doi:10.11005/jbm.2020.27.3.151.
120. Loumaye, A.; Thissen, J.-P. Biomarkers of Cancer Cachexia. *Clinical Biochemistry* **2017**, *50*, 1281–1288, doi:10.1016/j.clinbiochem.2017.07.011.
121. Loumaye, A.; de Barys, M.; Nachit, M.; Lause, P.; Frateur, L.; van Maanen, A.; Trefois, P.; Gruson, D.; Thissen, J.-P. Role of Activin A and Myostatin in Human Cancer Cachexia. *The Journal of Clinical Endocrinology & Metabolism* **2015**, *100*, 2030–2038, doi:10.1210/jc.2014-4318.
122. Loumaye, A.; de Barys, M.; Nachit, M.; Lause, P.; van Maanen, A.; Trefois, P.; Gruson, D.; Thissen, J.-P. Circulating Activin A Predicts Survival in Cancer Patients: Circulating ActivinA. *Journal of Cachexia, Sarcopenia and Muscle* **2017**, *8*, 768–777, doi:10.1002/jcsm.12209.
123. Ishitobi, M.; Haginoya, K.; Zhao, Y.; Ohnuma, A.; Minato, J.; Yanagisawa, T.; Tanabu, M.; Kikuchi, M.; Iinuma, K. Elevated Plasma Levels of Transforming Growth Factor $\alpha 1$ in Patients with Muscular Dystrophy. *3*.
124. Režen, T.; Kovanda, A.; Eiken, O.; Mekjavic, I.B.; Rogelj, B. Expression Changes in Human Skeletal Muscle miRNAs Following 10 Days of Bed Rest in Young Healthy Males. *Acta Physiol* **2014**, *210*, 655–666, doi:10.1111/apha.12228.
125. Garros, R.F.; Paul, R.; Connolly, M.; Lewis, A.; Garfield, B.E.; Natanek, S.A.; Bloch, S.; Mouly, V.; Griffiths, M.J.; Polkey, M.I.; et al. MicroRNA-542 Promotes Mitochondrial Dysfunction and SMAD Activity and Is Elevated in Intensive Care Unit–Acquired Weakness. *Am J Respir Crit Care Med* **2017**, *196*, 1422–1433, doi:10.1164/rccm.201701-0101OC.
126. Zimmers, T.A. Induction of Cachexia in Mice by Systemically Administered Myostatin. *Science* **2002**, *296*, 1486–1488, doi:10.1126/science.1069525.
127. Chen, J.L.; Walton, K.L.; Winbanks, C.E.; Murphy, K.T.; Thomson, R.E.; Makanji, Y.; Qian, H.; Lynch, G.S.; Harrison, C.A.; Gregorevic, P. Elevated Expression of Activins Promotes Muscle Wasting and Cachexia. *FASEB j.* **2014**, *28*, 1711–1723, doi:10.1096/fj.13-245894.
128. Latres, E.; Mastaitis, J.; Fury, W.; Miloscio, L.; Trejos, J.; Pangilinan, J.; Okamoto, H.; Cavino, K.; Na, E.; Papatheodorou, A.; et al. Activin A More Prominently Regulates Muscle Mass in Primates than Does GDF8. *Nat Commun* **2017**, *8*, 15153, doi:10.1038/ncomms15153.

129. McFarlane, C.; Plummer, E.; Thomas, M.; Hennebry, A.; Ashby, M.; Ling, N.; Smith, H.; Sharma, M.; Kambadur, R. Myostatin Induces Cachexia by Activating the Ubiquitin Proteolytic System through an NF-KB-Independent, FoxO1-Dependent Mechanism. *J. Cell. Physiol.* **2006**, *209*, 501–514, doi:10.1002/jcp.20757.
130. Zimmers, T.A.; Jiang, Y.; Wang, M.; Liang, T.W.; Rupert, J.E.; Au, E.D.; Marino, F.E.; Couch, M.E.; Koniaris, L.G. Exogenous GDF11 Induces Cardiac and Skeletal Muscle Dysfunction and Wasting. *Basic Res Cardiol* **2017**, *112*, 48, doi:10.1007/s00395-017-0639-9.
131. Sartori, R.; Milan, G.; Patron, M.; Mammucari, C.; Blaauw, B.; Abraham, R.; Sandri, M. Smad2 and 3 Transcription Factors Control Muscle Mass in Adulthood. *American Journal of Physiology-Cell Physiology* **2009**, *296*, C1248–C1257, doi:10.1152/ajpcell.00104.2009.
132. Tando, T.; Hirayama, A.; Furukawa, M.; Sato, Y.; Kobayashi, T.; Funayama, A.; Kanaji, A.; Hao, W.; Watanabe, R.; Morita, M.; et al. Smad2/3 Proteins Are Required for Immobilization-Induced Skeletal Muscle Atrophy. *J. Biol. Chem.* **2016**, *291*, 12184–12194, doi:10.1074/jbc.M115.680579.
133. Winbanks, C.E.; Weeks, K.L.; Thomson, R.E.; Sepulveda, P.V.; Beyer, C.; Qian, H.; Chen, J.L.; Allen, J.M.; Lancaster, G.I.; Febbraio, M.A.; et al. Follistatin-Mediated Skeletal Muscle Hypertrophy Is Regulated by Smad3 and MTOR Independently of Myostatin. *Journal of Cell Biology* **2012**, *197*, 997–1008, doi:10.1083/jcb.201109091.
134. Hillege, M.M.; Shi, A.; Galli, R.A.; Wu, G.; Bertolino, P.; Hoogaars, W.M.; Jaspers, R.T. Lack of Tgfr1 and Acvr1b Synergistically Stimulates Myofibre Hypertrophy and Accelerates Muscle Regeneration. *eLife* **2022**, *11*, e77610, doi:10.7554/eLife.77610.
135. Goodman, C.A.; McNally, R.M.; Hoffmann, F.M.; Hornberger, T.A. Smad3 Induces Atrogin-1, Inhibits MTOR and Protein Synthesis, and Promotes Muscle Atrophy In Vivo. *Molecular Endocrinology* **2013**, *27*, 1946–1957, doi:10.1210/me.2013-1194.
136. Bollinger, L.M.; Witczak, C.A.; Houmard, J.A.; Brault, J.J. SMAD3 Augments FoxO3-Induced MuRF-1 Promoter Activity in a DNA-Binding-Dependent Manner. *Am J Physiol Cell Physiol* **2014**, *307*, C278–C287, doi:10.1152/ajpcell.00391.2013.
137. Trendelenburg, A.U.; Meyer, A.; Rohner, D.; Boyle, J.; Hatakeyama, S.; Glass, D.J. Myostatin Reduces Akt/TORC1/P70S6K Signaling, Inhibiting Myoblast Differentiation and Myotube Size. *American Journal of Physiology-Cell Physiology* **2009**, *296*, C1258–C1270, doi:10.1152/ajpcell.00105.2009.
138. Amirouche, A.; Durieux, A.-C.; Banzet, S.; Koulmann, N.; Bonnefoy, R.; Mouret, C.; Bigard, X.; Peinnequin, A.; Freyssenet, D. Down-Regulation of Akt/Mammalian Target of Rapamycin Signaling Pathway in Response to Myostatin Overexpression in Skeletal Muscle. *Endocrinology* **2009**, *150*, 286–294, doi:10.1210/en.2008-0959.
139. Retamales, A.; Zuloaga, R.; Valenzuela, C.A.; Gallardo-Escarate, C.; Molina, A.; Valdés, J.A. Insulin-like Growth Factor-1 Suppresses the Myostatin Signaling Pathway during Myogenic Differentiation. *Biochemical and Biophysical Research Communications* **2015**, *464*, 596–602, doi:10.1016/j.bbrc.2015.07.018.
140. Timmer, L.T.; Hoogaars, W.M.H.; Jaspers, R.T. The Role of IGF-1 Signaling in Skeletal Muscle Atrophy. In *Muscle Atrophy*; Xiao, J., Ed.; Advances in Experimental Medicine and Biology; Springer Singapore: Singapore, 2018; Vol. 1088, pp. 109–137 ISBN 9789811314346.

141. Barbé, C.; Bray, F.; Gueugneau, M.; Devassine, S.; Lause, P.; Tokarski, C.; Rolando, C.; Thissen, J.-P. Comparative Proteomic and Transcriptomic Analysis of Follistatin-Induced Skeletal Muscle Hypertrophy. *J. Proteome Res.* **2017**, *16*, 3477–3490, doi:10.1021/acs.jproteome.7b00069.
142. Tiano, J.P.; Springer, D.A.; Rane, S.G. SMAD3 Negatively Regulates Serum Irisin and Skeletal Muscle FNDC5 and Peroxisome Proliferator-Activated Receptor γ Coactivator 1- α (PGC-1 α) during Exercise. *Journal of Biological Chemistry* **2015**, *290*, 7671–7684, doi:10.1074/jbc.M114.617399.
143. Böhm, A.; Hoffmann, C.; Irmeler, M.; Schneeweiss, P.; Schnauder, G.; Sailer, C.; Schmid, V.; Hudemann, J.; Machann, J.; Schick, F.; et al. TGF- β Contributes to Impaired Exercise Response by Suppression of Mitochondrial Key Regulators in Skeletal Muscle. *Diabetes* **2016**, *65*, 2849–2861, doi:10.2337/db15-1723.
144. VanderVeen, B.N.; Fix, D.K.; Carson, J.A. Disrupted Skeletal Muscle Mitochondrial Dynamics, Mitophagy, and Biogenesis during Cancer Cachexia: A Role for Inflammation. *Oxidative Medicine and Cellular Longevity* **2017**, *2017*, 1–13, doi:10.1155/2017/3292087.
145. Abrigo, J.; Rivera, J.C.; Simon, F.; Cabrera, D.; Cabello-Verrugio, C. Transforming Growth Factor Type Beta (TGF- β) Requires Reactive Oxygen Species to Induce Skeletal Muscle Atrophy. *Cellular Signalling* **2016**, *28*, 366–376, doi:10.1016/j.cellsig.2016.01.010.
146. Ismaeel, A.; Kim, J.-S.; Kirk, J.S.; Smith, R.S.; Bohannon, W.T.; Koutakis, P. Role of Transforming Growth Factor- β in Skeletal Muscle Fibrosis: A Review. *Int J Mol Sci* **2019**, *20*, doi:10.3390/ijms20102446.
147. Hu, H.-H.; Chen, D.-Q.; Wang, Y.-N.; Feng, Y.-L.; Cao, G.; Vaziri, N.D.; Zhao, Y.-Y. New Insights into TGF- β /Smad Signaling in Tissue Fibrosis. *Chemico-Biological Interactions* **2018**, *292*, 76–83, doi:10.1016/j.cbi.2018.07.008.
148. Lee, S.-J. Quadrupling Muscle Mass in Mice by Targeting TGF- β Signaling Pathways. *PLoS ONE* **2007**, *2*, e789, doi:10.1371/journal.pone.0000789.
149. Chen, J.L.; Walton, K.L.; Hagg, A.; Colgan, T.D.; Johnson, K.; Qian, H.; Gregorevic, P.; Harrison, C.A. Specific Targeting of TGF- β Family Ligands Demonstrates Distinct Roles in the Regulation of Muscle Mass in Health and Disease. *Proc Natl Acad Sci USA* **2017**, *201620013*, doi:10.1073/pnas.1620013114.
150. Morvan, F.; Rondeau, J.-M.; Zou, C.; Minetti, G.; Scheufler, C.; Scharenberg, M.; Jacobi, C.; Brebbia, P.; Ritter, V.; Toussaint, G.; et al. Blockade of Activin Type II Receptors with a Dual Anti-ActRIIA/IIB Antibody Is Critical to Promote Maximal Skeletal Muscle Hypertrophy. *Proc. Natl. Acad. Sci. U.S.A.* **2017**, *114*, 12448–12453, doi:10.1073/pnas.1707925114.
151. Ojima, C.; Noguchi, Y.; Miyamoto, T.; Saito, Y.; Orihashi, H.; Yoshimatsu, Y.; Watabe, T.; Takayama, K.; Hayashi, Y.; Itoh, F. Peptide-2 from Mouse Myostatin Precursor Protein Alleviates Muscle Wasting in Cancer-associated Cachexia. *Cancer Sci* **2020**, *111*, 2954–2964, doi:10.1111/cas.14520.
152. Jude, B.; Tissier, F.; Dubourg, A.; Droguet, M.; Castel, T.; Léon, K.; Giroux-Metges, M.-A.; Pennec, J.-P. TGF- β Pathway Inhibition Protects the Diaphragm From Sepsis-Induced Wasting and Weakness in Rat. *Shock* **2020**, *53*, 772–778, doi:10.1097/SHK.0000000000001393.

153. Liu, M.; Hammers, D.W.; Barton, E.R.; Sweeney, H.L. Activin Receptor Type IIB Inhibition Improves Muscle Phenotype and Function in a Mouse Model of Spinal Muscular Atrophy. *PLoS ONE* **2016**, *11*, e0166803, doi:10.1371/journal.pone.0166803.
154. Lee, S.-J.; Lehar, A.; Meir, J.U.; Koch, C.; Morgan, A.; Warren, L.E.; Rydzik, R.; Youngstrom, D.W.; Chandok, H.; George, J.; et al. Targeting Myostatin/Activin A Protects against Skeletal Muscle and Bone Loss during Spaceflight. *Proc. Natl. Acad. Sci. U.S.A.* **2020**, *117*, 23942–23951, doi:10.1073/pnas.2014716117.
155. Zhou, X.; Wang, J.L.; Lu, J.; Song, Y.; Kwak, K.S.; Jiao, Q.; Rosenfeld, R.; Chen, Q.; Boone, T.; Simonet, W.S.; et al. Reversal of Cancer Cachexia and Muscle Wasting by ActRIIB Antagonism Leads to Prolonged Survival. *Cell* **2010**, *142*, 531–543, doi:10.1016/j.cell.2010.07.011.
156. Cohen, T.V.; Kollias, H.D.; Liu, N.; Ward, C.W.; Wagner, K.R. Genetic Disruption of Smad7 Impairs Skeletal Muscle Growth and Regeneration: Genetic Disruption of Smad7 Impairs Skeletal Muscle. *J Physiol* **2015**, *593*, 2479–2497, doi:10.1113/JP270201.
157. Winbanks, C.E.; Murphy, K.T.; Bernardo, B.C.; Qian, H.; Liu, Y.; Sepulveda, P.V.; Beyer, C.; Hagg, A.; Thomson, R.E.; Chen, J.L.; et al. Smad7 Gene Delivery Prevents Muscle Wasting Associated with Cancer Cachexia in Mice. *Science Translational Medicine* **2016**, *8*, 348ra98-348ra98, doi:10.1126/scitranslmed.aac4976.
158. Huang, Q.K.; Qiao, H.-Y.; Fu, M.-H.; Li, G.; Li, W.-B.; Chen, Z.; Wei, J.; Liang, B.-S. MiR-206 Attenuates Denervation-Induced Skeletal Muscle Atrophy in Rats Through Regulation of Satellite Cell Differentiation via TGF- β 1, Smad3, and HDAC4 Signaling. *Med Sci Monit* **2016**, *22*, 1161–1170, doi:10.12659/MSM.897909.
159. Becker, C.; Lord, S.R.; Studenski, S.A.; Warden, S.J.; Fielding, R.A.; Recknor, C.P.; Hochberg, M.C.; Ferrari, S.L.; Blain, H.; Binder, E.F.; et al. Myostatin Antibody (LY2495655) in Older Weak Fallers: A Proof-of-Concept, Randomised, Phase 2 Trial. *The Lancet Diabetes & Endocrinology* **2015**, *3*, 948–957, doi:10.1016/S2213-8587(15)00298-3.
160. Amato, A.A.; Hanna, M.G.; Machado, P.M.; Badrising, U.A.; Chinoy, H.; Benveniste, O.; Karanam, A.K.; Wu, M.; Tankó, L.B.; Schubert-Tennigkeit, A.A.; et al. Efficacy and Safety of Bimagrumab in Sporadic Inclusion Body Myositis: Long-Term Extension of RESILIENT. *Neurology* **2021**, *96*, e1595–e1607, doi:10.1212/WNL.0000000000011626.
161. Hofbauer, L.C.; Witvrouw, R.; Varga, Z.; Shiota, N.; Cremer, M.; Tanko, L.B.; Rooks, D.; Auberson, L.Z.; Arkuszewski, M.; Fretault, N.; et al. Bimagrumab to Improve Recovery after Hip Fracture in Older Adults: A Multicentre, Double-Blind, Randomised, Parallel-Group, Placebo-Controlled, Phase 2a/b Trial. *The Lancet Healthy Longevity* **2021**, *2*, e263–e274, doi:10.1016/S2666-7568(21)00084-2.
162. Rooks, D.; Swan, T.; Goswami, B.; Filosa, L.A.; Bunte, O.; Panchaud, N.; Coleman, L.A.; Miller, R.R.; Garcia Garayoa, E.; Praestgaard, J.; et al. Bimagrumab vs Optimized Standard of Care for Treatment of Sarcopenia in Community-Dwelling Older Adults: A Randomized Clinical Trial. *JAMA Netw Open* **2020**, *3*, e2020836, doi:10.1001/jamanetworkopen.2020.20836.
163. Polkey, M.I.; Praestgaard, J.; Berwick, A.; Franssen, F.M.E.; Singh, D.; Steiner, M.C.; Casaburi, R.; Tillmann, H.-C.; Lach-Trifilieff, E.; Roubenoff, R.; et al. Activin Type II Receptor Blockade for Treatment of Muscle Depletion in Chronic Obstructive Pulmonary Disease. A Randomized Trial. *Am J Respir Crit Care Med* **2019**, *199*, 313–320, doi:10.1164/rccm.201802-0286OC.

164. Abrigo, J.; Simon, F.; Cabrera, D.; Cordova, G.; Trollet, C.; Cabello-Verrugio, C. Central Role of Transforming Growth Factor Type Beta 1 in Skeletal Muscle Dysfunctions: An Update on Therapeutic Strategies. *CPPS* **2018**, *19*, 1189–1200, doi:10.2174/1389203718666171117101916.
165. Wang, R.N.; Green, J.; Wang, Z.; Deng, Y.; Qiao, M.; Peabody, M.; Zhang, Q.; Ye, J.; Yan, Z.; Denduluri, S.; et al. Bone Morphogenetic Protein (BMP) Signaling in Development and Human Diseases. *Genes & Diseases* **2014**, *1*, 87–105, doi:10.1016/j.gendis.2014.07.005.
166. Sartori, R.; Schirwis, E.; Blaauw, B.; Bortolanza, S.; Zhao, J.; Enzo, E.; Stantzou, A.; Mouisel, E.; Toniolo, L.; Ferry, A.; et al. BMP Signaling Controls Muscle Mass. *Nat Genet* **2013**, *45*, 1309–1318, doi:10.1038/ng.2772.
167. Winbanks, C.E.; Chen, J.L.; Qian, H.; Liu, Y.; Bernardo, B.C.; Beyer, C.; Watt, K.I.; Thomson, R.E.; Connor, T.; Turner, B.J.; et al. The Bone Morphogenetic Protein Axis Is a Positive Regulator of Skeletal Muscle Mass. *The Journal of Cell Biology* **2013**, *203*, 345–357, doi:10.1083/jcb.201211134.
168. Sartori, R.; Hagg, A.; Zampieri, S.; Armani, A.; Winbanks, C.E.; Viana, L.R.; Haidar, M.; Watt, K.I.; Qian, H.; Pezzini, C.; et al. Perturbed BMP Signaling and Denervation Promote Muscle Wasting in Cancer Cachexia. *Sci. Transl. Med.* **2021**, *13*, eaay9592, doi:10.1126/scitranslmed.aay9592.
169. Scimeca, M.; Piccirilli, E.; Mastrangeli, F.; Rao, C.; Feola, M.; Orlandi, A.; Gasbarra, E.; Bonanno, E.; Tarantino, U. Bone Morphogenetic Proteins and Myostatin Pathways: Key Mediator of Human Sarcopenia. *J Transl Med* **2017**, *15*, 34, doi:10.1186/s12967-017-1143-6.
170. Neppl, R.L.; Wu, C.-L.; Walsh, K. LncRNA Chronos Is an Aging-Induced Inhibitor of Muscle Hypertrophy. *Journal of Cell Biology* **2017**, *216*, 3497–3507, doi:10.1083/jcb.201612100.
171. Le Goff, C.; Mahaut, C.; Abhyankar, A.; Le Goff, W.; Serre, V.; Afenjar, A.; Destrée, A.; di Rocco, M.; Héron, D.; Jacquemont, S.; et al. Mutations at a Single Codon in Mad Homology 2 Domain of SMAD4 Cause Myhre Syndrome. *Nat Genet* **2012**, *44*, 85–88, doi:10.1038/ng.1016.
172. Zhang, Y.E. Non-Smad Signaling Pathways of the TGF- β Family. *Cold Spring Harb Perspect Biol* **2017**, *9*, a022129, doi:10.1101/cshperspect.a022129.
173. Kim, S.I. TGF- β -Activated Kinase-1_ New Insights into the Mechanism of TGF- β Signaling and Kidney Disease. **2012**, *12*.
174. Boergermann, J.H.; Kopf, J.; Yu, P.B.; Knaus, P. Dorsomorphin and LDN-193189 Inhibit BMP-Mediated Smad, P38 and Akt Signalling in C2C12 Cells. *The International Journal of Biochemistry & Cell Biology* **2010**, *42*, 1802–1807, doi:10.1016/j.biocel.2010.07.018.
175. Yamashita, M.; Fatyol, K.; Jin, C.; Wang, X.; Liu, Z.; Zhang, Y.E. TRAF6 Mediates Smad-Independent Activation of JNK and P38 by TGF- β . *Molecular Cell* **2008**, *31*, 918–924, doi:10.1016/j.molcel.2008.09.002.
176. Paul, P.K.; Bhatnagar, S.; Mishra, V.; Srivastava, S.; Darnay, B.G.; Choi, Y.; Kumar, A. The E3 Ubiquitin Ligase TRAF6 Intercedes in Starvation-Induced Skeletal Muscle Atrophy through Multiple Mechanisms. *Molecular and Cellular Biology* **2012**, *32*, 1248–1259, doi:10.1128/MCB.06351-11.
177. Paul, P.K.; Gupta, S.K.; Bhatnagar, S.; Panguluri, S.K.; Darnay, B.G.; Choi, Y.; Kumar, A. Targeted Ablation of TRAF6 Inhibits Skeletal Muscle Wasting in Mice. *The Journal of Cell Biology* **2010**, *191*, 1395–1411, doi:10.1083/jcb.201006098.

178. Paul, P.K.; Kumar, A. TRAF6 Coordinates the Activation of Autophagy and Ubiquitin-Proteasome Systems in Atrophying Skeletal Muscle. *Autophagy* **2011**, *7*, 555–556, doi:10.4161/auto.7.5.15102.
179. Sun, Y.-S.; Ye, Z.-Y.; Qian, Z.-Y.; Xu, X.-D.; Hu, J.-F. Expression of TRAF6 and Ubiquitin mRNA in Skeletal Muscle of Gastric Cancer Patients. *J Exp Clin Cancer Res* **2012**, *31*, 81, doi:10.1186/1756-9966-31-81.
180. Ding, H.; Zhang, G.; Sin, K.W.T.; Liu, Z.; Lin, R.-K.; Li, M.; Li, Y.-P. Activin A Induces Skeletal Muscle Catabolism via P38 β Mitogen-Activated Protein Kinase: Activin A Induces Skeletal Muscle Catabolism. *Journal of Cachexia, Sarcopenia and Muscle* **2017**, *8*, 202–212, doi:10.1002/jcsm.12145.
181. Xu, D.; Zhao, L.; Li, S.; Huang, X.; Li, C.; Sun, L.; Li, X.; Zhang, L.; Jiang, Z. Catalpol Counteracts the Pathology in a Mouse Model of Duchenne Muscular Dystrophy by Inhibiting the TGF-B1/TAK1 Signaling Pathway. *Acta Pharmacol Sin* **2021**, *42*, 1080–1089, doi:10.1038/s41401-020-00515-1.
182. Hindi, S.M.; Sato, S.; Xiong, G.; Bohnert, K.R.; Gibb, A.A.; Gallot, Y.S.; McMillan, J.D.; Hill, B.G.; Uchida, S.; Kumar, A. TAK1 Regulates Skeletal Muscle Mass and Mitochondrial Function. *JCI Insight* **2018**, *3*, e98441, doi:10.1172/jci.insight.98441.
183. Roy, A.; Sharma, A.K.; Nellore, K.; Narkar, V.A.; Kumar, A. TAK1 Preserves Skeletal Muscle Mass and Mitochondrial Function through Redox Homeostasis. *FASEB BioAdvances* **2020**, *2*, 538–553, doi:10.1096/fba.2020-00043.
184. Roy, A.; Kumar, A. Supraphysiological Activation of TAK1 Promotes Skeletal Muscle Growth and Mitigates Neurogenic Atrophy. *Nat Commun* **2022**, *13*, 2201, doi:10.1038/s41467-022-29752-0.
185. Black, B.L.; Olson, E.N. TRANSCRIPTIONAL CONTROL OF MUSCLE DEVELOPMENT BY MYOCYTE ENHANCER FACTOR-2 (MEF2) PROTEINS. *Annu. Rev. Cell Dev. Biol.* **1998**, *14*, 167–196, doi:10.1146/annurev.cellbio.14.1.167.
186. Richter, E.A.; Hargreaves, M. Exercise, GLUT4, and Skeletal Muscle Glucose Uptake. *Physiological Reviews* **2013**, *93*, 993–1017, doi:10.1152/physrev.00038.2012.
187. Anderson, C.M.; Hu, J.; Barnes, R.M.; Heidt, A.B.; Cornelissen, I.; Black, B.L. Myocyte Enhancer Factor 2C Function in Skeletal Muscle Is Required for Normal Growth and Glucose Metabolism in Mice. *Skeletal Muscle* **2015**, *5*, 7, doi:10.1186/s13395-015-0031-0.
188. Wu, Z.; Woodring, P.J.; Bhakta, K.S.; Tamura, K.; Wen, F.; Feramisco, J.R.; Karin, M.; Wang, J.Y.J.; Puri, P.L. P38 and Extracellular Signal-Regulated Kinases Regulate the Myogenic Program at Multiple Steps. *Mol Cell Biol* **2000**, *20*, 3951–3964, doi:10.1128/MCB.20.11.3951-3964.2000.
189. Zetser, A.; Gredinger, E.; Bengal, E. P38 Mitogen-Activated Protein Kinase Pathway Promotes Skeletal Muscle Differentiation. *Journal of Biological Chemistry* **1999**, *274*, 5193–5200, doi:10.1074/jbc.274.8.5193.
190. Xiao, F.; Wang, H.; Fu, X.; Li, Y.; Wu, Z. TRAF6 Promotes Myogenic Differentiation via the TAK1/P38 Mitogen-Activated Protein Kinase and Akt Pathways. *PLoS ONE* **2012**, *7*, e34081, doi:10.1371/journal.pone.0034081.
191. Liu, D.; Black, B.L.; Derynck, R. TGF- β Inhibits Muscle Differentiation through Functional Repression of Myogenic Transcription Factors by Smad3. *17*.

192. Loumaye, A.; Lause, P.; Zhong, X.; Zimmers, T.A.; Bindels, L.B.; Thissen, J.-P. Activin A Causes Muscle Atrophy through MEF2C-Dependent Impaired Myogenesis. *Cells* **2022**, *11*, 1119, doi:10.3390/cells11071119.
193. Costa-Mattioli, M.; Walter, P. The Integrated Stress Response: From Mechanism to Disease. *Science* **2020**, *368*, eaat5314, doi:10.1126/science.aat5314.
194. Pakos-Zebrucka, K.; Koryga, I.; Mnich, K.; Ljujic, M.; Samali, A.; Gorman, A.M. The Integrated Stress Response. *EMBO reports* **2016**, *17*, 1374–1395, doi:10.15252/embr.201642195.
195. Vattem, K.M.; Wek, R.C. Reinitiation Involving Upstream ORFs Regulates ATF4 MRNA Translation in Mammalian Cells. *6*.
196. Ameri, K.; Harris, A.L. Activating Transcription Factor 4. *The International Journal of Biochemistry & Cell Biology* **2008**, *40*, 14–21, doi:10.1016/j.biocel.2007.01.020.
197. B'chir, W.; Maurin, A.-C.; Carraro, V.; Averous, J.; Jousse, C.; Muranishi, Y.; Parry, L.; Stepien, G.; Fafournoux, P.; Bruhat, A. The EIF2 α /ATF4 Pathway Is Essential for Stress-Induced Autophagy Gene Expression. *Nucleic Acids Research* **2013**, *41*, 7683–7699, doi:10.1093/nar/gkt563.
198. Kilberg, M.S.; Shan, J.; Su, N. ATF4-Dependent Transcription Mediates Signaling of Amino Acid Limitation. *Trends in Endocrinology & Metabolism* **2009**, *20*, 436–443, doi:10.1016/j.tem.2009.05.008.
199. Han, S.; Zhu, L.; Zhu, Y.; Meng, Y.; Li, J.; Song, P.; Yousafzai, N.A.; Feng, L.; Chen, M.; Wang, Y.; et al. Targeting ATF4-Dependent pro-Survival Autophagy to Synergize Glutaminolysis Inhibition. *Theranostics* **2021**, *11*, 8464–8479, doi:10.7150/thno.60028.
200. Kojima, E.; Takeuchi, A.; Haneda, M.; Yagi, F.; Hasegawa, T.; Yamaki, K.-I.; Takeda, K.; Akira, S.; Shimokata, K.; Isobe, K.-I. The Function of GADD34 Is a Recovery from a Shutoff of Protein Synthesis Induced by ER Stress—Elucidation by GADD34-deficient Mice. *FASEB j.* **2003**, *17*, 1–18, doi:10.1096/fj.02-1184fje.
201. Teske, B.F.; Fusakio, M.E.; Zhou, D.; Shan, J.; McClintick, J.N.; Kilberg, M.S.; Wek, R.C. CHOP Induces Activating Transcription Factor 5 (ATF5) to Trigger Apoptosis in Response to Perturbations in Protein Homeostasis. *MBoC* **2013**, *24*, 2477–2490, doi:10.1091/mbc.e13-01-0067.
202. Iurlaro, R.; Püschel, F.; León-Annicchiarico, C.L.; O'Connor, H.; Martin, S.J.; Palou-Gramón, D.; Lucendo, E.; Muñoz-Pinedo, C. Glucose Deprivation Induces ATF4-Mediated Apoptosis through TRAIL Death Receptors. *Mol Cell Biol* **2017**, *37*, e00479-16, doi:10.1128/MCB.00479-16.
203. Qing, G.; Li, B.; Vu, A.; Skuli, N.; Walton, Z.E.; Liu, X.; Mayes, P.A.; Wise, D.R.; Thompson, C.B.; Maris, J.M.; et al. ATF4 Regulates MYC-Mediated Neuroblastoma Cell Death upon Glutamine Deprivation. *Cancer Cell* **2012**, *22*, 631–644, doi:10.1016/j.ccr.2012.09.021.
204. B'chir, W.; Chaveroux, C.; Carraro, V.; Averous, J.; Maurin, A.-C.; Jousse, C.; Muranishi, Y.; Parry, L.; Fafournoux, P.; Bruhat, A. Dual Role for CHOP in the Crosstalk between Autophagy and Apoptosis to Determine Cell Fate in Response to Amino Acid Deprivation. *Cellular Signalling* **2014**, *26*, 1385–1391, doi:10.1016/j.cellsig.2014.03.009.
205. Byles, V.; Cormerais, Y.; Kalafut, K.; Barrera, V.; Hughes Hallett, J.E.; Sui, S.H.; Asara, J.M.; Adams, C.M.; Hoxhaj, G.; Ben-Sahra, I.; et al. Hepatic mTORC1 Signaling Activates ATF4 as Part of Its Metabolic Response to Feeding and Insulin. *Molecular Metabolism* **2021**, *53*, 101309, doi:10.1016/j.molmet.2021.101309.

206. Malmberg, S.E.; Adams, C.M. Insulin Signaling and the General Amino Acid Control Response. *Journal of Biological Chemistry* **2008**, *283*, 19229–19234, doi:10.1074/jbc.M801331200.
207. Ebert, S.M.; Rasmussen, B.B.; Judge, A.R.; Judge, S.M.; Larsson, L.; Wek, R.C.; Anthony, T.G.; Marcotte, G.R.; Miller, M.J.; Yorek, M.A.; et al. Biology of Activating Transcription Factor 4 (ATF4) and Its Role in Skeletal Muscle Atrophy. *The Journal of Nutrition* **2022**, *152*, 926–938, doi:10.1093/jn/nxab440.
208. Adams, C.M. Role of the Transcription Factor ATF4 in the Anabolic Actions of Insulin and the Anti-Anabolic Actions of Glucocorticoids. *Journal of Biological Chemistry* **2007**, *282*, 16744–16753, doi:10.1074/jbc.M610510200.
209. Park, Y.; Reyna-Neyra, A.; Philippe, L.; Thoreen, C.C. mTORC1 Balances Cellular Amino Acid Supply with Demand for Protein Synthesis through Post-Transcriptional Control of ATF4. *Cell Reports* **2017**, *19*, 1083–1090, doi:10.1016/j.celrep.2017.04.042.
210. Jin, H.-O.; Seo, S.-K.; Woo, S.-H.; Choe, T.-B.; Hong, S.-I.; Kim, J.-I.; Park, I.-C. Nuclear Protein 1 Induced by ATF4 in Response to Various Stressors Acts as a Positive Regulator on the Transcriptional Activation of ATF4. *IUBMB Life* **2009**, *61*, 1153–1158, doi:10.1002/iub.271.
211. Deegan, S.; Koryga, I.; Glynn, S.A.; Gupta, S.; Gorman, A.M.; Samali, A. A Close Connection between the PERK and IRE Arms of the UPR and the Transcriptional Regulation of Autophagy. *Biochemical and Biophysical Research Communications* **2015**, *456*, 305–311, doi:10.1016/j.bbrc.2014.11.076.
212. Luhr, M.; Torgersen, M.L.; Szalai, P.; Hashim, A.; Brech, A.; Staerk, J.; Engedal, N. The Kinase PERK and the Transcription Factor ATF4 Play Distinct and Essential Roles in Autophagy Resulting from Tunicamycin-Induced ER Stress. *Journal of Biological Chemistry* **2019**, *294*, 8197–8217, doi:10.1074/jbc.RA118.002829.
213. Shao, L.; Xiong, X.; Zhang, Y.; Miao, H.; Ren, Y.; Tang, X.; Song, J.; Wang, C. IL-22 Ameliorates LPS-Induced Acute Liver Injury by Autophagy Activation through ATF4-ATG7 Signaling. *Cell Death Dis* **2020**, *11*, 970, doi:10.1038/s41419-020-03176-4.
214. Sciarretta, S.; Zhai, P.; Shao, D.; Zablocki, D.; Nagarajan, N.; Terada, L.S.; Volpe, M.; Sadoshima, J. Activation of NADPH Oxidase 4 in the Endoplasmic Reticulum Promotes Cardiomyocyte Autophagy and Survival During Energy Stress Through the Protein Kinase RNA-Activated-Like Endoplasmic Reticulum Kinase/Eukaryotic Initiation Factor 2 α /Activating Transcription Factor 4 Pathway. *Circ Res* **2013**, *113*, 1253–1264, doi:10.1161/CIRCRESAHA.113.301787.
215. Wang, H.; Wilson, G.J.; Zhou, D.; Lezmi, S.; Chen, X.; Layman, D.K.; Pan, Y.-X. Induction of Autophagy through the Activating Transcription Factor 4 (ATF4)-Dependent Amino Acid Response Pathway in Maternal Skeletal Muscle May Function as the Molecular Memory in Response to Gestational Protein Restriction to Alert Offspring to Maternal Nutrition. *Br J Nutr* **2015**, *114*, 519–532, doi:10.1017/S0007114515002172.
216. Rouschop, K.M.A.; van den Beucken, T.; Dubois, L.; Niessen, H.; Bussink, J.; Savelkoul, K.; Keulers, T.; Mujcic, H.; Landuyt, W.; Voncken, J.W.; et al. The Unfolded Protein Response Protects Human Tumor Cells during Hypoxia through Regulation of the Autophagy Genes MAP1LC3B and ATG5. *J. Clin. Invest.* **2010**, *120*, 127–141, doi:10.1172/JCI40027.

217. Rzymiski, T.; Milani, M.; Pike, L.; Buffa, F.; Mellor, H.R.; Winchester, L.; Pires, I.; Hammond, E.; Ragoussis, I.; Harris, A.L. Regulation of Autophagy by ATF4 in Response to Severe Hypoxia. *Oncogene* **2010**, *29*, 4424–4435, doi:10.1038/onc.2010.191.
218. Vanhoutte, D.; Schips, T.G.; Vo, A.; Grimes, K.M.; Baldwin, T.A.; Brody, M.J.; Accornero, F.; Sargent, M.A.; Molkentin, J.D. Thbs1 Induces Lethal Cardiac Atrophy through PERK-ATF4 Regulated Autophagy. *Nat Commun* **2021**, *12*, 3928, doi:10.1038/s41467-021-24215-4.
219. Luo, B.; Lin, Y.; Jiang, S.; Huang, L.; Yao, H.; Zhuang, Q.; Zhao, R.; Liu, H.; He, C.; Lin, Z. Endoplasmic Reticulum Stress EIF2 α -ATF4 Pathway-Mediated Cyclooxygenase-2 Induction Regulates Cadmium-Induced Autophagy in Kidney. *Cell Death Dis* **2016**, *7*, e2251–e2251, doi:10.1038/cddis.2016.78.
220. Deegan, S.; Saveljeva, S.; Gorman, A.M.; Samali, A. Stress-Induced Self-Cannibalism: On the Regulation of Autophagy by Endoplasmic Reticulum Stress. *Cell. Mol. Life Sci.* **2013**, *70*, 2425–2441, doi:10.1007/s00018-012-1173-4.
221. Ye, J.; Kumanova, M.; Hart, L.S.; Sloane, K.; Zhang, H.; De Panis, D.N.; Bobrovnikova-Marjon, E.; Diehl, J.A.; Ron, D.; Koumenis, C. The GCN2-ATF4 Pathway Is Critical for Tumour Cell Survival and Proliferation in Response to Nutrient Deprivation. *EMBO J* **2010**, *29*, 2082–2096, doi:10.1038/emboj.2010.81.
222. Ravindran, R.; Loebbermann, J.; Nakaya, H.I.; Khan, N.; Ma, H.; Gama, L.; Machiah, D.K.; Lawson, B.; Hakimpour, P.; Wang, Y.-C.; et al. The Amino Acid Sensor GCN2 Controls Gut Inflammation by Inhibiting Inflammasome Activation. *Nature* **2016**, *531*, 523–527, doi:10.1038/nature17186.
223. Kouroku, Y.; Fujita, E.; Tanida, I.; Ueno, T.; Isoai, A.; Kumagai, H.; Ogawa, S.; Kaufman, R.; Kominami, E.; Momoi, T. ER Stress (PERK/EIF2 α Phosphorylation) Mediates the Polyglutamine-Induced LC3 Conversion, an Essential Step for Autophagy Formation. *Cell Death and Differentiation* **10**.
224. Kroemer, G.; Mariño, G.; Levine, B. Autophagy and the Integrated Stress Response. *Molecular Cell* **2010**, *40*, 280–293, doi:10.1016/j.molcel.2010.09.023.
225. Behrends, C.; Sowa, M.E.; Gygi, S.P.; Harper, J.W. Network Organization of the Human Autophagy System. *Nature* **2010**, *466*, 68–76, doi:10.1038/nature09204.
226. Suárez-Rivero, J.M.; Pastor-Maldonado, C.J.; Povea-Cabello, S.; Álvarez-Córdoba, M.; Villalón-García, I.; Talaverón-Rey, M.; Suárez-Carrillo, A.; Munuera-Cabeza, M.; Reche-López, D.; Cilleros-Holgado, P.; et al. Activation of the Mitochondrial Unfolded Protein Response: A New Therapeutic Target? *Biomedicines* **2022**, *10*, 1611, doi:10.3390/biomedicines10071611.
227. Quirós, P.M.; Prado, M.A.; Zamboni, N.; D’Amico, D.; Williams, R.W.; Finley, D.; Gygi, S.P.; Auwerx, J. Multi-Omics Analysis Identifies ATF4 as a Key Regulator of the Mitochondrial Stress Response in Mammals. *Journal of Cell Biology* **2017**, *216*, 2027–2045, doi:10.1083/jcb.201702058.
228. Münch, C.; Harper, J.W. Mitochondrial Unfolded Protein Response Controls Matrix Pre-RNA Processing and Translation. *Nature* **2016**, *534*, 710–713, doi:10.1038/nature18302.
229. Mick, E.; Titov, D.V.; Skinner, O.S.; Sharma, R.; Jourdain, A.A.; Mootha, V.K. Distinct Mitochondrial Defects Trigger the Integrated Stress Response Depending on the Metabolic State of the Cell. *eLife* **2020**, *9*, e49178, doi:10.7554/eLife.49178.

230. Guo, X.; Aviles, G.; Liu, Y.; Tian, R.; Unger, B.A.; Lin, Y.-H.T.; Wiita, A.P.; Xu, K.; Correia, M.A.; Kampmann, M. Mitochondrial Stress Is Relayed to the Cytosol by an OMA1–DELE1–HRI Pathway. *Nature* **2020**, *579*, 427–432, doi:10.1038/s41586-020-2078-2.
231. Bilen, M.; Benhammouda, S.; Slack, R.S.; Germain, M. The Integrated Stress Response as a Key Pathway Downstream of Mitochondrial Dysfunction. *Current Opinion in Physiology* **2022**, *27*, 100555, doi:10.1016/j.cophys.2022.100555.
232. Favaro, G.; Romanello, V.; Varanita, T.; Andrea Desbats, M.; Morbidoni, V.; Tezze, C.; Albiero, M.; Canato, M.; Gherardi, G.; De Stefani, D.; et al. DRP1-Mediated Mitochondrial Shape Controls Calcium Homeostasis and Muscle Mass. *Nat Commun* **2019**, *10*, 2576, doi:10.1038/s41467-019-10226-9.
233. Kasai, S.; Yamazaki, H.; Tanji, K.; Engler, M.J.; Matsumiya, T.; Itoh, K. Role of the ISR-ATF4 Pathway and Its Cross Talk with Nrf2 in Mitochondrial Quality Control. *J Clin Biochem Nutr* **2019**, *64*, 1–12, doi:10.3164/jcfn.18-37.
234. Romanello, V.; Scalabrin, M.; Albiero, M.; Blaauw, B.; Scorrano, L.; Sandri, M. Inhibition of the Fission Machinery Mitigates OPA1 Impairment in Adult Skeletal Muscles. *Cells* **2019**, *8*, 597, doi:10.3390/cells8060597.
235. Miyake, M.; Kuroda, M.; Kiyonari, H.; Takehana, K.; Hisanaga, S.; Morimoto, M.; Zhang, J.; Oyadomari, M.; Sakaue, H.; Oyadomari, S. Ligand-Induced Rapid Skeletal Muscle Atrophy in HSA-Fv2E-PERK Transgenic Mice. *PLoS ONE* **2017**, *12*, e0179955, doi:10.1371/journal.pone.0179955.
236. Gallot, Y.S.; Bohnert, K.R.; Straughn, A.R.; Xiong, G.; Hindi, S.M.; Kumar, A. PERK Regulates Skeletal Muscle Mass and Contractile Function in Adult Mice. *FASEB j.* **2019**, *33*, 1946–1962, doi:10.1096/fj.201800683RR.
237. Bohnert, K.R.; Gallot, Y.S.; Sato, S.; Xiong, G.; Hindi, S.M.; Kumar, A. Inhibition of ER Stress and Unfolding Protein Response Pathways Causes Skeletal Muscle Wasting during Cancer Cachexia. *FASEB j.* **2016**, *30*, 3053–3068, doi:10.1096/fj.201600250RR.
238. Guo, Y.; Wang, H.; Tang, Y.; Wang, Y.; Zhang, M.; Yang, Z.; Nyirimigabo, E.; Wei, B.; Lu, Z.; Ji, G. GCN2 Deficiency Protects Mice from Denervation-Induced Skeletal Muscle Atrophy via Inhibiting FoxO3a Nuclear Translocation. *Protein Cell* **2018**, *9*, 966–970, doi:10.1007/s13238-018-0504-0.
239. Eley, H.L.; Skipworth, R.J.E.; Deans, D.A.C.; Fearon, K.C.H.; Tisdale, M.J. Increased Expression of Phosphorylated Forms of RNA-Dependent Protein Kinase and Eukaryotic Initiation Factor 2 α May Signal Skeletal Muscle Atrophy in Weight-Losing Cancer Patients. *Br J Cancer* **2008**, *98*, 443–449, doi:10.1038/sj.bjc.6604150.
240. Eley, H.L.; Tisdale, M.J. Skeletal Muscle Atrophy, a Link between Depression of Protein Synthesis and Increase in Degradation. *Journal of Biological Chemistry* **2007**, *282*, 7087–7097, doi:10.1074/jbc.M610378200.
241. Chen, D.; Wang, Y.; Chin, E.R. Activation of the Endoplasmic Reticulum Stress Response in Skeletal Muscle of G93A*SOD1 Amyotrophic Lateral Sclerosis Mice. *Front. Cell. Neurosci.* **2015**, *9*, doi:10.3389/fncel.2015.00170.
242. Ebert, S.M.; Monteys, A.M.; Fox, D.K.; Bongers, K.S.; Shields, B.E.; Malmberg, S.E.; Davidson, B.L.; Suneja, M.; Adams, C.M. The Transcription Factor ATF4 Promotes Skeletal Myofiber Atrophy during Fasting. *Molecular Endocrinology* **2010**, *24*, 790–799, doi:10.1210/me.2009-0345.

243. de Theije, C.C.; Schols, A.M.W.J.; Lamers, W.H.; Neumann, D.; Köhler, S.E.; Langen, R.C.J. Hypoxia Impairs Adaptation of Skeletal Muscle Protein Turnover- and AMPK Signaling during Fasting-Induced Muscle Atrophy. *PLoS ONE* **2018**, *13*, e0203630, doi:10.1371/journal.pone.0203630.
244. Haddad, F.; Roy, R.R.; Zhong, H.; Edgerton, V.R.; Baldwin, K.M. Atrophy Responses to Muscle Inactivity. II. Molecular Markers of Protein Deficits. *Journal of Applied Physiology* **2003**, *95*, 791–802, doi:10.1152/jappphysiol.01113.2002.
245. Camerino, G.M.; Desaphy, J.-F.; De Bellis, M.; Capogrosso, R.F.; Cozzoli, A.; Dinardo, M.M.; Caloiero, R.; Musaraj, K.; Fonzino, A.; Conte, E.; et al. Effects of Nandrolone in the Counteraction of Skeletal Muscle Atrophy in a Mouse Model of Muscle Disuse: Molecular Biology and Functional Evaluation. *PLoS ONE* **2015**, *10*, e0129686, doi:10.1371/journal.pone.0129686.
246. Ebert, S.M.; Dyle, M.C.; Kunkel, S.D.; Bullard, S.A.; Bongers, K.S.; Fox, D.K.; Dierdorff, J.M.; Foster, E.D.; Adams, C.M. Stress-Induced Skeletal Muscle Gadd45a Expression Reprograms Myonuclei and Causes Muscle Atrophy. *Journal of Biological Chemistry* **2012**, *287*, 27290–27301, doi:10.1074/jbc.M112.374777.
247. Ebert, S.M.; Dyle, M.C.; Bullard, S.A.; Dierdorff, J.M.; Murry, D.J.; Fox, D.K.; Bongers, K.S.; Lira, V.A.; Meyerholz, D.K.; Talley, J.J.; et al. Identification and Small Molecule Inhibition of an Activating Transcription Factor 4 (ATF4)-Dependent Pathway to Age-Related Skeletal Muscle Weakness and Atrophy. *Journal of Biological Chemistry* **2015**, *290*, 25497–25511, doi:10.1074/jbc.M115.681445.
248. Fox, D.K.; Ebert, S.M.; Bongers, K.S.; Dyle, M.C.; Bullard, S.A.; Dierdorff, J.M.; Kunkel, S.D.; Adams, C.M. P53 and ATF4 Mediate Distinct and Additive Pathways to Skeletal Muscle Atrophy during Limb Immobilization. *American Journal of Physiology-Endocrinology and Metabolism* **2014**, *307*, E245–E261, doi:10.1152/ajpendo.00010.2014.
249. Sacheck, J.M.; Hyatt, J.K.; Raffaello, A.; Thomas Jagoe, R.; Roy, R.R.; Reggie Edgerton, V.; Lecker, S.H.; Goldberg, A.L. Rapid Disuse and Denervation Atrophy Involve Transcriptional Changes Similar to Those of Muscle Wasting during Systemic Diseases. *FASEB j.* **2007**, *21*, 140–155, doi:10.1096/fj.06-6604com.
250. Ebert, S.M.; Bullard, S.A.; Basisty, N.; Marcotte, G.R.; Skopec, Z.P.; Dierdorff, J.M.; Al-Zougbi, A.; Tomcheck, K.C.; DeLau, A.D.; Rathmacher, J.A.; et al. Activating Transcription Factor 4 (ATF4) Promotes Skeletal Muscle Atrophy by Forming a Heterodimer with the Transcriptional Regulator C/EBP β . *Journal of Biological Chemistry* **2020**, *295*, 2787–2803, doi:10.1074/jbc.RA119.012095.
251. Markofski, M.M.; Dickinson, J.M.; Drummond, M.J.; Fry, C.S.; Fujita, S.; Gundermann, D.M.; Glynn, E.L.; Jennings, K.; Paddon-Jones, D.; Reidy, P.T.; et al. Effect of Age on Basal Muscle Protein Synthesis and MTORC1 Signaling in a Large Cohort of Young and Older Men and Women. *Experimental Gerontology* **2015**, *65*, 1–7, doi:10.1016/j.exger.2015.02.015.
252. Joseph, G.A.; Wang, S.X.; Jacobs, C.E.; Zhou, W.; Kimble, G.C.; Tse, H.W.; Eash, J.K.; Shavlakadze, T.; Glass, D.J. Partial Inhibition of MTORC1 in Aged Rats Counteracts the Decline in Muscle Mass and Reverses Molecular Signaling Associated with Sarcopenia. *Mol Cell Biol* **2019**, *39*, e00141-19, doi:10.1128/MCB.00141-19.
253. Galvan, E.; Arentson-Lantz, E.; Lamon, S.; Paddon-Jones, D. Protecting Skeletal Muscle with Protein and Amino Acid during Periods of Disuse. *Nutrients* **2016**, *8*, 404, doi:10.3390/nu8070404.

254. Welle, S.; Brooks, A.I.; Delehanty, J.M.; Needler, N.; Bhatt, K.; Shah, B.; Thornton, C.A. Skeletal Muscle Gene Expression Profiles in 20–29 Year Old and 65–71 Year Old Women. *Experimental Gerontology* **2004**, *39*, 369–377, doi:10.1016/j.exger.2003.11.011.
255. Gonzalez de Aguilar, J.-L.; Niederhauser-Wiederkehr, C.; Halter, B.; De Tapia, M.; Di Scala, F.; Demougin, P.; Dupuis, L.; Primig, M.; Meininger, V.; Loeffler, J.-P. Gene Profiling of Skeletal Muscle in an Amyotrophic Lateral Sclerosis Mouse Model. *Physiological Genomics* **2008**, *32*, 207–218, doi:10.1152/physiolgenomics.00017.2007.
256. Banduseela, V.C.; Ochala, J.; Chen, Y.-W.; Göransson, H.; Norman, H.; Radell, P.; Eriksson, L.I.; Hoffman, E.P.; Larsson, L. Gene Expression and Muscle Fiber Function in a Porcine ICU Model. *Physiological Genomics* **2009**, *39*, 141–159, doi:10.1152/physiolgenomics.00026.2009.
257. Llano-Diez, M.; Fury, W.; Okamoto, H.; Bai, Y.; Gromada, J.; Larsson, L. RNA-Sequencing Reveals Altered Skeletal Muscle Contraction, E3 Ligases, Autophagy, Apoptosis, and Chaperone Expression in Patients with Critical Illness Myopathy. *Skeletal Muscle* **2019**, *9*, 9, doi:10.1186/s13395-019-0194-1.
258. Ehmsen, J.T.; Kawaguchi, R.; Kaval, D.; Johnson, A.E.; Nachun, D.; Coppola, G.; Höke, A. GADD45A Is a Protective Modifier of Neurogenic Skeletal Muscle Atrophy. *JCI Insight* **2021**, *6*, e149381, doi:10.1172/jci.insight.149381.
259. Bullard, S.A.; Seo, S.; Schilling, B.; Dyle, M.C.; Dierdorff, J.M.; Ebert, S.M.; DeLau, A.D.; Gibson, B.W.; Adams, C.M. Gadd45a Protein Promotes Skeletal Muscle Atrophy by Forming a Complex with the Protein Kinase MEK4. *Journal of Biological Chemistry* **2016**, *291*, 17496–17509, doi:10.1074/jbc.M116.740308.
260. Bongers, K.S.; Fox, D.K.; Ebert, S.M.; Kunkel, S.D.; Dyle, M.C.; Bullard, S.A.; Dierdorff, J.M.; Adams, C.M. Skeletal Muscle Denervation Causes Skeletal Muscle Atrophy through a Pathway That Involves Both Gadd45a and HDAC4. *Am J Physiol Endocrinol Metab* **2013**, *305*, E907–E915, doi:10.1152/ajpendo.00380.2013.
261. Stevenson, E.J.; Giresi, P.G.; Koncarevic, A.; Kandarian, S.C. Global Analysis of Gene Expression Patterns during Disuse Atrophy in Rat Skeletal Muscle. *The Journal of Physiology* **2003**, *551*, 33–48, doi:10.1113/jphysiol.2003.044701.
262. Atherton, P.J.; Greenhaff, P.L.; Phillips, S.M.; Bodine, S.C.; Adams, C.M.; Lang, C.H. Control of Skeletal Muscle Atrophy in Response to Disuse: Clinical/Preclinical Contentions and Fallacies of Evidence. *American Journal of Physiology-Endocrinology and Metabolism* **2016**, *311*, E594–E604, doi:10.1152/ajpendo.00257.2016.
263. Bongers, K.S.; Fox, D.K.; Kunkel, S.D.; Stebounova, L.V.; Murry, D.J.; Pufall, M.A.; Ebert, S.M.; Dyle, M.C.; Bullard, S.A.; Dierdorff, J.M.; et al. Spermine Oxidase Maintains Basal Skeletal Muscle Gene Expression and Fiber Size and Is Strongly Repressed by Conditions That Cause Skeletal Muscle Atrophy. *American Journal of Physiology-Endocrinology and Metabolism* **2015**, *308*, E144–E158, doi:10.1152/ajpendo.00472.2014.
264. Wu, C.-L.; Kandarian, S.C.; Jackman, R.W. Identification of Genes That Elicit Disuse Muscle Atrophy via the Transcription Factors P50 and Bcl-3. *PLoS ONE* **2011**, *6*, e16171, doi:10.1371/journal.pone.0016171.
265. Choi, R.H.; McConahay, A.; Jeong, H.-W.; McClellan, J.L.; Hardee, J.P.; Carson, J.A.; Hirshman, M.F.; Goodyear, L.J.; Koh, H.-J. Tribbles 3 Regulates Protein Turnover in Mouse Skeletal Muscle.

- Biochemical and Biophysical Research Communications* **2017**, *493*, 1236–1242, doi:10.1016/j.bbrc.2017.09.134.
266. Shang, G.; Han, L.; Wang, Z.; Liu, Y.; Yan, S.; Sai, W.; Wang, D.; Li, Y.; Zhang, W.; Zhong, M. Sarcopenia Is Attenuated by TRB3 Knockout in Aging Mice via the Alleviation of Atrophy and Fibrosis of Skeletal Muscles. *Journal of Cachexia, Sarcopenia and Muscle* **2020**, *11*, 1104–1120, doi:10.1002/jcsm.12560.
267. Choi, R.H.; McConahay, A.; Silvestre, J.G.; Moriscot, A.S.; Carson, J.A.; Koh, H.-J. TRB3 Regulates Skeletal Muscle Mass in Food Deprivation–Induced Atrophy. *FASEB J* **2019**, *33*, 5654–5666, doi:10.1096/fj.201802145RR.
268. Stenvinkel, P.; Avesani, C.M.; Gordon, L.J.; Schalling, M.; Shiels, P.G. Biomimetics Provides Lessons from Nature for Contemporary Ways to Improve Human Health. *J. Clin. Trans. Sci.* **2021**, *5*, e128, doi:10.1017/cts.2021.790.
269. Balkenende, D.W.R.; Winkler, S.M.; Messersmith, P.B. Marine-Inspired Polymers in Medical Adhesion. *European Polymer Journal* **2019**, *116*, 134–143, doi:10.1016/j.eurpolymj.2019.03.059.
270. Shoffstall, A.J. A Mosquito Inspired Strategy to Implant Microprobes into the Brain. *SCIEnTifc REPOrtS* **2018**, *10*.
271. Chen, Z.; Zhang, Z. Recent Progress in Beetle-Inspired Superhydrophilic-Superhydrophobic Micropatterned Water-Collection Materials. *Water Science and Technology* **2020**, wst2020238, doi:10.2166/wst.2020.238.
272. Whitney, M.R.; Sidor, C.A. Evidence of Torpor in the Tusks of *Lystrosaurus* from the Early Triassic of Antarctica. *Commun Biol* **2020**, *3*, 471, doi:10.1038/s42003-020-01207-6.
273. Geiser, F. Seasonal Expression of Avian and Mammalian Daily Torpor and Hibernation: Not a Simple Summer-Winter Affair†. *Front. Physiol.* **2020**, *11*, 436, doi:10.3389/fphys.2020.00436.
274. Heldmaier, G.; Ortman, S.; Elvert, R. Natural Hypometabolism during Hibernation and Daily Torpor in Mammals. *Respiratory Physiology & Neurobiology* **2004**, *141*, 317–329, doi:10.1016/j.resp.2004.03.014.
275. Barnes, B.M. Freeze Avoidance in a Mammal: Body Temperatures Below 0°C in an Arctic Hibernator. *Science* **1989**, *244*, 1593–1595, doi:10.1126/science.2740905.
276. Watts, P.D.; Britsland, N.A.; Jonkel, C.; Ronald, K. MAMMALIAN HIBERNATION AND THE OXYGEN CONSUMPTION OF A DENNING BLACK BEAR. *3*.
277. Hissa, R.; Siekkinen, J.; Hohtola, E.; Saarela, S.; Hakala, A.; Pudas, J. Seasonal Patterns in the Physiology of the European Brown Bear (*Ursus Arctos Arctos*) in Finland. *Comparative Biochemistry and Physiology Part A: Physiology* **1994**, *109*, 781–791, doi:10.1016/0300-9629(94)90222-4.
278. Tøien, Ø.; Blake, J.; Edgar, D.M.; Grahn, D.A.; Heller, H.C.; Barnes, B.M. Hibernation in Black Bears: Independence of Metabolic Suppression from Body Temperature. *Science* **2011**, *331*, 906–909, doi:10.1126/science.1199435.
279. Evans, A.L.; Singh, N.J.; Friebe, A.; Arnemo, J.M.; Laske, T.G.; Frøbert, O.; Swenson, J.E.; Blanc, S. Drivers of Hibernation in the Brown Bear. *Front Zool* **2016**, *13*, 7, doi:10.1186/s12983-016-0140-6.

280. Tjøien, Ø.; Blake, J.; Barnes, B.M. Thermoregulation and Energetics in Hibernating Black Bears: Metabolic Rate and the Mystery of Multi-Day Body Temperature Cycles. *J Comp Physiol B* **2015**, *185*, 447–461, doi:10.1007/s00360-015-0891-y.
281. Hitrec, T.; Luppi, M.; Bastianini, S.; Squarcio, F.; Berteotti, C.; Lo Martire, V.; Martelli, D.; Occhinegro, A.; Tupone, D.; Zoccoli, G.; et al. Neural Control of Fasting-Induced Torpor in Mice. *Sci Rep* **2019**, *9*, 15462, doi:10.1038/s41598-019-51841-2.
282. Hrvatin, S.; Sun, S.; Wilcox, O.F.; Yao, H.; Lavin-Peter, A.J.; Cicconet, M.; Assad, E.G.; Palmer, M.E.; Aronson, S.; Banks, A.S.; et al. Neurons That Regulate Mouse Torpor. *Nature* **2020**, *583*, 115–121, doi:10.1038/s41586-020-2387-5.
283. Takahashi, T.M.; Sunagawa, G.A.; Soya, S.; Abe, M.; Sakurai, K.; Ishikawa, K.; Yanagisawa, M.; Hama, H.; Hasegawa, E.; Miyawaki, A.; et al. A Discrete Neuronal Circuit Induces a Hibernation-like State in Rodents. *Nature* **2020**, *583*, 109–114, doi:10.1038/s41586-020-2163-6.
284. Cerri, M.; Hitrec, T.; Luppi, M.; Amici, R. Be Cool to Be Far: Exploiting Hibernation for Space Exploration. *Neuroscience & Biobehavioral Reviews* **2021**, *128*, 218–232, doi:10.1016/j.neubiorev.2021.03.037.
285. Collins, D.M. Ursidae. In *Fowler's Zoo and Wild Animal Medicine, Volume 8*; Elsevier, 2015; pp. 498–508 ISBN 978-1-4557-7397-8.
286. Johnson, H.E.; Lewis, D.L.; Verzuh, T.L.; Wallace, C.F.; Much, R.M.; Willmarth, L.K.; Breck, S.W. Human Development and Climate Affect Hibernation in a Large Carnivore with Implications for Human-Carnivore Conflicts. *J Appl Ecol* **2018**, *55*, 663–672, doi:10.1111/1365-2664.13021.
287. Manchi, S.; Swenson, J.E. Denning Behaviour of Scandinavian Brown Bears *Ursus Arctos*. *Wildlife Biology* **2005**, *11*, 123–132, doi:10.2981/0909-6396(2005)11[123:DBOSBB]2.0.CO;2.
288. Craighead, F.C.; Craighead, J.J. Data on Grizzly Bear Denning Activities and Behavior Obtained by Using Wildlife Telemetry. *Bears: Their Biology and Management* **1972**, *2*, 84, doi:10.2307/3872573.
289. Folk, G.E.; Larson, A.; Folk, M.A. Physiology of Hibernating Bears. *Bears: Their Biology and Management* **1976**, *3*, 373, doi:10.2307/3872787.
290. Scholander, P.F.; Hock, R.; Walters, V.; Johnson, F.; Irving, L. HEAT REGULATION IN SOME ARCTIC AND TROPICAL MAMMALS AND BIRDS. *The Biological Bulletin* **1950**, *99*, 237–258, doi:10.2307/1538741.
291. Svihla, A.; Bowman, H.S. Hibernation in the American Black Bear. *American Midland Naturalist* **1954**, *52*, 248, doi:10.2307/2422063.
292. Nelson, O.L.; Robbins, C.T. Cardiac Function Adaptations in Hibernating Grizzly Bears (*Ursus Arctos Horribilis*). *J Comp Physiol B* **2010**, *180*, 465–473, doi:10.1007/s00360-009-0421-x.
293. Jørgensen, P.G.; Evans, A.; Kindberg, J.; Olsen, L.H.; Galatius, S.; Frøbert, O. Cardiac Adaptation in Hibernating, Free-Ranging Scandinavian Brown Bears (*Ursus Arctos*). *Sci Rep* **2020**, *10*, 247, doi:10.1038/s41598-019-57126-y.
294. Laske, T.G.; Garshelis, D.L.; Iazzo, P.A. Monitoring the Wild Black Bear's Reaction to Human and Environmental Stressors. *BMC Physiol* **2011**, *11*, 13, doi:10.1186/1472-6793-11-13.

295. Brown, D.; Mulhausen, R.; Andrew, D.; Seal, U. Renal Function in Anesthetized Dormant and Active Bears. *American Journal of Physiology-Legacy Content* **1971**, *220*, 293–298, doi:10.1152/ajplegacy.1971.220.1.293.
296. Stenset, N.E.; Lutnæs, P.N.; Bjarnadóttir, V.; Dahle, B.; Fossum, K.H.; Jigsved, P.; Johansen, T.; Neumann, W.; Opseth, O.; Rønning, O.; et al. Seasonal and Annual Variation in the Diet of Brown Bears *Ursus Arctos* in the Boreal Forest of Southcentral Sweden. *Wildlife Biology* **2016**, *22*, 107–116, doi:10.2981/wlb.00194.
297. Farley, S.D.; Robbins, C.T. Lactation, Hibernation, and Mass Dynamics of American Black Bears and Grizzly Bears. *Can. J. Zool.* **1995**, *73*, 2216–2222, doi:10.1139/z95-262.
298. Shimozuru, M.; Nagashima, A.; Tanaka, J.; Tsubota, T. Seasonal Changes in the Expression of Energy Metabolism-Related Genes in White Adipose Tissue and Skeletal Muscle in Female Japanese Black Bears. *Comparative Biochemistry and Physiology Part B: Biochemistry and Molecular Biology* **2016**, *196–197*, 38–47, doi:10.1016/j.cbpb.2016.02.001.
299. Hissa, R.; Siekkinen, J.; Hohtola, E.; Saarela, S.; Hakala, A.; Pudast, J. Seasonal Patterns in the Physiology of the European Brown Bear (*Ursus Ursinus*) in Finland. **11**.
300. Swenson, J.E.; Adamič, M.; Huber, D.; Stokke, S. Brown Bear Body Mass and Growth in Northern and Southern Europe. *Oecologia* **2007**, *153*, 37–47, doi:10.1007/s00442-007-0715-1.
301. Lohuis, T.D.; Harlow, H.J.; Beck, T.D.I. Hibernating Black Bears (*Ursus Americanus*) Experience Skeletal Muscle Protein Balance during Winter Anorexia. *Comparative Biochemistry and Physiology Part B: Biochemistry and Molecular Biology* **2007**, *147*, 20–28, doi:10.1016/j.cbpb.2006.12.020.
302. Tinker, D.B.; Harlow, H.J.; Beck, T.D.I. Protein Use and Muscle-Fiber Changes in Free-Ranging, Hibernating Black Bears. *Physiological Zoology* **1998**, *71*, 414–424, doi:10.1086/515429.
303. Ahlquist, D.A.; Nelson, R.A.; Steiger, D.L.; Jones, J.D.; Ellefson, R.D. Glycerol Metabolism in the Hibernating Black Bear. *J Comp Physiol B* **1984**, *155*, 75–79, doi:10.1007/BF00688794.
304. Fedorov, V.B.; Goropashnaya, A.V.; Tøien, Ø.; Stewart, N.C.; Gracey, A.Y.; Chang, C.; Qin, S.; Perteu, G.; Quackenbush, J.; Showe, L.C.; et al. Elevated Expression of Protein Biosynthesis Genes in Liver and Muscle of Hibernating Black Bears (*Ursus Americanus*). *Physiological Genomics* **2009**, *37*, 108–118, doi:10.1152/physiolgenomics.90398.2008.
305. Shimozuru, M.; Kamine, A.; Tsubota, T. Changes in Expression of Hepatic Genes Involved in Energy Metabolism during Hibernation in Captive, Adult, Female Japanese Black Bears (*Ursus Thibetanus Japonicus*). *Comparative Biochemistry and Physiology Part B: Biochemistry and Molecular Biology* **2012**, *163*, 254–261, doi:10.1016/j.cbpb.2012.06.007.
306. Fedorov, V.B.; Goropashnaya, A.V.; Tøien, Ø.; Stewart, N.C.; Chang, C.; Wang, H.; Yan, J.; Showe, L.C.; Showe, M.K.; Barnes, B.M. Modulation of Gene Expression in Heart and Liver of Hibernating Black Bears (*Ursus Americanus*). **2011**, *15*.
307. Jansen, H.T.; Trojahn, S.; Saxton, M.W.; Quackenbush, C.R.; Evans Hutzenbiler, B.D.; Nelson, O.L.; Cornejo, O.E.; Robbins, C.T.; Kelley, J.L. Hibernation Induces Widespread Transcriptional Remodeling in Metabolic Tissues of the Grizzly Bear. *Commun Biol* **2019**, *2*, 336, doi:10.1038/s42003-019-0574-4.
308. Vella, C.A.; Nelson, O.L.; Jansen, H.T.; Robbins, C.T.; Jensen, A.E.; Constantinescu, S.; Abbott, M.J.; Turcotte, L.P. Regulation of Metabolism during Hibernation in Brown Bears (*Ursus Arctos*):

- Involvement of Cortisol, PGC-1 α and AMPK in Adipose Tissue and Skeletal Muscle. *Comparative Biochemistry and Physiology Part A: Molecular & Integrative Physiology* **2020**, *240*, 110591, doi:10.1016/j.cbpa.2019.110591.
309. Stenvinkel, P.; Jani, A.H.; Johnson, R.J. Hibernating Bears (Ursidae): Metabolic Magicians of Definite Interest for the Nephrologist. *Kidney International* **2013**, *83*, 207–212, doi:10.1038/ki.2012.396.
310. Chazarin, B.; Storey, K.B.; Ziemianin, A.; Chanon, S.; Plumel, M.; Chery, I.; Durand, C.; Evans, A.L.; Arnemo, J.M.; Zedrosser, A.; et al. Metabolic Reprogramming Involving Glycolysis in the Hibernating Brown Bear Skeletal Muscle. *Front Zool* **2019**, *16*, 12, doi:10.1186/s12983-019-0312-2.
311. Owen, O.E.; Smalley, K.J.; D'Alessio, D.A.; Mozzoli, M.A.; Dawson, E.K. Protein, Fat, and Carbohydrate Requirements during Starvation: Anaplerosis and Cataplerosis. *The American Journal of Clinical Nutrition* **1998**, *68*, 12–34, doi:10.1093/ajcn/68.1.12.
312. Rigano, K.S.; Gehring, J.L.; Evans Hutzenbiler, B.D.; Chen, A.V.; Nelson, O.L.; Vella, C.A.; Robbins, C.T.; Jansen, H.T. Life in the Fat Lane: Seasonal Regulation of Insulin Sensitivity, Food Intake, and Adipose Biology in Brown Bears. *J Comp Physiol B* **2017**, *187*, 649–676, doi:10.1007/s00360-016-1050-9.
313. Rynders, C.A.; Blanc, S.; DeJong, N.; Bessesen, D.H.; Bergouignan, A. Sedentary Behaviour Is a Key Determinant of Metabolic Inflexibility: Sedentary Behaviour and Metabolic Flexibility. *J Physiol* **2018**, *596*, 1319–1330, doi:10.1113/JP273282.
314. Galgani, J.E.; Bergouignan, A.; Rieusset, J.; Moro, C.; Nazare, J.-A. Editorial: Metabolic Flexibility. *Front. Nutr.* **2022**, *9*, 946300, doi:10.3389/fnut.2022.946300.
315. Pedrelli, M.; Parini, P.; Kindberg, J.; Arnemo, J.M.; Bjorkhem, I.; Aasa, U.; Westerståhl, M.; Walentinsson, A.; Pavanello, C.; Turri, M.; et al. Vasculoprotective Properties of Plasma Lipoproteins from Brown Bears (*Ursus Arctos*). *Journal of Lipid Research* **2021**, *62*, 100065, doi:10.1016/j.jlr.2021.100065.
316. Berg von Linde, M.; Arevström, L.; Fröbert, O. Insights from the Den: How Hibernating Bears May Help Us Understand and Treat Human Disease: Hibernating Bears and Human Disease. *Clinical And Translational Science* **2015**, *8*, 601–605, doi:10.1111/cts.12279.
317. MmRS, P.G.; NELSON'an, R.A. CHANGES IN SKELET, 4G BEARS (URSUS AME. 4.
318. Harlow, H.J.; Lohuis, T.; Beck, T.D.I.; Iazzo, P.A. Muscle Strength in Overwintering Bears. *Nature* **2001**, *409*, 997–997, doi:10.1038/35059165.
319. Hershey, J.D.; Robbins, C.T.; Nelson, O.L.; Lin, D.C. Minimal Seasonal Alterations in the Skeletal Muscle of Captive Brown Bears. *Physiological and Biochemical Zoology* **2008**, *81*, 138–147, doi:10.1086/524391.
320. Riley, D.A.; Van Dyke, J.M.; Vogel, V.; Curry, B.D.; Bain, J.L.W.; Schuett, R.; Costill, D.L.; Trappe, T.; Minchev, K.; Trappe, S. Soleus Muscle Stability in Wild Hibernating Black Bears. *American Journal of Physiology-Regulatory, Integrative and Comparative Physiology* **2018**, *315*, R369–R379, doi:10.1152/ajpregu.00060.2018.
321. Miyazaki, M.; Shimozuru, M.; Tsubota, T. Skeletal Muscles of Hibernating Black Bears Show Minimal Atrophy and Phenotype Shifting despite Prolonged Physical Inactivity and Starvation. *PLoS ONE* **2019**, *14*, e0215489, doi:10.1371/journal.pone.0215489.

322. Rennie, M.J.; Selby, A.; Atherton, P.; Smith, K.; Kumar, V.; Glover, E.L.; Philips, S.M. Facts, Noise and Wishful Thinking: Muscle Protein Turnover in Aging and Human Disuse Atrophy. *Scandinavian Journal of Medicine & Science in Sports* **2010**, *20*, 5–9, doi:10.1111/j.1600-0838.2009.00967.x.
323. de Boer, M.D.; Selby, A.; Atherton, P.; Smith, K.; Seynnes, O.R.; Maganaris, C.N.; Maffulli, N.; Movin, T.; Narici, M.V.; Rennie, M.J. The Temporal Responses of Protein Synthesis, Gene Expression and Cell Signalling in Human Quadriceps Muscle and Patellar Tendon to Disuse. *J Physiol* **2007**, *585*, 241–251, doi:10.1113/jphysiol.2007.142828.
324. Rourke, B.C.; Cotton, C.J.; Harlow, H.J.; Caiozzo, V.J. Maintenance of Slow Type I Myosin Protein and mRNA Expression in Overwintering Prairie Dogs (*Cynomys Leucurus* and *Ludovicianus*) and Black Bears (*Ursus Americanus*). *J Comp Physiol B* **2006**, *176*, 709–720, doi:10.1007/s00360-006-0093-8.
325. Salmov, N.N.; Vikhlyantsev, I.M.; Ulanova, A.D.; Gritsyna, Yu.V.; Bobylev, A.G.; Saveljev, A.P.; Makariushchenko, V.V.; Maksudov, G.Yu.; Podlubnaya, Z.A. Seasonal Changes in Isoform Composition of Giant Proteins of Thick and Thin Filaments and Titin (Connectin) Phosphorylation Level in Striated Muscles of Bears (*Ursidae*, *Mammalia*). *Biochemistry Moscow* **2015**, *80*, 343–355, doi:10.1134/S0006297915030098.
326. Lohuis, T.D.; Harlow, H.J.; Beck, T.D.I.; Iazzo, P.A. Hibernating Bears Conserve Muscle Strength and Maintain Fatigue Resistance. *Physiological and Biochemical Zoology* **2007**, *80*, 257–269, doi:10.1086/513190.
327. Harlow, H. Muscle Protein and Strength Retention by Bears During Winter Fasting and Starvation. In *Comparative Physiology of Fasting, Starvation, and Food Limitation*; McCue, M.D., Ed.; Springer Berlin Heidelberg: Berlin, Heidelberg, 2012; pp. 277–296 ISBN 978-3-642-29055-8.
328. Lin, D.C.; Hershey, J.D.; Mattoon, J.S.; Robbins, C.T. Skeletal Muscles of Hibernating Brown Bears Are Unusually Resistant to Effects of Denervation. *J Exp Biol* **2012**, *215*, 2081–2087, doi:10.1242/jeb.066134.
329. Fedorov, V.B.; Goropashnaya, A.V.; Stewart, N.C.; Tøien, Ø.; Chang, C.; Wang, H.; Yan, J.; Showe, L.C.; Showe, M.K.; Barnes, B.M. Comparative Functional Genomics of Adaptation to Muscular Disuse in Hibernating Mammals. *Mol Ecol* **2014**, *23*, 5524–5537, doi:10.1111/mec.12963.
330. Barboza, P.S.; Farley, S.D.; Robbins, C.T. Whole-Body Urea Cycling and Protein Turnover during Hyperphagia and Dormancy in Growing Bears (*Ursus Americanus* and *U. Arctos*). *Can. J. Zool.* **1997**, *75*, 2129–2136, doi:10.1139/z97-848.
331. Græsli, A.R.; Evans, A.L.; Fahlman, Å.; Bertelsen, M.F.; Blanc, S.; Arnemo, J.M. Seasonal Variation in Haematological and Biochemical Variables in Free-Ranging Subadult Brown Bears (*Ursus Arctos*) in Sweden. *BMC Vet Res* **2015**, *11*, 301, doi:10.1186/s12917-015-0615-2.
332. Luu, B.E.; Lefai, E.; Giroud, S.; Swenson, J.E.; Chazarin, B.; Gauquelin-Koch, G.; Arnemo, J.M.; Evans, A.L.; Bertile, F.; Storey, K.B. MicroRNAs Facilitate Skeletal Muscle Maintenance and Metabolic Suppression in Hibernating Brown Bears. *J Cell Physiol* **2020**, *235*, 3984–3993, doi:10.1002/jcp.29294.
333. Mugahid, D.A.; Sengul, T.G.; You, X.; Wang, Y.; Steil, L.; Bergmann, N.; Radke, M.H.; Ofenbauer, A.; Gesell-Salazar, M.; Balogh, A.; et al. Proteomic and Transcriptomic Changes in Hibernating Grizzly Bears Reveal Metabolic and Signaling Pathways That Protect against Muscle Atrophy. *Sci Rep* **2019**, *9*, 19976, doi:10.1038/s41598-019-56007-8.

334. Frøbert, A.M.; Brohus, M.; Roesen, T.S.; Kindberg, J.; Frøbert, O.; Conover, C.A.; Overgaard, M.T. Circulating Insulin-like Growth Factor (IGF) System Adaptations in Hibernating Brown Bears Indicate Increased Tissue IGF Availability. *Am. J. Physiol.* **46**.
335. Boyer, C.; Cussonneau, L.; Brun, C.; Deval, C.; Pais de Barros, J.-P.; Chanon, S.; Bernoud-Hubac, N.; Daira, P.; Evans, A.L.; Arnemo, J.M.; et al. Specific Shifts in the Endocannabinoid System in Hibernating Brown Bears. *Front Zool* **2020**, *17*, 35, doi:10.1186/s12983-020-00380-y.
336. Deval, C.; Capel, F.; Laillet, B.; Polge, C.; Béchet, D.; Taillandier, D.; Attaix, D.; Combaret, L. Docosahexaenoic Acid-Supplementation Prior to Fasting Prevents Muscle Atrophy in Mice: Docosahexaenoic Acid Limits Muscle Wasting in Fasted Mice. *Journal of Cachexia, Sarcopenia and Muscle* **2016**, *7*, 587–603, doi:10.1002/jcsm.12103.
337. Chazarin; Ziemianin; Evans; Meugnier; Loizon; Chery; Arnemo; Swenson; Gauquelin-Koch; Simon; et al. Limited Oxidative Stress Favors Resistance to Skeletal Muscle Atrophy in Hibernating Brown Bears (*Ursus Arctos*). *Antioxidants* **2019**, *8*, 334, doi:10.3390/antiox8090334.
338. Cadenas, S. Mitochondrial Uncoupling, ROS Generation and Cardioprotection. *Biochimica et Biophysica Acta (BBA) - Bioenergetics* **2018**, *1859*, 940–950, doi:10.1016/j.bbabi.2018.05.019.
339. Giroud, S.; Chery, I.; Arrivé, M.; Prost, M.; Zumsteg, J.; Heintz, D.; Evans, A.L.; Gauquelin-Koch, G.; Arnemo, J.M.; Swenson, J.E.; et al. Hibernating Brown Bears Are Protected against Atherogenic Dyslipidemia. *Sci Rep* **2021**, *11*, 18723, doi:10.1038/s41598-021-98085-7.
340. Fuster, G.; Busquets, S.; Almendro, V.; López-Soriano, F.J.; Argilés, J.M. Antiproteolytic Effects of Plasma from Hibernating Bears: A New Approach for Muscle Wasting Therapy? *Clinical Nutrition* **2007**, *26*, 658–661, doi:10.1016/j.clnu.2007.07.003.
341. Chanon, S.; Chazarin, B.; Toubhans, B.; Durand, C.; Chery, I.; Robert, M.; Vieille-Marchiset, A.; Swenson, J.E.; Zedrosser, A.; Evans, A.L.; et al. Proteolysis Inhibition by Hibernating Bear Serum Leads to Increased Protein Content in Human Muscle Cells. *Sci Rep* **2018**, *8*, 5525, doi:10.1038/s41598-018-23891-5.
342. Miyazaki, M.; Shimozuru, M.; Tsubota, T. Supplementing Cultured Human Myotubes with Hibernating Bear Serum Results in Increased Protein Content by Modulating Akt/FOXO3a Signaling. *PLoS ONE* **2022**, *17*, e0263085, doi:10.1371/journal.pone.0263085.
343. Brooks, N.E.; Myburgh, K.H.; Storey, K.B. Myostatin Levels in Skeletal Muscle of Hibernating Ground Squirrels. *Journal of Experimental Biology* **2011**, *214*, 2522–2527, doi:10.1242/jeb.055764.
344. Kornfeld, S.F.; Biggar, K.K.; Storey, K.B. Differential Expression of Mature MicroRNAs Involved in Muscle Maintenance of Hibernating Little Brown Bats, *Myotis Lucifugus*: A Model of Muscle Atrophy Resistance. *Genomics, Proteomics & Bioinformatics* **2012**, *10*, 295–301, doi:10.1016/j.gpb.2012.09.001.
345. Nowell, M.M.; Choi, H.; Rourke, B.C. Muscle Plasticity in Hibernating Ground Squirrels (*Spermophilus Lateralis*) Is Induced by Seasonal, but Not Low-Temperature, Mechanisms. *J Comp Physiol B* **2011**, *181*, 147–164, doi:10.1007/s00360-010-0505-7.
346. Mamady, H.; Storey, K.B. Coping with the Stress: Expression of ATF4, ATF6, and Downstream Targets in Organs of Hibernating Ground Squirrels. *Archives of Biochemistry and Biophysics* **2008**, *477*, 77–85, doi:10.1016/j.abb.2008.05.006.

347. Zhang, J.; Wei, Y.; Qu, T.; Wang, Z.; Xu, S.; Peng, X.; Yan, X.; Chang, H.; Wang, H.; Gao, Y. Prosurvival Roles Mediated by the PERK Signaling Pathway Effectively Prevent Excessive Endoplasmic Reticulum Stress-induced Skeletal Muscle Loss during High-stress Conditions of Hibernation. *Journal Cellular Physiology* **2019**, *234*, 19728–19739, doi:10.1002/jcp.28572.
348. Marzuca-Nassr, G.N.; Vitzel, K.F.; Murata, G.M.; Márquez, J.L.; Curi, R. Experimental Model of HindLimb Suspension-Induced Skeletal Muscle Atrophy in Rodents. In *Pre-Clinical Models*; Guest, P.C., Ed.; Springer New York: New York, NY, 2019; Vol. 1916, pp. 167–176 ISBN 978-1-4939-8993-5.
349. Sasabe, R.; Sakamoto, J.; Goto, K.; Honda, Y.; Kataoka, H.; Nakano, J.; Origuchi, T.; Endo, D.; Koji, T.; Okita, M. Effects of Joint Immobilization on Changes in Myofibroblasts and Collagen in the Rat Knee Contracture Model: IMMOBILIZATION-INDUCED JOINT CAPSULE FIBROSIS. *J. Orthop. Res.* **2017**, *35*, 1998–2006, doi:10.1002/jor.23498.
350. Kawanishi, N.; Funakoshi, T.; Machida, S. Time-Course Study of Macrophage Infiltration and Inflammation in Cast Immobilization-Induced Atrophied Muscle of Mice: Macrophage Infiltration and Muscle Atrophy. *Muscle Nerve* **2018**, *57*, 1006–1013, doi:10.1002/mus.26061.
351. Cussonneau, L.; Boyer, C.; Brun, C.; Deval, C.; Loizon, E.; Meugnier, E.; Gueret, E.; Dubois, E.; Taillandier, D.; Polge, C.; et al. Concurrent BMP Signaling Maintenance and TGF- β Signaling Inhibition Is a Hallmark of Natural Resistance to Muscle Atrophy in the Hibernating Bear. *Cells* **2021**, *10*, 1873, doi:10.3390/cells10081873.
352. Williams, D.R.; Epperson, L.E.; Li, W.; Hughes, M.A.; Taylor, R.; Rogers, J.; Martin, S.L.; Cossins, A.R.; Gracey, A.Y. Seasonally Hibernating Phenotype Assessed through Transcript Screening. *Physiological Genomics* **2006**, *24*, 13–22, doi:10.1152/physiolgenomics.00301.2004.
353. Yan, J.; Barnes, B.M.; Kohl, F.; Marr, T.G. Modulation of Gene Expression in Hibernating Arctic Ground Squirrels. *Physiol Genomics* *32*, 12.
354. Knight, J.E.; Narus, E.N.; Martin, S.L.; Jacobson, A.; Barnes, B.M.; Boyer, B.B. mRNA Stability and Polysome Loss in Hibernating Arctic Ground Squirrels (*Spermophilus Parryii*). *MOL. CELL. BIOL.* **2000**, *20*, 6.
355. Pan, P.; van Breukelen, F. Preference of IRES-Mediated Initiation of Translation during Hibernation in Golden-Mantled Ground Squirrels, *Spermophilus Lateralis*. *American Journal of Physiology-Regulatory, Integrative and Comparative Physiology* **2011**, *301*, R370–R377, doi:10.1152/ajpregu.00748.2010.
356. Pelt, D.W.V.; Hettinger, Z.R.; Dupont-Versteegden, E.E. Cold Shock RNA-Binding Protein RBM3 as a Potential Therapeutic Target to Prevent Skeletal Muscle Atrophy. *binding protein* *5*.
357. Liu, Y.; Beyer, A.; Aebersold, R. On the Dependency of Cellular Protein Levels on mRNA Abundance. *Cell* **2016**, *165*, 535–550, doi:10.1016/j.cell.2016.03.014.
358. Glock, C.; Heumüller, M.; Schuman, E.M. mRNA Transport & Local Translation in Neurons. *Current Opinion in Neurobiology* **2017**, *45*, 169–177, doi:10.1016/j.conb.2017.05.005.
359. Miyazono, K.; Miyazawa, K. Id: A Target of BMP Signaling. *Sci. STKE* **2002**, *2002*, doi:10.1126/stke.2002.151.pe40.
360. Katagiri, T.; Imada, M.; Yanai, T.; Suda, T.; Takahashi, N.; Kamijo, R. For Inhibition of Myogenesis. *12*.

361. Kusanagi, K.; Inoue, H.; Ishidou, Y.; Mishima, H.K.; Kawabata, M.; Miyazono, K. Characterization of a Bone Morphogenetic Protein-Responsive Smad-Binding Element. *MBoC* **2000**, *11*, 555–565, doi:10.1091/mbc.11.2.555.
362. Zhao, Z.; Bo, Z.; Gong, W.; Guo, Y. Inhibitor of Differentiation 1 (Id1) in Cancer and Cancer Therapy. *Int. J. Med. Sci.* **2020**, *17*, 995–1005, doi:10.7150/ijms.42805.
363. Goumans, M.-J.; Valdimarsdottir, G.; Itoh, S.; Rosendahl, A.; Sideras, P. Balancing the Activation State of the Endothelium via Two Distinct TGF- β Type I Receptors. **11**.
364. Jen, Y.; Weintraub, H.; Benezra, R. Overexpression of Id Protein Inhibits the Muscle Differentiation Program: In Vivo Association of Id with E2A Proteins. *Genes Dev.* **1992**, *6*, 1466–1479, doi:10.1101/gad.6.8.1466.
365. Gundersen, K.; Merlie, J.P. Id-1 as a Possible Transcriptional Mediator of Muscle Disuse Atrophy. *Proc. Natl. Acad. Sci. U.S.A.* **1994**, *91*, 3647–3651, doi:10.1073/pnas.91.9.3647.
366. Buford, T.W.; Cooke, M.B.; Shelmadine, B.D.; Hudson, G.M.; Redd, L.L.; Willoughby, D.S. Differential Gene Expression of FoxO1, ID1, and ID3 between Young and Older Men and Associations with Muscle Mass and Function. *Aging Clin Exp Res* **2011**, *23*, 170–174, doi:10.1007/BF03324957.
367. Raja, E.; Tzavlaki, K.; Vuilleumier, R.; Edlund, K.; Kahata, K.; Zieba, A.; Morén, A.; Watanabe, Y.; Voytyuk, I.; Botling, J.; et al. The Protein Kinase LKB1 Negatively Regulates Bone Morphogenetic Protein Receptor Signaling. *Oncotarget* **2016**, *7*, 1120–1143, doi:10.18632/oncotarget.6683.
368. Macias, M.J.; Martin-Malpartida, P.; Massagué, J. Structural Determinants of Smad Function in TGF- β Signaling. *Trends in Biochemical Sciences* **2015**, *40*, 296–308, doi:10.1016/j.tibs.2015.03.012.
369. Aragón, E.; Goerner, N.; Zaromytidou, A.-I.; Xi, Q.; Escobedo, A.; Massagué, J.; Macias, M.J. A Smad Action Turnover Switch Operated by WW Domain Readers of a Phosphoserine Code. *Genes Dev.* **2011**, *25*, 1275–1288, doi:10.1101/gad.2060811.
370. Demagny, H.; Araki, T.; De Robertis, E.M. The Tumor Suppressor Smad4/DPC4 Is Regulated by Phosphorylations That Integrate FGF, Wnt, and TGF- β Signaling. *Cell Reports* **2014**, *9*, 688–700, doi:10.1016/j.celrep.2014.09.020.
371. Dijke, P.; Baker, D. Controlling Smad4 Signaling with a Wip. *EMBO Rep* **2020**, *21*, doi:10.15252/embr.202050246.
372. Kubota, S.; Takigawa, M. Cellular and Molecular Actions of CCN2/CTGF and Its Role under Physiological and Pathological Conditions. *Clinical Science* **2015**, *128*, 181–196, doi:10.1042/CS20140264.
373. Sun, G.; Haginoya, K.; Wu, Y.; Chiba, Y.; Nakanishi, T.; Onuma, A.; Sato, Y.; Takigawa, M.; Iinuma, K.; Tsuchiya, S. Connective Tissue Growth Factor Is Overexpressed in Muscles of Human Muscular Dystrophy. *Journal of the Neurological Sciences* **2008**, *267*, 48–56, doi:10.1016/j.jns.2007.09.043.
374. Vial, C.; Zúñiga, L.M.; Cabello-Verrugio, C.; Cañón, P.; Fadic, R.; Brandan, E. Skeletal Muscle Cells Express the Profibrotic Cytokine Connective Tissue Growth Factor (CTGF/CCN2), Which Induces Their Dedifferentiation. *J. Cell. Physiol.* **2008**, *215*, 410–421, doi:10.1002/jcp.21324.

375. Hillege, M.; Galli Caro, R.; Offringa, C.; de Wit, G.; Jaspers, R.; Hoogaars, W. TGF- β Regulates Collagen Type I Expression in Myoblasts and Myotubes via Transient Ctgf and Fgf-2 Expression. *Cells* **2020**, *9*, 375, doi:10.3390/cells9020375.
376. Abreu, J.G.; Ketpura, N.I.; Reversade, B.; De Robertis, E.M. Connective-Tissue Growth Factor (CTGF) Modulates Cell Signalling by BMP and TGF- β . *Nat Cell Biol* **2002**, *4*, 599–604, doi:10.1038/ncb826.
377. Furumatsu, T.; Kanazawa, T.; Miyake, Y.; Kubota, S.; Takigawa, M.; Ozaki, T. Mechanical Stretch Increases Smad3-Dependent CCN2 Expression in Inner Meniscus Cells: STRETCH-INDUCED CCN2 IN THE MENISCUS. *J. Orthop. Res.* **2012**, *30*, 1738–1745, doi:10.1002/jor.22142.
378. Song, Y.; Yao, S.; Liu, Y.; Long, L.; Yang, H.; Li, Q.; Liang, J.; Li, X.; Lu, Y.; Zhu, H.; et al. Expression Levels of TGF-B1 and CTGF Are Associated with the Severity of Duchenne Muscular Dystrophy. *Experimental and Therapeutic Medicine* **2017**, *13*, 1209–1214, doi:10.3892/etm.2017.4105.
379. Kular, L.; Pakradouni, J.; Kitabgi, P.; Laurent, M.; Martinerie, C. The CCN Family: A New Class of Inflammation Modulators? *Biochimie* **2011**, *93*, 377–388, doi:10.1016/j.biochi.2010.11.010.
380. Nguyen, T.Q.; Roestenberg, P.; van Nieuwenhoven, F.A.; Bovenschen, N.; Li, Z.; Xu, L.; Oliver, N.; Aten, J.; Joles, J.A.; Vial, C.; et al. CTGF Inhibits BMP-7 Signaling in Diabetic Nephropathy. *JASN* **2008**, *19*, 2098–2107, doi:10.1681/ASN.2007111261.
381. Khattab, H.M.; Aoyama, E.; Kubota, S.; Takigawa, M. Physical Interaction of CCN2 with Diverse Growth Factors Involved in Chondrocyte Differentiation during Endochondral Ossification. *J. Cell Commun. Signal.* **2015**, *9*, 247–254, doi:10.1007/s12079-015-0290-x.
382. Morales, M.G.; Gutierrez, J.; Cabello-Verrugio, C.; Cabrera, D.; Lipson, K.E.; Goldschmeding, R.; Brandan, E. Reducing CTGF/CCN2 Slows down Mdx Muscle Dystrophy and Improves Cell Therapy. *Human Molecular Genetics* **2013**, *22*, 4938–4951, doi:10.1093/hmg/ddt352.
383. Desai, A.J.; Miller, L.J. Changes in the Plasma Membrane in Metabolic Disease: Impact of the Membrane Environment on G Protein-Coupled Receptor Structure and Function: Membrane Impact on Receptor Function. *British Journal of Pharmacology* **2018**, *175*, 4009–4025, doi:10.1111/bph.13943.
384. Maulucci, G.; Cohen, O.; Daniel, B.; Sansone, A.; Petropoulou, P.I.; Filou, S.; Spyridonidis, A.; Pani, G.; De Spirito, M.; Chatgililoglu, C.; et al. Fatty Acid-Related Modulations of Membrane Fluidity in Cells: Detection and Implications. *Free Radical Research* **2016**, *50*, S40–S50, doi:10.1080/10715762.2016.1231403.
385. Chen, C.L.; Chen, C.Y.; Chen, Y.P.; Huang, Y.B.; Lin, M.W.; Wu, D.C.; Huang, H.T.; Liu, M.Y.; Chang, H.W.; Kao, Y.C.; et al. Betulinic Acid Enhances TGF- β Signaling by Altering TGF- β Receptors Partitioning between Lipid-Raft/Caveolae and Non-Caveolae Membrane Microdomains in Mink Lung Epithelial Cells. *J Biomed Sci* **2016**, *23*, 30, doi:10.1186/s12929-016-0229-4.
386. Chen, Y.-G. Endocytic Regulation of TGF- β Signaling. *Cell Res* **2009**, *19*, 58–70, doi:10.1038/cr.2008.315.
387. Yakymovych, I.; Yakymovych, M.; Heldin, C.-H. Intracellular Trafficking of Transforming Growth Factor β ; Receptors. *ABBS* **2018**, *50*, 3–11, doi:10.1093/abbs/gmx119.

388. Chen, C.-L.; Liu, I.-H.; Fliesler, S.J.; Han, X.; Huang, S.S.; Huang, J.S. Cholesterol Suppresses Cellular TGF- β Responsiveness: Implications in Atherogenesis. *Journal of Cell Science* **2007**, *120*, 3509–3521, doi:10.1242/jcs.006916.
389. Hartung, A.; Bitton-Worms, K.; Rechtman, M.M.; Wenzel, V.; Boergermann, J.H.; Hassel, S.; Henis, Y.I.; Knaus, P. Different Routes of Bone Morphogenic Protein (BMP) Receptor Endocytosis Influence BMP Signaling. *Mol Cell Biol* **2006**, *26*, 7791–7805, doi:10.1128/MCB.00022-06.
390. Ball, R.W.; Warren-Paquin, M.; Tsurudome, K.; Liao, E.H.; Elazzouzi, F.; Cavanagh, C.; An, B.-S.; Wang, T.-T.; White, J.H.; Haghighi, A.P. Retrograde BMP Signaling Controls Synaptic Growth at the NMJ by Regulating Trio Expression in Motor Neurons. *Neuron* **2010**, *66*, 536–549, doi:10.1016/j.neuron.2010.04.011.
391. Bayat, V.; Jaiswal, M.; Bellen, H.J. The BMP Signaling Pathway at the Drosophila Neuromuscular Junction and Its Links to Neurodegenerative Diseases. *Current Opinion in Neurobiology* **2011**, *21*, 182–188, doi:10.1016/j.conb.2010.08.014.
392. Kelly, C.E.; Thymiakou, E.; Dixon, J.E.; Tanaka, S.; Godwin, J.; Episkopou, V. Rnf165/Ark2C Enhances BMP-Smad Signaling to Mediate Motor Axon Extension. *PLoS Biol* **2013**, *11*, e1001538, doi:10.1371/journal.pbio.1001538.
393. Yilmaz, A.; Kattamuri, C.; Ozdeslik, R.N.; Schmiedel, C.; Mentzer, S.; Schorl, C.; Oancea, E.; Thompson, T.B.; Fallon, J.R. MuSK Is a BMP Co-Receptor That Shapes BMP Responses and Calcium Signaling in Muscle Cells. *Sci. Signal.* **2016**, *9*, ra87–ra87, doi:10.1126/scisignal.aaf0890.
394. Fish, L.A.; Fallon, J.R. Multiple MuSK Signaling Pathways and the Aging Neuromuscular Junction. *Neuroscience Letters* **2020**, *731*, 135014, doi:10.1016/j.neulet.2020.135014.
395. Zhang, W.; Wu, X.; Pei, Z.; Kiess, W.; Yang, Y.; Xu, Y.; Chang, Z.; Wu, J.; Sun, C.; Luo, F. GDF5 Promotes White Adipose Tissue Thermogenesis via P38 MAPK Signaling Pathway. *DNA and Cell Biology* **2019**, *38*, 1303–1312, doi:10.1089/dna.2019.4724.
396. Hinoi, E.; Nakamura, Y.; Takada, S.; Fujita, H.; Iezaki, T.; Hashizume, S.; Takahashi, S.; Odaka, Y.; Watanabe, T.; Yoneda, Y. Growth Differentiation Factor-5 Promotes Brown Adipogenesis in Systemic Energy Expenditure. *Diabetes* **2014**, *63*, 162–175, doi:10.2337/db13-0808.
397. Davis, W.L.; Goodman, D.B.P.; Crawford, L.A.; Cooper, O.J.; Matthews, J.L. Hibernation Activates Glyoxylate Cycle and Gluconeogenesis in Black Bear Brown Adipose Tissue. *Biochimica et Biophysica Acta (BBA) - Molecular Cell Research* **1990**, *1051*, 276–278, doi:10.1016/0167-4889(90)90133-X.
398. Jones, J.D.; Burnett, P.; Zollman, P. The Glyoxylate Cycle: Does It Function in the Dormant or Active Bear? *Comparative Biochemistry and Physiology Part B: Biochemistry and Molecular Biology* **1999**, *124*, 177–179, doi:10.1016/S0305-0491(99)00109-1.
399. Zhang, Z.; Yang, D.; Xiang, J.; Zhou, J.; Cao, H.; Che, Q.; Bai, Y.; Guo, J.; Su, Z. Non-Shivering Thermogenesis Signalling Regulation and Potential Therapeutic Applications of Brown Adipose Tissue. *Int. J. Biol. Sci.* **2021**, *17*, 2853–2870, doi:10.7150/ijbs.60354.
400. Bonewald, L. Use It or Lose It to Age: A Review of Bone and Muscle Communication. *Bone* **2019**, *120*, 212–218, doi:10.1016/j.bone.2018.11.002.
401. Lloyd, S.A.; Lang, C.H.; Zhang, Y.; Paul, E.M.; Laufenberg, L.J.; Lewis, G.S.; Donahue, H.J. Interdependence of Muscle Atrophy and Bone Loss Induced by Mechanical Unloading: MUSCLE

- ATROPHY AND BONE LOSS DURING UNLOADING. *J Bone Miner Res* **2014**, *29*, 1118–1130, doi:10.1002/jbmr.2113.
402. Essex, A.L.; Pin, F.; Huot, J.R.; Bonewald, L.F.; Plotkin, L.I.; Bonetto, A. Bisphosphonate Treatment Ameliorates Chemotherapy-Induced Bone and Muscle Abnormalities in Young Mice. *Front. Endocrinol.* **2019**, *10*, 809, doi:10.3389/fendo.2019.00809.
403. Pin, F.; Bonetto, A.; Bonewald, L.F.; Klein, G.L. Molecular Mechanisms Responsible for the Rescue Effects of Pamidronate on Muscle Atrophy in Pediatric Burn Patients. *Front. Endocrinol.* **2019**, *10*, 543, doi:10.3389/fendo.2019.00543.
404. Dallas, S.L.; Rosser, J.L.; Mundy, G.R.; Bonewald, L.F. Proteolysis of Latent Transforming Growth Factor- β (TGF- β)-Binding Protein-1 by Osteoclasts. *Journal of Biological Chemistry* **2002**, *277*, 21352–21360, doi:10.1074/jbc.M111663200.
405. Morikawa, M.; Derynck, R.; Miyazono, K. TGF- β and the TGF- β Family: Context-Dependent Roles in Cell and Tissue Physiology. *Cold Spring Harb Perspect Biol* **2016**, *8*, a021873, doi:10.1101/cshperspect.a021873.
406. Buehring, B.; Binkley, N. Myostatin – The Holy Grail for Muscle, Bone, and Fat? *Curr Osteoporos Rep* **2013**, *11*, 407–414, doi:10.1007/s11914-013-0160-5.
407. Zou, M.-L.; Chen, Z.-H.; Teng, Y.-Y.; Liu, S.-Y.; Jia, Y.; Zhang, K.-W.; Sun, Z.-L.; Wu, J.-J.; Yuan, Z.-D.; Feng, Y.; et al. The Smad Dependent TGF- β and BMP Signaling Pathway in Bone Remodeling and Therapies. *Front. Mol. Biosci.* **2021**, *8*, 593310, doi:10.3389/fmolb.2021.593310.
408. Dankbar, B.; Fennen, M.; Brunert, D.; Hayer, S.; Frank, S.; Wehmeyer, C.; Beckmann, D.; Paruzel, P.; Bertrand, J.; Redlich, K.; et al. Myostatin Is a Direct Regulator of Osteoclast Differentiation and Its Inhibition Reduces Inflammatory Joint Destruction in Mice. *Nat Med* **2015**, *21*, 1085–1090, doi:10.1038/nm.3917.
409. Umezu, T.; Nakamura, S.; Sato, Y.; Kobayashi, T.; Ito, E.; Abe, T.; Kaneko, M.; Nomura, M.; Yoshimura, A.; Oya, A.; et al. Smad2 and Smad3 Expressed in Skeletal Muscle Promote Immobilization-Induced Bone Atrophy in Mice. *Biochemical and Biophysical Research Communications* **2021**, *582*, 111–117, doi:10.1016/j.bbrc.2021.10.043.
410. Puolakkainen, T.; Ma, H.; Kainulainen, H.; Pasternack, A.; Rantalainen, T.; Ritvos, O.; Heikinheimo, K.; Hulmi, J.J.; Kiviranta, R. Treatment with Soluble Activin Type IIB-Receptor Improves Bone Mass and Strength in a Mouse Model of Duchenne Muscular Dystrophy. *BMC Musculoskelet Disord* **2017**, *18*, 20, doi:10.1186/s12891-016-1366-3.
411. Bialek, P.; Parkington, J.; Li, X.; Gavin, D.; Wallace, C.; Zhang, J.; Root, A.; Yan, G.; Warner, L.; Seeherman, H.J.; et al. A Myostatin and Activin Decoy Receptor Enhances Bone Formation in Mice. *Bone* **2014**, *60*, 162–171, doi:10.1016/j.bone.2013.12.002.
412. Jeong, Y.; Daghlas, S.A.; Xie, Y.; Hulbert, M.A.; Pfeiffer, F.M.; Dallas, M.R.; Omosule, C.L.; Pearsall, R.S.; Dallas, S.L.; Phillips, C.L. Skeletal Response to Soluble Activin Receptor Type IIB in Mouse Models of Osteogenesis Imperfecta: SKELETAL RESPONSE TO SOLUBLE ACTIVIN RECEPTOR TYPE IIB IN OI. *J Bone Miner Res* **2018**, *33*, 1760–1772, doi:10.1002/jbmr.3473.
413. Donahue, S.W.; Wojda, S.J.; McGee-Lawrence, M.E.; Auger, J.; Black, H.L. Osteoporosis Prevention in an Extraordinary Hibernating Bear. *Bone* **2021**, *145*, 115845, doi:10.1016/j.bone.2021.115845.

414. Nasoori, A.; Okamatsu-Ogura, Y.; Shimozuru, M.; Sashika, M.; Tsubota, T. Hibernating Bear Serum Hinders Osteoclastogenesis In-Vitro. *PLoS ONE* **2020**, *15*, e0238132, doi:10.1371/journal.pone.0238132.
415. Smullen, S.; McLaughlin, N.P.; Evans, P. Chemical Synthesis of Febrifugine and Analogues. *Bioorganic & Medicinal Chemistry* **2018**, *26*, 2199–2220, doi:10.1016/j.bmc.2018.04.027.
416. Pines, M.; Spector, I. Halofuginone — The Multifaceted Molecule. *Molecules* **2015**, *20*, 573–594, doi:10.3390/molecules20010573.
417. Kamberov, Y.G.; Kim, J.; Mazitschek, R.; Kuo, W.P.; Whitman, M. Microarray Profiling Reveals the Integrated Stress Response Is Activated by Halofuginone in Mammary Epithelial Cells. *BMC Res Notes* **2011**, *4*, 381, doi:10.1186/1756-0500-4-381.
418. Keller, T.L.; Zocco, D.; Sundrud, M.S.; Hendrick, M.; Edenius, M.; Yum, J.; Kim, Y.-J.; Lee, H.-K.; Cortese, J.F.; Wirth, D.F.; et al. Halofuginone and Other Febrifugine Derivatives Inhibit Prolyl-TRNA Synthetase. *Nat Chem Biol* **2012**, *8*, 311–317, doi:10.1038/nchembio.790.
419. Chaveroux, C.; Carraro, V.; Canaple, L.; Averous, J.; Maurin, A.-C.; Jousse, C.; Muranishi, Y.; Parry, L.; Mesclon, F.; Gatti, E.; et al. In Vivo Imaging of the Spatiotemporal Activity of the EIF2 α -ATF4 Signaling Pathway: Insights into Stress and Related Disorders. *Sci. Signal.* **2015**, *8*, doi:10.1126/scisignal.aaa0549.
420. Roffe, S.; Hagai, Y.; Pines, M.; Halevy, O. Halofuginone Inhibits Smad3 Phosphorylation via the PI3K/Akt and MAPK/ERK Pathways in Muscle Cells: Effect on Myotube Fusion. *Experimental Cell Research* **2010**, *316*, 1061–1069, doi:10.1016/j.yexcr.2010.01.003.
421. Duan, M.; Wei, X.; Cheng, Z.; Liu, D.; Fotina, H.; Xia, X.; Hu, J. Involvement of EIF2 α in Halofuginone-Driven Inhibition of TGF-B1-Induced EMT. *J Biosci* **2020**, *45*, 71, doi:10.1007/s12038-020-00042-5.
422. Luo, Y.; Xie, X.; Luo, D.; Wang, Y.; Gao, Y. The Role of Halofuginone in Fibrosis: More to Be Explored? *J Leukoc Biol* **2017**, *102*, 1333–1345, doi:10.1189/jlb.3RU0417-148RR.
423. Cussonneau, L.; Coudy-Gandilhon, C.; Deval, C.; Chaouki, G.; Djelloul-Mazouz, M.; Delorme, Y.; Hermet, J.; Gauquelin-Koch, G.; Polge, C.; Taillandier, D.; et al. Induction of ATF4-Regulated Atrogenes Is Uncoupled from Muscle Atrophy during Disuse in Halofuginone-Treated Mice and in Hibernating Brown Bears. *IJMS* **2022**, *24*, 621, doi:10.3390/ijms24010621.
424. Li, T.-F.; Yukata, K.; Yin, G.; Sheu, T.; Maruyama, T.; Jonason, J.H.; Hsu, W.; Zhang, X.; Xiao, G.; Konttinen, Y.T.; et al. BMP-2 Induces ATF4 Phosphorylation in Chondrocytes through a COX-2/PGE2 Dependent Signaling Pathway. *Osteoarthritis and Cartilage* **2014**, *22*, 481–489, doi:10.1016/j.joca.2013.12.020.
425. Egawa, T.; Goto, A.; Ohno, Y.; Yokoyama, S.; Ikuta, A.; Suzuki, M.; Sugiura, T.; Ohira, Y.; Yoshioka, T.; Hayashi, T.; et al. Involvement of AMPK in Regulating Slow-Twitch Muscle Atrophy during Hindlimb Unloading in Mice. *American Journal of Physiology-Endocrinology and Metabolism* **2015**, *309*, E651–E662, doi:10.1152/ajpendo.00165.2015.
426. Li, Y.; Zheng, W.; Lu, Y.; Zheng, Y.; Pan, L.; Wu, X.; Yuan, Y.; Shen, Z.; Ma, S.; Zhang, X.; et al. BNIP3L/NIX-Mediated Mitophagy: Molecular Mechanisms and Implications for Human Disease. *Cell Death Dis* **2022**, *13*, 14, doi:10.1038/s41419-021-04469-y.

427. Hanna, R.A.; Quinsay, M.N.; Orogo, A.M.; Giang, K.; Rikka, S.; Gustafsson, Å.B. Microtubule-Associated Protein 1 Light Chain 3 (LC3) Interacts with Bnip3 Protein to Selectively Remove Endoplasmic Reticulum and Mitochondria via Autophagy. *Journal of Biological Chemistry* **2012**, *287*, 19094–19104, doi:10.1074/jbc.M111.322933.
428. Springer, M.Z. COMMITTEE ON CANCER BIOLOGY. 143.
429. Harding, H.P.; Zhang, Y.; Zeng, H.; Novoa, I.; Lu, P.D.; Calton, M.; Sadri, N.; Yun, C.; Popko, B.; Paules, R.; et al. An Integrated Stress Response Regulates Amino Acid Metabolism and Resistance to Oxidative Stress. *Molecular Cell* **2003**, *11*, 619–633, doi:10.1016/S1097-2765(03)00105-9.
430. Korchynskiy, O.; ten Dijke, P. Identification and Functional Characterization of Distinct Critically Important Bone Morphogenetic Protein-Specific Response Elements in the Id1 Promoter. *Journal of Biological Chemistry* **2002**, *277*, 4883–4891, doi:10.1074/jbc.M111023200.
431. Zawel, L.; Le Dai, J.; Buckhaults, P.; Zhou, S.; Kinzler, K.W.; Vogelstein, B.; Kern, S.E. Human Smad3 and Smad4 Are Sequence-Specific Transcription Activators. *Molecular Cell* **1998**, *1*, 611–617, doi:10.1016/S1097-2765(00)80061-1.
432. Zhou, Y.; Zhou, B.; Pache, L.; Chang, M.; Khodabakhshi, A.H.; Tanaseichuk, O.; Benner, C.; Chanda, S.K. Metascape Provides a Biologist-Oriented Resource for the Analysis of Systems-Level Datasets. *Nat Commun* **2019**, *10*, 1523, doi:10.1038/s41467-019-09234-6.

Résumé

L'atrophie musculaire impacte des millions de personnes à travers le monde, incluant des personnes âgées, des personnes atteintes de maladies ou encore des personnes immobilisées pendant de longues périodes. La perte de masse musculaire conduit à un déclin de l'autonomie, favorise l'apparition de maladies, augmente la résistance aux traitements mis en place, et est associée à une augmentation de la mortalité. De ce fait, l'atrophie musculaire constitue un problème majeur de santé publique. Enormément de mécanismes biomoléculaires ont été documentés pouvant expliquer l'apparition de l'atrophie musculaire, principalement grâce à l'utilisation de modèle de rongeurs de laboratoire. Pourtant, aucun traitement n'est réellement efficace et/ou adaptable pour tous aujourd'hui.

L'objectif principal de cette thèse était de trouver de nouveaux mécanismes sous-jacents qui pourraient devenir des cibles thérapeutiques pour combattre l'atrophie musculaire chez l'Homme. Nous avons choisi une approche basée sur le biomimétisme. Notre stratégie a été (1) de réaliser une étude de physiologie comparée entre le modèle de l'ours brun naturellement résistant à l'atrophie pendant hibernation et la souris suspendue sensible à l'atrophie musculaire, (2) d'étudier le rôle des voies de signalisations ATF4 et TGF- β /BMP dans ces deux modèles, et enfin (3) d'initier des études sur des cellules musculaires humaines pour valider les hypothèses issues des deux premières études.

Dans notre première étude, la stratégie a été d'identifier les gènes différenciellement régulés dans les muscles de l'ours brun entre la période d'hibernation et la période d'activité. Ensuite, nous les avons comparés à ceux différenciellement régulés dans les muscles de la souris suspendue par rapport à la souris contrôle. Nous avons montré que la concomitance de l'inhibition de la signalisation TGF- β et de l'induction de la signalisation BMP semblait être cruciale pour le maintien de la masse musculaire en condition d'inactivité physique prolongée. Dans notre deuxième étude, nous avons montré que l'induction de la voie de signalisation d'ATF4 dans le muscle était découplée de l'atrophie musculaire chez la souris saine ou soumise à une situation d'inactivité physique lorsqu'elles étaient préalablement traitées par la molécule d'halofuginone, et également chez l'ours hibernant. Dans ces 3 situations, le maintien de la masse musculaire était associé à la fois à l'induction de la signalisation d'ATF4 et de BMP et à l'inhibition de TGF- β . Enfin, des résultats préliminaires obtenus en cultivant des cellules musculaires humaines avec du sérum d'ours brun hibernant suggèrent la présence d'un composé actif circulant pouvant reproduire certaines caractéristiques observées dans le muscle de l'ours brun hibernant résistant à l'atrophie. En conclusion, ces travaux ouvrent de nombreuses perspectives dans la modulation de la balance des voies de signalisation TGF- β et BMP dans des situations d'inactivité physique prolongée. De plus, ils ouvrent de nouvelles recherches sur l'identification de composés actifs dans le sérum de l'ours pouvant être utilisables en clinique humaine afin de limiter ou prévenir l'apparition d'atrophie musculaire lors de l'immobilisation ou dans d'autres conditions physiopathologiques.

Abstract

Muscle wasting affects millions of people around the world, including the elderly, people with illnesses, and people who are immobilised for long periods of time. The loss of muscle mass leads to a decline in independence, promotes disease, increases resistance to treatment, and is associated with increased mortality. As a result, muscle wasting is a major public health problem. Many biomolecular mechanisms have been documented to explain the occurrence of muscle wasting, mainly through the use of laboratory rodent models. However, no treatment is really effective and/or adaptable for all today. The main objective of this thesis was to find new underlying mechanisms that could become therapeutic targets to combat muscle atrophy in humans. We chose an approach based on biomimicry. Our strategy was (1) to perform a comparative physiology study between the brown bear model naturally resistant to atrophy during hibernation and the unloading mouse sensitive to muscle atrophy, (2) to study the role of the ATF4 and TGF- β /BMP signalling pathways in these two models, and finally (3) to initiate studies on human muscle cells to validate the hypotheses from the first two studies. In our first study, the strategy was to identify genes differentially regulated in brown bear muscle between the hibernation and active periods. Then we compared them to those differentially regulated in the muscles of the unloading mouse versus the control mouse. We showed that the concomitance of inhibition of TGF- β signalling and induction of BMP signalling appeared to be crucial for the maintenance of muscle mass under conditions of prolonged physical inactivity. In our second study, we showed that the induction of the ATF4 signalling pathway in muscle was uncoupled from muscle atrophy in healthy and physically inactive mice when previously treated with the halofuginone molecule, and also in hibernating bears. In all three situations, the maintenance of muscle mass was associated with both the induction of ATF4 and BMP signalling and the inhibition of TGF- β . Finally, preliminary results obtained by cultivating human muscle cells with hibernating brown bear serum suggest the presence of a circulating active compound that may mimic some of the characteristics observed in atrophy-resistant hibernating brown bear muscle. In conclusion, this work provides numerous perspectives in the modulation of the balance of TGF- β and BMP signalling pathways in situations of prolonged physical inactivity. In addition, it opens up new research on the identification of active compounds in bear serum that could be used in the human clinic to limit or prevent the onset of muscle atrophy during immobilisation or in other pathophysiological conditions.